Departament de Biologia Evolutiva, Ecologia i Ciències Ambientals
Programa de Doctorat de Biodiversitat

The bathyal connections between the Mediterranean Sea and the Northeastern Atlantic Ocean: an assessment using deep-water sponges as a case study

Memòria presentada per Cèlia Sitjà Poch per optar al grau de doctora per la Universitat de Barcelona

Cèlia Sitjà Poch
Centre d'Estudis Avançats de Blanes (CEAB-CSIC)
Barcelona, juliol del 2020

Director:
Dr. Manuel Maldonado Barahona
Investigador Científic CSIC
Centre d'Estudis Avançats de Blanes

Co-director:
Dr. José Luis Rueda Ruiz
Investigador Titular IEO
Centro Oceanográfico de Málaga

Tutora:
Dra. Conxita Avila Escartín
Professora catedràtica d'universitat
Universitat de Barcelona

Sitjà, C., 2020. The bathyal connections between the Mediterranean Sea and the Northeastern Atlantic Ocean: an assessment using deep-water sponges as a case study. Doctoral thesis. Universitat de Barcelona. 360 pp.

Cover design: Sílvia Bancells Aulet and Cèlia Sitjà Poch.
Picture: Pipoca mud volcano seabed with *Asconema setubalense* and *Petrosia crassa* on methane-derived authigenic carbonates. Picture taken with a ROV during the LIFE+INDEMARES-Chica expeditions performed by the Spanish Institute of Oceanography (IEO).

Als meus pares

Agraïments

Tots els que esteu dins de les pròximes pàgines m'heu recolzat, ensenyat, acompanyat i animat durant els meus anys de doctoranda. A tots us estic immensament agraïda i em sento afortunada d'haver-nos trobat. Sapigueu que us dono unes gràcies de les de veritat, de tot cor, perquè ja sabia que no em fallaríeu però sobretot perquè he après molt més que ciència al vostre costat. Sabia que podia comptar amb vosaltres, però no era conscient de tot el que em regalaríeu al llarg d'aquests anys. Per donar-vos les gràcies he resumit en unes frases i un petit text el que més valoro de tot allò que m'heu aportat cada un de vosaltres:

"Hay que marcarse objetivos lejanos"

Cada día he tenido en frente un ejemplo de perseverancia, esfuerzo y ambición. Manuel, gracias no solo por buscar el material y financiación para esta tesis, sino también por darme ejemplo pensando siempre en grande y lejos. Al final no te he dejado cuadricular mi "mente poética", como tú la llamas, pero sin duda la has ayudado a tener capacidad crítica y puntos de vista mucho más amplios de lo que yo podía imaginar. Gracias por darme unas herramientas tan valiosas, estoy deseando sacarles el mejor provecho en el futuro.

"La distancia es relativa"

Nunca un director a tantos quilómetros ha estado tan cerca y tan presente. Tu predisposición, vocación y positivismo me llegaban a través de cada uno de tus mails. Los volcanes de fango son muy interesantes, pero los del Golfo de Cádiz tienen un encanto especial gracias a tu valiosa forma de transmitir tus conocimientos sobre ellos. Por favor José, dirige muchas tesis más y enseña a tantos estudiantes como puedas contagiándolos con tus ánimos y entusiasmo.

"Un pont sòlid i pràctic "

La distancia entre Blanes i la UB s'ha escurçat gràcies a una bona tutora. Sempre disponible quan ho he necessitat, t'agraeixo, Conxita, la teva ajuda, comentaris i ànims.

"En el Riesgo Lab todo es posible"

Siempre con un "sí" listo, en este grupo todo son facilidades y *primers*! Sois la combinación perfecta de trabajo y compañerismo. No hay otro laboratorio con tan buenos científicos y un grupo de watsapp tan activo. Ana y Sergi son capaces de convertir el mismo *National History Museum* de Londres en tu casa des del momento en que lo pisas y pasas a formar parte del Riesgo Lab. Y encima tuve la suerte de compartirlo con Jenny, Carlos, Vassia, Nathan… you were all excellent labmates, always ready to help, and also ready to have fun! Thanks to all of you my short-time stay in London became a great stay!

"Mucho más que muestras"

Muchas de las muestras usadas en esta tesis han pasado por Málaga en algún momento. Gracias a ellas conocí a Carmen y Serge, que me ofrecieron todo lo que tenían mientras esperábamos a poder embarcar para la campaña de Alborán. No solo confiasteis en mí para procesar las muestras, también lo hicisteis para recibirme en vuestra casa, o más bien adoptarme! Muchas gracias a los dos por vuestra confianza y calidez. Gracias también a Javi, por convertirse en el mejor guía de Málaga y asegurarse de que mi estancia allí fuera la mejor.

Y por supuesto también quiero agradecer a todos los participantes en la campaña a bordo del Isla de Alborán esos fantásticos días embarcados. ¿Cómo puede ser que en un barco que se tambalea tanto se cree un equilibrio tan sano entre trabajo y risas? Gracias a la tripulación, y a todos los compañeros de campaña por hacer del trabajo duro un *hobbie*. Y gracias en especial al jefe de campaña, Serge, para asegurarse de que así fuera.

No puedo olvidarme de nombrar al Oceanográfico de Málaga por cedernos las muestras de los volcanes de fango del Golfo de Cádiz. El esfuerzo de muchas personas invertido en las campañas del Golfo de Cádiz hizo que unos años más tarde las muestras recolectadas cayeran en mis manos junto con un montón de datos. A todos los involucrados en esas campañas les doy unas grandes gracias, en especial a Carlos, por el gigantesco trabajo de identificación que hizo con muchas de las muestras antes de que yo me las llevara a Blanes. Mil gracias a todos por vuestra generosidad y confianza.

Las muestras de Malta tuvieron una historia similar a las de los volcanes de fango. En este caso nos las cedió la ONG OCEANA, que dejó en mis manos todo el material de esponjas que habían colectado previamente en Malta. Y literalmente lo dejaron en mis manos, porque gracias al entendimiento entre Manuel y Ricardo, un buen día llegaron al Ceab unas cajas con esponjas maltesas listas para ser identificadas. Más fácil no me lo pudisteis poner, así que muchísimas gracias.

"Técnicos siempre dispuestos a ayudar"

¿Había que pasar unas láminas a tinta? Gustavo sin duda dominaba la técnica y era mucho más rápido que yo. ¿Había que metalizar muestras para el SEM? María José, Xavi, Maria, lo hacían tan pronto como podían. Todos estabais siempre dispuestos a colaborar a pesar de que lo que os pedía no formaba parte de vuestras actividades habituales. Gracias por encontrar siempre un hueco para ayudarme.

"Algunes son capaces d'elevar el concepte d'equip a un altre nivell"

María, Marta y Cris. Nombrades per odre d'arribada al Ceab, perquè no se us pot ordenar de cap altra manera. Al nostre equip no hi ha hagut mai desigualtats, només dones preparades per col·laborar i facilitar la vida de les demés. Alguna de vosaltres sap com explicar als lectors el que significuem les unes per les altres? No hem estat només companyes de feina, perquè les companyes de feina no es tenen el respecte i afecte que ens tenim nosaltres. Tampoc podem dir-nos només amigues, perquè és impossible posar un grup d'amigues a treballar, i que s'entenguin tan fàcilment com nosaltres per obtenir resultats. Un dia podíem estar treballant al despatx i el següent anàvem al mar a buscar larves. I acabàvem muntant una *nursery* d'esponges a la sala de cultius. O començàvem organitzant un congrés i acabàvem repartint cafès i entrepans als participants…Totes sempre a punt per participar en el que fes falta. I no puc oblidar-me de tu, Jana! Ja saps que sense tu, a l'equip li faltaria una part, molt important!. Amb vosaltres una pot fer tot el que es proposi. La nostra unió ha donat resultats inesperats, i seguirà donant-ne. M'inspireu amb la vostra força, suport i humilitat, i em sento immensament afortunada d'haver estat al vostre equip. Corregeixo, EQUIP.

"Algunos son capaces de convertirse en imprescindibles"

A vosotros os doy gracias especiales porque nuestra complicidad ha llegado más lejos de lo que podría imaginar. Me enorgullece que personas buenas y generosas como vosotros sean mis amigos. Sara, en qué gran momento empezamos a ser vecinas! ¡Lo que vino a partir de entonces fueron todo risas, confianza y diversión! Con Leyre lo que vino fue mucho *glamour* y dignidad. Nadie como ella para compartir té y buenas conversaciones. Queridas, no veo la hora de reunirnos otra vez, gracias infinitas por esos años tan bonitos. Sin duda, el más polifacético y artista de todos es Rudi. Querido, gracias por los *brunch* playeros y por tener siempre tan estupendo carácter, contigo todo fluye y todo es fácil. Y gracias también a Elliot por aparecer y desaparecer cuando menos te lo esperas sin dejar de preocuparse de que todo esté en orden. Gracias por aportar esa espontaneidad que tanta falta me hacía cuando la rutina chafaba los ánimos.

"Blanes es el nuevo destino de Erasmus"

Un día una amiga no ceabina describió mi vida en Blanes como un Erasmus. Ceabinos, salíamos de fiesta casi todos los findes, y cuando Blanes hibernaba nos montábamos nuestras propias fiestas en casa. Éramos todos de diferentes lugares, compartíamos pisos, compartíamos lugar de trabajo… Con vosotros empezaron el "NDT", las "Meriendas de gordacos", las "Cenas de Tronos" y el "Cine Palacine". ¿Qué no hemos inventado? ¡Creo que mi amiga tenía razón y nos montamos un Erasmus sin darnos cuenta! Desde entonces ya ha pasado un tiempo, y he acumulado grandes recuerdos de esa etapa, por los que estoy muy, muy agradecida. Kathrin, Anna, Carla, Íbor, Vicente, Clus, Carlos, Ari, João, Magda, Donatella, Xavi, Luis Fran, Nayeli, Mateus, Miquel, Mirco, Nuria …Tantísimas personas con quien compartir momentazos! ¡Gracias por esa sensación constante de compañerismo y alegría!

Por si esto fuera poco, nuevas personas igualmente geniales han aparecido en los últimos años, cogiendo el relevo a los anteriores y dando nuevos aires a mi última etapa de tesis. Carmen, Nerea, Candela, Anna, Jan, Mateu, Marta, Xavi, Jorge, Mario, Edu, Roger, … Gracias a todos por los buenos ratos y por las buenas charlas, sois compañía de calidad.

"Vosotras sois un gran descubrimiento"

Sara, Sílvia, Yanet, Anna,… Habéis sido una compañía excelente, me habéis aportado el toque de variedad que tanto me gusta. Todas tan diferentes pero todas tan buenas y transparentes. Sara, la más decidida; Sílvia, la més dolça; Yanet, la más sabia y Anna, la més moderna. ¿Qué nos queda por contarnos? Gracias a vosotras desconectaba del trabajo y podía hablar sobre un sinfín de temas, a cuál más extraño! Habéis sido un gran apoyo y estoy felicísima de habernos conocido. ¡Ya tengo ganas de saber por dónde irán nuestras próximas charlas!

"Vosaltres sou la meva aposta segura"

Sou la definició perfecta d'amistat de tota la vida, un pilar segur, no falleu i m'encanteu. Gràcies per tot el suport i per tots els moments que passem sempre que ens trobem. Né, Noe i Ari, es un honor ser amiga vostra. Vosaltres em coneixeu i em deixeu que faci i desfaci plans, que arribi tard, que desaparegui, que em presenti de cop…Entre nosaltres no ens hem de preocupar d'aquestes coses perquè ja sabem que ens tenim. Gràcies de veritat.

"I vosaltres sou el meu refugi"

A vegades se'n van les forces o apareixen entrebancs que no t'esperaves. En aquests moments busco una bombolla que em protegeixi de tots aquests imprevistos i que em doni energia per superar els obstacles. Sé perfectament on trobar aquesta bombolla. Sol ser a Sils, a vegades a Palamós, fins i tot pot expandir-se i contraure's cap a Vilobí, Girona i Sant Hilari. És molt flexible però també és fortíssima. Entres i en surts quan vols, amb llibertat i sense explicacions, com a mi m'agrada. Al centre de la bombolla sempre hi ha en Joan i la Roser, els meus pares, sempre. Entrant i sortint hi ha la Marta, la Bel, en Joan, en Santi, i jo mateixa. I a vegades la resta de la família també apareix i desapareix. Vosaltres sempre heu creat les condiciones perfectes perquè em llenci a fer tot el que em proposo i també per recuperar-me quan no me'n surto o estic massa cansada. Gràcies per ensenyar-me a ser forta i perseverant, i per donar-me sempre llibertat per decidir el meu camí. Per últim, nombro al petit que m'ha regalat alegria incondicional des del primer moment que va aparèixer i que em va acompanyar des del principi d'aquesta tesi. Gràcies a tu també, Atsu.

Financial support

The research conducted in this thesis has been supported by several grants. The Spanish Ministry of Economy and Competitiveness funded the POR-Si (CTM2012-37787) and the PBS (MINECO– CTM2015-6722-1R). The Spanish National Research Council financed an Intramural CSIC Research Grant (PIE, PN-2013). Founds were also provided by the European Community grants LIFE+INDEMARES (Project 46P.PR9999), LIFE+INDEMARES (07/NAT/E/000732), LIFE-IP INTEMARES (LIFE15 IPE/ES/000012) and Horizon 2020 SponGES (no. 679849). This research has also benefited from a SYNTHESYS fellowship within the FP7 Capacities Programme awarded to the author by the European Community Research Infrastructure Action. The LIFE BaHAR for N2K (LIFE12 NAT/MT/000845) project also funded this research, coordinated by the Environment and Resources Authority (ERA) in partnership with the Non-Governmental Organization OCEANA, the Ministry for Sustainable Development of Environment and Climate Change (MSDEC) of Malta, the Department of Fisheries and Aquaculture (MSDEC-DFA), and the Biology Department of the University of Malta (UoM-DoB).

Directors' report

Dr. Manuel Maldonado Barahona, and Dr. José Luis Rueda Ruiz, supervisors of the PhD thesis entitled "**The bathyal connections between the Mediterranean Sea and the Northeastern Atlantic Ocean: an assessment using deep-water sponges as a case study**", report on the contribution of Cèlia Sitjà Poch on the co-authored chapters and publications that constitute her PhD thesis. Two chapters are already published, one is accepted, and two others are currently being prepared as manuscripts for submission.

List of manuscripts of this thesis, organized by chapters, with indication of journal impact factor (IF), quartile (Q), publication stage and contributions of Cèlia Sitjà Poch in each of them:

Chapter 1. Sitjà C.[1], Maldonado M.[1], Farias C.[2] and Rueda J.L[3]. (2019) Deep-water sponge fauna from the mud volcanoes of the Gulf of Cadiz (North Atlantic, Spain). *Journal of the Marine Biological Association of the United Kingdom*, 99 (4): 807 - 831.5. IF (2019) = 1.181, Q = Q3

Contributions: Taxonomic identifications and descriptions, illustrations, photography and paper writing.

Chapter 2. Sitjà C.[1], Maldonado M.[1], Taboada, S. [4], Riesgo, A[4]. Characterization of some rare deep sponges from the Gulf of Cádiz, North East Atlantic, through integrative taxonomy. To be submitted to *Journal of the Marine Biological Association of the United Kingdom*. In preparation. IF (2019) = 1.181, Q = Q3

Contributions: Taxonomic identifications and descriptions, illustrations, photography, DNA extraction and amplification and manuscript writing.

Chapter 3. Sitjà C.[1] and Maldonado M. [1](2014) New and rare sponges from the deep shelf of the Alboran Island (Alboran Sea, Western Mediterranean). *Zootaxa*, 3760(2), 141-179. IF (2019) = 0.906, Q = Q3

Contributions: Collection of samples, taxonomic identifications and descriptions, illustrations, photography and paper writing.

Chapter 4. Sitjà C., Maldonado M., Farias C. and Rueda J.L. Export of bathyal benthos to the Atlantic through the Mediterranean outflow: sponges from the mud volcanoes of the Gulf of Cádiz as a case study. *Deep-sea Research Part I – Oceanographic Research Papers*. Accepted. IF (2019) = 2.606, Q = Q2

Contributions: Statistical analyses, illustrations, bibliographic research and database elaboration, interpretation of the results and paper writing.

Chapter 5. Sitjà C.[1], Maldonado M.[1] and Aguilar, R.[5] The distribution of Mediterranean deep-sea sponges influenced by the Levantine Intermediate Water across the Strait of Sicily: The case of Maltese sponges. To be submitted to *Biodiversity and Conservation*. In preparation. IF (2019) = 2.935, Q = Q1/Q2/Q2

Contributions: Taxonomic identifications and descriptions, statistical analyses, illustrations, photography, interpretation of the results and manuscript writing.

Dr. Manuel Maldonado Barahona
CEAB - CSIC Research scientist

Dr. José Luis Rueda Ruiz
CO Málaga - IEO Senior scientist

Authors affiliations:

[1] Department of Marine Ecology, Centre for Advanced Studies of Blanes (CEAB-CSIC), Blanes, Girona, Spain
[2] Oceanography Centre of Cádiz (IEO), Cádiz, Spain
[3] Oceanography Centre of Málaga (IEO), Fuengirola, Spain
[4] Life Sciences Department, Natural History Museum of London, London, UK
[5] OCEANA, Madrid, Spain

Summary

Sponges are common representatives of the marine benthos and play functional roles in the ecosystems as recyclers of dissolved and particulate organic matter, as reservoirs and sinks of silicon, and as habitat builders that increase the three-dimensional structure of the benthic communities and their associated biodiversity. In this study, sponges are also used as a tool to deep-sea biogeography.

The Mediterranean Sea is connected to the Atlantic Ocean by the Strait of Gibraltar, through which the North Atlantic Surface (NAS) water enters the Mediterranean. The Intermediate Levantine Water (LIW) current, originated at the Mediterranean, in the eastern basin, runs westwards between 200 and 800 m depth, until it reaches the westernmost part of the Mediterranean Sea. The LIW is the main contributor to the Mediterranean Outflow Water (MOW), which enters the Atlantic Ocean in the opposite direction to the NAS at 300 m depth.

This thesis addresses the potential of these Mediterranean outgoing water masses to export fauna to the North Atlantic. Deep-water sponges are used as a case study.

The deep-water sponge fauna was taxonomically investigated in three areas across the Atlantic-Mediterranean trajectory, which, despite being hypothesized as crucial to understand the biogeographical effects of the MOW and LIW, remain poorly known in terms of sponge fauna. These locations were the mud volcano fields of the Gulf of Cádiz (Northeastern Atlantic) and the shelfs and slopes of the Alboran Island (Western Mediterranean) and the Maltese Islands (Central Mediterranean). A total of 5 new species were described during the taxonomic inventories, together with

3 new records for the Atlantic and 6 for the Mediterranean. A faunal matrix of 461 spp. was built for a total of 20 biogeographical zones defined along an Atlantic-Mediterranean deep-sea gradient. A bias in the sampling effort at the Mediterranean was evidenced, being the deep-water sponge fauna from the eastern basin poorly explored. The analysis of faunal affinities suggested a distribution of the deep-water sponge species in the Mediterranean related to the trajectory of the LIW, while higher affinities between the Mediterranean areas and the easternmost Atlantic study area, the Gulf of Cádiz, evidenced a transfer of Mediterranean deep-water sponge species into this area favoured by the MOW.

This study supports the idea of the faunal transport by the MOW of deep-water fauna from the Mediterranean to the Northeast Atlantic, showing that sponges are a suitable tool to assess faunal shifts. This is of interest to predict and manage future transfers of non-indigenous bathyal benthic species in the Mediterranean and Northeast Atlantic, as well as to improve the management of key biodiversity and conservation areas.

Contents

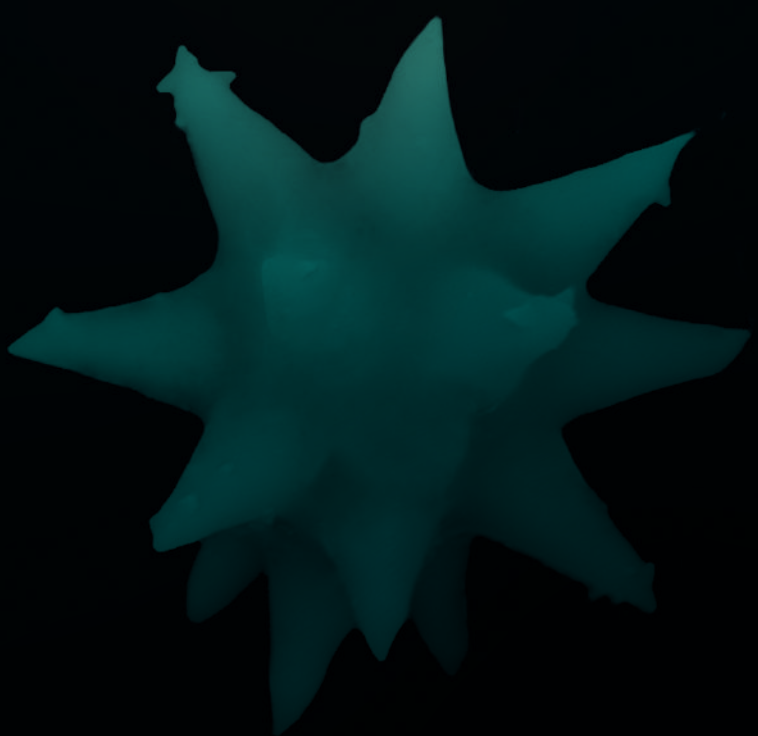

General introduction

The phylum Porifera

Sponges (Phylum Porifera Grant, 1836) represent a common sessile biological component of marine benthos (Bell, 2008; Wulff, 2012; Maldonado et al., 2017). These metazoans are anatomically very simple and lack most of tissues or organs that characterize other animal phyla. Yet, their physiological activity renders them important. They are very active filter feeders that process huge amounts of carbon, but also inorganic nutrients (Gili & Coma, 1998; Maldonado et al., 2012; Ludeman et al., 2017). Sponges can feed on a wide range of food sources, such as dissolved and particulate organic carbon, bacteria, protozoans and phytoplankton (Reiswig, 1971; Frost, 1980; Pile et al., 1996; Ribes et al., 1999; Pile & Young, 2006). Some of them have developed symbiotic associations with photosynthetic microorganisms such as cyanobacteria (Cheshire et al., 1997; Steindler et al., 2002; Taylor et al., 2007) and chemosynthetic bacteria (Harrison et al., 1994; Vacelet et al., 1995; Arellano et al., 2013). Others have evolved towards a carnivorous diet based on zooplankton, showing a reduced filtering system (Vacelet & Boury-Esnault, 1995). Through their biological activity, sponges play a variety of important services to the ecosystems such as habitat providers (Bell, 2008), sometimes even growing abundantly, forming sponge grounds (Klitgaard & Tendal, 2004; Hogg et al., 2010; Maldonado et al., 2017), and creating singular communities, some of which have been included in the OSPAR habitats directive. Sponges are also food providers (Bell, 2008) and contribute to the benthic-pelagic coupling of biogeochemical cycles (Pile & Young, 2006; Jiménez & Ribes, 2007; Coppari et al., 2016). They act as recyclers of

dissolved organic matter into particulate matter, which can be used by organisms at higher trophic levels (de Goeij et al., 2013; Rix et al., 2016) and they can become a silicon reservoir, playing a significant role to the silicon cycle in the ocean (Maldonado et al., 2005; Maldonado et al., 2010; Maldonado et al., 2019). They are also producers of chemical compounds that mediate interactions with other organisms (Webster & Taylor, 2012; Wulff, 2012). Due to the biotechnological potential of some of their chemical compounds (Ehrlich et al., 2010; Lin et al., 2011; Leal et al., 2012; Bhatnagar et al., 2016), sponges are becoming again commercially attractive to the human kind.

Sponges are one of the most ancient animal groups on Earth. The fossil record has traditionally located their origin in the Early Cambrian, (Antcliffe et al., 2014), being the Precambrian sponge fossil record remarkably poor. However, a recent work suggested that Precambrian sponges showed weakly biomineralized skeletons or even lacked spicules, which would explain such a poor fossil record (Tang et al., 2019). This new approach is consistent with sponge specific biomarkers and molecular clock analyses, which also locate their origin in the Precambrian (Love et al., 2009; Sperling et al., 2010). Several phylogenetic studies have placed them at the base of the Metazoan tree (Feuda et al., 2017; Simion et al., 2017; Pett et al., 2019), but with some debate generated by other studies that alternatively claimed Ctenophores or Placozoa to occupy this basal position (Borowiec et al., 2015; Shen et al., 2017; Whelan et al., 2017).

Sponges are a highly diverse group, accounting for ca. 9100 marine and fresh-water species (Van Soest et al., 2020), but with ca. 22000 species that are estimated to remain undescribed (Appeltans et al., 2012; Van Soest et al., 2012). The phylum is divided in four classes: Demospongiae Sollas, 1885, including a large part of the living sponges (84% of the species); Calcarea Bowerbank, 1862 (8%), Hexactinellida Schmidt, 1870 (7%) and Homoscleromorpha Bergquist, 1978 (1%). The taxonomy and the classification of sponges have been traditionally based on morphometric characters, such as external shape, composition, arrangement and size of their skeletal pieces (Boury-Esnault & Rützler, 1997). However, laboratory experiments have shown that siliceous sponges (those with a skeleton made of biogenic

silica) under different silicic acid concentrations can change the composition, shape and size of their skeletal pieces (Maldonado et al., 1999; Mercurio et al., 2000), suggesting that the taxonomic system cannot be merely based on skeletal traits. The advent of molecular phylogenetic analyses has further proved that morphometric features can sometimes be remarkably homoplasic (Erpenbeck et al., 2006; Cárdenas et al., 2011).

The pillars of the current accepted classification of Demospongiae (Morrow & Cárdenas, 2015) are already based on molecular relationships. The sponge classification remains in continuous change and refinement, seeking for integration and congruence between molecular and phenetic sources of information. Therefore, there is a need for establishing a reliable framework based on relevant molecular and morphological markers that can definitively unravel the taxonomy and the phylogeny of sponges.

Deep-sea biogeography of sponges in the Northeastern Atlantic and the Mediterranean

The deep sea is the largest biome of our planet comprising about 90% of the oceans (Ramirez-Llodra et al., 2010; Ramirez-Llodra et al., 2011) and is considered to start bellow 200 m depth. Functionally, it is defined by the 10ºC permanent thermocline and characterized by a progressive pressure increase with depth as well as by the absence of photosynthesis, what makes food availability poorer, compared to shallow water ecosystems (Gage & Tyler, 1991; Thistle, 2003). Deep-sea ecosystems are often characterized by slow-growing, long-living organisms, such as sponges, that are highly vulnerable because of their low capability to recover from anthropogenic disturbances (Ramirez-Llodra et al., 2011).

In addition to the potential ecological relevance of the sponge fauna to the deep-sea ecosystems remaining little investigated, the knowledge on the global distribution of deep-sea sponges is also poor. It is largely biased by the trajectories of historical deep-sea expeditions – such as those of the H.M.S. Porcupine (Thomson, 1873; Carter, 1876), the Challenger (Ridley & Dendy, 1887; Schulze, 1887; Sollas, 1888),

Hirondelle and Princesse Alice of *Prince Albert I de Monaco* (Topsent, 1892, 1904, 1928) *Président Théodore-Tissier* (Lévi & Vacelet, 1958; Vacelet, 1960, 1961), Calypso (Vacelet, 1959, 1961, 1969) and Balgim (Boury-Esnault et al., 1994) – and is markedly fragmented at the regional scale (Hogg et al., 2010; Van Soest et al., 2012). The information on deep-sea sponges has also been traditionally limited by logistic problems to work in deep sea. Since the first expeditions, many other studies have addressed the composition of the sponge faunas in different areas of the deep Northeastern Atlantic and Mediterranean, but their connectivity remains poorly studied. More importantly, the deep-water sponge fauna from fundamental transition areas where water exchange occurs between the Atlantic Ocean and the Mediterranean Sea – the Strait of Gibraltar – and between the Eastern and Western Mediterranean – the Strait of Sicily – remain poorly explored.

The recent technological advances have provided tools for better mapping and exploration of the deep sea, facilitating a variety of scientific approaches to study the composition and distribution of deep-sea sponge faunas. During the last ten years, several oceanographic expeditions have been performed under the framework of the EU LIFE programme, aimed to list and designate marine areas for the Nature 2000 Network. Some of the expeditions were conducted in the Strait of Gibraltar and the Strait of Sicily and explored their deep-water benthic communities. This thesis results from the effort of assembling the sponge collections obtained from these expeditions, in order to gain knowledge on the deep-water sponge fauna of these transition areas.

The sponge material collected from the transition area of the Strait of Gibraltar was obtained from the INDEMARES-CHICA (Chimeneas de Cádiz - *Cádiz chimneys*) expeditions in the mud volcanoes of the Gulf of Cádiz (Díaz del Río et al., 2014), at the Atlantic side of the Strait of Gibraltar, and the INDEMARES-ALBORAN expeditions in the Alboran Island (Gofas et al., 2014) at the Mediterranean side. The sponge material collected from the transition area of the Strait of Sicily consists of a smaller set of sponge samples collected during the LIFE BaHAR expeditions, at the Maltese Islands, South of the Strait of Sicily.

Not only these are strategic areas for biogeographic studies, they also encompass Sites of Community Importance (SCI) included in the

Natura 2000 network and host rich benthic communities, for which they were expected to provide abundant and diverse sponge material. In the study area of the Gulf of Cádiz, sampling was achieved on a mud volcano field between 380 – 1146 m depth. Mud volcanoes are fluid venting submarine structures known to harbour benthic communities related to methane-derived authigenic carbonates such as slabs, crusts and chimneys. These carbonate structures originate in the sediment, and once they are exhumed, become available for colonization of sessile fauna like sponges (Fig. 1A). Some studies have suggested that the pioneering fauna, known as a provider of habitat and food, facilitates the settlement of other organisms, triggering an increase of the diversity of these communities (Freiwald & Roberts, 2005; Levin, 2005; Cordes et al., 2009; Palomino et al., 2016). Contrastingly, in the mud volcano field where methane-derived authigenic carbonates are scarce, the benthic fauna is that typically found in bathyal soft bottoms (Fig. 1B).

The study area at the Mediterranean side of the Strait of Gibraltar, in the central part of the Alboran Sea, is the tiny Alboran Island, which emerges from a large submerged shelf, remnant of an ancient volcanic cone. The upper part of the shelf was already known to host rich benthic communities (Templado et al., 2006), including sponges, which have been widely studied (Templado et al., 1986; Pansini, 1987; Maldonado & Benito, 1991; Maldonado, 1992, 1993; Maldonado & Uriz, 1995; Rosell & Uriz, 2002; Templado et al., 2006). Contrarily, the deeper part of the shelf (down to 200 m) (Fig. 1C-D) and the upper slope, which conform the area studied in this thesis (40 – 290 m depth), remained poorly explored before the LIFE+INDEMARES-ALBORAN expeditions.

The study area nearby the key transition area of the central Mediterranean, the Strait of Sicily, was at the Maltese Islands, between 50 and 1000 m depth. Their deep-water sponge fauna had seldom been studied (Calcinai et al., 2013). Additionally, some studies have dealt with the sponge fauna of other areas of the Strait of Sicily (Zibrowius & Taviani, 2005; Aguilar et al., 2011; Calcinai et al., 2013), although its current knowledge is still at an initial level when compared to other Mediterranean areas (Calcinai et al., 2013).

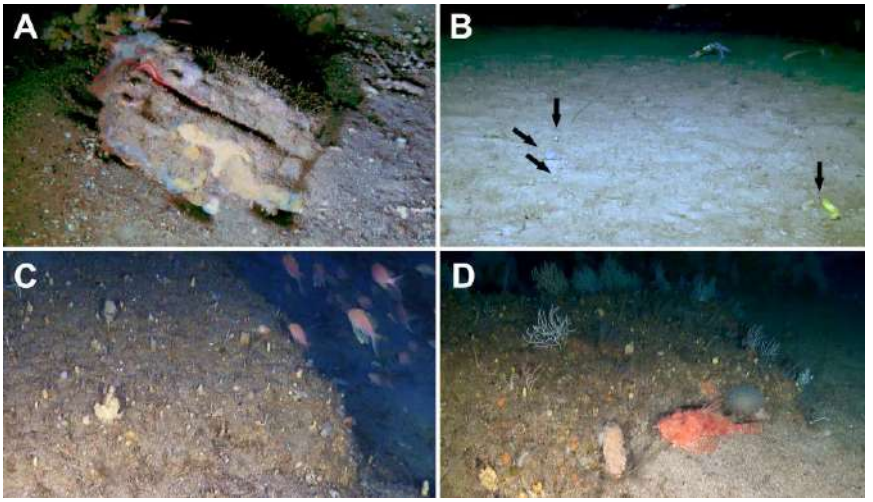

Figure 1. Some of the deep bottoms explored in the Gulf of Cádiz and the Alboran Sea. (A) Methane-derived authigenic carbonate formations from mud volcanoes of the Gulf of Cádiz providing substrate for sponges and other sessile fauna. (B) A deep soft bottom of the mud volcano field where some sponges occur (pointed with arrows). (C-D) Benthic communities from the deep shelf of the Alboran Island, where a variety of sponges were detected.

The Straits of Gibraltar and Sicily are transition areas involving several Atlantic and Mediterranean water currents. The Levantine Intermediate Water (LIW) current, originated at the Eastern Mediterranean, flows westwards between 200 and 800 m depth, crossing the Strait of Sicily and flowing westwards until it reaches the westernmost part of the Mediterranean, the Alboran Sea. The LIW becomes the main contributor to the formation of the Mediterranean Outflow Water (MOW), which crosses the Gibraltar Strait and ultimately enters the Atlantic Ocean flowing down from 300 m depth (Sánchez-Leal et al., 2017). Flowing above these water currents, from surface to about 150 m depth, the North Atlantic Surface (NAS) water enters the Mediterranean through the Strait of Gibraltar and runs eastwards across the Mediterranean.

While the shallow sponge fauna of the Strait of Sicily has been reported to be influenced by the NAS flow (Pansini, 1987; Xavier & Van Soest, 2012), the effect of the LIW on the bathyal sponge fauna

across the Strait of Sicily remains unknown. Similarly, the effect of the NAS is known to favour the entry of Atlantic sessile species to the westernmost part of the Mediterranean Sea, the Alboran Sea, (Pérès & Picard, 1964; Templado et al., 2006), and this has been largely proved for the sponge fauna of this area (Templado et al., 1986; Maldonado, 1992, 1993; Maldonado & Uriz, 1995; Xavier & Van Soest, 2012). Nevertheless, little is known about the transfer of deep benthic fauna derived from the MOW, existing only one study comparing the deep-water sponge fauna of both sides of the Strait of Gibraltar (Boury-Esnault et al., 1994).

The study of the deep-water sponges from these transition areas will provide fundamental data to assess their faunal affinities along the Northeast Atlantic and the Mediterranean. Such affinities can be used to achieve the main objective of this thesis, providing a case study to approach the connectivity of the deep-water fauna along a North Atlantic-Mediterranean gradient.

Objectives

Objectives

The general outline of this thesis is to assess the potential of the Mediterranean water masses to transport deep-sea fauna towards the Atlantic Ocean. By examining the effects that the bathyal water mases moving from the Eastern Mediterranean basin towards the Northeastern Atlantic Ocean may have on the relationships of the deep-water sponge fauna, a case study is provided. Prior to using the sponge fauna as a deep-water biogeographic tool, new collections of deep-sea sponges needed to be conducted in order to increase the faunal resolution at the two most important transition areas across the bathyal trajectory from the Eastern Mediterranean to the Atlantic, the Strait of Gibraltar and the Strait of Sicily, which remained poorly studied. In this context, the specific objectives of this thesis are as it follows:

1. **To complete the previous limited knowledge on the deep-water sponge fauna at key transition areas along the trajectory of the bathyal water mases.**

   1.1. To provide the missing qualitative and quantitative knowledge of the bathyal sponge fauna at the most Eastern-Atlantic side of the Strait of Gibraltar, focusing on a mud volcano system at the Gulf of Cádiz that spans the entire range of bathyal depths.

   1.2. To underpin the qualitative and quantitative knowledge of the deep-water sponge fauna at the most Western-Mediterranean side of the Strait of Gibraltar, focusing on the deep shelf and upper slope of the Alboran Island.

   1.3. To underpin the qualitative knowledge of the deep-water sponge fauna at the Eastern-Mediterranean side of the Strait of Sicily, focusing on the deep shelf and slope of the Maltese Islands.

   1.4. To put into practice basic genetic techniques to aid in the identification of species that remain unresolvable through the classical phenetic approach, providing an example case for a more integrative sponge taxonomy.

2. **To assess the effects of local environmental variables on the qualitative and quantitative distribution of abundances of the sponges across a complete bathymetric bathyal range, focussing on the mud volcanoes of the Gulf of Cádiz as a case study.**

3. **To examine the affinities of the deep-water sponge fauna across the trajectory of the bathyal water masses running from the Eastern Mediterranean to the Northeastern Atlantic.**

Objectives *versus* chapters

The inter-regional nature of the objectives and the large geographical area encompassed in this work have required the progressive integration of samples and data produced by four different major research grants (LIFE-Alboran, LIFE-*Chimeneas de Cádiz*, LIFE BaHAR, H2020-SponGES), in a process that has extended for seven years. This long-term, accretive process of building data and publishing results has caused that each publication (i.e., Ph.D. Thesis chapter) cannot exactly match an objective. A matching which is also disrupted by the thematic scope of the various international journals selected to publish the results. The exact correspondence between the scientific global objectives and the scope of the publications and chapters is at it follows:

Objective 1: Chapters 1, 2, 3 and 5
- **Objective 1.1:** Chapter 1
- **Objective 1.2:** Chapter 3
- **Objective 1.3:** Chapter 5
- **Objective 1.4:** Chapter 2

Objective 2: Chapters 1 and 4

Objective 3: Chapters 4 and 5

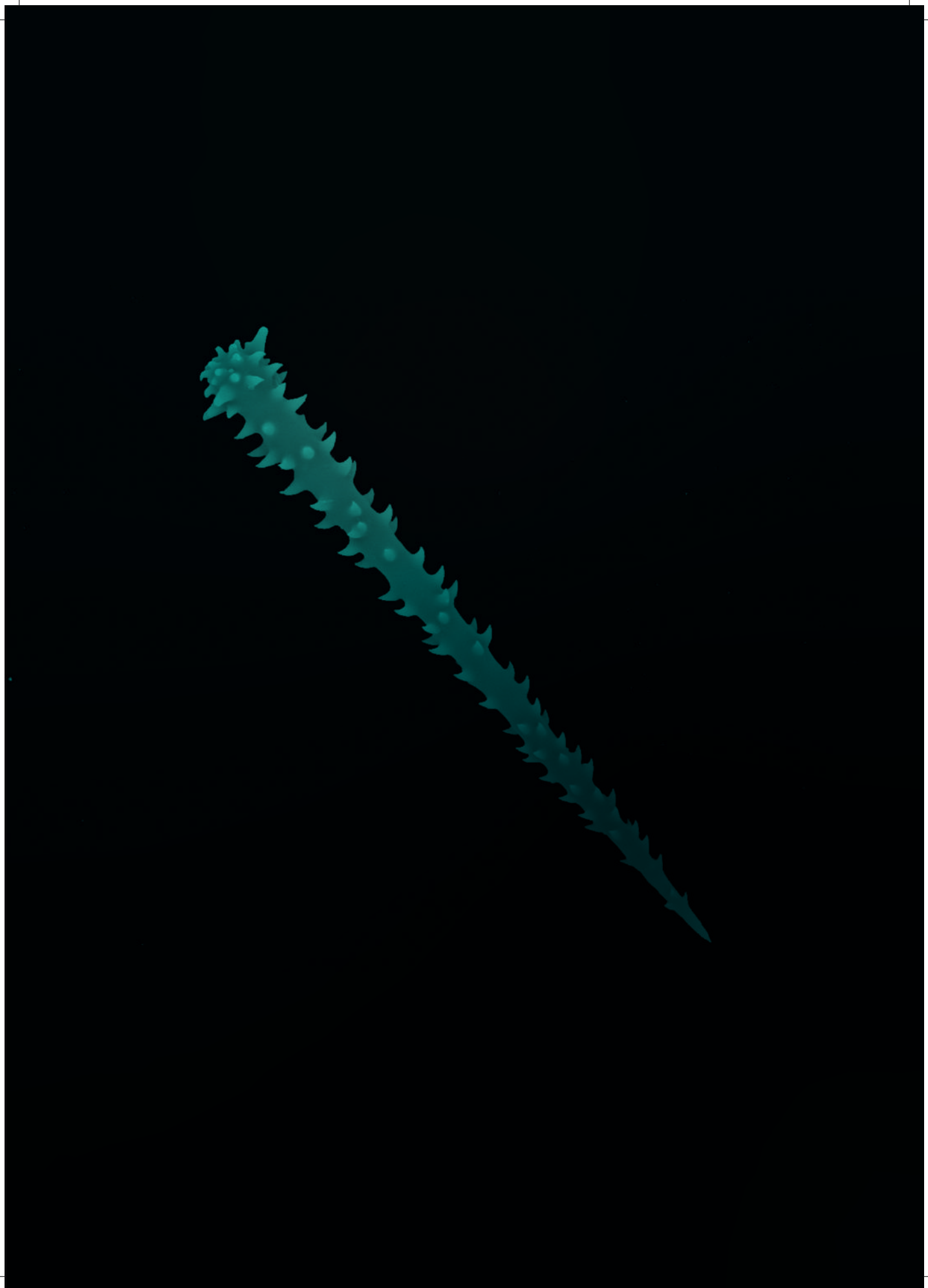

Chapter 1

Deep-water sponge fauna from the mud volcanoes of the Gulf of Cádiz (North Atlantic, Spain)

Abstract

Mud volcanoes are singular seafloor structures classified as "sensitive habitats". Here we report on the sponge fauna from a field of 8 mud volcanoes located in the Spanish margin of the northern Gulf of Cádiz (northeastern Atlantic), at depths ranging from 380 to 1,146 m. Thirty-eight beam-trawl samplings were conducted (covering over 61,000 m^2) from 2010 to 2012, in the frame of a EC-LIFE+ INDEMARES grant. A total of 1,659 specimens were retrieved, belonging to 82 species, from which 79 were in the Class Demospongiae and 3 in Hexactinellida. Two species were new to science (*Jaspis sinuoxea* nov. sp.; *Myrmekioderma indemaresi* nov.sp.) and three others recorded for the first time in the Atlantic Ocean (*Geodia anceps*, *Coelosphaera cryosi* and *Petrosia raphida*). Five additional species were "Atlantic oddities", since this study provides their second record in the Atlantic Ocean (*Lanuginella* cf. *pupa*, *Geodia* cf. *spherastrella*, *Cladocroce spathiformis*, *Cladocroce fibrosa* and *Haliclona pedunculata*). Basic numerical analyses indicated a significant linear relationship between the species richness per m^2 and the number of sponge individuals per m^2, meaning that in most volcanoes many species occur in equivalent, moderate abundance. Likewise, sponge species richness increased with depth, while the abundance of hard substrata resulting from carbonate precipitation and the fishing activities around the volcanoes had no detectable effect on the sponge fauna. However, in the latter case, a negative trend —lacking statistical support— underlaid the analyses, suggesting that a more extensive sampling would be necessary to derive more definitive conclusions in this regard.

Introduction

The confluence of the Atlantic Ocean and the Mediterranean Sea is an area of special interest to monitor the flux of invasive marine fauna in either direction and to identify natural patterns of North-Atlantic vs. Mediterranean endemicity (Pérès & Picard, 1964; Bouchet & Taviani, 1992; Coll et al., 2010). Biodiversity studies have shown how the taxonomic composition of the benthic fauna of the westernmost zone of the Mediterranean Sea (i.e., the Alboran Sea) is naturally influenced by the North Atlantic Surface (NAS) water inflow (0 to about 150 m depth), which has historically imported shallow-water Atlantic species into the Alboran Sea (Pérès & Picard, 1964; Templado et al., 2006). This general pattern has also been confirmed specifically for the sponge fauna of the Alboran Sea (Topsent, 1928; Templado et al., 1986; Pansini, 1987; Maldonado, 1992, 1993; Maldonado & Uriz, 1995; Sitjà & Maldonado, 2014), including the African Mediterranean coasts (Schmidt, 1868; Topsent, 1901, 1938; Maldonado et al., 2011). However, the reverse effect is worse known. How the outflow of Intermediate Mediterranean water (MOW), originated at 500 m depth, impacts on the diversity and taxonomic composition of the benthic faunal assemblages at the Atlantic side of the Gilbraltar Strait remains poorly investigated. The MOW deviates North along the Portuguese continental margin upon passing the Camarinal Sill (280 m depth) of the Gibraltar Strait. Although the MOW is thoroughly mixed North of the Iberian Peninsula, its physical characteristics have been hypothesized to somehow affect positively the development of cold-water coral communities so distant to the North as the Galicia Bank seamount, the Aviles Canyon, Le Danois Bank seamount, and the Porcupine Seabight (de Mol et al., 2005; Van Rooij et al., 2010; Sánchez et al., 2014). However, the impact on the fauna of the bathyal bottoms at the Gulf of Cádiz, where the MOW could yet have an important influence because it remains

still unmixed, has seldom been addressed, particularly regarding the sponge fauna (Arnesen, 1920; Topsent, 1927, 1928). Most of the available information on the deep-water sponge fauna in that Atlantic region derives from Azores archipelago due to intensive sampling by French cruises (Topsent, 1892, 1898, 1904, 1928) and some more recent Portuguese initiatives (Carvalho et al., 2015; Xavier et al., 2015). The Azores archipelago is, however, too distant from the Gibraltar Strait as to reflect clearly the role of the MOW in exporting benthic fauna. Therefore, to our knowledge, there is only a single study dealing with the deep-water sponge fauna from Atlantic locations close to the Gibraltar Strait (Boury-Esnault et al., 1994).

In the last decade of the 20th century, an exciting, new deep-water habitat was discovered in the Gulf of Cádiz: fields of mud volcanoes extending between the Moroccan, Portuguese and Spanish continental margins (Kenyon et al., 2000; Gardner, 2001; Pinheiro et al., 2003). More than 60 mud volcanoes have been identified to date, distributed in four main fields, which constitute one of the most extensive gas seepage areas of the Northeastern Atlantic (Gardner, 2001; Pinheiro et al., 2003; León et al., 2007; Medialdea et al., 2009; Palomino et al., 2016). The bubbling of methane (and other hydrocarbons seeping in smaller amounts, such as propane, butane and ethane) provides the carbon that highly specialized microorganisms (i.e., methanotrophic) will consume anaerobically. This process results in precipitation of methane-derived authigenic carbonates (MDAC), such as slabs and chimneys (Levin, 2005; Suess, 2014). These structures generated by carbonate precipitation around the methane seeps are a source of new hard substrate suitable for colonization by deep-sea sessile fauna (sponges, gorgonians, cold-water corals, etc.), which in turn appears to attract demersal fauna, unchaining a global increase of benthic biodiversity (León et al., 2007; Rueda et al., 2012; Palomino et al., 2016). In European waters, mud volcanoes are classified as sensitive habitats: habitat 1180 "Submarine structures made by leaking gases" (Habitats Directive 92/43/EEC), and, to date, the sponge fauna occurring in these mud volcano systems remains largely unexplored. The main objective of this study is to describe the diversity of the sponge fauna at some of the mud volcanoes, with the subsequent purpose (Chapter 4) of assessing quantitatively its relationships with sponge faunas of bathyal bottoms in both Northern Atlantic and Western Mediterranean adjacent areas.

Material and methods

In the frame of the EC Grant LIFE+ INDEMARES —leg CHICA (Chimneys of Cádiz)— the mud volcanoes of the Spanish margin of the Gulf of Cádiz were explored and subsequently declared SCI (Site of Community Importance), which has now become part of the Nature 2000 Network in Spanish territorial waters. The current study has benefited from a variety of tasks conducted by the research consortium during four oceanographic cruises (INDEMARES CHICA 0610 – IEO, 0211 – IEO, 1011 – IEO, 0412 – IEO) in 2010, 2011 and 2012, as it follows: (1) Elaboration of a high-resolution bathymetric profile of the mud volcano fields at the upper and medium continental slope using a sound velocity sensor SV Plus, a multibeam echosounder Simrad EM-3002D, a multifrequency echosounder EK-60, and a topographic parametric sonar TOPAS PS 28 (Fig. 1) and (2) video recording of the benthic communities of the SCI using both, the towed observation vehicle, VOR Aphia 2012, and the ROV Liropus 2000. These tasks resulted in about 28 VOR and 7 ROV digital video transects, involving about 14 and 12 hours of seafloor recordings, respectively. Information from mapping and video records has been used to complement this study of the sponge fauna.

The sponge specimens herein examined were collected using a 2m-wide beam trawl at a total of 38 sampling stations distributed across 8 mud volcanoes, namely Gazul, Anastasya, Tarsis, Pipoca, Chica, Hesperides, Almazan and Aveiro (Fig. 1). The total trawled area across the mud volcano field accounted for over 61,000 m^2. The exact location of each trawling is depicted in Fig. 1 and additional details (pathway coordinates, depth, trawled area, type of bottom, etc.) are summarized in Table 1. The sampled mud volcanoes were located at different depths, ranging from 380 and 1,146 m (Table 2).

In addition to depth, there were also between-volcano differences in the abundance of methane-derived authigenic carbonate (MDAC) formations. Samples retrieved by the trawls were used to assess between-volcano differences in the abundance of MDAC formations, such as chimneys, crusts and slabs (Table 2). This information, when possible, was confronted with underwater images obtained during ROV transects. The abundance of these

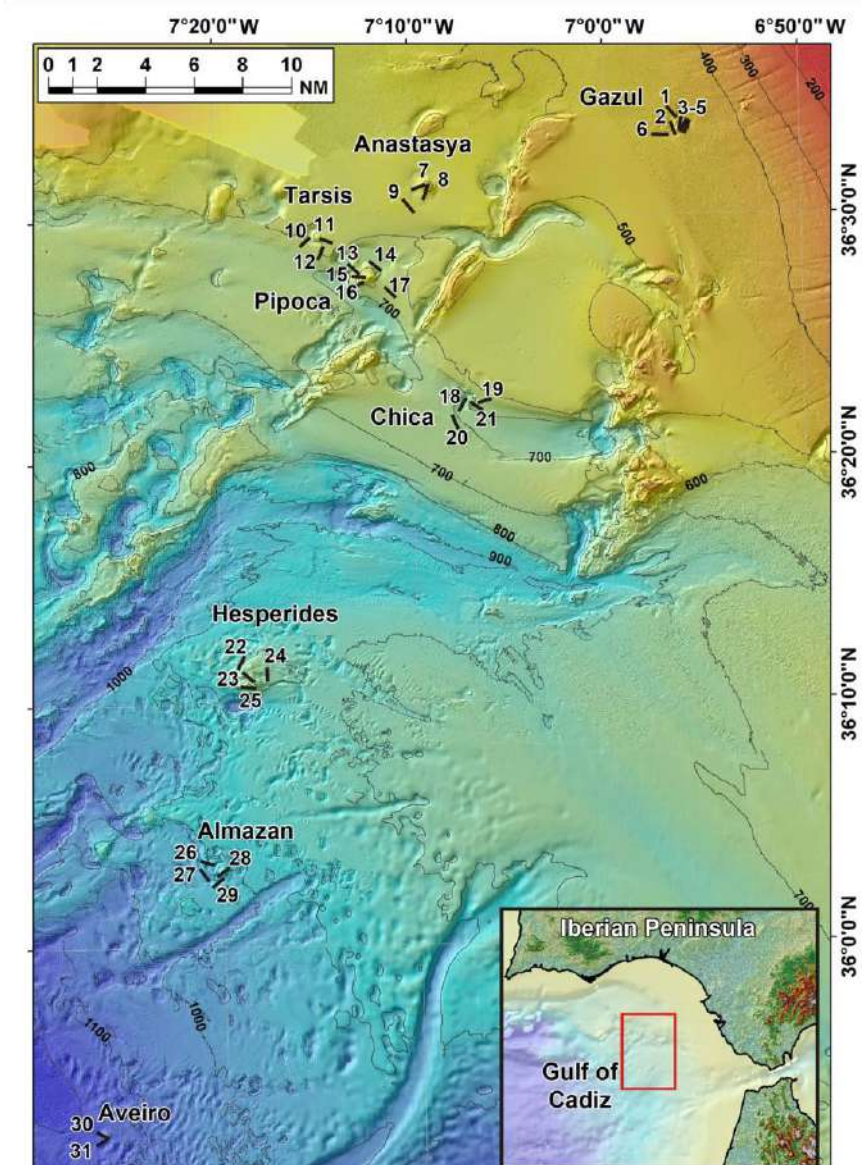

Figure 1. Location of the 31 studied beam trawl transects (see also Table 1). Transect numbers in map correspond to trawling codes at the data base of the Spanish Institute of Oceanography (IEO) cruises as it follows: 1: 10BT03; 2: 10BT04; 3: 10BT06; 4: 10BT08; 5: 10BT07; 6: 10BT02; 7: 11BT08; 8: 11BT01; 9: 11BT14; 10: 11BT10; 11: 11BT02; 12: 11BT11; 13: 11BT16; 14: 11BT15; 15: 11BT18; 16: 11BT17; 17: 11BT20; 18: 11BT31; 19: 11BT05; 20: 11BT19; 21: 11BT06; 22: 11BT21; 23: 11BT24; 24: 11BT22; 25: 11BT23; 26: 11BT30; 27: 11BT26; 28: 11BT29; 29: 11BT25; 30: 11BT27; 31: 11BT28.

hard substrata is a factor hypothesized to favour locally sponge abundance and species richness. The MDAC abundance was semiquantitatively categorized from 0 to 3 for each of the beam trawls, according to the following criteria: 0= no MDAC piece retrieved per trawl, 1= 1 MDAC piece retrieved per trawl, 2= two to five MDAC pieces retrieved, and 3= more than five MDAC pieces retrieved, often larger than 50 cm in length. Finally, the abundance of MDAC formations for a given volcano was calculated as the mean (±SD) of the semiquantitative value for the set of beam trawl transects conducted in such a mud volcano.

Besides depth and MDAC differences, there were also between-volcano differences in the intensity of the fishing activity by the trawling fleet. The intensity of trawling activity has herein been quantified by tracking the activity of each vessel in the fleet for the period January to December 2011 using the Vessel Monitoring System (VMS) datasets supplied by the Spanish General Secretary of Fisheries (Spanish Ministry of Agriculture and Fisheries). The value of fishing activity at each mud volcano (Table 2) was then calculated as the mean (±SD) of the semi-quantitative value inferred for each of the beam trawl transects in that volcano, according to the following criteria: 0= no trawling vessel operating in that area during 2011; 1= 1 trawling vessel; 2= 2-5 trawling vessels; 3= >5 trawling vessels.

The relationship between the values of species richness (i.e., number of species) and sponge abundance (i.e., number of individuals) found in each mud volcano and normalized per the extension of the sampled area were analyzed by Pearson correlation. The relationships between each of these two faunal variables, the average volcano depth, the MDAC abundance, and the level of fishing activity in each mud volcano (Table 2) were also examined pairwise using the Spearman rank correlation.

Immediately after beam-trawl retrieval, the sponges were directly preserved in 70% ethanol. In some cases, the sponges were damaged in diverse grade during trawling. Taxonomic identification of the stored material followed the standard protocols for phenetic taxonomy, based on features of the external morphology and skeleton using dissecting and compound light microscopes. When high-resolution observations of skeletal elements were required, spicules were nitric acid-cleaned, mounted on aluminum stubs, dried and then

Table 1: Summary of beam-trawl sampling stations that retrieved sponges. MDAC: Methane-derived authigenic carbonates; CWC: Cold-water corals.

			Beam trawl start			Beam trawl end				
Map code	**Haul**	**Mud volcano**	**Latitude**	**Longitude**	**Depth (m)**	**Latitude**	**Longitude**	**Depth (m)**	**Sampled area (m^2)**	**Seabed characteristics**
1	10BT03	Gazul	36º 34.02' N	6º 56.17' W	462	36º 34.26' N	6º 56.41' W	460	1864	Muddy medium sand with sea urchins, *Flabellum chunii* & sponges
2	10BT04	Gazul	36º 33.48' N	6º 56.31' W	495	36º 33.20' N	6º 56.19' W	483	1902	Gravel coarse and fine sand with MDAC, *Cidaris cidaris* & *Hyalinoecia tubicola*
3	10BT06	Gazul	36º 33.33' N	6º 56.07' W	422	36º 33.59' N	6º 55.59' W	450	1778	Fine sand with MDAC, *Leptometra phalangium*, sponges & *Madrepora oculata*
4	10BT08	Gazul	36º 33.27' N	6º 56.01'W	380	36º 33.54' N	6º 55.44' W	455	1990	Muddy gravel and fine sand with MDAC, *L. phalangium*, sponges & *M. oculata*
5	10BT07	Gazul	36º 33.22' N	6º 55.51' W	420	36º 33.52' N	6º 56.36' W	459	2088	Muddy fine sand with MDAC, *L. phalangium*, sponges & *M. oculata*
6	10BT02	Gazul	36º 33.17' N	6º 56.43' W	477	36º 33.19' N	6º 57.27' W	478	2424	Medium and fine sand with *Actinauge richardi*
7	11BT08	Anastasya	36º 31.37' N	7º 9.23' W	478	36º 31.56' N	7º 8.59' W	550	2155	Sandy mud with seapens (*Kophobelemnon. stelliferum, Funiculina quadrangularis*)
8	11BT01	Anastasya	36º 31.14' N	7º 8.86' W	489	36º 31.76' N	7º 8.67' W	546	2424	Sandy mud with seapens (*K. stelliferum, F. quadrangularis*) & *Thenea muricata*
9	11BT14	Anastasya	36º 30.70' N	7º 10.00' W	540	36º 31.20' N	7º 10.50' W	539	2343	Sandy mud with seapens (*K. stelliferum, F. quadrangularis*)
10	11BT10	Tarsis	36º 29.37' N	7º 15.12' W	639	36º 29.71' N	7º 14.64' W	598	1911	Sandy mud with seapens and *F. chunii*.
11	11BT02	Tarsis	36º 29.24' N	7º 14.27' W	579	36º 29.19' N	7º 14.99' W	620	2159	Sandy mud with seapens (*K. stelliferum, F. quadrangularis*)
12	11BT11	Tarsis	36º 28.85' N	7º 14.19' W	591	36º 29.30' N	7º 13.91' W	584	1882	Muddy sand with seapens (*K. stelliferum, F. quadrangularis*) & bamboo coral (*Isidella*)
13	11BT16	Pipoca	36º 28.18' N	7º 12.98' W	627	36º 28.57' N	7º 13.47' W	719	2051	Muddy sand with seapens (*K. stelliferum, F. quadrangularis*) & *T. muricata*
14	11BT15	Pipoca	36º 28.28' N	7º 11.88' W	675	36º 28.62' N	7º 12.40' W	670	1987	Muddy sand with *Cidaris cidaris*
15	11BT18	Pipoca	36º 27.74' N	7º 12.48' W	565	36º 27.70' N	7º 11.87' W	557	1805	Sandy mud with MDAC, sponges & small gorgonians (*Acanthogorgia hirsuta*)
16	11BT17	Pipoca	36º 27.38' N	7º 12.52' W	573	36º 27.61' N	7º 11.97' W	530	1848	Sandy mud with MDAC, sponges & small gorgonians (*A. hirsuta*)
17	11BT20	Pipoca	36º 27.18' N	7º 11.12' W	625	36º 27.54' N	7º 11.60' W	616	1914	Muddy sand with seapens (*K. stelliferum, F. quadrangularis*) & *T. muricata*
18	11BT31	Chica	36º 22.60' N	7º 7.22' W	729	36º 23.02' N	7º 6.88' W	604	1863	Sandy mud awith MDAC, *C. cidaris*, sponges & gorgonians
19	11BT05	Chica	36º 22.38' N	7º 6.41' W	655	36º 22.23' N	7º 7.08' W	682	2212	Muddy sand with seapens (*K. stelliferum, F. quadrangularis*) & *F. chunii*
20	11BT19	Chica	36º 21.88' N	7º 7.86' W	690	36º 22.36'N	7º 8.11' W	690	1935	Sandy mud with *C. cidaris* & *A. richardi*.
21	11BT06	Chica	36º 22.56' N	7º 6.79' W	660	36º 22.86' N	7º 7.31' W	673	2065	Muddy sand with MDAC, *T. muricata*, seapens & gorgonians
22	11BT21	Hesperides	36º 12.21' N	7º 18.73' W	817	36º 12.66' N	7º 18.42' W	845	1897	Muddy sand with *Radicipes* cf. *fragilis* & *F. chunii*
23	11BT24	Hesperides	36º 11.17' N	7º 18.42' W	704	36º 10.82' N	7º 17.95' W	734	1876	Muddy sand with MDAC, CWC remains, *F. chunii*, gorgonians & black corals
24	11BT22	Hesperides	36º 11.22' N	7º 17.50' W	758	36º 10.76' N	7º 17.48' W	801	1713	Muddy sand with MDAC, CWC remains, *F. chunii*, gorgonians & black corals
25	11BT23	Hesperides	36º 10.83' N	7º 18.69' W	703	36º 10.87' N	7º 19.31' W	756	1856	Muddy sand with MDAC, CWC remains, hydrozoans, siboglinids, *F. chunii* & black corals
26	11BT30	Almazan	36º 3.67' N	7º 20.15' W	912	36º 3.52' N	7º 19.56' W	904	1842	Sandy mud with *R.* cf. *fragilis, Isidella* & *Pheronema carpenteri*
27	11BT26	Almazan	36º 2.90' N	7º 20.59' W	941	36º 2.48' N	7º 20.22' W	893	1892	Sandy mud with MDAC, CWC remains, *Isidella, R.* cf. *fragilis* and gorgonians.
28	11BT29	Almazan	36º 3.17' N	7º 20.33' W	860	36º 2.88' N	7º 20.87' W	928	1948	Sandy mud with MDAC, CWC remains, *P. carpenteri, Isidella*, gorgonians & black corals
29	11BT25	Almazan	36º 3.29' N	7º 19.72' W	894	36º 3.61' N	7º 19.22' W	896	1871	Sandy mud with MDAC, CWC remains, gorgonians, *C. cidaris*, siboglinids & crinoids
30	11BT27	Aveiro	35º 52.03' N	7º 25.83' W	1099	35º 51.79' N	7º 25.30' W	1114	1809	Mud with siboglinids, *Isidella* & *Nymphaster arenatus*
31	11BT28	Aveiro	35º 51.74' N	7º 26.72' W	1146	35º 51.51' N	7º 27.28' W	1136	1871	Sandy mud with *T. muricata, Isidella* & *P. carpenteri*

gold-coated to be examined through a HITACHI TM3000 Scanning Electron Microscope (SEM). Molecular approaches have also been conducted for a minority of species, but the results will be reported elsewhere (Chapter 2).

Description of body features, spicules, and skeletal arrangements have been made according to the sponge morphology thesaurus (Boury-Esnault & Rützler, 1997). When required, the features of the collected material were compared to those of holotypes and additional material borrowed from the sponge collections of the Muséum National d'Histoire Naturelle of Paris (MNHN) and the Museo Civico di Storia Naturale Giacomo Doria of Genoa (MSNG). All material herein described as part of INDEMARES-CHICA cruises, holotypes included, will be stored in the Invertebrate Collection of the National Museum of Natural Sciences (MNCN), Madrid, Spain.

Table 2. Summary of features of the mud volcanoes, including N= number of beam-trawl transects conducted, total sampled area (m^2), mean (±SD) depth of trawls (m), abundance of methane-derived authigenic carbonates (MDAC), level of intensity of benthic fishing activity (trawling) in the sampled areas, total number of sponge species identified, and total number of individuals retrieved. The MDAC abundance and fishing intensity in each mud volcano have been calculated as semiquantitative indexes (mean±SD) from the values of each beam-trawl transect (see Methods).

Mud volcano	N	Sampled area (m^2)	Mean depth (m)	MDAC abundance	Fishing intensity	Species richness	Abundance (ind.)
Gazul	6	12046	453 ± 32	2.00 ± 0.89	0.50 ± 0.84	15	370
Anastasya	3	6923	524 ± 32	0.00 ± 0.00	2.67 ± 0.58	8	42
Tarsis	3	5954	602 ± 23	0.33 ± 0.58	2.33 ± 1.15	9	99
Pipoca	5	9608	616 ± 60	0.60 ± 0.89	0.40 ± 0.89	38	249
Chica	4	8078	673 ± 36	0.75 ± 0.50	1.00 ± 1.41	27	299
Hesperides	4	7344	765 ± 52	1.75 ± 1.50	0.00 ± 0.00	19	105
Almazan	4	7555	904 ± 25	1.00 ± 0.82	0.00 ± 0.00	27	270
Aveiro	2	3681	1124 ± 21	0.00 ± 0.00	0.00 ± 0.00	9	225

Results

General faunal assessment

Out of the 38 sampling stations, 7 provided no sponges and the remaining 31 retrieved a total of 1,659 sponges. There were preserved a total of 671 specimens, while 988 others, which were easily identifiable as representatives of common species already preserved, were only counted as collected material and returned to the sea. The collected sponges represented a total of 82 species, as listed in Appendix I. Most of them belonged to the class Demospongiae (79 species), being the class Hexactinellida represented by 3 species only, *Asconema setubalense* Kent, 1870; *Pheronema carpenteri* (Thomson, 1869) and *Lanuginella* cf. *pupa* Schmidt, 1870. Calcarea and Homoscleromorpha species were not collected. Such a species richness increases the number of previously recorded species (86 spp) in the Gulf of Cádiz in 43 leading to a total of 125 spp and representing a 35% increase. Ten species were considered as taxonomically or faunistically relevant (12% of the total identified species) and are herein described in detail. Two of them are new to science (*Jaspis sinuoxea* nov. sp.; *Myrmekioderma indemaresi* nov. sp.). Three others are recorded in the Atlantic Ocean for the first time; *Geodia anceps* (Vosmaer, 1894) previously known from Western Mediterranean, *Coelosphaera* (*Histodermion*) *cryosi* (Boury-Esnault, Pansini & Uriz, 1994), from the Mediterranean Moroccan coast, and P*etrosia* (*Petrosia*) *raphida* (Boury-Esnault, Pansini & Uriz, 1994), hitherto known only from deep Mediterranean waters close to the Gibraltar Strait. *G. anceps* was found at Almazan mud volcano, while both *C. cryosi* and *P. raphida* at Pipoca mud volcano, which largely meet the MOW, so these records could reflect a natural species transfer from the Mediterranean to the Atlantic. Other five species are considered as rare because this study provides their second record for the Atlantic Ocean: the hexactinellid *Lanuginella* cf *pupa* Schmidt, 1870 and the demosponges *Geodia* cf. *spherastrella* Topsent, 1904; *Cladocroce spathiformis* Topsent, 1904, *Cladocroce fibrosa* (Topsent, 1890) and *Haliclona (Rhizoniera) pedunculata* (Boury-Esnault, Pansini & Uriz, 1994).

Another relevant finding was a "micro-aggregation" of individuals of the carnivorous sponge *Lycopodina hypogea* (Vacelet & Boury-Esnault, 1996): a total of 71 individuals in close proximity to each other on a flattened MDAC boulder of 35 cm^2 collected from Gazul mud volcano at a depth of about

490 m. The presence of this species in this same mud volcano had previously been suggested from a ROV study based on video recording (Chevaldonné et al., 2015). Deep-water records of this species in the Mediterranean are scarce and it is rarely found in such high densities (Chevaldonné et al., 2015). Because this sponge has been mostly reported from the Mediterranean and from shallow Atlantic waters, a detailed description of the skeleton of these deep-water individuals was considered worth to contribute to the understanding of intraspecific skeletal variability.

Regarding abundances, the most abundant species was the demosponge *Thenea muricata* (Bowerbank, 1858) with 366 collected individuals. Because its relatively small size and the capability to form aggregations on soft bottoms (which are extensive in the studied fields of mud volcanoes), these high abundances are not surprising. The only demosponge forming real aggregations on hard bottoms was *Petrosia (Petrosia) crassa* (Carter, 1876), represented in the samples by 169 individuals. The demosponge *Desmacella inornata* (Bowerbank, 1866) was also very abundant, with 110 individuals. The abundance of two hexactinellids, *Pheronema carpenteri* (Thomson, 1869), with 181 individuals, and *Asconema setubalense* Kent, 1870, with 117 individuals, made evident that aggregations of these large species also occur even when methane seeping happens (see Appendix I).

A comparison of the species richness and total sponge abundance (individual counts) revealed large between-volcano differences in these parameters (Table 2). Yet there are also large differences in the sampling effort between mud volcanoes (Table 2), being the sampled area (12,046 m^2) in Gazul (the shallowest and best sampled mud volcano) almost 4-fold larger than that sampled (3,681 m^2) in Aveiro (the deepest and least sampled volcano). When species richness and abundance are normalized by sampled area, the mud volcano Pipoca (located at an intermediate depth) emerged as hosting the highest species richness per square meter and Aveiro (the deepest one) as having the highest abundance per square meter (Table 2; Fig. 2). A Pearson correlation involving the 8 mud volcanoes revealed no relationship between the species richness and the average density of sponges per m^2 of sampled bottom ($n= 8$, $r^2= 0.127$, $P= 0.386$; Fig. 2A). The main reason for the lack of correlation is that the pattern is largely disrupted by the sponge fauna of the shallowest (Gazul) and the deepest (Aveiro) volcanoes. The Aveiro fauna consists of a moderate number of species per m^2 but a very high

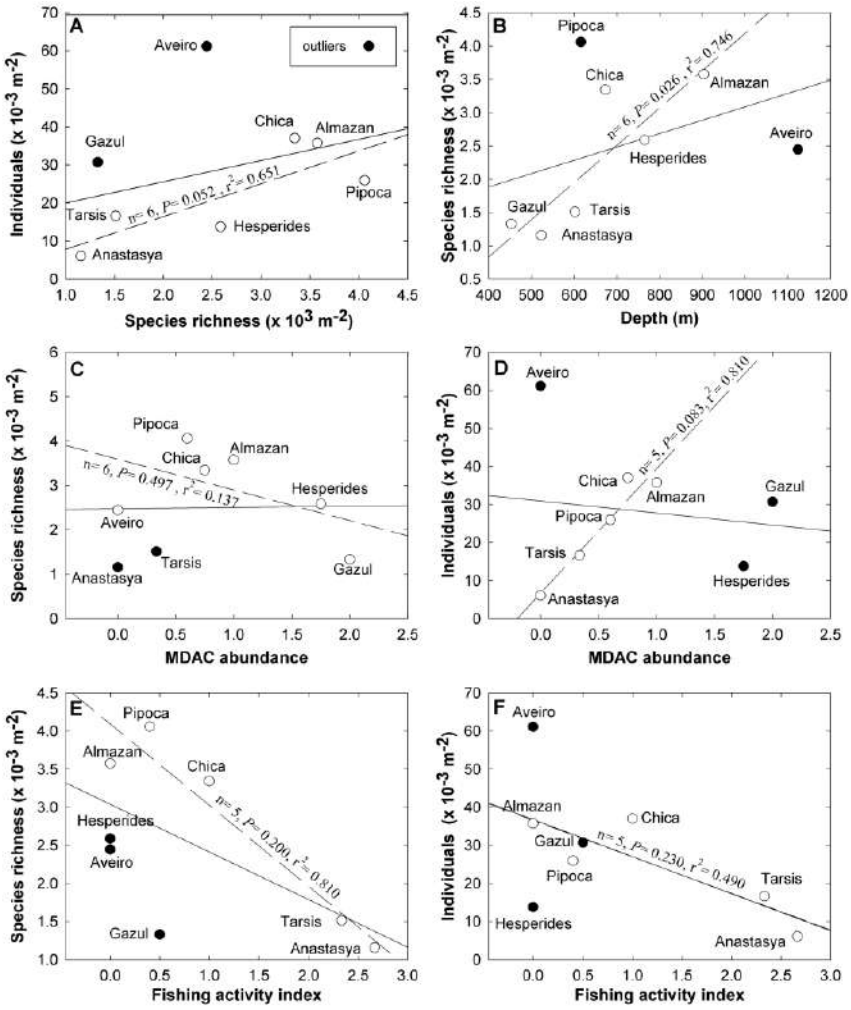

Figure 2. Pairwise relationships between the faunal parameters (species richness per m^2 and abundance of individuals per m^2) and some features of the volcanoes (average depth, abundance of methane-derived authigenic carbonates, and fishing activity). In each graph, the solid lines represent a correlation analysis (either Pearson or Spearman, as explained in the Method section) involving the 8 studied volcanoes. The dashed line represents a "revised" version of the correlation analysis after excluding the outliers (i.e., those volcanoes indicated with solid circles), for which the basic test statistics are given adjacent to the correlation line.

number of individuals. This is so because the species *Thenea muricata* occurs in this mud volcano forming dense aggregations, represented in the samples for a total of 139 individuals. On the other hand, the Gazul fauna consists of a

low number of species but several of them represented with high abundances, such as *Asconema setubalense* (27 individuals), *Lycopodina hypogea* (71), *Poecillastra compressa* (59), and *Petrosia crassa* (85). Both ROV and VOR images and collected material confirmed that most of these sponges are able to form at some point aggregations, as also documented preliminarily for some of them in a technical report of the grant results (Díaz del Río et al., 2014). When the Gazul and Aveiro mud volcanoes were excluded from the correlation analysis for being outliers, a nearly significant relationship between species richness per m^2 and abundance of individuals per m^2 emerged for the remaining mud volcanoes (n= 6, *P*= 0.052, r^2= 0.651; Fig. 2A). Such a relationship means that, in most volcanoes, most of the species are not spatially overrepresented through aggregations, but just scattered with low or moderate abundances that do not differ much between species. When the species richness per m^2 was plotted versus the average depth of each mud volcano (Fig. 2B), no significant correlation emerged (n= 8, *P*= 0.328, r^2= 0.158), but it became statistically significant when the outlier volcanoes Pipoca and Aveiro were excluded from the analysis (n= 6, *P*= 0.026, r^2= 0.746; Fig. 2B). This shift indicates that, as a general trend, the species richness per m^2 increases with increasing depth within the bathymetric range of these mud volcanoes. Such a pattern was altered by the fauna of Pipoca, which is richer than expected given its intermediate depth, and by the fauna of Aveiro, which is poorer than expected given that it is the deepest mud volcano. This general pattern appears to support the classical view that biodiversity of benthic fauna peaks at intermediate depths on the continental slope.

The underwater images revealed marked between-transect differences in the intensity of the seeping activity in the different mud volcanoes. Likewise, the number of fragments of MDAC formations retrieved by the beam trawl also varied across transects (Table 2). The highest mean abundance of MDAC structures was found in Gazul (averaged as 2), followed by Hesperides (1.75) and Almazan (1). MDAC abundance was comparatively low at Chica, Pipoca and Tarsis (averaged as 0.75, 0.60 and 0.33, respectively). The rest of volcanoes (i.e., Anastasya and Aveiro) lacked MDAC formations (scored as 0). The abundance of hard substrate is a feature that was predicted to affect the general composition and abundance of the sponge fauna. Yet when the pairwise relationship between abundance of MDAC formations in each mud volcano and its respective species richness and abundance of sponges per m^2 were examined through rank correlation, no significant

pattern was revealed, even when two and up to three outliers were eliminated (Fig. 2C-D).

When the faunal parameters were confronted against the level of impact that the trawling activity in each of the mud volcanoes may have, a negative general trend was noticed, suggesting that the greater the fishery activity the smaller the sponge richness (Fig. 2E) and abundance (Fig. 2F). Yet, this trend was never statistically significant, even when up to three outliers were progressively eliminated (Fig. 2E-F).

Systematics

Phylum PORIFERA Grant, 1836
Class HEXACTINELLIDA Schmidt, 1870
Subclass HEXASTEROPHORA Schulze, 1886
Order LYSSACINOSIDA Zittel, 1877
Family ROSSELLIDAE Schulze, 1885
Genus *Lanuginella* Schmidt, 1870

Diagnosis: (Tabachnick, 2002)

Lanuginella cf *pupa* Schmidt, 1870

(Figures 3A, 4)

Material examined: One specimen collected from Stn. 20: P75-11BT19

Macroscopic description: Ovate specimen measuring 6 mm in length and 3 mm in diameter, attached to a rock, basiphytose, with smooth surface and a single oscule. Consistency is fragile and colour after preservation in ethanol is white (Fig. 3A).

Spicules: Spicules are diactins often flexuous, with four centrally located tubercles, and rough pointed ends (Fig.4A-B). They measure 325 – 3000 x 3.75 – 6.8 μm. Choanosomal hexactins occur bearing rays of different lengths, sometimes flexuous, with smooth or rough pointed ends (Fig. 4A, C). Size of the rays is 250 – 850 x 5.6 – 12.5 μm. Hypodermal pentactins are common (Fig. 4A, D), characterized by rays with acerate ends measuring 170 – 850 x 4 – 10 μm and a proximal ray measuring 242 – 950 x 7.5 – 11.5 μm with

Figure 3. Pictures showing the general aspect of some studied specimens: (A) *Lanuginella* cf *pupa* (P75-11BT19) growing on a small rock. (B) Some representatives of the specimens of *Lycopodina hypogea* (P203-10BT04) growing

…continued in the next page

in close proximity on a boulder. (C) *Coelosphaera (Histodermion) cryosi* (P03C-11BT18). (D) Specimen of *Jaspis sinuoxea* nov. sp. designed as holotype (P70-11BT17A). (E) Specimen of *Geodia anceps* (P224-11BT25) growing on a rock, marked as 'Ga'. (F) Fragment of a specimen of *Geodia* cf *spherastrella* (P14E-11BT17A) showing what remains of its hispidation, ectosome and choanosome. (G) Specimen of *Myrmekioderma indemaresi* nov. sp. designed as holotype (P10-10BT06) with a patent cerebriform surface. (H) Fragment of *Petrosia (Petrosia) raphida* (P200-11BT17) attached to a rock. (I-J) Specimen of *Cladocroce fibrosa* (P54-11BT17). (K) Specimen of *Cladocroce spathiformis* (P05-10BT03A). (L) Specimens of *Haliclona (Rhizoniera) pedunculata* (from left to right P23B-11BT20D, P23B-11BT20C, and P23B-11BT20D) showing slightly different morphologies, being that on the left the most common.

microspinned end. Abundant stauractins occur (Fig. 4A, E-G) along with scarce pentactins, tauactins (Fig. 4A) and hexactins. They are evenly microspined, with conical ends and rays measuring 42.5 – 140 x 2 – 5.64 μm. Atrialia hexactins moderately happen (Fig. 4A, H), being less rough than the dermalia spicules, almost smooth, and measuring 46.46 – 150 x 2 – 6.25 μm. Microscleres are discohexasters showing a total diameter of 30 – 70 μm with a primary rosette being 6.3 – 10.45 μm in diameter and discs of 3-5 points (Fig. 4A, I-J). Strobiloplumicomes were not observed.

Skeletal structure: Choanosomal skeleton is composed of diactins, hexactins and microscleres. Hypodermal pentactins are tangential to the surface with their proximal ray directed inwards the body of the sponge. Dermalia is mainly composed of stauractins, and sometimes pentactins, tauactins and hexactins. The atrialia presents hexactins smaller and less rough than the choanosomal ones.

Distribution and ecology notes: Specimen collected from depths of 690 m, growing on a small MDAC slab from a sandy mud bottom from the Chica mud volcano (Table 1). It makes the second record of the species in the Atlantic Ocean, having previously been recorded 12 specimens from Cape Verde by Schmidt (1870) and Tabachnick (2002). Schulze and Ijima (1904) reported some specimens from the Pacific Ocean but their assignation to *L. pupa* is currently considered "inaccurate" according to the World Porifera Database (Van Soest et al., 2018).

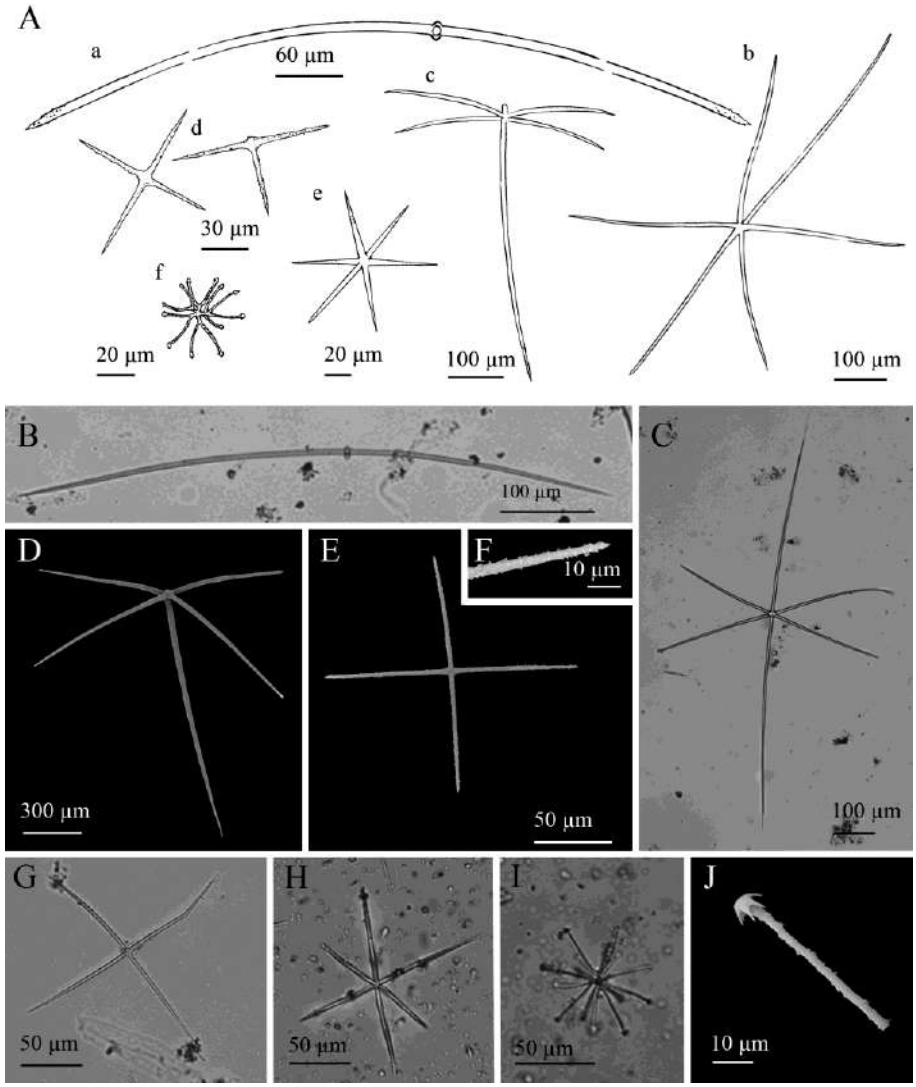

Figure 4. *Lanuginella* cf *pupa* Schmidt, 1870: (A) Line drawing summarizing the skeletal complement of the specimen herein described. Diactins are (a) bent or flexuous and show four tubercles at the centre of their shaft. Choanosomal hexactins (b) also occur with often differently sized rays, as well as hypodermal pentactins (c). Dermalia is mainly formed by microspined stauractins and, less frequently other variations as tauactins (d), while the atrialia contains hexactins, smoother than the previous (e). Microscleres are microspinned discohexasters (f). (B) Light microscope view of a diactine.

…continued in the next page

(C) Light microscope view of a choanosomal hexactine, with differently long, somewhat flexuous rays. (D) SEM view of an hypodermal pentactine. (E) SEM view of a tauractine. (F) SEM detail of a spinned ray of a tauractine. (G) Light microscope view of a tauractine with an abnormal ray. (H) Light microscope view of an atrialia hexactine. (I) Light microscope view of a discohexaster. (J) SEM detail of a ray of a discohexaster in which the microspines can be observed.

Taxonomic remarks: Since the holotype of the species is not available, the features of our specimen were compared with those reported in the original description (Schmidt, 1870). Being this holotype description somewhat imprecise, a more complete and accurate description of another specimen off Palmeira, Cape Verde was also consulted (Tabachnick, 2002). According with them, our specimen shares the same habit and skeletal structure, being the skeletal composition mostly coincident but with two small differences: 1) the atrialia hexactins (46.46 – 150 x 2 – 6.25 μm) from our specimen were slightly smaller than those from the Cape Verde specimens (68 – 243 x 7 μm), and 2) strobiloplumicomes were neither observed in our specimen nor mentioned in the holotype, while they were described by Tabachnik (2002). Regarding other species from subfamily Lanuginellinae, they all bear strobiloplumicomes, and none of them resembles the rest of skeletal features better than *Lanuginella pupa*.

Class DEMOSPONGIAE Sollas, 1885
Subclass HETEROSCLEROMORPHA Cárdenas, Perez & Boury-Esnault, 2012
Order POECILOSCLERIDA Topsent, 1928
Family CLADORHIZIDAE Dendy, 1922
Genus *Lycopodina* Lundbeck, 1905

Diagnosis: (Hestetun et al., 2016)

***Lycopodina hypogea* (Vacelet & Boury-Esnault, 1996)**
(Figures 3B, 5)

Material examined: Three of seventy-one specimens collected from Stn. 2: P203-10BT04 A-BS.

Macroscopic description: Oval body, 0.72 – 1.5 mm long and 0.58 – 1 mm in diameter, with a stalk of 1.2 – 1.83 mm in length and 0.09 – 0.18 mm in diameter. Filaments project from the body, varying in number and length among individuals, depending on the digestive stage. Whitish colour after preservation in ethanol (Fig. 3B).

Spicules: Megascleres are styles and subtylostyles (Fig. 5A-B), measuring 200 – 550 x 2.5 – 6.6 μm. Megascleres in the stalk are slightly thinner while those at the basal plate are shorter (100 – 300 μm) and more robust (4.5 – 6 μm). Microscleres are abundant palmate anisochela, 8.75 – 11.5 μm in length, with a frontal long tooth of 4.4 – 5.86 x 2.17 – 3.09 μm (Fig. 5C). No forceps was observed, suggesting absence of reproductive elements at the time of collection.

Skeletal structure: The stalk contains a central axis of styles and subtylostyles, which branches radially at the body, forming progressively thinner tracts that finally enter the filamentous, feeding projections. The main ramifications of the axis are surrounded by styles and subtylostyles in confusion. Anisochela are abundant, projecting the largest ala from the

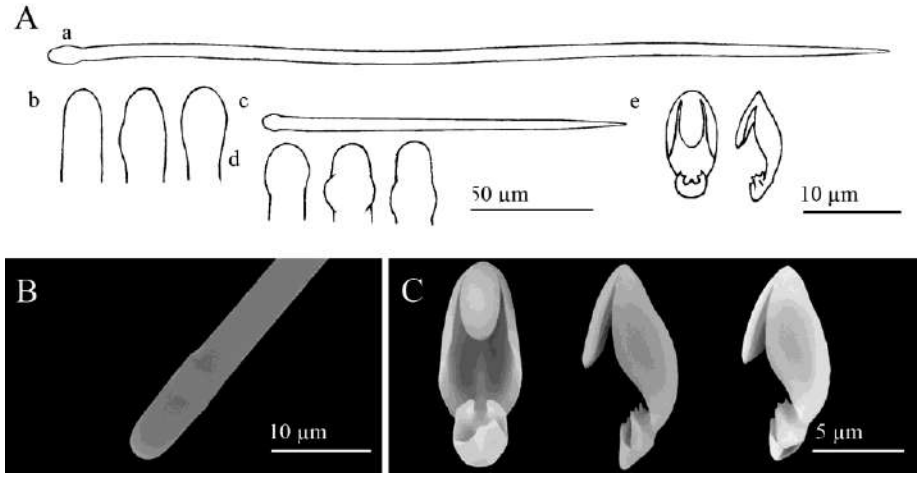

Figure 5. *Lycopodina hypogea*: (A) Line drawing summarizing the skeletal complement of the species. Megascleres are (subtylo-)styles (a) with rome to faintly subtylote ends (b). The basal plate of the sponge shows shorter subtylostyles (c) with more evident subtyles (d). Microscleres are palamate anisochela (e). (B) SEM detail of a blunt end of a style with a very subtle subterminal swelling. (C) SEM detail of anisochelae.

epithelium of the hunting filaments. The attachment base contains smaller subtylostyles and/or styles in confusion and desma were never found.

Distribution and ecology notes: Noticeable aggregation of seventy-one individuals on a flattened slab of merely 35 cm^2 from Gazul mud volcano, at depths of 483 – 495 m (Table 1). Previously, *L. hypogea* had been reported from the Mediterranean and shallow depths in the Atlantic. The bathyal occurrence of the species in the area had only tentatively been proposed from a ROV video record (Chevaldonné et al., 2015). All previous Mediterranean deep-water records reports individuals in low numbers rather than in aggregations.

Taxonomic remarks: Some of the previously described shallow-water specimens of *L. hypogea* show longer subtylostyles in the stalk than in the body (Vacelet & Boury-Esnault, 1996; Chevaldonné et al., 2015), while some others show no length differences (Chevaldonné et al., 2015).

Family COELOSPHAERIDAE Dendy, 1922
Genus *Coelosphaera* Thomson, 1873
Subgenus *Coelosphaera (Histodermion)* Topsent, 1927

Diagnosis: (Van Soest, 2002)

Coelosphaera (Histodermion) cryosi (Boury-Esnault, Pansini & Uriz, 1994)

(Figures 3C, 6)

Material Examined: Two specimens, collected from Stn. 13: P03C-11BT16 and Stn. 15: P03C-11BT18.

Macroscopic Description: Specimen with a body collapsed as a result of being trawled and exposed to air on board during its collection process. The sponge looks coating, with an irregular shape, covering a surface of 15 mm in length and 30 mm in wideness. It shows an evident ectosome and a loose, somewhat hollow choanosome. Surface is smooth and shows 12 fistulas with no patent openings. Oscules and pores are not observed, consistency is fragile

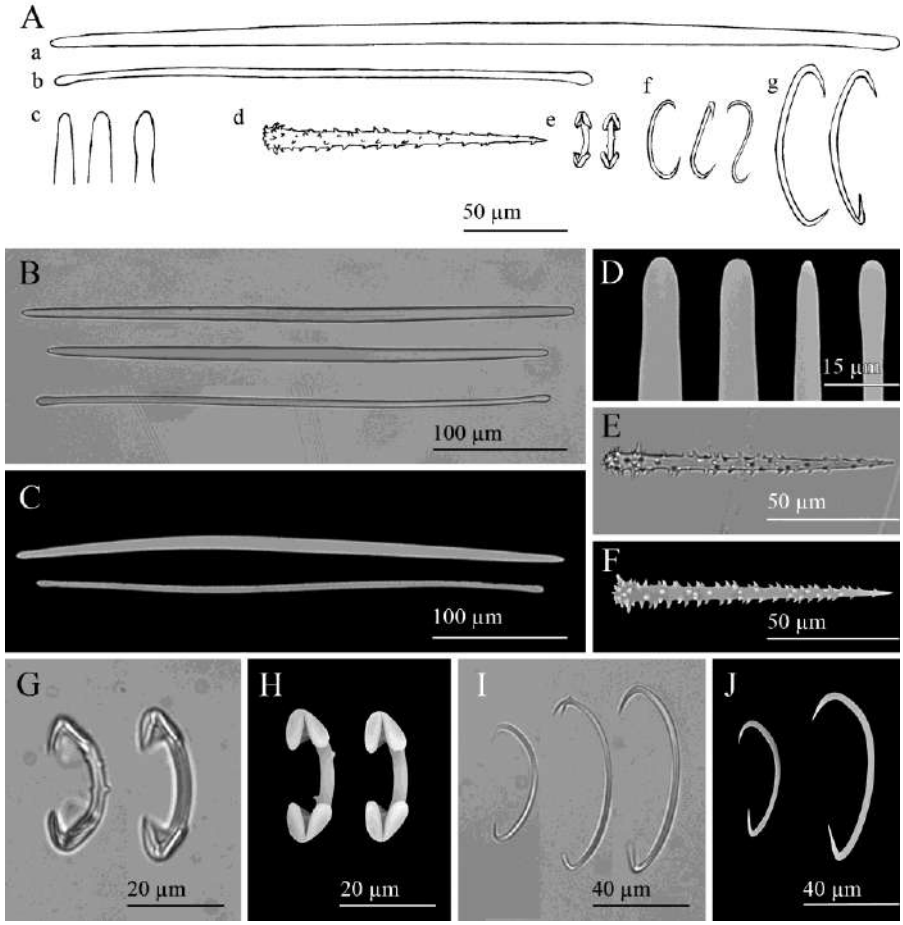

Figure 6. *Coelosphaera (Histodermion) cryosi*: A) Line drawing summarizing the skeletal complement of the species. Megascleres are abundant iso- and anisostrongyles (a) that sometimes occur in thinner shapes (b). Their ends range from narrow to lanceolate, and are tylote in the thinner shapes (c). Accessory megascleres are subtylote acanthostyles with conspicuous spines curved upwards at the shaft (d). Microscleres are arcuate isochelae that sometimes bear sparse microspines (e) and C and S shaped sigmata in two size categories (f-g). (B) Light microscope view of anisostrongyles. (C) SEM view of anisostrongiles. (D) SEM detail of different strongyle tips. (E) Light microscope view of an acanthostyle. (F) SEM vie of an acanthostyle. (G) Light microscope view of a spiny and a smooth isochelae. (H) SEM view of a spiny and a smooth isochelae. (I) Light microscope view of sigmata in two size categories with regular and bifid tips. (J) SEM view of sigmata in two size categories.

and easy to steer with tweezers, and colour after preservation in ethanol is cream (Fig. 3C).

Spicules: Megascleres are abundant iso- and anisostrongyles (Fig. 6A-C) with variable strongylote ends that range from narrow to lanceolate (Fig. 6A, D). Fusiform and slightly sinuous shapes sometimes happen, as well as tylote developing stages (Fig. 6A-C). They measure 335 – 470 μm in length and 8.75 – 15 μm in diameter. Accessory megascleres are subtylote acanthostyles, straight or slightly bent, with conspicuous spines curved upwards at the shaft (Fig. 6A, E-F). They measure 60 – 240 μm in length by 10 – 15 μm in diameter. Microscleres are abundant, arcuate isochelae that sometimes bear sparse microspines (Fig. 6A, G-H), measuring 27.5 – 37.5 μm in length and 3.5 – 7.5 μm in wideness, and C and S shaped sigmata (Fig. 6A, I-J). Sigmata occur in two categories, measuring the smallest 22.5 -50 μm in length and 1.8 – 2.5 μm in diameter, while the largest comprises sizes of 58.5 – 85 μm in length and 1.8 – 2.5 μm in wideness, and sometimes shows bifid ends.

Skeletal Structure: Choanosomal skeleton is formed by loose bundles of strongyles echinated by some acanthostyles. Microscleres are present overall the choanosome and are especially abundant at the base, where also some acanthostyles lie perpendicularly to the substrate. Ectosome is a tangential and compact layer of strongyles and microscleres, showing the fistula the same structure.

Distribution and ecology notes: The specimens were collected from Pipoca mud volcano, growing on small MDAC piece found on muddy sand (627-719 m deep) and sandy mud (565-557 m deep) bottoms respectively (Table 1). This is the second record for this species, being previously reported from the Mediterranean Moroccan coast, at a 170m-deep bottom of shell debris (Boury-Esnault et al., 1994).

Taxonomic remarks: The collected specimen fits closely the diagnosis of the genus *Coalosphaera (Histodermion)*, sharing most of its characteristics with *C. cryosi* except for two minor differences. Our specimen has ectosomal diactines with ends widely variable in shape, from narrowing to lanceolated, to even tylote. In the holotype all the ectosomal diactines have tylote end. Differences in the isochelae also occur, showing our specimen a single category which can show microspines, while the holotype shows two categories with no reported microspines. These differences are here considered to be intraspecific variability, since tylote stages of megascleres happen in both the studied and

the type material and the isochela size of our specimen fall between the two size categories described in the holotype, suggesting that the existence or not of the two categories could also have resulted from a subjective author criterion during categorization.

Regarding body shape, the mud volcano specimen resembles *Coelosphaera (Histodermion) dividuum* (Topsent, 1927) from Azores, which is the only other species in this subgenus hitherto recorded from the Atlantic. They both bear anisostrongyles and only one category of isochelae. Nevertheless, our specimen only has anisostrongyles while *C. dividuum* has anisostrongyles and tylotes, measuring the lasts 425 – 740 x 8 – 15 μm (size of anisostrongyles is not specified in the original description). Also the acanthostyles of our specimen are smaller than those of *C. dividuum*, which measure 450 – 470 x 13 – 16 μm, and it bears two categories of sigmata while *C. dividuum* lacks them.

Order TETRACTINELLIDA Marshall, 1876
Family ANCORINIDAE Schmidt, 1870
Genus *Jaspis* Gray, 1867

Diagnosis: (Uriz, 2002)

***Jaspis sinuoxea* nov. sp.**
(Figures 3D, 7)

Material examined: Holotype P70-11BT17A from Stn. 16 (36º 27.38'N 7º12.52'W – 36º 27.61'N 7º 11.97'W). Four paratypes designated: P70-11BT17B & C from Stn. 16; P70-11BT18 A & B from Stn. 15 (36º 27.74'N 7º 12.48'W – 36º 27.70'N 7º11.87'W).

E**tymology:** This species is named after the evident sinuous shape of its oxeas.

Macroscopic description: Encrusting to thickly encrusting, patchily growing on small rocks. Some fragmented specimens collected with no attached substrate. They measure 3 – 25 mm in length, 5 – 50 mm in wideness and 1 – 3 mm in thickness. Oscules only observed in holotype as two non-elevated "pores" of 0.25mm in diameter and with some faint radiating "veins". Sponge

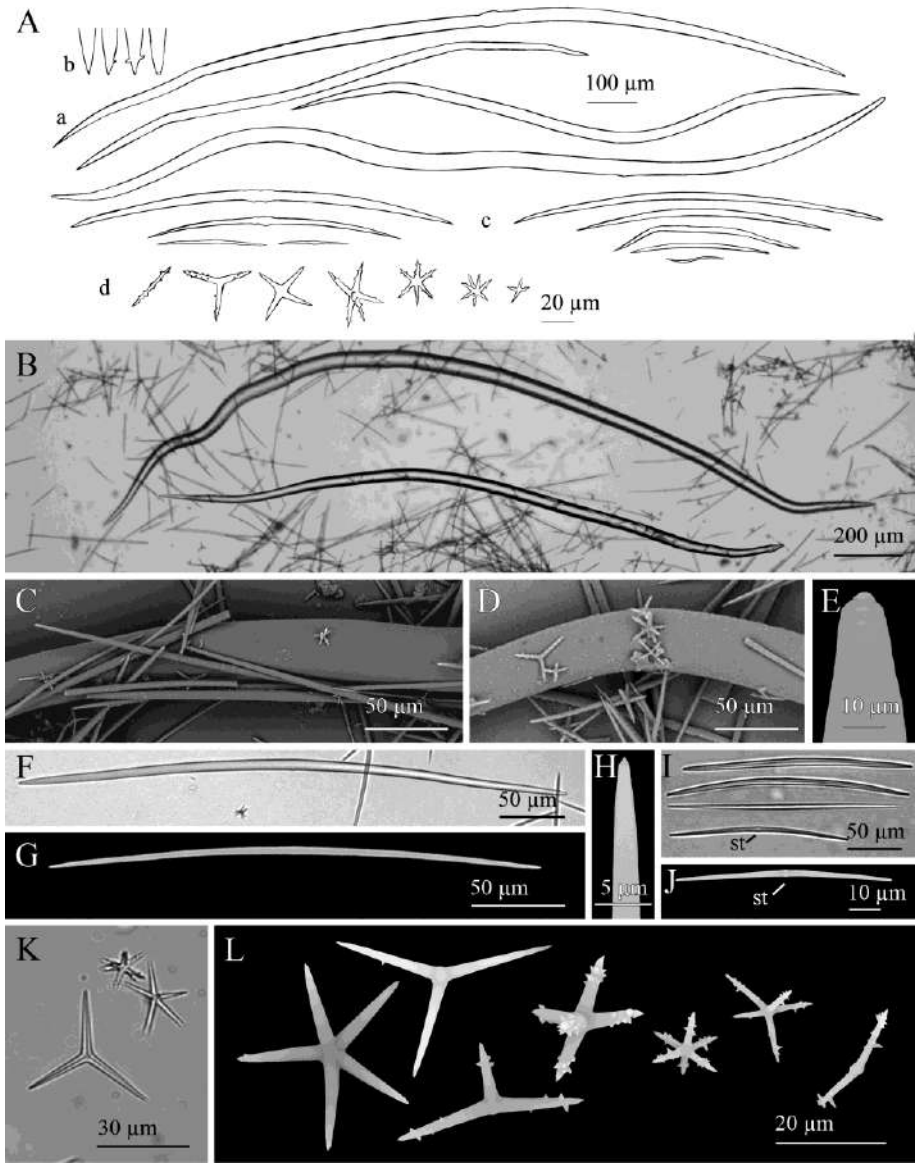

Figure 7. *Jaspis sinuoxea* nov. sp.: (A) Line drawing summarizing the skeletal complement of the species. Choanosomal oxeas are from bent to sinuous, sometimes with a subtyle more or less centrally located (a) and with acerate or mucronate ends that occasionally bear one or two spines (b). Ectosomal oxeas are once or twice slightly or evenly bent, occasionally slightly sinuous and sometimes show centrotylotism (c). Microscleres are oxyasters in a wide size range, with few to abundant spines, rarely smooth (d).

…continued in the next page

(B) Light microscope view of sinuous choanosomal oxeas, which can be hardly to evenly sinuous. (C-D) SEM detail of choanosomal oxea sections surrounded by ectosomal oxeas and oxyasters. (E) SEM detail of a choanosomal oxea mucronate end. (F) Light microscope view of an ectosomal oxea. (G) SEM view of an ectosomal oxea. (H) SEM detail of an ectosomal oxea conical end. (I) Light microscope view of small ectosomal oxeas, which are from straight to softly bent and sometimes bear a faint subtyle (st). (J) SEM detail of a small ectosomal oxea with a central subtyle (st). (K) Light microscope view of widely variable oxyasters, from large with three smooth actines to small and bearing seven spined actines. (L) SEM detail of oxyasters in a wide range of shapes and sizes. All kind of shapes can be found independently from size, but large oxyasters frequently show few nearly smooth actines while smaller ones generally bear abundant spined actines.

surface is smooth, although large megascleres from the choanosome occasionally hispidate it. Consistency is friable, especially in the choanosome, colour after preservation in ethanol is whitish beige (Fig. 3D)

S**picules:** Megascleres are oxeas in a wide size range (Fig. 7A), not divisible into discrete size categories but by location and shape. Choanosomal oxeas (Fig. 7A-D) measure 450 – 2875 x 8.5 – 75 μm, they are more or less fusiform, bent or more often sinuous, the ends are usually softly mucronated (Fig. 7E) or blunt, resulting in strongyloxeas (Fig. 7A); sometimes they are acerate. Centrotylotism is fairly common and scarce spines at the ends may occasionally occur as well. Ectosomal oxeas (Fig. 7A, F-G, I-J) measure 65 – 550 x 1.25 – 12.5 μm, they are from slightly to evenly fusiform, once or twice slightly or markedly bent. Occasionally they are subtly sinuous, and can show centrotylotism. Ends are acerate or conical (Fig. 7H). Microscleres are oxyasters variable in shape and size but with no discernible categories (Fig. 7A, K-L). They measure 7.5 – 45 μm in diameter and bear 2 – 9 conical actines, which can be either smooth or spiny. Generally, oxyasters smaller than 15 – 30 μm in diameter (depending on the specimen) show spines, while those of larger diameters can be either smooth or spiny, but most of the largest ones are actually entirely or almost entirely smooth.

Skeletal structure: Ectosome is a crust-like layer of tangential and compacted ectosomal oxeas and oxyasters. The organization of the choanosomal skeleton is in confusion, with all spicule types arranged without a recognisable pattern.

Distribution and ecology notes: The individuals were collected at 530 – 573 m from a deep sandy mud bottom with MDAC piece at Pipoca mud volcano (Table 1).

Taxonomic remarks: The specimens from the volcanoes fit the diagnosis of genus *Jaspis*, which in the Atlantic and the Mediterranean is represented by species lacking sinuous oxeas. However, sinuous megascleres have been recorded in *Jaspis stellifera* (Carter, 1879) from Australia and *Jaspis serpentina* Wilson, 1925 from Philippines. The former has slightly flexuous oxeas (Kennedy, 2000) and the latter more markedly sinuous strongyles or oxeas. Yet the microscleres from those two species do not match the features of those in our specimens. Interestingly, a combination of euasters and sinuous diactines occurs in some species of the genus *Paratimea* Hallman, 1917. However, the global spicule complement and skeletal arrangement in the specimens here collected do not meet those characterizing *Paratimea* spp.

Family GEODIIDAE Gray, 1867
Genus *Geodia* Lamarck, 1815

Diagnosis: (Cárdenas et al., 2013)

Geodia anceps (Vosmaer, 1894)
(Figures 3E, 8)

Material examined: One specimen: P224-11BT25 from Stn. 29.

Macroscopic description: Irregularly globular shape, measuring 65 mm in height, and 50 mm x 25 mm in width. Smooth surface, with uniporal oscules and ostioles. Some small buds occur scattered on the sponge surface. Consistency is slightly compressible and colour in ethanol is beige (Fig. 3E).

Spicules: Megascleres are oxeas, orthotriaenes and dichotriaenes. Oxeas, softly curved and fusiform with slightly blunt ends, measure 2122 – 3406 x 16 – 42.3 μm (Fig. 8A-B). Orthotriaenes show clads of 96.8 – 580 x 12 – 68.86 μm and a rhabdome of 375 – 2770 x 13.5- 70 μm (Fig. 8A, C). Dichotriaenes with rhabdomes measuring 800 – 2700 x 30 – 55 μm and protoclads and deuteroclads measuring respectively 122 – 378 x 30 – 53.4 μm and 121 – 338 x 39 – 53 μm (Fig. 8A, D). Anatriaenes (Fig. 8A) have been mostly observed

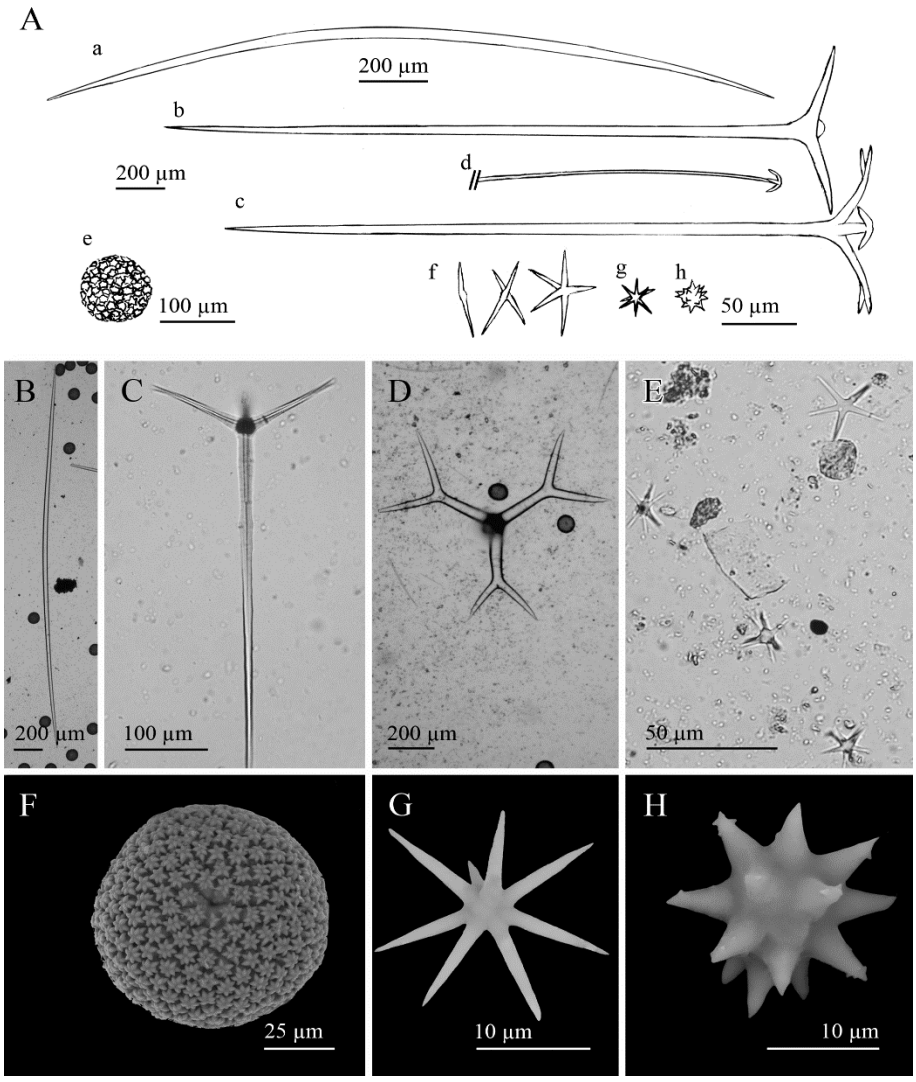

Figure 8. *Geodia anceps* (Vosmaer 1894): (A) Line drawing summarizing the skeletal complement of the species. Megascleres are fusiform oxeas (a), orthotriaenes (b), dichotriaenes (c) and flexuous anatriaenes (d). Microscleres are sterrasters (e), oxyasters in two different categories, oxyasters I, scarce and bigger (f) and oxyasters II, more abundant, smaller and with more actines (g), and spheroxyasters with abundant spines (h). (B) Light microscope view of a softly bent oxea. (C) Light microscope view of a orthotriaene. (D) Light microscope view of a dichotriaene. (E) Light microscope view of an oxyaster I on the upper left and three smaller oxyasters II. (F) SEM view of a sterraster. (G) SEM view of an oxyaster II. (H) SEM view of a spheroxyaster with sparse microspines.

as broken, isodiametric and somewhat flexuous rhabdomes of 6 – 8 μm in diameter and lengths of up to1500 μm. Microscleres are somewhat compressed sterrasters, with a diameter of 76.6 – 91.1 μm (Fig. 8A, F). Also smooth oxyasters in two categories. The first one consisting of scarce oxyasters with a diameter of 30.8 – 50 μm (generally smaller than 36 μm) and only 2 to 5 actines (Fig. 8Af, E); the second one, being a more abundant category of oxyasters with diameter of 18 – 30 μm and 6 to 8 actines and a centrum slightly thicker (Fig. 8Ag, E, G). Spheroxyasters of 13.2 – 28.5 μm in total diameter, with a large centrum (6.2 – 14.5 μm in diameter) and abundant actines which can show sparse microspines (Fig. 8Ah, H).

Skeletal structure: The inner choanosome shows oxea and oxyasters in confusion, becoming radially arranged in loose bundles towards the ectosome. The cortex is 500 μm thick, being the inner cortex reinforced by oxea and clades of triaenes, with their rhabdomes towards the choanosome. The external cortex consists of two layers, an inner layer of sterrasters and an outer layer of oxyspherasters. Anatrianes project their clads out from the sponge surface.

Distribution and ecology notes: The specimen was collected from Almazan mud volcano, on a sandy mud bottom with MDAC at a depth of 894 – 896 m (Table 1). It represents the first record for the species in the Atlantic Ocean, although it is noteworthy to mention that several specimens were recently found by Ríos and Cárdenas in the Avilés Canyon, Atlantic northern coast of Spain (Cárdenas, pers. comm.). To date, it was only recorded from the Mediterranean, that is, from the Bay of Naples at 150 – 200 m depth (Vosmaer, 1894) and, from the same area, at a 120-135m deep muddy bottom with stones (Pulitzer-Finali, 1970). Maldonado (1992) provided another record from 70-120 m deep bottom in Alboran Sea with red coral. Also, it was recorded from a white coral reef located south of Cape S. Maria di Leuca (southern Italy) at 738 – 809 m depth (Longo et al., 2005).

Taxonomic remarks: The skeletal structure and composition of our specimen fits that of *Geodia anceps*. Sterrasters were found to be somewhat bigger than those from the holotype with a larger centrum. Specimens recently found in the Avilés canyon by Ríos and Cárdenas are also characterized by comparatively larger sterrasters (Cárdenas, pers. comm.), for which this could represent a common character of the Atlantic specimens. It is also remarkable

the presence of small buds at the sponge surface of the collected specimen, which, to our knowledge, makes the first budding report in this species.

Geodia cf. *spherastrella* Topsent, 1904

(Figures 3F, 9)

Material examined: Four specimens: P14E-11BT17A to D from Stn. 16.

Comparative material: Geodia spherastrella Topsent, 1904. Holotype: A spicules slide (MNHN no. D.T. 842 122P.A. 1897); Princesse-Alice cruise to Azores, station 866 (Terceira Island: 38º52'50"N 27º23'05"W); collected on 2nd August 1897 from a coarse sand bottom at 599 m depth.

Macroscopic description: Two cushion-shaped specimens of 2 – 3 mm in diameter, with no discernible openings, sparse, long hispidation, and hard consistency. A third specimen only conserved its base and part of the lateral body wall, showing a 0.5 mm thick cortex and an unevenly distributed hispidation and three sparse ostia (Fig. 3F). A fourth individual only had its base (30 mm in diameter) preserved.

Spicules: Megascleres are oxeas, fusiform and softly bent, with acerate to blunt ends, sometimes mucronate, measuring 445 – 4153 x 9 – 22.5 μm (Fig. 9A-B). Those longer than 2500 - 3000μm are often hispidating and sometimes show a slightly flexuous shape, but no categories can be established since size overlapping occurs between hispidating and choanosomal oxeas. Orthotriaenes also occur, with clads measuring 165 – 360 x 15 – 23 μm and rhabdomes of 752 – 1149 x 16.5 – 29 μm (Fig. 9A, C). Microscleres are abundant sterrasters with ellipsoidal shape and a maximum diameter of 100 – 130 μm (Fig. 9A, D, G), being often observed developing stages which measure down to 60μm. Sparse spheroxyasters of 17.8 – 27 μm in diameter occur, showing a marked centrum and smooth and microspined actines (Fig. 9A, E, H). Moderately abundant sphero-strongylasters are also present, measuring 8.5 – 11.6 μm in diameter and bearing more or less regular actines, which can be short to slightly long and always with spined ends (Fig. 9. A, E, I).

Skeletal structure: The deepest choanosome skeleton consists mostly of oxeas in confusion and sparse microscleres, but the structure becomes more radially arranged towards the ectosome. Oxeas often hispidate the surface and orthotrianes are placed with clads in the ectosome without crossing it.

Ectosome consists of highly packed sterrasters together with spheroxyasters and sphero-strongylasters.

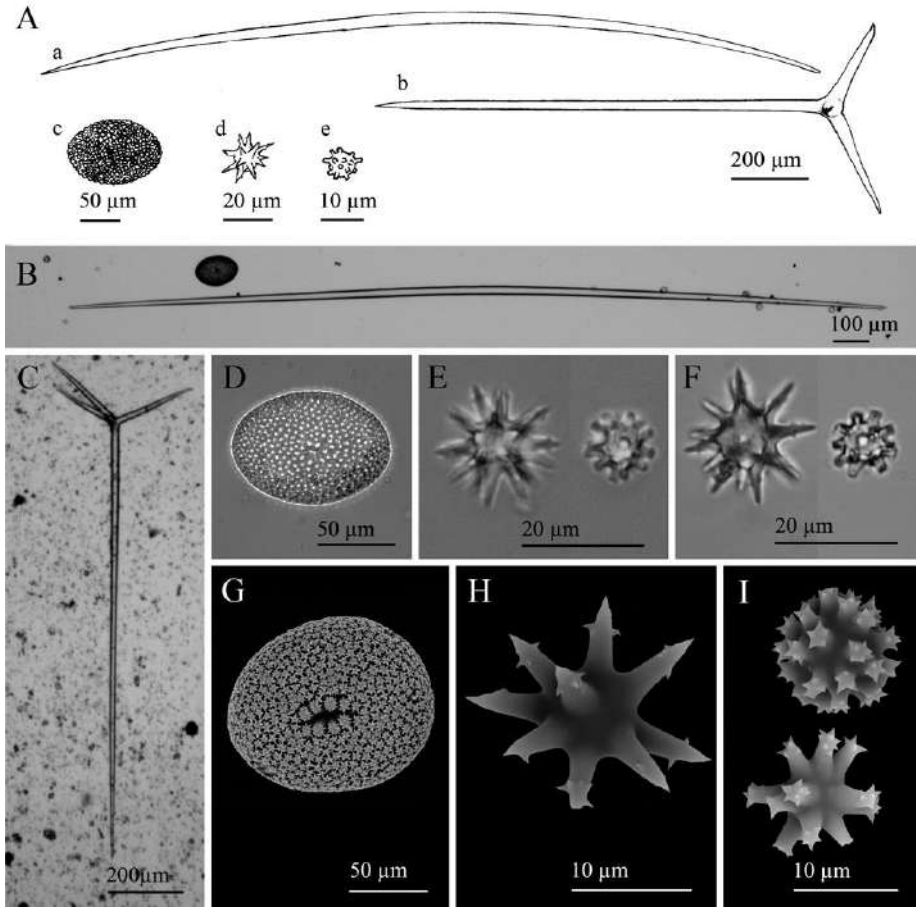

Figure 9. *Geodia* cf. *spherastrella* Topsent, 1904: (A) Line drawing summarizing the skeletal complement of the species. Megascleres are oxeas, normally fusiform and bent (a), and orthotrianes (b). Microscleres are ellipsoid sterrasters (c), spheroxyasters (d) and sphero-strongylasters (e). (B) Light microscope view of a softly bent oxea. (C) Light microscope view of an orthotriaene. (D) Light microscope view of an sterraster. (E) Light microscope view of a spheroxyaster and a sphero-strongylaster. (F)) Light microscope view from the type material of a spheroxyaster and a sphero-strongylaster. Note the similarities between "E" and "F". (G) SEM view of a sterraster. (H) SEM view of a spherostrongylaster. (H) SEM view of two sphero-strongylasters. Note the differences on the length of the rays and their spinned ends.

Distribution and ecology notes: The specimens were collected from Pipoca mud volcano, all from a sandy mud bottom with MDAC at a depth of 530 – 573 m (Table 1). This material makes the second record of this species in the Atlantic Ocean, being previously known one specimen from the vicinities of Terceira Island in Azores that was collected at a coarse sand bottom at 599 m depth (Topsent, 1904).

Taxonomic remarks: The skeletal composition of our specimens strongly resembles that of the holotype of *Geodia spherastrella*, which is represented by a mere spicules slide. The examination of the type slide revealed oxeas of 558.7 – 3519 x 27.6 – 40.32 μm, similar in shape to those of the collected specimens. Orthotrianes were not observed in the holotype slide although Topsent (1904) mentioned them in the original description of the species. For this reason, we consider that the lack of orthotrianes in the type slide is an unfortunate mishap that subsequent authors should keep in mind if using it. Microscleres from the holotype also coincide in shape and size with those of our specimens, measuring sterrasters 90 – 125.5 μm in diameter, spheroxyasters 19.3 – 30.2 μm, and sphero-strongylasters, 7.6 – 14.8 μm. It is worth noting that, in the type description from Topsent (1904), "sterraster-like ends" of the sphero-strongylaster actines were mentioned, and they were observed both in the holotype slide through light microscope and in our specimens through scanning microscopy (Fig. 9I).

Little is known about the habit and skeletal structure of the type. According to the original description, it was irregularly shaped, white, smooth and with encrusted small pebbles. The specimens collected from the mud volcanoes conserved a small part of their surface and it seems to be smooth with some irregularly hispid regions and no encrusted pebbles.

Order AXINELLIDA Lévi, 1953
Family HETEROXYIDAE Dendy, 1905
Genus *Myrmekioderma* Elhers, 1870

Diagnosis: (Hooper, 2002)

Myrmekioderma indemaresi nov. sp.

(Figures 3G, 10)

Material examined: Two specimens collected: Holotype P10-10BT06 from Stn. 3(36º33.33'N 6º56.07'W – 36º33.59'N 6º55.59'W); paratype P10-10BT08 from Stn 4 (36º33.27'N 6º56.01'W – 36º33.54'N 6º55.44'W).

Comparative material: Holotype of *Myrmekioderma spelaea* (Pulitzer – Finali, 1983) originally designated as *Raphisia spelaea* Pulitzer-Finali, 1983; MSNG - (PTRE12) from Cala Sorrentino, Tremiti Island, 2 – 3 m deep

Etymology: This species is named after the acronym (i.e., INDEMARES) of the EC LIFE+ grant that funded the exploration and sampling of the mud volcanoes.

Macroscopic description: Massive nearly entire individuals, measuring 40 – 60 mm in height, 40 – 65 mm in wideness, and 5 – 20 mm in thickness. Four oscules observed in P10-10BT08 being 2 – 3 mm in diameter. Ostioles not evident. Surface is cerebriform (where it is well preserved), shortly hispid, incorporating sparse debris. Colour after preservation in ethanol is creamy-white. Consistency is firm and fleshy, somewhat friable (Fig. 3G).

Skeletal structure: Ectosome shows a layer of oxeas perpendicular to surface (Fig. 10I), sometimes hispidating it. The choanosome shows multispicular tracts of oxeas, with some sparse oxeas in between that become more evident in the subectosomal region, where they run radially to surface. A moderate amount of collagen is present in the tracts. Trichodragmata occur in all regions of the skeleton.

Spicules: Megascleres are oxeas in a wide size range of 200 – 1020 x 3.5 – 30 μm. They are from slightly to evenly, once or twice, bent, with acerate ends (Fig. 10A-D) that sometimes are blunt (Fig. 10F-E), mucronated or stepped. Oxeas located in the ectosome are shorter, showing a maximum size of 520 x 15 μm. Microscleres are moderately abundant raphides in wispy trichodragmata (Fig. 10G-H). Raphides are from straight to slightly sinuous and measure 35 – 212.5 x 1.2 – 1.4 μm.

Distribution and ecology notes: The specimens were collected from Gazul mud volcano. One of them from a fine sand with MDAC bottom at a depth of 422 – 450. The other individual proceed from a bottom of muddy gravel and fine sand with MDAC at 380 – 455 m depth (Table 1). The collected material makes the first deep-sea record of this genus, since its deepest record is 73m depth. To date *Myrmekioderma* species were known from the Indian and

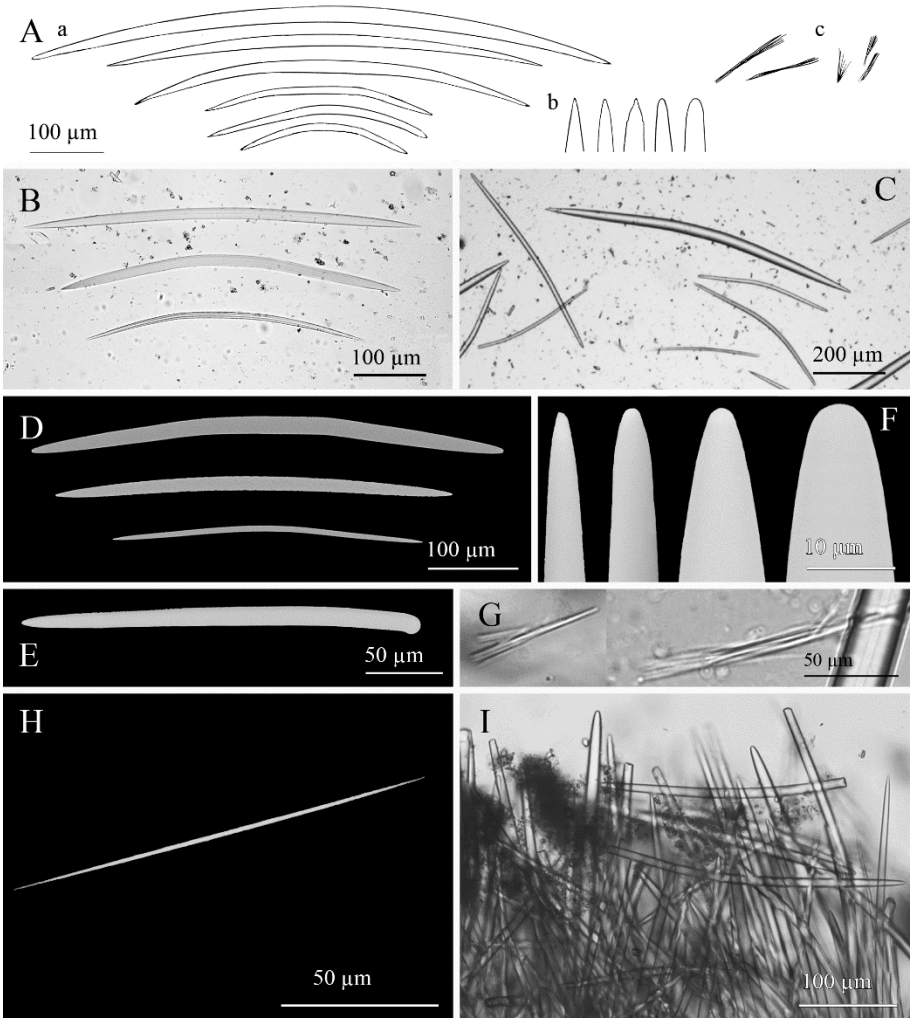

Figure 10. *Myrmekioderma indemaresi* nov. sp.: (A) Line drawing summarizing the skeletal complement of the species. Oxeas occur in a wide variety of sizes and are once or twice bent (a) with variable ends that can be acerate, mucronate, stepped or blunt (b). Raphides occur in wispy trichodragmata in two different categories (c). (B) Light microscope view of oxeas once and twice bent. (C) Light microscope view of oxeas of different sizes. (D) SEM view of oxeas nearly straight and softly bent. (E) SEM view of an oxea with a blunt, almost subtylote end modification. (F) SEM detail of slight to even blunt ends of oxeas. (G) Raphides in trichodragmata. (H) SEM view of a raphide. (I) Light microscope view of ectosomal oxeas perpendicular to surface.

Pacific oceans, the western Atlantic and the Mediterranean. This is the first record of *Myrmekioderma* in the eastern Atlantic.

Taxonomic remarks: Among the *Myrmekioderma* species from the Atlantic and Mediterranean, the spicule complement of the collected specimens shows some resemblance with that of *Myrmekioderma spelaea* (Pulitzer-Finali, 1983) from the Mediterranean. However, the examination of the holotype of *M. spelaea* has revealed a smooth non-tuberculated surface, the presence of often anisostrongylote oxea measuring 82.5 – 680 x 2.5 – 25 μm and trichodragmata measuring 30 – 150 x 5 – 8 μm. Its choanosome is confused while its ectosome is arranged tangentially and easily detachable. Also its distribution in depth is different, since it is recorded from 5 m depth. The specimens here described also coincide in showing similar oxeas and trichodragmata with *Epipolasis spissa* (Topsent, 1892), recorded from Azores and Mediterranean. But it bears toxas (Topsent, 1892, 1904) and its skeletal structure is described as a subhalichondroid reticule (De Weerdt, 2002). Since no other species comparable to the collected specimens have been hitherto described, we consider them to constitute a new species to science.

There is little doubt that our two specimens fit the diagnosis of genus *Myrmekioderma,* concerning habit and spicules complement. However, during our examination of the holotype of *M. spelaea*, we have noticed that this species appears to fit better in the current diagnosis of the genus *Epipolasis* than in *Myrmekioderm*a. Van Soest *et al.* (1990) transferred *Raphisia spelaea* to *Myrmekioderma spelaea* when the latter was still considered a halichondrid and genus *Epipolasis* a synonym of *Myrmekioderma*. Given the noticed similarities between the holotype of *M. spelaea*, including a detachable ectosome, and current *Epipolasis* diagnosis (Erpenbeck & Van Soest, 2002), a genus transfer for such a species, that is, *Epipolasis spelaea* (Pulitzer-Finali, 1983), should be advisable.

Order HAPLOSCLERIDA Topsent, 1928
Family PETROSIIDAE Van Soest, 1980
Genus *Petrosia* Vosmaer, 1885
Subgenus *Petrosia (Petrosia)* Vosmaer, 1885

Diagnosis (Desqueyroux-Fáundez & Valentine, 2002)

***Petrosia* (*Petrosia*) *raphida* Boury-Esnault, Pansini & Uriz, 1994**
(Figures 3H, 11)

Material examined: Specimen P200-11BT17 collected from Stn. 16.

Macroscopic description: Fragment of a specimen, measuring 20 mm in length, 10 mm in wideness and 1 – 5 mm in thickness, attached to a rock. Oscules are not observed (probably due to the fragment condition of the specimen) but ostioles of 0.2 – 0.5 mm in diameter are abundantly scattered over the scarce areas of preserved surface, which is smooth to the touch and crust-like in consistency. Choanosome is friable and somewhat loose. Colour after preservation in ethanol is creamy beige (Fig. 3H).

Spicules: Megascleres are strongyloxeas (Fig. 11A-B, E), moderately once or twice bent, although nearly straight and marked curvatures sometimes occur. They are mostly isodiametric, with ends ranging from slightly acerate to strongylote. Both iso- and anisoxeas happen, being the firsts the usual form. Conical, mucronated, stepped, polyactine and tuberculated ends are fairly common (Fig. 11A, C, F). Size is 290 – 500 x 20 – 25 μm and diameters down to 7.5 μm are occasional. Microscleres are abundant raphides (Fig. 11A, D, G), from straight to centrally bent, with microspines, regularly spread or more abundant at the ends. More rarely, the microspination is nearly lacking (Fig. 11H). Raphides measure 75 – 100 x 0.95 – 1.15 μm.

Skeletal structure: The skeleton of the ectosome is a tangential net of multispicular tracts of a diameter of 150 – 300 μm made by strongyloxeas and raphides. Choanosome is a three-dimensional net of multispicular tracts of strongyloxeas and raphides forming more or less roundish meshes of 50 – 165 μm in wideness. Spongin not observed.

Distribution and ecology notes: The specimen was collected from depths of 530 – 573 m, growing on a small MDAC piece from a sandy mud bottom at Pipoca mud volcano (Table 1). It makes the first record of the species in the Atlantic Ocean, being so far known two individuals from the Mediterranean side of the Strait of Gibraltar, at 580 m depth (Boury-Esnault et al. 1994).

Taxonomic remarks: Our specimen fits the holotype description of *P. raphida*, with two minor differences. One relates with megascleres tips, being those of the type specimen usually strongylote, sometimes varying to narrower or swollen ends. The other difference is the presence of microspines in

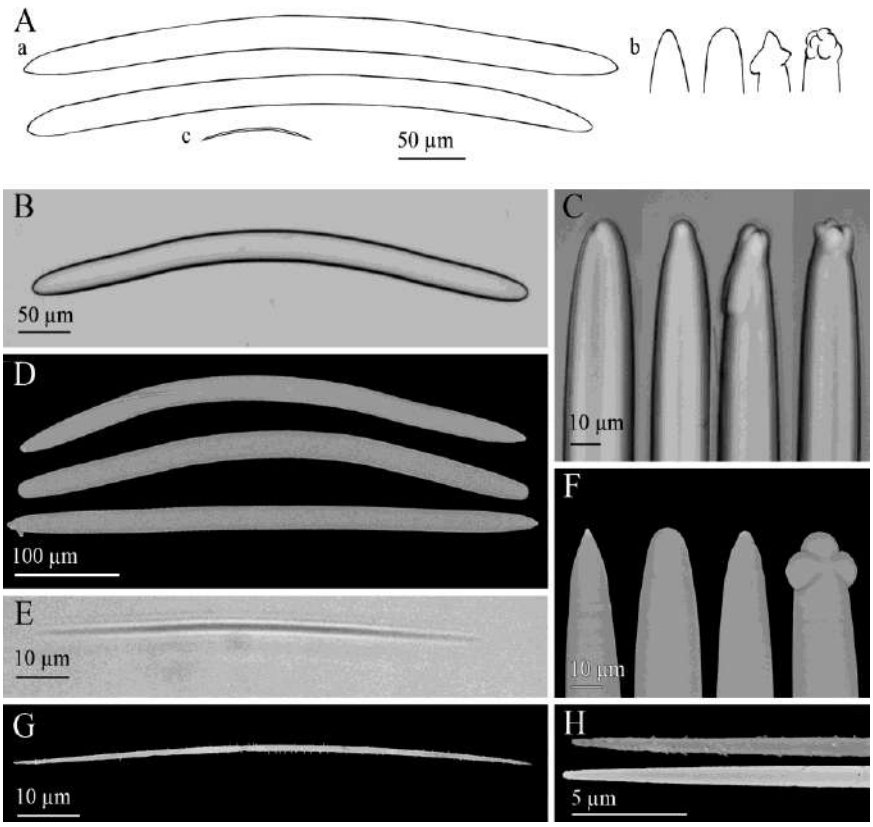

Figure 11. *Petrosia* (*Petrosia*) *raphida* Boury-Esnault, Pansini & Uriz, 1994: (A) Line drawing summarizing the skeletal complement of the volcano specimen. Strongyloxeas (a) are usually bent and show variable ends from slightly to markedly strongylote and sometimes polyactine or tuberculate (b). Raphides (c) are strait or centrally bent and microspined. (B) Light microscope view of a strongyloxea. (C) Light microscope view of strongylote, mucronate or polyactine strongyloxea ends. (D) SEM view showing the variable shapes and ends of strongyloxeas (E) Light microscope view of a raphide. (F) SEM detail of conic, strongylote, mucronated and tuberculate ends of strongyloxeas. (G) SEM view of a raphide with microspines. (H) SEM detail of raphides ends with spines, and

raphides, not reported in the original description, although, admittedly, these spines are only observable through scanning electron microscopy. Since the collected material fits the spicule complement and skeletal structure of *P. raphida* and it was collected not geographically far from the holotype collection

site, the two minor differences above reported are considered as intraspecific variability of those characters.

The literature of additional *Petrosia* species recorded from the Atlantic and the Mediterranean have been considered, being *Petrosia (Strongylophora) davilai* (Alcolado, 1979), from Cuba, the only one which bears raphides. Nevertheless, it shows smaller strongyles (29 – 311 x 3 – 9 μm) and microxeas, which are not present in our specimens.

The genus *Petrosia* is currently divided in two subgenera, mainly differentiated by: (i) the number of size categories of oxeas or strongyles (subgenus *Petrosia* shows 2 or 3 categories while subgenus *Strongylophora* Dendy, 1905 shows 3 to 5); (ii) the ectosomal skeleton architecture (unispicular ectosomal network in *Petrosia* and dense irregular tangential ectosomal reticulation of free strongyles and oxeas of different sizes echinated by small centrangulate microxeas in *Strongylophora*; (iii) absence and presence of microscleres in *Petrosia* and *Strongylophora* respectively (Desqueyroux-Fáundez & Valentine, 2002). It is worth noting that *P. raphida* is close to the current diagnosis of subgenus *Petrosia* but it differs from it by having only a category of megascleres, microscleres and a multispicular tangential network. Therefore, a readjustment of the subgenus diagnosis would be advisable, as it is herein suggested: Subgenus *Petrosia* characterized by a tangential specialised ectosomal uni- or multispicular network, and a very dense lamellate-isotropic choanosomal skeletal network of thickly crowded spicule tracts producing rounded meshes, forming layers parallel to the surface. A dense interstitial reticulation of free spicules gives the sponge a stony texture. Megascleres are in one to three distinct size categories of oxeote or strongylote spicules. Microscleres occasionally present.

Family CHALINIDAE Gray, 1867
Genus *Cladocroce* Topsent, 1892

Diagnosis: (De Weerdt, 2002)

Cladocroce fibrosa (Topsent, 1890)

(Figures 3I-J, 12)

Material examined: One of four specimens collected from the mud volcanoes of Gulf of Cádiz: P54-11BT17 from Stn. 16; P54-11BT06A to C from Stn. 21.

Macroscopic description: Foliaceous body, erect on a cylindrical stalk. Its body measures 130 mm in length, 50mm in wideness and 2 mm in thickness. The stalk is 80mm in height and 3 mm in diameter at its base, reaching up to 11 mm at the junction with the body, where it ramifies in 3 main branches. The surface at the best preserved areas is hispid and pores of 0.5 – 3 mm are abundantly spread on both faces. The body is flexible but collapses outside the water while the stalk is robust and keeps its shape. Colour after preservation in ethanol is beige, being the stalk darker than the body (Fig. 3I-J).

Skeletal structure: The skeleton of the stalk is made of highly compacted oxeas longitudinally arranged, with moderately abundant spongin in-between. The skeleton of the stalk ramifies at its upper extreme in three main multispicular tracts that run longitudinally along the body. They anastomose in thinner multispicular tracts, which are connected by uni- and paucispicular tracts and single oxeas that make a diffuse triangular net with oval meshes (Fig. 12E-F). As a consequence, the skeleton of the body is reticulate. There is no ectosomal skeleton differentiated.

Spicules: Oxeas softly bent, sometimes straight or markedly bent, occasionally asymmetric (Fig. 12A-C). Ends are acerate, more or less sharp (Fig. 12D). They measure 410 – 610 x 10 – 17 μm.

Distribution and ecology notes: The specimen was collected from a 530 – 573 m depth range, on a sandy mud bottom with MDAC from Pipoca mud volcano (Table 1). It makes the second Atlantic record. One specimen was previously collected on sand and mud bottom at 1300 m depth in Azores (Topsent 1892), and two more individuals from a mud bottom of Planier Canyon, off Marseille, at 352 m depth, in the western Mediterranean (Vacelet, 1996). Also (Fourt et al., 2017) provided seven records off the Mediterranean French coasts (Calvi, Cassidaigne, Planier, Porquerolles and Sicié Canyons and Banc de Magaud) and Corse (Ajaccio Canyon) between 250 – 510 m depth.

Taxonomic remarks: Several species of *Cladocroce* occur in the Atlantic, and some of them show a lamellate habit: *Cladocroce spatula* (Lundbeck, 1902), *Cladocroce spathiformis* Topsent, 1904 and *Cladocroce osculosa* Topsent, 1927, the latest one lacking a stalk. Nevertheless, *C. fibrosa* is the only one bearing

evident, thick, oxea fibres that rise from the base and ramify longitudinally as they become thinner. Likewise, none of the *Cladocroce* spp. has oxeas out of the size range 62 – 375 x 2 – 25 μm, except for *C. fibrosa*. The oxeas of the latter are reported to measure 600 x 18 μm by Topsent (1892) and 445 – 570 x 14 – 20 μm by Vacelet (1996), data which are also consistent with the sizes in our specimen.

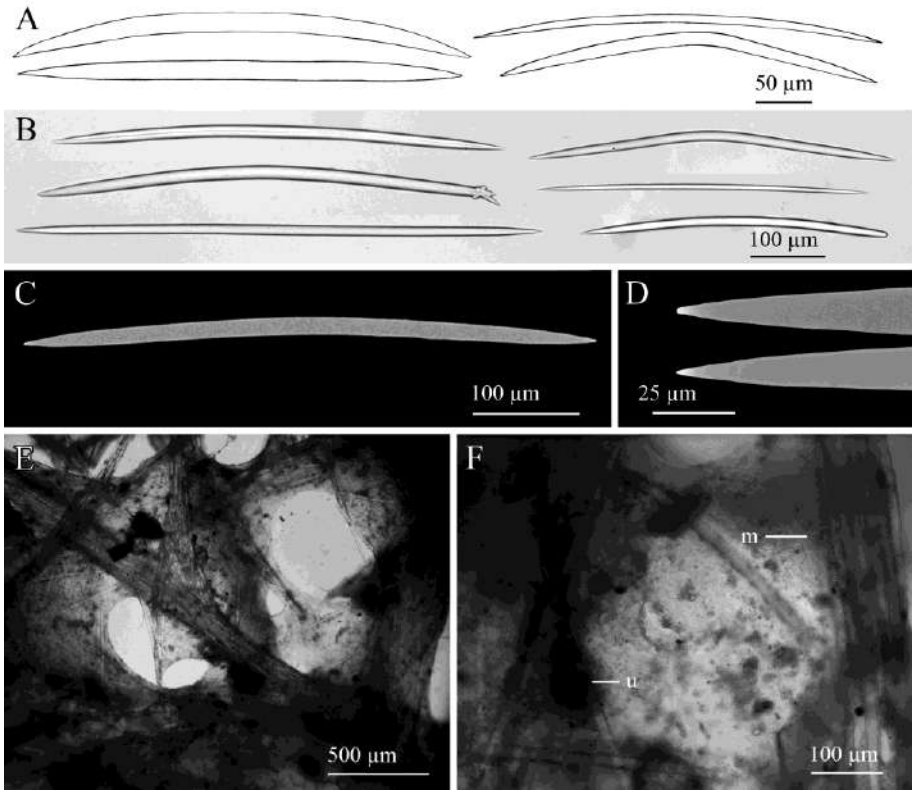

Figure 12. *Cladocroce fibrosa* (Topsent, 1890): (A) Line drawing summarizing the skeletal complement of the volcano specimen. Oxeas are usually slightly bent but range from straight to markedly bent, with normally acerate ends. (B) Light microscope view of oxeas variable in shape and ends. (C) SEM view of an oxea, (D) SEM detail of more or less sharpen acerate ends of oxeas. (E) Light microscope view of skeletal structure of the body with multispicular tracts of oxeas in between which single oxeas form a diffuse triangular net. (F) Light microscope detail of a multispicular tract (m) and three unispicular tracts (u) forming a triangular net.

Cladocroce spathiformis Topsent, 1904

(Figures 3K, 13)

Material examined: Eight specimens collected from the mud volcanoes of Gulf of Cádiz: P05-10BT03A to E from Stn. 1; P05-11BT17 from Stn.16; P05-11BT18 from Stn. 15 and P05-11BT31 from Stn. 18.

Macroscopic description: Lamellar fragments of 58 mm in length, 47mm in wideness and 8 mm in thickness, one is conserving the attachment base. The surface is porous, and oscula of 1 – 2 mm in diameter are all located at one face. The surface is slightly hispid and shows spared sand rests observed under binocular microscope. Consistency is fleshy, firm and friable, poorly flexible. Colour after preservation in ethanol ranges from beige to brown (Fig. 3K).

Skeletal structure: Ectosomal skeleton is a tangential, triangular reticule of uni- and paucispicular tracts, also with some debris. Spongin is only visible at nodes. The choanosomal skeleton at the base of the body is an anisotropic reticule of multispicular (Fig. 13F) tracts of oxea, measuring about 60-175 μm in diameter, connected by paucispicular (Fig. 13E), some unispicular tracts and free spicules. At the upper part of the body multispicular tracts are scarce, being mainly pauci- and unispicular along with free oxeas. They form a more or less triangular mesh with some detrital inclusions in some specimens.

Spicules: Isodiametric oxeas, usually softly bent (Fig. 13A-C), sometimes straight or markedly bent once or twice. Ends are often mucronate, stepped, or sometimes strongylote (Fig. 13D). They measure 312 – 422 x 5 – 17 μm.

Distribution and ecology notes: The specimens were collected from 460 – 729 m. Five came from a muddy medium sand bottom from Gazul mud volcano, two others were collected from sandy mud bottoms with MDAC from Pipoca, and an eighth one came from a sandy mud with MDAC bottom from Chica mud volcano (Table 1). They constitute the second record of the species, being hitherto known only one specimen collected from a muddy sand bottom at 1165 m depth in Azores (Topsent, 1904).

Taxonomic remarks: The collected specimens fit the holotype of *C. spathiformis*, which was described to be brown and lamellate, with several aquiferous openings and oxeas measuring 375 x 17 μm. The collected material slightly resembled *Cladocroce osculosa* Topsent 1927, recorded from the Ibero-

Morrocan Gulf (Topsent, 1928), in being lamellate and brown with numerous aquiferous openings, but our specimens are much thicker than those of *C. osculosa* (1.5 mm thick) and show larger oxea than C. *osculosa* (225 x 9 μm). Similarly, our specimens share a lamellate habit with *Cladocroce spatula* (Lundbeck, 1902), recorded from Iceland and Greenland, but our specimens have larger oxeas than those of *C. spatula* (190 – 220 x 10 – 12 μm). They also

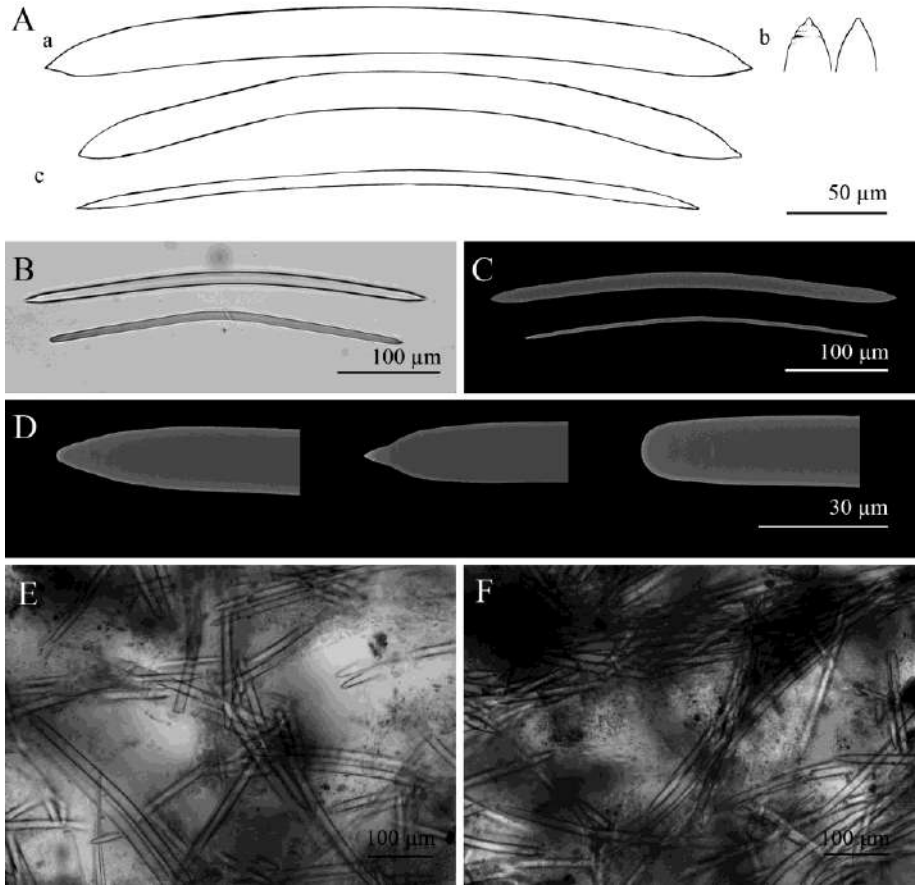

Figure 13. *Cladocroce spathiformis* Topsent, 1904: (A) Line drawing summarizing the skeletal complement of the volcano specimen. Oxeas are usually once or twice softly bent (a) and often show mucronate and stepped ends (b). Thinner oxea sometimes occur (c). (B) Light microscope view of two oxea. (C) SEM view of two oxea. (D) SEM detail of slightly stepped, mucronate and strongylote oxea ends. (E) Light microscope view of paucispicular tracts of oxea. (F) Light microscope view of multispicular tracts of oxea.

have multi-spicular choanosomal tracts, distinguishable from uni- or paucispicular primary tracts characterizing *C. spatula* choanosomal skeleton (Lundbeck, 1902).

Genus *Haliclona* Grant, 1836
Subgenus *Haliclona* (*Rhizoniera*) Griessinger, 1971

Diagnosis: (De Weerdt, 2002)

Haliclona (*Rhizoniera*) *pedunculata* (Boury-Esnault, Pansini & Uriz, 1994)

(Figures 3L, 14, Table 3)

Material examined: Seven of forty-nine specimens collected from the mud volcanoes of Gulf of Cádiz: P23B-11BT01 from Stn. 8; P23B-11BT05A to J from Stn. 19; P23B-11BT06A to N from Stn. 21; P23B-11BT11A to H from Stn. 12; P23B-11BT16A & B from Stn. 13; P23B-11BT20A to N from Stn. 17.

Comparative material: Holotype of *Haliclona (Rhizoniera) rhizophora* (Vacelet, 1969) as *Reniera rhizophora* (MNHN-JV-68-13) from Standia, North of Crete (Stn. 12; 35° 29' 7" N 25° 14' 6" E, 150 m deep, 1984); Holotype of *Haliclona* (*Rhizoniera*) *pedunculata* (Boury-Esnault, Pansini & Uriz, 1994) as *Rhizoniera pedunculata* (MNHN D-NBE.MP.MV-3) from off Sant Vincent Cape, Portugal (Stn. DW16-187; 36.7º N 9.4º W, 1280-1285 m deep, 1984).

Macroscopic description: Stalked, with inverted pyriform and somewhat compressed body, which is 8 – 15 mm long and 5 – 8 mm wide (one specimen showed an irregularly shaped, flattened body measuring 13 mm wide). The stalk is flexible and cylindrical, measuring 4 – 17 mm long and 0.3 – 1.5 mm wide. At its distal extreme, the stalk divides radially along the body base so that it conforms a supporting structure. The stalk also ramifies at its basal end in 2 – 7 rhizomes that are 4 – 25 mm long and 0.1 - 1 wide. Some specimens show partially or totally broken rhizomes and one of them bears two stalks. Oscule normally not observed, probably contracted, with the exception of one individual with an oscular tube. Surface shows abundant pores of up to 0.75

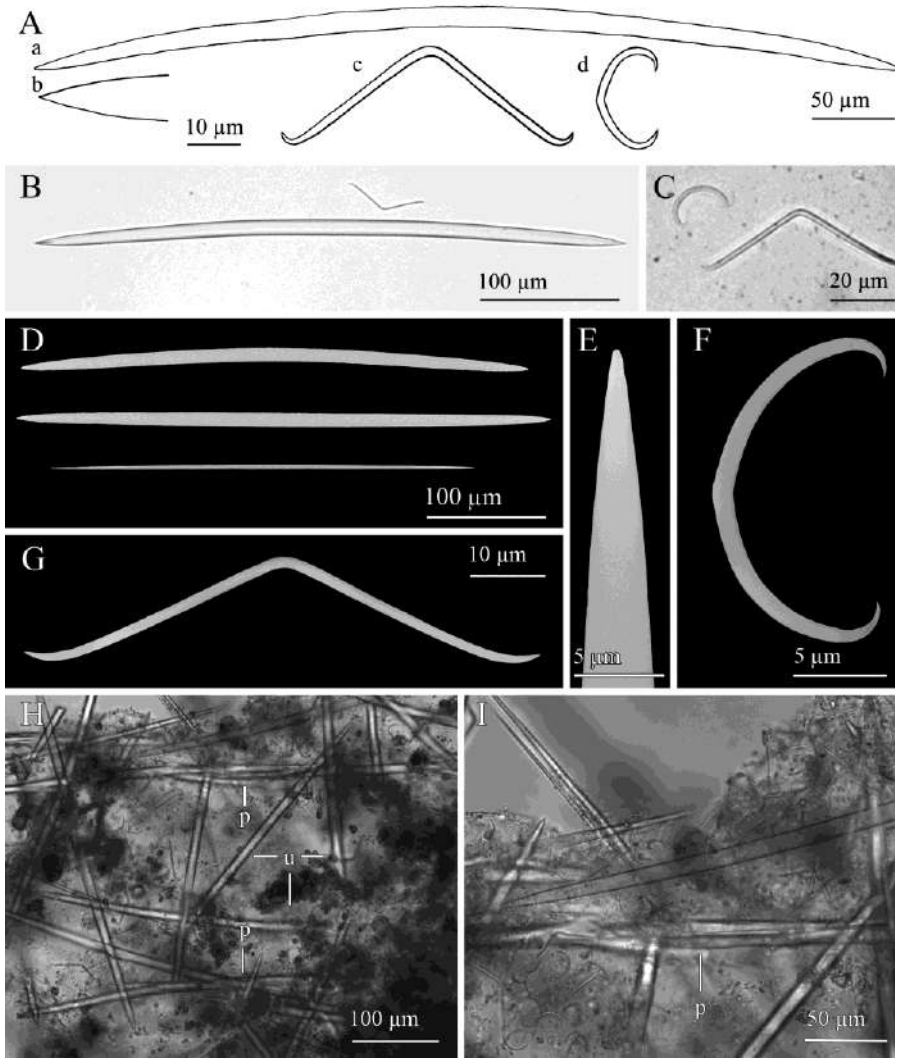

Figure 14. *Haliclona (Rhizoniera) pedunculata* (Boury-Esnault, Pansini & Uriz, 1994): (A) Line drawing summarizing the skeletal complement of the collected specimens. Oxeas (a) are somewhat fusiform and softly bent with acerate ends (b). Microscleres are toxas (c) markedly bent and sigmata (d) slightly angulate. (B) Light microscope view of an oxea and a toxa. (C) Light microscope view of a toxa and a sigma. (D) SEM view of slightly different oxeas and a developing one. (E) SEM detail of an end of an oxea. (F) SEM detail of a sigma. (G) SEM detail of a toxa. (H) Light microscope view of the reticulate skeleton with paucispicular tracts (p) connected by unispicular tracts of oxeas or single oxeas (u). (I) Light microscope detail of a pauciscpicular tract. Note microscleres spared all around the skeleton.

mm. Texture is spongy and fragile, colour after preservation in ethanol is light brown at the body and beige at the stalk (Fig. 3L)

Skeletal structure: There is no ectosomal skeleton differentiated. The choanosomal skeleton is an anisotropic somewhat irregular reticule of paucispicular tracts of oxeas forming primary lines which are interconnected by a net of unispicular tracts of oxeas (Fig.14H-I). Spongin is hardly observed and microscleres are scattered all over the body. Stalk is made of densely packed ascending multispicular tracts of oxeas.

Spicules: Megascleres are oxeas softly bent, sometimes straight (Fig.14A-B, D), with acerate ends (Fig.14A, E). They are 350 – 470 x 8 – 12.5 μm. Thin developing stages (Fig.14D) are sometimes observed in some specimens, measuring down to 270 x 2.5μm. Microscleres generally are fairly abundant toxas, markedly bent and with ends curved upwards (Fig.14A, C, G). They measure 47.43 – 74 x 1 – 1.9 μm. There are also abundant sigmata, with a slightly angulate shape at the center of their shaft (Fig.14A, C, F), measuring 13.75 – 24 x 0.6 – 1.6 μm. Yet, although the seven specimens studied in full detail showed consistently a single sigmata category and presence of toxa, some variability was noticed regarding the microscleres when the microscleres of the remaining 43 specimens were examined. A total of four specimens showed not one but two size categories of sigmata (12.5 – 25 x 1.5 – 2.5 μm and 27.5 – 37.5 x 1.25 – 2 μm for pooled data; for individual data see Table 3), two other specimens had a single sigmata category but lacked toxa, showing one of them a wide size range of sigmata not discernible in two categories (Table 3).

Distribution and ecology notes: The individuals were collected at muddy sand and sandy mud bottoms at depths between 489 – 719 m from Anastasya,

Table 3. Summary of microsclere size in the six individuals of *Haliclona (Rhizoniera) pedunculata* that showed an atypical microsclere composition out of the 49 collected individuals.

Specimen	Sigmata I (μm)	Sigmata II (μm)	Toxa (μm)
P23B-11BT05A	12.5 – 25.0 x 2.0 – 2.5	32.5 – 37.5 x 1.25 – 2.0	60.6 – 70.0 x 1.3 – 1.7
P23B-11BT05B	17.5 – 20.0 x 2.0 – 2.5	30.0 – 35.0 x 1.25 – 2.0	53.8 – 66.1 x 1.4 – 1.8
P23B-11BT05C	15.0 – 21.0 x 2.0 – 2.5	27.5 – 33.2 x 1.20 – 2.0	56.4 – 70.4 x 1.5 – 2.6
P23B-11BT06A	15.0 – 23.0 x 1.5 – 2.0	27.5 – 36.0 x 1.25 – 1.5	58.2 – 65.4 x 1.3 – 2.0
P23B-11BT06B	20.0 – 27.0 x 1.3 – 1.8	absent	absent
P23B-11BT06C	16.1 – 32.5 x 1.0 – 1.8	absent	absent

Tarsis, Pipoca and Chica mud volcanoes (Table 1). Despite being notably common across different mud volcanoes, the collected specimens constitute the second record for the species, which had previously been recorded from a nearby area of the Atlantic (36º 43'N, 9º 24' W), where three specimens were collected from depths of 1141 and 1283 m (Boury-Esnault et al., 1994).

Taxonomic remarks: The collected specimens fit well the features of subgenus *Haliclona (Rhizoniera)* (De Weerdt, 2002) except, in some of them, for the presence of microscleres. However, the variability in the microscleres across the herein studied individuals indicated that their presence/absence can be a matter of intra-specific variability. Examination of the holotype revealed that the stalk was broken, for which rhizomes could not be observed, and that toxas were actually present but scarce, measuring 64 – 74.28 x 1.6 – 2.5 μm. This result is important because it is modifying the original description of the species, which was thought to lack toxa. Yet there are two minor differences between the collected and the type material. The holotype bears a small oscular tube, which has been only observed in one of the specimens from the Gulf of Cádiz and is therefore assumed to be contracted in the rest of them. The other difference concerns the sigmata, since the holotype shows two categories with a wider size range (16.25 – 29.35 x 0.7 – 1.4 μm and 35 – 70 x 2 – 3.75 μm). Four of the Gulf of Cádiz specimens have been found two show two categories as well, but two others had only one category and lacked toxa, showing one of them sigmata in a wide size range not separable in categories. Therefore, the microsclere spicule complement is assumed to be subject of important intraspecific variability.

Due to the high number of collected specimens, it is no longer possible to consider *H. pedunculata* as an isolated case of a microscleres-bearing individual in the subgenus *Rhizoniera*. Rather, an amendment of its current diagnosis is suggested as follows to consider that stalked species with microscleres are to be included in this subgenus: Sponges thickly encrusting, cushion-shaped with oscular chimneys or mounds, or massive, rarely stalked. Consistency soft to moderately firm, sometimes viscous. Surface frequently slightly hispid through projecting spicules of the primary lines. Colour brown, pink, purple or bluish-grey. Megascleres usually slender oxeas with acerated points. Microscleres are rarely present sigmas and toxas. Consistency soft to moderately firm (amended from De Weerdt, 2002).

Discussion

The study of the sponge fauna of eight mud volcanoes from the Gulf of Cádiz resulted in the identification of 1655 specimens belonging to 82 species. Two of them were new to science and several others were little known previously. Apart from the taxonomic value of the gathered collection, three of the species, *Geodia anceps*, *Coelosphaera (Histodermion) cryosi* and *Petrosia (Petrosia) raphida* were hitherto known from the Alboran Sea. Their present discovery in the Gulf of Cádiz mud volcanoes bathed by the MOW could well testify for a natural export towards the Atlantic of deep-sea Mediterranean benthic fauna. The occurrence of *G. anceps* in the Avilés Canyon (Cantabrian Sea) has also being recently corroborated (Cárdenas; pers. comm.), which suggest dispersal from the Mediterranean following the northwards MOW's along Portuguese coasts. A similar effect has been detected for crinoids, with large bathyal fields of the typically-Mediteranean species *Leptometra phlangium* growing at the Pipoca mud volcano (Palomino et al., 2016), which is located in the pathway of the MOW. In contrast, in those bathyal areas of the Gulf of Cádiz that are located out of the MOW pathway, the crionid aggregations are formed by a typically Atlantic species, *Leptometra celtica* (Fonseca et al., 2014). According to the scarce available information, the natural transfer of Mediterranean species towards the Gulf of Cádiz could be interpreted as being of much lower intensity than in the other way around. In the only previous study addressing this issue (Boury-Esnault et al., 1994), it was found that the Atlantic stations bathed by the outgoing MOW did not show noticeable values of species richness. Only about 18% of the species collected in that study were present in both the Atlantic and the Mediterranean side of the Gibraltar Strait. Six species considered to that date as Mediterranean endemisms were collected for the first time in the Gulf of Cádiz (Boury-Esnault et al., 1994). Combining this literature data and our new records, it appears that out of the 62 species known to occur both in the northeastern Atlantic and the western Mediterranean, about 26 are from deep-sea locations bathed by the MOW. Therefore, it could be that the natural export of Mediterranean deep-sea benthos by the MOW is more important than previously believed from the few available studies.

Some elemental numerical analyses of the species richness and sponge abundance have been made, but the results have to be very cautiously

interpreted since the gathered sponge collection is affected by large between-volcano differences in sampling effort. Because of logistic limitations, the deep mud volcanoes were systematically sampled less extensively than the shallow ones. For this reason, it cannot be discarded the possibility that the fauna of some of the deeper volcanoes could be seriously underrepresented in the gathered sponge collection. With available data, it appears that the mud volcanoes located at mid depths on the continental slope host a richer sponge fauna that those placed in shallower and deeper waters. A previous study using a manned submersible to record sponge abundance over a transect along the upper part of a tropical continental slope found a moderated increase in the species richness between 400 and 500 m depths (Maldonado & Young, 1996). From the present approach, the abundance of MDAC, which was *a priori* predicted to act as source of new hard substrate suitable for sessile fauna, emerges as having no significant rol in increasing the species richness per m^2 in the sponge fauna of the mud volcanoes. Likewise, the abundance of MDAC substrate did not correlate positively with the number of sponge individuals. Rather sponge abundance per m^2 peaked in areas of soft bottom, where highly specialized species are known to form large aggregations. This situation is paradigmatically summarized by the mud volcano Aveiro, which, despite lacking authigenic carbonates, holds the highest values of sponge abundance due to the high abundance of *Thenea muricata* individuals. Therefore, the theoretical role of MDAC in favouring somehow the sponge fauna cannot be demonstrated in practice, at least from the available data.

Likewise, from the current data, no statistically significant effect can be put forward for the fishing activity concerning either the species richness or the sponge abundance, beyond just mere negative trends which lacks statistical support (Fig. 2D-E). These trends would suggest that both the species richness and the abundance would decrease with increasing fishing activity, except for some mud volcanoes where the faunal parameters are low despite being subjected to no or very low fishing activity. Yet, to derive more definitive conclusion in this regard it would be necessary a more extensive and homogeneous sampling of the mud volcanoes located deeper than 500 m, as well as the inclusion of a greater number of mud volcanoes in the analyses.

The combined effect of depth, occurrence of MDAC formations and fishing activity on the sponge communities of the volcanoes has not been assessed here, being these multivariate analyses part of a further, separate

study (Chapter 4) that is specifically dealing with faunal and biogeographic affinities.

References

Arnesen, E. (1920) Spongia. *Report on the Scientific Results of the "Michael Sars" North Atlantic Deep-Sea Expedition 1910,* 3(2), 1-29.

Bouchet, P. and Taviani, M. (1992) The Mediterranean deep-sea fauna: pseudopopulations of Atlantic species. *Deep Sea Research Part A. Oceanographic Research Papers,* 39(2), 169-148.

Boury-Esnault, N., Pansini, M. and Uriz, M. J. (1994) Spongiaires bathyaux de la mer d'Alboran et du golfe ibéro-marocain. *Mémoires. Muséum National d'Histoire Naturelle,* 160, 1-174.

Boury-Esnault, N. and Rützler, K. (1997) Thesaurus of sponge morphology. *Smithsonian Contributions to Zoology,* 596, 1-55.

Cárdenas, P., Rapp, H. T., Klitgaard, A. B., Best, M., Thollesson, M. and Tendal, O. S. (2013) Taxonomy, biogeography and DNA barcodes of Geodia species (Porifera, Demospongiae, Tetractinellida) in the Atlantic boreo-arctic region. *Zoological Journal of the Linnean Society,* 169(2), 251-311.

Carvalho, F. C., Pomponi, S. A. and Xavier, J. R. (2015) Lithistid sponges of the upper bathyal of Madeira, Selvagens and Canary Islands, with description of a new species of *Isabella. Journal of the Marine Biological Association of the United Kingdom,* 95(7), 1287-1296.

Chevaldonné, P., Pérez, T., Crouzet, J.-M., Bay-Nouailhat, W., Bay-Nouailhat, A., Fourt, M., Almón, B., Pérez, J., Aguilar, R. and Vacelet, J. (2015) Unexpected records of 'deep-sea' carnivorous sponges *Asbestopluma hypogea* in the shallow NE Atlantic shed light on new conservation issues. *Marine Ecology,* 36(3), 475-484.

Coll, M., Piroddi, C., Steenbeek, J., Kaschner, K., Ben Rais Lasram, F., Aguzzi, J., Ballesteros, E., Bianchi, C. N., Corbera, J., Dailianis, T., Danovaro, R., Estrada, M., Froglia, C., Galil, B. S., Gasol, J. M., Gertwagen, R., Gil, J., Guilhaumon, F., Kesner-Reyes, K., Kitsos, M.-S., Koukouras, A., Lampadariou, N., Laxamana, E., López-Fé de la Cuadra, C. M., Lotze,

H. K., Martin, D., Mouillot, D., Oro, D., Raicevich, S., Rius-Barile, J., Saiz-Salinas, J. I., San Vicente, C., Somot, S., Templado, J., Turon, X., Vafidis, D., Villanueva, R. and Voultsiadou, E. (2010) The biodiversity of the Mediterranean Sea: Estimates, patterns, and threats. *PLoS One,* 5(8), e11842.

de Mol, B., Henriet, J. P. and Canals, M. (2005) Development of coral banks in Porcupine Seabight: do they have Mediterranean ancestors? *In:* A. Freiwald and J. M. Roberts (Eds), *Cold-water corals and ecosystems*. Springer, Berlin, pp. 515-533.

de Weerdt, W. H. (2002) Family Chalinidae Gray, 1867. *In:* J. N. A. Hooper and R. W. M. Van Soest (Eds), *Systema Porifera. A guide to the classification of sponges,* 1. Kluwer Academic/Plenum, New York, pp. 852-873.

Desqueyroux-Fáundez, R. and Valentine, C. A. (2002) Family Niphatidae Van Soest, 1980. *In:* J. N. A. Hooper and R. W. M. Van Soest (Eds), *Systema Porifera. A guide to the classification of sponges,* 1. Kluwer Academic/ Plenum New York, pp. 874-890.

Díaz del Río, V., Bruque, G., Fernández-Salas, L. M., Rueda, J. L., González, E., López, N., Palomino, D., López, F. J., Farias, C., Sánchez, R., Vázquez, J. T., Rittierott, C. C., Fernández, A., Marina, P., Luque, V., Oporto, T., Sánchez, O., García, M., Urra, J., Bárcenas, P., Jiménez, M. P., Sagarminaga, R. and Arcos, J. M. Volcanes de fango del golfo de Cádiz, Proyecto LIFE + INDEMARES. Fundación Biodiversidad del Ministerio de Agricultura, Alimentación y Medio Ambiente. (2014).

Erpenbeck, D. and Van Soest, R. W. M. (2002) Family Halichondriidae Gray, 1867. *In:* J. N. A. Hooper and R. W. M. Van Soest (Eds), *Systema Porifera. A guide to the classification of sponges,* 1. Kluwer Academic/Plenum, New York, pp. 787-816.

Fonseca, P., Abrantes, F., Aguilar, R., Campos, A., Cunha, M., Ferreira, D., Fonseca, T. P., García, S., Henriques, V., Machado, M., Mechó, A., Relvas, P., Rodrigues, C. F., Salgueiro, E., Vieira, R., Weetman, A. and Castro, M. (2014) A deep-water crinoid *Leptometra celtica* bed off the Portuguese south coast. *Marine Biodiversity,* 44(2), 223-228.

Fourt, M., Goujard, A., Pérez, T. and Chevaldonné, P. (2017) Guide de la faune profonde de la mer Méditerranée. Explorations des roches et des

canyons sous-marins des côtes françaises. *Patrimoines naturels. Publications scientifiques du Muséum national d'Histoire naturelle Paris,* 751-184.

Gardner, J. M. (2001) Mud volcanoes revealed and sampled on Western Moroccan continental margin. *Geophysical Research Letters,* 28(2), 339-342.

Hestetun, J. T., Vacelet, J., Boury-Esnault, N., Borchiellini, C., Kelly, M., Ríos, P., Cristobo, J. and Rapp, H. T. (2016) The systematics of carnivorous sponges. *Molecular Phylogenetics and Evolution,* 94, Part A, 327-345.

Hooper, J. N. A. (2002) Family Desmoxyidae Hallmann, 1916. *In:* J. N. A. Hooper and R. W. M. Van Soest (Eds), *Systema Porifera. A guide to the classification of sponges,* 1. Kluwer Academic/Plenum, New York, pp. 755-772.

Ijima, I. (1904) Studies on the Hexactinellida. Contribution IV. (Rossellidae). *Journal of the College of Science, Imperial University of Tokyo,* 18(7), 1-307.

Kennedy, J. A. (2000) Resolving the 'Jaspis stellifera' complex. *Memoirs of the Queensland Museum,* 45(2), 453-476.

Kenyon, N. H., Ivanov, M. K., Akhmetzhanov, A. M and G.G. Akhmanov. Multidisciplinary study of geological processes on the North East Atlantic and Western Mediterranean margins. IOC Technical Series No. 56, UNESCO (2000)

León, R., Somoza, L., Medialdea, T., González, F. J., Díaz-del-Río, V., Fernández-Puga, M. C., Maestro, A. and Mata, M. P. (2007) Sea-floor features related to hydrocarbon seeps in deepwater carbonate-mud mounds of the Gulf of Cádiz: from mud flows to carbonate precipitates. *Geo-Marine Letters,* 27(2), 237-247.

Levin, L. A. (2005) Ecology of cold seep sediments: Interactions of fauna with flow, chemistry and microbes *Oceanography and Marine Biology. Annual review,* 43, 1-46.

Longo, C., Mastrototaro, F. and Corriero, G. (2005) Sponge fauna associated with a Mediterranean deep-sea coral bank. *Journal of the Marine Biological Association of the United Kingdom,* 85(06), 1341-1352.

Lundbeck, W. (1902) Porifera. Part I. Homorrhaphidae and Heterorhaphidae. *In: The Danish Ingolf Expedition.* Bianco Luno, Copenhagen*,* 6(1), 1-108.

Maldonado, M. (1992) Demosponges of the red coral bottoms from the Alboran Sea. *Journal of Natural History,* 26, 1131-1161.

Maldonado, M. (1993). *Demosponjas litorales de Alborán. Faunística y Biogeografía*. (Philosophical Dissertation). University of Barcelona, Barcelona.

Maldonado, M., Sánchez-Tocino, L., López-Acosta, M. and Sitjà, C. Invertebrados claves del sistema infralitoral y circalitoral rocoso de las Islas Chafarinas: estudio con vistas a futuras estrategias de conservación. (2011).

Maldonado, M. and Uriz, J. M. (1995) Biotoic affinities in a transitional zone between the Atlantic and the Mediterranean: a biogeographical approach based on sponges. *Journal of Biogeography,* 22, 89-110.

Maldonado, M. and Young, C. M. (1996) Effects of physical factors on larval behavior, settlement and recruitmet of four tropical demosponges. *Marine Ecology Progress Series,* 138, 169-180.

Medialdea, T., Somoza, L., Pinheiro, L. M., Fernández-Puga, M. C., Vázquez, J. T., León, R., Ivanov, M. K., Magalhaes, V., Díaz-del-Río, V. and Vegas, R. (2009) Tectonics and mud volcano development in the Gulf of Cádiz. *Marine Geology,* 261(1), 48-63.

Palomino, D., López-González, N., Vázquez, J. T., Fernández-Salas, L. M., Rueda, J. L., Sánchez-Leal, R. and Díaz-del-Río, V. (2016) Multidisciplinary study of mud volcanoes and diapirs and their relationship to seepages and bottom currents in the Gulf of Cádiz continental slope (northeastern sector). *Marine Geology,* 378, 196-212.

Pansini, M., Vacelet, J. and Boury-Esnault, N. (1987) Littoral demosponges from the banks of the straits of Sicily and the Alboran Sea. *In:* J. Vacelet and N. Boury-Esnault (Eds), *Taxonomy of Porifera,* G 13. Springer Verlag, Berlin, Heidelberg, pp. 149-186.

Pérès, J. M. and Picard, J. (1964) Nouveau manuel de bionomie benthique de la mer Méditerranée. *Recueil des Travaux de la Station Marine d'Endoume,* 31(47), 1-137.

Pinheiro, L. M., Ivanov, M. K., Sautkin, A., Akhmanov, G., Magalhães, V. H., Volkonskaya, A., Monteiro, J. H., Somoza, L., Gardner, J., Hamouni, N. and Cunha, M. R. (2003) Mud volcanism in the Gulf of Cádiz: results from the TTR-10 cruise. *Marine Geology,* 195, 131-151.

Pulitzer-Finali, G. (1970) Report on a collection of sponges from the Bay of Naples. I. Sclerospongiae, Lithistida, Tetractinellida, Epipolasida. *Pubblicazioni della Stazione Zoologica di Napoli*, 328-354.

Rueda, J. L., Díaz-del-Río, V., Sayago-Gil, M., López-González, N., Fernández-Salas, L. M. and Vázquez, J. T. (2012) Fluid venting through the seabed in the Gulf of Cadiz (SE Atlantic Ocean, Western Iberian Peninsula): Geomorphic features, habitats, and associated fauna *In:* P. T. Harris and E. K. Baker (Eds), *Seafloor geomorphology as benthic habitat*. Elsevier, London, pp. 831-841.

Sánchez, F., González-Pola, C., Druet, M., García-Alegre, A., Acosta, J., Cristobo, J., Parra, S., Ríos, P., Altuna, A., Gómez-Ballesteros, M., Muñoz-Recio, A., Rivera, J. and Díaz del Río, G. (2014) Habitat characterization of deep-water coral reefs in La Gaviera Canyon (Avilés Canyon System, Cantabrian Sea). *Deep-Sea Research Part II: Topical Studies in Oceanography,* 106, 118-140.

Schmidt, O. (1868) *Die Spongien der Küste von Algier. Mit Nachträgen zu den Spongien des Adriatischen Meeres*. Wilhelm Engelmann, Leipzig, 1-44 pp.

Schmidt, O. (1870) *Grundzüge einer Spongien-Fauna des Atlantischen Gebietes*. Wilhelm Engelmann, Leipzig, 1-88 pp.

Sitjà, C. and Maldonado, M. (2014) New and rare sponges from the deep shelf of the Alboran Island (Alboran Sea, Western Mediterranean). *Zootaxa,* 3760(2), 141-179.

Suess, E. (2014) Marine cold seeps and their manifestations: geological control, biogeochemical criteria and environmental conditions. *International Journal of Earth Sciences,* 103(7), 1889-1916.

Tabachnick, K. P. (2002) Family Rossellidae Schulze, 1885. *In:* J. N. A. Hooper and R. W. M. Van Soest (Eds), *Systema Porifera. A guide to the classification of sponges,* 2. Kluwer Academic/Plenum, New York, pp. 1441-1505.

Templado, J., Calvo, M., Moreno, D., Flores, A., Conde, F., Abad, R., Rubio, J., López-Fé, C. M. and Ortiz, M. (2006) *Flora y fauna de la reserva marina y reserva de pesca de la isla de Alborán*. Ministerio de Agricultura, Pesca y Alimentación. Secretaría General de Pesca Marítima, Madrid.

Templado, J., García-Carrascosa, M., Baratech, L., Capaccioni, R., Juan, A., López-Ibor, A., Silvestre, R. and Massó, C. (1986) Estudio preliminar de la fauna asociada a los fondos coralígenos del mar de Alborán (SE de España). *Boletín del Instituto Español de Oceanografía,* 3(4), 93-104.

Topsent, E. (1892) Contribution a l'étude des Spongiaires de l'Atlantique Nord (Golfe de Gascogne, Terre-Neuve, Açores). *Résultats des Campagnes Scientifiques accomplies par le Prince Albert I.* Monaco, 2, 1-165.

Topsent, E. (1898) Eponges nouvelles des Açores, 1ère série. *Mémoires de la Société Zoologique de France,* 11, 225-255.

Topsent, E. (1901) Considérations sur la faune des Spongiaires des côtes d'Algerie. Eponges de La Calle. *Archives de Zoologie Expérimentale et Générale,* 3ème série, 9, 327-370.

Topsent, E. (1904) Spongiaires des Açores. *Résultats des Campagnes Scientifiques accomplies par le Prince Albert I.* Monaco, 25, 1-279.

Topsent, E. (1927) Diagnoses d'Eponges nouvelles recueillies par le Prince Albert I de Monaco. *Bulletin de l'Institut Océanographique de Monaco,* 502, 1-19.

Topsent, E. (1928) Spongiaires de l'Atlantique et de la Méditerranée, provenant des croissières du Prince Albert I de Monaco. *Résultats des Campagnes Scientifiques accomplies par le Prince Albert I.* Monaco, 74, 1-376.

Topsent, E. (1938) Contribution nouvelle à la connaisance des Eponges des côtes d'Algerie. Les espéces nouvelles d'O. Schmidt, 1868. *Bulletin de l'Institut Océanographique de Monaco,* 7581-32.

Uriz, M. J. (2002) Family Ancorinidae Schmidt, 1870. *In:* J. N. A. Hooper and R. W. M. Van Soest (Eds), *Systema Porifera: a guide to the classification of Sponges,* 1. Kluwer Academic/Plenum Publishers, New York, pp. 108-126.

Vacelet, J. (1996) Nouvelles signalisations d'éponges profondes en Méditerranée. *Mesogee,* 55107-114.

Vacelet, J. and Boury-Esnault, N. (1996) A new species of carnivorous sponge (Demospongiae: Cladorhizidae) from a Mediterranean cave. *Bulletin de l'Institut Royal des Sciences Naturelles de Belgique,* 66 suppl., 109-115.

Van Rooij, D., De Mol, L., Le Guilloux, E., Réveillaud, J., Hernández-Molina, F. J., Llave, E., Léon, R., Estrada, F., Mienis, F., Moeremans, R., Blamart, D., Vanreusel, A. and Henriet, J. (2010) Influence of the Mediterranean Outflow Water on benthic ecosystems : answers and questions after a decade of observations. *GeoTemas,* 11, 179-180.

Van Soest, R. W. M. (2002) Family Coelosphaeridae Dendy, 1922. *In:* J. N. A. Hooper and R. W. M. Van Soest (Eds), *Systema Porifera. A guide to the*

classification of sponges, 1. Kluwer Academic/Plenum, New York, pp. 528-546.

Van Soest, R. M. W., Boury-Esnault, N., Hooper, J. N. A., Rützler, K., de Voogd, N. J., Alvarez de Glasby, B., Hajdu, E., Pisera, A., Manconi, R., Schönberg, C. H. L., Janussen, D., Tabachnick, K. R., Klautau, M., Picton, B. E., Kelly, M., Vacelet, J., Dohrmann, M. and Díaz, M. C.(2020). World Porifera database. Accessed at http://www.marinespecies.org/porifera on 24/05/2018 on 2470572018.

Van Soest, R. W. M., Díaz, M. C. and Pomponi, S. A. (1990) Phylogenetic classification of the Halichondrids (Porifera, Demospongiae). *Beaufortia. Series of Miscellaneous Publications,* 40(2), 15-62.

Vosmaer, G. C. J. (1894) Preliminary notes on some Tetractinellids of the Bay of Naples. *Tijdschrift der Nederlandsche Dierkundige Vereeniging,* 4(2), 269-286.

Xavier, J. R., Cárdenas, P., Cristobo, J., Van Soest, R. W. M. and Rapp, H. T. (2015) Systematics and biodiversity of deep-sea sponges of the Atlanto-Mediterranean region. *Journal of the Marine Biological Association of the United Kingdom,* 95(7), 1285-1286.

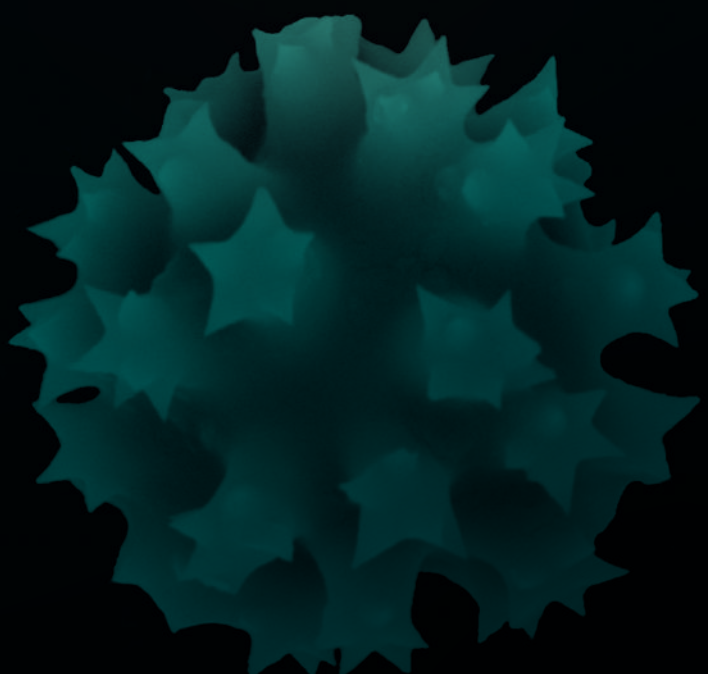

Chapter 2

Characterization of some rare bathyal sponges from the Gulf of Cádiz, Northeastern Atlantic, through integrative taxonomy.

Abstract

The ecological importance of the marine area encompassing the mud volcanoes from the Gulf of Cádiz, Northeastern Atlantic, is evidenced by a wide variety of bathyal fauna inhabiting their seabeds, being sponges one of their most diverse benthic groups. A previous taxonomic study based on phenetic characteristics has shown that many uncommon sponge species occur in this area and has also raised some concerns regarding their taxonomic position. The present study phylogenetically analyses 11 specimens belonging to five rare species from the mud volcanoes of the Gulf of Cádiz using *COI*, *18S* rRNA, and *28S* rRNA markers. This is intended to integrate the new phylogenetic results with their already described morphometric characteristics. The specimens analysed constitute second records for their species in the Atlantic Ocean and were previously identified as *Suberites hirsutus, Geodia* cf. *spherastrella, Petrosia* (*Petrosia*) *raphida, Cladocroce spathiformis* and *Haliclona* (*Rhizoniera*) *bouryesnaultae*. The results from the phylogenetic analyses have questioned their current taxonomic status, but they are considered as preliminary analyses, conducted with a limited set of sequences. This makes evident a need for further efforts on obtaining more molecular markers to help in characterizing ecologically relevant deep-sea habitats.

Introduction

The mud volcanoes from the Gulf of Cádiz, their main habitats and its associated fauna were studied and characterized within the frame of the EC LIFE+INDEMARES project – *Chimeneas de Cádiz* (CHICA) (2009-2013). Several oceanographic expeditions revealed the ecological importance of this area, resulting in the discovery of some sensitive habitats of the Habitats Directive (92/43/EEC) such as the 1180 'Submarine structures made by leaking gases' and the 1170 'Reefs' (Díaz del Río et al., 2014). A combination of sampling methods retrieved a variety of samples that revealed sponges to be among the most diverse and abundant faunistic groups (Chapter 1; also Sitjà et al., 2019), together with cnidarians, molluscs, and decapods (Díaz del Río et al., 2014; González-García et al., 2020). Additionally, they are located close to a transition area between the North Atlantic Ocean and the Mediterranean Sea, becoming a strategic location for studying the faunal connectivity between these two basins.

The composition of the bathyal sponge fauna collected from the expeditions resulted in 82 different sponge species out of 1659 specimens studied (Chapter 1). Two new species were described, and most of them were unequivocally identified, representing 8 of them first and second records for the Atlantic Ocean. Some of these rare species generated different taxonomic considerations which remained in need for further analyses (Chapter 1). These problematic species are: *Suberites hirsutus* Topsent, 1904; *Geodia* cf. *spherastrella* Topsent, 1904; *Petrosia* (*Petrosia*) *raphida* Boury-Esnault, Pansini & Uriz, 1994; *Cladocroce spathiformis* Topsent, 1904; and *Haliclona* (*Rhizoniera*) *bouryesnaultae* Van Soest & Hooper, 2020 (formerly called *Haliclona* (*Rhizoniera*) *pedunculata* Boury-Esnault, Pansini & Uriz, 1994 as it is in Chapter 1). The aim of the

present work is to provide an integrative molecular characterization of these poorly known species with their morphological taxonomic characteristics. Additionally, other four common species also present in the mud volcanoes of the Gulf of Cádiz have been newly sequenced for comparative purposes: *Suberites carnosus* (Johnston, 1842); *Petrosia* (*Strongylophora*) *vansoesti* Boury-Esnault, Pansini & Uriz, 1994; *Petrosia* (*Petrosia*) *crassa* (Carter, 1876) and *Cladocroce fibrosa* (Topsent, 1890). To achieve this, different molecular markers were sequenced for the nine taxa mentioned above. This integrative approach is expected to improve knowledge on the sponge fauna of this Site of Community Importance (SCI) and provide new bathyal sponge sequences, necessary for further monitoring of the deep-sea.

Material and methods

Samples collection

The bathyal sponge fauna from the mud volcanoes and fluid venting related structures of the Gulf of Cádiz (Northeast Atlantic and South West of the Iberian Peninsula) were collected in two different expeditions of the LIFE+INDEMARES project (INDEMARES CHICA 0610 and 0211). These were Gazul, Tarsis, Pipoca, Chica and Almazan, which are located at a

Table 1. List of the studied specimens collected from the mud volcanoes, indicating their codes, mud volcano, station and depth as stated in Chapter 1.

Specimens studied	Specimen code	Volcano	Station	Depth (m)
Suberites hirsutus	P202-11BT16	Pipoca	13	627-719
Suberites carnosus	P206-11BT06	Gazul	3	422-450
Geodia cf. *spherastrella*	P14E-11BT17	Pipoca	16	573-530
Cladocroce spathiformis	P05-11BT18	Pipoca	15	565-557
Cladocroce fibrosa	P54-11BT17	Pipoca	16	573-530
Petrosia (Petrosia) raphida	P200-11BT17	Pipoca	16	573-530
Petrosia (Petrosia) crassa	P06-11BT25_A	Almazan	29	703-756
Petrosia (Strongylophora) vansoesti	P67-11BT18	Pipoca	18	557-565
Haliclona (Rhizoniera) bouryesnaultae	P23B-11BT05_A	Chica	19	655-682
Haliclona (Rhizoniera) bouryesnaultae	P23B-11BT05_C	Chica	19	655-682
Haliclona (Rhizoniera) bouryesnaultae	P23B-11BT05_D	Chica	19	655-682

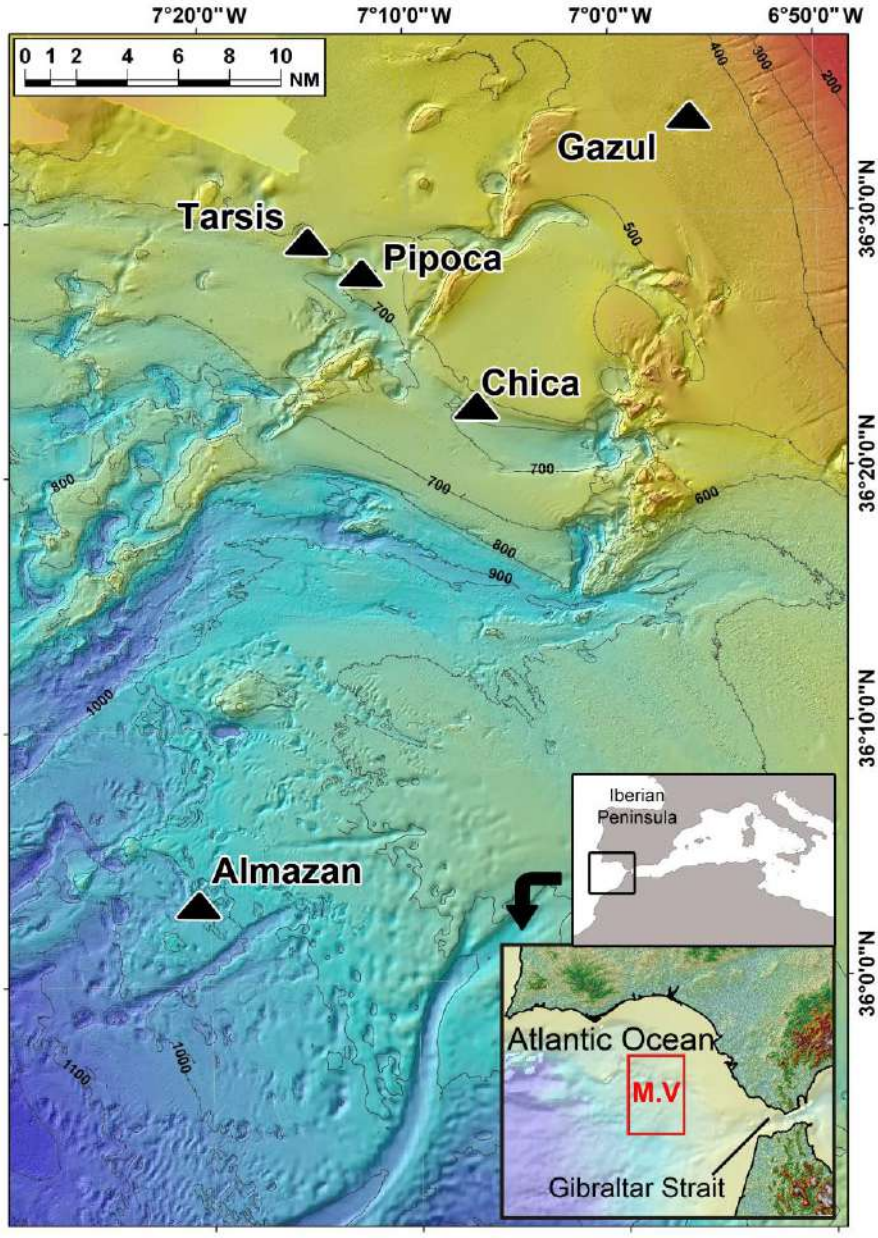

Fig. 1 Map displaying the location of the SCI of the mud volcanoes in the Gulf of Cádiz from which the specimens were collected. The bottom right image shows the South Western Iberian Peninsula and the SCI limits (red square) in the Atlantic Ocean.

bathymetric range of 422-756 m depth (Table 1, Fig. 1). Details on the sampling areas and methods used for collecting the sponge fauna can be found in Chapter 1. The present study analyses 11 specimens belonging to nine species, which were preserved in 70% ethanol and kept at room temperature.

The taxonomic identification and spicule composition and arrangement of the 11 specimens (nine species) studied here was provided in Chapter 1. An exception to this is the case of *Suberites hirsutus*, whose taxonomic description is provided here. Briefly, observation of external and skeletal morphometric characters was conducted by binocular and light microscopy, using standard techniques. When required, nitric acid-cleaned spicules were mounted on aluminium stubs, critically point-dried, gold-coated, and studied through a HITACHI TM3000 Scanning Electron Microscope (SEM). The description of body features, spicules, and skeletal arrangements was accomplished according to the Sponge Thesaurus of morphology (Boury-Esnault and Rützler, 1997).

DNA extraction, amplification and sequencing

DNA was extracted from a piece of tissue (approximately 1 cm^3) using the DNeasy Blood & Tissue Kit (QIAGEN, CA, USA), following manufacturer's instructions except for a longer incubation in lysis buffer (overnight) and double elution in 50 µl (100 µl total final volume). Given that the preservation conditions of the specimens were not optimal, a suite of primers from different markers including cytochrome *c* oxidase I (*COI*), 18S rRNA (*18S*), and 28S rRNA (*28S*) (Appendix I), was first assessed in order to test their performance. Two different primer sets were used to amplify a fragment of *COI*: the universal Folmer primers LCO1490 and HCO2198 (Folmer et al., 1994), and PorCOI2fwd (AATATGNGGGCNCCNGGNATNAC) and PorCOI2rev (ACTGCCCCCATNGATAAAACAT) (Xavier et al., 2010). For both of them, the amplifications followed the following PCR protocols: 94ºC, 5min; (94ºC, 30s; 48ºC, 30s; 72ºC, 30s) x 30 cycles; 72ºC, 5 min; and 94ºC, 5 min; (94ºC, 30s; 48ºC - 0.5ºC per cycle, 30s; 72ºC, 30s) x 10 cycles; (94ºC, 30s; 45ºC, 30s; 72ºC, 30s) x 20 cycles; 72ºC, 5 min (Morrow et al., 2012). Several primers were used for the amplification of the entire *18S* in the following fragments: 18S400F - 18S1080R, 18S830F - 18S1350R, 18S1200F - 18S1340R,

Sp18aF and Sp18gR (Redmond et al., 2007; Redmond et al., 2013), using the following PCR protocol: 94ºC, 5min; (94ºC, 30s; 55ºC - 0.5ºC per cycle, 30s; 72ºC, 30s) x 10 cycles; (94ºC, 30s; 53ºC, 30s; 72ºC, 30s) x 20 cycles; 72ºC, 5min. Finally, the primers we used for the amplification of the *28S* were 28Sa (GAC CCG TCT TGA AAC ACG GA) and 28S-rD5b (5CCA CAG CGC CAG TTC TGC TTA C) (Whiting et al., 1997; Giribet et al., 2002), using the same PCR protocol as for *18S*.

PCR products were purified and sequenced in both directions using an ABI 3730xl DNA analyser (Applied Biosystems) at the sequencing facility of the Natural History Museum of London. The sequences were cleaned from the primers with Geneious® 10.2.2 (Drummond et al., 2009) and then checked by BLAST searching against the nr database of Genbank. We trimmed poor quality regions, assembled forward and reverse reads into contigs, checked for incongruities and obtained the consensus sequences using Geneious.

Phylogenetic analyses

We used MAFFT v. 5 (Katoh & Standley, 2013) as implemented in Geneious for the alignment of the sequences using L-INS-I settings, as well as MUSCLE (Edgar, 2004) in SEAVIEW (Galtier et al., 1996) depending on the marker.

For the analyses of family Suberitidae, containing *Suberites hirsutus* and *Suberites carnosus,* we concatenated the alignments of *COI* (551 bp) and *28S* (1337 bp). The *28S* alignment was trimmed of poorly aligned regions and gaps using Gblocks (Castresana, 2000) using the default settings.

Another alignment of *COI* for family Geodiidae with 612 bp, allowed to assess the phylogenetic position of *Geodia* cf. *spherastrella.* This alignment contained the sequences of both a specimen from the mud volcanoes of the Gulf of Cádiz (Chapter 1) plus that of another specimen from the Mediterranean, previously sequenced and identified as *Geodia sp.* by Cárdenas et al. (2011) and suspected to be also *G. spherastrella* (Cárdenas, pers. comm.).

The remaining species (*Petrosia raphida*, *Petrosia crassa*, *Petrosia vansoesti*, *Cladocroce spathiformis, Cladocroce fibrosa and Haliclona bouryesnaultae*) were included in two alignments, one for *18S* (2004 bp) and another for *COI* (639 bp), for order Haplosclerida. These two alignments were not concatenated because of scarce overlap for the two markers among taxa available at NCBI.

RAxML v.8 (Stamatakis, 2014) was used to obtain all phylogenetic hypotheses with Maximum Likelihood, using the GTR + G + I model obtained in jModelTest (Guindon & Gascuel, 2003; Darriba et al., 2012) for all markers. Ten runs and 100 replicates were used for bootstrapping. The specimens used in this study and their GenBank accession numbers are available in Appendix II.

Results

Systematics

Phylum PORIFERA Grant, 1836
Class DEMOSPONGIAE Sollas, 1885
Order SUBERITIDA Chombard & Boury-Esnault, 1999
Family SUBERITIDAE Schmidt, 1870
Genus *Suberites* Nardo, 1833

Diagnosis: (van Soest, 2002)

***Suberites hirsutus* Topsent, 1927**

(Fig. 2)

Material examined: Specimen P202-11BT16 collected from Stn. 13 (36°28.18'N 7°12.98'W – 627 36°28.57'N 7°13.47'W) at the Pipoca mud volcano from the Gulf of Cádiz.

Comparative material: Holotype of *Protosuberites rugosus* (Topsent, 1893) originally described as *Prosuberites rugosus* (MNHN DT 2469) from Cap l'Abeille, South Gulf of Lion France (2° 28' 0" N – 3° 9' 0" E)

Macroscopic description: Encrusting specimen, covering an area of about 50 mm^2, on both a gastropod shell and partly a solitary coral skeleton attached to the shell. Thickness of 1-1.5 mm, aquiferous openings not observed and surface showing a dense hispidation visible to the naked eye. Colour after preservation in ethanol is beige (Fig. 2A).

Spicules: Megascleres are straight tylostyles, sometimes slightly curved in the longest sizes, softly to more markedly fusiform (Fig. 2C-E), with tyles mucronated or subterminal that often bear discrete tubercles and vesicles (Fig. 2C, F-G). Pointed end usually acerate and sometimes slightly stepped

(Fig. 2C, G). Tylostyles occur in a wide size range of 320–2425 x 13–20 μm, no size categories are discernible, although those longer than 850 μm are often hispidating while those shorter than 500 μm are less abundant.

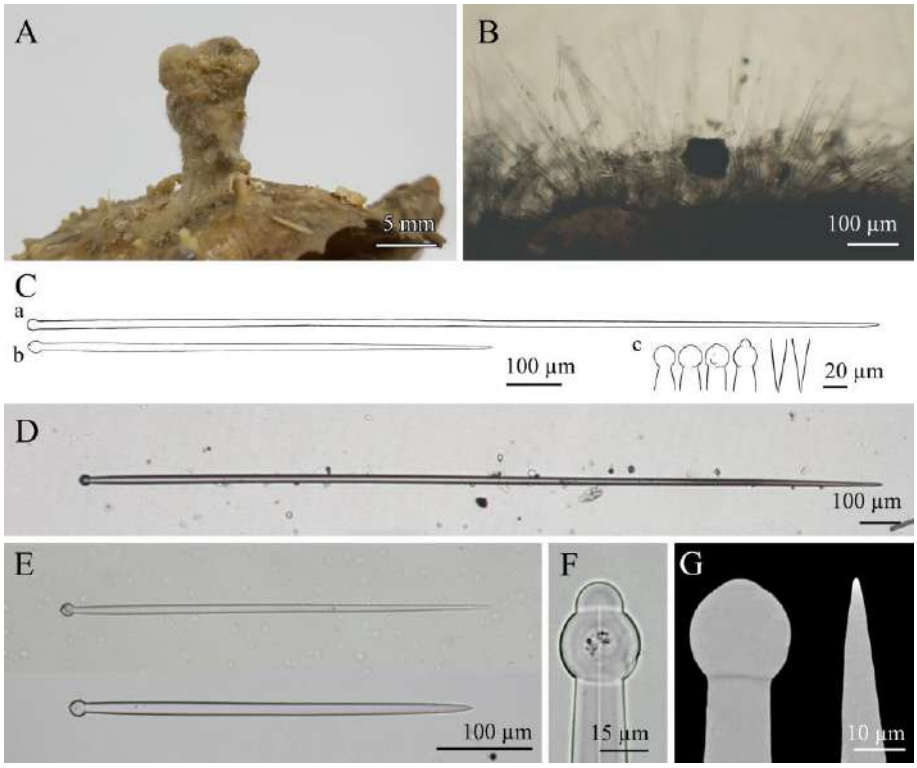

Fig. 2 *Suberites hirsutus* Topsent, 1927: (A) Photograph showing the encrusting habit of the specimen, growing on a skeleton of a death coral. (B) Light microscope view of a section of the surface of the specimen, displaying the long hispidating tylostyles. (C) Line drawing summarizing the skeletal complement of the specimen. Tylostyles are often straight and occur in a wide size range (a-b), they show spherical tyles subtly to markedly mucronated and acerate pointed ends (c). (D) Light microscope view of a long, hispidating tylostyle. (E) Light microscope view of shorter, fusiform tylostyles. (F) Light microscope view of a markedly mucronated tyle with some vesicles. (G) Electron microscopy image of a typical tyle and an acerate end of a tylostyle.

Skeletal structure: Choanosome formed by sparse bundles of tylostyles in confusion that become more tightly packed as they reach the ectosome, where they form bundles that run more or less perpendicular to the surface, ending in hispidating tufts. Longest tylostyles (Fig. 2B) are the hispidating ones. The choanosome is fleshier, measuring 500–1000 μm in thickness, while the ectosome is more compact and is 500 – 800 μm thick.

Distribution and ecology notes: Specimen collected from depths of 627–719 m, on a muddy sand bottom from the Pipoca mud volcano (Table 1). It constitutes the second record for the species. It was previously recorded from Azores (Topsent, 1927; 1928), where seven specimens growing on polyp skeletons were collected from a mud and globigerinids bottom (2,460 m depth).

Taxonomic remarks: Our specimen fits habit, skeletal structure and spicule complement of the description of the holotype of *Suberites hirsutus* Topsent, 1927. The specimen from the mud volcanoes differed only from the size of tylostyles, which in the holotype shows a maximum size of 1540 x 15 μm. We consider this size difference minor. Our observations coincide with the original description in showing no discernible size categories and showing the longest styles as the hispidating ones. The shape of the tylostyles is also coincident with the original description of the species (i.e., straight, fusiform and mucronated).

Our *S. hirsutus* from the Gulf of Cádiz is similar to *Protosuberites rugosus* (Topsent, 1893), since it is also coating and hispid, with tylostyles showing spherical tyles and measuring 200–1200 x 8–12 μm. However, the tylostyles of *P. rugosus* are arranged perpendicularly to the surface with their tyles on the substrate and form no bundles. Another resembling species is *Protosuberites ferrerhernandezi* (Boury-Esnault & Lopes, 1985), which is also encrusting and finely hispid, but it can be papillated and its megascleres differ in shape and size from those of the specimen in our study, since they are trilobate and smaller tylostyles (135.5–965.6 x 2.7–20.7 μm). Its skeletal structure is also different, with ectosomal smaller, hispidating tylostyle tufts and lacking a choanosomal layer of tylostyles.

S*uberites hirsutus* shows a skeletal arrangement structured in less evident layers than that typically diagnosed for *Suberites* Nardo, 1833 (i.e., inner choanosome of densely packed tylostyles in confusion, peripheral

choanosome with packed strands of tylostyles and ectosome of densely packed, usually smaller, tylostyles perpendicular to surface) (Van Soest, 2002). Since *S. hirsutus* lacks an ectosome of densely packed tylostyles, raises the possibility for this species to be placed in another genus within the family Suberitidae, although it is worth mentioning that its skeletal features do not fit into any of the remaining genera of the family. Comparison with those genera in Suberitidae that share some similarities with our specimen sowed that *Protosuberites* Swartschewsky, 1905 presents a different choanosomal skeleton arrangement, bearing a choanosome with spicules single or in tracts running from substrate to surface, and an ectosome of usually smaller tylostyles densely packed in tufts. Other encrusting genera such as *Pseudosuberites* Topsent, 1896 and *Terpios* Duchassaing & Michelotti, 1864, show a clearly different skeletal structure, bearing the former a confused choanosomal skeleton with a tangential ectosome, and the latter, a weakly developed choanosome of spicule strands with brush-like ends that form the ectosome (Van Soest, 2002).

Phylogenetic analyses

Phylogenetic placement of *Suberites hirsutus* and *Suberites carnosus*

The phylogenetic tree based on the concatenated *COI* and *28S* alignment recovered three different clades, here named *Suberitidae* clade I, *Suberitidae* clade II, and *Suberitdae* clade III, although with low to moderate support (Fig. 3). *Suberites hirsutus* appeared in a clade with a moderate support, '*Suberitidae* clade I', also including *Rhizaxinella* sp. and *Suberites* sp. 1. This subclade was sister to another one with other taxa from the genus *Suberites,* including *S. diversicolor* and *S. aurantiacus*.

The 'Suberitidae clade II', containing the type species for the genus *S. domuncula,* was not robustly supported and showed a sister relationship with a larger clade (clade III) containing different *Suberites* spp. in a polyphyletic organization, together with other encrusting genera like *Protosuberites* and *Pseudosuberites,* with less complex skeletal structures than *Suberites*. The support values were very low in clade III except for the subclade containing *Protosuberites* and *Pseudosuberites* (Fig. 3). Our sequence for *Suberites carnosus*, displayed an unclear phylogenetic relationship clustering in clade III despite showing the typical skeletal features recognized in the genus *Suberites*.

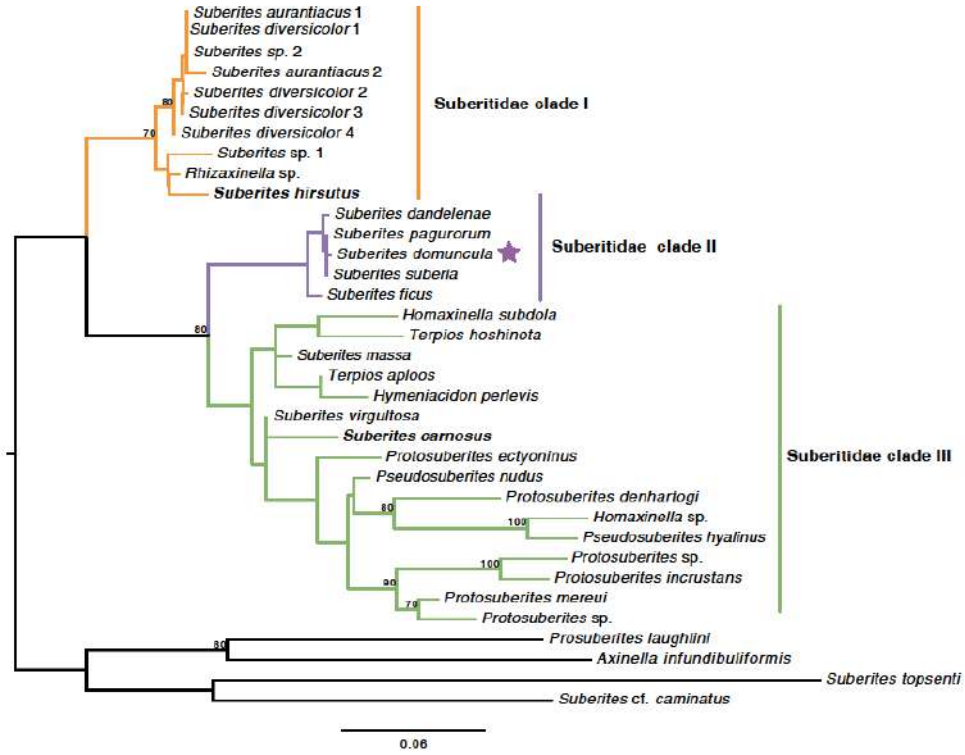

Fig. 3 Phylogenetic tree for the family Suberitidae using Maximum Likelihood on an alignment of a concatenated set of *28S* and *COI* from 32 taxa. Only bootstrap values >70 were considered.

Phylogenetic placement of *Geodia* cf. *spherastrella*

The phylogenetic tree based on the *COI* alignment of 62 taxa from the order Tetractinellida with the two *Geodia spherastrella* recovered the family Geodiidae as monophyletic although with moderate bootstrap support (Fig. 4). Most of the *Geodia* species in the phylogenetic tree clustered in the same clade, although the genus was recovered as polyphyletic. Importantly, our analysis recovered *G. spherastrella* 1 and *G.* cf. *spherast*rella 2 in two different clades.

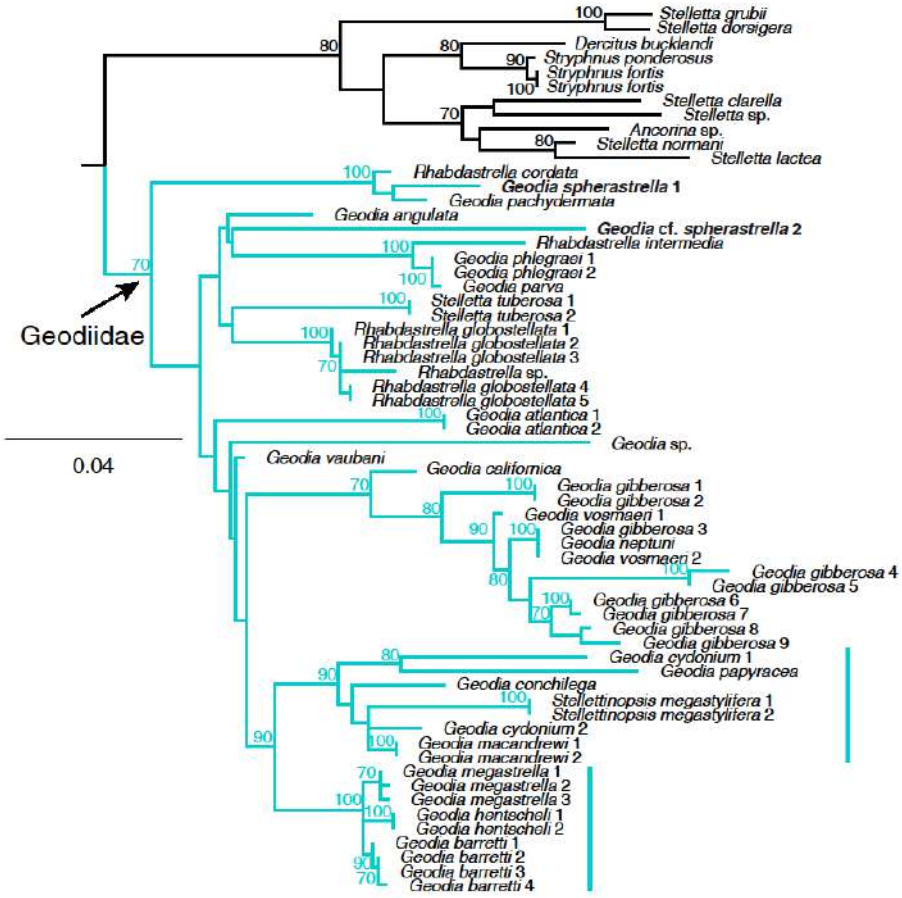

Fig. 4 Phylogenetic tree for Geodiidae and Ancorinidae using Maximum Likelihood on an alignment of *COI* sequences from 35 taxa. Only bootstrap values >70 were considered.

Phylogenetic placement of *Petrosia* (*Petrosia*) *raphida*, *Cladocroce spathiformis*, *Cladocroce fibrosa* and *Haliclona* (*Rhizoniera*) *bouryesnaultae*

Two molecular phylogenetic trees were recovered for *COI* (50 taxa) and *18S* (38 taxa) including our specimens and other members of the order Haplosclerida Topsent, 1928 (Fig. 5).

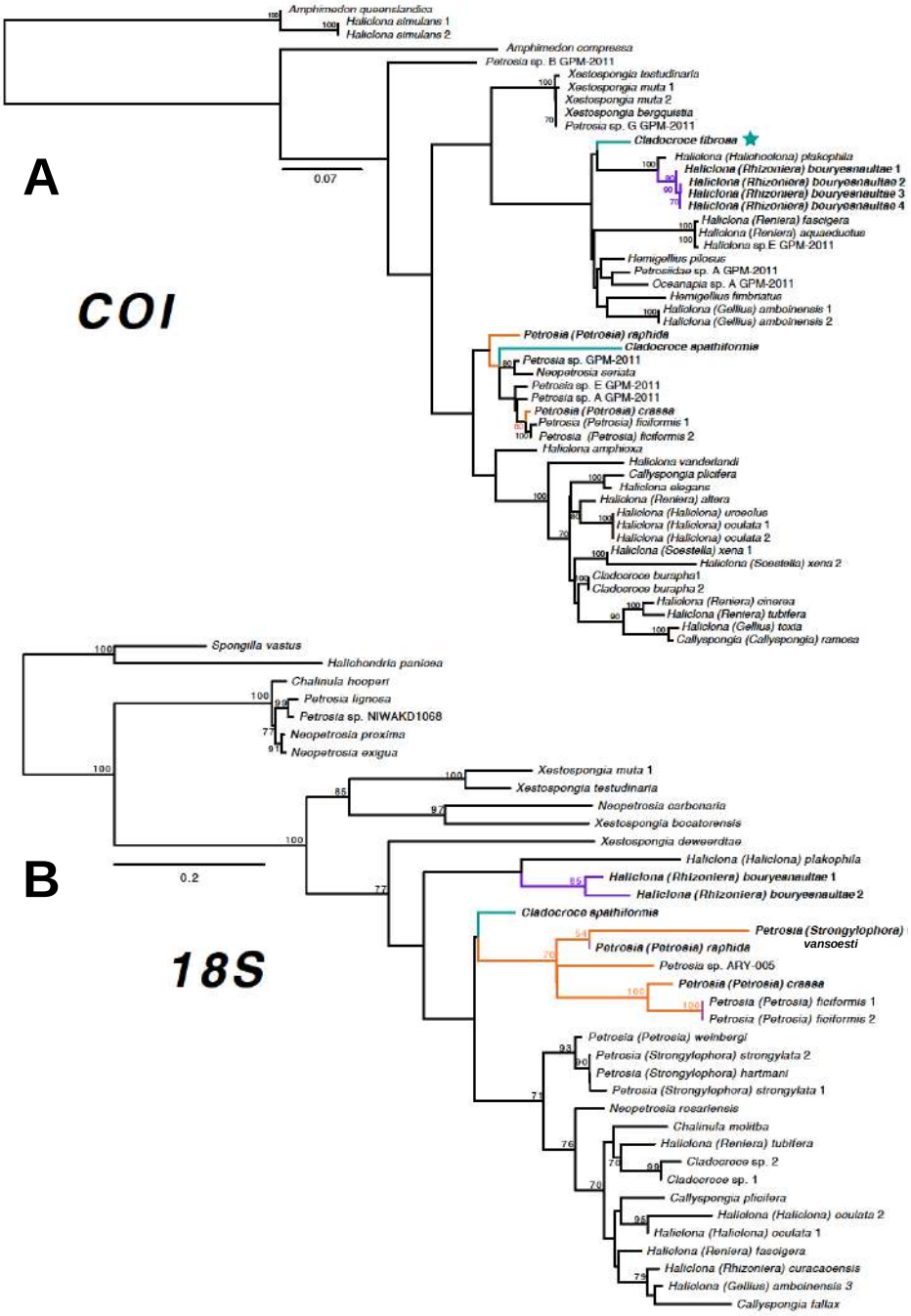

Fig. 5 Phylogenetic trees of Haplosclerida using Maximum Likelihood: (A) Phylogeny of Haplosclerida using *COI* of 40 Haplosclerida taxa and (B) using *18S* of 34 Haplosclerida taxa. Only bootstrap values >70 were considered.

The *COI* phylogenetic tree placed *Petrosia (Petrosia*) *raphida* with other members of the genus *Petrosia* (*Petrosia*), *Neopetrosia* and *Cladocroce spathiformis*, although this clade was not supported in our analysis (Fig. 5A). Unfortunately, no *COI* sequences of *Petrosia* (*Strongylophora*) *vansoesti* could be obtained for comparison between subgenera of *Petrosia*. In the *18S* tree, *P. vansoesti* was sister to *P. raphida*, and together formed a poorly supported clade, sister to other *Petrosia* species. Altogether, they formed a moderately supported clade. Additionally, other *Petrosia* (*Strongylophra)* sequences, from NCBI, appeared in another different clade.

The molecular analyses for *Cladocroce spathiformis* (*COI* and *18S*) and *Cladocroce fibrosa* (*COI*) recovered polyphyly for the genus in both cases. *C. spathiformis* was found closely related to *Petrosia* species on both trees, although poorly supported (Fig. 5). *C. fibrosa*, which is the type species of its genus, was only present in the *COI* analysis where was distantly located from *C. spathiformis* as sister to a clade including *Haliclona* (*Halichoclona*) *plakophila* and *Haliclona* (*Rhizoniera*) *bouryesnaultae,* also with a low support (Fig. 5A).

Four *COI* sequences and two *18S* sequences of specimens of *Haliclona* (*Rhizoniera*) *bouryesnaultae* showing some variations in the composition of their microscleres complement were analysed to confirm that such differences could be considered as intraspecific variation of its skeletal characters. Unfortunately, all attempts to obtain the sequences of other specimens, such as the type material, were unsuccessful. The results showed for both trees that *H. bouryesnaultae* sequences were located in the same clade with strong support in both trees. However, in the *COI* tree, they were distributed in different sister subclades within a main clade.

Discussion

Phylogenetic analyses were conducted in order to gain more insight into the characterization of five rare bathyal sponge species whose taxonomical position, previously determined by phenetic taxonomy (Chapter 1 and present Chapter), remained in need for verification. Such need was caused by the occurrence of some differing morphometric characters in the studied

specimens, which are herein exposed and integrated with the phylogenetic results.

The specimen of *Suberites hirsutus* collected from the mud volcanoes of the Gulf of Cádiz represents the second record for this species, being the type species recorded from Azores (Topsent, 1927). The specimen was sequenced in an attempt to clarify its affiliation to genus *Suberites* since this species lacks a palisade of tylostyles forming the ectosomal skeleton. This is a differing feature from the regular skeletal structure of genus *Suberites*, which shows a palisade of small tylostyles forming the ectosomal skeleton. The analyses allocated the specimen in a moderately supported clade, 'clade I', which contained species of both *Suberites* and other genera such as *Rhizaxinella*, but did not contain the type species of the genus, *Suberites domuncula*, which appeared in 'clade II'. These results allowed no confirmation that S*uberites hirsutus* actually belongs to the genus *Suberite*s, but the low support of the clades prevents from raising any changes in the taxonomy of the genus *Suberites*. Since the analysed specimen represents the second record for this species to science, and the holotype was unavailable for sequencing, further assumptions regarding its classification will remain unclear until more specimens can be sequenced.

Geodia cf. *spherastrella* is a poorly known species hitherto recorded only once from the Azores Islands (Topsent, 1904) and whose holotype remains as a spicule slide preparation. Little is known about the habit and skeletal structure of the type, being the only information available its original description, which states that the type specimen was irregularly shaped, white, smooth and with encrusted small pebbles. The specimens collected from the mud volcanoes (Chapter 1) conserved a small part of their surface, which seemed to be smooth with some irregularly hispid regions and no encrusted pebbles. Given the discrepancies in the external shape and the lack of information about the skeletal structure of the type, phylogenetic analyses were intended to contribute to the characterization of this species. The comparison of the sequences of a specimen from the mud volcanoes (*Geodia* cf. *spherastrella* 2) and another specimen from the Mediterranean (*Geodia spherastrella* 1) (Cárdenas, et al, 2011) was also expected to contribute to the characterization of such a rare species. Unexpectedly, these two specimens appeared as two phylogenetically different species, despite showing similar skeletal characters. Considering that they show small sizes, it is hypothesized

that the lack of differences in their spicule complement could be due to an early growth stage of the specimens in which spicules are not totally developed. However, this should be tested with further exhaustive morphometric comparison of the specimens and more phylogenetic analyses. Until then, the results indicate that the identification of possible *G spherastrella* specimens should be cautiously conducted.

Petrosia (Petrosia) raphida was found in the Gulf of Cádiz (Chapter 1), constituting the second record for this species, previously described from the Strait of Gibraltar (Boury-Esnault et al., 1994). It differs from some of the defining features of the subgenus *Petrosia (Petrosia)* Vosmaer, 1885 in having only a category of megascleres, microscleres and a multispicular tangential network (Desqueyroux-Faúndez & Valentine, 2002). The phylogenetic analyses were intended to confirm its affiliation in subgenus *Petrosia*, for which a specimen of *Petrosia (Strongylophora) vansoesti* and another of *Petrosia (Petrosia) crassa* were also sequenced as comparative material, being the first a species found for the second time in the Atlantic Ocean and the latter a common Atlantic species. However, comparison with *P. vansoesti* was only possible in the *18S* alignment, since no *COI* sequences could be successfully obtained for this species. The fact that *P. raphida* appeared as sister to *P. vansoesti* in the *18S* alignment is in contrast with the fact that these two species were closer to the main *Petrosia* subgenus clade than to the *Strongylophora* subgenus clade. Since the relationship with *P. raphida* and *P. vansoesti* was poorly supported, *Petrosia raphida* is suggested to belong to subgenus *Petrosia*, until the analysis of more sequences of *P. vansoesti* can clarify its affilitation and relationship with *P. raphida*.

The genus *Cladocroce* represented by three different species in our *COI* phylogenetic analysis, resulted to be polyphyletic, evidencing a need for a further review of this genus. While *C. spathiformis*, clustered within a clade containing species of the genus *Petrosia*, *C. fibrosa,* the type species of the genus, appeared as the sister group of *Haliclona* (*Halichoclona*) *plakophila* and *Haliclona* (*Rhizoniera*) *bouryesnaultae.* Interestingly, *C. fibrosa* and *H. bouryesnaultae* are both stipitate species with a long peduncle made of highly packed oxea longitudinally arranged (Topsent, 1892; Boury-Esnault et al., 1994; Sitjà et al., 2019). Most of *Haliclona* (*Rhizoniera*) species are not stalked and show a skeletal choanosome of multispicular primary lines connected by unispicular secondary lines (de Weerdt, 2002). Contrastingly, the stalked morphology of

H. bouryesnaultae, and also the type species of this subgenus, *Haliclona* (*Rhizoniera*) *rhizophora,* (Vacelet, 1969) is sustained by a skeleton of multispicular lines anastomosing from the main multispicular tract that forms the stalk (Boury-Esnault et al., 1994; de Weerdt, 2002). The phenetic resemblances between *C. fibrosa* and *H. bouryesnaultae* should be considered in further phylogenetic analyses, being currently not possible to make further assumptions based on the low support of their relationship in the phylogenetic tree. The allocation of the haplosclerid species has been partly resolved, but the monophyletic status of several genera, including *Cladocroce*, remains untested (Redmond et al., 2007). Our results evidence a need for further analyses to confidently allocate the genus *Cladocroce* within Haplosclerida.

Haliclona (Rhizoniera) bouryesnaultae was abundantly collected from the mud volcanoes of the Gulf of Cádiz (Chapter 1), being hitherto recorded only once, also from the Gulf of Cádiz. The holotype of this species shows two categories of sigmata and one category of toxa (Boury-Esnault et al., 1994). Contrastingly, only 4 out of the 49 specimens studied in Chapter 1 showed two categories of sigmata, and 2 others showed only one category of sigmata but lacked toxa. Since the rest of the morphometric characters of the specimens fit those of the holotype, these differences were considered in Chapter 1 as intraspecific variation. *COI* sequences were initially intended to be obtained from the holotype and also from specimens representing all kind of skeletal variations. However, the final successfully sequenced specimens were only those collected from the mud volcanoes of the Gulf of Cádiz, specifically, the obtained sequences belonged to specimens that showed either 1 or 2 categories of sigmata and also showed toxa. Therefore, the phylogenetic relationships herein assessed allow to compare specimens with either one or two sigma categories. The *COI* tree showed all the *H. bouryesnaultae* sequences distributed in different subclades that constituted a larger clade. Therefore, despite their close relationship, it is not possible to confidently consider that all the specimens belong to the same species. However, these will remain as a tentative assumption until more sequences representing a wider range of skeletal differences are analysed, especially considering that intraspecific differences in the skeletal composition are known to occur in different sponge species. For instance, the importance of the environmental conditions such as wave force, environmental stability, depth and temperature in skeletal phenotypic plasticity has been previously noticed in species like *Halichondria*

panicea (Palumbi, 1984), *Petrosia ficiformis* and *Volzia azzaroliae* (Bavestrello et al., 1993a), *Cliona celata* (Bell et al., 2002), *Tetilla* sp. (Meroz-Fine et al., 2005) and *Xestospongia testudinaria* (Subagio et al., 2017). Nutrient availability, especially silica concentration, can also affect spicule size as proved for *Crambe crambe* (Maldonado et al., 1999) and *Halichondria semitubulosa* (Mercurio et al., 2000). Bavestrello et al., (1993b) notted the annual cycle of *Chondrilla nucula* as another determining factor for the spicule size and shape of this species.

It should be stressed that all the specimens showing two categories of sigmata or lacking toxa were collected from the same mud volcano, called Chica, together with other 20 specimens with only one sigma category. This is actually a mud volcano/diapir complex (Palomino et al., 2016) located between two of the most relevant contourite channels in the area, Gusano and Cádiz channels, excavated by the MOW (García et al., 2009). Being this the main differential feature between this and the rest of the volcanoes included in this study, strong hydrodynamics could explain such differences if future studies confirm them to be intraspecific.

The present study evidences the singularity of the bathyal sponge assemblages from the SCI of 'Volcanes de fango del golfo de Cádiz' (Mud volcanoes of the Gulf of Cádiz), improving the current knowledge of the biodiversity of this ecologically relevant area (Rueda et al., 2012; Díaz del Río et al., 2014; González-García et al., 2020), which is also a transitional area between the Atlantic and the Mediterranean. Such knowledge is fundamental for further management and preservation of this SCI, which also hosts some important fishery grounds used by the Spanish trawling fleet (González-García et al., 2020), being some mud volcanoes potentially exposed to severe trawling impacts (Delgado et al., 2013; Díaz del Río et al., 2014).

Knowledge on the deep sea is still poor despite covering more than a 50% of The Earth and the increasing anthropogenic activities such as resource extraction industries (Ramirez-Llodra et al., 2011). Environmental DNA (eDNA) metabarcoding allows the detection or the inventory of target organisms using their DNA directly extracted from soil, water, or air samples (Taberlet et al., 2012a). The use of eDNA can also be applied to biomonitoring and ecosystem biodiversity assessment (Baird & Hajibabaei, 2012; Bohmann et al., 2014), representing a useful tool for uneasily accessible areas like the deep-sea. However, despite the dynamic expansion of deep-sea eDNA studies (Sinniger et al., 2016; Mariani et al., 2019), little metabarcoding

information is still available for benthic diversity at bathyal and abyssal depths (Pawlowski et al., 2011). Advances in ocean monitoring and conservation depend on the availability of large amounts of inexpensive, standardised and tractable samples from across the world (Mariani et al., 2019). For this reason, sequences like the ones obtained in the present study can favour the elaboration of exhaustive sequence databases of deep-sea species.

References

Baird, D. J. and Hajibabaei, M. (2012) Biomonitoring 2.0: a new paradigm in ecosystem assessment made possible by next-generation DNA sequencing. *Molecular Ecology*, 21(8), 2039-2044.

Bavestrello, G., Bonito, M. and Sará, M. (1993a) Influence of depth on the size of sponge spicules. *Scientia Marina*, 57(4), 415-420.

Bavestrello, G., Bonito, M. and Sarà, M. (1993b) Silica content and spicular size variation during an annual cycle in Chondrilla nucula Schmidt (Porifera, Demospongiae) in the Ligurian Sea. *Scientia Marina*, 57(4), 421-425.

Bell, J. J., Barnes, D. K. A. and Turner, J. R. (2002) The importance of micro and macro morphological variation in the adaptation of a sublittoral demosponge to current extremes. *Marine Biology*, 140(1), 75-81.

Bohmann, K., Evans, A., Gilbert, M. T. P., Carvalho, G. R., Creer, S., Knapp, M., Yu, D. W. and de Bruyn, M. (2014) Environmental DNA for wildlife biology and biodiversity monitoring. *Trends in Ecology & Evolution*, 29(6), 358-367.

Boury-Esnault, N. and Lopes, M. T. (1985) Les Démosponges littorales de l'Archipel des Açores. *Annales de l'Institut océanographique*, 61(2), 149-225.

Boury-Esnault, N., Pansini, M. and Uriz, M. J. (1994) Spongiaires bathyaux de la mer d'Alboran et du golfe ibéro-marocain. *Mémoires. Muséum National d'Histoire Naturelle,* 160, 1-174.

Boury-Esnault, N. and Rützler, K. (1997) Thesaurus of sponge morphology. *Smithsonian Contributions to Zoology*, 596, 1-55.

Castresana, J. (2000) Selection of conserved blocks from multiple alignments for their use in phylogenetic analysis. *Molecular Biology and Evolution*, 17(4), 540-552.

Darriba, D., Taboada, G. L., Doallo, R. and Posada, D. (2012) jModelTest 2: more models, new heuristics and parallel computing. *Nature Methods*, 9(8), 772-772.

de Weerdt, W. H. (2002) Family Chalinidae Gray, 1867. In: J. N. A. Hooper and R. W. M. Van Soest (Eds), *Systema Porifera. A guide to the classification of sponges*, 1. Kluwer Academic/Plenum, New York, pp. 852-873.

Delgado, M., Rueda, J. L., Gil, J., Burgos, C. and Sobrino, I. (2013) Spatial characterization of megabenthic epifauna of soft bottoms around mud volcanoes in the Gulf of Cádiz. *Journal of Natural History*, 47(25-28), 1803-1831.

Desqueyroux-Faúndez, R. and Valentine, C. (2002) Family Petrosiidae Van Soest, 1980. In: J. N. A. Hooper and R. W. M. Van Soest (Eds), *Systema Porifera. A guide to the classification of sponges*, 1. Kluwer Academic/ Plenum, New York, pp. 906-917.

Díaz del Río, V., Bruque, G., Fernández-Salas, L. M., Rueda, J. L., González, E., López, N., Palomino, D., López, F. J., Farias, C., Sánchez, R., Vázquez, J. T., Rittierott, C. C., Fernández, A., Marina, P., Luque, V., Oporto, T., Sánchez, O., García, M., Urra, J., Bárcenas, P., Jiménez, M. P., Sagarminaga, R. and Arcos, J. M. Volcanes de fango del golfo de Cádiz, Proyecto LIFE + INDEMARES. A. y. M. A. Fundación Biodiversidad del Ministerio de Agricultura. (2014).

Drummond, A. J., Ashton, B., Cheung, M., Heled, J., Kearse, M., Moir, R., Stones-Havas, S., Thierer, T. and Wilson, A. (2009) Geneious v10.2.2.

Edgar, R. C. (2004) MUSCLE: multiple sequence alignment with high accuracy and high throughput. *Nucleic Acids Research*, 32(5), 1792-1797.

Folmer, O., Black, M., Hoeh, W., Lutz, R. and Vrijenhoek, R. (1994) DNA primers for amplification of mitochondrial cytochrome c oxidase subunit I from diverse metazoan invertebrates. *Molecular Marine Biology and Biotechnology*, 3(5), 294-299.

Galtier, N., Gouy, M. and Gautier, C. (1996) SEAVIEW and PHYLO_WIN: two graphic tools for sequence alignment and molecular phylogeny. *Bioinformatics*, 12(6), 543-548.

García, M., Hernández-Molina, F. J., Llave, E., Stow, D. A. V., León, R., Fernández-Puga, M. C., Díaz del Rio, V. and Somoza, L. (2009) Contourite erosive features caused by the Mediterranean Outflow Water in the Gulf of Cadiz: Quaternary tectonic and oceanographic implications. *Marine Geology*, 257(1-4), 24-40.

Giribet, G., Edgecombe, G. D., Wheeler, W. C. and Babbitt, C. (2002) Phylogeny and systematic position of Opiliones: A combined analysis of chelicerate relationships using morphological and molecular data. *Cladistics*, 18(1), 5-70.

González-García, E., Mateo-Ramírez, Á., Urra, J., Farias, C., Marina, P., Lozano, P., López-González, P. J., Megina, C., Raso, J. E. G., Gofas, S., López, E., Moreira, J., López-González, N., Sánchez-Leal, R. F., Fernández-Salas, L. M. and Rueda, J. L. (2020) Composition, structure and distribution of epibenthic communities within a mud volcano field of the northern Gulf of Cádiz in relation to environmental variables and trawling activity. *Journal of Sea Research,* 160-161, 101892.

Guindon, S. and Gascuel, O. (2003) A simple, fast, and accurate algorithm to estimate large phylogenies by maximum likelihood. *Systematic Biology*, 52(5), 696-704.

Katoh, K. and Standley, D. M. (2013) MAFFT Multiple Sequence Alignment Software Version 7: Improvements in Performance and Usability. *Molecular Biology and Evolution*, 30(4), 772-780.

Maldonado, M., Carmona, M. C., Uriz, M. J. and Cruzado, A. (1999) Decline in Mesozoic reef-building sponges explained by silicon limitation. *Nature*, 401, 785-788.

Mariani, S., Baillie, C., Colosimo, G. and Riesgo, A. (2019) Sponges as natural environmental DNA samplers. *Current Biology*, 29(11), R401-R402.

Mercurio, M., Correiro, G., Liaci, L. S. and Gaino, E. (2000) Silica content and spicule size variations in Pellina semitubulosa (Porifera: Demospongiae). *Marine Biology*, 137(1), 87-92.

Meroz-Fine, E., Shefer, S. and Ilan, M. (2005) Changes in morphology and physiology of an East Mediterranean sponge in different habitats. *Marine Biology*, 147, 243-250.

Morrow, C. C., Picton, B. E., Erpenbeck, D., Boury-Esnault, N., Maggs, C. A. and Allcock, A. L. (2012) Congruence between nuclear and mitochondrial genes in Demospongiae: A new hypothesis for relationships within the G4 clade (Porifera: Demospongiae). *Molecular Phylogenetics and Evolution*, 62(1), 174-190.

Palomino, D., López-González, N., Vázquez, J.-T., Fernández-Salas, L.-M., Rueda, J.-L., Sánchez-Leal, R. and Díaz-del-Río, V. (2016) Multidisciplinary study of mud volcanoes and diapirs and their relationship to seepages and bottom currents in the Gulf of Cádiz continental slope (northeastern sector). *Marine Geology*, 378, 196-212.

Palumbi, S. R. (1984) Tactics of Acclimation: Morphological Changes of Sponges in an Unpredictable Environment. *Science*, 225(4669), 1478-1480.

Pawlowski, J., Christen, R., Lecroq, B., Bachar, D., Shahbazkia, H. R., Amaral-Zettler, L. and Guillou, L. (2011) Eukaryotic Richness in the Abyss: Insights from Pyrotag Sequencing. *PLoS One*, 6(4), e18169.

Ramirez-Llodra, E., Tyler, P. A., Baker, M. C., Bergstad, O. A., Clark, M. R., Escobar, E., Levin, L. A., Menot, L., Rowden, A. A., Smith, C. R. and Van Dover, C. L. (2011) Man and the Last Great Wilderness: Human Impact on the Deep Sea. *PLoS One*, 6(8), e22588.

Redmond, N. E., Morrow, C. C., Thacker, R. W., Diaz, M. C., Boury-Esnault, N., Cárdenas, P., Hajdu, E., Lôbo-Hajdu, G., Picton, B. E., Pomponi, S. A., Kayal, E. and Collins, A. G. (2013) Phylogeny and Systematics of Demospongiae in Light of New Small-Subunit Ribosomal DNA (18S) Sequences. *Integrative and Comparative Biology*, 53(3), 388-415.

Redmond, N. E., van Soest, R. M. W., Kelly, M., Raleigh, J., Travers, S. A. A. and McCormack, G. P. (2007) Reassessment of the classification of the Order Haplosclerida (Class Demospongiae, Phylum Porifera) using 18S rRNA gene sequence data. *Molecular Phylogenetics and Evolution*, 43, 344-352.

Rueda, J. L., Díaz-del-Río, V., Sayago-Gil, M., López-González, N., Fernández-Salas, L. M. and Vázquez, J. T. (2012) Fluid venting through

the seabed in the Gulf of Cadiz (SE Atlantic Ocean, Western Iberian Peninsula): Geomorphic features, habitats, and associated fauna In: P. T. Harris and E. K. Baker (Eds), *Seafloor geomorphology as benthic habitat*. Elsevier, London, pp. 831-841.

Sinniger, F., Pawlowski, J., Harii, S., Gooday, A. J., Yamamoto, H., Chevaldonne, P., Cedhagen, T., Carvalho, G. and Creer, S. (2016) Worldwide Analysis of Sedimentary DNA Reveals Major Gaps in Taxonomic Knowledge of Deep-Sea Benthos. *Frontiers in Marine Science*, 3, 92.

Sitjà, C., Maldonado, M., Farias, C. and Rueda, J. L. (2019) Deep-water sponge fauna from the mud volcanoes of the Gulf of Cadiz (North Atlantic, Spain). *Journal of the Marine Biological Association of the United Kingdom*, 99(4), 807-831.

Stamatakis, A. (2014) RAxML version 8: a tool for phylogenetic analysis and post-analysis of large phylogenies. *Bioinformatics*, 30(9), 1312-1313.

Subagio, I. B., Setiawan, E., Hariyanto, S. and Irawan, B. (2017) Spicule size variation in Xestospongia testudinaria Lamarck, 1815 at Probolinggo-Situbondo coastal. AIP Conference Proceedings, 1854(1), 020034.

Topsent, E. (1892) Contribution a l'étude des Spongiaires de l'Atlantique Nord (Golfe de Gascogne, Terre-Neuve, Açores). *Résultats des Campagnes Scientifiques accomplies par le Prince Albert I.* Monaco*,* 2, 1-165.

Topsent, E. (1893) Nouvelle série de diagnoses d'Éponges de Roscoff et de Banyuls. *Archives de Zoologie Expérimentale et Générale*, 3ème série(10), XXXIII-XLIII.

Topsent, E. (1904) Spongiaires des Açores. *Résultats des Campagnes Scientifiques accomplies par le Prince Albert I.* Monaco, 25, 1-279.

Topsent, E. (1927) Diagnoses d'Eponges nouvelles recueillies par le Prince Albert I de Monaco. *Bulletin de l'Institut Océanographique de Monaco*, 502, 1-19.

Topsent, E. (1928) Spongiaires de l'Atlantique et de la Méditerranée, provenant des croisières de Prince Albert I de Monaco. *Résultats des Campagnes Scientifiques accomplies par le Prince Albert I.* Monaco, 74, 1-376.

Van Soest, R. W. M. (2002) Family Suberitidae Schmidt, 1870. In: J. N. A. Hooper and R. W. M. Van Soest (Eds), *Systema Porifera. A guide to the*

classification of sponges, 1. Kluwer Academic/Plenum, New York, pp. 227-244.

Whiting, M. F., Carpenter, J. C., Wheeler, Q. D. and Wheeler, W. C. (1997) The strepsiptera problem: Phylogeny of the holometabolous insect orders inferred from 18S and 28S ribosomal DNA sequences and morphology. *Systematic Biology*, 46(1), 1-68.

Xavier, J. R., Rachello-Dolmen, P. G., Parra-Velandia, F., Schonberg, C. H. L., Breeuwer, J. A. J. and van Soest, R. W. M. (2010) Molecular evidence of cryptic speciation in the "cosmopolitan" excavating sponge Cliona celata (Porifera, Clionaidae). *Molecular Phylogenetics and Evolution*, 56(1), 13-20.

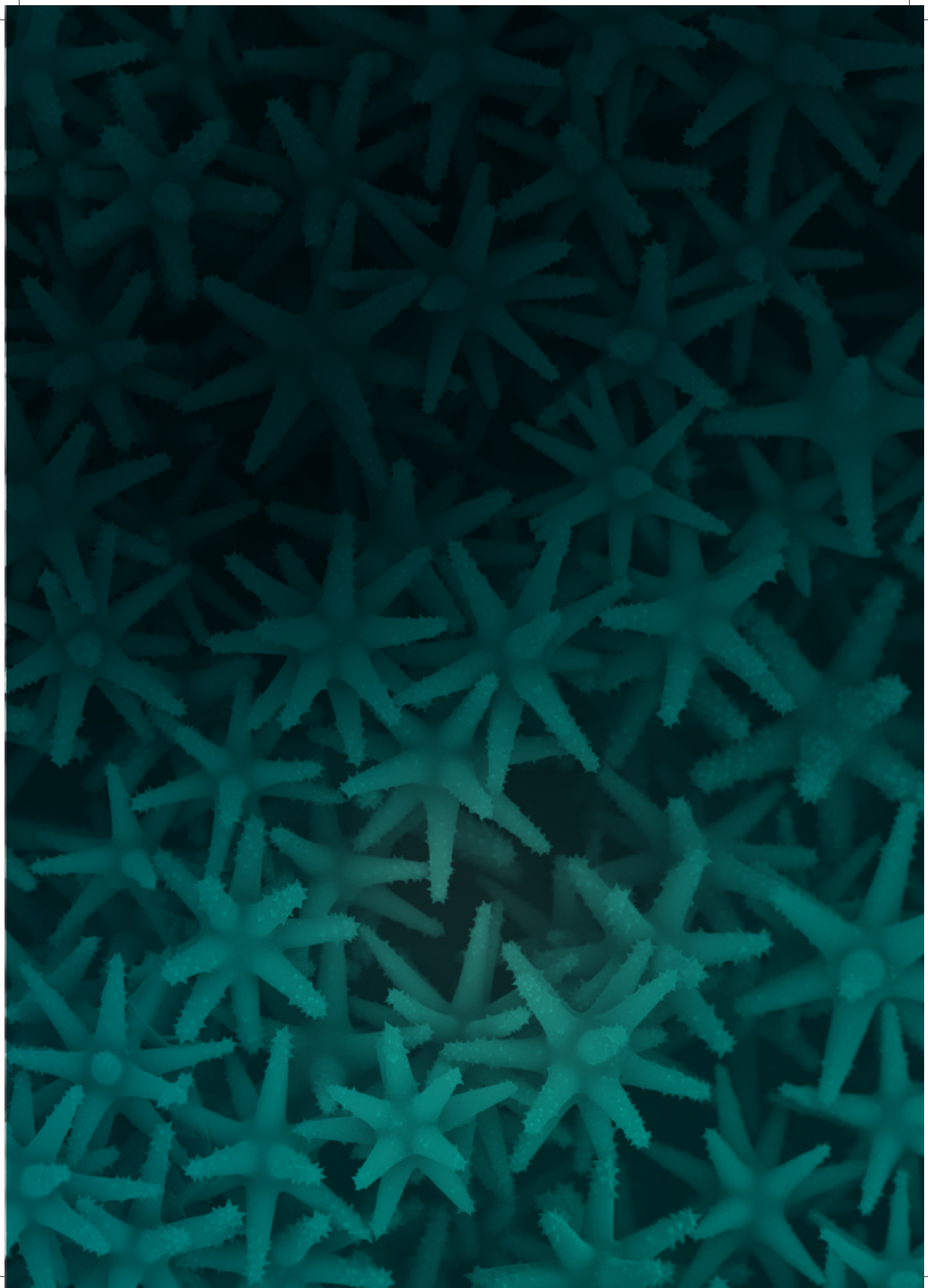

Chapter 3

New and rare sponges from the deep shelf of the Alboran Island (Alboran Sea, Western Mediterranean)

Abstract

The sponge fauna from the deep shelf (70 to 200 m) of the Alboran Island (Alboran Sea, Western Mediterranean) was investigated using a combination of ROV surveys and collecting devices in the frame of the EC LIFE+ INDEMARES Grant aimed to designate marine areas of the Nature 2000 Network within Spanish territorial waters. From ROV surveys and 351 examined specimens, a total of 87 sponge species were identified, most belonging in the Class Demospongiae, and one belonging in the Class Hexactinellida. Twenty-six (29%) species can be regarded as either taxonomically or faunistically relevant. Three of them were new to science (*Axinella alborana* nov. sp.; *Axinella spatula* nov. sp.; *Endectyon filiformis* nov. sp.) and 4 others were Atlantic species recorded for the first time in the Mediterranean Sea (*Jaspis eudermis* Lévi & Vacelet, 1958; *Hemiasterella elongata* Topsent, 1928; *Axinella vellerea* Topsent, 1904; *Gelliodes fayalensis* Topsent, 1892). Another outstanding finding was a complete specimen of *Rhabdobaris implicata* Pulitzer-Finali, 1983, a species only known from its holotype, which had entirely been dissolved for its description. Our second record of the species has allowed a neotype designation and a restitution of the recently abolished genus *Rhabdobaris* Pulitzer-Finally, 1983, also forcing a slight modification of the diagnosis of the family Bubaridae. Additionally, 12 species were recorded for the first time from the shelf of the Alboran Island, including a few individuals of the large hexactinellid *Asconema setubalense* Kent, 1877 that provided the second Mediterranean record of this "North Atlantic" hexactinellid. ROV explorations also revealed that sponges are an important component of the deep-shelf benthos, particularly on rocky bottoms, where they make peculiar sponge gardens characterized by a wide diversity of small, erect species forming a dense "undergrowth" among a scatter of large sponges and gorgonians. The great abundance and the taxonomic singularities of the sponge fauna occurring in these deep-shelf bottoms strongly suggest these habitats to be considered within the environmental protection of the Nature 2000 Network.

Introduction

The Alboran Sea occupies the westernmost basin of the Mediterranean. It is known to be a transitional region between the North Atlantic Ocean and the Mediterranean *sensu stricto*, in terms of both hydrography and organismal distributions. The influx of North Atlantic surface water during most of the Quaternary and in Recent times favors the penetration of many "Atlantic species" in this western Mediterranean zone (Péres & Picard, 1964). Consequently, the sublittoral communities in this area often present high biodiversity relative to equivalent communities in nearby Lusitanian and Mauritanian areas (Templado et al., 2006; Coll et al., 2010).

At the heart of the Alboran basin, the Island of Alboran (Fig. 1), a tiny (642 m long and 265 m wide) islet made of volcanic rocks, emerges from a large (45 km long and 10 km wide) submerged shelf, remnant of an ancient (7-16 my old) volcanic cone. This cone is in turn part of an ancient submerged volcanic chain that crosses the Alboran basin with Northeast-Southwest direction. The bottom of the basin in this area reaches a maximum depth of 1500 m and consists of a thinned crustal microplate formed during the Lower Miocene (about 18 my ago) at an important seismic area where the Eurasian and African plates collided (Comas et al., 1992; Martínez-García et al., 2010).

Although the hydrography of the Alboran Sea is quite complex, it has been well documented that in the central area where the Alboran Island is located, the incoming Atlantic seawater forms a low-salinity (~36.5 ‰), 150-200 m thick, upper layer above the underlying Mediterranean water (~38.2‰), influencing to a varying extent all the communities on the shelf of the island. The singularity and ecological relevance of the benthic communities on the upper shelf (above 70 m) of the Alboran Island has long been recognized (reviewed in Templado et al., 2006), and is currently protected under both

Spanish and European legislation by declaration of a Marine Reserve, a Fish Reserve, a Special Area of Mediterranean Importance (SPAMI), and a Site of Community Importance (SCI). Additionally, the shelf of the Alboran Island, due to its strategic location at the Mediterranean entry, provides a unique reference site for early detection of migration and invasion processes into the Mediterranean by Atlantic organisms.

Previously available information on the sponge fauna of the Alboran Sea (Templado et al., 1986; Pansini et al., 1987; Maldonado & Benito, 1991; Maldonado, 1992; Boury-Esnault et al., 1994; Maldonado & Uriz, 1996, 1999; Rosell & Uriz, 2002; Templado et al., 2006) strongly suggests that sponges may be an important component of the benthos at the still ill-known deep shelf of the Alboran Island. Interestingly, the deep-shelf sponge fauna of the Alboran Island bears some similarities with that reported from the easternmost areas of the western Mediterranean, such as the Ligurian Sea and the Strait of Sicily (Pansini et al., 1987; Maldonado & Uriz, 1995; Bertolino et al., 2013a; Bertolino et al., 2013b). Additionally, some studies have suggested a continued input of sponge species from the Lusitanian region into the Alboran Sea over the Quaternary (Maldonado & Uriz, 1995), despite sponges being sessile organisms with short-living planktonic larvae lacking recognizable strategies for long-distance dispersal (Maldonado, 2006). Since global warming enhances northward migration of subtropical marine species (Coll et al., 2010), it is urgent to improve our knowledge of these deep-shelf Alboranian communities before the immigrants get integrated in them and further complicate discrimination of the pre-warming original fauna and the understanding of future Mediterranean faunal shifts (Vermeij, 2012).

Material and methods

Within the frame of an EC Grant LIFE+ INDEMARES aimed to list and designate marine areas for the Nature 2000 Network in Spanish territorial waters, we explored the deep shelf (70 to 200 m) of the Alboran Island, using a remotely operated underwater vehicle (ROV) along with traditional dredging and trawling devices to collect benthic fauna.

Prior to any collecting tasks, scientific partners of the INDEMARES-Alboran grant developed a detailed bathymetric profiling of the island shelf using side scan sonar (Geotecnia, Hidrología and Medio Ambiente S.L.) and outlined the location of the most relevant benthic communities through suspended still video (information available through Juan Goutayer). Using this basic information, a first detailed assessment of the benthic communities at the deep shelf of the Alboran Island was carried out by running 9 transects (19 hours of recording) at depths ranging from 65 to 205 m in September 2011, using a SEAEYE FALCON ROV. A second research stage involved collecting cruises in 2011 and 2012, during which a total of 44 sites were sampled in the 25-290 m depth range, using a small beam trawl on soft bottoms and a dredge on hard bottoms. Here we are reporting on the sponge fauna collected in 25 sampling stations (Fig. 1; Table 1), incorporating, whenever possible, the information available from the video transects. Collected specimens were fixed in 4% formalin for 2-3 months, rinsed in distilled water, and subsequently transferred to 70% ethanol. Because of an initial fixation step in formalin, the collected sponge material

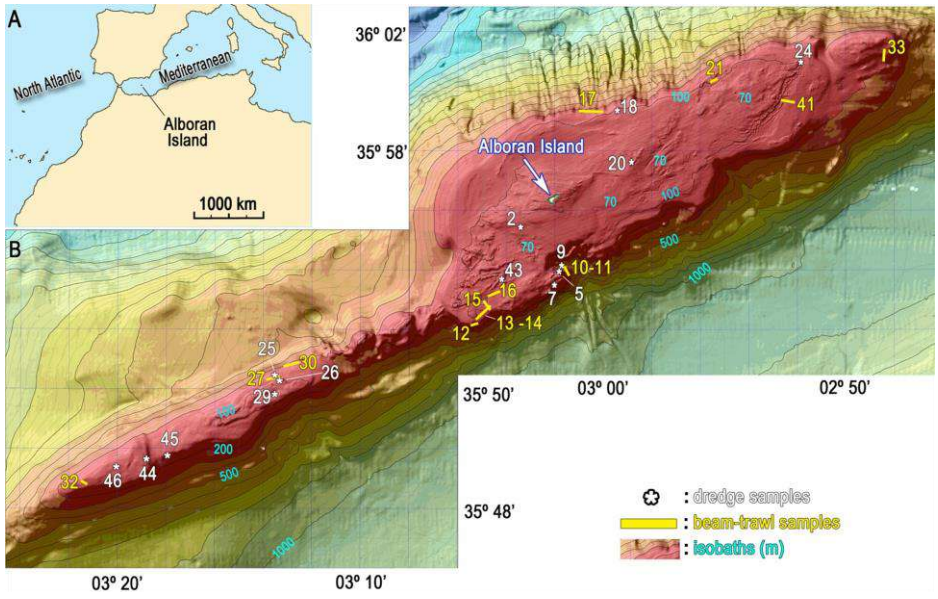

Figure 1. (A) Localization of the Alboran Island in the Mediterranean. (B) Distribution of the 25 studied sampling stations over the bathymetric map of the shelf of the Alboran Island.

Table 1. Information on sampling stations, indicating station number (Stn. #), type of collecting device (DR= dredge; BV= beam trawl), geographical coordinates of starting and end point of sampling transects, depth range (m) during the transect, and bottom type (R= rocky, G= gravel, OG= Organogenic gravel, RH= Rhodolith bed, LS= Lava stone bed).

Station number	Collection device	Transect start point (lat. and long.)	Transect end point (lat. and long.)	Starting depth (m)	Ending depth (m)	Bottom type
02	DR	35°55.422'N 03°03.307'W	35°55.452'N 03°03.378'W	54	52	RH
05	DR	35°53.980'N 03°01.806'W	35°53.917'N 03°01.810'W	130	109	R
07	DR	35°53.506'N 03°02.092'W	35°53.416'N 03°02.051'W	87	92	RH
10	BV	35°53.990'N 03°01.570'W	35°54.116'N 03°01.610'W	214	290	G
11	BV	35°54.068'N 03°01.613'W	35°53.811'N 03°01.413'W	243	240	G
12	BV	35°52.222'N 03°05.215'W	35°52.167'N 03°05.388'W	120	112	OG
13	BV	35°52.379'N 03°05.182'W	35°52.825'N 03°04.591'W	99	95	G
14	BV	35°52.723'N 03°04.668'W	35°52.340'N 03°05.265'W	96	100	G
15	BV	35°52.668'N 03°04.656'W	35°52.900'N 03°04.924'W	96	96	G
16	BV	35°53.103'N 03°04.738'W	35°53.256'N 03°04.289'W	92	82	RH
17	BV	35°59.326'N 03°00.044'W	35°59.364'N 03°01.000'W	121	169	G
18	DR	35°59.395'N 02°59.396'W	35°59.386'N 02°59.460'W	92	94	R
20	DR	35°57.663'N 02°58.848'W	35°57.672'N 02°58.810'W	48	42	RH
21	BV	36°00.399'N 02°55.318'W	36°00.288'N 02°55.570'W	101	93	OG
25	DR	35°50.413'N 03°13.390'W	35°50.421'N 03°13.491'W	111	114	OG
26	DR	35°50.294'N 03°13.248'W	35°50.251'N 03°13.304'W	94	97	OG
27	BV	35°50.415'N 03°13.245'W	35°50.398'N 03°13.722'W	109	100	OG
29	DR	35°49.768'N 03°13.090'W	35°49.996'N 03°13.432'W	93	94	OG /RH
30	BV	35°50.756'N 03°13.165'W	35°50.896'N 03°12.434'W	180	163	OG
32	BV	35°46.869'N 03°21.413'W	35°46.843'N 03°21.301'W	125	122	R
33	BV	36°01.034'N 02°48.487'W	36°01.397'N 02°48.433'W	173	134	G
41	BV	35°59.617'N 02°52.077'W	35°59.677'N 02°52.666'W	112	102	G
44	DR	35°47.716'N 03°17.986'W	35°47.820'N 03°17.902'W	152	135	R /G
45	DR	35°47.589'N 03°18.679'W	35°47.560'N 03°18.769'W	134	120	G
46	DR	35°47.404'N 03°19.984'W	35°47.437'N 03°20.037'W	103	104	G/ LS

is not suitable for molecular analysis. Taxonomic identifications were accomplished by considering the external morphology and skeleton, using standard techniques to prepare spongin fibres and spicules for light microscopy observation. Body features, spicules, and skeletal arrangements were described according to the thesaurus of sponge morphology (Boury-Esnault & Rützler 1997). When required, acid-cleaned spicules were mounted on aluminum stubs, gold-coated, and studied through a HITACHI TM3000 Scanning Electron Microscope (SEM), following standard protocols for samples preparation. Features of the collected material were compared, when required, to those of holotypes and additional material borrowed from sponge collections of the Muséum National d'Histoire Naturelle (MNHN) of Paris, the Musée Océanographique of Monaco (MOM), and the Museo Civico di Storia Naturale Giacomo Doria of Genoa (MSNG). All collected material during the INDEMARES-Alboran cruises, holotypes included, has been stored in the Invertebrate Collection of the National Museum of Natural Sciences (MNCN), Madrid, Spain.

Results and discussion

Taxonomic and ecological singularities

Taxonomic identification of 351 collected specimens along with additional identifications derived from ROV video monitoring yielded a list of 87 sponge species (Appendix I), most belonging to the Class Demospongiae. The Hexactinellida were represented by only one species, *Asconema setubalense* Kent, 1870, identified through ROV recordings. Eleven specimens of Calcarea were collected, but they were not taxonomically investigated. The results of the present study have increased the previous number of sponge species known from the island shelf and its surrounding bathyal bottoms by 33, leading to a total of 196 species (Appendix II).

Twenty-six (29%) out of 87 identified species were considered as relevant from either a taxonomical or faunal point of view. Three of them were new to science (*Axinella alborana* nov. sp.; *Axinella spatula* nov. sp.; *Endectyon filiformis* nov. sp.) and 4 others were recorded in the Mediterranean Sea for the first time (*Jaspis eudermis* Lévi & Vacelet, 1958; *Hemiasterella elongata* Topsent, 1928; *Axinella vellerea* Topsent, 1904; *Gelliodes fayalensis* Topsent,

1892). Another outstanding finding was a complete specimen of *Rhabdobaris implicata* Pulitzer-Finali, 1983, a species only known from the holotype, which was entirely dissolved for the preparation of a spicule slide. Twelve additional species were recorded for the first time from the shelf of the Alboran Island: *Acanthella acuta* Schmidt, 1862; *Calthropella recondita* Pulitzer-Finali, 1983; *Dendroxea lenis* (Topsent, 1892); *Endectyon delaubenfelsi* Burton, 1930; *Erylus discophorus* (Schmidt, 1862); *Eurypon lacazei* (Topsent, 1891); *Prosuberites longispinus* Topsent, 1893; *Rhizaxinella gracilis* (Lendenfeld, 1898); *Spongosorites intricatus* (Topsent, 1892); *Hexadella racovitzai* Topsent, 1896; *Terpios fugax* Duchassaing & Michelotti, 1864; and *Asconema setubalense*. From a conservation point of view, there were 4 rare Mediterranean endemic species (*Axinella salicina* Schmidt, 1868; *Crambe tailliezi* Vacelet & Boury-Esnault, 1982; *Sarcotragus pipetta* Schmidt, 1868; *Vulcanella aberrans* (Maldonado & Uriz, 1996), and 2 other species, *Tethya aurantium* (Pallas, 1766) and *Axinella polypoides* Schmidt, 1862, listed as vulnerable in the current environmental legislation (Templado et al. 2004).

Collecting devices and ROV explorations revealed that sponges are relevant or dominant benthic organisms in 3 major habitats of the deep shelf: 1) the rhodolith beds (60-120 m; Fig. 2A-B); 2) the rocky plains moderately sloping, which correspond to the flanks of the ancient volcanic cone (80-120 m; Fig. 2C-D); and 3) the isolated rocky outcrops surrounded by soft sediments (Fig. 2E-F).

The rhodolith beds occupied vast areas in the 60-100 m depth range. Although the species composition of the general sessile fauna varied widely from one rhodolith to another, a wide variety of encrusting sponges was often abundant on them (Fig. 2B). Species such as *Bubaris vermiculata* (Bowerbank, 1866), *Diplastrella bistellata* (Schmidt, 1862), *Dercitus (Stoeba) plicatus* (Schmidt, 1868), and several members of the genera *Eurypon* Gray, 1867 were common. Small submassive and erect species of the genera *Axinella*, *Suberites*, *Phakellia* or *Poecillastra compressa* were also frequent.

The slopy rocky plains, which showed moderate charges of fine sediments, often hosted important populations of flabellate and lamellate, erect and massive sponges, typically including *Phakellia robusta* (Fig. 2C), *Phakellia ventilabrum*, *Poecillastra compressa* (Fig. 2C), *Characella pachastrelloides* (Carter, 1876), *Pachastrella monilifera* Schmidt, 1868, *Vulcanella aberrans* (Fig. 2D), along with a lower abundance of other large astrophorids and

halichondrids. Among the scatter of large sponges, there was a dense, peculiar "undergrowth" made of a variety of small erect sponges (Fig. 2C). Stipitate or lollipop morphologies, such as *Podospongia lovenii* Bocage, 1869, *Rhizaxinella elongata* (Ridley & Dendy, 1886), *Rhizaxinella gracilis* or *Crella (Yvesia) pyrula* (Carter, 1876), and digitate or poorly-branching morphologies, such as *Axinella vellerea* Topsent, 1904, *Axinella pumila* Babic, 1922, *Stelligera stuposa* (Ellis & Solander, 1786), and *Stelligera rigida* (Montagu, 1818), were common in the undergrowth (Fig. 2C-D, G-H). These communities can indeed be regarded as Mediterranean "sponge gardens", characterized by high diversity and abundance of small erect species growing among the large astrophorids and axinellids that typically build the "sponge gardens" or "sponge grounds" at similar depth ranges on North-Atlantic margins (Hogg et al., 2010). On the deepest zone of the sloping rocky flats some isolated individuals of the large hexactinellid *Asconema setubalense* also occurred (e.g., 181 m deep; 35º 53.190' N, 03º 02.111' W), providing the second Mediterranean record of this species. Whether a denser population of *A. setubalense* occurs deeper in the slope remains to be explored. This hexactinellid had traditionally been reported from greater depths in the North Atlantic Ocean, but it was recently recorded first in the Mediterranean during the ROV exploration of another deep site (> 250 m) of the Alboran Sea, the "Seco de los Olivos" (Chella Seamount; Pardo et al. 2011).

The rocky outcrops standing out from soft bottoms, with their impressive rocky crests, walls, overhangs, and crevices, provided an optimal substrate for suspension feeders, often hosting a large variety of sponges, cnidarians, brachiopods, molluscs, sabellid tube worms, ascidians, etc (Fig. 2E). The ROV inspections revealed that encrusting, branching, and massive sponges often co-occurred on the outcrops, favored by the multiplicity of microhabitats that these tortuous rocky structures offer. Common sponges were *Dysidea fragilis* (Montagu, 1818), *Sarcotragus pipetta*, *Hexadella racovitzai*, *Penares helleri* (Schmidt, 1864), *Crambe tailliezi*, *Terpios fugax*, *Caminus vulcani* Schmidt, 1862, *Dercitus plicatus*, *Craniella cranium* (Müller, 1776), and also several species of *Suberites*, *Calthropella* Sollas, 1888, *Erylus* Gray, 1867, *Haliclona* Grant, 1836, *Spongosorites* Topsent, 1896, and *Phorbas* Duchassaing & Michelotti, 1864. Large astrophorids (Fig. 2F), such as *Geodia* spp., *Stelletta* spp., *Pacahastrella monilifera*, *Poecillastra compressa*, *Characella pachastrelloides*,

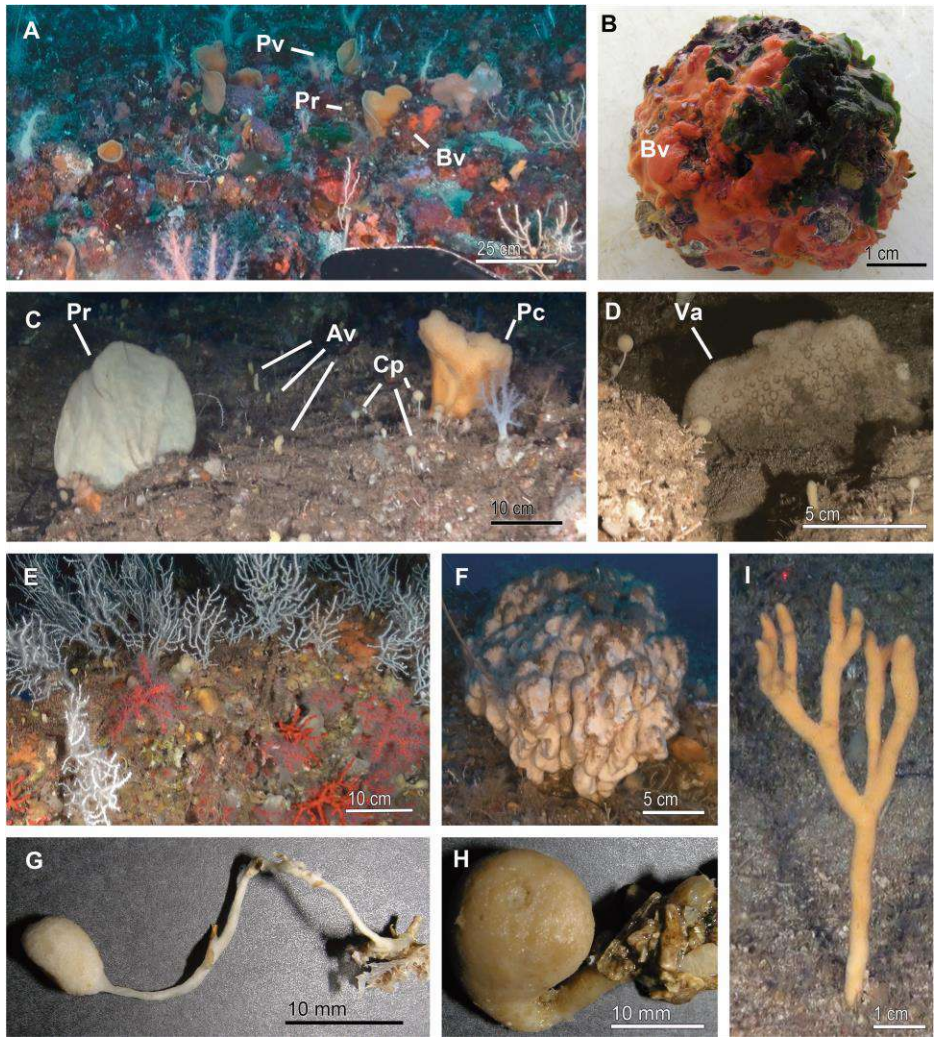

Figure 2. Benthic communities on the deep shelf of the Alboran Island in which sponges are important members. (A) View of a rhodoliths bottom dominated by cnidaria and sponges. The most abundant sponges were *Phakellia ventilabrum* (Pv), *Phakellia robusta* (Pr), and *Bubaris vermiculata* (Bv). (B) Detail of a rodolith, largely encrusted by *Bubaris vermiculata* (Bv). (C) View of a gently sloping rocky bottom, showing large specimens of *Phakellia robusta* (Pr) and *Poecillastra compressa* (Pc) together with a dense "canopy" of small digitiform, claviform and globiform sponges, such as *Axinella vellerea* (Av) and *Crella pyrula* (Cp). (D) Individual of *Vulcanella aberrans* (Va) surrounded by small globiform and digitiform sponges.

…*continued in the next page*

(E) Benthic community on the outcrops dominated by cnidarians, including the octocoral *Corallium rubrum*. Abundant massive, submassive and encrusting sponges are common under the gorgonian forest. (F) Large astrophorid sighted from the ROV on the top of an outcrop, probably belonging to the genera *Geodia* or *Stelletta*. (G) Collected specimen of *Crella (Yvesia) pyrula* (MNHN-Sp136-DR44). (H) Collected specimen of *Rhizaxinella gracilis* (MNHN-Sp22-BV14). (I) A solitary specimen of *Axinella salicina* located by the ROV on a coarse-sand and gravel bottom, a substrate type that generally shows a low abundance of sponges.

Vulcanella aberrans, along with small digitate and stalked sponges were also present, though in lower abundance.

Large areas of the deep shelf were covered with soft bottom, particularly on the north side of the island. The substrate mostly consisted of coarse sand mixed with calcareous gravel, more rarely incorporating a low proportion of mud. In contrast to the above-described hard-bottom communities, the soft bottoms were poor in sponges. Nevertheless, despite their general low sponge abundance, this bottom type hosted scattered individuals of rare and/or endemic species, such as *Axinella salicina* (Fig. 2I) and a new species of the genus *Endectyon*.

A total of 631 demosponges *sensu lato*: (i.e., Demospongiae + Homoscleromorpha) have been listed for the Mediterranean (Voultsiadou 2009; Calcinai et al. 2013; the present study). Interestingly, the shelf of the Alboran Island by itself hosts 194 demosponge species (Appendix II), which means about 30.4% of the total Mediterranean demosponge fauna. Such a remarkable percentage points clearly this island shelf to be a remarkable biodiversity hotspot in terms of demosponge fauna (and probably of several other groups of benthic invertebrates as well). Altogether, the abundance and taxonomic singularity of the sponge fauna occurring in these deep-shelf bottoms strongly suggest these habitats to be accommodated within the environmental protection of the Nature 2000 Network.

Systematics

Herein we are providing full taxonomic description of 8 collected demosponges that have been considered of special interest because being new to science, providing new records for the Mediterranean Sea, or being exceptionally rare species.

Phylum PORIFERA Grant, 1836
Class DEMOSPONGIAE Sollas, 1885
Order ASTROPHORIDA Sollas, 1887
Family ANCORINIDAE Schmidt, 1870
Genus *Jaspis* Gray, 1867

Diagnosis: Encrusting or massive sponges without triaenes; choanosomal skeleton composed of oxeas irregularly interlaced, ectosomal skeleton formed by a layer of paratangential oxeas generally smaller than those in the choanosome; microscleres are euasters without a centrum; never being spherasters (*sensu* Uriz 2002).

Jaspis eudermis Lévi & Vacelet, 1958

(Figs. 3A, 4; Appendix I)

Material examined: Specimen MNCN-Sp71-BV10 collected from Stn. 10 (Table 1; Fig 1).

Comparative material: Holotype of *Jaspis eudermis* Lévi & Vacelet, 1957 (MNHN DCL-738) from Princess Alice Bank, Azores (Stn. 62; 37º47'N 29º03'W, 330 m deep, 1955-1956).

Macroscopic description: Creamy white (in alcohol), cushion-shaped sponge, being 45 x 23 mm in size (Fig. 3A). Consistency firm, but friable. Surface nearly glabrous, covered by a friable, detachable, thick membrane (crust-like), with no discernible aquiferous openings. At the zones where the ectosomal crust is lost, subdermal aquifer canals of up to 1mm in diameter are evident.

Spicules: Megascleres are oxeas, which seem to occur in two categories. Oxeas I are 1125-2000 x 20-40 μm and fairly abundant. They are once or twice

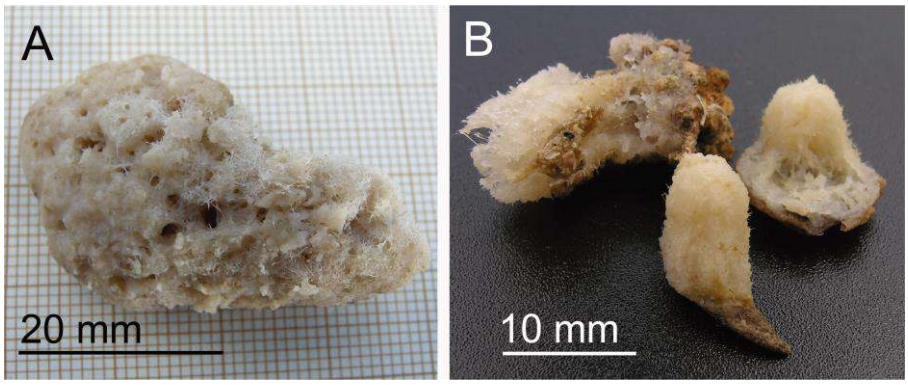

Figure 3. (A) Specimen of *Jaspis eudermis* Lévi & Vacelet, 1958 collected from Alboran and photographed on graphic paper (MNCN-Sp71-BV10). (B) Three Alboranian specimens of *Hemiasterella elongata* Topsent, 1928 (from left to right, MNCN-Sp66-BV21, MNCN-Sp66 B & A).

slightly bent, frequently asymmetric, usually with acerate tips, occasionally blunt (Fig. 4A-B). Oxeas I showing irregular shapes are also occasional (Fig. 4C). Oxeas II are 390-1500 x 5-10 μm, and comparatively quite scarce; they are slightly curved, sometimes centrotylote, and with conical or acerate ends (Fig. 4A). Microscleres are oxyasters, with 12-20 conical, smooth actines (Fig. 4A, D); their total diameter ranges from 20 to 65 μm, but with no discernible size categories.

Skeletal structure: There is an ectosomal, crust-like skeleton consisting of abundant oxyasters and tangential oxeas (mostly type II) irregularly disposed in small groups. The choanosomal skeleton consists of oxeas in disordered arrangement, along with abundant oxyasters.

Distribution and ecology notes: Rare species, previously known only from Azores (Northeastern Atlantic). The only specimen herein collected from a gravel bottom at depths of 214-290 m provides the first record of the species in the Mediterranean Sea.

Taxonomic remarks: Several species of *Jaspis* occur in the Mediterranean or in the adjacent eastern North-Atlantic zone, but most of them have spicules clearly smaller than those of *J. eudermis*. The only exception is *Jaspis incrustans* (Topsent, 1890), which has fairly large oxeas that reach 1250 μm in length. Nevertheless, oxyasters of *J. incrustans* measure only up to 26 μm in total

diameter and their actines are clearly spiny rather than smooth (Maldonado, 1993).

Our material fits reasonably the only brief description available for *J. eudermis*, which corresponds to the holotype, a fragmentary, 2 x 2 x 1 cm, cushion-shaped sponge. It was reported to have a single category of 1200-1650 x 45 μm oxeas (versus two in our specimens) and 35-45 μm oxyasters. The oxyasters were pictured by Lévi & Vacelet (1958) as having more than 10

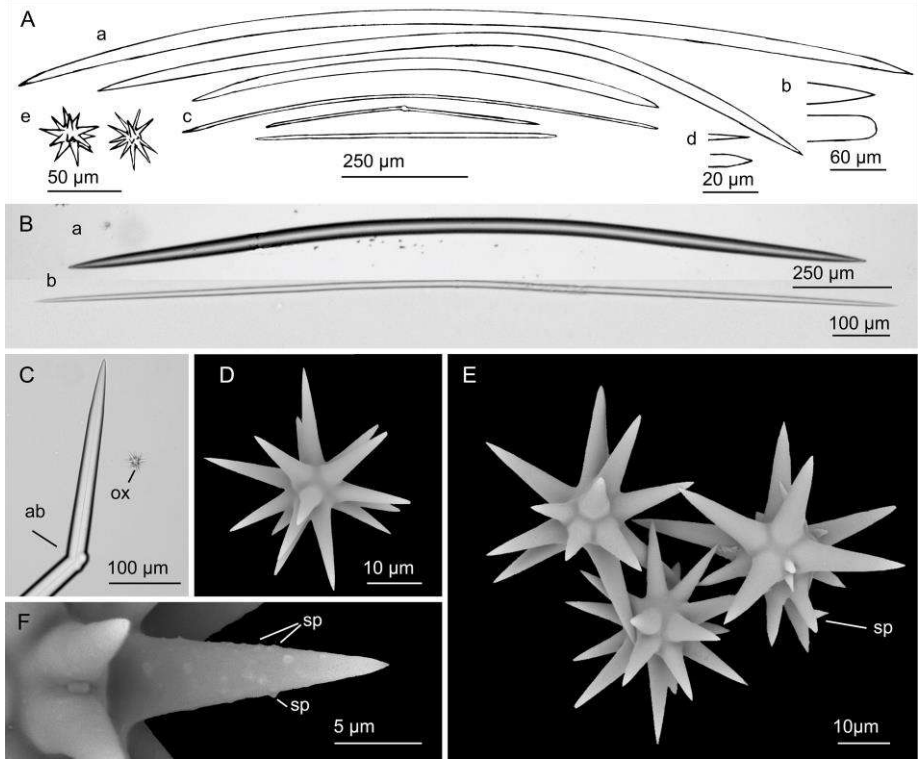

Figure 4. *Jaspis eudermis* Lévi & Vacelet, 1958: (A) Line drawing of the spicule complement of the Alboranian specimen (MNCN-Sp71-BV10), consisting of oxeas I (a) with acerate or blunt ends (b), oxeas II (c) with acerate or conical ends (d), and oxyasters (e). (B) Light microscope micrographs of oxeas I (a) and oxeas II (b). (C) An abnormal end (ab) of an oxea I next to an oxyaster (ox). (D) SEM micrograph of an entirely smooth oxyaster. (E) SEM image of several oxyasters of the holotype of *J. eudermis* (Stn. 62 MNHN DCL738), one having some large spines (sp) on the actine. (F) Detail of an oxyaster actine of the holotype showing minute spines (sp).

actines with a smooth (not spiny) surface. Our revision of the holotype indicates that there are indeed two size categories of oxeas, discernible not only because of their thickness (1225-1725 x 30-60 μm and 660-850 x 8-10 μm, with some occasional transitional stage), but also because of their shape, being the smaller category isodiametric and more markedly curved than the fusiform oxeas of the larger category. This reinterpretation of the oxea size distribution brings our specimen and the holotype in full skeletal agreement, as they also share the general traits of the macroscopic morphology and skeletal architecture. Furthermore, they both are the only *Jaspis* material in the Atlantic-Mediterranean region having large, "smooth" oxyasters with more than eleven actines. In this regard, our SEM re-examination of the holotype provides new interesting information. The oxyasters of the holotype measure 30-55μm in total diameter and have 16 to 20 actines. Most of the actines are entirely smooth (Fig.4E), as it also happens consistently in the Alboranian specimen (Fig.4D). Nevertheless, under high SEM magnification approximately 20% of the oxyasters of the holotype show subtle microspines in one or more of their actines (Fig. 4F). In very few occasions, large, isolated spines also occur (Fig. 4E). Therefore, the "smooth" nature of the actines of *J. eudermis* is to be assessed in further detail when more specimens are collected.

Order HADROMERIDA Topsent, 1894
Family HEMIASTERELLIDAE Lendenfeld, 1889
Genus *Hemiasterella* Carter, 1879

Diagnosis: Hemiasterellidae with vasiform, plate-like, flattened branching or massive growth form; choanosomal and peripheral skeletons are loosely organized, vaguely plumoreticulate, without apparent axial compression or differentiation between axial and extra-axial regions. The spicule complement consists of styles and/or oxeas without functional arrangement to any particular part of skeleton and euasters predominantly located in peripheral region of the sponge but not forming a surface crust. The euasters typically show thick, acanthose, strongylote, curved, asymmetrical or branching actines; sometimes calthrop-like, reduced in number to 2–4 actines (*sensu* Hooper 2002a).

Hemiasterella elongata Topsent, 1928

(Figs. 3B, 5; Appendix I)

Material examined: Four specimens collected: MNCN-Sp66-BV21 from Stn. 21; MNCN-Sp04-DR29 from Stn. 29 m; and MNCN-Sp20-BV33A & B from Stn. 33 (Table 1, Fig. 1).

Macroscopic description: Specimens with columnar shape, measuring 5-15 x 4-7 mm (Fig. 3B). The individuals are settled on rock pieces, over which slightly expand their base. The surface shows irregularly shallow folds and grooves, mostly running parallel to the longest body axis. The ectoderm is membrane-like and bears a sparse and uneven hispidation. Pore-like aquiferous opening are visible, especially in the lower half of the body. Color is bright to creamy white both in life and after preservation in ethanol.

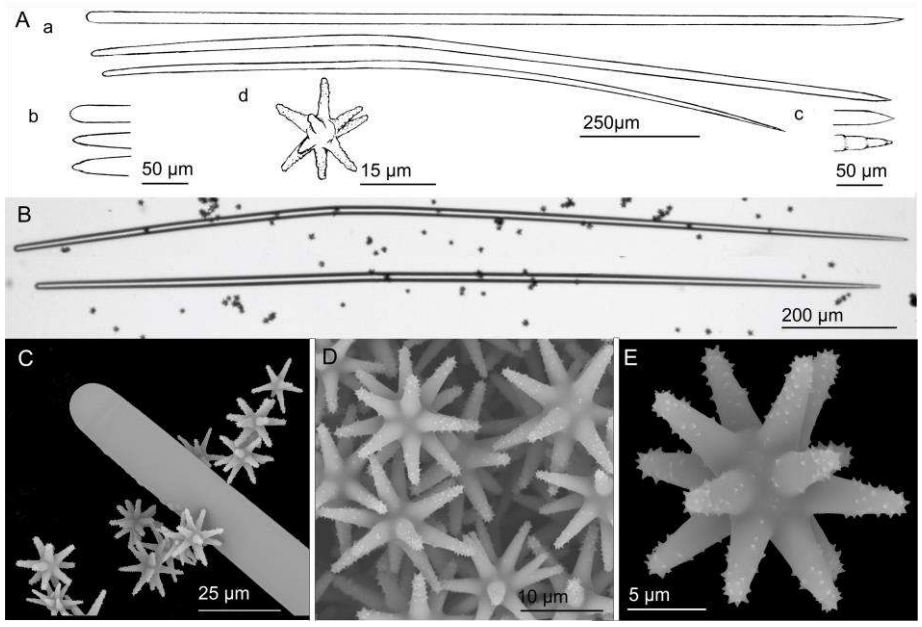

Figure 5. *Hemiasterella elongata* Topsent, 1928: (A) Line drawing summarizing the skeletal complement of the Alboranian specimens, consisting of long, isodiametric styles (a) with a round to strongylote end (b) and an acerate or stepped distal end (c), and spiny spherostrongylasters (d). (B) Light microscope view of two differently curved styles. (C) SEM micrograph of a typical round end of a style surrounded by spherostrongylasters. (D-E) SEM details of spherostrongylasters, with spiny actines.

Spicules: Megascleres are styles, measuring 1316-2250 x 10-30 μm. They are straight, markedly curved, or just with a slight asymmetrical curvature (Fig. 5A-B). The round end of the styles may also be in a stronglyoxea fashion; the pointing end is regularly acerate or, less frequently, stepped, not very sharp (Fig. 5A-C). Styles with both ends modified into oxea are very rare (e.g., one of 1825 x 10 μm per slide) or absent, depending on the individuals. Microscleres are abundant spherostrongylasters, with only a moderately developed centrum and 10-15 strongylote, slightly conical, spiny actines (Fig. 5A, C-E). Spines are denser toward the end of the actines. Spherostrongylasters range from 14 to 23 μm in total diameter.

Skeletal structure: The skeletal arrangement shows no axial condensation. Ascending plumose pauci- or multispiculate tracts of styles that ramify below the ectosome and may end in plumose tufts that make an hispid surface. There is scarce spongin connecting and packing the spicules in the tracts. Spherostrongylasters are very abundant overall the skeleton, but especially at the periphery, where they make a layer reinforcing the ectosome.

Distribution and ecology notes: Rare species, previously known only from its holotype collected at Cape Verde Islands, eastern North Atlantic (Topsent 1928). The herein collected individuals provide the first record of the species for the Mediterranean Sea. All the collected specimens inhabited 93 to 173 m deep, soft bottoms rich in organogenic gravel, occasionally mixed with pieces of dead rhodoliths.

Taxonomic remarks. The collected specimens bear overall similarity with the holotype described by Topsent (1928). Nevertheless, some morphological differences occur. The holotype shows two incipient branches, while the Alboranian specimens show no sign of branching. Another difference is that the Alboranian individuals have thinner styles (10-30 μm) than the holotype (25-60 μm).

Hemiasterella aristoteliana Voultsiadou-Koukoura & Van Soest, 1991, the only *Hemiasterella* representative recorded in the Mediterranean previously, occurs in the northern Aegean Sea. Although it has also styles and strongylasters as the only spicule types, the species is clearly distinguishable from *H. elongata*, because the former has much longer styles (1800-3000 x 18-37 μm) and its asters are commonly reduced to forms with only 1 to 3 actines (Voultsiadou-Koukoura & van Soest, 1991).

As noted by Topsent (1928), there are some similarities between *H. elongata* and *Hemiasterella vasiformis* (Kirkpatrick, 1903) from South Africa. Nevertheless, the latter has a caliculate body shape, many styles becoming tylostyles and strongyles, and a bit larger asters (up to 30 μm of diameter) (Kirkpatrick, 1903).

Together with the Antarctic *Hemiasterella digitata* Burton, 1929, *H. elongata* shows an uncommon shape within the genus, but that of *H. digitata* is better described as palmo – digitate, with a surface strongly hispid in small patches and neither oscules nor pores visible (Burton, 1929).

Order HALICHONDRIDA Gray, 1867
Family AXINELLIDAE Carter, 1875
Genus *Axinella* Schmidt, 1862

Diagnosis: Ramose, bushy or lamellate habit. Surface generally smooth, with choanosomal spicules projecting slightly. Oscules, when visible, with stellate morphology (i.e., superficial canals leading to opening 'imprinted' in superficial skeleton). Ectosome without specialized skeleton. Choanosomal skeleton differentiated in axial and extra-axial regions; axial skeleton compressed or vaguely reticulated. Extra-axial skeleton plumose or plumoreticulate. Megascleres styles, or styles and oxeas, or oxeas; when both present, one type may be rare; modifications of megascleres common in several species. Microscleres, if present, microraphides and raphides, mostly in tightly packed trichodragmata (*sensu* Alvarez & Hooper, 2002).

Remarks: Recent molecular work based on 18S rRNA, 28S rRNA, and CO1 has suggested that the genus *Axinella* is polyphyletic, containing at least two major clades (Gazave et al., 2010; Morrow et al., 2012). One of the clades—the proper "Axinella clade"—revolves around the type species, *Axinella polypoides* Schmidt, 1862, while the other, which includes species such as *Axinella damicornis* (Esper, 1794), *Axinella verrucosa* (Esper, 1794), and *Axinella corrugata* (George & Wilson, 1919), shows greater affinities to agelasid sponges than to the *A. polypoides* clade. The name "Cymbaxinella clade" has been proposed to allude these latter molecular-based group, following the phylocode (Gazave et al., 2010). As no morphological synapomorphies can be found to decide when an "Axinella-like" species should be allocated to the "Cymbaxinella" clade or the "Axinella" clade (Gazave et al., 2010), whenever the molecular

information is not available for a species a serious practical gap rises between the phylocode proposal and the traditional Linnean classification. Subsequent work based on 28S rRNA and CO1 molecular markers has revealed that the "Axinella-like" members of the "Cymbaxinella" clade are closer to encrusting species, such *Hymerhabdia typica* Topsent, 1892 (formerly in Bubaridae) and *Prosuberites* spp. (formerly in Suberitidae), than to *Agelas* spp. On those arguments, a new family Hymerhabdiidae was erected in the Order Agelasida to assemble together *Prosuberites* spp. *Hymerhabdia* spp., those "Axinella" species in the "Cymbaxinella" clade, and some species formerly in the genus *Stylissa* (Morrow et al., 2012). But again, no morphological clues have been provided to decide in the absence of molecular information when either a newly described or an old, revisited "Axinella-like" species could belong to this new family. Tentatively, Morrow and co-workers (2012) have suggested that "true Axinella" species, such as *A. polypoides*, have raphides in trichodragmata, while those in the "Cymbaxinella" clade of Agelasida "apparently lack this spicule type". Following, this tentative argument, we cannot rule out the possibility that at least one of new species herein described as *Axinella* but lacking raphides (i.e., *Axinella alborana* nov. sp.) could be reallocated into another genus in the future if newly collected specimens can ever be analyzed by molecular methods and the emerging molecular clades are finally given taxonomic status. Likewise, this could also be the case of the rare *Axinella vellerea* Topsent, 1904, which is herein morphologically revisited in detail.

Axinella alborana sp. nov.

(Figs. 6A-C, 7; Tables 2, 3; Appendix I)

Etymology: This species is named after the Alboran Island, where it occurs abundantly.

Material examined: Holotype MNCN-Sp155-DR44A from type locality Stn. 44 (Table 1, Fig. 1), a rocky bottom at depths of 135 to152 m on the Alboran Island shelf. Thirty-three paratypes designated: MNCN-Sp03DR05A to C from Stn. 5; MNCN-Sp13-DR07A & B from Stn. 7; MNCN-Sp14-BV13A & B from Stn. 13; MNCN-Sp34-BV14A to F from

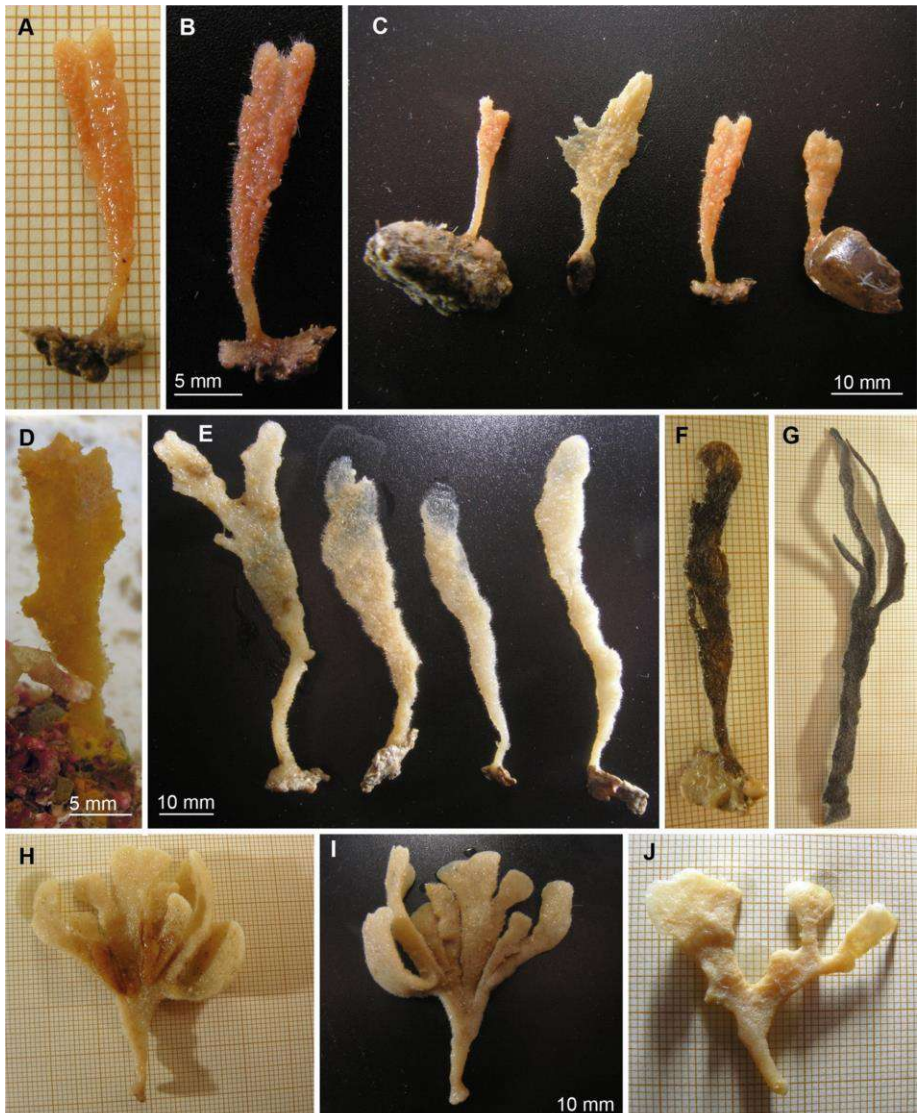

Figure 6. (A-B) Holotype of *Axinella alborana* sp. nov. seen from its both sides (MNCN-Sp155-DR44A). (C) Four additional, collected specimens of *A. alborana* sp. nov. (from left to right, MNCN-Sp3-DR05A, MNCN-Sp146-BV33A, MNCN-Sp155-DR44A, MNCN-Sp146-BV33B). (D) Specimen of *Axinella spatula* sp. nov. photographed on board immediately after collection. (E) Preserved specimens of *A. spatula* sp. nov., being the first (from left to right, MNCN-Sp145) the holotype; the remaining specimens are BV33B, MNCN-Sp116-BV15A & B, and MNCN-Sp65-BV21B.

…continued in the next page

(F-G) Blackish specimens (MNCN-Sp57-BV21A and MNCN-Sp57-BV21B, respectively) of *A. spatula* sp. nov. The former shows an incipient branching, while the latter is clearly branched and with no narrowing at the stalk. (H-J) Syntypes of *Tragosia flustra* (Topsent, 1892) collected by Topsent in 1888 (Stn. 247. M. O. M. 040272) and in 1886 (Stn. 58. M. O. M. 040044), respectively. The former (H-I) is shown on its both sides, being profusely ramified, while the latter (J) shows only 2 to 3 branches.

Stn. 14; MNCN-Sp19-DR29A to D from Stn. 29 m; MNCN-Sp146-BV33 A to N from Stn. 33; MNCN-Sp191-BV41 from Stn. 41; and MNCN-Sp155-DR44B from Stn. 44 (Table 1, Fig. 1).

Comparative material: Syntype material of *Axinella flustra* (Topsent, 1892) = *Tragosia flustra* Topsent, 1892, since no holotype was designated by Topsent (1892) for this species (Table 3). Syntypes were two specimens (MOM-040044) from Bay of Biscay (Stn. 58; 43º40'N 8º55'W, 134 m deep, 7 August 1886) and two specimens (MOM-040272) from Azores (Stn. 247; 38º23.500'N 30º20.333'W, 318 m deep, 30 August 1888).

Macroscopic description: Erect, stalked, flattened sponge, typically attached to small fragments of rocks or shell fragments (Fig. 6A-C; Table 2). The stalk is either cylindrical or compressed, no longer than one quarter of the total sponge length, and hardly recognizable in some specimens. The flattened part of the body is flexible and relatively rectangular, except for the apical margin of the lamina that may be irregularly lobate. Some specimens show an incipient, terminal ramification; none is markedly divided nor further branched. The sponges measure 10-28 mm in height, with a lamina up to 19 mm in wideness and 1-2 mm in thickness. The surface is irregularly hispid, with no aquiferous opening discernible. The color ranges from creamy to reddish orange in life, clearing after preservation in ethanol.

Spicules: Megascleres are styles and oxeas (Table 2). Styles are slightly curved at a third of their length (Fig. 7A-B), with a regular round end that occasionally forms one or two slight subtyles and/or annular swellings (Fig. 7C). The pointed end is usually sharp, but rarely blunt ends occur. Styles measure 630-2375 x 5-20 μm, although two specimens showed a low proportion (<1%) of abnormally shorter or longer styles, measuring respectively down to 580 μm and up to 3000 μm in length (Table 2). Oxeas are slightly or markedly

Table 2. Comparative data of *Axinella alborana* sp. nov. specimens, including branching level, color after preservation, and size range of styles and oxeas.

Specimen	Branching	Colour (alcohol)	Styles (μm)	Oxeas (μm)
MNCN-Sp03-DR05A	unbranched	orange	990-1800 x 10-20	270-560 x 5-20
MNCN-Sp03-DR05B	2 incipient branches	reddish orange	1100-2375 x 1-20	180-580 x 7.5-15
MNCN-Sp14-BV13A	2 incipient branches	pale orange	630-2075 x 5-20	260-650 x 5-20
MNCN-Sp34-BV14A	2 incipient branches	pale orange	580-1300 x 10-20	125-620 x 5-15
MNCN-Sp34-BV14B	2 incipient branches	whitish orange	975-2000 x 10-20	360-630 x 10-20
MNCN-Sp19-DR29A	damaged	pale orange	710-1625 x 7.5-15	360-610 x 7.5-20
MNCN-Sp146-BV33A	2 incipient branches	pale orange	630-1400 x 7.5-20	290-580 x 10-20
MNCN-Sp146-BV33B	2 incipient branches	pale orange	730-2250 x 5-20	280-620 x 5-20
MNCN-Sp191-BV41A	unbranched	whitish orange	825-1750 x 7.5-20	350-550 x 10-20
MNCN-Sp155-DR44A	2 incipient branches	reddish orange	1000-3000 x 10-20	390-600 x 15-20

fusiform, curved once or twice, either symmetrically or asymmetrically (Fig. 7A, D). Points are usually acerate; anisoxeas are fairly common and variations like mucronate and blunt ends are frequent, depending on the specimen (Fig. 7D). Occasionally they are centrotylote, with annular or subspherical swellings (Fig. 7D) being smooth or rarely rugose. They measure 260-650 x 5-20 μm, but shorter oxeas, down to 180 and 125 μm in length, occur respectively in 2 of the studied specimens. As a rule of thumb, oxeas are more abundant than styles.

Skeletal structure: An axial skeleton is discernible in the stalk, made of ascending compact tracts of oxeas embedded by spongin and crossed by isolated (i.e., not packed) oxeas arranged confusedly. From the axial skeleton, an extra-axial plumoreticulate skeleton emerges, consisting of ascending loose pauci- and multispicular tracts of oxeas reinforced with some spongin (Fig. 7G). In the extra-axial region, there are isolated inter-crossed oxeas forming a confusing reticule-like arrangement (Fig. 7H). Long styles, either isolated or in small groups (2-4), project outward from the spongin cover of the extra-axial tracts, piercing the sponge surface to make it hispid.

Distribution and ecology notes: The individuals were collected at the deep shelf (87 to 173 m) of the Alboran Island, from rocky, detritic-organogenic gravel, and rhodolith bottoms.

Taxonomic remarks: No previously known *Axinella* spp. in the Atlantic-Mediterranean area have characteristics similar to those of the new species (Table 3). The external morphology of *A. alborana* sp. nov. bears some external resemblance to *A. flustra* (Fig. 6H-J), especially to Topsent's (1904) syntypes from Stn. 247 (Fig. 6H-I). Nevertheless, both species strongly differ skeletally, including *A. flustra* having trichodragmata and shorter oxeas (Table 3). *Axinella vaceleti* Pansini, 1984 is also a flabellate species, but with a marked fan-

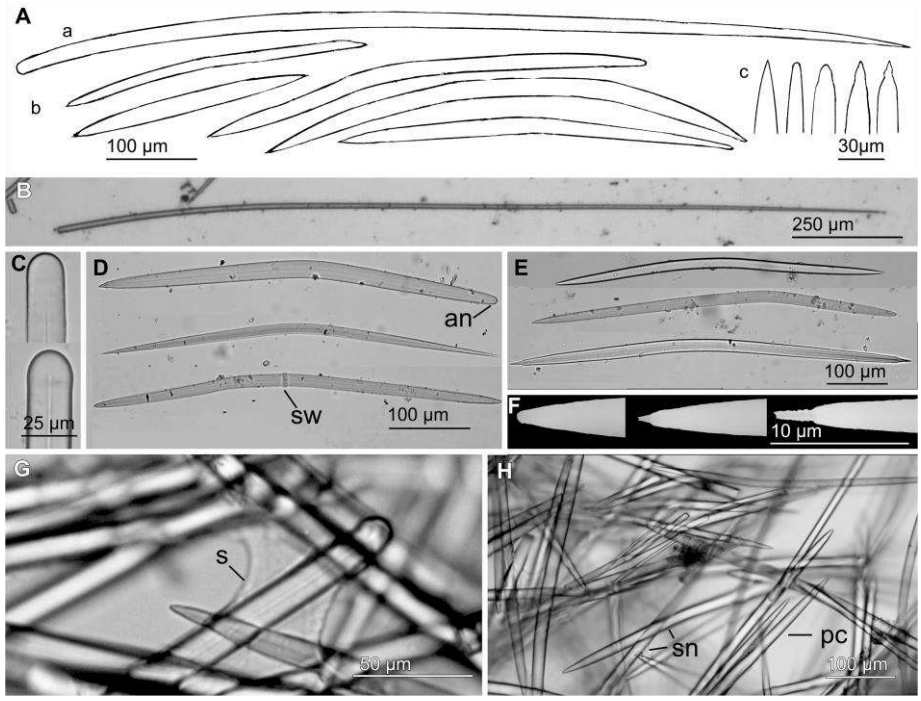

Figure 7. *Axinella alborana* sp. nov.: (A) Line drawing summarizing the skeletal complement of the Alboranian specimens, consisting of styles (a) and oxeas (b) with acerate, blunt or mucronate ends (c). (B-C) Light microscope view of a style, with examples of the round end. (D-E) Light microscope views of oxeas. Note the varying curving angle, the anisoxea (an) character in some spicules, and the annular swelling (sw) of others. (F) SEM details of oxea ends, being typically either blunt or mucronate. (G) Light microscope view of the skeletal arrangement, showing a style embedded in spongin (s) in the extra-axial skeleton. (H) Light microscope view of oxeas at the extra-axial plumoreticulate skeleton occurring either in paucispicular tracts (pc) or free (sn).

Table 3. Summary of sponge standing Comparative data of *Axinella* spp. previously described from the Atlantic-Mediterranean zone and skeletally and/or morphologically related to those reported in the present study (bottom of species list). Numbers in brackets following the species name indicate bibliographic references, as it follows: (1) Descatoire, 1966; (2) present study (2); (3) Topsent, 1892; (4) Topsent, 1896; (5) Topsent, 1928; (6) Lendenfeld, 1897; (7) Lévi, 1957; (8) Pulitzer – Finali, 1983; (9) Babiç, 1922; (10) Boury-Esnault et al.,1994; (11) Pansini, 1984; (12) Topsent, 1904; (13) Burton, 1931. Dashes refer to the absence of data in the references and blanks in the "Styles" or "Oxeas" columns indicate the absence of a particular spicule type. Abbreviations for skeletal structure are: pl= plumose; pr= plumoreticulate.

***Axinella* spp. (references)**	**Distribution**	**Shape and size (length x width in mm)**	**Color**	**Styles (µm)**	**Oxeas (µm)**	**Trichodrag-mata (µm)**	**Skeletal structure**
A. alba (11)	Glénan Islands (Atlantic Ocean)	encrusting base (25mm long) with 3 erect processes (15 x 5-8)	white	250-1200 x 15-18 (I) 260-950 x 3-10 (II)	700-1000 x 15-18	40-60 (raphides)	pl
A. flustra (3)	Bay of Biscay, Azores (Atlantic Ocean)	erect, stalked, with flattened branches (50 x 50)	beige (in alcohol)	870 x 16	185 x 7 (axis) 255 x 13 (body)		pr
A. flustra, revised syntypes (15)	Bay of Biscay, Azores (Atlantic Ocean)	erect, stalked , with 1-8 flattened branches (24-50 x 30-50)	yellowish white (in alcohol)	190->900 x 10-20	160-340 x 7.5-15	47-50	pr
A. flustra, as *A. padina* (4)	Gulf of Lion (Mediterranean Sea)	erect, foliaceous , with 4 spatula-shaped lobes (40x35)	_____	650-900 x 8-10	250-275 x 3-6	40 (raphides)	pr
A. flustra, as *Tragosia flustra* (8)	Cape Verde (Atlantic Ocean)	erect, stalked, foliaceous (30-40 x 35-40)	orange yellow (in vivo)	300- >1000 x 10-20	160-320 x 3-15	25-36 x 3-5	pr
A.infundibuliformis, as *Trinachophora microdragma* (5)	Rockall bank (Atlantic Ocean)	flabellate or caliculate (no size given)	_____	300-600 x 12-16	250-500 x 10-15	15-20 x 5-6	pr

Axinella spp. (references)	Distribution	Shape and size (length x width in mm)	Color	Styles (µm)	Oxeas (µm)	Trichodragmata (µm)	Skeletal structure
A. minuta (10)	Gabes Gulf , Alexandria (Western Mediterranean)	cushion-shaped encrusting base from which some processes rise up (2 x 2)	_____	120-300 (I) 1200 (II)	120-300		pr
A. minuta (13)	Corse (Mediterranean Sea)	Incipiently and irregularly branched (15 x 11)	_____	150-490 x 5.5-14 (I) 1300-1700 x 11.5-30 (II)	180-600 x 4.5-14		_____
A. pumila (7)	Adriatic Sea (Mediterranean Sea)	encrusting, resembling a grass lawn (no size given)	yellowish pink (in alcohol)	255-935 x 8-6 (I) 2000 x 19 (II)	170-730 x 2-18		_____
A. pumila (14)	Alboran Sea (Mediterranean)	massive (no size given)	white (in alcohol)	790-1300 x 20-25	350-520 x 12-15		pr
A. vaceleleti (12)	Portofino,Marseille, Marconi Gulf (Mediterranean Sea)	Flabellate (50-60 x 40-50)	orange (in vivo); white (in alcohol)	270-1450 x 2.5-14	250-370 x 2-12		pl
A. vellerea (6)	Azores (Atlantic Ocean)	clavate or stalked and branched (45-90 x 17)	yellowish white (in alcohol)	1000 x 30-40 (I) 1800 (II)			pl
A. vellerea, revised syntypes (15)	Azores (Atlantic Ocean)	markedly or slightly branched (45-97 x 18-40)	ochre (in alcohol)	825-1625 x 12-35			pl
A vellerea (9)	Folden Fiord (Norwegian Sea)	massive, as incipient, erect columns (no size given)	yellowish white (in alcohol)	_____	_____		_____
A. vellerea (15)	Alboran Island (Mediterranean Sea)	columnar, undivided or with 2-3 incipient lobule-like branches (10-30 x 5-8)	ochre to light brown (in alcohol)	470-1725 x 11-30	700-1120 x 5-20		pr
A. alboranica sp. nov.(15)	Alboran Island (Mediterranean Sea)	erect, stalked , and flattened, sometimes with incipient branches (10-28 x 2-19)	pale to bright orange (in alcohol)	630-2375 x 5-20	260-650 x 5-20		pr
A.spatula sp.nov. beige specimens(12)	Alboran Island (Mediterranean Sea)	erect, flabellate, undivided or with 2 branches (35-75 x 6-13)	beige (in alcohol)	119-1400 x 3-30	180-750 x 2.5-20	25-35 x 5-7.5	pr
A. spatula sp.nov. black specimens (12)	Alboran Island (Mediterranean Sea)	erect, flabellate, undivided or with 2-3 branches (35-100 x 2-8)	black (in alcohol)	350-1400 x 5-20	120-500 x 2.5-20	25-30 x 6-10	pr

shaped, undulating lamina, which is also larger (50-60 mm high) and thicker (4-5 mm) than that of the *A. alborana* sp. nov. specimens. Additionally, *A. vaceleti* has smaller spicules, specially the styles, ranging from 270 to 1450 μm (Pansini, 1984).

Specimens of *Axinella alborana* sp. nov. were investigated for the first time about twenty years ago, as part of a study on the deep-shelf Alboranian sponges carried out by Maldonado (1993). Nevertheless, no description of material was published at that time because of the risk that the small individuals now described as *A. alborana* sp. nov. might correspond to juvenile stages of some poorly known, large *Axinella* spp. growing at the ill-known deep shelf. However, our recent exploration of those deep-shelf habitats using an ROV has revealed that there is no dense population of any other large *Axinella* spp. in the areas where *A. alborana* sp. nov. occurs. In the light of these findings, the idea that the dense undergrowth of small individuals might correspond to juvenile sponges makes no sense and these small sponges can indeed be identified as adults of *A. alborana* sp. nov.

Axinella spatula sp. nov.

(Figs. 6D-G, 8; Tables 3, 4; Appendix I)

Etymology: The species is named after the "spatula" tool (a diminutive form of the Latin "spatha"), which bears resemblance to the external shape of the specimens.

Material examined: Holotype MNCN-Sp145-BV33B collected from type locality Stn. 33 (Table 1, Fig 1), a 134 to 173 m deep, gravel bottom at the deep shelf of the Alboran Island.

Twenty-two paratypes designated: MNCN-Sp28-BV14A to C from Stn. 14; MNCN-Sp116-BV15A to I from Stn.15; MNCN-Sp57-BV21A to C (blackish specimens) and MNCN-Sp65-BV21A & B from Stn. 21; MNCN-Sp145-BV33A & C to D from Stn. 33; MNCN-Sp188-BV41A & B from Stn. 41 (Table 1, Fig. 1).

Comparative material: Syntype material of *Axinella flustra* (Topsent, 1892) = *Tragosia flustra* Topsent, 1892, since no holotype was designated by Topsent

Table 4. Comparative data of *Axinella spatula* sp. nov. specimens, including branching level, color after preservation, and size range of styles and oxeas.

Specimen	Branching	Colour (alcohol)	Styles (µm)	Oxeas (µm)	Trichodragmata (µm)
MNCN-Sp28- BV14A	unbranched	beige	170-1300 x 8-20	180-430 x 5-12	22.5-32.5 x 8-10
MNCN-Sp28- BV14B	unbranched	beige	310-1250 x 5-10	210-450 x 4-10	25-28 x 5-8
MNCN-Sp57- BV21A	unbranched	black	350-1400 x 5-20	220-500 x 2.5-20	25-30 x 6.25-10
MNCN-Sp57- BV21B	2 incipient branches	black	245-1225 x 8-18	120-432 x 9-12	25-30 x 6-10
MNCN-Sp65 -BV21A	unbranched	beige	220-1100 x 5-30	220-520 x 5-10	25-30 x 9-10
MNCN-Sp145-BV33A	2 incipient branches	beige	165-1050 x 3-15	180-520 x 2.5-15	25-30 x 5-8
MNCN-Sp188- BV41A	unbranched	beige	119-1400 x 4-15	190-750 x 5-20	25-35 x 5-8

(1892) for this species (Table 3). Syntypes were two specimens (MOM-040044) from Bay of Biscay (Stn. 58; 43º40'N 8º55'W, 134 m deep, 7 August 1886) and two specimens (MOM-040272) from Azores (Stn. 247; 38º23.500'N 30º20.333'W, 318 m deep, 30 August 1888).

Macroscopic description: Erect, flabellate sponges (Fig. 6E-G; Table 4). They are 35-100 mm in height, with a basal stalk-like region in which the lamina progressively increases in wideness from the attachment point up to about 1/4 of the height, where it becomes approximately rectangular (3-9 mm in wideness). The lamina is thin (1-1.5 mm) and flexuous. It can be undivided, or, in some individuals, forming two or three flattened branches, all with a regular apical margin (Fig. 6E). The sponge surface is porous to the dissecting microscope, largely and irregularly hispid. Most collected individuals are pale orange when alive, turning into yellowish white after ethanol preservation. Nevertheless, three of the specimens show remarkable color dissimilarity, being dark brown to black, at least after preservation in ethanol (Fig. 6F-G). Some of these blackish specimens (part of the paratype series) also account for the largest sizes (up to 100 mm in height) and have the stalk-like region more flattened than the orange-beige individuals.

Spicules: Megascleres are styles and oxeas (Table 4). Styles occur in a wide variety of size and shape, with abundant intermediate forms that prevent making putative categories. Styles are often slightly curved, either symmetrically or asymmetrically; sometimes they have more than one flexion point and can even be angulated and, more rarely, slightly sinuous (Fig. 8A-

C). The round end is usually regular, occasionally with an annular swelling (Fig. 8A). The distal end is of variable morphology, from sharp hastate or acerate type to stepped, mucronate, and almost blunt (strongyloxea-like) type (Fig. 8A). Styles measure 119-1400 x 3-30 μm, not being further categorizable according to their size. They are also difficult to separate according to their location, but most of those in the choanosomal region are not larger than 550-

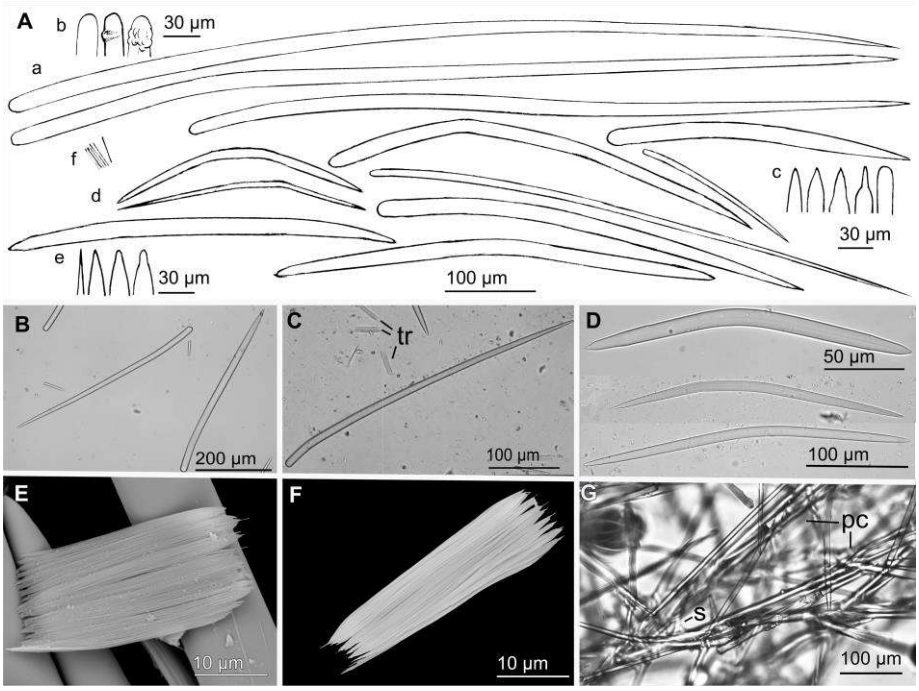

Figure 8. *Axinella spatula* sp. nov.: (A) Line drawing summarizing the skeletal complement of the Alboranian specimens. It consists of styles (a) in a wide range of sizes, with a round end that occasionally shows one or more swellings (b) and a distal end that can be acerate, stepped or blunt (c). Oxeas of varying shape (d), with acerate to mucronate ends (e). Raphides (f) are in trichodragmata. (B-C) Light microscope views of styles and trichodragmata (tr). (D) Light microscope view of oxeas. (E) SEM micrograph of the flattened trichodragmata typically found in the beige specimens (e.g., in MNCN-Sp65-BV21A). (F) SEM micrograph of a more cylindrical trichodragmata typically found in blackish specimens (e.g., in MNCN-Sp57-BV21A). (G) Detail of the plumoreticulate and somewhat irregular skeletal arrangement at the lamina region of the sponge. Note the spongin (s) is embedding the paucispicular tracts (pc).

620 x 10-20 μm. Styles in the black specimens have a size range (245-1400 x 5-20 μm) virtually identical to that of the orange-beige individuals, although predominating sizes are usually over 800 x 10 μm. Oxeas, some more abundant than the styles, are also relatively variable in size and shape, but variability ranges are similar among specimens. They can be slightly or markedly curved, once or twice, and symmetrically or asymmetrically (Fig. 8A, D). Tips are usually acerate or blunt, although mucronate ends also occur (Fig. 8A). They measure 180-750 x 2.5-20 μm in the orange-beige specimens and 120-500 x 2.5-20 μm in blackish individuals. Microscleres in both orange-beige and blackish individuals are raphides in highly packed trichodragmata (Fig. 8E-F), measuring 22.5-35 x 5-13.7 μm. Although no evident size difference exists in trichodragmata between orange-beige and blackish individuals, their shape can be flattened or cylindrical in the orange-beige ones (Fig. 8E), but only cylindrical trichodragmata (Fig. 8F), and in higher abundance, were found in the blackish ones.

Skeletal structure: The skeletal structure is plumoreticulate. There is a clear axial skeleton in the stalk-like region, built by multispiculate tracts of oxeas. In the thin lamina there is no clear distinction between axial and extra-axial skeleton. Rather, there are pauci- and multispicular, ascending and ramifying tracts, compressed in the sense of the lamina and consisting of mainly oxeas, with sparse styles (Fig. 8G). These tracts are looser than in the axial skeleton of the stalk, and are connected each other by an irregular reticule that becomes more apparent in the thinnest parts of the lamina. In the three blackish specimens, the styles in the ascending tracts are somewhat more abundant and usually slightly longer than those in the orange-beige specimens. There are peripheral styles with their round end embedded in the tracts, piercing perpendicularly surface and making it hispid. The hispidating styles are usually long and occur isolated or in plumose tufts of up to 7 styles. Trichodragmata are predominantly located near the surface, especially in the blackish specimens. Spongin is abundant in the axial skeleton although it does not entirely embed all the spicules. It occurs moderately in the plumose tracts of the lamina (Fig. 8G).

Distribution and ecology notes: All the collected specimens came from gravel bottoms, sometimes with organogenic components, at depths ranging from 93 to173 m.

Taxonomic remarks: Except for color, the morphological and skeletal differences between the orange-beige individuals and the blackish ones are minor (Table 4) and we judged them not enough to support a differentiation into two separated species. Both color varieties share relevant features, such as similar body morphology and plumoreticulate skeleton with the same spicule categories and similar size ranges. In addition to the obvious color differences, it can be noticed: 1) a higher abundance of cylindrical trichodragmata in the blackish individuals; 2) a slightly more organized reticule-like arrangement linking the plumose tracts in the orange-beige individuals; and 3) higher frequencies of short styles in the orange-beige specimens. Even though we are herein assuming that these differences correspond to ill-known aspects of intraspecific variation, we cannot discard that future studies based on new collections and/or "in vivo" observations may led to a species split.

Trichodragmata similar to those in *A. spatula* sp. nov. are also found in some other *Axinella* spp. (Table 3), such as *Axinella infundibuliformis* (Linnaeus, 1759). Nevertheless, this latter species has a caliculate or fan-like body shape, a plumoreticulate skeleton of oxeas and styles clearly smaller (300-600 x 12-16 μm), and smaller (15-20 μm long) trichodragmata (Lendenfeld, 1897; Arndt et al., 1935). It is also worth noting that the earliest descriptions of *A. infundibuliformis* were little accurate and apparently overlooked the small trichodragmata (Johnston, 1842; Bowerbank, 1866; Hansen et al., 1885; Fristedt, 1887). *Axinella alba* (Descatoire, 1966) also shows trichodragmata, but it is an encrusting species and has oxeas (700-1000 x 15-18 μm) longer than those of *A. spatula* sp. nov. Trichodramata and styles also occur in *Axinella flustra* (Descatoire, 1966), but, again, although these styles and trichodragmata are in a size range similar to those of *A. spatula* sp. nov., the branching body shape (Fig. 6H-J) and shorter oxeas make *A. flustra* easily distinguishable (Table 3).

Some members of the axinellid genus *Dragmacidon* Hallman, 1917 (Table 3) bear some vague resemblance to *A. spatula* sp. nov., namely occurrence of raphides and the absence of a clear axial and extra-axial skeleton differentiation. Furthermore, phylogenetic analyses based on 18SrRNA, 28S rRNA and CO1 have brought *Dragamacidon* species and raphide-bearing *Axinella* species into a same clade (Gazave et al., 2010; Morrow et al., 2012). *Dragmacidon tuberosum* (Topsent, 1928) is the only geographically close species

in the genus having trichodragmata, but those are distinctive, having the raphides projecting from each side of the packets; besides, this species has shorter styles (Topsent, 1928).

Axinella vellerea Topsent, 1904

(Figs. 2B, 9, 10; Table 3; Appendix I)

Material examined: Thirteen specimens collected from the deep shelf of Alboran Island: MNCN-Sp51-DR05A & B from Stn. 5; MNCN-Sp148-BV33 from Stn. 33; MNCN-Sp196-BV41 from Stn. 41; MNCN-Sp142-DR44 A to I from Stn. 44 (Table 1, Fig. 1)

Comparative material: Syntype material of *Axinella vellerea* Topsent, 1904 (since no holotype was originally designated by Topsent), consisting of two specimens from Stn. 866 at Azores Islands (38º52.833'N 27º23.083'W; water depth: 599 m; 2 August 1897), and currently stored at the Monaco Museum (MOM-040631).

Macroscopic description: Specimens are erect, columnar, undivided or with two-tree incipient, lobule-like ramifications (Fig. 9A-H). The sponges measure 10-30 x 5-8 mm. The consistency is fleshy but hardly flexible. The surface is irregular, grooved, and porous. In some specimens, the oscules can be observed in the translucent epithelium folding the grooves, which run usually vertically, parallel to the longest axis of the body. The hispidation of the ectosome is short and not very dense, mostly verifiable under the dissecting microscope. The animal color in ethanol is ochre or pale brown.

Spicules: Megascleres are only styles and, in some individuals, a very low number of oxeas. Styles occur in a wide range of shapes and sizes, but without making discernible categories. They are slightly curved to somewhat angulate, some curved nearly the round end, similarly to rhabdostyles (Fig. 10A-B). The round end may be regular, but subtyles and annular swellings are also common, either in terminal or subterminal position (Fig. 10A-C). The point is usually acerate, but sometimes stepped or even blunt (Fig. 10A). Spicule malformations occasionally occur as well. Styles measure 470-1725 x 11-30 μm, but diameters smaller than 15 μm are uncommon. Some scattered oxeas have been observed in some specimens, in which case they are angulated or

have a two-point curvature (Fig. 10D), sometimes asymmetrical; they may also be centrotylote. When present, they measure 700-1120 x 5-20 μm.

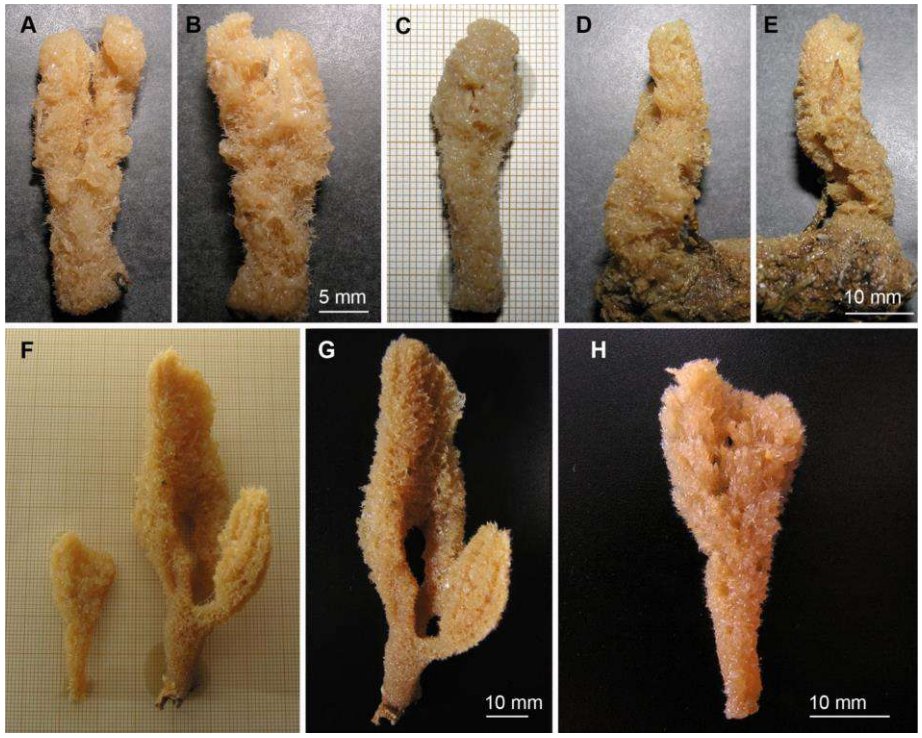

Figure 9. *Axinella vellerea* Topsent, 1904. (A-B) One of the collected Alboranian specimens (MNCN-Sp51-DR05A) shown on its both sides and bearing an incipient branching. (C) A branchless Alboranian specimen (MNCN-SP51-DR05B) of *A. vellerea* photographed on graphic paper. (D-E) Another unbranched Alboranian specimen (MNCN-Sp142-DR44A) attached to a piece of gravel, shown on its both sides. (F) Photograph of the holotype (the large sponge to the left) and the syntype (to the right) of *A. vellerea*, collected by Topsent in 1897 (Stn. 866. M. O. M. 040631). (G) Close up of the holotype of *A. vellerea*, being clearly ramified and larger than most specimens collected by us from the Alboran Island. (H) Close up of the syntype of *A. vellerea*, showing an incipient branch.

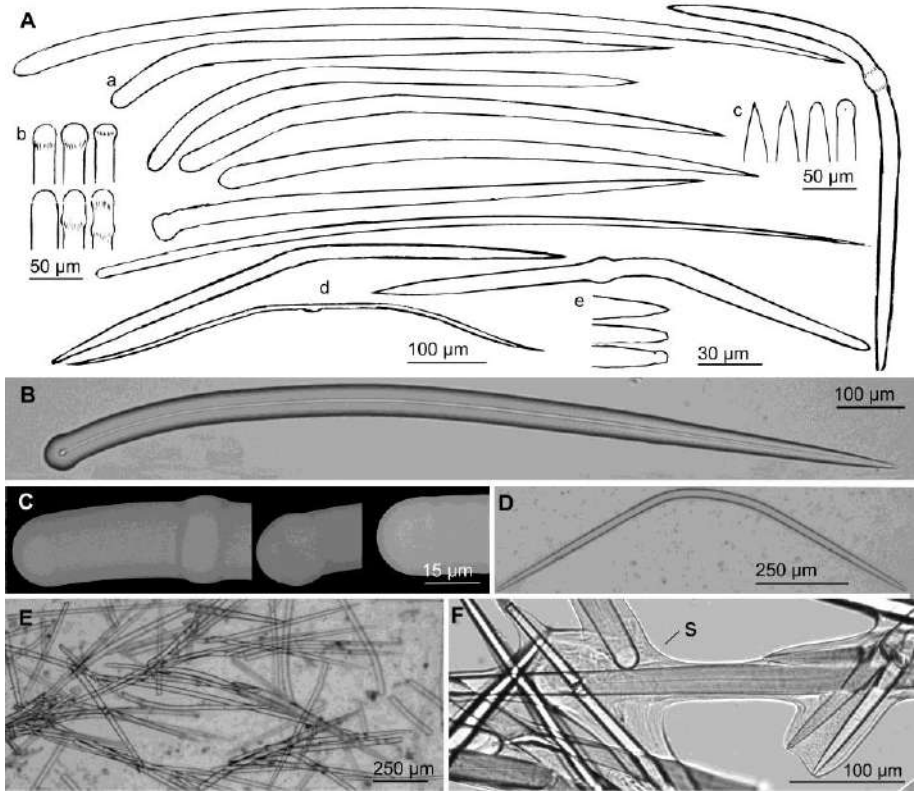

Figure 10. *Axinella vellerea* Topsent, 1904: (A) Line drawing summarizing the skeletal complement of the Alboranian specimens. Styles (a) are in a wide variety of shapes, with a round end that can be regular or showing one or more swellings (b) and a distal end (c) that can be regular to blunt, sometimes with mucronate variations. Oxeas (d) occur in varying size and shapes, with ends ranging from acerate to mucronate (e). (B) Light microscope view of a style with a subtylote end. (C) SEM detail of three typical morphologies (i.e., subterminal ring, subtylote, and regular) of the round end of styles. (D) Light microscope view of a double-bent oxea. (E) Light microscope view of plumose arrangement in the extra-axial skeleton. (F) Detail of styles embedded by spongin (s).

Skeletal structure: The skeletal arrangement consists of a somewhat central, compressed, plumoreticulate axis from which a plumoreticulate extra-axial skeleton spreads (Fig. 10E). The ascending extra-axial tracts become thinner as they reach the surface, and their terminal styles pierce the ectosome causing

hispidation. Moderate spongin embeds the spicules but without forming fibres (Fig. 10F); spongin becomes less abundant in the extra-axial region.

Distribution and ecology notes: The individuals were collected from depths ranging from 102 to 173 m, on rock, gravel or dead rhodolith pieces. The collected material makes the first Mediterranean record of this rare species. To date only four specimens had previously been reported: three of them collected from a 599 m deep, gravel bottom at Azores (Topsent, 1904), and one from 200-290 m depths at the Folden fiord of the Norwegian Sea (Burton, 1931).

Taxonomic remarks: The size of the examined syntypes of *A. vellerea* (97 x 40 mm and 45 x 18 mm) is slightly larger than that of any of the Alboranian individuals, being the remaining aspects of the external morphology notably similar between both specimen groups (Fig. 9A-H). The largest syntype also show two branches better developed (Fig. 9F-G) than the incipient branches often characterizing the Alboranian individuals (Fig. 9A-E). Regarding the spicules, the Alboranian specimens and the syntypes of *A. vellerea* show styles in nearly identical size and shape ranges (Table 3). A small skeletal difference is that oxeas are not found in neither the original description by Topsent (1904) nor in our re-examination of the syntypes. Burton (1931) did report occasional "oxeote styles" in his Norwegian specimen. In the Alboranian, specimens, we found oxeas in only a minority of individuals and always in low abundance. Therefore, the oxeas appear to be a variable element in the spicule complement of *A. vellerea*, as it is also the case of other *Axinella* spp.

As previously noticed by Topsent (1904), *A. vellerea* and *Axinella vasonuda* Topsent, 1904 bear similarity in both their external morphology and the skeletal organization. Nevertheless, *A. vasonuda* is characterized by having oxeas as main spicule type, showing only scarce styles, the occurrence of which is limited to the peripheral zones of the skeleton.

Family BUBARIDAE Topsent, 1894
Genus *Rhabdobaris* Pulitzer-Finali, 1983

Diagnosis. Monotypic genus of Bubaridae, characterized by stalked and flabellate body shape, possessing long hispidating styles and a plumoreticulate internal skeleton made of choanosomal rhabdostyles, oxeas, and strongyles,

with smooth and spiny forms co-occurring. Microscleres are raphides in trichodragmata (genus diagnosis herein redefined after *Rhabdobaris* being restituted as a valid genus; not a junior synonym of *Cerbaris* Topsent, 1898).

Remarks. See the "Taxonomic remarks" section of *Rhabdobaris implicata* for further discussion and concerns about the morphological affinity of the herein restituted genus *Rhabdobaris* and members of the family Raspailiidae.

Rhabdobaris implicata Pulitzer-Finali, 1983

(Figs. 11A-B, 12; Appendix I)

Synonymy: Cerbaris implicatus (Pulitzer-Finali, 1983): Alvarez & Van Soest, 2002, 751-752.

Material examined: Only one individual (MNCN-Sp23-BV14) collected from Stn. 14 (Table 1, Fig. 1), a 96-100 m deep, gravel bottom on the deep shelf of the island. The collected individual is herein designated the neotype, given that the previously available holotype specimen was entirely acid-dissolved to obtain a spicule slide. We are reasoning herein (see the "Taxonomic remarks" section) that type material in which the macroscopic body features and the skeletal arrangement can be evaluated is crucial to recognize the distinct nature of the monotypic genus *Rhabodobaris* within the family Bubaridae and, therefore, to support the nomenclatorial restitution of the genus. These "exceptional circumstances" strongly advice the neotype designation to preserve the stability of the nomenclature, following article 75 of the International Code of Zoological Nomenclature.

Comparative material: Original holotype of *Rhabdobaris implicata* Pulitzer-Finali, 1983. The only available material of the original holotype is the spicule slide (MSNG-47170) resulting from boiling in nitric acid the small specimen collected off Calvi, N-W of Corse, at 121-149 m depth (Pulitzer-Finali, 1983).

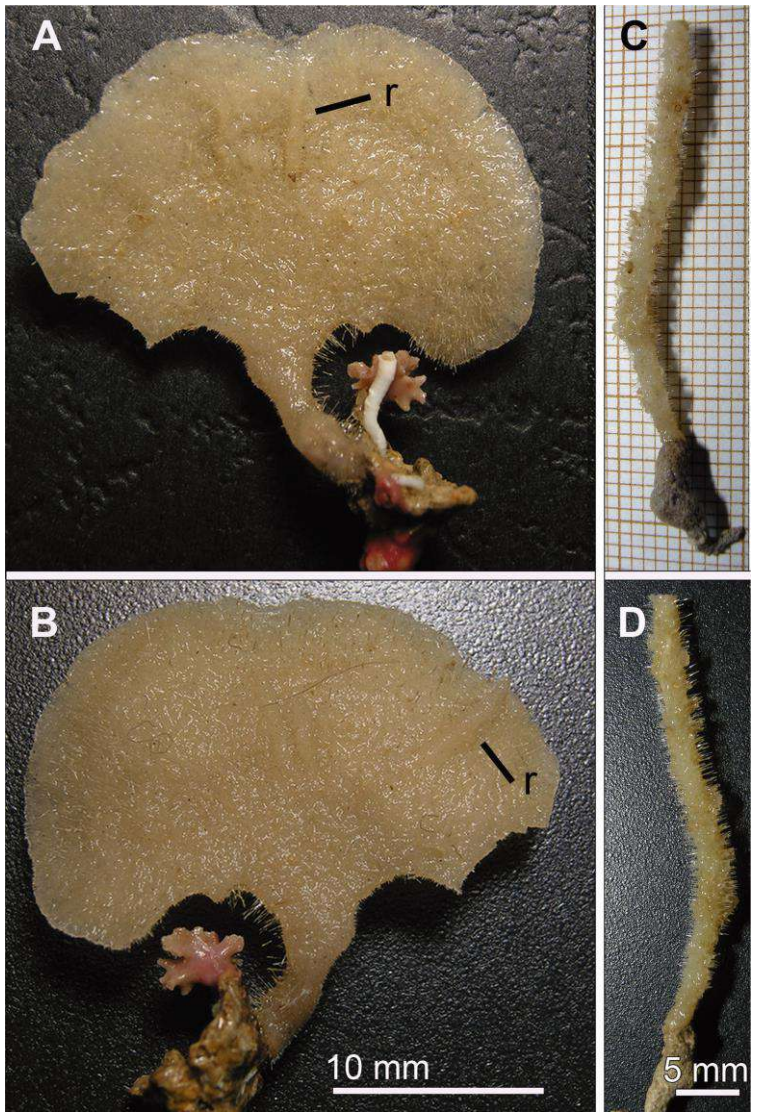

Figure 11. (A-B) Neotype (MNCN-Sp23-BV14) of *Rhabdobaris implicata* Pulitzer-Finali, 1983 collected from the Alboran Island and photographed on its both sides. Note some ribs (r) on the lamina. (C-D) Holotype of *Endectyon (Hemectyon) filiformis* sp. nov. (MNCN-Sp69 BV21) attached on a small piece of gravel, photographed on its both sides.

Macroscopic description: Stalked, flabellate sponge (Fig. 11A-B), with a thin lamina measuring 15 mm long x 25 mm wide x 1 mm thick; the stalk, somewhat compressed, measures 7 mm in length x 2.5 mm in wideness. There are 3 and 4 reinforcement ribs at each side of the lamina (Fig. 11A-B), making the lamina poorly flexible. There are no aquiferous openings discernible with naked eye. The surface of the lamina is markedly hispid, with long spicules protruding uniformly at moderated density. The stalk is less hispid. The color of the alcohol-preserved specimen is creamy white.

Spicules: Megascleres are in seven categories: long hispidating styles, rhabdostyles, oxeas, styrongyles, acanthoxeas, acanthostyles, acanthostrongyles. Microscleres are raphides in trichodragmata. Hispidating styles are long, gently conical, nearly straight or softly curved, with a regular round end and a sharp, acerate or hastate point (Fig. 12A-B). They are 754-1557 μm long and 8-16 μm wide. Rhabdostyles have a slight to marked curvature on their first ¼ of their length (Fig. 12A, C), rarely becoming regular styles. Other variations occurring in the rhabdostyles are annular or irregular swellings in the vicinity of the round end and polyaxial malformations in the vicinity of the pointing end (Fig. 12C); the points can be acerate, stepped, or even bifid (Fig. 12A). Rhabdostyles measure 137-304 x 5-13 μm, although some thinner, growing stages (Fig. 12A) can occasionally be observed, measuring 107-212 x 3-6 μm. Oxeas are isodiametric, in a wide range of morphologies, showing from one to three, flexion points, more asymmetrical (Fig. 12A, E); they can occasionally be centrotylote, sometimes with the swelling placed asymmetrically. Oxea ends are acerate, conical, mucronate or stepped, with bifid and polyaxonic malformations also occurring (Fig. 12A, E). Oxeas measure 222-405 x 5-10 μm, although, as it happens in the rhabdostyles, thinner growing stages (Fig. 12A) measuring 185-285 x 1-3 μm occasionally occur. Strongyles are curved once or twice, regularly or irregularly (Fig. 12A), occasionally symmetrically or asymmetrically centrotylote, measuring 160-310 x 14-15 μm. Strongyles are clearly less abundant that rhabdostyles and oxeas. The rhabdostyles, the oxeas and the strongyles have "acanthose versions", which usually are slightly smaller and less abundant than their respective smooth counterparts. Acanthorhabdostyles measure 125-187 x 6-11 μm and show from scarce to abundant small spines, equally or unequally distributed along the spicule and

not necessarily confined to one of the ends (Fig. 12D). Acanthoxeas measure 120-280 x 7-9 μm and show few to abundant spines, often more concentrated towards the ends (Fig. 12A, F). In few acanthoxeas, the spines were relatively thick and blunt, becoming a sort of tubercles. Acanthostrongyles measure 129-409 x 5-12 μm, being entirely or partially spiny (Fig. 12A). Microscleres

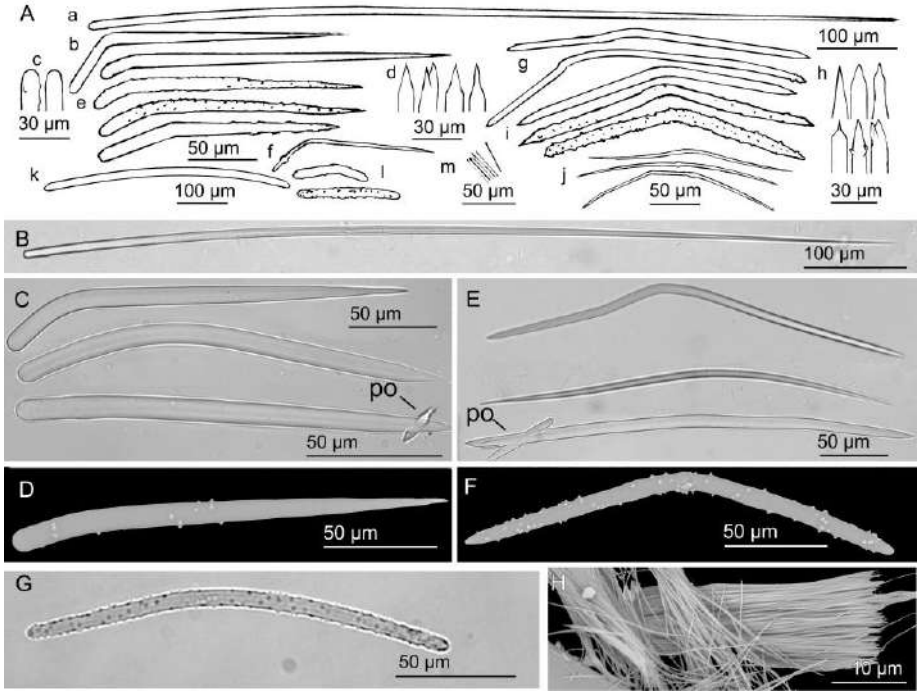

Figure 12. *Rhabdobaris implicata* Pulitzer-Finali, 1983: (A) Line drawing summarizing the skeletal complement of the Alboranian specimen (MNCN-Sp23-BV14), consisting of hispidating styles (a), smooth rhabdostyles (b) with a regular or swollen round end (c) and acerate, bifid to polyactinal, or stepped distal end (d), acanthostyles (e), small styles (f), smooth oxeas (g) with acerate, stepped, mucronate or polyactinal ends (h), acanthoxeas (i), developing stages of oxeas (j), strongyles (k), acanthostrongyles (l), and toxiform raphides in trichodragmata (m). (B-D) Light microscope views of an hispidating style (B) and choanosomal rhabdostyles (C), sometimes with abnormal, polyactinal points (po). (D) SEM view of an acanthostyle. (E) Light microscope view of oxeas in various shapes, sometimes showing polyactinal ends (po). (F) SEM micrograph of an acanthoxea. (G) Light microscope view of an acanthostrongyle of the holotype *Rhabdobaris implicata* Pulitzer-Finali, 1983 (MSNG-47170). (H) SEM image of two overlapped trichodragmata of toxiform raphides in the Alboranian specimen.

are toxiform raphides, occurring in trichodragmata (Fig. 12A, H) that measure 22-50 x 10-20 μm.

Skeletal structure: The skeletal architecture is plumoreticulate. The stalk contains a compact plumoreticulate skeleton with ascending multispiculate tracts including all categories of choanosomal megascleres (i.e., except the long hispidating styles) embedded in moderate spongin. Nevertheless, in order not to damage the stalk, we only sampled a tiny peripheral portion of stalk tissue and cannot discard the occurrence of a pure axial skeleton in its central region. In the lamina, the ascending tracts ramify and reticulate irregularly, compressed in the plane of the lamina; there are also free oxeas and styles arranged obliquely to the ascending tracts. Long hispidating styles with their round end embedded in the ascending tracts protrude largely the surface of the sponge at the lamina. Additionally, among the long hispidating styles, there is also a short, dense and uniform hispidation caused mostly by non-acanthose rhabdostyles and oxeas. Likewise, the hispidation of the stalk is only due to these shorter spicules, lacking the long hispidating styles.

Distribution and ecology notes: Rare species, only known previously from the holotype (Pulitzer-Finali, 1983), a specimen collected at 121-149 m, off Calvi (Corse Island, Western Mediterranean). Our Alboranian specimen, collected from a 96-100 m deep, gravel bottom with a very rich associated invertebrate fauna, provides the second record of the species in the Mediterranean.

Taxonomic remarks: The body shape and the spicule complement of the newly collected material matches notably well with the original description of *Rhabdobaris implicata* by Pulitzer-Finali (1983), who indicated that it was a new "stipitate" genus in the family Bubaridae. The only difference is that acanthostrongyles (Fig. 12G) are more abundant than acanthoxeas in the holotype, while it is the opposite in the Alboranian individual.

The genus *Rhabdobaris* Pulitzer-Finali, 1983 was declared a junior synonym of *Cerbaris* by Alvarez & Van Soest (2002) on the argument that they both share the occurrence of acanthose diactines in the basal, choanosomal skeleton. However, the features of the newly collected individual of *R. implicata* make clear that it does not fit the genus diagnosis of *Cerbaris* provided by Alvarez & Van Soest (2002). *Cerbaris*, among other traits, is characterized by encrusting sponges, with a choanosomal skeleton consisting of a basal layer

of acanthose and smooth diactines and monactines projecting perpendicularly to the substratum. Therefore, the current diagnosis of *Cerbaris* reflects several major mismatches relative to the features of *Rhabdobaris implicata*: 1) *R. implicata* is a stalked, flabellate sponge (Fig. 11A-B), rather than an encrusting form; 2) the skeleton is not a basal layer, but consists of a plumoreticulate structure of ascending tracts; 3) it lacks the distinct ceroxas (M-shaped oxeas) of *Cerbaris*; 4) *Rhabdobaris implicata* has acanthostyles in great abundance, a spicule type often missing in *Cerbaris*. Altogether, the differences in body shape, spicule complement and skeletal organization advice to re-establish the original genus *Rhabdobaris* erected by Pulitzler-Finali (1983) in the family Bubaridae. Likewise, the existence of *Rhabdobaris* makes compulsory a modification of the current definition for family Bubaridae, as it is currently defined by Alvarez & Van Soest (2002) only to host sponges with an encrusting growth habit supported by a basal layer of interlacing choanosomal diactines.

A comparison of the spicule complement of our Alboranian specimen to *Cerbaris* spp. occurring in or near the Western Mediterranean region reveals only vague resemblance to *Cerbaris* (formerly *Bubaropsis*) *curvisclera* (Lévi & Vacelet, 1958) from Azores and *Cerbaris* (formerly *Rhabdoploca*) *curvispiculifer* (Carter 1880), originally described from the Indian Ocean (Gulf of Manaar) and subsequently found in Azores (Topsent, 1904) and Banyuls (Vacelet, 1969). These two latter *Cerbaris* species are encrusting forms that also lack the plumoreticulate skeleton. In addition, *C. curvispiculifer* lacks raphides, having a spicule complement that varies across described specimens. For instance, it lacks both smooth and acanthose oxeas in the Indian and North-Atlantic specimens, but not in the Mediterranean material. *Cerbaris curvisclera* has raphides and smooth oxeas, but lacks any kind of style or acanthostyle. Therefore, *R. implicata* is clearly distinguishable from *Cerbaris* spp.

Although the genus *Rhabdobaris* is herein restituted within the original family in which it was erected, that is Bubaridae, there are concerns that *Rhabdobaris* could be a raspailiid. Indeed, the body shape, the spicule complement, and the general skeletal organization match better the traits characterizing the family Raspailiidae than those of the family Bubaridae. Nevertheless, *Rhabdobaris* lacks the hispidating bouquets around the long hispidating styles, which typically characterize most−but not all−raspailiids. Therefore, a definitive family assignation may require further inference of the phylogenetic relationships of *Rhabdobaris* using molecular markers.

Order POECILOSCLERIDA Topsent, 1928
Suborder MIICROCIONINA Hajdu, van Soest & Hooper, 1994
Family RASPAILIIDAE Nardo, 1833
Subfamily RASPAILIINAE Nardo, 1833
Genus *Endectyon* Topsent, 1920

Diagnosis: Prominently hispid, conulose surface, and typically arborescent growth form. Skeleton with marked axial and extra-axial differentiation; axial skeleton with well-developed spongin fibres forming a compressed reticulation, cored by stout choanosomal styles; extra-axial subectosomal skeleton being radial or plumose, with multi- or paucispicular tracts of long subectosomal styles (subgenus *Endectyon*) or choanosomal styles (subgenus *Hemectyon*), sometimes connected by unispicular tracts forming hexagonal meshes, usually protruding the surface. Ectosomal skeleton varies from typical raspailiid condition, with thin ectosomal styles grouped in brushes around protruding subectosomal styles (subgenus *Endectyon*), to surface brushes composed of subectosomal styles only (nominal genus *Basiectyon*), to brushes of acanthostyles surrounding choanosomal styles (subgenus *Hemectyon*). Erect brushes of echinating acanthostyles located on the outer margin of the axial skeleton, making a boundary between the extra-axial and axial regions, or forming plumose brushes along the length of the extra-axial tracts, or localized exclusively at the base of the sponge (nominal genus *Basiectyon*). Structural megascleres are smooth styles of 2-3 size categories, along with echinating acanthostyles and/or acanthostrongyles with peculiar strongly curved (clavulate) hooks on the shaft, base, and/or apex. Microscleres are absent (*sensu* Hooper, 2002b).

Subgenus *Hemectyon* Topsent, 1920

Diagnosis: Erect, probably undivided (see "Taxonomic Remarks"), growth form. Skeletal organization with recognizable axial, extra-axial and ectosomal regions. Axial skeleton of multispiculate-cored fibres densely reticulated. Extra-axial skeleton consisting of a more lax reticulum of pauci- to multispicular radiating primary tracts intercrossed by uni- to paucispicular secondary tracts. Spongin fibres and tracts of the axial and extra-axial regions

are cored by smooth choanosomal styles; the radiating primary tracts of the extra-axial skeleton may be sparsely echinated by acanthostyles, particularly in their subectosomal regions. In the subectosomal region, the peripheral nodes of the extra-axial network serve as basis for small bouquets of longer (subectosomal) styles, which pierce the sponge ectosome to make a long, dense hispidation. At the point where each of these protruding bouquets of styles pierce the sponge ectosome, a surrounding brush consisting mostly of acanthostyles (but also incorporating some choanosomal styles) occurs, being this skeletal trait a distinct character for the subgenus *Hemectyon* (modified herein to accommodate the features of the new species).

Endectyon (Hemectyon) filiformis sp. nov.

(Figs. 11C-D, 13; Appendix I)

Etymology: This species is named after its erect, undivided body shape.

Material examined: Holotype: Specimen MNCN-Sp69 BV21, from type locality Stn. 21 (Table 1, Fig. 1), a 93 to 101 m deep, gravel bottom on the deep shelf of the island.

Macroscopic description: Flexible, slender, thread-like sponge, measuring 54 mm in height and 3 mm in diameter, attached to a gravel piece. The surface is densely and markedly hispid (Fig. 11C-D), with no obvious oscules. The color in life is bright orange, turning into creamy white in ethanol.

Spicules: Megascleres in 4 spicule categories: Subectosomal styles, choanosomal styles, occasional oxeas, and acanthostyles. The subectosomal styles are long and slender, slightly curved at the centre or near the round end, with a regular round end, and an acerate point that can be sometimes softly stepped or, in the thinner growth stages, hastate (Fig. 13A); they measure 713-1465 x 3.2-20 μm. The choanosomal styles measure 187.4-272.5 x 6.4-9 μm, being irregularly curved once or twice, sometimes in a rhabdostyle fashion, with hastate or acerate points (Fig. 13A-B). These styles may show a slight swelling either near the round end or towards central positions. The oxeas are less common than the previous categories, typically curved at the middle, with sharp conical ends that can be slightly different (Fig. 13A, C), measuring 234-277 x 3-9 μm. The acanthostyles are nearly straight or slightly curved and show

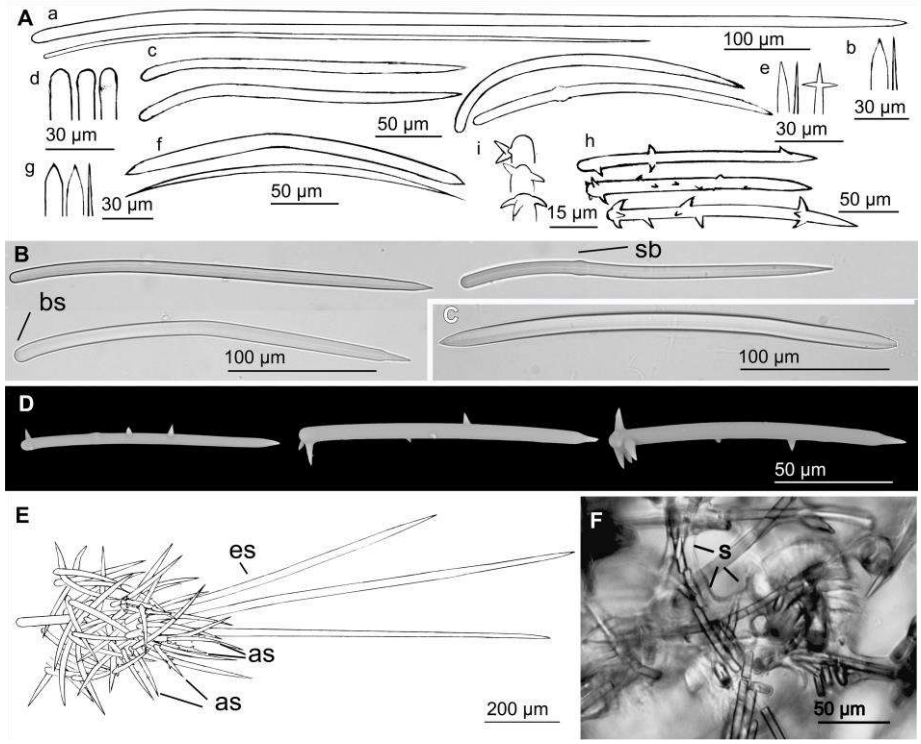

Figure 13. *Endectyon (Hemectyon) filiformis* sp. nov.: (A) Line drawing summarizing the spicule complement of the holotype (MNCN-Sp69-BV21). There are subectosomal styles (a) with a round end and an acerate or hastate distal end (b) and choanosomal styles with a regular or swollen round end (d) and an acerate, hastate or polyaxonic distal end (e). There are also oxeas (f) with conical to hastate ends (g) and acanthostyles (h) with large spines that can be clavulate at the round end (i). (B) Light microscope view of choanosomal styles, with slight subterminal swelling (bs) or a subtle subtyle (sb). (C) Light microscope view of an oxea. (D) SEM micrographs of acanthostyles. (E) Line drawing sketching of the organization of the ectosomal skeleton, which consists of the subectosomal styles (es) surrounded by an hispidating brush of acanthostyles (as). (F) Light microscope view of the choanosomal skeleton where spongin (s) can be observed embedding the choanosomal styles.

scarce, large, conical spines. Spines are usually sparse over the spicule length, mostly making a sort of verticillate cluster at the round end, producing a clavulate acanthostyle; very rarely the spines appear around the sharp end of the spicule. The number of spines varies from one to four at the round end

and from one to ten over the shaft length, and they can be straight, curved toward the spicule points or in the opposite direction (Fig. 13A, D). The acanthostyles are far less abundant than the choanosomal styles and measure 114-150 x 6-7 μm.

Skeletal structure: Axial and extra-axial skeleton are poorly differentiated. The axial skeleton is a relatively more compact reticule of pauci- and multispicular tracts of choanosomal styles surrounded by moderate spongin (Fig. 13F). The reticule becomes progressively less compact towards the periphery (extra-axial region?) and is built with thinner tracts (pauci- and unispiculate) of choanosomal styles and occasional oxeas. From the periphery of this extra-axial network, groups of 2 to 10, long subectosomal styles project radially (Fig. 13E), piercing the surface and causing the long hispidation of the surface. At the point where one of these radiating tracts of long subectosomal styles pierces the sponge ectosome, a surrounding brush consisting mostly of acanthostyles (but also incorporating some oxea or choanosomal style) occurs (Fig. 13E); this skeletal trait is a diagnostic character for the subgenus *Hemectyon*.

Distribution and ecology notes: The only individual of *Endectyon (Hemectyon) filiformis* sp. nov. was collected from a 93 to 100 m deep, organogenic-gravel bottom.

Taxonomic remarks: Members of the genus *Endectyon* are the only raspailiids having echinating acanthostyles with clavulate morphology and located outside the axial skeleton (Hooper, 1991; Hooper, 2002b). Within the subgenus *Hemectyon*, only one species has been described to date: *Endectyon (Hemectyon) hamatum* (Schmidt, 1870). This species was originally reported from the Caribbean (Schmidt, 1870; Topsent, 1920). It was subsequently cited from the East Africa (North Kenya) by Pulitzer-Finali (1993), but a revision of that specimen assignation would be advisable, as it contains abundant raphides and the brief skeletal description suggests it to be a raspailiid different from *Endectyon* spp.

The occurrence of acanthostyle brushes surrounding the groups of hispidating styles clearly indicates that the newly described Alboranian material belongs to the subgenus *Hemectyon*, making the second known species in this subgenus. The differences between *E. (H.) hamatum* and *E. (H.) filifomis* sp. nov. are clear: 1) the axial and extra-axial differentiation is less marked in

the new species, as well as the differentiation between radiating primary tracts and secondary intercrossing tracts; 2) the primary radiating tracts are only very rarely echinated by the acanthostyles in the new species; 3) the acanthostyles do not have clavulate spines at the round end in *E. (H.) hamatum*, but they do have them in the new species; 4) The hispidating styles in *E. (H.) hamatum* are relatively small (220-275 x 2 μm) and shorter than those coring the choanosomal fibres and tracts (270-615 x 6-18 μm), whereas they are notably longer (up to 1465 x 20 μm) in the new species; and 5) the new species contains occasional oxeas, while they do not occur in *E. (H.) hamatum*. Indeed, oxeas are an uncommon spicule type in *Endectyon* spp., although occasional modifications of styles into oxeas and strongyles have already been recorded in *Endectyon (Endectyon) tenax* (Schmidt, 1870) from North Carolina by Wells et al. (1960) and *Endectyon (Endectyon) multidentatum* (Burton, 1948) from Congo Coast (Burton, 1948).

To accommodate the skeletal features of this new species, it is necessary to modify herein the last accepted diagnosis of subgenus *Hemectyon*, which was proposed by Hooper (2002b) on the basis of the only species available at that time.

An additional reason to revise the subgenus diagnosis is the growth habit. Originally, *Hemectyon* was erected on a partial sponge fragment that was assumed to be part of a larger, branched individual (Schmidt, 1870; Topsent, 1920). Ever since, the successive genus diagnoses have included terms such as "rameuse" (Topsent, 1920) or "arborescent" (Hooper, 2002b), a branching condition that has never been corroborated objectively. Given that the holotype of *E. (H.) hamatum* is an undivided cylindrical fragment (23mm x 3.5) and that the complete holotype of *E. (H.) filiformis* sp. nov. is also an undivided, digit-like growth form, there is no reason to support any longer that the sponges of the subgenus *Hemectyon* are arboresecent. Rather, they should be postulated as erect, branchless growth forms, at least until future collections of new material disprove it.

Order HAPLOSCLERIDA Topsent, 1928

Suborder HAPLOSCLERINA Topsent, 1928

Family NIPHATIDAE Van Soest, 1980

Genus *Gelliodes* Ridley, 1884

Diagnosis: Thickly incrusting to massive, tubular growth form, intricately branching, long cylindrical stems irregularly ramified and anastomosing at points of contact (single branches attain a length of about 100 mm), rampant or erect, arising from a common basal portion. Oscules usually numerous, unevenly scattered over the surface and often conspicuous. Surface uneven, membranous, strongly aculeated at intervals of about 2-5mm, sustained by strong, slender, sharp ramified spines, 2-3 mm long (Fig. 3D) surface may be also ridged or tuberculate or smooth, and finely hispid or velvety. Texture very hard. Ectosomal skeleton is a tangential network of secondary fibres, free oxeas and abundant sigmas, often interrupted by the ends of the strong primary longitudinal fibres protruding from the choanosomal skeleton to form the spines. Choanosomal skeleton composed of primary longitudinal-radial multispicular and ramified primary fibres, distinct and very compact. Primary fibres form rectangular to rounded meshes, subdivided irregularly by secondary fibres, and mesh containing abundant free spicules. Megascleres consist of robust oxeas with sharp apices. Microscleres are abundant sigmata (sensu Desqueyroux-Fáundez & Valentine, 2002).

***Gelliodes fayalensis* Topsent, 1892**

(Figs. 14, 15; Appendix I)

Synonymy: Adocia fayalensis (Topsent, 1892): Burton, 1956, 145.

Material examined: Specimen MNCN-Sp137 DR07 collected from Stn. 7 (Table 1, Fig 1).

Macroscopic description: Ovate, cushion-shaped sponge, attached to a small piece of rhodolith (Fig. 14A-B). It measures 30 x 20 mm and is fouled around its basal region by a thickly encrusting individual of *Haliclona* sp. Surface is smooth, consisting of a thin, delicate, translucent membrane. The ectosomal membrane is damaged in many areas of the body, showing a highly cavernous subectosomal tissue. Ectosome damage makes difficult to discriminate the occurrence of oscules from ectosome breakages. The consistency is hard but friable. The color in alcohol is beige.

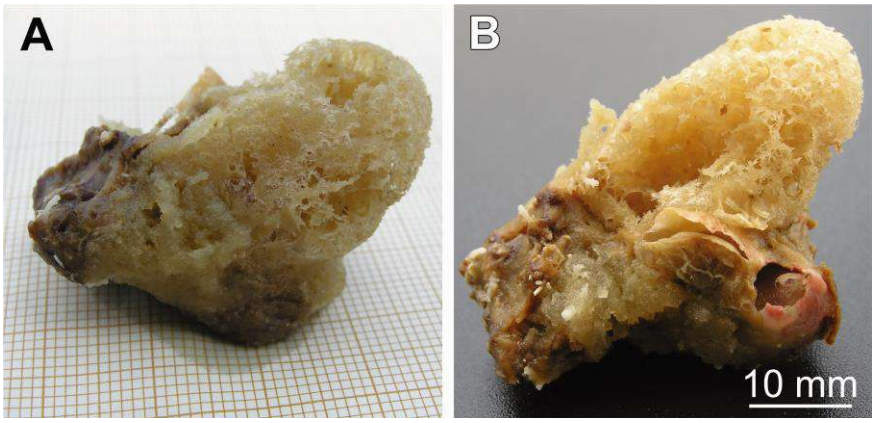

Figure 14. *Gelliodes fayalensis* Topsent, 1892. Specimen from the Alboran Island (MNCN-Sp137-DR07), photographed on its both sides while attached to a rhodolith fragment.

Spicules: Megascleres are oxeas in a size range that could well represent two categories. The oxeas in the large category measure 280-400 x 10-15 μm and are slightly curved, typically showing two flexion points (Fig. 15A-B, E). The ends are acerate, with occasional malformations (Fig. 15A, C). The oxeas in the small category are less abundant, measure 200-270 x 2-5 μm, are regularly curved over their entire length (Fig. 15A, D-E), and have relatively regular hastate ends (Fig. 15A). Nevertheless, we cannot discard that the smaller oxeas are early developing stages of the larger oxeas. Microscleres are abundant sigmata, 15-27 μm in maximum length (Fig. 15A, E-F).

Skeletal structure: The ectosomal skeleton is a reticule of tangential oxeas made of uni- or paucispicular lines. The choanosomal skeleton is an irregular network (Fig. 15G) consisting of compact, primary multispicular tracts of oxeas with moderate spongin (Fig. 15H), which branch and subdivide when running from the deep choanosome towards the periphery. Primary tracts are 250-625 μm wide and connect each other by secondary, pauci- or multispicular secondary tracts, which are 125-200 μm wide. Microscleres are abundant at the subectosomal region, also occur in the choanosome, some partially embedded in the oxea tracts.

Distribution and ecology notes: Rare species, known from the original description of 5 individuals from Azores (Topsent, 1892, 1904), all coming from the Fayal Channel (Azores), growing on gravel bottoms rich in organogenic elements, at depths of 98-100 m. The herein described Alboranian specimen, collected from a rhodolith bottom at depths ranging from 109 and 130 m, provides the first record of the species in the Mediterranean Sea.

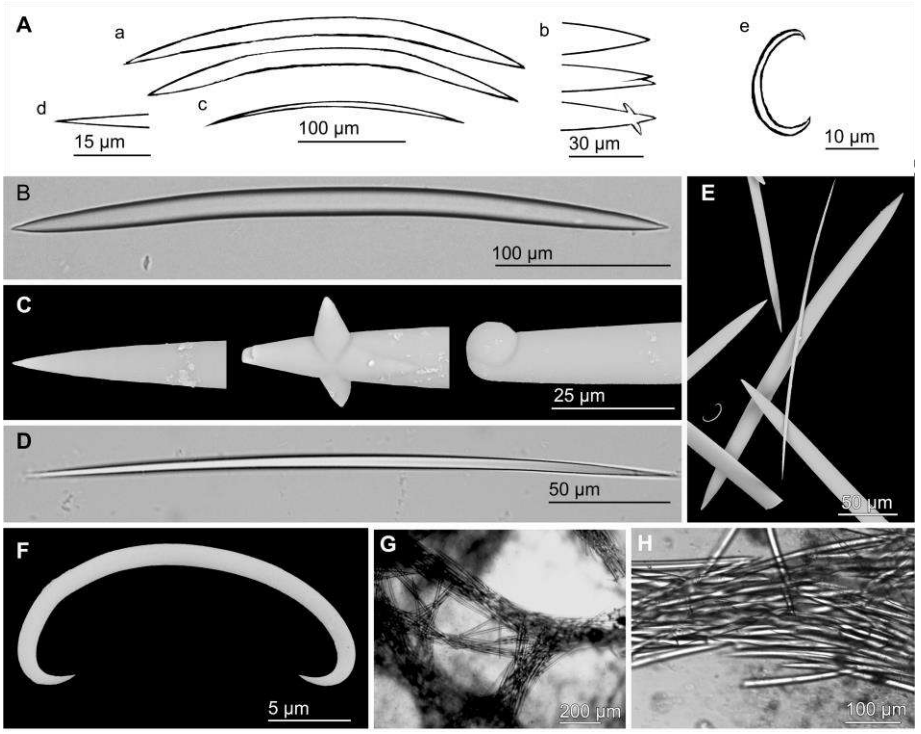

Figure 15. *Gelliodes fayalensis* Topsent, 1892: (A) Line drawing summarizing the spicule complement of the Alboranian specimen (MNCN-Sp137-DR07), consisting of fusiform oxeas I (a) with acerate to malformed ends (b), isodiametric oxeas II (c) with acerate ends (d), and sigmata (e). (B) Light microscope view of Oxea I. (C) SEM detail of regular and abnormal ends of oxea I. (D) Light microscope view of isodiametric Oxea II. (E) SEM view oxeas I and II and a sigma. (F) SEM detail of a sigma. (G) Light microscope view of multispiculate tracts of oxeas I and II forming a network. (H) Light microscope detail of a multispiculate tract.

Taxonomic remarks: The spicule complement, the spicule size, and the skeletal organization of the Alboranian individual are strongly similar to those of *Gelliodes fayalensis* Topsent, 1892. A minor difference is that Topsent (1892) did not split the oxeas of *G. fayalensis* into two size categories. Nevertheless, we are not completely certain that the smaller oxeas that we are herein describing are a size category themselves; they could rather be early growth stages. The only size data for oxeas in Topsent's description (1892) is 270 x 9 μm, which approximately represents the median of the size range found in the oxeas of the Alboran specimen.

All specimens described from Azores by Topsent (1892, 1904) were reported to have several distinct oscules. The preservation condition of our Alboranian specimen did prevent us to discriminate oscules from the frequent ectosomal breakages and, indeed, hindered a relevant comparison in terms of external morphology features.

Concluding remarks

The bottoms of the Alboran Island are characterized by elevated sponge richness and substantial diversity, hosting representatives of about 30 % of the known Mediterranean demosponges. Among this fauna, there are also a good number of Mediterranean endemisms and rare species, along with numerous "Atlantic" species that appear to have penetrated in this westernmost Mediterranean area and that, surprisingly, may reach notable abundances (e.g., *Axinella vellerea*). While recent invasions of shallow habitats by sponges have relatively been easy to detect in several oceans and seas (e.g., *Mycale grandis*, *Terpios hoshinota*, *Paralleucilla magna*), faunal expansions taking place in deep-sea habitats can go unnoticed for decades. It remains unclear whether the common occurrence of "North-Atlantic" deep-shelf immigrants that has been detected in this and previous sponge studies at the Alboran Island reflects only vestiges of ancestral faunal expansions during the Quaternary interglacial periods or it is also partially derived from recent northward expansions favored by man-driven global warming. While the former mechanism is more likely the main cause, our results contribute to reinforce the idea that the Alboran shelf provides a privileged natural laboratory from where to document past, present, and future biotic exchange between the Mediterranean and the Atlantic (Aguilar et al., 2011; Vermeij,

2012). From this notion, two major actions would be advisable for the immediate future: 1) To complete timely an exhaustive, global characterization of the benthic assemblages of the deep shelf of the Alboran Island, establishing a crucial baseline for further monitoring steps; 2) To extend the environmental protection currently given to the shallow-shelf communities of the Alboran Island to the singular and ecologically valuable deep-shelf bottoms, taking the opportunity of the currently developing frame of the Nature 2000 Network.

References

Aguilar, R., Aksissou, M., Templado, J. and Romani, M. (2011) Scientific rationale for the proposed CIESM Near Atlantic Marine Peace Park - A CIESM proposal. *In:* Briand, F. (Ed) *Marine peace parks in the Mediterranean*. CIESM, Monaco, pp. 43-49.

Alvarez, B. and Hooper, J.N.A. (2002) Family Axinellidae Carter, 1875. *In:* J.N.A Hooper. and R.W.M. Van Soest (Eds) *Systema Porifera: A guide to the classification of sponges,*1. Kluwer Academic/Plenum Publishers, New York, pp. 724-747.

Alvarez, B. and Van Soest, R.W.M. (2002) Family Bubaridae Topsent, 1894. *In:* J.N.A Hooper. and R.W.M. Van Soest (Eds) *Systema Porifera: A guide to the classification of sponges,*1. Kluwer Academic/ Plenum Publishers, New York, pp. 748-754.

Arndt, W., Grimpie and Wagler. (1935) *Porifera. Die Tierwelt der Nord-und Ostsee.* Berlin. 1-140 pp.

Babiç, K. (1922) Monactinellida und Tetractinellida des Adriatischen Meeres. *Zoologische Jahrbücher, Abteilung für Systematik, Geographie und Biologie der Tiere*, 46(2), 217-302.

Bertolino, M., Bo, M., Canese, S., Bavestrello, G. and Pansini, M. (2013a) Deep sponge communities of the Gulf of St Eufemia (Calabria, southern Tyrrhenian Sea), with description of two new species. *Journal of the Marine Biological Association of the United Kingdom*, FirstView, 1-17.

Bertolino, M., Cerrano, C., Bavestrello, G., Carella, M., Pansini, M. and Calcinai, B. (2013b) Diversity of Porifera in the Mediterranean

coralligenous accretions, with description of a new species. *ZooKeys*, 336, 1-37.

Boury-Esnault, N., Pansini, M. and Uriz, M.J. (1994) Spongiaires bathyaux de la mer d'Alboran et du golfe ibéro-marocain. *Mémoires. Muséum National d'Histoire Naturelle*, 160, 1-174.

Boury-Esnault, N. and Rützler, K. (1997) Thesaurus of sponge morphology. *Smithsonian Contributions to Zoology*, 596, 1-55.

Bowerbank, J.S. (1866) A monograph of the British Spongiadae. II. Synopsis of Genera. *Ray Society of London*, London, 1-388 pp.

Burton, M. (1929) Porifera. Part II. Antarctic Sponges. *British Antarctic Terra Nova Expedition. 1910-1913, Zoology*, 6, 393-458.

Burton, M. (1931) The Folden Fiord. Report on the sponges collected by Mr. Soot-Ryven in the Folden Fiord in the year 1923. *Tromsø Museum Skrifter*, 1, 1-8.

Burton, M. (1948) Marine sponges of Congo coast. *Institut Royal Colonial Belge Bulletin des Séances* 19, 753-758.

Burton, M. (1956) The Sponges of West Africa. *Atlantide Report. (Scientific Results of the Danish Expedition to the Coasts of Tropical West Africa, 1945-1946, Copenhaguen)*. 4, 111-147.

Calcinai, B., Moratti, V., Martinelli, M., Bavestrello, G. and Taviani, M. (2013) Uncommon sponges associated with deep coral bank and maerl habitats in the Strait of Sicily (Mediterranean Sea). *Italian Journal of Zoology*, 80, 412-423.

Carter, H.J. (1880) Report on Specimens dredged up from the Gulf of Manaar and presented to the Liverpool Free Museum by Capt. W. H. Cawne Warren. *Annals and Magazine of Natural History*, 6(31), 35-61, 129-156.

Coll, M., Piroddi, C., Steenbeek, J., Kaschner, K., Ben Rais Lasram, F., Aguzzi, J., Ballesteros, E., Bianchi, C.N., Corbera, J., Dailianis, T., Danovaro, R., Estrada, M., Froglia, C., Galil, B.S., Gasol, J.M., Gertwagen, R., Gil, J., Guilhaumon, F., Kesner-Reyes, K., Kitsos, M.-S., Koukouras, A., Lampadariou, N., Laxamana, E., López-Fé de la Cuadra, C.M., Lotze, H.K., Martin, D., Mouillot, D., Oro, D., Raicevich, S., Rius-Barile, J., Saiz-Salinas, J.I., San Vicente, C., Somot, S., Templado, J., Turon, X., Vafidis, D., Villanueva, R. and Voultsiadou, E. (2010) The biodiversity

of the Mediterranean Sea: Estimates, patterns, and threats. *PLoS One*, 5, e11842.

Comas, M.C., García-Dueñas, V. and Jurado, M.J. (1992) Neogene tectonic evolution of the Alboran Sea. *Geo-Marine Letters*, 12, 157-164.

Descatoire, A. (1966) Sur quelques Démosponges de l'Archipel de Glénan. *Cahiers de Biologie Marine*, 7, 231-246.

Desqueyroux-Fáundez, R. and Valentine, C.A. (2002) Family Niphatidae Van Soest, 1980. *In:* J.N.A Hooper. and R.W.M. Van Soest (Eds) *Systema Porifera: A guide to the classification of sponges,*1. Kluwer Academic/ Plenum New York, pp. 874-890.

Fristedt, K. (1887) Sponges from the Atlantic and Arctic Oceans and the Behring Sea. Vega-Expeditionens Vetenskap. *Iakttagelser (Nordenskiöld)*, 4, 401-471.

Gazave, E., Carteron, S., Chenuil, A., Richelle-Maurer, E., Boury-Esnault, N. and Borchiellini, C. (2010) Polyphyly of the genus *Axinella* and of the family Axinellidae (Porifera: Demospongiaep). *Molecular Phylogenetics and Evolution*, 57, 35-47.

Hansen, G.A., Grondal and Sons, B. (1885) *Spongiadae. Den Norske Nordhavs-Expedition 1876-1878*. Grondal and Sons Bogtrykkeri, Christiania, 1-25 pp.

Hogg, M. M., Tendal, O. S., Conway, K. W., Pomponi, S. A., van Soest, R. W. M., Gutt, J., Krautter, M. and Roberts, J. M. (2010) *Deep-sea sponge grounds: Reservoirs of biodiversity* . UNEP-WCMC Biodiversity Series No. 32 UNEP-WCMC, Cambridge.

Hooper, J.N.A. (1991) Revision of the Family Raspailiidae (Porifera: Demospongiae), with Description of Australian Species. *Invertebrate Taxonomy*, 5, 1179-1418.

Hooper, J.N.A. (2002a) Family Hemiasterellidae Lendenfeld, 1889. *In:* J.N.A Hooper. and R.W.M. Van Soest (Eds) *Systema Porifera: A guide to the classification of sponges,*1. Kluwer Academic/Plenum Publishers, New York, pp. 186-195.

Hooper, J.N.A. (2002b) Family Raspailiidae Hentschel, 1923. *In:* J.N.A Hooper. and R.W.M. Van Soest (Eds) *Systema Porifera: A guide to the*

*classification of sponges,*1. Kluwer Academic/ Plenum New York, pp. 469-510.

Johnston, G. (1842) A history of British sponges and lithophytes. W.H. Lizars, Edinburgh, 1-264 pp.

Kirkpatrick, R. (1903) Descriptions of South African sponges. Part III. *Marine Investigations in South Africa*, 2, 233-261.

Lendenfeld, R.V. (1897) On the Spongida. Notes on Rockall Island and Banks. *Transactions of the Royal Irish Academy*, 31, 82-88.

Lévi, C. (1957) Spongiaires des côtes d'Israel. *Bulletin of the Research Council of Israel*, 6B(3-4), 201-212.

Lévi, C. and Vacelet, J. (1958) Eponges récoltées dans l'Atlantique Oriental par le "President Theodore Tissier" (1955-1956). *Revue des Travaux de l'Institut des Pêches Maritimes*, 22, 225-246.

Maldonado, M. (1992) Demosponges of the red coral bottoms from the Alboran Sea. *Journal of Natural History*, 26, 1131-1161.

Maldonado, M. (1993) Demosponjas litorales de Alborán. Faunística y Biogeografía, 1-496 pp. Philosophical Dissertation. University of Barcelona, Barcelona.

Maldonado, M. (2006) The ecology of the sponge larva. *Canadian Journal of Zoology*, 84, 175-194.

Maldonado, M. and Benito, J. (1991) *Crambe tuberosa* n. sp. (Demospongiae, Poecilosclerida): a new Mediterranean poecilosclerid with lithistid affinities. *Cahiers de Biologie Marine*, 32, 323-332.

Maldonado, M. and Uriz, J.M. (1995) Biotoic affinities in a transitional zone between the Atlantic and the Mediterranean: a biogeographical approach based on sponges. *Journal of Biogeography*, 22, 89-110.

Maldonado, M. and Uriz, M.J. (1996) A new species of *Sphinctrella* (Demospongiae: Astrophorida) and remarks on the status of the genus in the Mediterranean. *Bulletin de l'Institut Royal des Sciences Naturelles de Belgique*, 66 suppl., 175-184.

Maldonado, M. and Uriz, M.J. (1999) A new dendroceratid sponge with reticulate skeleton. *Memoirs of the Queensland Museum*, 44, 353-359.

Martínez-García, P., Soto, J.I. and Comas, M. (2010) Structural analysis and recent tectonics in the central Alboran Sea. *Trabajos de Geología, Universidad de Oviedo*, 30, 44-48.

Morrow, C.C., Picton, B.E., Erpenbeck, D., Boury-Esnault, N., Maggs, C.A. and Allcock, A.L. (2012) Congruence between nuclear and mitochondrial genes in Demospongiae: A new hypothesis for relationships within the G4 clade (Porifera: Demospongiae). *Molecular Phylogenetics and Evolution*, 62, 174-190.

Pansini, M. (1984) Notes on some Mediterranean *Axinella* with description of two new species. *Bollettino dei Musei e degli Istituti Biologici della Università di Genova*, 50; 51, 79-98.

Pansini, M. (1987) Littoral demosponges from the banks of the straits of Sicily and the Alboran Sea. *In:* J. Vacelet & N. Boury-Esnault (Eds), *Taxonomy of Porifera,* G13. Springer-Verlag, Berlin, Heidelberg, pp. 149-186.

Pardo, E., Aguilar, R., García, S., de la Torriente, A. and Ubero, J. (2011) Documentación de arrecifes de corales de agua fría en el Mediterráneo occidental (Mar de Alborán). *Chronica Naturae*, 1, 20-34.

Pérès, J.M. and Picard, J. (1964) Nouveau manuel de bionomie benthique de la mer Méditerranée. *Recueil des Travaux de la Station Marine d'Endoume*, 31, 1-137.

Pulitzer-Finali, G. (1983) A collection of Mediterranean Demospongiae (Porifera) with, in appendix, a list of the Demospongiae hitherto recorded from the Mediterranean Sea. *Annali del Museo Civico di Storia Naturale Giacomo Doria*, 84, 445-621.

Pulitzer-Finali, G. (1993) A collection of marine sponges from East Africa. *Annali del Museo Civico di Storia Naturale Giacomo Doria*, 89, 247-350.

Rosell, D. and Uriz, M.J. (2002) Excavating and endolithic sponge species (Porifera) from the Mediterranean: species descriptions and identification key. *Organisms, Diversity and Evolution*, 2(1), 55-86.

Schmidt, O. (1870) *Grundzüge einer Spongien-Fauna des Atlantischen Gebietes.* Wilhelm Engelmann, Leipzig, 1-88 pp.

Templado, J., Calvo, M., Luque, A.A., Garvía, A., Maldonado, M. and Moro, L. (2004) *Guía de invertebrados y peces marinos protegidos por la legislación*

nacional e internacional. Ministerio de Medio Ambiente/Consejo Superior de Investigaciones Científicas, Madrid, 1-214 pp.

Templado, J., Calvo, M., Moreno, D., Flores, A., Conde, F., Abad, R., Rubio, J., López-Fé, C.M. and Ortiz, M. (2006) *Flora y fauna de la reserva marina y reserva de pesca de la isla de Alborán*. Ministerio de Agricultura, Pesca y Alimentación. Secretaría General de Pesca Marítima, Madrid, 1-126 pp.

Templado, J., García-Carrascosa, M., Baratech, L., Capaccioni, R., Juan, A., López-Ibor, A., Silvestre, R. and Massó, C. (1986) Estudio preliminar de la fauna asociada a los fondos coralígenos del mar de Alborán (SE de España). *Boletin del Instituto Español de Oceanografía*, 3, 93-104.

Topsent, E. (1892) Contribution a l'étude des Spongiaires de l'Atlantique Nord (Golfe de Gascogne, Terre-Neuve, Açores). Résultats des Campagnes Scientifiques accomplies par le Prince Albert I. Monaco, 2, 1-165.

Topsent, E. (1896) Matériaux pour servir à l'étude de la Faune des Spongiaires de France. *Mémoires de la Société Zoologique de France*, 9, 113-133.

Topsent, E. (1904) Spongiaires des Açores. *Résultats des Campagnes Scientifiques accomplies par le Prince Albert I*. Monaco, 25, 1-279.

Topsent, E. (1920) Spongiaires du Musée Zoologique de Strasbourg. Monaxonides. *Bulletin de l'Institut Océanographique de Monaco*, 381, 1-36.

Topsent, E. (1928) Spongiaires de l'Atlantique et de la Méditerranée, provenant des croissières du Prince Albert I de Monaco. *Résultats des Campagnes Scientifiques accomplies par le Prince Albert I*. Monaco, 74, 1-376.

Uriz, M.J. (2002) Family Ancorinidae Schmidt, 1870. *In:* Hooper, J.N.A. and Van Soest, R.W.M. (Eds) *Systema Porifera: a guide to the classification of Sponges*. Kluwer Academic/Plenum Publishers, New York, pp. 108-126.

Vacelet, J. (1969) Eponges de la Roche du Large et de l'étage bathyal de Méditerranée (récoltées de la Soucoupe plongeante cousteau et dragages). *Mémoires. Muséum National d'Histoire Naturelle*, série A, 59, 145-219.

Vermeij, G.J. (2012) The tropical history and future of the Mediterranean biota and the West African enigma. *Journal of Biogeography*, 39, 31-41.

Voultsiadou-Koukoura, E. and van Soest, R.W.M. (1991) *Hemiasterella aristoteliana* n. sp. (Porifera, Hadromerida) from the Aegean Sea with a

discussion on the family Hemiasterellidae. *Bijdragen tot de Dierkunde*, 61, 43-49.

Voultsiadou, E. (2009) Reevaluating sponge diversity and distribution in the Mediterranean Sea. *Hydrobiologia*, 628, 1-12.

Wells, H.W., Wells, M.J. and Gray, I.E. (1960) Marine sponges of North Carolina. *Journal of the Elisha Mitchell Scientific Society*, 76, 200-245.

Chapter 4

Export of bathyal benthos to the Atlantic through the Mediterranean outflow: sponges from the mud volcanoes of the Gulf of Cádiz as a case study

Abstract

The Mediterranean is a semi-enclosed sea, with a narrow natural connection —the Strait of Gibraltar— through its western basin to the North Atlantic. Many studies have investigated how the inflow of North Atlantic Surface water into the Mediterranean shapes the faunal composition and abundance of the shallow-water benthic communities of the Western Mediterranean. However, the reverse effect remains little explored, that is, at what level the relatively deep (>200 m deep) outflow of Mediterranean water (MOW) exports bathyal Mediterranean benthos into the North Atlantic and what is the fate of the exported fauna. In this study, we have investigated that process, using the bathyal sponge fauna known from a total of 9 biogeographical areas in the Northeastern Atlantic and 9 in the Western and Central Mediterranean, which accounted for a total of 456 spp. Prior to this general analysis, an exhaustive description of the bathyal sponge fauna (82 spp.) associated to 8 mud volcanoes located in the Gulf of Cádiz (Eastern North Atlantic) was conducted. This was necessary because the bathyal sponge fauna in the North Atlantic zone adjacent to the Strait of Gibraltar remained relatively poorly studied and that situation hindered relevant comparisons with the much better known bathyal fauna of the Western Mediterranean. The results of the clustering, ordination and regression analyses first revealed that the bathyal sponge fauna described from the mud volcanoes field in the Gulf of Cádiz was not essentially different from that previously described in pre-existing studies of other bathyal environments in the Gulf of Cádiz. The large scale subsequent assessment across the Atlantic-Mediterranean biogeographical gradient revealed that the sponge faunas of all Western Mediterranean areas form a relative cohesive group, except for the idiosyncratic nature of the Tyrrhenian Sea. More importantly, the deep-sea sponge fauna of the Gulf of

Cádiz (in the easternmost Atlantic side of the Atlantic-Mediterranean gradient) showed more affinity with the fauna of the Western Mediterranean than with the fauna of the remaining Northeastern Atlantic areas considered in the study (i.e., Cape Verde, Canary Islands, Madeira, the Moroccan slope, Lusitanian Banks, Southern Azores Banks and Azores). The Mediterranean area with the highest faunal similarity to the Gulf of Cádiz was the Alboran Sea, followed by the Gulf of Lion, the Strait of Sicily and, the Gulf of Taranto, sharing collectively about 17% of their species. These patterns of faunal affinities clearly illustrate the importance of the MOW in transporting components of the Mediterranean deep-sea sponge communities towards the bathyal communities of the Gulf of Cádiz. The contrasting low faunal affinity between the deep-water sponge fauna of the Gulf of Cádiz and the remaining North Atlantic areas considered in the analyses also revealed that the Mediterranean faunal export is largely circumscribed to the Gulf of Cádiz. It is likely that the North-Atlantic trajectory of the MOW, turning north after the Strait of Gibraltar and staying attached to the slope of the Iberian margin, hinders subsequent colonization of the slopes of the Macaronesia region by the deep-water Mediterranean sponges exported to the Gulf of Cádiz. The results of this study, combined with previous literature on biogeographical sponge transport by marine currents, suggest that the sponge fauna provides a useful tool to reveal the future shifts in the biogeographic patterns predicted in our man-impacted and changing ocean.

Introduction

The north-eastern Atlantic Ocean and the western Mediterranean Sea are connected through the Strait of Gibraltar. The North Atlantic Surface (NAS) water (0 to about 150 m depth) enters the westernmost area of the Mediterranean (i.e., Alboran Sea), while the Mediterranean Outflow Water (MOW) runs below (at 200-300 m) in the opposite direction and spreads along the North-Atlantic Gulf of Cádiz, divided in two main branches at depths of *ca*. 400 - 800 m and 1200 - 1500 m (Madelain, 1967; Zenk & Armi, 1990; Baringer and Price, 1999; Gasser et al., 2017; Sánchez-Leal et al., 2017), flowing close to the sea bottom. Two Mediterranean water masses contribute to the MOW: the Mediterranean Levantine Intermediate Water (LIW), originated in the Eastern Mediterranean, and the Western Mediterranean Deep Water (WMDW), originated in the Gulf of Lion. The former runs along the western basin at depths between 200 – 800 m and acts as the major contributor to the MOW, being responsible for 90% of the MOW's composition. The WMDW, responsible for a 10%, flows under the LIW (Stommel et al., 1973; Bryden and Stommel, 1984; Lascaratos et al., 1993; Malanotte-Rizzoli, 2001).

It has already been documented that the NAS brings the presence of Atlantic sessile species into the Alboran Sea, the westernmost basin of the Mediterranean (Pérès & Picard, 1964; Templado et al., 2006). Biogeographical studies specifically focused on the sponge fauna also reflect such a process (Templado et al., 1986; Pansini, 1987; Maldonado, 1992, 1993; Maldonado & Uriz, 1995; Maldonado et al., 2011; Xavier & Van Soest, 2012). However, little is known about the effects of a putative faunal transport in the opposite direction, that is, from the deep Mediterranean into the North Atlantic, which would be due to the MOW. Very few studies have assessed whether the MOW

exports Mediterranean benthic invertebrates to the Atlantic deep-sea communities and which could be the fate of the exported fauna. Most available information comes from the results of the French oceanographic cruises "Balgim", which sampled the benthos at the continental slope of the Ibero-Moroccan Gulf and the western zone of the Alboran Sea from May 25 to June 22 in 1984. Two Balgim studies based on 24 species of ascidians (Monniot & Monniot, 1988) and 146 species of bryozoans (Harmelin & d'Hondt, 1993) suggested minimal presence of Mediterranean species exported to the Atlantic communities, but the one based on sponges (Boury-Esnault et al., 1994) suggested a different pattern: from a total of 96 sponge species collected, 50 were present exclusively at the Atlantic side, 28 at the Mediterranean side and 17 occurred in both. Since the Balgim times, the study of the North Atlantic and the Mediterranean depths has been tremendously facilitated by progressive improvements of the technologies for deep-sea exploration during the past 30 years. As a result, numerous subsequent records on deep-sea benthos have been obtained, which need to be considered in updated faunal analysis. Herein we are re-examining the "biogeographical message" of the deep sponge fauna after expanding considerably the database used for this analyses (up to 456 spp.) relative to that in previous studies. Our main objective was to conduct a comprehensive re-examination of the MOW role in the interrelationships between the bathyal faunas of the Eastern North Atlantic and the Mediterranean, using sponges as a case study.

The faunal comparison in the concerned area for this study incorporates all taxonomic studies on sponges subsequent to Boury-Esnault et al. (1994), including diverse locations within both the eastern North Atlantic and the Western Mediterranean. Yet, the sponge fauna of the bathyal communities in the Gulf of Cádiz, despite being in a Northeastern Atlantic zone strongly affected by the MOW trajectory, was less known than its bathymetric equivalent in the Western Mediterranean, a situation that prevented reliable comparisons. For this reason, prior to the global analysis at a large-scale Atlantic-Mediterranean gradient, we conducted a detailed analysis of the rich sponge fauna (82 spp.) recently described from mud volcano habitats in the Gulf of Cádiz (Fig. 1). Since the late 90's, a variety of hydrocarbon fluid venting structures, including mud volcanoes, has progressively been described at the Gulf of Cádiz, with more than 70 mud volcanoes discovered to date, at

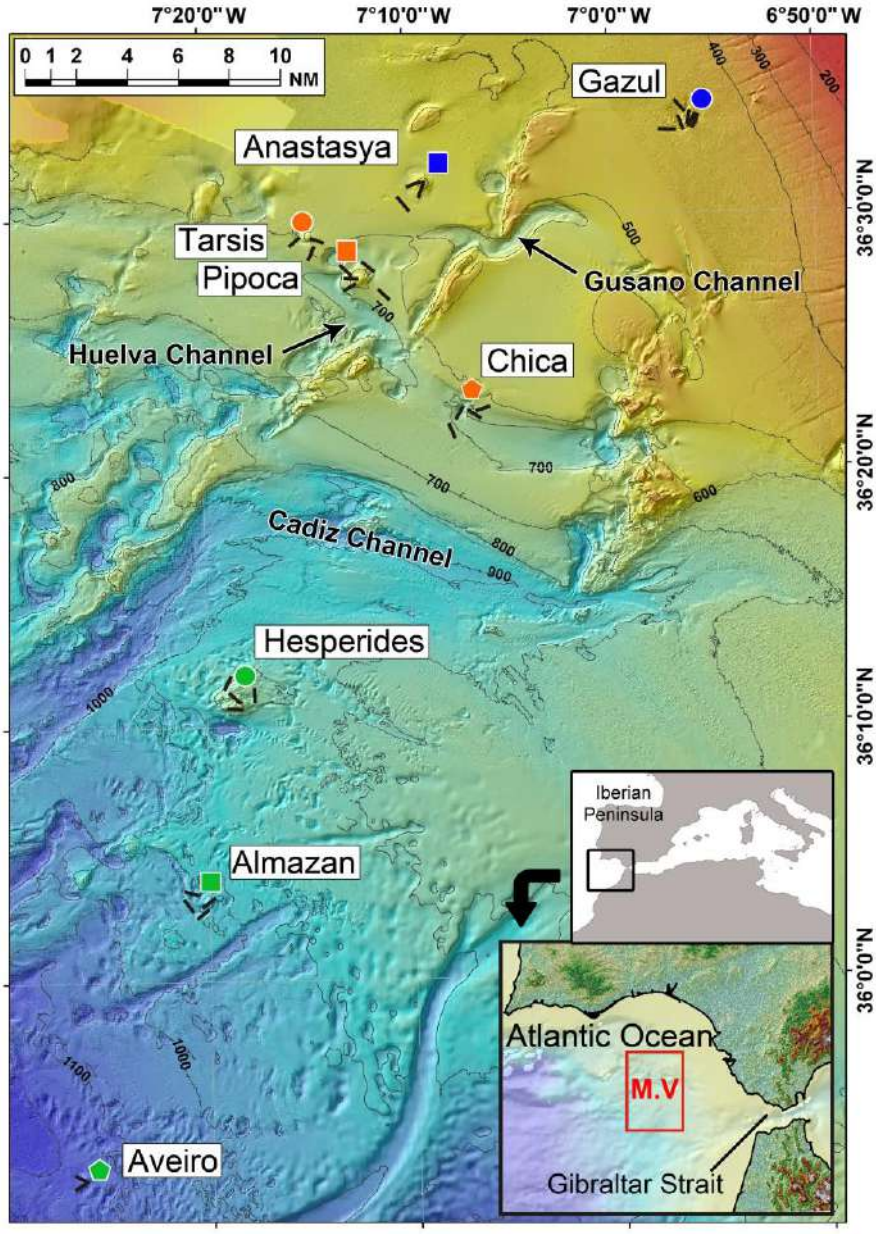

Fig. 1. Map showing the location of the eight sampled mud volcanoes investigated in the mud volcano fields of the Gulf of Cádiz. The insets show the general location of the mud volcanoes into the Atlantic-Mediterranean at two different spatial scales. The mud volcanoes (indicated by color symbols in the largest map) were located in zones across three depth ranges:

…continued in the next page

upper zone (blue symbols; 300-550 m), intermediate zone (orange symbols; 600-730 m) and deep zone (green symbols; 800-1200 m). The black lines indicate the location of beam trawl transects where the sponges were collected. The arrows indicate the location of some of the erosive channels produced by the Mediterranean Outflow Water (MOW) on the Gulf of Cádiz slope.

depths from 200 to 4000 m (Gardner, 2001; Pinheiro et al., 2003; Somoza et al., 2003). The presence of hydrocarbons (mainly consisting of methane) facilitates the proliferation of consortia of archaea and bacteria that live out of anaerobic methane oxidation coupled with sulphate reduction (Boetius et al., 2000; Boetius and Suess, 2004). The methane venting is also relevant to sessile invertebrates, since it results in precipitation of methane-derived authigenic carbonate structures (hereafter referred to as carbonates), such as slabs, crusts and chimneys (Hovland et al., 1987; Suess, 2014). Once venting ceases, the carbonate structures provide suitable hard substrates for subsequent colonization by deep-sea sessile fauna (sponges, gorgonians, cold-water corals, etc.). This pioneering fauna may in turn facilitate the arrival of additional organisms, triggering a global increase of the benthic biodiversity on the carbonates (Levin, 2005; Rueda et al., 2012; González-García et al., 2020). In European waters, mud volcanoes are classified as sensitive habitats: habitat 1180 "Submarine structures made by leaking gases" EUR 27, 2007, and their sponge fauna has only recently been explored (Fig 2). After the recent taxonomic description of the main sponge fauna associated to a field of mud volcanoes located at bathyal depths in the northern Gulf of Cádiz (Chapter 1), this study further investigates between-volcano faunal patterns. More importantly, the sponge fauna of those mud volcanoes is herein collectively incorporated as a crucial element to undertake a more representative Atlantic-Mediterranean assessment of the transport of bathyal fauna by the MOW.

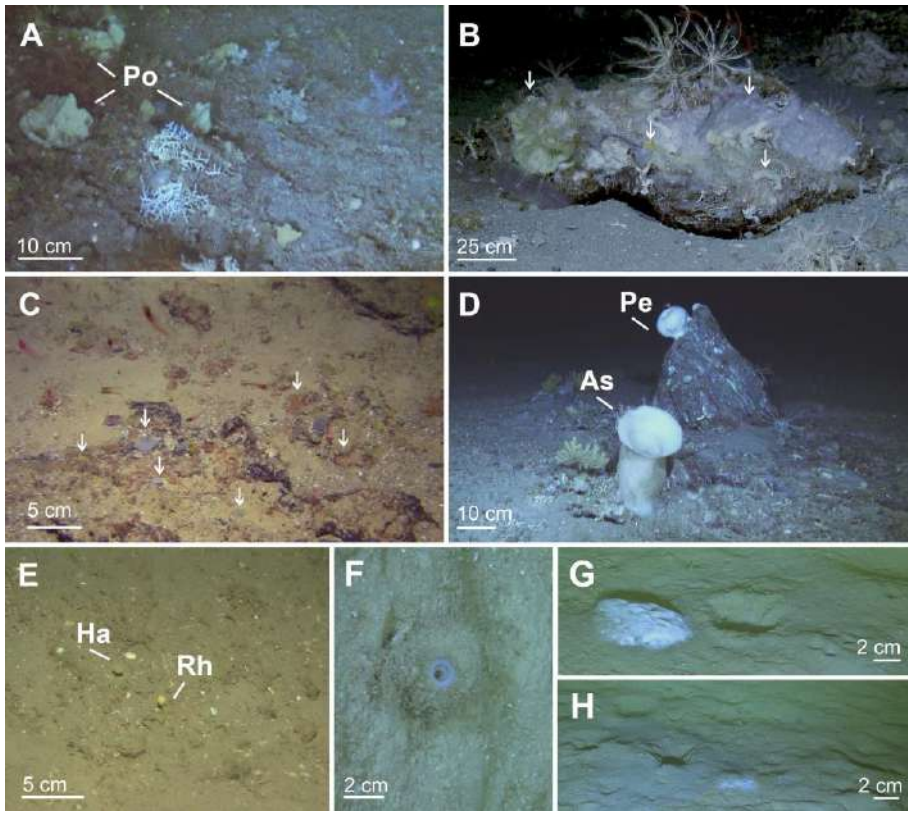

Fig. 2. Images of the sponge fauna of the mud volcanoes recorded by the Liropus ROV. (A-B) The hard substratum offered by the abundant carbonate slabs at Gazul mud volcano facilitated a rich benthic fauna of filter and suspension feeders. The sponge *Poecillastra compressa* (Po) is common in picture A. Likewise, abundant unidentifiable sponges occur on the carbonate slab in picture B, which are marked by arrows. (C) Carbonate slabs at Hesperides mud volcano showing a variety of small unidentified sponges (marked with arrows). (D) Bottom at Pipoca mud volcano characterized by predominant soft sediment with scarce carbonate slabs, which host the sponges *Asconema setubalense* (As) and *Petrosia crassa* (Pe). (E) Soft bottom at Chica mud volcano showing two different lollypop-shaped sponge species, *Haliclona bouryesnaultae* (Ha) and *Rhyzaxinella pyrifera* (Rh). (F) Soft bottom at Almazan volcano showing the hexactinellid *Pheronema carpenteri,* an abundant species at this volcano. (G-H) Soft bottoms at Anastasya mud volcano deprived from sponges and showing white mats of sulphur-reducing bacteria.

Material and methods

Study area at the Gulf of Cádiz

The Gulf of Cádiz is situated at the Northeast Atlantic, between the SW Iberian margin and the NW Moroccan margin (Fig. 1). The sponge fauna collected from eight mud volcanoes located on the continental slope from 300 to 1200 m depths in the northern Gulf of Cádiz was recently described by our team (Chapter 1 – also Sitjà et al., 2019). Strictly speaking, the eight studied mud volcanoes are indeed six mud volcanoes and two diapir-mud volcanoes, but for the sake of simplicity they will be referred to hereafter as mud volcanoes. The mud volcanoes are distributed in three zones (Fig. 1). The shallowest, consisting of Gazul and Anastasya, is located in the upper continental slope, from 300 to 550 m. Tarsis, Pipoca and Chica are located at intermediate depths of 600 to 730 m. Hesperides, Almazan and Aveiro make the deepest zone, from 800 to 1200m depths. This deepest zone is physically separated from the two others by the Cádiz Contourite Channel (Fig. 1), an orographic incision of the substrate caused by the erosive effect of the MOW. There are two others MOW-eroded contourite channels, one at the intermediate zone, called the Gusano Channel, relatively close to Anastasya volcano, and the other, the Huelva Channel, close to Chica and Pipoca volcanoes (Fig. 1). Therefore, there is strong evidence that the MOW trajectory directly impacts on the studied mud volcanoes (Sánchez-Leal et al., 2017).

Sampling procedures at the Gulf of Cádiz

A total of 38 collecting transects (hauls) were performed by beam trawl, sampling collectively about 75,000 m^2. Sampling was conducted in the frame of the EU LIFE+ INDEMARES project (subproject "Chimeneas de Cádiz"). Information on number of beam trawl transects and mean (± SD) sampling depth in each volcano is given in Table 1. Information on the area sampled at each volcano is given in section 2.4 "*Between-volcano faunal affinities"*. Details on the expeditions, sampling and taxonomic identification procedures of the sponge fauna are given elsewhere (Chapter 1). Further "in vivo" details of the sponge communities and their environment were documented during the cruises using both an underwater towed observation vehicle VOR 'Aphia

Table 1. Summary of major features of the studied mud volcanoes, including total number of beam trawl transects (N bt), number of beam trawl transects retrieving sponges (N sbt), average (±SD) depth (=D, in m) for the set of beam trawl transects conducted at each volcano, average (±SD) abundance of authigenic carbonates (Carbonate= C) as scored from a semi-quantitative approach (0 to 3), average (±SD) venting activity of methane-rich fluid (Methane= M) as scored from a semi-quantitative approach (0 to 3), and intensity of bottom fishing activity (Fishing= F) as scored from a semi-quantitative approach (0 to 3). Averages (±SD) were calculated considering only trawls that retrieved sponges. Sponge species richness (N sp), total number of sponge individuals (N ind), and density of individuals (N ind x 10^{-3} m^{-2}) at each mud volcano are also shown.

Mud volcano	N bt	N sbt	Depth (m)	Carbonate	Methane	Fishing	N sp	N ind	N ind ($x10^{-3}$ m^{-2})
Gazul	7	6	453 ± 32	2.00 ± 0.89	0.50 ± 0.55	0.50 ± 0.84	15	370	30.72
Anastasya	6	3	524 ± 32	0.00 ± 0.00	2.00 ± 1.73	2.67 ± 0.58	8	42	6.07
Tarsis	6	3	602 ± 23	0.33 ± 0.58	0.67 ± 1.15	2.33 ± 1.15	9	99	16.63
Pipoca	5	5	616 ± 60	0.60 ± 0.89	0.80 ± 1.10	0.40 ± 0.89	38	249	25.92
Chica	4	4	673 ± 36	0.75 ± 0.50	0.00 ± 0.00	1.00 ± 1.41	27	299	37.01
Hesperides	4	4	765 ± 52	1.75 ± 1.50	1.50 ± 1.73	0.00 ± 0.00	19	105	14.30
Almazan	4	4	904 ± 25	1.00 ± 0.82	1.00 ± 1.15	0.00 ± 0.00	27	270	35.74
Aveiro	2	2	1124 ± 21	0.00 ± 0.00	1.50 ± 2.12	0.00 ± 0.00	9	225	61.12

2012' and the ROV 'Liropus 2000'. Four environmental variables were recorded for each sampling transect: depth (D), semi-quantitative abundance of methane-derived authigenic carbonates (C), methane-rich fluid emission (M), and a semi-quantitative assessment of the intensity of bottom fishing (F) activities by the trawling fleet. The semi-quantitative assessment of the C, M, and F parameters consisted on scoring them from 0 to 3 for each sampling station, based on observations, as it follows: 1) Carbonate formations (C), such as chimneys, crusts and slabs, were scored by their abundance in the samples retrieved by the trawls and, when possible, these data were confronted with underwater images obtained during VOR and ROV transects. The criteria for the semi-quantitative categorization was 0= no carbonate piece retrieved per trawl, 1= one C piece retrieved per trawl, 2= two to five C pieces retrieved, and 3= more than five C pieces retrieved, often larger than 50 cm in length. 2) The scoring of the methane-rich fluid emission was ranked according to

the presence of chemosynthetic bacterial mats and the abundance of chemosymbiotic invertebrates recovered by the trawls and box corers from the various mud volcanoes. It was categorized as 0= no evidence of chemosynthetic-chemosymbiotic communities; 1= <50 individuals of chemosymbiotic invertebrates m^{-2}; 2= 51-500 individuals of chemosymbiotic invertebrates m^{-2}; 3= >500 individuals of chemosymbiotic invertebrates m^{-2}. 3) The trawl fishing activity was assessed by tracking the activity of each vessel of the trawling fleet for the period January to December 2011, using the Vessel Monitoring System (VMS) datasets supplied by the Spanish General Secretary of Fisheries (Spanish Ministry of Agriculture and Fisheries). Categories were 0= no trawling vessel operating in that area during 2011; 1= 1 trawling vessel; 2= 2-5 trawling vessels; 3= >5 trawling vessels.

The final score given to a mud volcano for each of the four environmental variables was the mean (±SD) value obtained from the set of beam trawl transects conducted in such a mud volcano (Table 1). Prior to any analysis, each of the 4 variables was standardized by its own maximum to render their ranges comparable.

Sampling effort at the Gulf of Cádiz

From the list of sponge species identified, a 'species x sample' matrix was created discriminating the number of individuals of each species (abundance) retrieved from each beam trawl transect. Previous to any analysis or standardization, the sampling effort performed on a mud volcano was tested through a species accumulation curve to examine at what level the collected fauna was representative of the global sponge fauna occurring at that volcano. The species accumulation curves were built following the Ugland, Gray and Ellingsen (UGE) method (Ugland et al., 2003) in the Plymouth Routines Multivariate Ecological Research (PRIMER 6) software (Clarke & Gorley, 2006). A curve was obtained for each volcano throughout 999 randomizations. Then, a global curve was built for the combination of all the samples of all volcanoes.

Between-volcano faunal affinities

To analyze the faunal affinities between volcanoes each 'species x volcano' matrix was collapsed across beam trawls, showing just the total number of individuals of each species for each volcano. The matrix included only the beam trawl transects that retrieved sponges (n= 31). When plotting the total trawled area versus either the area with sponge occurrence for each volcano or the total number of collected individuals (Fig. 3), it was made evident that

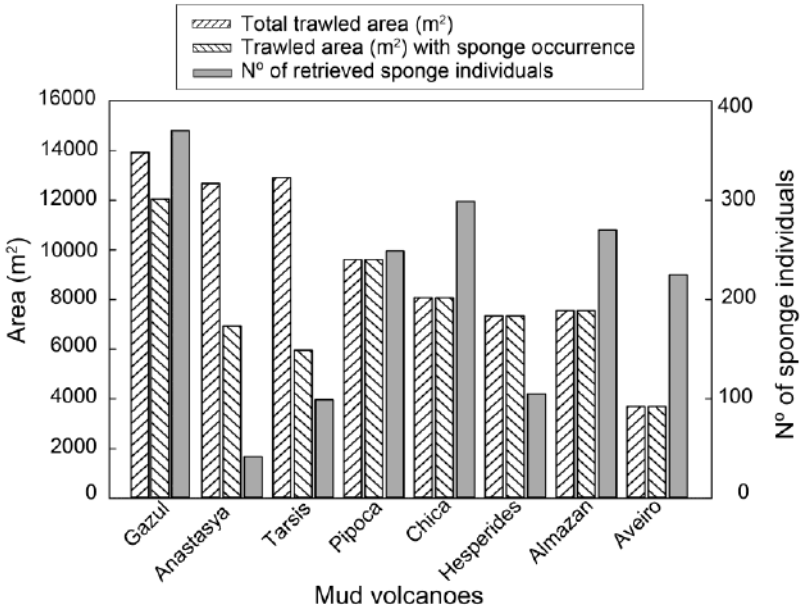

Fig. 3. Plot summarizing the total trawled area (m^2), the trawled area where sponges were found (m^2) and the number of collected sponge individuals (grey-shaded columns) for the sampled volcanoes

some trawl transects at Gazul, Anastasya and Tarsis collected no sponge. This was probably due to the fact that some hauls had initially been designed in the project frame for purposes other than the collecting sponges and targeted specific habitats in which sponges are typically absent.

Before any analysis, the number of individuals of each species in each volcano was standardized to total trawled area and such abundance per m^2 was then square root transformed in order to minimize the effect of highly abundant species in the subsequent multivariate analyses. By using the

PRIMER 6 software, the affinities between pairs of volcanoes based on the Bray-Curtis similarity index were calculated and represented in a dendrogram accompanied by a similarity profile (SIMPROF) permutation analysis to test for evidence of a genuine (statistically significant) clustering within our set of mud volcanoes. Following, a similarity percentages (SIMPER) test was run to obtain the percentage contribution of the species to the clustering pattern among volcanoes.

To assess the influence of the recorded environmental variables on the faunal patterns among the mud volcanoes, correspondence analyses were performed using the software for Canonical Community Ordination, CANOCO 4.5. To avoid distortion of ordination scores by rare species the 'down-weight option' available in the software was used. The explainable faunal variation in our 'species x volcano' matrix was assessed by using a correspondence analysis (CA) to reveal how the species were distributed along the volcanoes with no constraint. Then, the portion of variation related to the environmental variables was estimated using canonical correspondence analysis (CCA). The statistical significance of the first canonical axis and all canonical axes of the resulting model was tested by the Monte-Carlo test using 500 permutations. Four environmental variables (C, D, F, and M) were initially considered for the CCA analysis. Subsequently, we discriminated between "natural" environmental variables (i.e., D, C and M) and "man-driven" environmental variables (i.e., F) and calculated the faunal variation uniquely explained by each of the sets, by the two sets together and that remaining unexplained by the analysis, following an analysis of variation partitioning (Borcard et al., 1992). The 'forward selection' option was then used to unmask co-variation and select the most relevant environmental variables in terms of explaining faunal variance, as indicated by Monte-Carlo permutation tests with 500 permutations and the variance inflation factors (VIF). Finally, a second CCA was performed constrained by only the most relevant environmental variables. Additionally, the relationship of the resulting environmental vectors and the main axes of the ordination space was examined by Spearman rank correlation for both models of four and two environmental variables.

Faunal affinities across the Atlantic-Mediterranean gradient

To examine the faunal affinities along the Atlantic-Mediterranean gradient, a presence/absence matrix was built containing all deep-sea sponge species (456 spp.) recorded for a variety of bathyal biogeographic areas distributed along the considered Atlantic–Mediterranean gradient (Appendix I Data File). Areas recognized as biogeographic entities were based in pre-existing literature (Pansini & Longo, 2003; Spalding et al., 2007). The approach included records from a total of 18 initial areas, including areas from the Central and Western regions of the Mediterranean and, in the Atlantic, the Gulf of Cádiz, southern Lusitania and Macaronesia (Fig. 4, Appendix II). The nine areas from the Atlantic were Azores (A-A), Southern Azores Banks (AB-A), Cape Verde (CV-A), Canary Islands (Ca-A), Madeira (Ma-A), Morocco (Mo-A), Lusitanian Banks (LB-A), the Gulf of Cádiz mud volcanoes (MV-A), and the remaining slope communities of the Gulf of Cádiz (GC-A). In the Mediterranean, nine areas were considered: Alboran Sea (Al-M), Balearic Sea (B-M), Gulf of Lion (GL-M), Ligurian Sea (L-M), West Corsica (C-M), Tyrrhenian Sea (T-M), Strait of Sicily (S-M), Gulf of Taranto (GT-M), and Adriatic Sea (A-M).

An exploratory Jaccard-based dendrogram and subsequent SIMPROF tests were performed (data not shown) to detect: 1) areas with strong affinities representing statistically significant genuine groups, which can be combined with each other into a single biogeographic area; and 2) cluster members with no statistically significant structure, which should stay independent for the analyses. These exploratory tests suggested that the fauna of the Canary Islands (Ca-A), Madeira (Ma-A) and Morocco (Mo-A) could be grouped into a unit, hereafter referred to as C+Ma+Mo-A. Following this readjustment, a total of 16 areas were finally submitted to the definitive analyses of the bathyal sponge fauna along an Atlantic-Mediterranean gradient impacted by the MOW. The geographical location of the initial and collapsed areas and their respective numbers of species are summarized in Fig. 4.

Because the available taxonomic studies for the sponge fauna of most locations often lacked robust and/or consistent information about the abundance of the species, the use of quantitative or semi-quantitative analyses was impracticable. The compiled database included only those records deeper than 200 m, this threshold being defined by the upper depth limit of the LIW

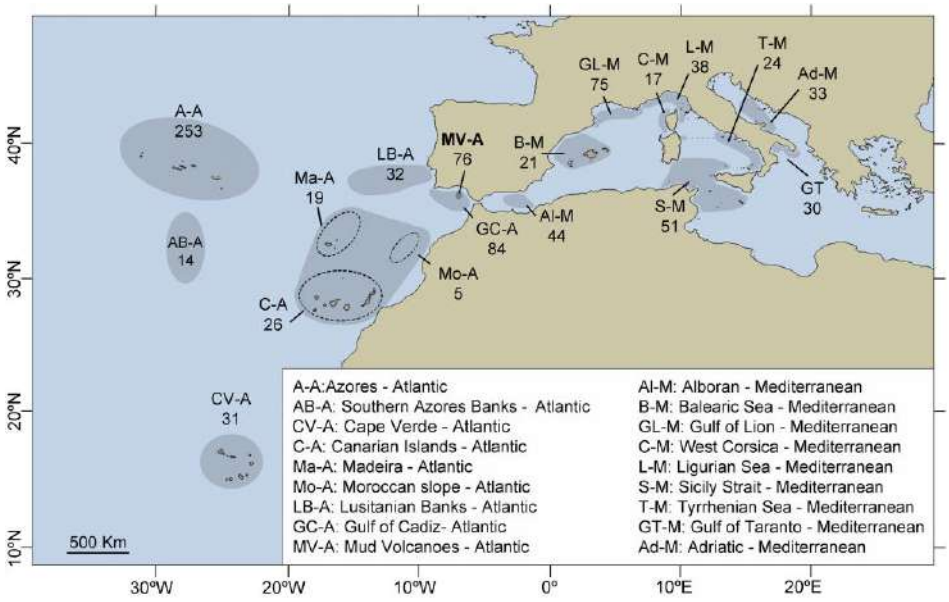

Fig. 4. Map of the Atlantic-Mediterranean region showing the biogeographical areas (grey shades) and their sub-areas (see codes in legend) considered for the comparison of affinities for the sponge fauna. Geographically close sub-areas which showed not significant faunal differences after exploratory Jaccard-based cluster analyses were unified into a larger area, but still indicated in the map by dashed lines. Each area and subarea is labelled with a code (see graphic legend). The number of sponge species recorded to date within the 200 - 1,500 m depth in each area and subareas is also indicated.

and the MOW. Since both the LIW and the WDMW contribute (in a 90% and 10%) to the composition of the MOW, no lower depth limit was settled for the Mediterranean records. Because the MOW spreads in the Atlantic at about 1500 m, this depth was established as the lower limit for the records in the Atlantic Ocean (Fig. 5). Therefore, the considered depth ranges facilitate the possibility that species living in the Mediterranean below 1500m can be detected into the Atlantic inventories if brought to shallower depths by the MOW trajectory in the North Atlantic region. All sponge records were double checked by contrasting them against the World Porifera Database (Van Soest et al., 2019), so that those currently considered as inaccurate or incorrect

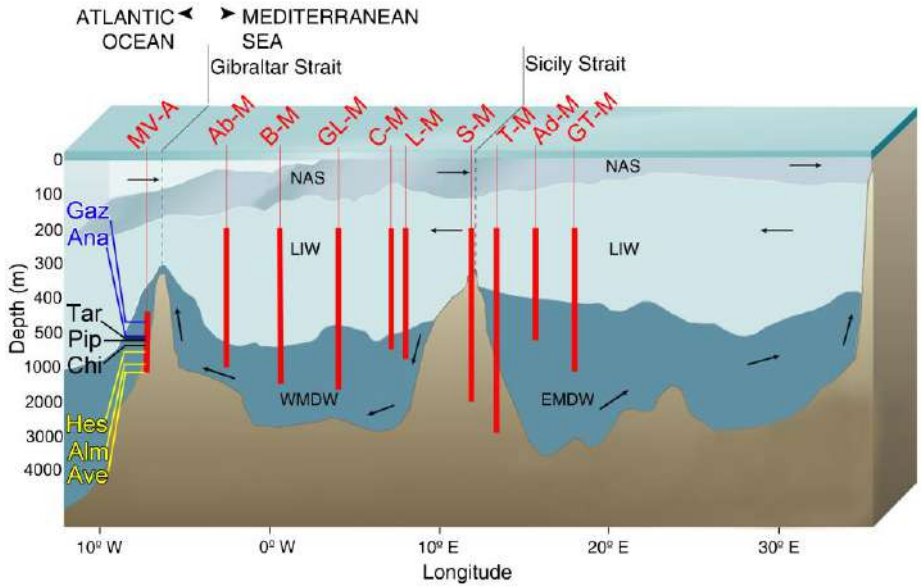

Fig. 5. Schematic profile of the Mediterranean and its connection to the North Atlantic (modified from GRID-Arendal, 2013), indicating the bathymetric range (thick red lines) and longitude of the Mediterranean areas and the mud volcanoes at the Gulf of Cádiz considered in this study. The major water masses (in black upper case) occurring in the depicted region and their prevailing direction (black arrows) are also indicated (NASW= North Atlantic Surface Water, LIW= Levantine Intermediate Water, WMDW & EMDW = Western & Eastern Mediterranean Deep Waters, respectively). Biogeographical areas (red uppercase labels) follow the codes given in Fig. 3 (Ab-M= Alboran – Mediterranean; B-M= Balearic Sea – Mediterranean; GL-M= Gulf of Lion – Mediterranean; L-M= Ligurian Sea – Mediterranean; C-M= West Corsica – Mediterranean; S-M= Sicily Strait – Mediterranean; T-M= Tyrrhenian Sea – Mediterranean; Ad-M= Adriatic Sea – Mediterranean; GT-M= Gulf of Taranto – Mediterranean). To the left, the blue, black and yellow, lower case labels for the mud volcanoes are Gaz= Gazul, Ana= Anastasya, Tar= Tarsis, Pip= Pipoca, Chi= Chica, Hes= Hesperides, Alm= Almazan and Ave= Aveiro.

taxonomic records in such database were excluded. Likewise, records identified as cf. (n=6) and those with an unknown collection depth were also discarded. The two controversial species *Leiodermatium lynceus* and *Leiodermatium pfeifferae* were included in the database as a single taxonomic entity called *Leiodermatium* spp. complex. This responds to their questionable validity as different species, since they have been reported to lack robust

differential characters (Carter, 1873; Kelly, 2007; Maldonado et al., 2015). The readjustments resulted in a total of 456 species. Appendix I Data File details all the species, sampling depths, geographic locations and bibliographic records.

To assess the sponge faunal affinities across the Atlantic-Mediterranean deep-sea gradient, the "species x area" matrix of presence/absence data was analyzed by PRIMER Vo. 6 software to conduct cluster analyses based on Jaccard similarity, along with SIMPROF tests. Jaccard similarity matrices were further processed by Multidimensional Scaling (MDS) to visualize affinity patterns in 2D ordination plots.

Subsequently, the putative effect of the MOW on the faunal affinities was also tested by linear regression analysis, under the assumption that, if the Mediterranean outflow has no major effect on shaping the faunal affinities, the geographical distances among the studied deep-sea areas should largely predict the faunal similarities: the greater the geographical distance between two areas, the lower their faunal affinity. Geographical distances were obtained by using Google Earth software. We considered the shortest possible distance between the centroids of two studied areas through the marine medium, meaning that all distances between Atlantic and Mediterranean areas were calculated from trajectories through the Strait of Gibraltar. The relationship between the pattern of faunal similarity and actual geographical distances among the areas was examined by linear regression using SigmaPlot Vo.13 software.

Results

Sampling effort and sponge abundance at the Gulf of Cádiz

The effectiveness of sampling, as analyzed by the UGE method, showed for each of the volcanoes a rising accumulation curve not reaching the asymptotic stage. This pattern suggests that probably additional sponge species would have been retrieved by increasing the sampling effort in all volcanoes (Fig. 6A). Uneven sampling effort across volcanoes was also detected, with shallower volcanoes typically being more sampled than the deepest ones (Fig. 3). The enormous logistic and economic effort required to increase sampling effort was simply not affordable. Therefore, these weaknesses in the approach

have been taken into consideration when conducting and interpreting the faunal analyses. Interestingly, the global sampling effort across the mud volcanoes field appears to be more representative. When pooling all volcanoes, the species accumulation curve starts describing a trajectory that approaches to an asymptotic stabilization (Fig. 6B).

From the 38 trawl transects performed in the eight mud volcanoes, seven of them retrieved no sponge and 31 provided a total of 1,659 sponge specimens belonging to 82 different species (Table 1). The volcanoes with high total numbers of sponge individuals were —in decreasing order from 370 to 225 individuals— Gazul, Chica, Almazan, Pipoca and Aveiro (Table 1, Fig. 7). A comparatively high number of species (i.e., richness) was found at Pipoca, Chica, Almazan, Hesperides and Gazul, ranging from 38 to 15 species (Table 1, Fig. 7).

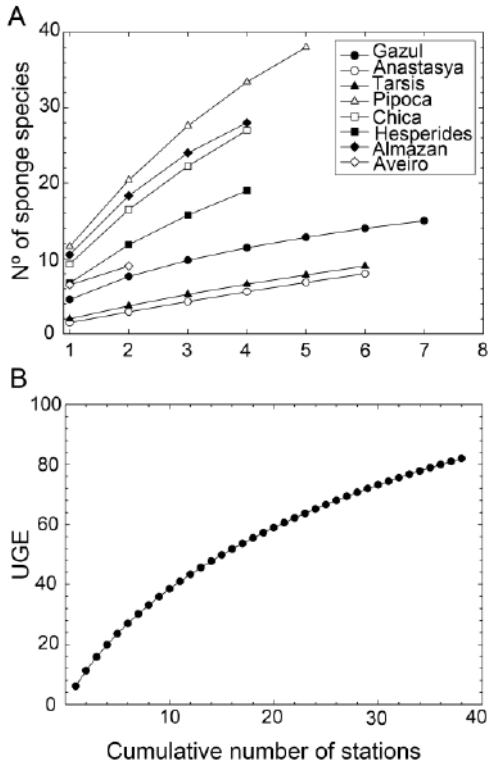

Fig. 6. (A) Species accumulation curves for each of the eight mud volcanoes obtained from randomizing samples through the Ugland, Gray and Ellingsen method (UGE). They show the increment in the number of different species with increasing numbers of trawl transects. (B) Species accumulation curves for data on number of species retrieved from trawl transects of all volcanoes are pooled together for analysis.

The pattern suggests a relatively even representativeness of the sponge species across the mud volcanoes, Gazul (the shallowest) and Aveiro (the deepest) being exceptions. The latter two showed a relatively low number of species in relation to the number of individuals because of disproportionate abundances of *Petrosia (Petrosia) crassa* (Carter, 1876) in Gazul

and *Thenea muricata* (Bowerbank, 1858) in Aveiro. The former species represented 40% of the collected individuals in Gazul and the latter about

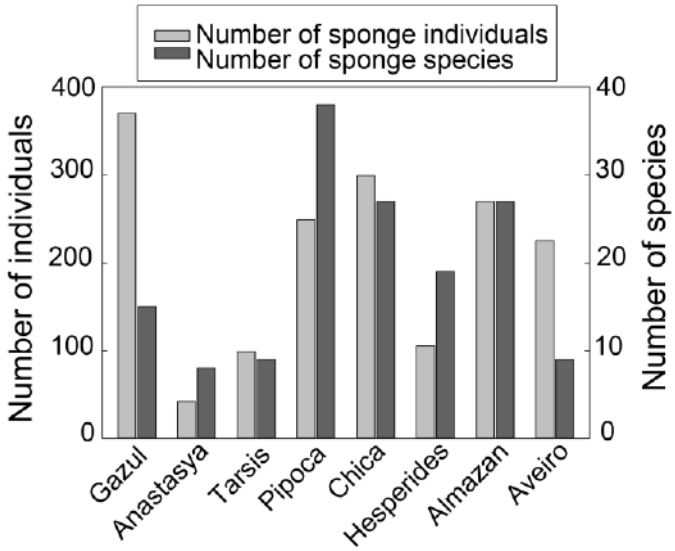

Fig. 7. Comparative summary of the number of individuals and species in the sponge fauna collected from each mud volcano.

60% of those collected in Aveiro. These results, together with ROV images, suggest that Gazul hosts aggregations of *P. crassa*, probably favored by an abundance of hard substrate in the form of carbonates, and that aggregations of *T. muricata,* a soft-bottom specialist, occur at Aveiro. Other mud volcanoes with lower but still fairly relevant abundances and high species richness were Pipoca, Chica, and Almazan. Interestingly, the first two are located close to the Huelva Channel, eroded by the MOW.

Taxonomically, the Class Hexactinellida represented 18% of the total of sponges identified and class Demospongiae 82%, both classes being present in all the studied volcanoes. The most abundant species were *T. muricata*, *Pheronema carpenteri* (Thomson, 1869) (Fig. 2F), *P. crassa* (Fig. 2D), *Asconema setubalense* Kent, 1870 (Fig. 2D), and *Desmacella inornata* (Bowerbank, 1866) (Table 2).

Between-volcano faunal affinities

The Bray-Curtis faunal similarity analysis distributed the mud volcanoes in two main groups (Fig. 8). At the global level, the within-group similarity was low (i.e., 16.8 and 25.4%, respectively) and none of the groups had its main node with statistical support. The main dichotomy in two volcano groups did not reflect a bathymetric pattern, since the smallest of the clusters (i.e., 16.8 % similarity) included the shallowest volcano (Gazul) along with two others of the deepest zone (Hesperides, Almazan). Likewise, the largest of the two clusters (25.48% similarity) contained volcanoes from the three bathymetric zones (Fig. 8). However, a more detailed analysis of the structure of this larger group in 3 subclusters revealed a clear effect of depth in the faunal affinities. There was a subcluster formed by Anastasya (from the shallow zone) and Tarsis (from the intermediate zone); they made a genuine group (50.45% similarity) with statistical support, probably because, although Tarsis was considered *a priori* a volcano from the shallow zone, it actually occurs in a transitional zone between the shallow and the intermediate zones. A second subcluster formed by the two volcanoes of the intermediate zone, Pipoca and Chica, showed even higher faunal similarity (53.26%) with statistical

Table 2. List of the most abundant species (i.e., those accounting each for more than 3% of the total abundance) in the total of the studied mud volcanoes. The taxonomic class to which they belong is indicated (Dem= Demospongiae; Hex= Hexactinellida), together with the abundance of each species along the total sampling stations (Ab), their abundance proportional to the total of sponge individuals (% Ab) and the number of trawls (N sbt) in which each of the species were present.

Class	Species	Ab	% Ab	N sbt
Dem	*Thenea muricata* (Bowerbank, 1858)	366	22.0	12
Hex	*Pheronema carpenteri* (Thomson, 1869)	181	11.0	8
Dem	*Petrosia (Petrosia) crassa* (Carter, 1876)	169	10.2	10
Hex	*Asconema setubalense* Kent, 1870	117	7.1	18
Dem	*Desmacella inornata* (Bowerbank, 1866)	110	6.6	16
Dem	*Haliclona (Gellius) angulata* (Bowerbank, 1866)	74	4.5	6
Dem	*Lycopodina hypogea* (Vacelet & Boury-Esnault, 1996)	71	4.3	1
Dem	*Poecillastra compressa* (Bowerbank, 1866)	64	3.9	8
Dem	*Stylocordyla borealis* (Lovén, 1868)	58	3.5	3
Dem	*Haliclona (Rhizoniera) bouryesnaultae* Van Soest & Hooper, 2020	49	3.0	6

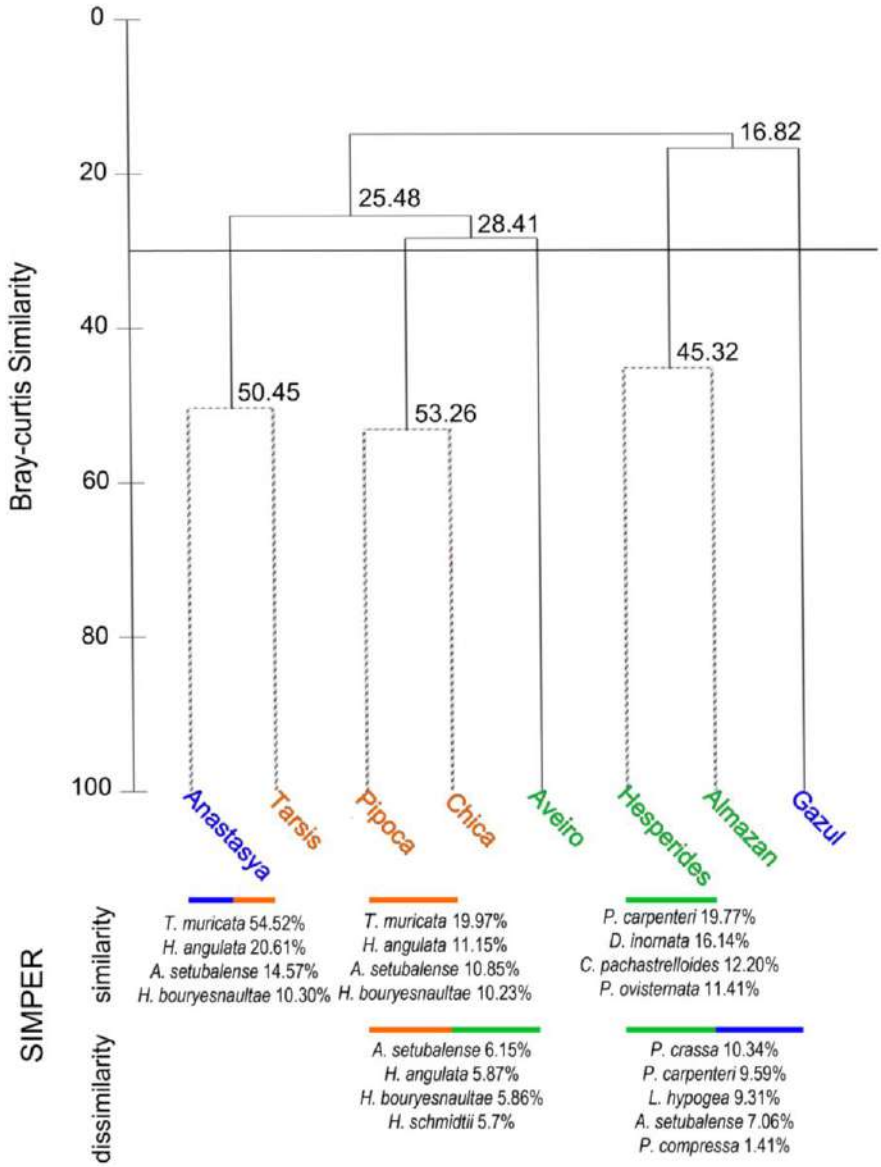

Fig. 8. Dendrogram based on Bray-Curtis similarity between the eight mud volcanoes, also summarizing the results of the SIMPROF and SIMPER tests. Mud volcanoes are labelled by colors according to the depth range of volcano zones they belong to (upper zone= blue, intermediate zone= orange, lower zone= green). The numerical values at the nodes correspond to the percentage of similarity of the sub-groups. The horizontal solid line represents the 30% similarity threshold.

…continued in the next page

Dashed lines represent genuine groups with statistical significance according to SIMPROF test. SIMPER results are shown at the bottom, indicating the species most contributing to the similarities or dissimilarities between the volcano clusters (see color lines for the cluster entities involved in the comparison). Species contribution is expressed in percentages. Length and color of the horizontal lines match the labels, indicating the subgroup to which the SIMPER results are referring to.

SIMPROF significance. Finally, Aveiro, the deepest volcano, became associated to the two intermediate volcanoes, although with only 28.41% and without statistical support. Therefore, under the structure of the large clusters there was some "depth pattern". The situation was similar for the smallest of the two main clusters (Fig. 8): Gazul, being at the shallower zone, shared only 16.82% (p= 0.001) of faunal similarity with Hesperides and Almazan, which are supported pair with 45.32% of similarity. It is also worth noticing that these three mud volcanoes clustered consistently with their features regarding authigenic carbonates features, being the mud volcanoes with highest abundance of such hard substrate (Table 1).

According to the SIMPER test, the species contributing to the formation of the larger group are *T. muricata, Haliclona angulata, A. setubalense* and *Haliclona bouryesnaultae* Van Soest and Hooper, 2020 (Fig. 8). The smallest cluster of volcanoes was mostly supported by the shared presence of *P. crassa*, *D. inornata* and *Poecillastra compressa* (Bowerbank, 1866) (Fig. 2A). The reasons for Gazul's distinctiveness were its singular abundance of *P. crassa* (10.34%) and the carnivorous sponge *Lycopodina hypogea* (Vacelet & Boury-Esnault, 1996) (9.31%) —of which 71 individuals were all found together in a single small boulder. The abundance of *A. setubalense* also contributed a 7.06%. Additionally, Gazul lacked *P. carpenteri* (9.59%), which was abundant in the two deep volcanoes of the group.

The bidimensional ordination space of an unconstrained CA (Fig. 9; Table 3) grouped the volcanoes in congruence with the results previously described from the dendrogram of Fig. 8. The first four axes explained a 75.3% of the faunal variation in the 'species x volcano' matrix (Table 4; Fig. 9). The first axis appeared related to depth and the second to the global number of sponge individuals at each volcano. Species like *Poecillastra compressa*

Table 3. Numerical coding used as labels for the scientific names of the sponge species in the ordination analyses in Figs. 9 to 11.

Code	Species	Code	Species
1	*Asconema setubalense*	42	*Jaspis incrustans*
2	*Pheronema carpenteri*	43	*Jaspis johnstonii*
3	*Lanuginella* cf. *pupa*	44	*Jaspis sinuoxea*
4	*Rhizaxinella elongata*	45	*Neoschrammeniella bowerbankii*
5	*Rhizaxinella pyrifera*	46	*Geodia anceps*
6	*Suberites carnosus*	47	*Penares euastrum*
7	*Topsentia glabra*	48	*Geodia* cf. *spherastrella*
8	*Stylocordyla borealis*	49	*Geodia megastrella*
9	*Cladorhiza abyssicola*	50	*Geodia pachydermata*
10	*Lycopodina hypogea*	51	*Characella pachastrelloides*
11	*Anisocrella hymedesmina*	52	*Characella tripodaria*
12	*Crella fusifera*	53	*Pachastrella monilifera*
13	*Crella pyrula*	54	*Pachastrella ovisternata*
14	*Coelosphaera tubifex*	55	*Nethea amygdaloides*
15	*Coelosphaera cryosi*	56	*Thenea muricata*
16	*Forcepia forcipis*	57	*Thrombus abyssi*
17	*Forcepia luciensis*	58	*Vulcanella gracilis*
18	*Hymedesmia koehleri*	59	*Discodermia ramifera*
19	*Hymedesmia mutabilis*	60	*Poecillastra compressa*
20	*Hymedesmia peachii*	61	*Rhabderemia profunda*
21	*Hymedesmia pennata*	62	*Bubaris vermiculata*
22	*Iotroata polydentata*	63	*Myrmekioderma indemaresi*
23	*Sceptrella insignis*	64	*Phakellia robusta*
24	*Clathria campecheae*	65	*Phakellia ventilabrum*
25	*Antho signata*	66	*Axinella vellerea*
26	*Antho erecta*	67	*Axinella* cf. *rugosa*
27	*Mycale lingua*	68	*Janulum spinispiculum*
28	*Myxilla incrustans*	69	*Eurypon clavatum*
29	*Myxilla rosacea*	70	*Acantheurypon pilosella*
30	*Podospongia lovenii*	71	*Petrosia crassa*
31	*Desmacella annexa*	72	*Petrosia raphida*
32	*Desmacella inornata*	73	*Petrosia vansoesti*
33	*Dragmatella aberrans*	74	*Cladocroce fibrosa*
34	*Hamacantha johnsoni*	75	*Cladocroce spathiformis*
35	*Hamacantha lundbecki*	76	*Haliclona* cf. *fulva*
36	*Hamacantha schmidtii*	77	*Haliclona angulata*
37	*Hamacantha papillata*	78	*Haliclona bouryesnaultae*
38	*Craniella cranium*	79	*Haliclona utriculus*
39	*Weberella verrucosa*	80	*Pleraplysilla spinifera*
40	*Leiodermatium pfeifferae*	81	*Dysidea fragilis*
41	*Jaspis* cf. *eudermis*	82	*Spongia officinalis*

(labelled as #60), *Axinella vellerea* Topsent, 1904 (#66) and *Petrosia crassa* (#71) were associated to the position of Gazul volcano in the ordination space (Fig. 9). A wide variety of species was associated to the group formed by Pipoca, Chica, Tarsis and Anastasya, some of them being encrusting species (typically in Pipoca and Chica) along with soft-bottom specialists occurring in all the volcanoes of the group. The encrusting species with relevant contribution to this group of volcanoes were *Hymedesmia (Hymedesmia) pennata* Brøndsted, 1932 (#21), *Jaspis sinuoxea* Sitjà, Maldonado, Farias and Rueda, 2019 (#44) and *Janulum spinispiculum* (Carter, 1876) (#68). The most relevant soft-bottom

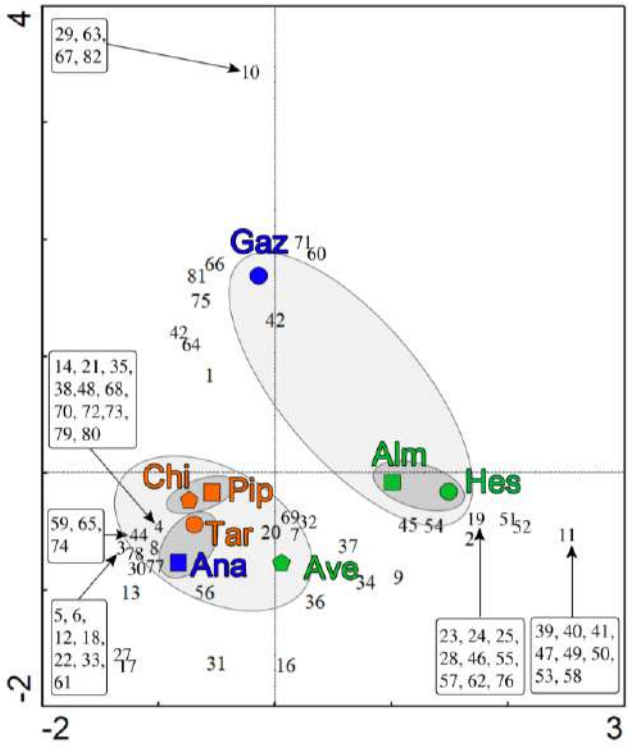

Fig. 9. Biplot showing the bidimensional space formed by the first and the second axes of an unconstrained CA depicting the relative position of the mud volcanoes —labelled in color (upper zone= blue, intermediate zone= orange, lower zone= green**)—** and their associated sponge species —labelled as numbers. Shaded areas correspond to the affinities observed from the dendrogram. Correspondence of each number to its respective species name is given in Table 3. Note that some species are clearly related to some volcanoes, such as *Poecillastra compressa* (#60) and *Petrosia crassa* (#71), which abound in Gazul volcano.

specialists were *Rhizaxinella elongata* (Ridley & Dendy, 1886) and *Haliclona bouryesnaultae*. Other soft-bottom specialists, such as *Thenea muricata* (#56) and *Haliclona angulata* (#77) were more typically associated to the Anastasya position. Although Aveiro showed abundant *T. muricata* too, it had a distinctive abundance of *Hamacantha* spp. (#34, 37, 36). The group formed by Almazan and Hesperides shared importantly species like *Neoschrammeniella bowerbankii* (Johnson, 1863) (#45) and *Pachastrella ovisternata* (#54).

The four main axes of a CCA analysis constrained by four environmental variables (Fig. 10) explained 63.7% of the faunal variation in the 'species x volcano' matrix (that is, less than the unconstrained CA) and 100% of variability in the 'species-environment' matrix (Table 4). The Monte-Carlo Permutation test indicated that the first axis of the ordination space was almost significant (p= 0.052), while all the canonical axes tested together resulted clearly significant (p=0.034), meaning that some of the environmental variables are responsible for at least some of the variation within the 'species x volcano' matrix.

Table 4. Summary of statistics for the correspondence analysis (CA) and canonical correspondence analyses (CCA) constrained by four and two environmental variables. Eigenvalues are shown for the first four axes, together with the sum of all unconstrained (T. inertia) and canonical (C. inertia) eigenvalues. The percentage of variance in both faunal data (%V_{sp}) and fauna-environment relation (%$V_{sp\text{-}env}$) explained by each axis is also given.

	CA		**4-var CCA**			**2-var CCA**		
	Eigen.	**% V_{sp}**	**Eigen.**	**% V_{sp}**	**% $V_{sp\text{-}env}$**	**Eigen.**	**% V_{sp}**	**% $V_{sp\text{-}env}$**
Axis 1	0.638	26.9	0.608	25.6	40.3	0.569	24	56.1
Axis 2	0.516	21.8	0.464	19.6	30.8	0.446	18.8	100
Axis 3	0.339	14.3	0.236	10.0	15.6	0.399	16.9	0
Axis 4	0.291	12.3	0.201	8.5	13.3	0.305	12.8	0
T. inertia	2.370	-	2.370	-	-	2.370	-	-
C. inertia	-	-	1.509	-	-	1.015	-	-

A subsequent variance partitioning analysis (Table 5) indicated that the variation explained by the set of natural variables (C=carbonates, D=depth, M=methane venting) was 47.64%, that is about 5 times more than that explained (9.20%) by the man-driven variable (F = bottom fishing activity).

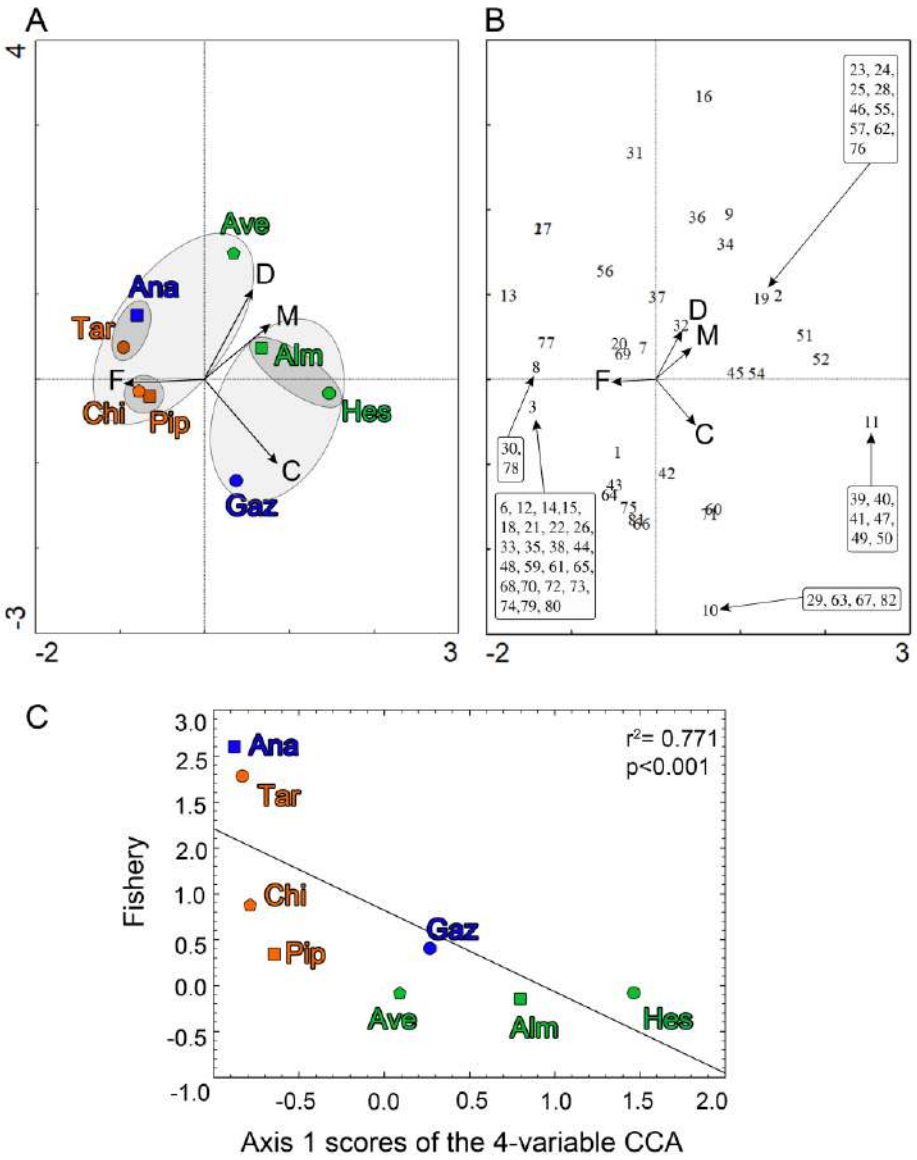

Fig. 10. (A) Bidimensional ordination space formed by the first and the second axes of a CCA constrained by four environmental variables. It depicts the relative position of the mud volcanoes with relation to the environmental variables represented as vectors (C= Average abundance carbonated hard substrata; D= average depth; M= average intensity of methane venting; F = average intensity of bottom fishing). Shaded areas correspond to the affinities observed from the dendrogram.

… continued in the next page

(B) Same CCA that in Fig. A, but showing the relative position of the sponge species in relation to the environmental variables. Species are labelled as numbers whose correspondence to scientific names is given in table 3. Some species, like *Podospongia lovenii* (#30) and *Haliclona bouryesnaultae* (#78) are closely related to the F vector. (C) Spearman correlation, showing the statistically significant association between the scores of the volcanoes along the first axis of the four-variable CCA and the average semi-quantitative scoring of the mud volcanoes relative to the intensity of bottom fishing in their benthic communities. The correlation coefficient and its "p" value are given at the top right corner.

The shared variation explained was low (6.84%), therefore, given the also low percentage of variation from the F variable, it can be concluded that most of the variation explained by F is also explained by the set of natural variables. The unexplained variation was 36.33%. Indeed, a subsequent step-forward process of the variables to the elaboration of the model indicated that the C and D environmental variables significantly explained part of the variability (Inflation Factors= 2.3 and 3.0, respectively; p= 0.034 and p= 0.036, respectively) while M and F variables resulted not statistically significant, despite having relatively low inflation factors that did not denote co-variation (Inflation Factors= 1.3 and 2.4, respectively; p= 0.414 and 0.642). However, although the step-forward addition process to examine the effect of each variable on the model in terms of explaining the faunal variation at the CCA ordination space indicated that variable F was not statistically significant, the CCA biplot revealed a strong relation between the F vector and the first ordination axis (Fig. 10A-B; Table 4), which was also supported by a subsequent Spearman rank correlation test (r^2= 0.771, p< 0.001; Fig. 10C).

The volcanoes Anastasya, Tarsis, Pipoca and Chica are the ones showing the strongest effects of bottom fishing activity (F) and are also characterized by soft-bottom sponge specialists, such as *Stylocordyla borealis* (Lovén, 1868) (#8), *Podospongia lovenii* Barboza du Bocage, 1869 (#30) and *Haliclona bouryesnaultae* (#78), since soft bottoms are preferred activity grounds of the fishery fleet.

Following the indications of the step-forward analysis of the environmental variables, a subsequent CCA constrained by only the two significant variables (C and D) was conducted (Fig. 11). Its 4 main axis

Table 5. Summary of the variance partitioning analysis and VIF based on the four-variable CCA. Abbreviations are as follows: D= average depth; C= average abundance of authigenic carbonates; M= average methane venting activity; F= average fishing activity.

Variation component	Explained variation (%)	Variance inflation factor (VIF)
Benthic variation	47.64	D = 3.05; C = 2.27; M = 1.31
Fishery variation	9.20	F = 2.405
Shared variation	6.84	
Unexplained variation	36.33	

explained collectively 72.5% of the faunal variation in the 'species x volcano' matrix, that is, more than in the two previous ordination analyses. It also explained 100% of variability in the 'species-environment' matrix (Table 4). The Monte-Carlo Permutation test indicated that the first axis of the ordination space was significant (p= 0.042), and also all the canonical axes when they were tested together (p= 0.002). These results suggested that the environmental variables D and C are responsible for at least some of the variation within the 'species x volcano' matrix.

The two-variable CCA biplot depicted a global pattern of relative faunal affinities similar to that in the CA analyses, but rotated and having Gazul, Almazan and Aveiro volcanoes moderately changed their positions in the biplot (Fig. 11A). Significant spearman rank correlations (Fig. 11C-D) revealed that the C variable was associated to axis 1 of the ordination space and D variable to axis 2 (C: r^2=0.552, p= 0.029; D: r^2=0.476, p= 0.047). The volcanoes with higher C values (Gazul, Hesperides, Almazan) were located at the negative side of axis 1 and the deepest volcanoes (Aveiro, Almazan) at the positive side of axis 2. Compared to the unconstrained biplot (Fig. 9), Gazul clearly moved its position in the 2-variable CCA towards the C vector, indicating the presence of carbonates has a strong influence on the abundance distribution of the sponge fauna of this volcano. Hesperides volcano, which conserved its position in the biplot despite the constraint, appeared relatively near the C vector, which can also be interpreted as a moderate influence of the carbonates on its sponge fauna. Almazan moderately moved towards the C vector, remaining in a central position between the C and the D, which can

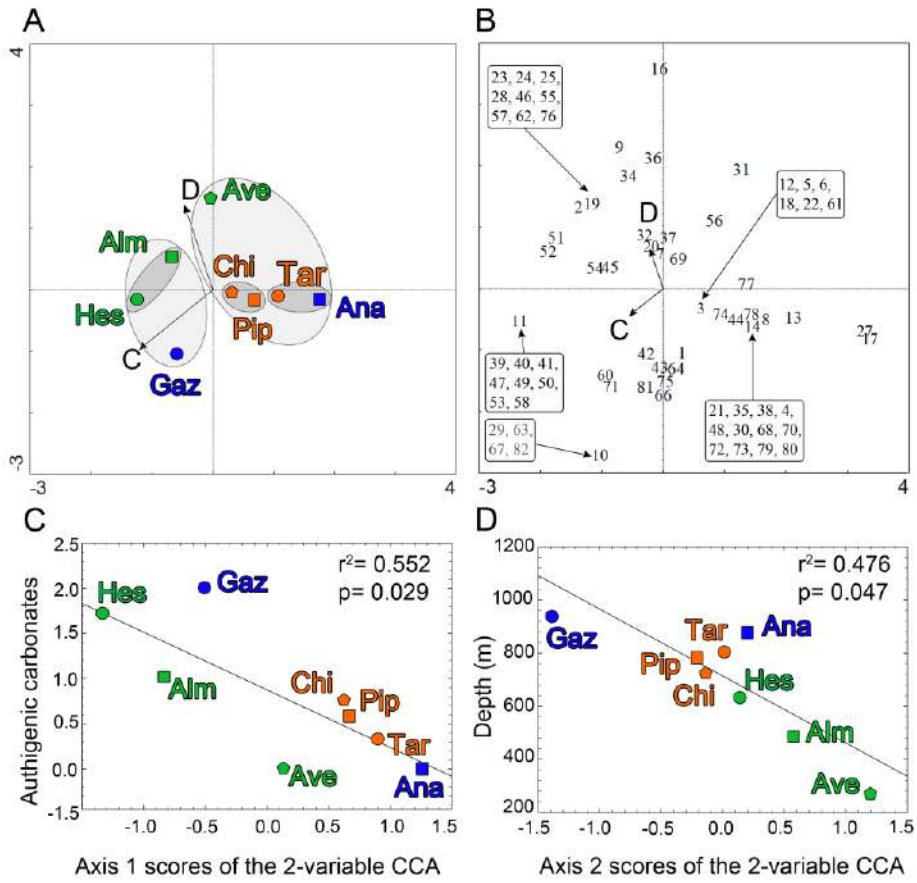

Fig. 11. (A) Bidimensional ordination space formed by the first and the second axes of a readjusted CCA constrained by only two of the four initial environmental variables (C= Average abundance of carbonated hard substrata and D= average depth), where volcanoes and environmental variables are represented. Shaded areas correspond to the affinities observed from the dendrogram. (B) Plot of the same CCA analysis, this time displaying the position of the sponge species and the environmental variables. The species are labelled as numbers which are referenced in table 3. Some species are evenly located near the vectors, indicating a major presence in determined environmental conditions. Note how some *Hamacantha* spp. (#34, 36, 37) occur near D vector, suggesting preference for deep habitats, while other species, such as *Petrosia crassa* (#71) and *Jaspis incrustans* (#42) occur near the C vector, suggesting dependence on hard carbonate substratum.

…continued in the next page

(C) Spearman rank correlation indicating statistically significant, negative association between the scores of the volcanoes along the first axis of the two-variable CCA and their average value of abundance in authigenic carbonates. (D) Spearman rank correlation indicating statistically significant, negative association between the scores of the volcanoes along the second axis of the two-variable CCA versus their average depth. Spearman correlation coefficient and its "p" value are given at the top right corner for both 'B' and 'C' plots.

be interpreted as a moderate influence of these two variables on its sponge fauna. Aveiro volcano subtly moved towards the center, and remained near the D variable, implying that depth was more markedly influencing its sponge composition. The remaining volcanoes, from the shallow and intermediate zones, and with moderate presence to lack of carbonates, seemed to be unaffected by these two environmental variables. The distribution of some species was closely related to these two environmental variables (Fig. 11B; Table 3). Species such as *D. inornata* (#32), *Hamacantha (Hamacantha) johnsoni* (Bowerbank, 1864) (#34), *Hamacantha (Hamacantha) schmidtii* (Carter, 1882) (#36) and *Hamacantha (Vomerula) papillata* Vosmaer, 1885 (#37) were close to D vector, with growing abundances with increasing depth. Other species, such as *Jaspis incrustans* (Topsent, 1890) (#42), *Poecillastra compressa* (#60) and *Petrosia crassa* (#71), were close to the C vector, indicating their preference or need for hard substrates.

Faunal affinities along a MOW-related Atlantic-Mediterranean gradient

Figure 12 summarizes the results of a cluster analysis based on the Jaccard similarity for a matrix of 456 sponge species from 9 deep-sea biogeographical areas of the Western Mediterranean and 7 from the Northeastern Atlantic — after pooling together the Canary Islands (C-A), Madeira islands (Ma-A), and the adjacent Moroccan slope (Mo-A). All Mediterranean areas were grouped together, except for the idiosyncratic Tyrrhenian Sea (T-M). The sponge fauna of the mud volcanoes (MV-A) and that previously known from other deep-sea environments in the Gulf of Cádiz (GC-A) were closely grouped together (28% similarity) with statistical

significance, indicating that the potentially singular environment at the volcanoes is not selecting for a singular composition of sponge species, that is, the occurrence of a sponge fauna specialized in mud volcanoes is not supported from our study. More importantly, the two faunas from the Gulf

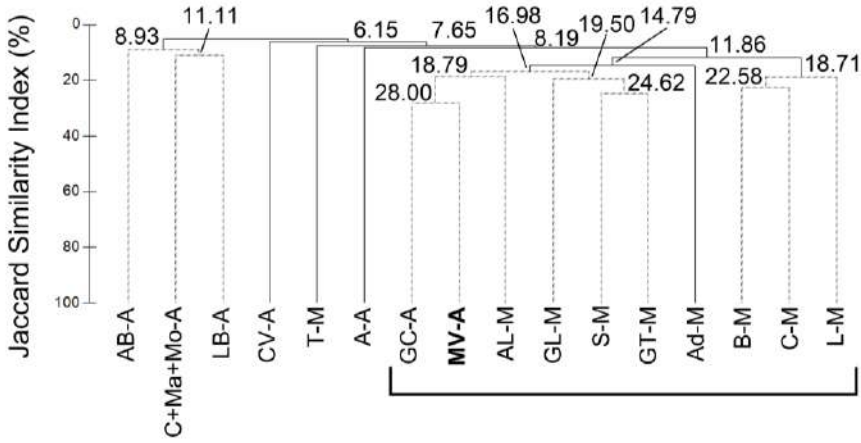

Fig. 12. Dendrogram based on Jaccard similarity displaying the affinities between the deep sponge fauna from different Atlantic and Mediterranean areas. Codes for biogeographical areas are as explained in Fig. 4. Values at the nodes correspond to the percentage of similarity between sub-groups. Dotted vertical lines represent genuine clusters with statistical support. Horizontal line at the bottom shows how the Mud volcanoes and Gulf of Cádiz group with all but one of the Mediterranean faunas considered in the study.

of Cádiz (GC-A+MV-A) did not become associated to other Atlantic areas. Rather they clustered with the westernmost Mediterranean Area, the Central Alboran Sea (Al-M), with 18.79% similarity. These three regions became the sister group (16.98% similarity) of three other Mediterranean regions, the Gulf of Lion, the slope of Sicily Island and its surroundings, and the slope of the Gulf of Taranto, forming collectively a genuine subgroup (19.50%) with statistical support (Fig. 12).

The statistical support for the Gulf of Cádiz-Western Mediterranean node clearly illustrates the effect that the MOW has in transporting

components of the Mediterranean deep-sea sponge communities towards the bathyal communities of the Gulf of Cádiz. The dendrogram also showed that the Atlantic areas considered in the analysis and not directly affected by the MOW trajectory (Azores, Southern Azores Banks, Cape Verde, Lusitanian Banks, and Canary-Madeira-Moroccan slopes) had surprising low levels of faunal similarity (from 6.15 to 8.19%) among them. Only the Lusitanian Banks shared a modest affinity with the Canary-Madeira-Moroccan slopes (11.11%), and the Southern Azores Banks (8.93% affinity) (Fig. 12). The analysis also showed that the Tyrrhenian Sea was not part of the main Mediterranean cluster, implying some dissimilarity between their deep sponge faunas.

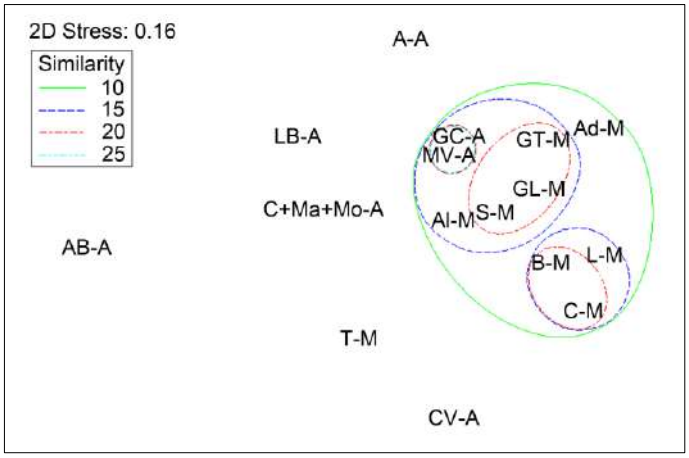

Fig. 13. MDS analysis based on the Jaccard similarity among the deep-sea biogeographical areas considered along the Atlantic-Mediterranean gradient. Color lines define 10,15, 20 or 25% clines of faunal affinities.

The MDS (Fig. 13) showed a global pattern similar to that of the dendrogram, identifying a cohesive group of Mediterranean areas to which the sponge fauna of the Gulf of Cádiz and the mud volcanoes (GC-A and MV-A) were also associated. This again reflected the importance of the MOW trajectory on the composition of the deep-water sponge fauna of the easternmost Atlantic areas. Within the Mediterranean cluster, the deep-water sponge faunas showing the highest similarity were, on the one side, those of Gulf of Lion, Gulf of Taranto and Sicily, and, on the other side, those of the Balearic Sea and the western slope of Corsica. The distinct nature of the deep-water sponges at the Tyrrhenian Sea relative to the rest of Mediterranean

deep-sea areas considered in the study was again highlighted by the analysis. The Atlantic areas not affected by the trajectory of the MOW did not form a cohesive group, but rather each area showed a relatively distinct fauna. While the distribution of the sponge faunas along the first ordination axis could not be related to a single predominant factor but to a mixed variety of them, the second axis appeared to be related to the latitude and the direction of the MOW. The Mediterranean areas (except for the idiosyncratic Tyrrhenian Sea) and those Atlantic areas impacted by the MOW, that is, the Gulf of Cádiz, the mud volcanoes, and, to a lesser extent, the Lusitanian Banks and Azores were located towards the top of the diagram. The Atlantic areas of Cape Verde, the Canary-Madeira-Moroccan slopes, and Southern Azores Banks were depicted towards the bottom of the ordination space.

The effect of the MOW in the faunal affinities was also tested by linear regression analysis, under the assumption that, if the MOW trajectory has no major effect on shaping the faunal affinities, the geographical distances among the studied deep-sea areas should largely predict the faunal similarities: the greater the geographical distance between two areas, the lower their faunal

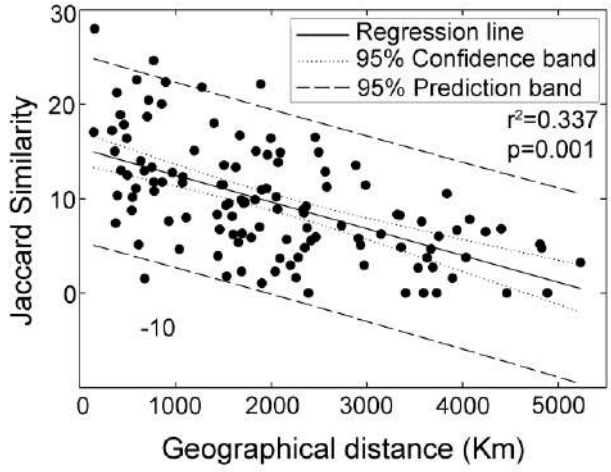

Fig. 14. Linear regression analysis showing that faunal distances between two areas (expressed as Jaccard faunal similarity) can only be predicted with confidence from the marine geographical distance in less than 34% of times. This poor predictive capability of the between-area geographical distances suggests that marine current (i.e., the MOW) is substantially affecting the pattern of faunal affinities.

affinity. A regression analysis showed a very weak support to this hypothesis, since faunal similarity could be predicted with confidence from the geographical distance in only 34% of cases (r^2= 0.337, p< 0.001; Fig. 14). Therefore, it can be concluded that the low association between geographical and faunal distances among the investigated deep-sea areas is largely the result of the MOW effect.

Out of the 456 species recorded for the considered depth range (≥200 m in the Mediterranean and 200 – 1500 m in the Atlantic) in the Atlantic-Mediterranean areas, a total of 280 (61%) species were only present in the Atlantic and 92 (20%) where present only in the Mediterranean. The number of species co-occurring in at least one Atlantic and one Mediterranean deep-sea area was 84 (18%). The deep-water sponge fauna of the Gulf of Cádiz, understood in this study as the combination of that in the mud volcanoes (MV-A) and that cited in the pre-existing literature of the Gulf of Cádiz (GC-A), consisted of 125 species, of which 63 were also present in the Mediterranean and 27 in their geographically nearest Mediterranean area, the Alboran Sea. Thirty-five species co-occurred at the MV and GC areas, from which 12 were also present at the Alboran Sea: *P. carpenteri*, *A. setubalense*, *Rhizaxinella pyrifera* (Delle Chiaje, 1828), *Cladorhiza abyssicola* Sars, 1872, *Crella (Yvesia) pyrula* Carter, (1876), *D. inornata*, *Hamacantha (Hamacantha) johnsoni* (Bowerbank, 1864), *Pachastrella monilifera* Schmidt, 1868, *T. muricata*, *Bubaris vermiculata* (Bowerbank, 1866), *Phakellia robusta* Bowerbank, 1866 and *Janulum spinispiculum*. This group of deep-water species makes the core of the faunal affinities between the Gulf of Cádiz and the westernmost Mediterranean. From those species, only three were also present in other four Mediterranean areas, which also showed faunal affinity with the Gulf of Cádiz (i.e., Al-M, Si-M, GT-M, NB+GL-M): *D. inornata*, *H. johnsoni* and *T. muricata*. Collectively, these results provide evidence that the composition of the deep-sea sponge communities of the mud volcanoes and, in general, of the Gulf of Cádiz is clearly affected by the outflow of Mediterranean water (MOW).

Discussion

The sponge fauna of the mud volcanoes

Previous studies on different groups of benthic organisms have been conducted across various mud volcanoes of the Gulf of Cádiz (Rodrigues et al., 2011; Rueda et al., 2012; Cunha et al., 2013; Delgado et al., 2013; González-García et al., 2020), but the sponge fauna remained hardly investigated until recently (Chapter 1, also Sitjà et al., 2019). Our study shows that the sponges of the mud volcanoes at the northern Gulf of Cádiz make a relatively cohesive fauna, which in turn shows significant affinities with the sponge fauna previously described from other bathyal communities within the Gulf of Cádiz. Between-volcano comparisons also revealed that differences in faunal composition existed, being depth and presence of carbonate substrate the most relevant factors affecting both the composition and the abundance distribution of the sponges. Volcanoes such as Gazul and Hesperides (Fig. 2A-C), which had abundant authigenic carbonates exhumed by erosive processes, hosted relatively large abundance of sponges in terms of number of individuals and species richness respectively. The presence of carbonates has been reported to have positive effects in the abundance of other sessile organisms as well (Díaz del Río et al., 2014; González-García et al., 2020). Interestingly, while Gazul had the highest abundance of sponges among all the herein studied volcanoes, it showed a relatively low species richness, because its fauna was dominated by aggregations of *P. crassa*. The modest sponge species richness in Gazul contrasts with previous reports for other sessile groups, such as cnidarians and bryozoans, found to be comparatively very diverse in this volcano (Oporto et al., 2012; Díaz del Río et al., 2014; González-García et al., 2020). Yet, the abundance of hard substrates was not the rule in most volcanoes, which were characterized by prevailing soft bottoms with interspersed carbonate structures at varying density levels (Fig. 2D-E), including extremely rare presence of hard substrata (Fig. 2F-H). As a general rule, wherever soft bottoms abounded, species richness decreased comparatively, as typically in Anastasya, Tarsis and Aveiro, where the sponge fauna was dominated by a few soft-bottom specialists, which, sometimes formed aggregations. As typically happening in many other marine environments, in those volcanoes with relatively balanced proportions of hard and soft bottom (Pipoca, Chica, Almazan), species richness showed the

highest values. This pattern has also been observed for other benthic organisms from Pipoca and Chica (González-García et al., 2020), in fact, their benthic communities have shown species accumulation curves similar to those herein obtained for sponges.

From a qualitative point of view, Gazul (the shallowest volcano) and Aveiro (the deepest volcano) hosted the most distinct sponge fauna relative to the other volcanoes. The main species responsible for the differentiation of Gazul from those mud volcanoes also characterized by hard substrates were *P. crassa* and *L. hypogea* —both occurring in small aggregations, along with *A. setubalense* and *P. compressa* (Fig. 2A). On the other side, the distinct nature of Aveiro derived from its aggregations of the soft-bottom sponge *T. muricata*. Another explanation might be the fact that the sampling methodologies favored the collection of larger species at this volcano, missing the small encrusting ones that might abound only on hard substrates.

The other environmental factor revealed by the CCA analyses as relevant to the sponge fauna of the volcanoes was depth, which has also been observed for the benthic communities of mud volcanoes in the depth ranges from Gazul to Tarsis (González-García et al., 2020). The general pattern for sponges, also pointed out previously (Chapter 1), was an increase in species richness with increasing depth. In the studied volcanoes, the analysis of the sponge fauna did not reveal significant detrimental effects by the bottom fishing activity. The CCA analyses indicated that fishing was not a significant variable for the constrained model addressing the explanation of the faunal variation in the "species x volcano" matrix. However, this could be a consequence of the fishing activity occurring with most intensity at the shallower volcanoes, which in turn are characterized by predominant soft bottoms (except Gazul). It is possible that the variation to be explained by the bottom fishing activity was confounded with that explained by the two other variables, depth (D) and soft bottom (measured in our analyses as 1-C, that is, lack of carbonate abundance). It is worth noting that the 4-variable CCA model revealed a strong alignment between the F vector and the first ordination axis (Fig. 10A-B), a relationship also supported by a statistically significant Spearman rank correlation (r^2= 0.771, p< 0.001; Fig. 10C). Therefore, a subsequent, more detailed study addressing the bottom fishing effects would be needed for this field of volcanoes, since in the current study fishing was processed as a semi-quantitative variable and the sampling effort

at the volcanos was suboptimal for the sponge fauna. Likewise, methane venting was found to have no effect on the sponge fauna, but this, again, should be taken as tentative conclusion that might be affected by a limited sponge sampling and an incomplete acquisition of proper quantitative environmental data for the analyses. In other cold seep systems, highly specific nutritional symbioses between some sponge species and microbial symbionts have been described (Vacelet et al., 1995; Maldonado & Young, 1998; Rubin-Blum et al., 2019), suggesting that methane venting favors occurrence of a little diverse but highly specialized sponge fauna. In the mud volcanoes from the Gulf of Cádiz, no extensive dominance by such sponge fauna was detected. Therefore, the real importance of methane venting will only be elucidated by additional, more detailed studies using oceanographic manned submersibles or remotely operated vehicles rather than just trawling to both quantify methane concentrations and sampling sponge fauna from venting zones specifically.

In addition to the four environmental variables considered in the CCA analyses, it is obvious that many other factors can affect both the abundance and diversity of the sponge communities at the mud volcanoes. Local patterns of current and regional geological processes are among them (Van Rooij et al., 2010; Lozano et al., 2019). For instance, Palomino et al. (2016) found that zones of low-velocity bottom currents favored development of benthic communities related to seepage, as it could also be the case in Anastasya. Conversely, high-velocity currents could promote erosive processes that prevent sediment deposition and lead to exposure of the authigenic carbonates and any other hard substratum, favoring settlement of sessile organisms. At the same time, strong hydrodynamics associated to internal waves could favor resuspension and supply of food particles. This could be the case of Gazul, located near the shelf-break and characterized by abundant filter feeders and suspension feeders, being also known to shelter cold water corals (Rueda et al., 2016; González-García et al., 2020). Other volcanoes, such as Chica and Pipoca, which are exposed to one of the main branches of the MOW running through the adjacent Huelva Channel, also show abundant filter feeders (Rueda et al., 2016; González-García et al., 2020), in agreement with rich and abundant sponge fauna herein described from them.

Faunal affinities along the Mediterranean-Atlantic gradient

The significant similarity between the sponge fauna of the mud volcanoes (MV-A) and that previously known from other bathyal communities of the Gulf of Cádiz (GC-A) indicated that there does not appear to exist a sponge fauna specialized in the environment of the mud volcanoes. The detected similarity in the deep-sea sponge fauna between the Gulf of Cádiz (understood herein as MV-A+GC-A areas) and the Alboran Sea is in agreement with the only previous study about this issue (Boury-Esnault et al., 1994), but our results even expand the intensity of such an affinity, making clear that the MOW has a crucial role in exporting bathyal sponge fauna from the Western Mediterranean into the easternmost North Atlantic. The low faunal affinity between the deep-water sponge fauna of the Gulf of Cádiz and the remaining North Atlantic areas considered in the analysis also reveals that the effect of the Mediterranean faunal export is largely circumscribed to the Gulf of Cádiz. The reasons of this spatial constraint are unclear from the scope of our study. Nevertheless, it is likely that the exported Mediterranean sponges may somehow need the presence of the MOW water to survive, since it appears that once exported to the Gulf of Cádiz, they cannot disperse easily towards additional northeastern Atlantic areas (e.g., Azores, etc.). It could also be that the North-Atlantic trajectory of the MOW, turning North after passing the Strait of Gibraltar to stay attached to the Lusitanian slope, is hindering the colonization of the slopes of the Macaronesia (i.e., Azores, Morocco, Canary Islands, Madeira Islands, Cape Verde). Another potential reason —but less likely— for such a distribution could be that the pre-existing Atlantic deep-sea sponge fauna outcompetes rapidly the Mediterranean immigrants and avoid their proliferation.

The markedly low affinity of the sponge fauna from the Tyrrhenian Sea region with the rest of the Mediterranean reflects the long known hydrographic and hydrobiological singularity of this Mediterranean basin (Cognetti et al., 2000). There are some structural features of the Tyrrhenian Sea that contribute to its singularity relative to adjacent basins. For instance, the continental shelf of the Tyrrhenian Sea is very narrow and depth exceeds 2000 m throughout virtually the whole of the basin, reaching maximum values of 3,840 m. Because the input from the continental waters is minimal, salinity remains constant at roughly 38 PSU. Temperature also remains constant all year in the deep sea, set at a relatively comfortable value of 13 ºC, which allows

survival in very deep water of species that in other Mediterranean areas can live only in shallower (i.e., warmer) ranges. There are many areas with active volcanism. The oxygen concentration (4.4 ppm) in deep waters is also comparatively low as well as primary productivity is in surface waters. In addition to those features, the known hydrodynamics also support a distinctive character. At depths of 200 to 800 m, the Tyrrhenian Sea gets an inflow of the LIW. After passing the Strait of Sicily, a major branch of the LIW flows towards the Algerian basin and a secondary one deviates towards the Gulf of Lion running across the Tyrrhenian Sea. In the Tyrrhenian Sea, it turns cyclonically forming the South Western Tyrrhenian Gyre (SWTG) and further breaking down into smaller LIW branches that run across Corsica and the Algerian basin (Pinardi et al., 2015). Most of the deep sponge species cited from the Tyrrhenian Sea were located where the SWTG occurs, meaning that they are located out of the main LIW pathway. Contrastingly, the sponge faunas from the rest of the Mediterranean regions considered in this study are directly bathed by the main LIW flow, which contributes to explain the low affinity of the Tyrrhenian deep sponges to those of adjacent Western Mediterranean areas.

Why the exporting role of the MOW appears to be more effective for the sponge fauna than for other sessile groups, such as bryozoans and ascidians (Monniot & Monniot, 1988; Harmelin & d'Hondt, 1993), remains unclear. Previous studies showed that the sponge fauna was very suitable to illustrate how the North Atlantic Superficial water entering into the Mediterranean was transporting shallow-water northeastern-Atlantic fauna (Maldonado & Uriz, 1995; Xavier & Van Soest, 2012). Likewise, our study shows again that the sponge fauna is suitable to retrace the export of bathyal Mediterranean fauna towards the Atlantic by the MOW. The export of deep-sea sponges by the MOW explains why about 18 % of the 456 species considered in our analysis of the global Atlantic-Mediterranean gradient co-occurred at both the Atlantic and the Mediterranean sides of the Strait of Gibraltar.

The global message is that the sponge faunas, either from shallow-water or deep-water, may be particularly suitable to detect early stages of between-sea faunal shifts (also ecological invasions at the deep-sea level) that might result from future alteration of major marine currents as foreseen for our future changing ocean.

References

Baringer, M. O. and Price, J. F. (1999) A review of the physical oceanography of the Mediterranean outflow. *Marine Geology,* 155, 63-82.

Boetius, A., Ravenschlag, K., Schubert, C. J., Rickert, D., Widdel, F., Gieseke, A., Amann, R., Jørgensen, B. B., Witte, U. and Pfannkuche, O. (2000) A marine microbial consortium apparently mediating anaerobic oxidation of methane. *Nature,* 407(6804), 623-626.

Boetius, A. and Suess, E. (2004) Hydrate Ridge: A natural laboratory for the study of microbial life fueled by methane from near-surface gas hydrates. *Chemical Geology,* 205, 291-310.

Borcard, D., Legendre, P. and Drapeau, P. (1992) Partialling out the spatial component of ecological variation. *Ecology,* 73(3), 1045-1055.

Boury-Esnault, N., Pansini, M. and Uriz, M. J. (1994) Spongiaires bathyaux de la mer d'Alboran et du golfe ibéro-marocain. *Mémoires du Muséum National d'Histoire Naturelle,* 160, 1-174.

Bryden, H. L. and Stommel, H. M. (1984) Limiting processes that determine basic features of the circulation in the Mediterranean Sea. *Oceanologica Acta,* 7(3), 289-296.

Clarke, K. R. and Gorley, R. N. (2006) *PRIMER v6: User Manual/Tutorial.*

Cunha, M. R., Rodrigues, C. F., Génio, L., Hilário, A., Ravara, A. and Pfannkuche, O. (2013) Macrofaunal assemblages from mud volcanoes in the Gulf of Cadiz: abundance, biodiversity and diversity partitioning across spatial scales. *Biogeosciences,* 10(4), 2553-2568.

Delgado, M., Rueda, J. L., Gil, J., Burgos, C. and Sobrino, I. (2013) Spatial characterization of megabenthic epifauna of soft bottoms around mud volcanoes in the Gulf of Cádiz. *Journal of Natural History,* 47(25-28), 1803-1831.

Díaz del Río, V., Bruque, G., Fernández-Salas, L. M., Rueda, J. L., González, E., López, N., Palomino, D., López, F. J., Farias, C., Sánchez, R., Vázquez, J. T., Rittierott, C. C., Fernández, A., Marina, P., Luque, V., Oporto, T., Sánchez, O., García, M., Urra, J., Bárcenas, P., Jiménez, M. P., Sagarminaga, R. and Arcos, J. M. Volcanes de fango del golfo de Cádiz, Proyecto LIFE + INDEMARES. Fundación Biodiversidad del Ministerio de Agricultura, Alimentación y Medio Ambiente (2014).

Gardner, J. M. (2001) Mud volcanoes revealed and sampled on Western Moroccan continental margin. *Geophysical Research Letters,* 28(2), 339 – 342.

Gasser, M., Pelegrí, J. L., Emelianov, M., Bruno, M., Gràcia, E., Pastor, M., Peters, H., Rodríguez-Santana, A., Salvador, J. and Sánchez-Leal, R. F. (2017) Tracking the Mediterranean outflow in the Gulf of Cadiz. *Progress in Oceanography,* 157, 47-71.

GRID-Arendal (2013) Mediterranean Sea water masses: vertical distribution. Accessed at: 851 http://www.grida.no/resources/5885 on 29/04/2019.

Harmelin, J.-G. and d'Hondt, J. L. (1993) Transfers of bryozoan species between the Atlantic Ocean and the Mediterranean Sea via the Strait of Gibraltar. *Oceanologica Acta,* 16 (1), 63-72.

Hovland, M., Talbot, M. R., Qvale, H., Olaussen, S. and Aasberg, L. (1987) Methane-related carbonate cements in pockmarks of the North Sea. *Journal of Sedimentary Research,* 57(5), 881-892.

Lascaratos, A., Williams, R. G. and Tragou, E. (1993) A mixed-layer study of the formation of Levantine intermediate water. *Journal of Geophysical Research: Oceans,* 98(C8), 14739-14749.

Levin, L. A. (2005) Ecology of cold seep sediments: Interactions of fauna with flow, chemistry and microbes. *In:* R. N. Gibson, R. J. A. Atkinson and J. D. M. Gordon (Eds), *Oceanography and marine biology: an annual review,* 43. CRC Press-Taylor and Francis Group, Boca Raton, pp. 1-46.

Lozano, P., Rueda, J., Gallardo-Núñez, M., Farias, C., Urra, J., Vila, Y., López-González, N., Palomino, D., Sánchez Guillamón, O., Vazquez, J.-T. and Fernández Salas, L. (2019) Habitat distribution and associated biota in different geomorphic features within a fluid venting area of the Gulf of Cádiz (South Western Iberian Peninsula, NE Atlantic Ocean). *In:* P. T. Harris and E. K. Baker (Eds), *Seafloor Geomorphology as Benthic Habitat*. Elsevier Science, London, pp. 717-726.

Madelain, F. (1967) Calculs dynamiques au large de la Peninsula Ibérique. *Cahiers Océanographiques,* 19, 181-194.

Malanotte-Rizzoli, P. (2001) Current Systems in the Mediterranean Sea. *In:* J. H. Steele (Ed), *Encyclopedia of Ocean Sciences (Second Edition)*. Academic Press, Oxford, pp. 744-751.

Maldonado, M. (1992) Demosponges of the red coral bottoms from the Alboran Sea. *Journal of Natural History,* 26, 1131-1161.

Maldonado, M. (1993). *Demosponjas litorales de Alborán. Faunística y Biogeografía*. (Philosophical Dissertation). University of Barcelona, Barcelona.

Maldonado, M., Sánchez-Tocino, L., López-Acosta, M. and Sitjà, C. Invertebrados claves del sistema infralitoral y circalitoral rocoso de las Islas Chafarinas: estudio con vistas a futuras estrategias de conservación. (2011).

Maldonado, M. and Uriz, J. M. (1995) Biotic affinities in a transitional zone between the Atlantic and the Mediterranean: a biogeographical approach based on sponges. *Journal of Biogeography,* 22, 89-110.

Maldonado, M. and Young, C. M. (1998) A new demosponge associated with methane seeps in the Gulf of Mexico. *Journal of the Marine Biological Association of the United Kingdom,* 78, 795-806.

Monniot, C. and Monniot, F. (1988) Ascidies profondes de chaque côté du seuil de Gibraltar (Campagne BALGIM). *Mémoires du Muséum National d'Histoire Naturelle (France),* A, 10(3), 415-428.

Oporto, T., Marina, P., López, F., Zambrano, A., G.Bruque, González-García, E., Sánchez Guillamón, O., López, E., Moreira, J., Gofas, S., García Raso, J., Fernández Salas, L., Díaz-del-Río, V., López-González, N. and Rueda, J. (2012) Sedimentological and faunistic characterization of summits of mud volcanoes of the Spanish margin (Gulf of Cádiz). *In: VI Simpósio sobre a Margem Ibérica Atlântica - MIA12*, Lisboa, December 2012.

Palomino, D., López-González, N., Vázquez, J.-T., Fernández-Salas, L.-M., Rueda, J.-L., Sánchez-Leal, R. and Díaz-del-Río, V. (2016) Multidisciplinary study of mud volcanoes and diapirs and their relationship to seepages and bottom currents in the Gulf of Cádiz continental slope (northeastern sector). *Marine Geology,* 378, 196-212.

Pansini, M. (1987) Littoral demosponges from the banks of the straits of Sicily and the Alboran Sea. *In:* J. Vacelet and N. Boury-Esnault (Eds), *Taxonomy of Porifera,* G13. Springer-Verlag, Berlin, Heidelberg, pp. 149-186.

Pérès, J. M. and Picard, J. (1964) Nouveau manuel de bionomie benthique de la mer Méditerranée. *Recueil des Travaux de la Station Marine d'Endoume,* 31(47), 1-137.

Pinheiro, L. M., Ivanov, M. K., Sautkin, A., Akhmanov, G., Magalhães, V. H., Volkonskaya, A., Monteiro, J. H., Somoza, L., Gardner, J., Hamouni, N. and Cunha, M. R. (2003) Mud volcanism in the Gulf of Cádiz: results from the TTR-10 cruise. *Marine Geology,* 195, 131-151.

Rodrigues, C. F., Paterson, G. L. J., Cabrinovic, A. and Cunha, M. R. (2011) Deep-sea ophiuroids (Echinodermata: Ophiuroidea: Ophiurida) from the Gulf of Cadiz (NE Atlantic). *Zootaxa,* 2754, 1-26.

Rubin-Blum, M., Antony, C. P., Sayavedra, L., Martínez-Pérez, C., Birgel, D., Peckmann, J., Wu, Y.-C., Cárdenas, P., MacDonald, I., Marcon, Y., Sahling, H., Hentschel, U. and Dubilier, N. (2019) Fueled by methane: deep-sea sponges from asphalt seeps gain their nutrition from methane-oxidizing symbionts. *The ISME Journal,* 13(5), 1209-1225.

Rueda, J. L., Díaz-del-Río, V., Sayago-Gil, M., López-González, N., Fernández-Salas, L. M. and Vázquez, J. T. (2012) Fluid venting through the seabed in the Gulf of Cadiz (SE Atlantic Ocean, Western Iberian Peninsula): Geomorphic features, habitats, and associated fauna *In:* P. T. Harris and E. K. Baker (Eds), *Seafloor geomorphology as benthic habitat*. Elsevier, London, pp. 831-841.

Rueda, J. L., González-García, E., Krutzky, C., López-Rodríguez, F. J., Bruque, G., López-González, N., Palomino, D., Sánchez, R. F., Vázquez, J. T., Fernández-Salas, L. M. and Díaz-del-Río, V. (2016) From chemosynthesis-based communities to cold-water corals: Vulnerable deep-sea habitats of the Gulf of Cadiz. *Marine Biodiversity,* 46(2), 473-482.

Sánchez-Leal, R. F., Bellanco, M. J., Fernández-Salas, L. M., García-Lafuente, J., Gasser-Rubinat, M., González-Pola, C., Hernandez-Molina, F. J., Pelegrí, J. L., Peliz, A., Relvas, P., Roque, D., Ruiz-Villarreal, M., Sammartino, S. and Sánchez-Garrido, J. C. (2017) The Mediterranean Overflow in the Gulf of Cadiz: A rugged journey. *Science Advances,* 3(11):eaao060911.

Sitjà, C., Maldonado, M., Farias, C. and Rueda, J. L. (2019) Deep-water sponge fauna from the mud volcanoes of the Gulf of Cadiz (North Atlantic,

Spain). *Journal of the Marine Biological Association of the United Kingdom,* 99(4), 807-831.

Somoza, L., Díaz-del-Río, V., Leon, R., Ivanov, M., Fernández-Puga, M. C., Gardner, J. M., Hernández-Molina, F. J., Pinheiro, L. M., Rodero, J., Lobato, A., Maestro, A., Vázquez, J. T., Medialdea, T. and Fernández-Salas, L. M. (2003) Seabed morphology and hydrocarbon seepage in the Gulf of Cadiz mud volcano area: Acoustic imagery, multibeam and ultra-high resolution seismic data. *Marine Geology,* 195(1-4), 153-176.

Stommel, H., Bryden, H. and Mangelsdorf, P. (1973) Does some of the Mediterranean outflow come from great depth? *pure and applied geophysics,* 105(1), 879-889.

Suess, E. (2014) Marine cold seeps and their manifestations: geological control, biogeochemical criteria and environmental conditions. *International Journal of Earth Sciences,* 103(7), 1889-1916.

Templado, J., Calvo, M., Moreno, D., Flores, A., Conde, F., Abad, R., Rubio, J., López-Fé, C. M. and Ortiz, M. (2006) *Flora y fauna de la reserva marina y reserva de pesca de la isla de Alborán*. Secretaría General de Pesca Marítima, MAPA, Madrid.

Templado, J., García-Carrascosa, M., Baratech, L., Capaccioni, R., Juan, A., López-Ibor, A., Silvestre, R. and Massó, C. (1986) Estudio preliminar de la fauna asociada a los fondos coralígenos del mar de Alborán (SE de España). *Boletín del Instituto Español de Oceanografía,* 3(4), 93-104.

Ugland, K. I., Gray, J. S. and Ellingsen, K. E. (2003) The Species-Accumulation Curve and Estimation of Species Richness. *Journal of Animal Ecology,* 72(5), 888-897.

Vacelet, J., Boury-Esnault, N., Fiala-Medioni, A. and Fisher, C. R. (1995) A methanotrophic carnivorous sponge. *Nature,* 377(6547), 296-296.

Van Rooij, D., De Mol, L., Le Guilloux, E., Réveillaud, J., Hernández-Molina, F. J., Llave, E., Léon, R., Estrada, F., Mienis, F., Moeremans, R., Blamart, D., Vanreusel, A. and Henriet, J. (2010) Influence of the Mediterranean Outflow Water on benthic ecosystems: answers and questions after a decade of observations. *Geo-Temas,* 11, 179-180.

Van Soest, R. M. W., Boury-Esnault, N., Hooper, J. N. A., Rützler, K., de Voogd, N. J., Alvarez de Glasby, B., Hajdu, E., Pisera, A., Manconi, R.,

Schönberg, C. H. L., Janussen, D., Tabachnick, K. R., Klautau, M., Picton, B. E., Kelly, M., Vacelet, J., Dohrmann, M. and Díaz, M. C.(2020). World Porifera database. Accessed at http://www.marinespecies.org/porifera on 24/06/2020. doi: 10.14284/359

Xavier, J. R. and Van Soest, R. W. M. (2012) Diversity patterns and zoogeography of the Northeast Atlantic and Mediterranean shallow-water sponge fauna. *Hydrobiologia,* 687(1), 107-125.

Zenk, W. and Armi, L. (1990) The complex spreading pattern of Mediterranean Water off the Portuguese continental slope. *Deep-Sea Research Part A. Oceanographic Research Papers,* 37(12), 1805-1823.

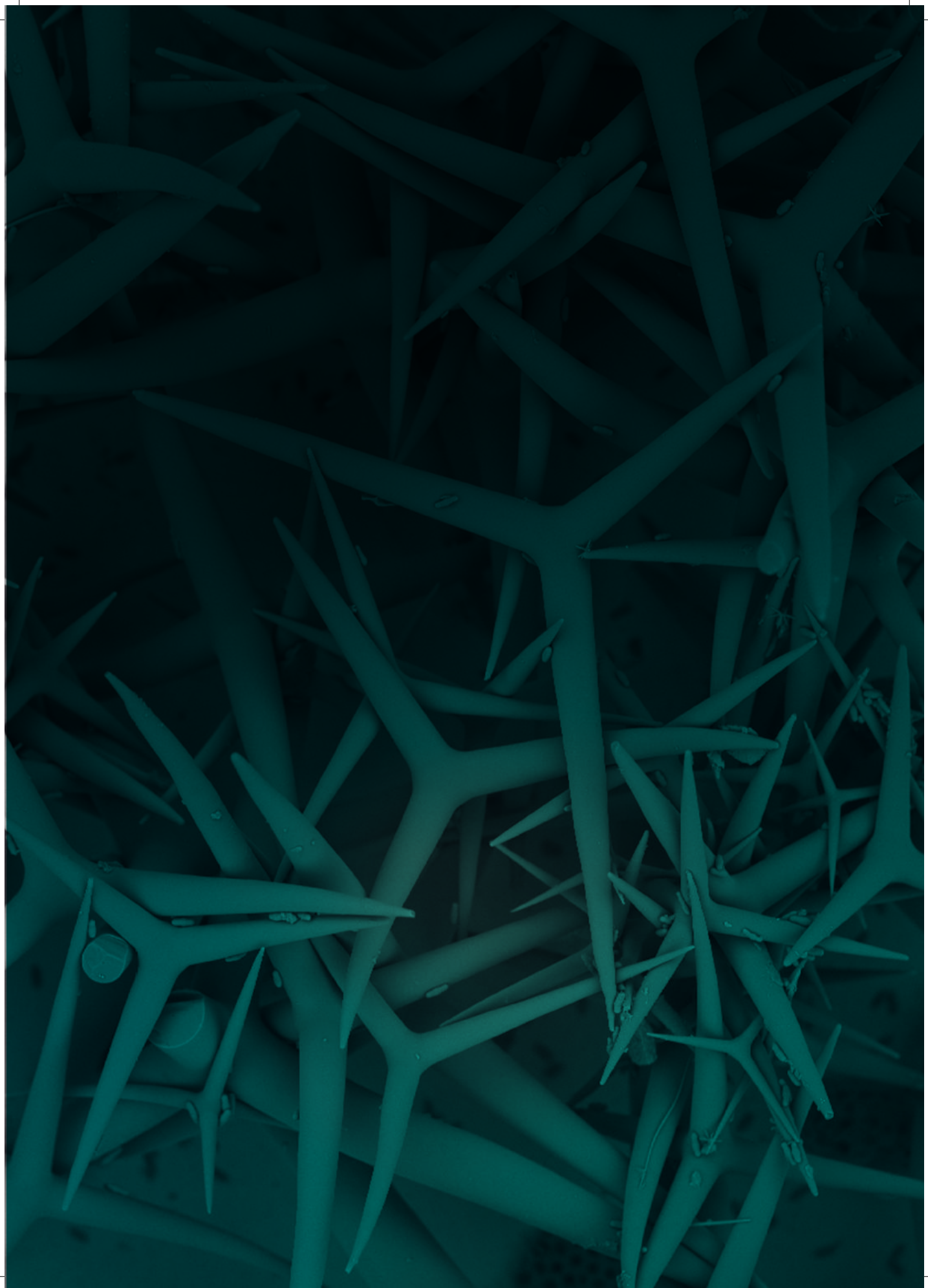

Chapter 5

The distribution of Mediterranean deep-sea sponges influenced by the Levantine Intermediate Water across the Strait of Sicily: The case of Maltese sponges

Abstract

Faunal exchange between the Atlantic and the Mediterranean occurs through their natural connection, the Strait of Gibraltar. This has been assessed elsewhere for both shallow and deep sponge faunas from the vicinities of the Strait of Gibraltar (i.e., Gulf o Cádiz, at the Atlantic, and Alboran Sea at the Mediterranean). In the case of deep-water sponge fauna, the Mediterranean Outflow Water (MOW), flowing through the Strait of Gibraltar at 300 m depth, favours the sponge transfer towards the Atlantic Ocean. The MOW is 90% constituted by another current originated at the easternmost Mediterranean, the Levantine Intermediate Water (LIW). Differently from the Strait of Gibraltar, the transfer of deep-water sponges occurring through the Strait of Sicily —the most important transitional zone between the Eastern and the Western Mediterranean— has been poorly studied. The present study assesses the influence of the LIW on the distribution pattern of the deep sponge fauna across the Mediterranean, with a special interest in the Strait of Sicily. Additionally, this study provides taxonomic data on a collection of deep-water sponges collected by ROV from the Maltese Islands, which encompass different Sites of Community Importance. The Maltese Islands are a key spot for the present biogeographical study since they are located at the South of the Strait of Sicily. A total of 36 sponge specimens belonging to 23 species were identified, all belonging to Class Demospongiae, except for one hexactinellid specimen. Two of these species are considered taxonomically and faunistically relevant, being Atlantic species recorded for the first time in the Mediterranean (*Pachastrella ovisternata* and *Higginsia thielei*). The results obtained suggest that sponges are a common benthic component of the deep bottoms of the Maltese Islands and that the distribution pattern of the deep sponge fauna across the Western Mediterranean is influenced by the LIW. Since the LIW is a main contributor to the MOW, it implies that the LIW has also an indirect effect on the final transfer of deep Mediterranean benthic species to the Atlantic Ocean through its incorporation into the MOW. The spatial patterns of benthic deep-sea fauna in the Mediterranean are poorly known compared to those of other ecosystems. Our taxonomic and biogeographic approaches have made evident the need for further knowledge on the deep benthic fauna of the eastern Mediterranean basin as a base for management and conservation of the Mediterranean biodiversity.

Introduction

The Mediterranean Sea has a large cycle of water mass formation, which is relatively well known in general terms. The Mediterranean Sea receives North Atlantic Surface water (NAS) through the Strait of Gibraltar, an influx that runs eastwards along the Mediterranean Sea from the surface to 100 – 150 m depth (Millot & Taupier-Letage, 2005; El-Geziry & Bryden, 2010; Pinardi et al., 2015; Sánchez-Leal et al., 2017). Below this water mass, the Levantine Intermediate Water (LIW) flows from the eastern Mediterranean to the opposite direction at depths of 200 – 800 m (Lascaratos et al., 1993; Malanotte-Rizzoli, 2001; El-Geziry and Bryden, 2010). Below the LIW, the Western and Eastern Deep Mediterranean Water currents (WDMW and EDMW) flow reaching the bottom. While the NAS and the LIW reach both the western and eastern basins through the Strait of Sicily, at the central Mediterranean, (Robinson et al., 2001), the deepest WDMW and EDMW are distinct between the two basins (Schroeder et al., 2012; Pinardi et al., 2015). They both run westwards at depths down from ca. 1200 m and are separated by two sills at the Strait of Sicily (460 and 330m) (Lascaratos et al., 1993; Astraldi et al., 1996), therefore, only the LIW reaches the western basin and finally flows through the Strait of Gibraltar together with the WDMW. Once these two water masses enter the Atlantic Ocean (flowing below the NAS), they constitute the Mediterranean Outflow Water (MOW) with a much higher contribution of the LIW (90% of the water) than of the WDMW (10%) (Bryden and Stommel, 1984; Malanotte-Rizzoli, 2001).

The water exchange occurring in the Strait of Gibraltar has been reported to favour the transfer of sponges between the Atlantic and the Mediterranean. The NAS favours the export of shallow Atlantic sponge species into the Mediterranean (Templado et al., 1986; Pansini, 1987;

Maldonado, 1992, 1993a; Xavier & Van Soest, 2012), and the MOW favours the export of deep Mediterranean sponge species into the Atlantic, (Chapter 4). The Strait of Sicily shares some similarities with the Strait of Gibraltar, (Pansini, 1987; Baringer & Price, 1999; Malanotte-Rizzoli, 2001; Lujan et al., 2011; Gasser et al., 2017). The Strait of Sicily is characterised by a very complicated bottom topography (Astraldi et al., 2002) and acts as a physical constraint for the Mediterranean water currents, affecting their paths (Astraldi et al., 1996; Malanotte-Rizzoli, 2001; Astraldi et al., 2002; Freiwald et al., 2009; Pinardi et al., 2015) and representing an important intersection for the distribution of benthic species along the two Mediterranean basins (Bianchi & Morri, 2000; Di Lorenzo et al., 2018). Some of the most relevant habitat-forming species of sessile megabenthic communities in the Mediterranean are cnidarians and sponges (Freiwald, 2009; Angeletti et al. 2015), and the Strait of Sicily is considered a biodiversity hotspot (Coll et al., 2010; Vega Fernández et al., 2012). Therefore, a biogeographical analysis of the sponge fauna around the Strait of Sicily can provide understanding on the influence of the LIW across the Mediterranean and its role in faunal transference from the Eastern Mediterranean basin towards the Western Mediterranean and, ultimately, to the Atlantic Ocean. While the shallow sponge fauna of the Strait of Sicily has been reported to be influenced by the NAS flow (Pansini, 1987; Xavier & Van Soest, 2012), the effect of the LIW on the bathyal sponge fauna across the Strait of Sicily remains poorly studied. Chapter 4 assessed the biogeographic patterns of the deep sponge fauna along an Atlanto-Mediterranean gradient, involving the Northeastern Atlantic, Western and Central Mediterranean, which included the Strait of Sicily. However, that study was focused on the effect of the MOW on the easternmost Atlantic deep sponge fauna, implying that the effect of the LIW in the distribution of the Mediterranean sponges was not explored in detail. The present study extends this previous biogeographical work by expanding the study area to the easternmost Mediterranean sectors that are, the Aegean Sea and the Israel slope. This is aimed to assess the bathyal sponge distribution along the entire Mediterranean Sea, focusing on the intermediate water running through the Strait of Sicily as a precursor of the MOW.

While the deep sponge fauna of the Alboran Sea and the Gulf of Cádiz is fairly well known (Thomson, 1873; Carter, 1876; Schulze, 1887; Sollas, 1888; Topsent, 1895; Arnesen, 1920; Templado et al., 1986; Pansini, 1987;

Maldonado & Benito, 1991; Maldonado, 1992, 1993a; Boury-Esnault et al., 1994; Maldonado & Uriz, 1995; Rosell & Uriz, 2002; Templado et al., 2006; Van Soest et al., 2013; Díaz del Río et al., 2014; Van Soest et al., 2014; Chevaldonné et al., 2015; Sitjà et al., 2019), similar studies around the Strait of Sicily are scarce but have revealed a noticeable sponge occurrence (Topsent, 1928, 1934; Vacelet, 1961; Rützler, 1973, 1976; Pansini, 1987; Ben Mustapha & Vacelet, 1991; Borg & Schembri, 1996; Ben Mustapha et al., 2003; Pansini & Longo, 2003; Zibrowius & Taviani, 2005; Aguilar et al., 2011). The knowledge on the bathyal sponge fauna from the Strait of Sicily still remains in a primary stage compared to that of other Mediterranean regions, and, in particular, the sponges from the Maltese Islands (South West of the Strait of Sicily) remain even less studied (Calcinai et al., 2013; Evans et al., 2016).

The non-governmental organization (NGO) OCEANA conducted two oceanographic expeditions under the framework of the LIFE BaHAR Project, which evidenced the importance of the marine biodiversity of the Maltese Islands (Evans et al., 2016). Previous to these expeditions, the seabed surrounding the Maltese Islands was already known to host a variety of communities like seagrass beds (Borg et al., 2009), maërl beds (Sciberras et al., 2009), and cold-water corals (Freiwald et al., 2009; Deidun et al., 2010; Deidun et al., 2015; Knittweis et al., 2016). The LIFE BaHAR expeditions allowed to list a variety of key marine habitats of the EU Habitats Directive (92/43/ECC) (habitats 1110 "Sandbanks which are slightly covered by sea water all the time", 1170 "Reefs" and 8330 "Submerged or partially submerged sea caves") found in a total of eight marine protected areas in the Islands. The results from that expedition indicated that the deep sea around Malta represents an important biodiversity hotspot with a variety of different assemblages dominated by suspension feeders (mainly cnidarians and sponges) as habitat-forming taxa (Evans et al., 2016). A collection of deep-sea sponges was accomplished during the exploration of the Maltese Islands by the LIFE BaHAR expeditions. The sponge material was later on taxonomically identified and included in the database for the study of the deep sponge faunal affinities along an Atlanto-Mediterranean gradient (Chapter 4). However, the taxonomically relevant findings derived from the identifications of the sponge material remained undescribed. The present work aims to provide further information on the collected sponge fauna from the shelf of

the Maltese Islands and to describe two new sponge records for the Mediterranean Sea.

Material and methods

Faunal affinities

In order to examine the faunal affinities along the Atlantic-Mediterranean gradient, data was extended and updated from a sponge presence/absence matrix previously built in Chapter 4. The original matrix contained 456 deep-sea sponge species recorded from nine biogeographic areas distributed along the Macaronesia, southern Lusitania and Gulf of Cádiz, in the Atlantic; and other nine areas distributed along the Western and Central Mediterranean. The areas from the Atlantic were Azores (A-A), Southern Azores Banks (AB-A), Cape Verde (CV-A), Canary Islands (Ca-A), Madeira (Ma-A), Morocco (Mo-A), Lusitanian Banks (LB-A), the mud volcanoes of the Gulf of Cádiz (MV-A), and the remaining slope communities of the Gulf of Cádiz (GC-A). In the Mediterranean Sea, the nine areas considered were Alboran Sea (Al-M), Balearic Sea (B-M), Gulf of Lion (GL-M), Ligurian Sea (L-M), West Corsica (C-M), Tyrrhenian Sea (T-M), Strait of Sicily (S-M), Gulf of Taranto (GT-M), and Adriatic Sea (A-M). The present study expands the original matrix by adding the extant deep sponge records of the easternmost Mediterranean, that is, the Aegean Sea (Ae-M) (Vamvakas, 1970; Voultsiadou, 2005; Boury-Esnault et al., 2017) and the slope of Israel in the Levantine Sea (I-M) (Ilan et al., 1994; Ilan et al., 2003). This update represents a total of 20 deep-sea biogeographical areas for this study, it also implies the addition of 5 sponge species to the data base, accounting for a total of 461 species, and 32 records of species, some newly and others formerly included in the database of Chapter 4 (Fig. 1; Appendix I). Following the directions of the former database, only records deeper than 200 m were considered, being this threshold similar to the upper depth limit of the LIW and the MOW (Malanotte-Rizzoli, 2001; Sánchez-Leal et al., 2017). Since both the LIW and the WDMW contribute to the composition of the MOW (in a 90% and 10% respectively), no maximum depth limit was settled for the Mediterranean records. Because the MOW spreads in the Atlantic at about 1500 m (Sánchez-Leal et al., 2017), this depth was established as the lower limit for the records

in the Atlantic Ocean. All sponge records were double checked by contrasting them against the World Porifera Database (Van Soest et al., 2020), so that those currently considered as inaccurate or incorrect taxonomic records in such database were excluded. Because the available taxonomic studies for the sponge fauna of most locations often lacked robust and/or consistent information about the abundance of the species, the use of quantitative or semi-quantitative analyses was impracticable.

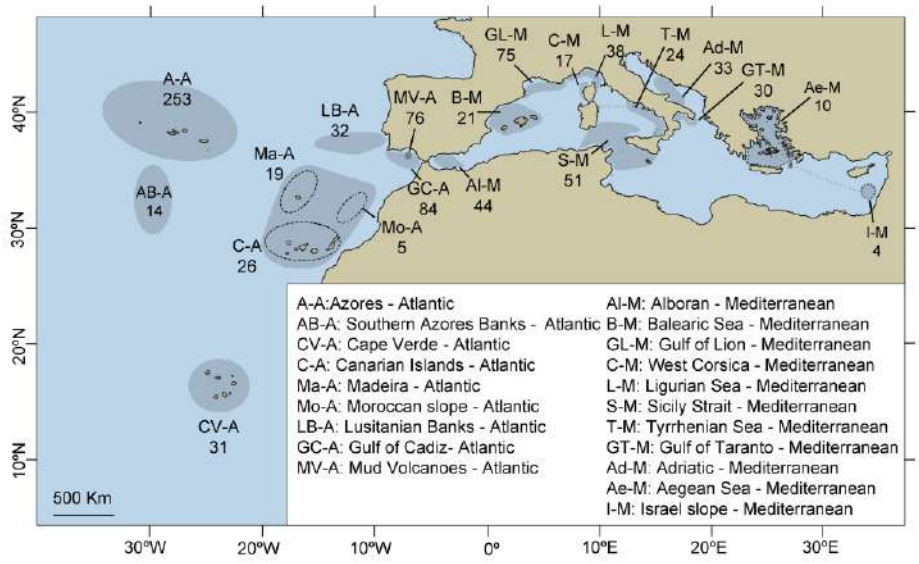

Fig. 1 Map of the Atlantic-Mediterranean region showing the biogeographical areas (grey shades) and their sub-areas (see codes in legend) considered for the comparison of affinities for the sponge fauna. Geographically close sub-areas which showed non-significant faunal differences after exploratory Jaccard-based cluster analyses were unified into a larger area, but still indicated in the map by dashed lines. Each area and subarea is labelled with a code (see graphic legend). The number of sponge species recorded to date within the 200 – 1,500 m depth in each area and subareas is also indicated.

An exploratory Jaccard-based dendrogram and subsequent SIMPROF test were performed (data not shown) to detect areas with strong affinities representing statistically significant genuine groups (which can be combined with each other into a single biogeographic area) and cluster members with

not statistically significant structure, which should stay independent for the analyses. These exploratory tests suggested that the fauna from the Canary Islands, Madeira and Morocco could be grouped into a unit, hereafter referred to as C+Ma+Mo-A. Additionally, some initial areas which are poorly studied and have a low number of taxonomic records had to be combined with their geographically closest area to minimize the impact of under-represented outliers on the analyses. Consequently, the Aegean Sea and the Israel slope, with 10 and 4 recorded deep sponge species, respectively, were collapsed as Ae+I-M. Following these readjustments, a total of 17 areas were finally submitted to the definitive analyses of the bathyal sponge fauna along an Atlantic-Mediterranean gradient impacted by the MOW. The geographical location of the initial and collapsed areas and their respective numbers of species are summarized in Fig. 1.

Taxonomic methods

The oceanographic expeditions that collected the sponge material from the Maltese Islands were conducted during the project LIFE BaHAR for N2K - Life+ Benthic Habitat Research for Marine Natura 2000 Site Designation. The NGO OCEANA, partner of the project, performed several Remotely Operated Vehicle (ROV) dives on board of the Oceana Ranger catamaran around the shelf of the Maltese Islands of Malta and Gozo (Fig. 2). A Saab

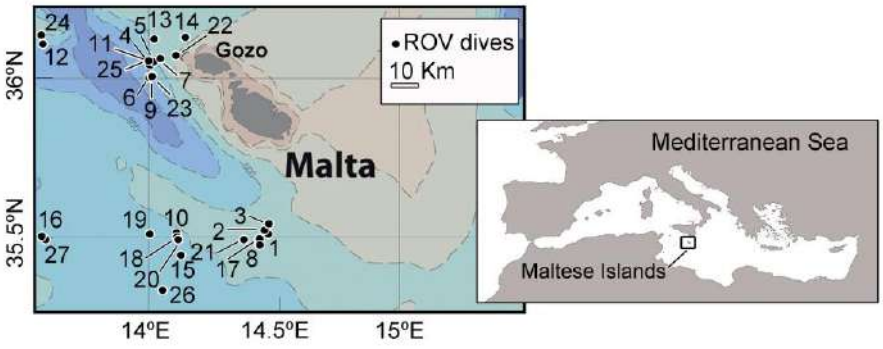

Fig. 2 Maps indicating the location of Malta in the Mediterranean Sea (right) and, in a closer view, the location of the ROV dives (left).

Seaeye Falcon DR ROV equipped with a High Definition Video (HDV) camera was used to record images in offshore areas of the islands, allowing the observation of around 650 m2 of the seabed per hour of exploration. Collection was conducted along 27 dives between 53 and 1007 m depth by means of a ROV mechanical arm. Dives are represented in Fig. 2 and sampling depth, geographic coordinates and date of collection are given in Table 1.

After collection, sponges were directly preserved in 100% and 70% ethanol for further taxonomic identification. Taxonomic identification followed the standard protocols for taxonomical identification based on features of the external morphology and skeleton, using dissecting and compound light microscopes. When high-resolution observations of skeletal elements were required, spicules were nitric acid-cleaned, mounted on

Table 1. Location, depth (m) and date of ROV dives (the label and original name of each dive) conducted in the LIFE BaHAR 2015 and 2016 expeditions which collected information and samples of deep-sea sponges in Malta.

Dive Label	Dive	Latitude	Longitude	Depth (m)	Collection Date
1	4.17	35º 53' 56.72"N	14º 45' 12.23"E	53	20/07/2015
2	4.3	35º 55' 43.88"N	14º 43' 53.28"E	95	06/07/2015
3	4.24	35º 56' 44.46"N	14º 44' 59.82"E	101	21/07/2015
4	7.4	36 04' 81.82"N	14º 04' 20.85"E	242	24/06/2015
5	7.3	36º 05' 97.17"N	14º 05' 75.58"E	247	21/06/2015
6	1.20	36º 00' 71.90"N	14º 04' 24.55"E	266	08/07/2015
7	7.1	36º 06' 50.25"N	14º 07' 24.67"E	278	06/06/2015
8	11.5	35º 48' 68.62"N	14º 41' 30.64"E	291	07/07/2015
9	7.5	36º 02' 12.60"N	14º 01' 49.06"E	298	03/07/2015
10	1.11	35º 52' 51.93"N	14º 10' 64.12"E	320	19/06/2015
11	7.3	36º 06' 01.61"N	14º 05' 58.25"E	332	21/06/2015
12	6.2	36º 10' 51.05"N	13º 56' 27.06"E	365	15/07/2015
13	7.6	36º 12' 82.57"N	14º 08' 52.44"E	372	04/07/2015
14	5.1	36º 13' 87.91"N	14º 18' 38.19"E	475	02/06/2015
15	11	35º 46' 34.42"N	14º 17' 37.84"E	621	09/06/2015
16	1.7	35º 51' 11.37"N	13º 53' 22.41"E	657	11/06/2015
17	1.25	35º 49' 52.46"N	14º 41' 95.54"E	760	18/07/2015
18	11.2	35º 47' 82.68"N	14º 14' 01.49"E	881	28/06/2015
19	1.22	35º 53' 60.12"N	14º 04' 79.88"E	955	12/07/2015
20	1.17	35º 49' 49.09"N	14º 11' 20.34"E	1007	05/07/2015
21	F27	35º 49,8858' N	14º 36,1595' E	91	08/07/2016
22	C04	36º 08,3810' N	14º 12,4660' E	235	05/06/2016
23	A04	36º 01,6339' N	14º 02,6400' E	256	31/05/2016
24	A32	36º 15,0651' N	13º 46,5741' E	340	29/07/2016
25	A24	36º 05,9894' N	14º 00,2098' E	556	10/07/2016
26	E15	35º 30,6360' N	14º 07,6150' E	431	05/07/2016
27	B09	35º 49,7109' N	13º 57,7781' E	752	12/07/2016

aluminium stubs, dried and then gold-coated to be examined through a HITACHI TM3000 Scanning Electron Microscope (SEM). Description of body features, spicules, and skeletal arrangements have been made according to the sponge morphology thesaurus (Boury-Esnault & Rützler, 1997). All the material herein described as part of OCEANA LIFE BaHAR cruises, holotypes included, will be stored at the University of Malta.

Results

Faunal affinities across the Mediterranean Sea related to the LIW

The results of a cluster analysis based on the Jaccard similarity index on a matrix of 461 sponge species from 10 deep-sea biogeographical areas of the Mediterranean and 7 from the Northeastern Atlantic (Fig. 3) showed that the Mediterranean areas were grouped in one main cluster that split in two clusters related with a statistically non-significant 10.34% of affinity. The largest of the two groups that formed the main Mediterranean cluster (group I, Fig. 3) included the central Mediterranean areas of the Strait of Sicily (S-M) and Gulf of Taranto (GT-M), which shared a 19.50% of statistically supported affinity with the Gulf of Lion (GL-M). It also included the Alboran Sea (A-M), the westernmost Mediterranean, and the two areas from the Gulf of Cádiz, the Mud volcanoes area and the remaining slope of the Gulf of Cádiz (MV-A, GC-A). All the above mentioned areas formed a group that shared a 14.79 % of affinity with the Adriatic Sea (Ad-M). The other Mediterranean group (group II, Fig. 3) included the Balearic Sea (B-M), the Corsica (C-M) and the Ligurian slopes (L-M), showing B-M and C-M the highest statistically significant affinity among them (22.58%). The group II also included the area formed from the combination of the Aegean Sea and Israel slope (Ae+I-M), which showed a statistically significant affinity of 14.84% with the rest of the members of this group. Contrarily to the rest of the Mediterranean areas, the Tyrrhenian Sea (T-M) was not included within the main Mediterranean group but between other Atlantic areas. The relationships between the remaining Atlantic Areas, and also the Tyrrhenian Sea, are further presented and discussed in Chapter 4.

Out of the 461 species recorded for the considered depth range in the Atlantic-Mediterranean areas (≥200 m in the Mediterranean and 200 – 1500 m in the Atlantic), 181 of them were present in the Mediterranean (about a 40%). Out of the total species recorded from the Mediterranean, 105 (59%) occurred only in the Western Mediterranean, while 31 (17%) occurred only in the Eastern Mediterranean. The number of species co-occurring in at least

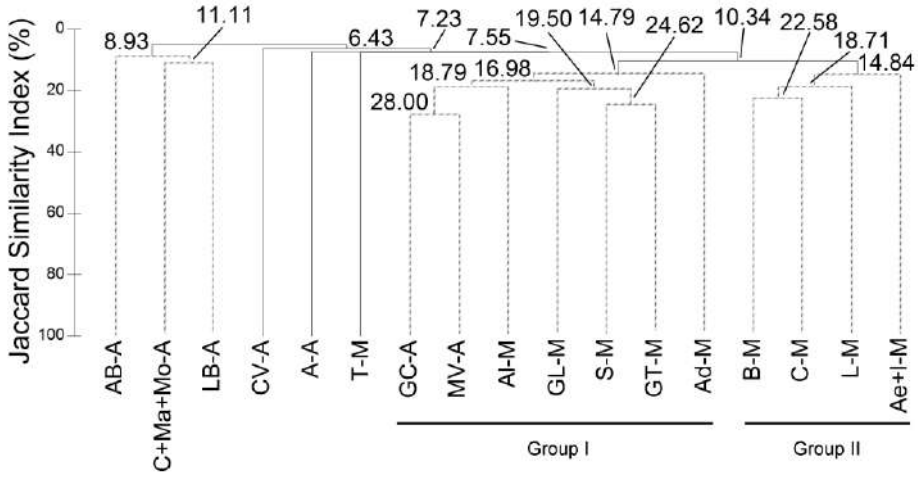

Fig.3 Dendrogram based on Jaccard similarity Index displaying the affinities between the deep sponge fauna from different Atlantic and Mediterranean areas. Values at the nodes represent the percentage of similarity between sub-groups. Dashed vertical lines represent genuine clusters with statistical support.

one Western and one Eastern Mediterranean deep-sea area was 45 (25%). The deep-water sponge fauna of the Strait of Sicily area accounted for 51 species, representing 28% of the total deep sponge species recorded in the Mediterranean Sea. The only Mediterranean area with higher number of records than the Strait of Sicily is the Gulf of Lion (75 species recorded), which is one of the most intensely sampled areas in the Mediterranean Sea. Likewise, the Strait of Sicily hosts 50% of the deep sponge species co-occurring in both eastern and western Mediterranean.

Taxonomic remarks on the deep sponge fauna of the Maltese Islands

The OCEANA LIFE BaHAR expeditions retrieved 36 sponge specimens belonging to 23 different species, obtained from 27 ROV dives. Five additional samples remained unidentifiable, being fragmentary specimens from the order Haplosclerida that were too small to provide reliable identifications. Most specimens of the collection belonged to the class Demospongiae with the exception of one member of the class Hexactinellida. No species belonging to the classes Calcarea and Homoscleromorpha were retrieved. The material collected is detailed in Table 2, summarising the species identification, number of individuals collected and their associated ROV dive information.

The sponge collection from the Maltese Islands provided only two taxonomically relevant findings. They both represented first Mediterranean records for the species *Pachastrella ovisternata* Lendenfeld, 1894 and *Higginsia thielei* Topsent, 1898, which previously were only known from the North Atlantic. These specimens accounting for new records are described in detail in the present study.

Systematics

Class DEMOSPONGIAE Sollas, 1885
Subclass HETEROSCLEROMORPHA Cárdenas, Perez andBoury-Esnault, 2012
Order TETRACTINELLIDA Marshall, 1876
Family PACHASTRELLIDAE Carter, 1875
Genus *Pachastrella* Schmidt, 1868

Diagnosis: (Maldonado, 2002)

***Pachastrella ovisternata* Lendenfeld, 1894**
(Figures 4-5)

Material examined: One specimen (M006.7-C04) from dive C04 and one specimen (M045-B09) from dive B09.

Macroscopic description: Each specimen consists of two fragments with somewhat subspherical shape. Those of specimen M006.7-C04 measured 1 x

3x 3 mm in thickness and 2 x 3x 3 mm in width (Fig. 4A). The two fragments of specimen M045-B09 are 3 x 4 x 1.5 mm and 1 x 1 x 1.5 mm. Surface is smooth with some areas showing an hispidation and others showing debris on the surface. Pores are not observed, probably due to the fragmentary character of the specimens. The consistency is hard and compact, although the choanosome is somewhat friable. Colour after preservation is light beige.

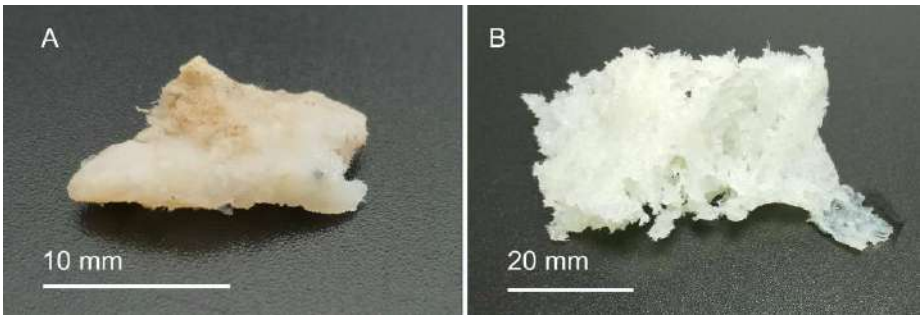

Fig. 4 Pictures showing the general aspect of some studied specimens: (A) *Pachastrella ovisternata* (M006.7-C04). (B) *Higgindia thielei* (M007-11.2)

Spicules: Spicules are softly curved oxeas with blunt ends of 765 – 4398x 15 – 47.55 μm (Fig.5A-B). Smaller softly bent oxeas of 90 – 338 x 3 – 8 μm are also observed (Fig. 5A, C). Abundant calthrops occur in a wide size range, measuring their clads 84 – 1027 x 11 – 22.5 μm. Abnormal shapes like blunt ends or evenly bent clads often happen (Fig. 5A, D-E). Short-shafted dichotrianes occur with a rhabdome measuring 29.7 – 35.5 x 5.6 – 8.4 μm, the protoclads 14.14 – 36.97 x 5.3 – 8.5 μm and the deuteroclads 26 – 65.3 x 5.7 – 9 μm (Fig.5A, E-F). Occasional larger sizes are also found with rhabdomes measuring up to 245.7 x 37.94 μm, their protoclads 188 x 22.69 μm and their deuteroclads 396.3 x 50.08 μm. Mesodichotrianes also occur in very similar sizes to the common dichotriaenes (Fig. 5A, G). Their epirhabdome is shorter than their clads and measures 28 – 55.6 x 6.4 – 10.3 μm. Both dicho- and mesodichotriaenes sometimes show variations like extra or blunt clads and irregular shapes (Fig. 5A, H). Microscleres are abundant oval microstrongyles with microspines, measuring 12.8 – 18.17 x 3 – 8.3 μm. Microrhabdose spiny streptasters with thin and long shapes are very scarce, and measure 16 – 33.19 x 1.3 – 1.9 μm (Fig. 5A, I). Amphiasters with microspines abundantly occur

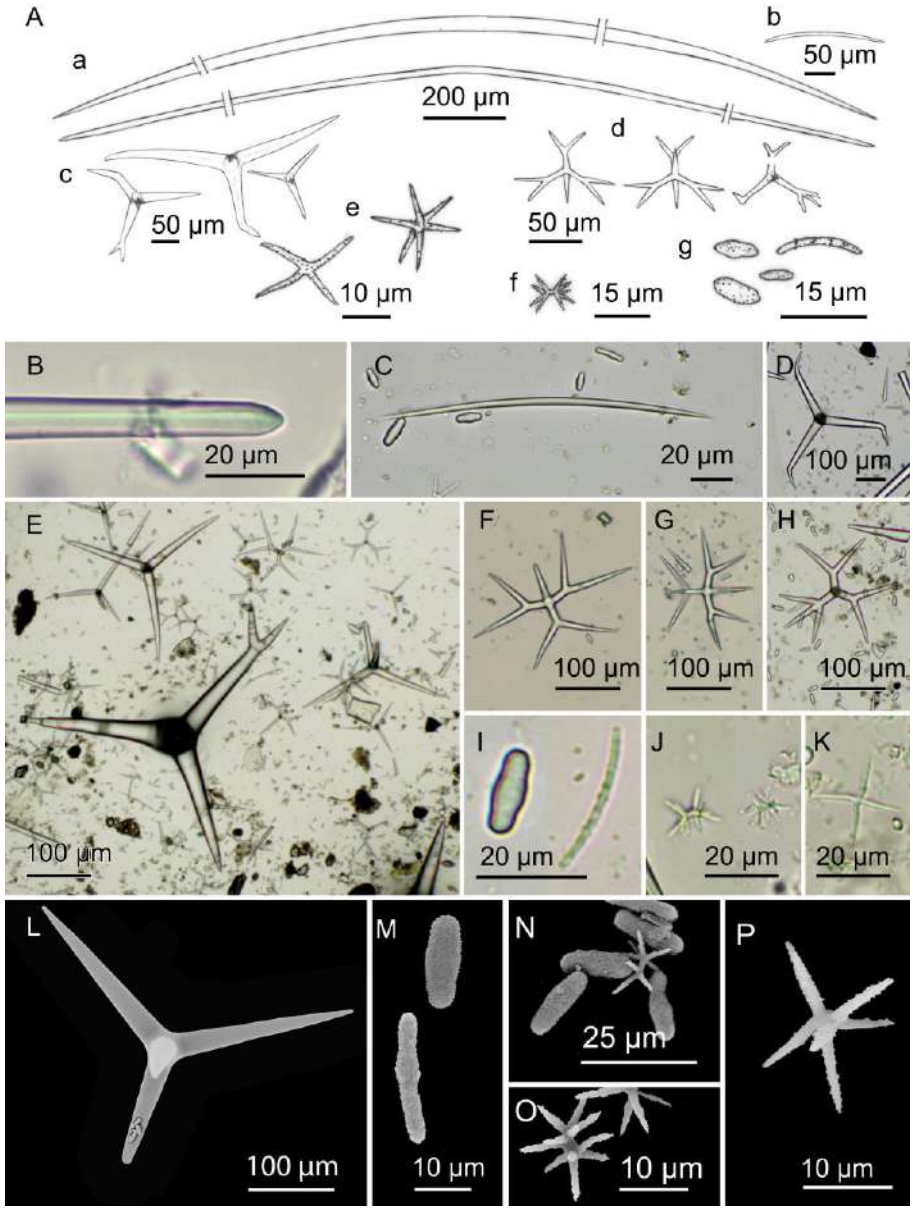

Fig. 5 *Pachastrella ovisternata*: (A) Line drawing summarizing the skeletal complement of the species. Megascleres are long oxeas (a) with rome ends (b), and another category of smaller oxeas (c). Calthrops are abundant (d), sometimes with abnormal formations (e). Dichotrianes (f) and mesodichotrianes (g) also occur, sometimes bearing extra clads (h). Microscleres bear all microspines and are microstrongyles (i), rare spiraster-like microstrongyles (j), amphiasters (k),

…continued in the next page

which occasionally become metasters (l) and plesiasters with 4 to 6 actines (m). (B) Light microscope view of a long oxea blunt end. (C) A small oxea. (D) Calthrop with bent ends. (E) General view of differently shaped calthrops and dichotrianes. (F) A dichotriane. (G) A mesodichotriaene. (H) A dichotriaene with an extra deuteroclad. (I) A microstrongyle and a thiner spiraster-like microstrongyle. (J) An amphiaster and a smaller metaster. (K) A plesiaster.

and measure 11.12 – 15.16 μm in length. Rarely, they are transformed into metasters (Fig. 5A, J). Moderately abundant plesiasters are observed bearing 4 – 6 actines, which measure 8.5 – 12 x 1 – 2 μm, being the total spicule length 14.3 – 26 μm (Fig. 5A, K).

Skeletal structure: The choanosome shows all the megascleres and streptasters in confusion, only being the larger oxeas arranged in more or less defined radial bundles running from choanosome towards the sponge surface, and sometimes hispidating the ectosome. The ectosome is a crust formed by densely packed microstrongyles.

Distribution and ecology notes: The holotype of this species is recorded off Portugal, Northeast Atlantic (Lendenfeld, 1894). It is also recorded from the North and Southwest Iberian Peninsula, at 557-928 m depth (Ferrer Hernández, 1914; Maldonado, 1993b; Ríos et al., 2017; Sitjà et al., 2019). The specimens from Malta described in the present study represent the first Mediterranean record of the species.

Taxonomic remarks: Maldonado (1993b) reported especially long (up to 7500 μm in lenght), flexuous oxeas in *P. ovisternata* specimens from the northeastern-Atlantic coast of Spain, longer than those measured in the specimens from Malta herein studied. However, since their characteristic blunt ends and lengths of more than 4000 μm have been observed, this difference is here considered as a consequence of the fragmentary condition of our material. The rest of the characteristics of the specimens herein studied fit those of *P. ovisternata*, which differentiate it from the similar *Pachastrella monilifera* Schmidt, 1868. That is, the presence of dichotrianes and mesodichotrianes (Maldonado, 1993b). It is worth to mention that in our specimens abnormal formations have been found in both of these spicule types, while Maldonado (1993) observed them only in the dichotrianes.

Order AXINELLIDA Lévi, 1953
Family STELLIGERIDAE Lendenfeld, 1898
Genus *Higginsia* Higgin, 1877

Diagnosis: (Hooper, 2002)

***Higginsia thielei* Topsent, 1898**
(Figures 4, 6)

Material examined: One specimen (M007-11.2) collected from dive 18.

Macroscopic description: A specimen consisting of two lamellar fragments of 30 x 60 x 4– 7 mm (Fig. 4B) and 10 x 15 x 4 mm in width, length and thickness respectively. The best preserved parts show a thin, smooth ectosomal membrane, while the inner body is porous. The consistency is firm but easily breakable, and the colour after preservation is white with a very subtle greenish tone.

Spicules: Megascleres are smooth styles in one size category (Fig. 6A, B), measuring 528.4 – 677.9 x 23 – 30 μm, they are slightly to markedly bent, with a shaft that becomes slightly thinner near the rounded end. Sometimes they show weakly subtylote rounded ends (Fig. 6A, C). Microscleres are spiny microxeas evenly bent at the centre (Fig. 6A, D), sometimes only softly bent or even straight, that measure 61.5 – 93.9 x 1.3 – 2 μm. Small spherules are abundant, measuring 1 – 3 μm in diameter (Fig. 6A, E).

Skeletal structure: The choanosome shows tracts of styles measuring 40 – 150 μm in diameter and arranged in a plumo-reticulated fashion. The ectosomal skeleton is composed of tangential styles, free or grouped in bundles of two to four spicules forming a vaguely defined mesh (Fig. 6F) and abundant spherules. Microxeas are abundantly found in the choanosome and the ectosome.

Distribution and ecology notes: This specimen was collected at 881 m depth and belongs to a species which was hitherto recorded only from the Atlantic. Topsent (1898) described the holotype from Azores at 523 m depth, plus two other specimens also from Azores at 200 m depth. Later he described

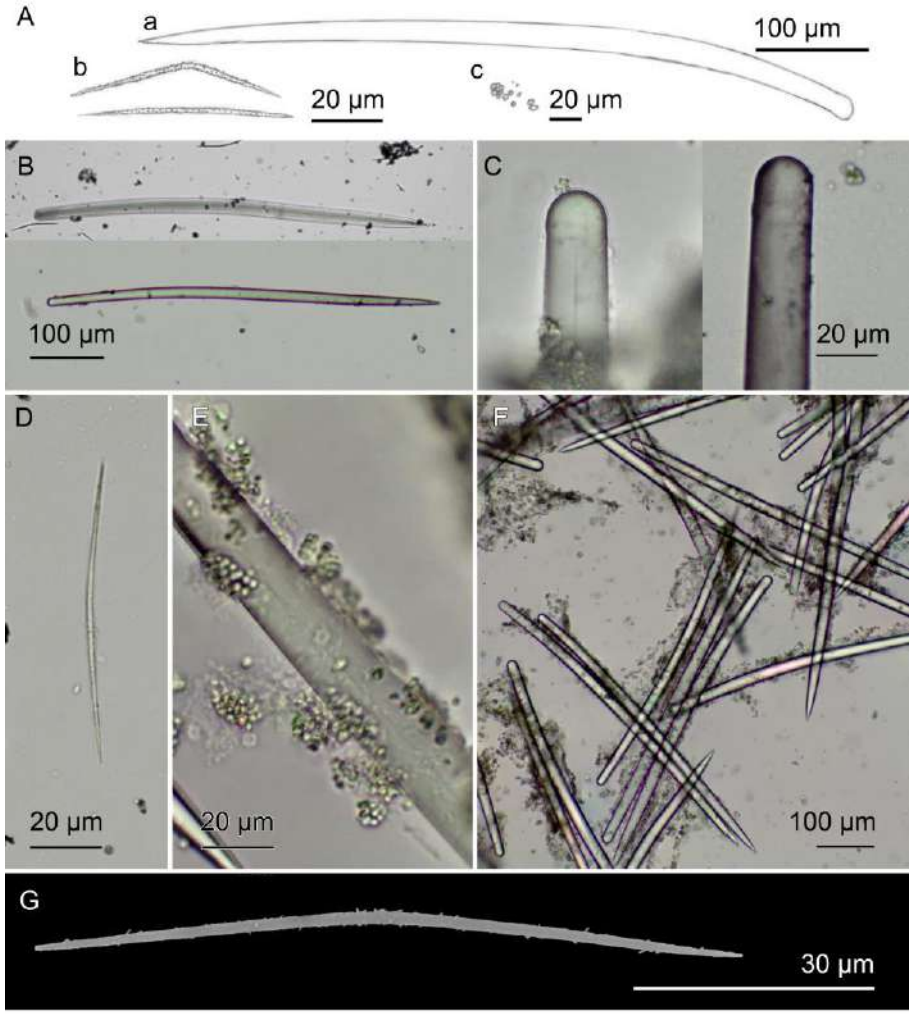

Fig.6 *Higginsia thielei*: (A) Line drawing summarizing the skeletal complement of the species. Megascleres are softly bent styles (a), sometimes with very subtle subtylotism (b). Microscleres are spinned microxea (c). Spherules occur abundantly (d). (B) Light microscope view of teo styles. (C) Blunt ends of styles showing very subtle swellings. (D) A microxea. (E) Spherules agregated arround a style. (F) Ectosomal skeleton view of tangential styles grouped in small bundles and surrounded by spherules and microxeas, forming a poorly definet mesh. (G) Scanning electron microscope view of a microxea.

two more specimens from Azores collected from 1095 and 1250 m depth (Topsent, 1904). Other three fragmentary specimens were recorded from Ireland between 457 – 1024 m depth (Stephens, 1920).

Taxonomic remarks: Other *Higginsia* species from the Mediterranean Sea were compared to our material, that is, *Higginsia ciccaresei* Pansini and Pesce, 1998 and *Higginsia mediterranea* Pulitzer-Finali, 1978. The first has oxeas and strongyles instead of styles, and the last shows styles and oxeas. Additionally, its styles are longer (600 – 900 x 14 μm) and show a different shape, being curved or flexuous, sometimes with an annular swelling and occasionally modified to strongyles. Other Eastern Atlantic species were also assessed for a comparison with the collected material. *Higginsia tethyoides* Lévi, 1960, and *Higginsia coralloides* var. *liberiensis Higgin*, 1877 are recorded both from West Africa, but they bear oxeas instead of styles. Since our specimen fits the characteristics of *H. thielei* described by Topsent we consider that the material from Malta constitutes a first record of this species in the Mediterranean Sea.

Discussion

The completion of a database containing sponge records for the whole Mediterranean allows a first assessment of the faunal affinities deeper than 200 m along the Eastern and Western Mediterranean. The biogeographic pattern of the deep sponge fauna of both the Mediterranean and Northeast Atlantic resulted very similar to that observed in Chapter 4, despite the addition of two new eastern Mediterranean areas (Aegean Sea and Israel Slope). This is not unexpected because the deep-water sponge fauna is still poorly sampled and the sponge records under 200 m depth in the easternmost Mediterranean are scarce (the analysed database was updated with 32 sponge records). In the Aegean Sea, with its depths also poorly investigated, 10 different bathyal sponge species are recorded (Vamvakas, 1970; Voultsiadou, 2005; Boury-Esnault et al., 2017), while only 4 are recorded from the Israel slope (Ilan et al., 1994; Ilan et al., 2003) (Appendix I). However, the improvement of the database containing sponge records for the whole Mediterranean allows a first assessment of the faunal affinities deeper than 200 m along the Eastern and Western Mediterranean. Despite the similarities with the previous results of the faunistic analyses of Chapter 4, the present analysis of the updated database focuses on the role of the Strait of Sicily

Table 2. Summary of sponge specimens collected for each species during the 27 ROV dives conducted in the LIFE BaHAR 2015 and 2016 expeditions. Sponge species are listed alphabetically by class (Cl), subclass (SCl), order (Or), family and species. Abbreviations for the taxonomic categories are: Dm= Demospongiae, Hx= Hexactinellida, Het= Heteroscleromorpha, Ly= Lyssacinosida,Ax= Axinellida, Bi= Biemnida, Bu= Bubarida, De= Desmacellida, Di= Dictyoceratida, Me= Merliida, Po= Poecilosclerida, Su= Suberitida, Te= Tetractinellida, Ly= Lyssacinosida, Ra= Raspailiidae, St= Stelligeridae, Rh= Rhabderemiidae, Bb= Bubaridade, Ds= Desmacellidae, Th=Thorectidae, Ch= Chalinidae, Hm= Hamacanthidae, Cl= Cladorhizidae, Hy= Hymedesmiidae, Hl=Halichondriidae, Sb= Suberitidae, An= Ancorinidae, Az= Azoricidae, Ca= Calthropellidae, Pa= Pachastrellidae, Tn= Theneidae, Vu= Vulcanellidae, Ro= Rossellidae

					Dive Label																						
Cl	**SCl**	**Or**	**Family**	**Species**	**1**	**2**	**3**	**4**	**5**	**6**	**7**	**8**	**9**	**10**	**11**	**12**	**13**	**14**	**15**	**16**	**17**	**18**	**19**	**20**	**21**	**22**	**23**	**24**	**25**	**26**	**27**
Dm	Het	Ax	Ra	*Eurypon hispidulum* (Topsent, 1904)																						1					
Dm	Het	Ax	St	*Higginsia thielei*																		1									
Dm	Het	Bi	Rh	*Rhabderemia* sp.																	1										
Dm	Het	Bu	Bb	*Bubaris subtyla* Pulitzer-Finali, 1983																						1					
Dm	Het	De	Ds	*Desmacella annexa* Schmidt, 1870					1																						
Dm	Het	De	Ds	*Desmacella inornata* (Bowerbank, 1866)						1	1				1																
Dm	Het	Di	Th	*Cacospongia mollior* Schmidt, 1862																					1						
Dm	Het	Ha	Ch	*Haliclona (Gellius) fibulata* (Schmidt, 1862)																	1										
Dm	Het	Ha	Ch	*Haliclona (Soestella) implexa* (Schmidt, 1868)	1		1																								
Dm	Het	Ha	Ch	*Haplosclerid 1*																				1							
Dm	Het	Ha	Ch	*Haplosclerid 2*		1																									
Dm	Het	Ha	Ch	*Haplosclerid 3*								1																			
Dm	Het	Ha	Ch	*Haplosclerid 4*																		1									
Dm	Het	Ha	Ch	*Haplosclerid 5*																							1				

					Dive Label																						
Cl	**SCl**	**Or**	**Family**	**Species**	**1**	**2**	**3**	**4**	**5**	**6**	**7**	**8**	**9**	**10**	**11**	**12**	**13**	**14**	**15**	**16**	**17**	**18**	**19**	**20**	**21**	**22**	**23**	**24**	**25**	**26**	**27**
Dm	Het	Me	Hm	*Hamacantha (Vomerula) falcula* (Bowerbank, 1874)										1																	
Dm	Het	Po	Cl	*Cladorhiza abyssicola* Sars, 1872																									1		
Dm	Het	Po	Hy	*Hymedesmia* cf. *pansa*																					1						
Dm	Het	Po	Hy	*Hymedesmia* sp.																					1						
Dm	Het	Su	Hl	*Ciocalypta hyalina* (Pulitzer-Finali, 1978)																					1						
Dm	Het	Su	Sb	*Aaptos aaptos* (Schmidt, 1864)																										1	
Dm	Het	Te	An	*Jaspis incrustans*(Topsent, 1890)								1					1			1								1			
Dm	Het	Te	Az	*Leiodermatium* sp. (Fossil)						1			1	1																	
Dm	Het	Te	Ca	*Calthropella (Calthropella) pathologica* (Schmidt, 1868)													2														
Dm	Het	Te	Pa	*Pachastrella ovisternata* Lendenfeld, 1894																					1						1
Dm	Het	Te	Tn	*Thenea muricata* (Bowerbank, 1858)														1													
Dm	Het	Te	Vu	*Poecillastra compressa* (Bowerbank, 1866)											1				1												
Dm	Het	Te	Vu	*Vulcanella gracilis* (Sollas, 1888)										1			1														1
Hx	He	Ly	Ro	*Sympagella delauzei* Boury-Esnault, Vacelet, Reiswig & Chevaldonné, 2015												1															

relative to the transfer of deep sponge fauna from the Eastern to the Western Mediterranean.

The Mediterranean area showing the highest affinity with the Strait of Sicily (S-M) was the Gulf of Taranto (GT-M) followed by the Gulf of Lion (GL-M) and the Adriatic Sea (Ad-M). A reason for the highest affinity between Strait of Sicily and Gulf of Taranto may be the geographical proximity of these two areas and the presence of the Northern Ionic Cyclonic Gyre (Pinardi et al., 2015), suggesting that it can connect the faunas from the Strait of Sicily and Gulf of Taranto. The group formed for all these Mediterranean areas (S-M, GT-M, GL-M and Ad-M) was faunistically related to the westernmost Mediterranean area, the Alboran Sea (Al-M), and the easternmost Atlantic areas of the Gulf of Cádiz (MV-A and GC-M). The relationship of the Strait of Sicily with areas from both the Eastern and the Western Mediterranean is indicative of its role as a transitional area for the deep sponge fauna of the Mediterranean. Such a role has also been suggested for other sessile invertebrates such as cnidarians (Freiwald et al., 2009; Di Lorenzo et al., 2018). Subsequently, the transport of deep sponge species from the Eastern to the Western Mediterranean through the Strait of Sicily is influencing at a certain extent the deep sponge components from the Western Mediterranean that might be transferred to the Gulf of Cádiz, as observed in Chapter 4.

Similarly, as the MOW in the Strait of Gibraltar, the LIW is suggested as a responsible for the deep sponge transfers from the Eastern to the Western Mediterranean basins through the Strait of Sicily. Pinardi et al. (2015) pointed that the preferred path for the LIW before reaching the Strait of Sicily is southwards, along the Gulf of Syrte as part of the anticyclonic Syrte Gyre. This trajectory can explain the lower affinity of the deep sponge fauna of the Adriatic Sea. Moreover, the isolated position of the Adriatic Sea, only connected through its southern basin to the rest of the Mediterranean, may also have an influence on its lower affinity. The other two easternmost areas, the Aegean Sea and Israel slope, also at the northern sector of the Eastern Mediterranean, may also be affected in a similar way by the southwards trajectory of the LIW. However, such assumption will remain untested until further deep-sea sponge records for these two areas can provide new data for subsequent analyses.

The cluster obtained from the analysis of similarities also supported the influence of the LIW in the Western Mediterranean. After passing the Strait of Sicily, a major branch of the LIW flows towards the Algerian basin, which is consistent with the affinities observed between the group formed by the Alboran Sea and the Gulf of Cádiz and the remaining Mediterranean areas. A secondary branch of the LIW deviates towards the Gulf of Lion running across the Tyrrhenian Sea. The path of this secondary branch explains the affinity between the Gulf of Lion and the Central Mediterranean area. The hydrodynamics of the Tyrrhenian Sea also supports the distinctive deep fauna recorded from this area, since the LIW breaks into smaller branches that run across Corsica and the Algerian basin due to the presence of the cyclonic South Western Tyrrhenian Gyre (SWTG). Most of the deep sponge species cited from the Tyrrhenian Sea were located where the SWTG occurs, meaning that they are located out of the main LIW pathway (Chapter 4). Why the areas of Balearic Sea, Corse and Ligurian slopes remained as a separate cluster from the rest of the Mediterranean areas is unclear. Pinardi et al (2015) noted some circulation structures like the Eastern Corsica Current, which turns cyclonically at the Northwestern Mediterranean, and the Western Corsica Current, that flows across the Ligurian Sea, which could connect the deep sponge faunas of these areas.

This study confirms that the LIW has a role on the export of the deep sponge fauna from the Eastern to the Western Mediterranean, while in Chapter 4 the MOW was observed to have a crucial role in exporting bathyal sponge fauna from the Western Mediterranean into the North Atlantic. The present study shows that the distribution pattern of the deep sponge fauna across the Mediterranean is influenced by the main contributor to the MOW, which is the LIW. Therefore, it can be considered that the LIW has an indirect effect on the transfer of species to the Atlantic Ocean.

This pattern illustrates the effect that the MOW has in transporting components of the Mediterranean deep-sea sponge communities towards the bathyal communities of the Gulf of Cádiz.

The fact that the Strait of Sicily hosted about 50% of the species that co-occur in both the Eastern and Western Mediterranean evidences its role as a connecting area between the two basins. The number of species only occurring in the Western Mediterranean is fairly higher than that of the Eastern Mediterranean (105 and 31 respectively). This is, in part, because the

deep-water benthic communities of the Eastern basin remain poorly explored. However, these results are also consistent with the general trend of the Western Mediterranean fauna displaying higher values of species richness (Coll et al., 2010; Danovaro et al., 2010) as has been proved for coastal sponges, reported to show a Northwest to Southeast richness gradient (Pansini & Longo, 2003; Voultsiadou, 2009; Xavier & Van Soest, 2012). While deep sponges from Western and Central Mediterranean areas have been intensely studied, sampling at the Strait of Sicily remains still scarce (Topsent, 1928; Zibrowius & Taviani, 2005; Calcinai et al., 2013) and that of the Eastern Mediterranean remains even scarcer (Pansini & Longo, 2003; Voultsiadou, 2005). Therefore, the current bias on the sampling effort of bathyal sponges across the Mediterranean is impacting negatively on the assessment of the relationships of deep sponge fauna of the eastern basins.

This study provides data on sponges inhabiting the Maltese Islands, being all but 3 of the reported species found below 200 m depth (Tables 1, 2). The material collected by ROV resulted in 23 different species identified, of which two are new records for the Mediterranean Sea (*Pachastrella ovisternata* and *Higginsia thielei*). Previously to this study, 40 deep sponge species were known from the Strait of Sicily, having been increased to 51, implying a 27% increase. The taxonomic results reinforce the conclusions of previous studies, confirming that the deep-water benthic communities of the Maltese Islands are faunistically rich and ecologically relevant area (Freiwald et al., 2009; Evans et al., 2016; Knittweis et al., 2016; Prampolini et al., 2018; Knittweis et al., 2019).

The Mediterranean is under intense pressure from a variety of human activities (Di Lorenzo et al., 2018). More importantly, the Strait of Sicily is the most important traffic lane for oil tankers towards the Black Sea, Suez and Gibraltar (Patruno, 2008), there is an increasing demand for oil drilling and mining (Velaoras et al., 2020) and an important part of the local community relays on fishing activity (Di Lorenzo et al., 2018). Some cold-water coral communities around the Maltese Islands have already been reported to become partially damaged by fishing activities and marine litter (Freiwald et al., 2009; Deidun et al., 2015). At the present, the knowledge of the natural resources of the deep Mediterranean ecosystems is imprecise; therefore, the best proxy for ecosystem services is represented by ecosystem-based marine spatial planning and identification of biodiversity (Manea et al., 2020).

The present study improves knowledge on both sponge diversity and spatial distribution of deep Mediterranean sponges, and on the scarcely known deep bottoms surrounding the Maltese Islands. It all shows that sponges can provide a suitable tool for tracing faunal shifts across basins, which might include ecological deep-sea invasions and other negative effects resulting from the increasing anthropogenic alterations. Thus, there is an urgent need for further research on the deep benthic communities from not only Malta but the entire Eastern Mediterranean, in order to obtain an accurate understanding of their composition and biogeographical relationships. These aspects may result critical in understanding the origin and evolution of the deep Mediterranean fauna, also to assess the current level of preservation and to trace future management plans.

References

Aguilar, R., López Correa, M., Calcinai, B., Pastor, X. and García, S. (2011) First records of Asbestopluma hypogea Vacelet and Boury-Esnault, 1996 (Porifera, Demospongiae Cladorhizidae) on seamounts and in bathyal settings of the Mediterranean Sea. *Zootaxa*, 2925, 33-40.

Arnesen, E. (1920) Spongia. *Report on the Scientific Results of the "Michael Sars" North Atlantic Deep-Sea Expedition, 1910*. 3(2), 1-29.

Astraldi, M., Gasparini, G. P., Sparnocchia, S., Moretti, M. and Sansone, E. (1996) The characteristics of the water masses and the water transport in the Sicily Strait at long time scales. In: F. Briand (Ed), *Dynamics of Mediterranean Straits and Channels,* CIESM Science Series, Monaco, 2, 95-115.

Astraldi, M., Gasparini, G. P., Vetrano, A. and Vignudelli, S. (2002) Hydrographic characteristics and interannual variability of water masses in the central Mediterranean: a sensitivity test for long-term changes in the Mediterranean Sea. *Deep Sea Research Part I: Oceanographic Research Papers*, 49(4), 661-680.

Baringer, M. O. and Price, J. F. (1999) A review of the physical oceanography of the Mediterranean outflow. *Marine Geology*, 155, 63-82.

Ben Mustapha, K. and Vacelet, J. (1991) État actuel des fonds spongiferes de Tunisie. In: C. F. Boudouresque, M. Avon and V. Gravez (Eds), *Les Espèces Marines à Protéger en Méditerranée. GIS Posidonie*, Marseille, 43-46.

Ben Mustapha, K., Zarrouk, S., Souissi, A. and El Abed, A. (2003) Diversité des Démosponges Tunisiennes. *Bulletin Institut national des Sciences et Technologies de la mer de Salammbô*, 30, 55-78.

Bianchi, C. N. and Morri, C. (2000) Marine Biodiversity of the Mediterranean Sea: Situation, Problems and Prospects for Future Research. *Marine Pollution Bulletin*, 40(5), 367-376.

Borg, J. A., Rowden, A. A., Attrill, M. J., Schembri, P. J. and Jones, M. B. (2009) Occurrence and distribution of different bed types of seagrass *Posidonia oceanica* around the Maltese Islands. *Mediterranean Marine Science*, 10(2), 45-62.

Borg, J. A. and Schembri, P. (1996) Preliminary data on the occurrence and distribution of shallow water marine sponges (Porifera) around Maltese coasts. *Xjenza*, 1(1), 24-28.

Boury-Esnault, N., Pansini, M. and Uriz, M. J. (1994) Spongiaires bathyaux de la mer d'Alboran et du golfe ibéro-marocain. *Mémoires du Muséum National d'Histoire Naturelle*, 160, 1-174.

Boury-Esnault, N. and Rützler, K. (1997) Thesaurus of sponge morphology. *Smithsonian Contributions to Zoology*, 596, 1-55.

Boury-Esnault, N., Vacelet, J., Dubois, M., Goujard, A., Fourt, M., Pérez, T. and Chevaldonné, P. (2017) New hexactinellid sponges from deep Mediterranean canyons. *Zootaxa*, 4236, 118-134.

Bryden, H. L. and Stommel, H. M. (1984) Limiting processes that determine basic features of the circulation in the Mediterranean Sea. *Oceanologica Acta*, 7(3), 289-296.

Calcinai, B., Moratti, V., Martinelli, M., Bavestrello, G. and Taviani, M. (2013) Uncommon sponges associated with deep coral bank and maerl habitats in the Strait of Sicily (Mediterranean Sea). *Italian Journal of Zoology*, 80(3), 412-423.

Carter, H. J. (1876) Descriptions and figures of deep-sea sponges and their spicules, from the Atlantic Ocean, dredged up on board H.M.S.

"Porcupine", chiefly in 1869 (concluded). *Annals and Magazine of Natural History*, 4(18), 225-479.

Chevaldonné, P., Pérez, T., Crouzet, J.-M., Bay-Nouailhat, W., Bay-Nouailhat, A., Fourt, M., Almón, B., Pérez, J., Aguilar, R. and Vacelet, J. (2015) Unexpected records of 'deep-sea' carnivorous sponges Asbestopluma hypogea in the shallow NE Atlantic shed light on new conservation issues. *Marine Ecology*, 36(3), 475-484.

Coll, M., Piroddi, C., Steenbeek, J., Kaschner, K., Ben Rais Lasram, F., Aguzzi, J., Ballesteros, E., Bianchi, C. N., Corbera, J., Dailianis, T., Danovaro, R., Estrada, M., Froglia, C., Galil, B. S., Gasol, J. M., Gertwagen, R., Gil, J., Guilhaumon, F., Kesner-Reyes, K., Kitsos, M.-S., Koukouras, A., Lampadariou, N., Laxamana, E., López-Fé de la Cuadra, C. M., Lotze, H. K., Martin, D., Mouillot, D., Oro, D., Raicevich, S., Rius-Barile, J., Saiz-Salinas, J. I., San Vicente, C., Somot, S., Templado, J., Turon, X., Vafidis, D., Villanueva, R. and Voultsiadou, E. (2010) The biodiversity of the Mediterranean Sea: Estimates, patterns, and threats. *PLoS One*, 5(8), e11842.

Danovaro, R., Company, J. B., Corinaldesi, C., D'Onghia, G., Galil, B., Gambi, C., Gooday, A. J., Lampadariou, N., Luna, G. M., Morigi, C., Olu, K., Polymenakou, P., Ramirez-Llodra, E., Sabbatini, A., Sardà, F., Sibuet, M. and Tselepides, A. (2010) Deep-Sea Biodiversity in the Mediterranean Sea: The Known, the Unknown, and the Unknowable. *PLoS One*, 5(8), e11832.

Deidun, A., Andaloro, F., Bavestrello, G., Canese, S., Consoli, P., Micallef, A., Romeo, T. and Bo, M. (2015) First characterisation of a Leiopathes glaberrima (Cnidaria: Anthozoa: Antipatharia) forest in Maltese exploited fishing grounds. *Italian Journal of Zoology*, 82(2), 271-280.

Deidun, A., Tsounis, G., Balzan, F. and Micallef, A. (2010) Records of black coral (Antipatharia) and red coral (Corallium rubrum) fishing activities in the Maltese Islands. *Marine Biodiversity Records*, 3, E90.

Di Lorenzo, M., Sinerchia, M. and Colloca, F. (2018) The North sector of the Strait of Sicily: a priority area for conservation in the Mediterranean Sea. *Hydrobiologia*, 821(1), 235-253.

Díaz del Río, V., Bruque, G., Fernández-Salas, L. M., Rueda, J. L., González, E., López, N., Palomino, D., López, F. J., Farias, C., Sánchez, R.,

Vázquez, J. T., Rittierott, C. C., Fernández, A., Marina, P., Luque, V., Oporto, T., Sánchez, O., García, M., Urra, J., Bárcenas, P., Jiménez, M. P., Sagarminaga, R. and Arcos, J. M. Volcanes de fango del golfo de Cádiz, Proyecto LIFE + INDEMARES. Fundación Biodiversidad del Ministerio de Agricultura, Alimentación y Medio Ambiente. (2014).

El-Geziry, T. M. and Bryden, I. G. (2010) The circulation pattern in the Mediterranean Sea: issues for modeller consideration. *Journal of Operational Oceanography*, 3(2), 39-46.

Evans, J., Aguilar, R., Alvarez, H., Borg, J. A., Garcia, S., Knittweis, L. and Schembri, P. J. Recent evidence that the deep sea around Malta is a biodiversity hotspot. Rapport du Congrès de la Commission Internationale pour l'Exploration Scientifique de la Mer Méditerranée Volume 41. Monaco: *La Commission Internationale pour l'Exploration Scientifique de la Mer Méditerranée*.

Ferrer Hernández, F. (1914) Esponjas del Cantábrico. Parte 2ª. III. Myxospongida. IV. Tetraxonida. V. Triaxonida. *Trabajos del Museo Nacional de Ciencias Naturales, Serie Zoologica*, 27, 1-52.

Freiwald, A., Beuck, L., Rueggeberg, A., Taviani, M. and Hebbeln, D. (2009) The White Coral Community in the Central Mediterranean Sea Revealed by ROV Surveys. *Oceanography*, 22(1), 58-74.

Gasser, M., Pelegrí, J. L., Emelianov, M., Bruno, M., Gracia, E., Pastor, M., Peters, H., Rodríguez-Santana, A., Salvador, J. and Sánchez-Leal, R. F. (2017) Tracking the Mediterranean outflow in the Gulf of Cadiz. *Progress in Oceanography*, 157, 47-71.

Ilan, M., Ben-Eliahu, M. N. and Galil, B. S. (1994) Three deep water sponges from the eastern Mediterranean and their associated fauna. *Ophelia*, 39(1), 45-54.

Ilan, M., Gugel, J., Galil, B. S. and Janussen, D. (2003) Small bathyal sponge species from east Mediterranean revealed by a non-regular soft bottom sampling technique. *Ophelia*, 57(3), 145-160.

Knittweis, L., Aguilar, R., Alvarez, H., Borg, J. A., Evans, J., Garcia, S. and Schembri, P. J. (2016) New depth record of the precious red coral *Corallium rubrum* for the Mediterranean. Rapport du Congrès de la Commission Internationale pour l'Exploration Scientifique de la Mer

Méditerranée, Monaco: *La Commission Internationale pour l'Exploration Scientifique de la Mer Méditerranée*. 41, 467.

Knittweis, L., Evans, J., Aguilar, R., Álvarez, H., Borg, J. A., García, S. and Schembri, P. (2019) Recent Discoveries of Extensive Cold-Water Coral Assemblages in Maltese Waters. In: C. Orejas and C. Jiménez (Eds), *Mediterranean Cold-Water Corals: Past, Present and Future*. Springer International Publishing AG, Switzerland, 253-255.

Lascaratos, A., Williams, R. G. and Tragou, E. (1993) A mixed-layer study of the formation of Levantine intermediate water. *Journal of Geophysical Research: Oceans*, 98(C8), 14739-14749.

Lendenfeld, R. von. (1894) Eine neue Pachastrella. Sitzungsberichte der Kaiserlichen Akademie der Wissenschaften. *Mathematisch-Naturwissenschaftliche Classe*, 103(1), 439-442.

Lujan, M., Crespo-Blanc, A. and Comas, M. (2011) Morphology and structure of the Camarinal Sill from high-resolution bathymetry: evidence of fault zones in the Gibraltar Strait. *Geo-Marine Letters*, 31(3), 163-174.

Malanotte-Rizzoli, P. (2001) Current Systems in the Mediterranean Sea. In: J. H. Steele (Ed), *Encyclopedia of Ocean Sciences* (Second Edition). Academic Press, Oxford, 744-751.

Maldonado, M. (1992) Demosponges of the red coral bottoms from the Alboran Sea. *Journal of Natural History*, 26, 1131-1161.

Maldonado, M. (1993a). Demosponjas litorales de Alborán. Faunística y Biogeografía. (Philosophical Dissertation). University of Barcelona, Barcelona.

Maldonado, M. (1993b) The taxonomic significance of the short-shafted mesotriaene reviewed by parsimony analysis: validation of Pachastrella ovisternata Von Ledenfeld (Demospongiae: Astrophorida). *Bijdragen tot de Dierkunde*, 63(3), 129-148.

Maldonado, M. and Benito, J. (1991) Crambe tuberosa n. sp. (Demospongiae, Poecilosclerida): a new Mediterranean poecilosclerid with lithistid affinities. *Cahiers de Biologie Marine*, 32, 323-332.

Maldonado, M. and Uriz, J. M. (1995) Biotic affinities in a transitional zone between the Atlantic and the Mediterranean: a biogeographical approach based on sponges. *Journal of Biogeography*, 22, 89-110.

Manea, E., Bianchelli, S., Fanelli, E., Danovaro, R. and Gissi, E. (2020) Towards an Ecosystem-Based Marine Spatial Planning in the deep Mediterranean Sea. *Science of the Total Environment*, 715, 136884.

Millot, C. and Taupier-Letage, I. (2005) Circulation in the Mediterranean Sea. In: A. Saliot (Ed), *The Mediterranean Sea. Handbook of Environmental Chemistry*. Springer, Berlin, Heidelberg, 5K, 29-66.

Pansini, M. (1987) Littoral demosponges from the banks of the straits of Sicily and the Alboran Sea. In: J. Vacelet and N. Boury-Esnault (Eds), *Taxonomy of Porifera*, G13. Springer-Verlag, Berlin, Heidelberg, 149-186.

Pansini, M. and Longo, C. (2003) A review of the Mediterranean Sea sponge biogeography with, in appendix, a list of the demosponges hitherto recorded from this sea. *Biogeographia*, 2457-73.

Patruno, R. (2008) Prevention of marine pollution from ships in the mediterranean region: Economic, legal and technical aspects. *Geografia Fisica e Dinamica Quaternaria*, 31(2), 211-214.

Pinardi, N., Zavatarelli, M., Adani, M., Coppini, G., Fratianni, C., Oddo, P., Simoncelli, S., Tonani, M., Lyubartsev, V., Dobricic, S. and Bonaduce, A. (2015) Mediterranean Sea large-scale low-frequency ocean variability and water mass formation rates from 1987 to 2007: A retrospective analysis. *Progress in Oceanography*, 132, 318-332.

Prampolini, M., Blondel, P., Foglini, F. and Madricardo, F. (2018) Habitat mapping of the Maltese continental shelf using acoustic textures and bathymetric analyses. *Estuarine, Coastal and Shelf Science*, 207, 483-498.

Ríos, P., Cristobo, J. and Sánchez, F. (2017) Porifera del cañón de la Gaviera (sistema de cañones de Avilés, mar Cantábrico). In: J. Cristobo and P. Ríos (Eds), *Avances en estudios de biología marina: contribuciones del XVIII SIEBM GIJÓN. Temas de Oceanografía*. Instituto Español de Oceanografía, Ministerio de Economía, Industria y Competitividad, Madrid, 10, 123-133.

Robinson, A. R., Leslie, W., Theocharis, A. and Lascaratos, A. (2001) *Mediterranean Sea Circulation.* In: J. H. Steele (Ed), *Encyclopedia of Ocean Sciences,* Academic Press, London, 1689-1705.

Rosell, D. and Uriz, M. J. (2002) Excavating and endolithic sponge species (Porifera) from the Mediterranean: species descriptions and identification key. Organisms, *Diversity and Evolution*, 2(1), 55-86.

Rützler, K. (1973) Clionid Sponges from the coast of Tunisia. Bulletin de l'Institut National *Scientifique et Technique d'Océanographie et de Pêche de Salammbô*, 2(4), 633-637.

Rützler, K. (1976) Ecology of Tunisian commercial Sponges. *Téthys*, 7(2-3), 249-264.

Sánchez-Leal, R. F., Bellanco, M. J., Fernández-Salas, L. M., García-Lafuente, J., Gasser-Rubinat, M., González-Pola, C., Hernández-Molina, F. J., Pelegrí, J. L., Peliz, A., Relvas, P., Roque, D., Ruiz-Villarreal, M., Sammartino, S. and Sánchez-Garrido, J. C. (2017) The Mediterranean Overflow in the Gulf of Cadiz: A rugged journey. *Science Advances*, 3(11), 11.

Schroeder, K., Lafuente, J., Josey, S., Artale, V., Buongiorno Nardelli, B., Gacic, M., Gasparini, G. P., Herrmann, M., Lionello, P., Ludwig, W., Millot, C., Özsoy, E., Pisacane, G., Sánchez-Garrido, J., Sannino, G., Santoleri, R., Somot, S., Struglia, M., Stanev, E. and Zodiatis, G. (2012) Circulation of the Mediterranean Sea and its variability. In: P. Lionello (Ed), *The Mediterranean climate: from past to future*. Elsevier, Amsterdam, 187-256.

Schulze, M. F. E. (1887) Report on the Hexactinellida collected by H.M.S. "Challenger" during the years 1873-1876. *Report of the Scientific Results of the Voyage of H.M.S. "Challenger" 1873-76, Zoology*, 211-513.

Sciberras, M., Rizzo, M., Mifsud, J. R., Camilleri, K., Borg, J. A., Lanfranco, E. and Schembri, P. J. (2009) Habitat structure and biological characteristics of a maerl bed off the northeastern coast of the Maltese Islands (central Mediterranean). *Marine Biodiversity*, 39(4), 251-264.

Sitjà, C., Maldonado, M., Farias, C. and Rueda, J. L. (2019) Deep-water sponge fauna from the mud volcanoes of the Gulf of Cadiz (North Atlantic, Spain). *Journal of the Marine Biological Association of the United Kingdom*, 99(4), 807-831.

Sollas, W. J. (1888) Report on the Tetractinellida collected by H.M.S. Challenger during the years 1873-76. *Report of the Scientific Results of the Voyage of H.M.S. Challenger 1873-76*, 25(part 63), 1-458.

Stephens, J. (1920) Sponges of the coast of Ireland. II. The tetraxonida. (concluded). Scientific Investigations. *Fisheries Branch, Department of Agriculture for Ireland*, 21-75.

Templado, J., Calvo, M., Moreno, D., Flores, A., Conde, F., Abad, R., Rubio, J., López-Fé, C. M. and Ortiz, M. (2006) Flora y fauna de la reserva marina y reserva de pesca de la isla de Alborán. Secretaría General de Pesca Marítima, MAPA, Madrid.

Templado, J., García-Carrascosa, M., Baratech, L., Capaccioni, R., Juan, A., López-Ibor, A., Silvestre, R. and Massó, C. (1986) Estudio preliminar de la fauna asociada a los fondos coralígenos del mar de Alborán (SE de España). *Boletín del Instituto Español de Oceanografía*, 3(4), 93-104.

Thomson, C. W. (1873) *The depths of the sea*. Macmillan and Co., London. 527 pp.

Topsent, E. (1895) Campagnes du Yacht "Princesse Alice". Notice sur les spongiaires recueillis en 1894 et 1895. *Bulletin de la Société Zoologique de France*, 20, 213-216.

Topsent, E. (1898) Eponges nouvelles des Açores. (Première série). *Mémoires de la Société Zoologique de France*, 11, 225-255.

Topsent, E. (1904) Spongiaires des Açores. *Résultats des Campagnes Scientifiques accomplies par le Prince Albert I.* Monaco, 25, 1-279.

Topsent, E. (1928) Spongiaires de l'Atlantique et de la Méditerranée, provenant des croisières de Prince Albert I de Monaco. *Résultats des Campagnes Scientifiques accomplies par le Prince Albert I.* Monaco, 74, 1-376.

Topsent, E. (1934) Eponges observées dans les parages de Monaco. Première Partie. *Bulletin de l'Institut Océanographique de Monaco*, 650, 1-42.

Vacelet, J. (1961) Quelques Eponges remarquables de Méditerranée. *Revue des Travaux de l'Institut des Pêches Maritimes*, 25(3), 351-354.

Vamvakas, C. E. (1970) Peuplements Benthiques des Substrats Meubles du Sud de la Mer Égée. *Téthys*, 2(1), 89-130.

Van Soest, R. M. W., Beglinger, E. J. and de Voogd, N. J. (2013) Microcionid sponges from Northwest Africa and the Macaronesian Islands (Porifera, Demospongiae, Poecilosclerida). *Zoologische mededeelingen*, 87(4), 275-404.

Van Soest, R. M. W., Beglinger, E. J. and de Voogd, N. J. (2014) Mycale species (Porifera: Poecilosclerida) of Northwest Africa and the Macaronesian Islands. *Zoölogische Mededelingen Leiden*, 88(4), 59-109.

Van Soest, R. M. W., Boury-Esnault, N., Hooper, J. N. A., Rützler, K., de Voogd, N. J., Alvarez de Glasby, B., Hajdu, E., Pisera, A., Manconi, R., Schönberg, C. H. L., Janussen, D., Tabachnick, K. R., Klautau, M., Picton, B. E., Kelly, M., Vacelet, J., Dohrmann, M. and Díaz, M. C. (2020). World Porifera database. Accessed at http://www.marinespecies.org/porifera on 24/06/2020.

Vega Fernández, T., Pace, M. L., Badalamenti, F., D'Anna, G., Fiorentino, F., Garofalo, G., Gristina, M., Knittweis, L., Mirto, M. and Pipitone, C. Application of the MESMA Framework. Case Study: Strait of Sicily. MESMA report. (2012).

Velaoras, D., Civitarese, G., Giani, M., Gogou, A., Rahav, E. and Zervoudaki, S. (2020) Revisiting the Eastern Mediterranean: Recent knowledge on the physical, biogeochemical and ecosystemic states and trends Volume II. *Deep Sea Research Part II: Topical Studies in Oceanography*, 171, 104725.

Voultsiadou, E. (2005) Demosponge distribution in the eastern Mediterranean: a NW-SE gradient. *Helgoland Marine Research*, 59(3), 237-251.

Voultsiadou, E. (2009) Reevaluating sponge diversity and distribution in the Mediterranean Sea. *Hydrobiologia*, 628, 1-12.

Xavier, J. R. and Van Soest, R. W. M. (2012) Diversity patterns and zoogeography of the Northeast Atlantic and Mediterranean shallow-water sponge fauna. *Hydrobiologia*, 687(1), 107-125.

Zibrowius, H. and Taviani, M. (2005) Remarkable sessile fauna associated with deep coral and other calcareous substrates in the Strait of Sicily, Mediterranean Sea. In: A. Freiwald and J. M. Roberts (Eds), *Cold-Water Corals and Ecosystems*. Springer Berlin Heidelberg, Berlin, 807-819.

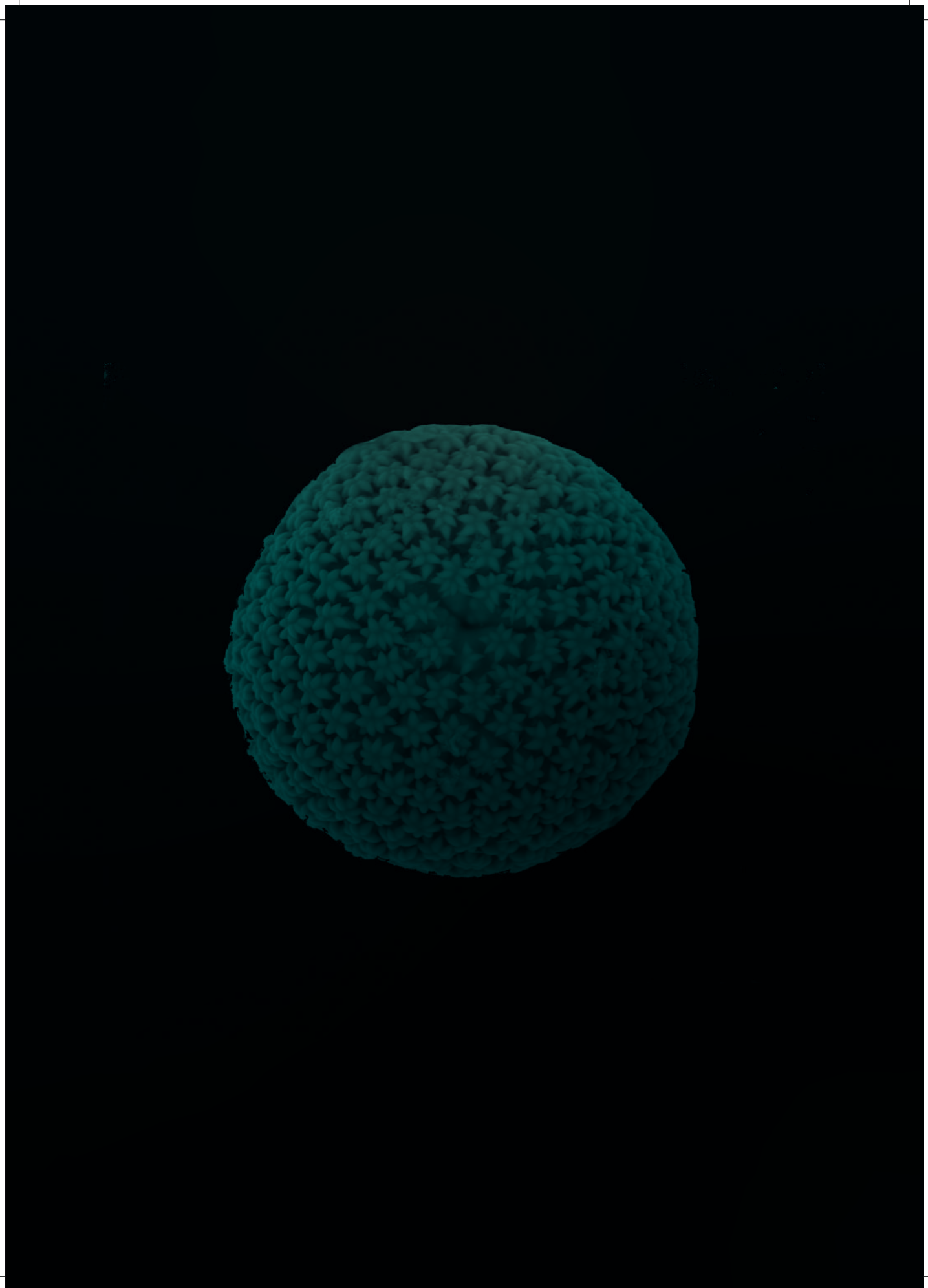

General discussion

Taxonomical contributions

The taxonomic results of this thesis have evidenced that the seabed of the mud volcanoes from the northern Gulf of Cádiz, the Alboran Island and the Maltese Islands harbour a rich deep sponge fauna that includes a variety of rare and new species to science. As part of this research, a total of 2,051 sponge individuals have been taxonomically identified: 1659 from the mud volcanoes of the Gulf of Cádiz, 351 from Alboran Island and 41 from the Maltese Islands. From this studied material, a total of 158 sponge species have been identified: 83 from the mud volcanoes of the Gulf of Cádiz, 87 from the Alboran Island and 23 from the Maltese Islands, co-occurring some of them in two or all the study areas. A total of 5 new species have been described, two from the mud volcanoes of the Gulf of Cádiz (*Jaspis sinuoxea* and *Myrmekioderma indemaresi*) and three from the Alboran Island (*Axinella alborana*, *Axinella spatula* and *Endectyon filiformis*). Additionally, 3 new records have been detected for the Atlantic Ocean (*Geodia anceps*, *Coelosphaera cryosi* and *Petrosia raphida*), and 6 for the Mediterranean Sea (*Jaspis eudermis*, *Hemiasterella elongata*, *Axinella vellerea*, *Gelliodes fayalensis*, *Higginsia thielei* and *Pachastrella ovisternata*). Summing up new species, and those found for first and second time in either the Atlantic Ocean or the Mediterranean Sea, a total of 21 rare species have been identified from the three study areas, evidencing their role as Sites of Community Importance (SCI) in favouring the preservation of the deep-water sponge fauna diversity.

In the mud volcanoes of the northern Gulf of Cádiz, the sponge fauna had been seldom studied previously to this thesis (preliminary data in Díaz del Río et al., 2014; Chevaldonné et al., 2015). Previous studies indicated the presence of 86 deep sponge species from the whole Gulf of Cádiz (Thomson, 1873; Carter, 1876; Schulze, 1887; Sollas, 1888; Topsent, 1895; Arnesen, 1920;

Topsent, 1928; Boury-Esnault et al., 1994; Van Soest et al., 2013, 2014) which were increased to 125 species after the taxonomic identifications of the sponge material from the mud volcanoes performed in the present work (Chapter 1). Therefore, this thesis has contributed with 30% of the species known to occur in the Gulf of Cádiz. Similarly, the lower shelf and upper slope of the Alboran Island remained poorly studied, while the upper shelf was already well known, with 163 sponge species recorded from the last extensive revision (Templado et al., 2006). After this thesis, the total number of sponge species known from the Alboran Island has increased to 196 (Chapter 3). The sponges from the Maltese Islands, and more generally the sponges from the Strait of Sicily, still remain at a beginning stage of knowledge (Calcinai et al., 2013). Previously to this thesis, 40 different deep-water sponge species were known from the Strait of Sicily (Topsent, 1928; Vacelet, 1960; Zibrowius & Taviani, 2005; Aguilar et al., 2011; Bo et al., 2012; Calcinai et al., 2013; Taviani et al., 2017; Bertolino et al., 2019). After the taxonomic study of the sponges collected from the Maltese Islands (Chapter 5), the number of deep-water sponge species recorded from the Strait of Sicily has increased to 51.

Some of the studied species represent endemisms from the Gulf of Cádiz, which have been abundantly collected, like *Haliclona bouryesnaultae* (formerly named *H. pedunculata*), and from the Alboran Island, like *Axinella alborana* and *Axinella spatula*. The occurrence of such rarities highlights the importance of these SCI for the preservation of the deep-sea biodiversity. Future management plans in the area should include specific actions and statements for the protection of the populations of these rare species. These are endemisms abundantly found in their respective study areas, for which their inclusion in the annex II of the Habitats directive of the Natura 2000 Network should be considered. *Axinella vellerea*, previously known only from Azores, was abundantly collected from both the mud volcanoes of the northern Gulf of Cádiz and the Alboran Island, which makes these two transitional areas crucial for inter-population connectivity of these rare species.

While it was logistically unfeasible to perform phylogenetic analyses of all the relevant specimens studied in this work, 18S rDNA, 28S rDNA and cytochrome c oxidase I (*COI*) sequences were phylogenetically analysed from a small set of taxonomically relevant sponge species collected from the mud

volcanoes of the Gulf of Cádiz, with the objective of showing how the incorporation of molecular tools can help synergistically more traditional taxonomic approaches (Chapter 2). The analyses revealed that some of the sequenced specimens were rare not only for their scarcity but also for their taxonomic characteristics. The phenetic discrepancies observed in Chapters 1 and 2 were also reflected in the phylogenetic trees (Chapter 2). The species analysed (S*uberites hirsutus*, *Geodia* cf. *spherastrella*, *Petrosia raphida* and *Haliclona bouryesnaultae*) showed a distribution in their respective trees mostly inconsistent with their current taxonomic status. However, low to moderate support of the clades prevented from any conclusive assumptions. For this reason, these results are considered as preliminary, and should be understood as a first approximation to the actual characterization of such singular species. Likewise, they evidence a need for further sequencing to conduct phylogenetic analysis with better resolution. Even if phylogeny represents a minor part of this thesis, it has provided 11 new sequences, contributing to further studies of sponge phylogenetic relationships, which are expected to change as new descriptions and sequencing of new species, use of new datasets and improvements in phylogenetic reconstruction methods appear (Cárdenas et al., 2012; Morrow & Cárdenas, 2015). Likewise, high resolution taxonomic techniques such as environmental DNA metabarcoding can be applied to ecosystem biodiversity assessment and biomonitoring (Baird & Hajibabaei, 2012; Bohmann et al., 2014), representing a useful tool for uneasily accessible areas like the deep-sea. To perform these type of analyses in the deep-sea, exhaustive sequence databases are required from tractable samples from across the world (Mariani et al., 2019). For this reason, sequences like the ones obtained in the present study can favour the elaboration of databases of deep-sea species.

Understanding local deep-water sponge assemblages and their conservation needs

After an initial taxonomic characterization of the sponges living in the studied deep-water assemblages, a remaining obvious question is how abundant those deep-sea species are and which is their basic ecology/biology. A previous study on the deep sponges from the Gulf of Cádiz (Boury-Esnault et al., 1994) revealed a high sponge biomass mainly due to three abundant species:

Pheronema carpenteri, *Thenea muricata* and *Phakellia hirondellei*. In the mud volcanoes, the first two have been also frequently found, together with *Petrossia crassa* (Chapter 4). The distribution of the sponges across the mud volcanoes of the northern Gulf of Cádiz emerged as being related to a variety of seafloor and environmental variables, such as depth, sediment and substrate types. This is consistent with studies on other benthic groups from the mud volcanoes of the northern Gulf of Cádiz, revealing that their differential benthic fauna is favoured by the variety of bottom types and habitats co-ocurring in this area (Rueda et al., 2012; Palomino et al., 2016; González-García et al., 2020). Del Río et al. (2014) already described different habitats to which a majorly predominant sponge species was associated. For instance, *Asconema setubalense* was typical from the habitat "Submarine structures made by leaking gases", where abundant methane-derived authigenic carbonates can be found, while *Thenea muricata* was characteristic from the bathyal muds where bottom trawling generally occurs. The results of this thesis revealed that depth and the abundance/scarcity of methane-derived authigenic carbonates are the main variables that influence the distribution of sponges across the field of mud volcanoes in the northern Gulf of Cádiz. Being bottom fishing a common activity in this area, it was also assessed as a possible anthropogenic factor that could have an impact on the sponge distribution. Although the graphic analyses suggested a trend for some effects, no statistically significant results were obtained indeed. Our approach in this sense should be understood as a mere initial approach to the issue that will require a more sophisticated experimental design and higher deep-sea technology to capture the real levels of impact. The most common fishing techniques used in this SCI are bottom trawling and bottom longlining, both of which can impact the sea bed and its benthic fauna (Delgado et al., 2013; Díaz del Río et al., 2014; González-García et al., 2020) and they have already been demonstrated to impact on deep-sponge grounds (Kenchington et al., 2019; Pham et al., 2019). Given that the mud volcanoes of the northern Gulf of Cádiz harbour a diverse deep sponge fauna, with rare and endemic species, bottom-trawling pressure is advised to be further evaluated, including other benthic groups, to provide a solid base for the management of this area.

The explorations of the shelf of the Alboran Island (Chapter 3) were performed through a combination of bottom trawling devices (e.g., beam trawl and benthic dredge) and ROV dives, but no environmental variables

could be obtained to contrast them with the sponge assemblages examined. Structurally complex bottoms are known to host diverse sponge fauna (Ramos-Esplá & Luque, 2004; Santín et al., 2018; Wilborn et al., 2018). This was clearly exemplified by the deep shelf of Alboran Island, where sponges were similarly abundant in habitats as different as rhodolith beds, rocky plains moderately sloping and on isolated rocky outcrops surrounded by soft sediments. On the rocky plains some peculiar aggregations of erect sponges resembled "sponge gardens". Unlike the typically known sponge grounds (Hogg et al., 2010; Maldonado et al., 2017), these sponge aggregations were characterized by diverse and abundant erect small sponge species growing around other larger astrophorid and axinellid sponges. Such a mixed composition had been observed neither in the real sponge grounds from Amendolara Bank and Bari Canyon in the Adriatic Sea (Bo et al., 2012), nor in other sponge assemblages like those associated to the cold coral banks off Santa Maria di Leuca in the Ionian Sea (Longo et al., 2005; Mastrototaro et al., 2010; Vertino et al., 2010). Given their singularity and composition, with rare sponges such as *Axinella alborana* and *Axinella vellerea*, these aggregations should be considered in further protection actions and better studied to assess whether they can be considered as actual sponge grounds (Hogg et al., 2010).

While the habitat mapping of the shelf of Malta is well known (Prampolini et al., 2018), the upper slope bottoms deeper than 260 m and the fauna inhabiting them remain poorly explored (Evans et al., 2016), as is generally the case for other areas (e.g., Alboran Island). Calcinai (2013) studied the sponge fauna associated to the deep cold water coral communities of Malta advancing that further studies would be necessary to provide a more comprehensive understanding of the sponge fauna inhabiting this type of habitat. The present work improves knowledge on the deep sponge fauna of the Maltese Islands (Chapter 5), confirming that sponges are a relevant part of the benthos and that further exploration is likely to retrieve more remarkable findings. The diversity of sponge species described in the present study reinforces previous works that confirm the ecological relevance of the surrounding bathyal waters of the Maltese Islands, mainly focused in cold-water corals (Freiwald et al., 2009; Evans et al., 2016; Knittweis et al., 2016; Prampolini et al., 2018; Knittweis et al., 2019). The Strait of Sicily is under many anthropogenic pressures, including, among others, fishery, deployment of pipes and cables for gas water transport, communication, and renewable

energy (e.g., wind turbines). Also transport is to be added to the list, since the Strait of Sicily is the most important traffic lane for crude oil crossing the Mediterranean (Patruno, 2008; Di Lorenzo et al., 2018; Velaoras et al., 2020). The LIFE BaHAR Project achieved the designation of five different bathyal SCI around the Maltese Islands, being now necessary management plans that help on the preservation of these sites. Sponges have already been reported associated to cold-water corals in Malta (Calcinai et al., 2013) and it is likely that they are also present in the other such-like communities already reported from these Islands. Further assessment of the bathyal sponges from the Maltese Islands is expected to provide a better understanding of their deep benthic communities, providing new tools for their preservation.

Sponges as deep-sea biogeographical tools

The analyses performed for the study of the affinities of the deep-water sponges from different areas across the environmental gradient running from the bathyal bottom of the eastern Mediterranean to those of the Northeastern Atlantic indicate that a bathyal connection can be retraced.

The pattern of faunal affinities suggested that the distribution of the deep sponge species in the Mediterranean is largely determined by the trajectory of the Levantine Intermediate Water (LIW) (Chapter 5). The assessment of the relationships of the deep-water sponge fauna of the eastern basin is negatively impacted by a bias on the sampling effort. This is due to the fact that deep-water sponges from Western and Central Mediterranean have been intensely studied, while sampling at the Strait of Sicily remains still scarce (Topsent, 1928; Zibrowius & Taviani, 2005; Calcinai et al., 2013) and that of the Eastern Mediterranean remains even scarcer (Pansini & Longo, 2003; Voultsiadou, 2005). The Strait of Sicily hosted about 50% of the species that co-occur in both the Eastern and Western Mediterranean, evidencing its role as a connecting area between these two basins.

An effect of the Mediterranean Outflow Water (MOW) on the distribution of the deep sponge species from the Gulf of Cádiz was also evidenced (Chapter 4). A previous study (Boury-Esnault et al., 1994) already detected that the bathyal sponges from the Alboran Sea were similar to the nearby Atlantic ones. The same study found no relationship between the sponge composition of the Gulf of Cádiz and the origin of the water masses.

However, sampling efforts for each side of the Strait of Gibraltar were uneven in that study, while more data are available in the present work. The fact that weak sponge faunal affinities were observed between the Gulf of Cádiz and the rest of the Atlantic areas analysed, suggests that the exported Mediterranean fauna is restricted to the Gulf of Cádiz. The reasons of this spatial constraint remain uncertain from the scope of our study. However, this pattern of affinities suggests that the exported Mediterranean sponges may require the presence of the MOW to survive, since it seems that once exported to the Gulf of Cádiz they cannot spread easily towards additional Northeastern Atlantic areas (e.g., Azores). It is also possible that the North-Atlantic trajectory of the MOW, which turns North after passing the Strait of Gibraltar and stays attached to the Lusitanian slope, is hindering the colonization of the slopes of the Macaronesia (i.e., Azores, Morocco, Canary Islands, Madeira Islands and Cape Verde). This contrasts with the large knowledge available on the role of the Atlantic Surface Water current to transport water masses and larvae of shelf and some bathyal species from the Gulf of Cádiz to the Alboran Sea. This results on the presence of typical Atlantic fauna, including species of subtropical affinity, on some shallow and deep areas of the Alboran Sea (García Raso et al., 2010; Gofas et al., 2011; Gofas et al., 2014; Gallardo-Roldan et al., 2015; Ordines et al., 2019).

Also, our analyses were based on qualitative data, reflecting the mere occurrence of deep-sea species across areas but disregarding the effects of their comparative abundances. The use of qualitative data, which are less conclusive that the quantitative approaches, was compelled by the lack of information associated in this regard to the 461 species making the "species x area" matrix to be analysed. This means that the results of the biogeographical analyses have to be interpreted cautiously and that future approaches based on quantitative assessments can increase the resolution when determining the intensity of the relationships across the areas considered in this study

In this thesis, emphasis has been made on improving the faunal information for three areas of strategic location, being transition zones along the trajectory of the deep mases of Mediterranean water towards the North Atlantic. The better faunal characterization allowed to make evident that the LIW acts as an exporting mechanism for deep-water sponge fauna (and probably also other benthic and demersal invertebrates) from the Eastern to the Western Mediterranean, indirectly affecting the transports of deep-water

sponge fauna favoured by the MOW from the Western Mediterranean to the Gulf of Cádiz, in the Atlantic Ocean.

In a short term, major shifts are expected in the distribution of marine species driven by temperature rises in the Mediterranean and the North Atlantic (Poloczanska et al., 2013; Cramer et al., 2018). This contribution to the knowledge of the Mediterranean and North-Atlantic distribution patterns of the deep-sea sponge fauna provides a case study that may help to predict and/or interpret future transfers of non-indigenous bathyal benthic species in the Mediterranean and Northeastern Atlantic related to the MOW and the LIW.

Increasing the knowledge on the composition and distribution of deep-sea benthic organisms is of paramount importance, especially if they are habitat-forming or rare species to be taken into account for management of deep-seea biodiversity and conservation areas (Maldonado et al., 2017; Kenchington et al., 2019; Pham et al., 2019). By improving the information on biodiversity and connectivity, this study intends to be of help in the development of management plans for future Special Areas of Conservation (SAC) in deep sea.

Conclusions

Conclusions

1. The mud volcanoes of the Gulf of Cádiz, and the deep shelf and upper slope of the Alboran and Maltese Islands, host a variety of rare deep-water sponge species, including 5 new species to science, 6 new records for the Mediterranean Sea and 3 for the Atlantic Ocean.

2. The deep-water sponge fauna from the Maltese Islands remains poorly studied, as that of the easternmost Mediterranean, in general. This thesis provides 23 species identifications from this area, suggesting the sponge fauna as a common component of its deep-sea benthos. Our results suggest the bathyal bottoms to the South of the Strait of Sicily as key areas for further biogeographic studies.

3. In the Alboran Island, 87 circalittoral and bathyal sponges were identified, being especially abundant on rhodolith beds, rocky plains moderately sloping and on isolated rocky outcrops surrounded by soft sediments, where small erect sponges occurred in aggregations resembling sponge gardens.

4. A total of 83 bathyal sponge species were identified from the mud volcanoes of the Gulf of Cádiz, where water depth and presence of authigenic carbonates were the most relevant factors affecting both the composition and the abundance of the sponge fauna.

5. Mud volcanoes with abundant authigenic carbonates showed either high sponge abundances, like Gazul with aggregations of *Petrosia crassa*, or relatively high species richness like Hesperides. When soft bottoms were predominant, sponge abundances and species richness generally decreased (i.e., Anastasya, Tarsis), except for Aveiro mud volcano, which hosted aggregations of *Thenea muricata*. Those volcanoes with relatively balanced proportions of hard and soft

bottoms (Pipoca, Chica, Almazan), generally showed the highest values of both sponge abundance and species richness.

6. Phylogenetic analyses of some rare species collected from the mud volcanoes of the Gulf of Cádiz have shown that species such as *Suberites hirsutus, Cladocroce spathiformis* and *Cladocroce fibrosa* are uncertainly assigned to their respective genera, remaining in need for further analyses.

7. Our faunal analyses indicate that the Mediterranean Outflow water favours the transfer of deep sponge fauna from the Mediterranean to the Atlantic through the Strait of Gibraltar. However, only the bathyal sponges from the Gulf of Cádiz show a strong affinity with those of the Mediterranean, suggesting that environmental conditions are unsuitable for a majority of Mediterranean sponges to colonize adjacent areas of the North Atlantic beyond the Gulf of Cádiz.

8. The Levantine Intermediate Water flowing from the Eastern to the Western Mediterranean through the Strait of Sicily acts as a connection between the deep sponge faunas of these two Mediterranean basins. As a main contributor to the Mediterranean Outflow Water, this intermediate water current indirectly affects the faunal transfer to the Atlantic Ocean.

9. The study of the faunal affinities of the deep sponges from the Northeast Atlantic and the Mediterranean have proved that sponges provide a useful biogeographical tool to indirectly address the issue of connectivity in deep sea.

General Bibliography

Aguilar, R., López Correa, M., Calcinai, B., Pastor, X. and García, S. (2011) First records of *Asbestopluma hypogea* Vacelet and Boury-Esnault, 1996 (Porifera, Demospongiae Cladorhizidae) on seamounts and in bathyal settings of the Mediterranean Sea. *Zootaxa,* 2925, 33-40.

Antcliffe, J. B., Callow, R. H. T. and Brasier, M. D. (2014) Giving the early fossil record of sponges a squeeze. *Biological Reviews,* 89(4), 972-1004.

Appeltans, W., Ahyong, Shane T., Anderson, G., Angel, Martin V., Artois, T., Bailly, N., Bamber, R., Barber, A., Bartsch, I., Berta, A., et al. (2012) The Magnitude of Global Marine Species Diversity. *Current Biology,* 22(23), 2189-2202.

Arellano, S. M., Lee, O. O., Lafi, F. F., Yang, J., Wang, Y., Young, C. M. and Qian, P.-Y. (2013) Deep Sequencing of *Myxilla* (*Ectyomyxilla*) *methanophila*, an Epibiotic Sponge on Cold-Seep Tubeworms, Reveals Methylotrophic, Thiotrophic, and Putative Hydrocarbon-Degrading Microbial Associations. *Microbial Ecology,* 65(2), 450-461.

Arnesen, E. (1920) Spongia. *Report on the Scientific Results of the "Michael Sars" North Atlantic Deep-Sea Expedition, 1910*. 3(II), 1-29.

Baird, D. J. and Hajibabaei, M. (2012) Biomonitoring 2.0: a new paradigm in ecosystem assessment made possible by next-generation DNA sequencing. *Molecular Ecology,* 21(8), 2039-2044.

Bell, J. J. (2008) The functional roles of marine sponges. *Estuarine, Coastal and Shelf Science,* 79(3), 341-353.

Bertolino, M., Ricci, S., Canese, S., Cau, A., Bavestrello, G., Pansini, M. and Bo, M. (2019) Diversity of the sponge fauna associated with white coral banks from two Sardinian canyons (Mediterranean Sea). *Journal of the Marine Biological Association of the United Kingdom,* 99(8), 1735-1751.

Bhatnagar, I., Pallela, R., Bramhachari, P. V. and Ealla, K. K. R. (2016) Chronicles of Sponge Biomaterials: The Saga in Biomedicine. *In*: R. Palella and H. Ehrlich (Eds), *Marine Sponges: Chemicobiological and Biomedical Applications*. Springer, New Delhi, pp.315 – 327.

Bo, M., Bertolino, M., Bavestrello, G., Canese , S., Giusti, M., Angiolillo, M., Pansini, M. and Taviani, M. (2012) Role of deep sponge grounds in the Mediterranean Sea: a case study in southern Italy. *Hydrobiologia,* 687(1), 163-177.

Bohmann, K., Evans, A., Gilbert, M. T. P., Carvalho, G. R., Creer, S., Knapp, M., Yu, D. W. and de Bruyn, M. (2014) Environmental DNA for wildlife biology and biodiversity monitoring. *Trends in Ecology and Evolution,* 29(6), 358-367.

Borowiec, M. L., Lee, E. K., Chiu, J. C. and Plachetzki, D. C. (2015) Extracting phylogenetic signal and accounting for bias in whole-genome data sets supports the Ctenophora as sister to remaining Metazoa. *BMC Genomics,* 1615.

Boury-Esnault, N., Pansini, M. and Uriz, M. J. (1994) Spongiaires bathyaux de la mer d'Alboran et du golfe ibéro-marocain. *Mémoires du Muséum National d'Histoire Naturelle,* 160, 1-174.

Boury-Esnault, N. and Rützler, K. (1997) Thesaurus of sponge morphology. *Smithsonian Contributions to Zoology,* 596, 1-55.

Calcinai, B., Moratti, V., Martinelli, M., Bavestrello, G. and Taviani, M. (2013) Uncommon sponges associated with deep coral bank and maerl habitats in the Strait of Sicily (Mediterranean Sea). *Italian Journal of Zoology,* 80(3), 412-423.

Cárdenas, P., Pérez, T. and Boury-Esnault, N. (2012) Sponge systematics facing new challenges. *Adv Mar Biol,* 61, 79-209.

Cárdenas, P., Xavier, J. R., Réveillaud, J., Schander, C. and Rapp, H. T. (2011) Molecular Phylogeny of the Astrophorida (Porifera, Demospongiaep) Reveals an Unexpected High Level of Spicule Homoplasy. *PLoS One,* 6(4), e18318.

Carter, H. J. (1876) Descriptions and figures of deep-sea sponges and their spicules, from the Atlantic Ocean, dredged up on board H.M.S. "Porcupine", chiefly in 1869 (concluded). *Annals and Magazine of Natural History,* 4(18), 225-479.

Cheshire, A. C., Wilkinson, C. R., Seddon, S. and Westphalen, G. (1997) Bathymetric and seasonal changes in photosynthesis and respiration of the phototrophic sponge *Phyllospongia lamellosa* in comparison with respiration by the heterotrophic sponge *Ianthella basta* on Davies Reef, Great Barrier Reef. *Marine and Freshwater Research,* 485, 89-599.

Chevaldonné, P., Pérez, T., Crouzet, J.-M., Bay-Nouailhat, W., Bay-Nouailhat, A., Fourt, M., Almón, B., Pérez, J., Aguilar, R. and Vacelet, J. (2015)

Unexpected records of 'deep-sea' carnivorous sponges *Asbestopluma hypogea* in the shallow NE Atlantic shed light on new conservation issues. *Marine Ecology,* 36(3), 475-484.

Coppari, M., Gori, A., Viladrich, N., Saponari, L., Canepa, A., Grinyó, J., Olariaga, A. and Rossi, S. (2016) The role of Mediterranean sponges in benthic-pelagic coupling processes: Aplysina aerophoba and Axinella polypoides case studies. *Journal of Experimental Marine Biology and Ecology,* 477, 57-68.

Cordes, E. E., Bergquist, D. C. and Fisher, C. R. (2009) Macro-Ecology of Gulf of Mexico Cold Seeps. *Annual Review of Marine Science,* 1, 143-168.

de Goeij, J. M., van Oevelen, D., Vermeij, M. J. A., Osinga, R., Middelburg, J. J., de Goeij, A. F. P. M. and Admiraal, W. (2013) Surviving in a marine desert: The sponge loop retains resources within coral reefs. *Science,* 342, 108-110.

Delgado, M., Rueda, J. L., Gil, J., Burgos, C. and Sobrino, I. (2013) Spatial characterization of megabenthic epifauna of soft bottoms around mud volcanoes in the Gulf of Cádiz. *Journal of Natural History,* 47(25-28), 1803-1831.

Di Lorenzo, M., Sinerchia, M. and Colloca, F. (2018) The North sector of the Strait of Sicily: a priority area for conservation in the Mediterranean Sea. *Hydrobiologia,* 821(1), 235-253.

Díaz del Río, V., Bruque, G., Fernández-Salas, L. M., Rueda, J. L., González, E., López, N., Palomino, D., López, F. J., Farias, C., Sánchez, R., Vázquez, J. T., Rittierott, C. C., Fernández, A., Marina, P., Luque, V., Oporto, T., Sánchez, O., García, M., Urra, J., Bárcenas, P., Jiménez, M. P., Sagarminaga, R. and Arcos, J. M. Volcanes de fango del golfo de Cádiz, Proyecto LIFE + INDEMARES. Fundación Biodiversidad del Ministerio de Agricultura, Alimentación y Medio Ambiente. (2014).

Ehrlich, H., Steck, E., Ilan, M., Maldonado, M., Muricy, G., Bavestrello, G., Kljajic, Z., Carballo, J. L., Schiaparelli, S., Ereskovsky, A., Schupp, P., Born, R., Worch, H., Bazhenov, V. V., Kurek, D., Varlamov, V., Vyalikh, D., Kummer, K., Sivkov, V. V., Molodtsov, S. L., Meissner, H., Richter, G., Hunoldt, S., Kammer, M., Paasch, S., Krasokhin, V., Patzke, G., Brunner, E. and Richter, W. (2010) Three-dimensional chitin-based scaffolds from Verongida sponges (Demospongiae:

Porifera). Part II: Biomimetic potential and applications. *International Journal of Biological Macromolecules,* 47(2), 141-145.

Erpenbeck, D., Breeuwer, J. A. J., Parra-Velandia, F. J. and Van Soest, R. W. M. (2006) Speculation with spiculation? - Three independent gene fragments and biochemical characters versus morphology in demosponge higher classification. *Molecular Phylogenetics and Evolution,* 38, 293-305.

Evans, J., Aguilar, R., Alvarez, H., Borg, J. A., Garcia, S., Knittweis, L. and Schembri, P. J. Recent evidence that the deep sea around Malta is a biodiversity hotspot. Rapport du Congrès de la Commission Internationale pour l'Exploration Scientifique de la Mer Méditerranée. Volume 41. Monaco: *La Commission Internationale pour l'Exploration Scientifique de la Mer Méditerranée.*

Feuda, R., Dohrmann, M., Pett, W., Philippe, H., Rota-Stabelli, O., Lartillot, N., Wörheide, G. and Pisani, D. (2017) Improved Modeling of Compositional Heterogeneity Supports Sponges as Sister to All Other Animals. *Current Biology,* 27(24), 3864-3870.e3864.

Freiwald, A., Beuck, L., Rueggeberg, A., Taviani, M. and Hebbeln, D. (2009) The White Coral Community in the Central Mediterranean Sea Revealed by ROV Surveys. *Oceanography,* 22(1), 58-74.

Freiwald, A. and Roberts, J. M. (2005) *Cold-water Corals and Ecosystems*. Springer, Heidelberg.

Frost, T. M. (1980) Selection in sponge feeding processes. *In:* D. C. Smith and Y. Tiffon (Eds), *Nutrition in the Lower Metazoa*. Pergamon Press, Oxford, pp. 33-44.

Gage, J. D. and Tyler, P. A. (1991) Deep-sea biology: a natural history of organisms at the deep-sea floor. *Journal of the Marine Biological Association of the United Kingdom,* 73(1), 251-252.

Gallardo-Roldan, H., Urra, J., García, T., Lozano, M., Antit, M., Bar, J. and Rueda, J. L. (2015) First record of the starfish *Luidia atlantidea* Madsen, 1950 in the Mediterranean Sea, with evidence of persistent populations. *Cahiers de Biologie Marine,* 56(3), 263-270.

García Raso, J. E., Salas, C., García Muñóz, J. E. and Gofas, S. (2010) Biodiversidad faunística en el litoral Malagueño. *Jábega,* 102, 18-30.

Gili, J.-M. and Coma, R. (1998) Benthic suspension feeders: their paramount role in littoral marine food webs. *Trends in Ecology and Evolution,* 13(8), 316-321.

Gofas, S., Goutayer, J., Luque, A. A. and Salas, C. Espacio Marino de Alborán. Proyecto LIFE+INDEMARES. Fundación Biodiversidad del Ministerio de Agricultura, Alimentación y Medio Ambiente (2014).

Gofas, S., Moreno, D. and Salas (coords.), C. (2011) *Moluscos marinos de Andalucía* Volume II. Servicio de Publicaciones e Intercambio Científico, Universidad de Málaga, Málaga.

González-García, E., Mateo-Ramírez, Á., Urra, J., Farias, C., Marina, P., Lozano, P., López-González, P. J., Megina, C., Raso, J. E. G., Gofas, S., López, E., Moreira, J., López-González, N., Sánchez-Leal, R. F., Fernández-Salas, L. M. and Rueda, J. L. (2020) Composition, structure and distribution of epibenthic communities within a mud volcano field of the northern Gulf of Cádiz in relation to environmental variables and trawling activity. *Journal of Sea Research,* 160-161, 101892.

Harrison, F. W., Gardiner, S. L., Rützler, K. and Fisher, C. R. (1994) On the occurrence of endosymbiotic bacteria in a new species of sponge from hydrocarbon seep communities in the Gulf of Mexico. *Transactions of the American Microscopical Society,* 113, 419–420.

Hogg, M. M., Tendal, O. S., Conway, K. W., Pomponi, S. A., van Soest, R. W. M., Gutt, J., Krautter, M. and Roberts, J. M. (2010) *Deep-sea sponge grounds: Reservoirs of biodiversity* . UNEP-WCMC Biodiversity Series No. 32 UNEP-WCMC, Cambridge.

Jiménez, E. and Ribes, M. (2007) Sponges as a source of dissolved organic nitrogen: Nitrification mediated by temperate sponges. *Limnology and Oceanography,* 52(3), 948-958.

Kenchington, E., Wang, Z. L., Lirette, C., Murillo, F. J., Guijarro, J., Yashayaev, I. and Maldonado, M. (2019) Connectivity modelling of areas closed to protect vulnerable marine ecosystems in the northwest Atlantic. *Deep-Sea Research Part I: Oceanographic Research Papers,* 143, 85-103.

Klitgaard, A. B. and Tendal, O. S. (2004) Distribution and species composition of mass occurrences of large-sized sponges in the northeast Atlantic. *Progress in Oceanography,* 61(1), 57-98.

Knittweis, L., Aguilar, R., Álvarez, H., Borg, J. A., Evans, J., Garcia, S. and Schembri, P. J. (2016) New depth record of the precious red coral *Corallium rubrum* for the Mediterranean. Rapport du Congrès de la Commission Internationale pour l'Exploration Scientifique de la Mer Méditerranée Volume 41. Monaco: *La Commission Internationale pour l'Exploration Scientifique de la Mer Méditerranée*. 467.

Knittweis, L., Evans, J., Aguilar, R., Álvarez, H., Borg, J. A., García, S. and Schembri, P. (2019) Recent Discoveries of Extensive Cold-Water Coral Assemblages in MalteseWaters. *In:* C. Orejas and C. Jiménez (Eds), *Mediterranean Cold-Water Corals: Past, Present and Future*. Springer International Publishing AG, pp. 253-255.

Leal, M. C., Puga, J., Serôdio, J., Gomes, N. C. M. and Calado, R. (2012) Trends in the Discovery of New Marine Natural Products from Invertebrates over the Last Two Decades – Where and What Are We Bioprospecting? *PLoS One,* 7(1), e30580.

Lévi, C. and Vacelet, J. (1958) Eponges récoltées dans l'Atlantique Oriental par le "President Theodore Tissier" (1955-1956). *Revue des Travaux de l'Institut des Pêches Maritimes,* 22(2), 225-246.

Levin, L. A. (2005) Ecology of cold seep sediments: Interactions of fauna with flow, chemistry and microbes. *In:* R. N. Gibson, R. J. A. Atkinson and J. D. M. Gordon (Eds), *Oceanography and marine biology: an annual review,* 43. CRC Press-Taylor and Francis Group, Boca Raton, pp. 1-46.

Lin, Z., Solomon, K. L., Zhang, X., Pavlos, N. J., Abel, T., Willers, C., Dai, K., Xu, J., Zheng, Q. and Zheng, M. (2011) In vitro Evaluation of Natural Marine Sponge Collagen as a Scaffold for Bone Tissue Engineering. *International Journal of Biological Sciences,* 7(7), 968-977.

Longo, C., Mastrototaro, F. and Corriero, G. (2005) Sponge fauna associated with a Mediterranean deep-sea coral bank. *Journal of the Marine Biological Association of the United Kingdom,* 85(06), 1341-1352.

Love, G. D., Grosjean, E., Stalvies, C., Fike, D. A., Grotzinger, J. P., Bradley, A. S., Kelly, A. E., Bhatia, M., Meredith, W., Snape, C. E., Bowring, S. A., Condon, D. J. and Summons, R. E. (2009) Fossil steroids record the appearance of Demospongiae during the Cryogenian period. *Nature,* 457(7230), 718-721.

Ludeman, D. A., Reidenbach, M. A. and Leys, S. P. (2017) The energetic cost of filtration by demosponges and their behavioural response to ambient currents. *Journal of Experimental Biology,* 220(24), 4743-4744.

Maldonado, M. (1992) Demosponges of the red coral bottoms from the Alboran Sea. *Journal of Natural History,* 26, 1131-1161.

Maldonado, M. (1993). *Demosponjas litorales de Alborán. Faunística y Biogeografía*. (Philosophical Dissertation). University of Barcelona, Barcelona.

Maldonado, M., Aguilar, R., Bannister, R. J., Bell, J. J., Conway, K. W., Dayton, P. K., Díaz, C., Gutt, J., Kelly, M., Kenchington, E. L. R., Leys, S. P., Pomponi, S. A., Rapp, H. T., Rützler, K., Tendal, O. S., Vacelet, J. and Young, C. M. (2017) Sponge Grounds as Key Marine Habitats: A Synthetic Review of Types, Structure, Functional Roles, and Conservation Concerns. *In:* S. Rossi, L. Bramanti, A. Gori and C. Orejas Saco del Valle (Eds), *Marine Animal Forests: The Ecology of Benthic Biodiversity Hotspots*. Springer International Publishing, Cham, pp. 1-39.

Maldonado, M. and Benito, J. (1991) *Crambe tuberosa* n. sp. (Demospongiae, Poecilosclerida): a new Mediterranean poecilosclerid with lithistid affinities. *Cahiers de Biologie Marine,* 32, 323-332.

Maldonado, M., Carmona, M. C., Uriz, M. J. and Cruzado, A. (1999) Decline in Mesozoic reef-building sponges explained by silicon limitation. *Nature,* 401, 785-788.

Maldonado, M., Carmona, M. C., Velásquez, Z., Puig, A., Cruzado, A., López, A. and Young, C. M. (2005) Siliceous sponges as a silicon sink: An overlooked aspect of the benthopelagic coupling in the marine silicon cycle. *Limnology and Oceanography,* 50(3), 799-809.

Maldonado, M., López-Acosta, M., Sitjà, C., Garcia-Puig, M., Galobart, C., Ercilla, G. and Leynaert, A. (2019) Sponge skeletons as an important sink of silicon in the global oceans. *Nature Geoscience,* 12(10), 815-822.

Maldonado, M., Ribes, M. and Van Duyl, F. C. (2012) Nutrient fluxes through sponges: biology, budgets, and ecological implications. *Advances in Marine Biology,* 62, 114-182.

Maldonado, M., Riesgo, A., Bucci, A. and Rützler, K. (2010) Revisiting silicon budgets at a tropical continental shelf: Silica standing stocks in sponges surpass those in diatoms. *Limnology and Oceanography,* 55(5), 2001-2010.

Maldonado, M. and Uriz, J. M. (1995) Biotic affinities in a transitional zone between the Atlantic and the Mediterranean: a biogeographical approach based on sponges. *Journal of Biogeography,* 22, 89-110.

Mariani, S., Baillie, C., Colosimo, G. and Riesgo, A. (2019) Sponges as natural environmental DNA samplers. *Current Biology,* 29(11), R401-R402.

Mastrototaro, F., D'Onghia, G., Corriero, G., Matarrese, A., Maiorano, P., Panetta, P., Gherardi, M., Longo, C., Rosso, A., Sciuto, F., Sanfilippo, R., Gravili, C., Boero, F., Taviani, M. and Tursi, A. (2010) Biodiversity of the white coral bank off Cape Santa Maria di Leuca (Mediterranean Sea): An update. *Deep-Sea Research II,* 57(5-6), 412-430.

Mercurio, M., Correiro, G., Liaci, L. S. and Gaino, E. (2000) Silica content and spicule size variations in Pellina semitubulosa (Porifera : Demospongiae). *Marine Biology,* 137(1), 87-92.

Morrow, C. and Cárdenas, P. (2015) Proposal for a revised classification of the Demospongiae (Porifera). *Frontiers in Zoology,* 7, 12.

Ordines, F., Ferriol, P., Moya, F., Farias, C., Rueda, J. L. and García-Ruiz, C. (2019) First record of the sea cucumber Parastichopus tremulus (Gunnerus, 1767) (Echinodermata: Holothuroidea: Aspidochirotida) in the Mediterranean Sea (Alboran Sea, western Mediterranean). *Cahiers de Biologie Marine,* 60(2), 111-115.

Palomino, D., López-González, N., Vázquez, J.-T., Fernández-Salas, L.-M., Rueda, J.-L., Sánchez-Leal, R. and Díaz-del-Río, V. (2016) Multidisciplinary study of mud volcanoes and diapirs and their relationship to seepages and bottom currents in the Gulf of Cádiz continental slope (northeastern sector). *Marine Geology,* 378, 196-212.

Pansini, M. (1987) Littoral demosponges from the banks of the straits of Sicily and the Alboran Sea. *In:* J. Vacelet and N. Boury-Esnault (Eds), *Taxonomy of Porifera,* G13. Springer-Verlag, Berlin, Heidelberg, pp. 149-186.

Pansini, M. and Longo, C. (2003) A review of the Mediterranean Sea sponge biogeography with, in appendix, a list of the demosponges hitherto recorded from this sea. *Biogeographia,* 24, 57-73.

Patruno, R. (2008) Prevention of marine pollution from ships in the mediterranean region: Economic, legal and technical aspects. *Geografia Fisica e Dinamica Quaternaria,* 31(2), 211-214.

Pérès, J. M. and Picard, J. (1964) Nouveau manuel de bionomie benthique de la mer Méditerranée. *Recueil des Travaux de la Station Marine d'Endoume,* 31(47), 1-137.

Pett, W., Adamski, M., Adamska, M., Francis, W. R., Eitel, M., Pisani, D. and Wörheide, G. (2019) The Role of Homology and Orthology in the Phylogenomic Analysis of Metazoan Gene Content. *Molecular Biology and Evolution,* 36(4), 643-649.

Pham, C. K., Murillo, F. J., Lirette, C., Maldonado, M., Coleco, A., Ottaviani, D. and Kenchington, E. (2019) Removal of deep-sea sponges by bottom trawling in the Flemish Cap area: conservation, ecology and economic assessment. *Scientific Reports,* 9, 15843.

Pile, A. J., Patterson, M. R. and Witman, J. D. (1996) In situ grazing on plankton <10 μm by the boreal sponge *Mycale lingua*. *Marine Ecology Progess Series,* 141, 95-102.

Pile, A. J. and Young, C. M. (2006) The natural diet of a hexactinellid sponge: Benthic-pelagic coupling in a deep-sea microbial food web. *Deep-Sea Research Part I: Oceanographic Research Papers,* 53(7), 1148-1156.

Prampolini, M., Blondel, P., Foglini, F. and Madricardo, F. (2018) Habitat mapping of the Maltese continental shelf using acoustic textures and bathymetric analyses. *Estuarine, Coastal and Shelf Science,* 207, 483-498.

Ramirez-Llodra, E., Brandt, A., Danovaro, R., De Mol, B., Escobar, E., German, C. R., Levin, L. A., Martinez Arbizu, P., Menot, L., Buhl-Mortensen, P., Narayanaswamy, B. E., Smith, C. R., Tittensor, D. P., Tyler, P. A., Vanreusel, A. and Vecchione, M. (2010) Deep, diverse and definitely different: unique attributes of the world's largest ecosystem. *Biogeosciences,* 7(9), 2851-2899.

Ramirez-Llodra, E., Tyler, P. A., Baker, M. C., Bergstad, O. A., Clark, M. R., Escobar, E., Levin, L. A., Menot, L., Rowden, A. A., Smith, C. R. and Van Dover, C. L. (2011) Man and the Last Great Wilderness: Human Impact on the Deep Sea. *PLoS One,* 6(8), e22588.

Ramos-Esplá, A. A. and Luque, A. A. (2004) Los fondos de "maerl". *In:* A. A. Luque (Ed), *Praderas y bosques marinos de Andalucía*. Consejería de Medio Ambiente, Junta de Andalucía, Sevilla, pp. 223-236.

Reiswig, H. M. (1971) Particle feeding in natural populations of three marine demosponges. *Biological Bulletin, Marine Biological Laboratory, Woods Hole,* 141, 568-591.

Ribes, M., Coma, R. and Gili, J. M. (1999) Natural diet and grazing rate of the temperate sponge *Dysidea avara* (Demospongiae, Dendroceratida) throughout an annual cycle. *Marine Ecology Progress Series,* 176, 179-190.

Ridley, S. O. and Dendy, A. (1887) Report on the Monaxonida collected by H.M.S."Challenger" during the years 1873-1876. *Report of the Scientific Results of the Voyage of H.M.S."Challenger" 1873-76,* Zool., 20 (Part LIX)1-275.

Rix, L., de Goeij, J. M., Mueller, C. E., Struck, U., Middelburg, J. J., van Duyl, F. C., Al-Horani, F. A., Wild, C., Naumann, M. S. and van Oevelen, D. (2016) Coral mucus fuels the sponge loop in warm- and cold-water coral reef ecosystems. *Scientific Reports,* 7(6), 618715.

Rosell, D. and Uriz, M. J. (2002) Excavating and endolithic sponge species (Porifera) from the Mediterranean: species descriptions and identification key. *Organisms, Diversity and Evolution,* 2(1), 55-86.

Rueda, J. L., Díaz-del-Río, V., Sayago-Gil, M., López-González, N., Fernández-Salas, L. M. and Vázquez, J. T. (2012) Fluid venting through the seabed in the Gulf of Cadiz (SE Atlantic Ocean, Western Iberian Peninsula): Geomorphic features, habitats, and associated fauna *In:* P. T. Harris and E. K. Baker (Eds), *Seafloor geomorphology as benthic habitat*. Elsevier, London, pp. 831-841.

Sánchez-Leal, R. F., Bellanco, M. J., Fernández-Salas, L. M., García-Lafuente, J., Gasser-Rubinat, M., González-Pola, C., Hernández-Molina, F. J., Pelegrí, J. L., Peliz, A., Relvas, P., Roque, D., Ruiz-Villarreal, M., Sammartino, S. and Sánchez-Garrido, J. C. (2017) The Mediterranean Overflow in the Gulf of Cadiz: A rugged journey. *Science Advances,* 3(11), eaao060911.

Santín, A., Grinyó, J., Ambroso, S., Uriz, M., Gori, A., Dominguez-Carrió, C. and Gili, J.-M. (2018) Sponge assemblages on the deep Mediterranean

continental shelf and slope (Menorca Channel, Western Mediterranean Sea). *Deep-Sea Research Part I: Oceanographic Research Papers,* 131, 75-86.

Schulze, M. F. E. (1887) Report on the Hexactinellida collected by H.M.S. "Challenger" during the years 1873-1876. *Report of the Scientific Results of the Voyage of H.M.S."Challenger" 1873-76,* Zoology, 211-513.

Shen, X.-X., Hittinger, C. T. and Rokas, A. (2017) Contentious relationships in phylogenomic studies can be driven by a handful of genes. *Nature Ecology andAmp; Evolution,* 1, 0126.

Simion, P., Philippe, H., Baurain, D., Jager, M., Richter, D. J., Di Franco, A., Roure, B., Satoh, N., Quéinnec, É., Ereskovsky, A., Lapébie, P., Corre, E., Delsuc, F., King, N., Wörheide, G. and Manuel, M. (2017) A Large and Consistent Phylogenomic Dataset Supports Sponges as the Sister Group to All Other Animals. *Current Biology,* 27(7), 958-967.

Sollas, W. J. (1888) Report on the Tetractinellida collected by H.M.S. Challenger during the years 1873-76. *Report of the Scientific Results of the Voyage of H.M.S. Challenger 1873-76,* 25(part 63), 1-458.

Sperling, E. A., Robinson, J. M., Pisani, D. and Peterson, K. J. (2010) Where's the glass? Biomarkers, molecular clocks, and microRNAs suggest a 200-Myr missing Precambrian fossil record of siliceous sponge spicules. *Geobiology,* 8(1), 24-36.

Steindler, L., Beer, S. and Ilan, M. (2002) Photosymbiosis in intertidal and subtidal tropical sponges. *Symbiosis,* 33(3), 263-273.

Tang, Q., Wan, B., Yuan, X., Muscente, A. D. and Xiao, S. (2019) Spiculogenesis and biomineralization in early sponge animals. *Nature Communications,* 10(1), 3348.

Taviani, M., Angeletti, L., Canese, S., Cannas, R., Cardone, F., Cau, A., Cau, A. B., Follesa, M. C., Marchese, F., Montagna, P. and Tessarolo, C. (2017) The "Sardinian cold-water coral province" in the context of the Mediterranean coral ecosystems. *Deep-Sea Research Part II: Topical Studies in Oceanography,* 145, 61-78.

Taylor, M. W., Radax, R., Steger, D. and Wagner, M. (2007) Sponge-associated microorganisms: Evolution, ecology, and biotechnological potential. *Microbiology and Molecular Biology Reviews,* 71(2), 295-347.

Templado, J., Calvo, M., Moreno, D., Flores, A., Conde, F., Abad, R., Rubio, J., López-Fé, C. M. and Ortiz, M. (2006) *Flora y fauna de la reserva marina y reserva de pesca de la isla de Alborán*. Secretaría General de Pesca Marítima, MAPA, Madrid.

Templado, J., García-Carrascosa, M., Baratech, L., Capaccioni, R., Juan, A., López-Ibor, A., Silvestre, R. and Massó, C. (1986) Estudio preliminar de la fauna asociada a los fondos coralígenos del mar de Alborán (SE de España). *Boletín del Instituto Español de Oceanografía,* 3(4), 93-104.

Thistle, D. (2003) The deep-sea floor: An overview. In: P. A. Tyler (Ed), *Ecosystems of the Deep Ocean (Ecosystems of the World)* Volume 28, Elsevier Science, pp. 5-38.

Thomson, C. W. (1873) *The depths of the sea*. Macmillan and Co., London.

Topsent, E. (1892) Contribution a l'étude des Spongiaires de l'Atlantique Nord. *Résultats des Campagnes Scientifiques accomplies par le Prince Albert I. Monaco,* 21-165.

Topsent, E. (1895) Campagnes du Yacht "Princesse Alice". Notice sur les spongiaires recueillis en 1894 et 1895. *Bulletin de la Societe Zoologique de France,* 20213-216.

Topsent, E. (1904) Spongiaires des Açores. *Résultats des Campagnes Scientifiques accomplies par le Prince Albert I. Monaco,* 251-279.

Topsent, E. (1928) Spongiaires de l'Atlantique et de la Méditerranée, provenant des croisières de Prince Albert I de Monaco. *Résultats des Campagnes Scientifiques accomplies par le Prince Albert I. Monaco,* 741-376.

Vacelet, J. (1959) Répartition générale des Eponges Cornées de la region de Marseille et de quelques stations méditerranées. *Recueil des Travaux de la Station Marine d'Endoume,* 16(26), 39-101.

Vacelet, J. (1960) Eponges de la Méditerranée nord-occidentale récoltées par le "President Théodore Tissier" (1958). *Revue des Travaux de l'Institut des Pêches Maritimes,* 24(2), 257-272.

Vacelet, J. (1961) Quelques Eponges remarquables de Méditerranée. *Revue des Travaux de l'Institut des Pêches Maritimes,* 25(3), 351-354.

Vacelet, J. (1969) Eponges de la Roche du Large et de l'étage bathyal de Méditerranée (récoltées de la Soucoupe plongeante cousteau et

dragages). *Mémoires du Muséum National d'Histoire Naturelle (France),* série A, 59(2), 145-219.

Vacelet, J. and Boury-Esnault, N. (1995) Carnivorous sponges. *Nature,* 373(6512), 333-335.

Vacelet, J., Boury-Esnault, N., Fiala-Medioni, A. and Fisher, C. R. (1995) A methanotrophic carnivorous sponge. *Nature,* 377(6547), 296-296.

Van Soest, R. M. W., Beglinger, E. J. and de Voogd, N. J. (2013) Microcionid sponges from Northwest Africa and the Macaronesian Islands (Porifera, Demospongiae, Poecilosclerida). *Zoologische mededeelingen,* 87(4), 275-404.

Van Soest, R. M. W., Beglinger, E. J. and de Voogd, N. J. (2014) Mycale species (Porifera: Poecilosclerida) of Northwest Africa and the Macaronesian Islands. *Zoölogische Mededelingen Leiden,* 88(4), 59-109.

Van Soest, R. M. W., Boury-Esnault, N., Hooper, J. N. A., Rützler, K., de Voogd, N. J., Alvarez de Glasby, B., Hajdu, E., Pisera, A., Manconi, R., Schönberg, C. H. L., Janussen, D., Tabachnick, K. R., Klautau, M., Picton, B. E., Kelly, M., Vacelet, J., Dohrmann, M. and Díaz, M. C.(2020). World Porifera database. Accessed at http://www.marinespecies.org/porifera on 20/07/2020.

Van Soest, R. W. M., Boury-Esnault, N., Vacelet, J., Dohrmann, M., Erpenbeck, D., De Voogd, N. J., Santodomingo, N., Vanhoorne, B., Kelly, M. and Hooper, J. N. A. (2012) Global Diversity of Sponges (Porifera). *PLoS One,* 7(4), e35105.

Velaoras, D., Civitarese, G., Giani, M., Gogou, A., Rahav, E. and Zervoudaki, S. (2020) Revisiting the Eastern Mediterranean: Recent knowledge on the physical, biogeochemical and ecosystemic states and trends Volume II. *Deep-Sea Research Part II: Topical Studies in Oceanography,* 171, 104725.

Vertino, A., Savini, A., Rosso, A., Di Geronimo, I., Mastrototaro, F., Sanfilippo, R., Gay, G. and Etiope, G. (2010) Benthic habitat characterization and distribution from two representative sites of the deep-water SML Coral Province (Mediterranean). *Deep-Sea Research Part II: Topical Studies in Oceanography,* 57, 380-396.

Voultsiadou, E. (2005) Demosponge distribution in the eastern Mediterranean: a NW-SE gradient. *Helgoland Marine Research,* 59(3), 237-251.

Webster, N. S. and Taylor, M. W. (2012) Marine sponges and their microbial symbionts: love and other relationships. *Environmental Microbiology,* 14(2), 335-346.

Whelan, N. V., Kocot, K. M., Moroz, T. P., Mukherjee, K., Williams, P., Paulay, G., Moroz, L. L. and Halanych, K. M. (2017) Ctenophore relationships and their placement as the sister group to all other animals. *Nature Ecology and Evolution,* 1(11), 1737-1746.

Wilborn, R., Rooper, C. N., Goddard, P., Li, L. B., Williams, K. and Towler, R. (2018) The potential effects of substrate type, currents, depth and fishing pressure on distribution, abundance, diversity, and height of cold-water corals and sponges in temperate, marine waters. *Hydrobiologia,* 811(1), 251-268.

Wulff, J. (2012) Ecological Interactions and the Distribution, Abundance, and Diversity of Sponges. *In:* M. A. Becerro, M. J. Uriz, M. Maldonado and X. Turon (Eds), *Advances in Marine Biology,* Volume 61. Academic Press, pp. 273-344.

Xavier, J. R. and Van Soest, R. W. M. (2012) Diversity patterns and zoogeography of the Northeast Atlantic and Mediterranean shallow-water sponge fauna. *Hydrobiologia,* 687(1), 107-125.

Zibrowius, H. and Taviani, M. (2005) Remarkable sessile fauna associated with deep coral and other calcareous substrates in the Strait of Sicily, Mediterranean Sea. *In:* A. Freiwald and J. M. Roberts (Eds), *Cold-Water Corals and Ecosystems*. Springer Berlin Heidelberg, Berlin, pp. 807-819.

Appendix

Chapter 1

Appendix I. Summary of individuals collected for each species during each of the 31 trawls in the several volcanoes (see Table 1, Fig 1). Sponge species are listed alphabetically by class (Cl), subclass (Sc), order (Or), family (Fa), genus and species. Abbreviations for the taxonomic categories are: Dm= Demospongiae, Hx= Hexactinellida, Het= Heteroscleromorpha, Ke= Keratosa, Ap= Amphidiscophora, Hex= Hexasterophora, Am= Amphidiscosida, Ax= Axinellida, Bi= Biemnida, Bu= Bubarida, De= Desmacellida, Di= Dictyoceratida, Ha= Haplosclerida, Ly= Lyssacinosida, Me= Merliida,, Pl= Polymastiida, Po= Poecilosclerida, Su= Suberitida, Te= Tetractinellida, Ph= Pheronematidae, Ai= Axinellidae, He= Heteroxyidae, Ra= Raspailiidae, Rh= Rhabderemiidae, Bb= Bubaridae, Ds= Desmacellidae, Dy= Dysideidae, So= Spongiidae, Ch= Chalinidae, Pe= Petrosiidae, Ro= Rossellidae, Hm= Hamacanthidae, Pm= Polymastiidae, Ce= Coelosphaeridae, Cl= Cladorhizidae, Cr= Crellidae, Hy= Hymedesmiidae, Io= Iotrochotidae, La= Latrunculiidae, Mc= Mycalidae, Mi= Microcionidae, Mx= Myxillidae, Pd= Podospongiidae, Hl= Halichondriidae, Sb= Suberitidae, St= Stylocordylidae, An= Ancorinidae, Az= Azoricidae, Co= Corallistidae, Ge= Geodiidae, Pa= Pachastrellidae, Tn= Theneidae, To= Theonellidae, Tr= Thrombidae, Tt= Tetillidae, Vu= Vulcanellidae). Names of species not found in the Mediterranean are accompanied with *.

					Mud volcanoes																											
					Gazul						Anastasya			Tarsis			Pipoca					Chica				Hespérides				Almazán				Aveiro	
Cl	Sc	Or	Fa	Species	1	2	3	4	5	6	7	8	9	10	11	12	13	14	15	16	17	18	19	20	21	22	23	24	25	26	27	28	29	30	31
Dm	Het	Ax	Ai	*Axinella* cf *rugosa* (Bowerbank, 1866)		1																												
Dm	Het	Ax	Ai	*Axinella vellerea* Topsent, 1904				8										1		4														
Dm	Het	Ax	Ai	*Phakellia robusta* Bowerbank, 1866	1			7											6				1		3									
Dm	Het	Ax	Ai	*Phakellia ventilabrum* (Linnaeus, 1767)														1					2											
Dm	Het	Ax	He	*Myrmekioderma indemaresi* nov.sp.*				1		1																								
Dm	Het	Ax	Ra	*Acantheurypon pilosella* (Topsent, 1904)															1															
Dm	Het	Ax	Ra	*Eurypon clavatum* (Bowerbank, 1866)														1	1											1				
Dm	Het	Ax	Ra	*Janulum spinispiculum* (Carter, 1876)															1															
Dm	Het	Bi	Rh	*Rhabderemia profunda* Boury-Esnault, Pansini & Uriz, 1994*																					1									
Dm	Het	Bu	Bb	*Bubaris vermiculata* (Bowerbank, 1866)																											1			
Dm	Het	De	Ds	*Desmacella annexa* Schmidt, 1870							1																							1

Cl	Sc	Or	Fa	Species	Mud volcanoes																												
					Gazul						Anastasya			Tarsis			Pipoca					Chica				Hespérides				Almazán			Aveiro	
					1	2	3	4	5	6	7	8	9	10	11	12	13	14	15	16	17	18	19	20	21	22	23	24	25	26	27	28	29	30	31
Dm	Het	De	Ds	*Desmacella inornata* (Bowerbank, 1866)	3		1	1		4				3			2		3	1		10	17		1		14	1		4		10			35
Dm	Het	De	Ds	*Dragmatella aberrans* (Topsent, 1890)										1				2				9	27											
Dm	Het	Ha	Ch	*Cladocroce fibrosa* (Topsent, 1890)															1				3											
Dm	Het	Ha	Ch	*Cladocroce spathiformis* Topsent, 1904*		5													1	1					1									
Dm	Het	Ha	Ch	*Haliclona angulata* (Bowerbank, 1866)							4				8						19	30	12											1	
Dm	Het	Ha	Ch	*Haliclona* cf *fulva* (Topsent, 1893)																										1		1			
Dm	Het	Ha	Ch	*Haliclona pedunculata* (Boury-Esnault, Pansini & Uriz, 1994)*							1				8			2			14	10	14												
Dm	Het	Ha	Ch	*Haliclona utriculus* (Topsent, 1904)*														4	2																
Dm	Het	Ha	Pe	*Petrosia crassa* (Carter, 1876)*			2	2	75	70									3						2		2		3	9		1			
Dm	Het	Ha	Pe	*Petrosia raphida* Boury-Esnault, Pansini & Uriz, 1994															1																
Dm	Het	Ha	Pe	*Petrosia vansoesti* Boury-Esnault, Pansini & Uriz, 1994*																1															
Dm	Het	Me	Hm	*Hamacantha johnsoni* (Bowerbank, 1864)														1								2				1		3		10	
Dm	Het	Me	Hm	*Hamacantha lundbecki* Topsent, 1904															4																
Dm	Het	Me	Hm	*Hamacantha papillata* Vosmaer, 1885										1																		1			
Dm	Het	Me	Hm	*Hamacantha schmidtii* (Carter, 1882)*															4							1						2		10	18
Dm	Het	Pl	Pm	*Weberella verrucosa* Vacelet, 1960																						8									
Dm	Het	Po	Ce	*Coelosphaera cryosi* (Boury-Esnault, Pansini & Uriz, 1994)														1		1			1												
Dm	Het	Po	Ce	*Coelosphaera tubifex* Thomson, 1873*													2	4																	
Dm	Het	Po	Ce	*Forcepia forcipis* (Bowerbank, 1866)*																														2	2
Dm	Het	Po	Ce	*Forcepia luciensis* (Topsent, 1888)							2																								
Dm	Het	Po	Cl	*Cladorhiza abyssicola* Sars, 1872																												2		1	
Dm	Het	Po	Cl	*Lycopodina hypogea* (Vacelet & Boury-Esnault, 1996)			71																												
Dm	Het	Po	Cr	*Anisocrella hymedesmina* Topsent, 1927																								4							
Dm	Het	Po	Cr	*Crella fusifera* Sarà, 1969																			1												
Dm	Het	Po	Cr	*Crella pyrula* (Carter, 1876)											3																				
Dm	Het	Po	Hy	*Hymedesmia koehleri* (Topsent, 1896)																				1											
Dm	Het	Po	Hy	*Hymedesmia mutabilis* (Topsent, 1904)																										1					

Cl	Sc	Or	Fa	Species	Mud volcanoes																										
					Gazul						Anastasya			Tarsis			Pipoca				Chica				Hespérides				Almazán				Aveiro	
					1	2	3	4	5	6	7	8	9	10	11	12	13	14	15	16	17	18	19	20	21	22	23	24	25	26	27	28	29	30	31
Dm	Het	Po	Hy	*Hymedesmia peachii* Bowerbank, 1882																			2								1			
Dm	Het	Po	Hy	*Hymedesmia pennata* Brøndsted, 1932*														1																
Dm	Het	Po	Io	*Iotroata polydentata* (Lundbeck, 1905)*																			1											
Dm	Het	Po	La	*Sceptrella insignis* (Topsent, 1890)																											1			
Dm	Het	Po	Mc	*Mycale lingua* (Bowerbank, 1866)							1																							
Dm	Het	Po	Mi	*Antho erecta* (Ferrer Hernández, 1923)*																1			1											
Dm	Het	Po	Mi	*Antho signata* (Topsent, 1904)																											1			
Dm	Het	Po	Mi	*Clathria campecheae* Hooper, 1996*																										1		1		
Dm	Het	Po	Mx	*Myxilla incrustans* (Johnston, 1842)																										1				
Dm	Het	Po	Mx	*Myxilla rosacea* (Lieberkühn, 1859)				1																										
Dm	Het	Po	Pd	*Podospongia lovenii* Barboza du Bocage, 1869							3							9					14											
Dm	Het	Su	Hl	*Topsentia glabra* (Topsent, 1898)														1					2							1		3		
Dm	Het	Su	Sb	*Rhizaxinella elongata* (Ridley & Dendy, 1886)														1																
Dm	Het	Su	Sb	*Rhizaxinella pyrifera* (Delle Chiaje, 1828)																			5											
Dm	Het	Su	Sb	*Suberites carnosus* (Johnston, 1842)																			1											
Dm	Het	Su	St	*Stylocordyla borealis* (Lovén, 1868)											21			4			33													
Dm	Het	Te	An	*Jaspis* cf *eudermis* Lévi & Vacelet, 1958																								3						
Dm	Het	Te	An	*Jaspis incrustans* (Topsent, 1890)	1	2													1	1											1			
Dm	Het	Te	An	*Jaspis johnstonii* (Schmidt, 1862)		1																			2									
Dm	Het	Te	An	*Jaspis sinuoxea* nov.sp.*															4	1					2									
Dm	Het	Te	Az	*Leiodermatium pfeifferae* (Carter, 1873)																							4							
Dm	Het	Te	Co	*Neoschrammeniella bowerbankii* (Johnson, 1863)															1	4									5		4			
Dm	Het	Te	Ge	*Geodia anceps* (Vosmaer, 1894)																										1				
Dm	Het	Te	Ge	*Geodia* cf *spherastrella* Topsent, 1904*															4															
Dm	Het	Te	Ge	*Geodia megastrella* Carter, 1876*																							1							
Dm	Het	Te	Ge	*Geodia pachydermata* (Sollas, 1886)																									1					
Dm	Het	Te	Ge	*Penares euastrum* (Schmidt, 1868)																								1	4					

Cl	Sc	Or	Fa	Species	Mud volcanoes																													
					Gazul						Anastasya			Tarsis			Pipoca					Chica				Hespérides				Almazán				Aveiro	
					1	2	3	4	5	6	7	8	9	10	11	12	13	14	15	16	17	18	19	20	21	22	23	24	25	26	27	28	29	30	31
Dm	Het	Te	Pa	*Characella pachastrelloides* (Carter, 1876)																					5		3	7		13				
Dm	Het	Te	Pa	*Characella tripodaria* (Schmidt, 1868)																					4			3						
Dm	Het	Te	Pa	*Nethea amygdaloides* (Carter, 1876)																								6		6				
Dm	Het	Te	Pa	*Pachastrella monilifera* Schmidt, 1868																						2								
Dm	Het	Te	Pa	*Pachastrella ovisternata* Lendenfeld, 1894*															3	3						4	6	4	2	2	3			
Dm	Het	Te	Tn	*Thenea muricata* (Bowerbank, 1858)							28			4	9	28		3	30		28	13	80								4		15	124
Dm	Het	Te	To	*Discodermia ramifera* Topsent, 1892*															1						1									
Dm	Het	Te	Tr	*Thrombus abyssi* (Carter, 1873)																								3		2				
Dm	Het	Te	Tt	*Craniella* sp.															3															
Dm	Het	Te	Vu	*Poecillastra compressa* (Bowerbank, 1866)		1		2	25	26									2								1		5		2			
Dm	Het	Te	Vu	*Vulcanella gracilis* (Sollas, 1888)																								1						
Dm	Ke	Di	Dy	*Dysidea fragilis* (Montagu, 1814)			2			1												1	1											
Dm	Ke	Di	Dy	*Pleraplysilla spinifera* (Schulze, 1879)															2															
Dm	Ke	Di	So	*Spongia officinalis* Linnaeus, 1759						1																								
Hx	Ap	Am	Ph	*Pheronema carpenteri* (Thomson, 1869)																					6		3	12		10	80	64	1	5
Hx	Hex	Ly	Ro	*Asconema setubalense* Kent, 1870		11	6	7	20	10			1	1		11	2	1	4	10	2	1	2	9		15					4			
Hx	Hex	Ly	Ro	*Lanuginella cf pupa* Schmidt, 1870*																				1										

Chapter 2

Appendix I: Oligonucleotide primers used to amplify and sequence fragments of the *COI*, *18S* and *28S* markers.

Primer name	Oligonucleotide Sequence (5'- 3')	Source
LCO1490	GGT CAA CAA ATC ATA AAG ATA TTG G	Folmer et al., 1994
HC02198	TAA ACT TCA GGG TGA CCA AAA AAT CA	Folmer et al., 1994
PorCOI2fwd	AATATGNGGGCNCCNGGNATNAC	Xavier et al., 2010
PorCOI2rev	ACTGCCCCCATNGATAAAACAT	Xavier et al., 2010
18S400F	CCT GAG AAA CGG CTA CCA CA	Redmond et al., 2007
18S1080R	CGG TAT CTW ATC GTC TTC G	Redmond et al., 2013
18S830F	TTC GGG ACG TTT ACT TTG	Redmond et al., 2013
18S1350R	CGG GAC TAG TTA GCA GGT TAA	Redmond et al., 2007
18S1200F	TAA TTT GAC TCA ACA CGG G	Redmond et al., 2007
18S1340R	ACT AGT TAG CAG GTT AAG GAC	Redmond et al., 2013
Sp18aF	CCT GCC AGT AGT CAT ATG CTT	Redmond et al., 2013
Sp18gR	CCT TGT TAC GAC TTT TAC TTC CTC	Redmond et al., 2013
28Sa	GAC CCG TCT TGA AGC ACG	Giribet et al., 2006
28SRD5b	CCA CAG CGC CAG TTC TGC TTA C	Giribet et al., 2006

Appendix II: List of taxa used in the phylogenetic analyses and their corresponding *COI*, *18S* and *28S* GenBank accession numbers. Newly accession numbers generated in this study are in bold. Sequences programmed to be included in GenBank, and still lack accession numbers are marked as 'in process'.

Species	COI	18S	28S
Amphimedon compressa	EU237474		-
Amphimedon queenslandica	DQ915601		-
Anaderma rancureli	LN624205		-
Ancorina sp.	HM592744		-
Antarctotetilla leptoderma	KT124328		-
Axinella infundibuliformis	HQ379410		HQ379199
Callipelta sp.	LN624197		-
Callyspongia ramosa	JN242194		-
Callyspongia fallax		EU863812	
Callyspongia plicifera	EU237477	EU702412	-
Calthropella geodioides 1	HM592734		-
Calthropella geodioides 2	HM592705		-
Caminella intuta	HM592740		-
Caminus vulcani	EU442205		-
Chalinula hooperi		DQ927319	
Chalinula molitba		KC902402	
Characella pachastrelloides 1	HM592709		-
Characella sp.	AB453834		-
Cinachyrella apion	HM592667		-
Cinachyrella paterifera	LT628343		-
Cladocroce burapha 1	KY565331		-
Cladocroce burapha 2	KY565328		-
Cladocroce fibrosa	**in process**		-
Cladocroce spathiformis	**in process**	**in process**	-
Cladocroce sp. 1		KC902202	
Cladocroce sp. 2		KT900335	
Craniella cf. *leptoderma*	JX177916		-
Craniella cranium 1	HM592669		-
Cymbaxinella damicornis	in process		-
Dercitus bucklandi	HM592674		-
Discodermia polymorpha	HM592686		-
Discodermia proliferans	KJ494347		-
Erylus aleuticus	EU442201		-
Erylus deficiens	EU442204		-
Erylus discophorus 1	EU442206		-
Erylus discophorus 2	HM592692		-
Erylus expletus	EU442208		-
Erylus granularis	HM592729		-
Erylus mamillaris	EU442207		-
Erylus sp.	HM592687		-
Erylus topsenti	HM592733		-
Exsuperantia sp.	HM592730		-

Species	COI	18S	28S
Geodia angulata	EU442203		-
Geodia atlantica 1	EU442195		-
Geodia atlantica 2	HM592679		-
Geodia barretti 1	KC574389		-
Geodia barretti 2	EU442194		-
Geodia barretti 3	in process		-
Geodia barretti 4	JX999061		-
Geodia californica	EU442200		-
Geodia conchilega	HM592739		-
Geodia cydonium 1	HM592715		-
Geodia cydonium 2	EU442199		-
Geodia gibberosa 1	JX912215		-
Geodia gibberosa 2	JX912214		-
Geodia gibberosa 3	JX912213		-
Geodia gibberosa 4	JX912216		-
Geodia gibberosa 5	JX912211		-
Geodia gibberosa 6	JX912210		-
Geodia gibberosa 7	JX912212		-
Geodia gibberosa 8	JX912208		-
Geodia gibberosa 9	JX912209		-
Geodia hentscheli 1	in process		-
Geodia hentscheli 2	EU442197		-
Geodia macandrewi 1	EU442198		-
Geodia macandrewi 2	in process		-
Geodia megastrella 1	HM592741		-
Geodia megastrella 2	HM592731		-
Geodia megastrella 3	HM592721		-
Geodia neptuni	AY320032		-
Geodia pachydermata	HM592732		
Geodia papyracea	AY561961		-
Geodia parva	HM592690		-
Geodia phlegraei 1	in process		-
Geodia phlegraei 2	EU442196		-
Geodia sp.	HM592680		-
Geodia spherastrella 1	HM592707		-
***Geodia* cf. *spherastrella* 2**	**in process**		-
Geodia vaubani	EU442202		-
Geodia vosmaeri 1	HM592711		-
Geodia vosmaeri 2	HM592722		-
Halichondria panicea		KC902238	
Haliclona amboinensis 1	KX894495	KX894467	-
Haliclona amboinensis 2	KY463320		-
Haliclona plakophila	KX668522	KX668499	-
Haliclona oculata 1	JN242199		-
Haliclona oculata 2	HQ379430		-
Haliclona urceolus	JN242207		-
Haliclona altera	LN850187		-

Species	COI	18S	28S
Haliclona aquaeductus	EF095186		-
Haliclona cinerea	JN242198		-
Haliclona curacaoensis		KC90240	
Haliclona fascigera	KX894499	KC902346	-
Haliclona tubifera	KR707694	KC902356	-
Haliclona xena 1	JN242209		-
Haliclona xena 2	JX999085		-
Haliclona amphioxa	AJ843892		-
Haliclona elegans	JX999087		-
Haliclona simulans 1	JN242200		-
Haliclona simulans 2	JN242201		-
Haliclona sp.E GPM-2011	JN242210		-
Haliclona toxia	JN242206		-
Haliclona vanderlandi	JN242208		-
***Haliclona bouryesnaultae* 1**	**in process**		-
***Haliclona bouryesnaultae* 2**	**in process**		-
***Haliclona bouryesnaultae* 3**	**in process**		-
***Haliclona bouryesnaultae* 4**	**in process**		-
Characella pachastrelloides 2	HM592672		-
Hemigellius fimbriatus	JN242211		-
Hemigellius pilosus	LN850186		-
Homaxinella sp.	LN850197		-
Homaxinella subdola	-		HQ379318
Hymeniacidon perlevis	JX477040		AY618715
Melophlus sp.	HM592688		-
Neamphius huxleyi	HM592682		-
Neoaulaxinia sp. 1	LN624199		-
Neoaulaxinia sp. 2	LN624202		-
Neoaulaxinia sp. 3	LN624198		-
Neoaulaxinia sp. 4	LN624201		-
Neoaulaxinia sp. 5	LN624200		-
Neopetrosia carbonaria		KC901937	
Neopetrosia exigua		KC902135	
Neopetrosia proxima		KC902252	
Neopetrosia seriata	in process		-
Oceanapia sp. A GPM-2011	JN242223		-
Pachymatisma johnstonia 1	EF564337		-
Pachymatisma johnstonia 2	EF564330		-
Pachymatisma johnstonia 3	EF564331		-
Pachymatisma normani 1	EF564322		-
Pachymatisma normani 2	EF564327		-
Penares candidata	HM592719		-
Petrosia crassa	**in process**		-
Petrosia ficiformis 1	JX999088		-
Petrosia ficiformis 2	KR911863		-
Petrosia lignosa		KC901970	
Petrosia raphida	**in process**	**in process**	-

Species	COI	18S	28S
Petrosia sp.		DQ927320	
Petrosia sp. A GPM-2011	JN242214		-
Petrosia sp. B GPM-2011	JN242215		-
Petrosia sp. GPM-2011	JN242219		-
Petrosia sp. E GPM-2011	JN242217		-
Petrosia sp. G GPM-2011	JN242218		-
Petrosiidae sp. A GPM-2011	JN242212		-
Pleroma menoui	LN624206		-
Poecillastra compressa	in process		-
Poecillastra laminaris	KM362735		-
Prosuberites laughlini	AY561960		AY561927
Prosuberites longispinus			HQ379245
Protosuberites denhartogi	KX601191		KX601207
Protosuberites ectyoninus	KX601188		KX601205
Protosuberites incrustans	KX601189		KX601206
Protosuberites mereui	-		KX601212
Protosuberites sp. 1	AY561915		-
Protosuberites sp. 2	KX601204		-
Pseudosuberites hyalinus	LN850222		-
Pseudosuberites nudus	LN850223		-
Pseudosuberites sp.	-		AY561913
Pseudosuberites sulphureus	-		HQ379246
Rhabdastrella cordata	HM592727		-
Rhabdastrella globostellata 1	KY625186		-
Rhabdastrella globostellata 2	HM592673		-
Rhabdastrella globostellata 3	KT180228		-
Rhabdastrella globostellata 4	KY947261		-
Rhabdastrella globostellata 5	KX894502		-
Rhabdastrella intermedia	HM592726		-
Rhabdastrella sp.	HM592676		-
Rhizaxinella sp.	AY561983		AY561910
Spongilla vastus		DQ167166	
Stelletta clarella	HM592736		-
Stelletta dorsigera	HM592750		-
Stelletta grubii	HM592743		-
Stelletta lactea	HM592752		-
Stelletta normani	EU442193		-
Stelletta sp.	HM592751		-
Stelletta tuberosa 1	HM592678		-
Stelletta tuberosa 2	HM592735		-
Stellettinopsis megastylifera 1	FJ711642		-
Stellettinopsis megastylifera 2	AY561980		-
Stryphnus fortis	in process		-
Stryphnus fortis	HM592697		-
Stryphnus ponderosus	HM592685		-
Stylissa carteri	in process		-
Suberites aurantiacus 1	-		KC869577

Species	COI	18S	28S
Suberites aurantiacus 2			AY626316
Suberites carnosus	-		**in process**
Suberites cf. *caminatus*	LN850254		-
Suberites hirsutus	**-**		**in process**
Suberites dandelenae	KY463456		-
Suberites diversicolor 1	KF568963		KF568965
Suberites diversicolor 2	KF568962		-
Suberites diversicolor 3	KF568961		-
Suberites diversicolor 4	KF568960		-
Suberites domuncula	JX999078		AJ620113
Suberites ficus	AJ843891		AY026381
Suberites massa	-		AY618723
Suberites pagurorum	KC869422		HQ379323
Suberites sp. 1	AY561966		-
Suberites sp.2	-		KC869500
Suberites suberia	-		AY618724
Suberites topsenti	LN850246		-
Suberites virgultosa	-		AY618725
Terpios aploos	-		KC869465
Terpios granulosa	-		HQ379250
Terpios hoshinota	-		HQ379250
Thenea levis	HM592717		-
Thenea muricata	HM592677		-
Thenea valdiviae	HM592703		-
Theonella cf. *cupola*	KJ494351		-
Theonella cf. *cylindrica*	KJ494353		-
Theonella deliqua	KJ494355		-
Theonella maricae	KJ494356		-
Theonella mirabilis	LN624208		-
Theonella sp. 1	LN624209		-
Theonella sp. 2	LN624210		-
Theonella sp. 3	KY625187		-
Theonella swinhoei	HM592745		-
Theonella xantha 1	KJ494361		-
Theonella xantha 2	KJ494365		-
Theonella xantha 3	KJ494367		-
Theonella xantha 4	KJ494363		-
Theonella xantha 5	KJ494362		-
Triptolemma intextum	HM592710		-
Vulcanella gracilis	HM592702		-
Xestospongia bergquistia	JN242222		-
Xestospongia bocatorensis		KC902039	
Xestospongia deweerdtae		KX668500	
Xestospongia muta 1	EF095185	KC902281	-
Xestospongia muta 2	NC010211		-
Xestospongia testudinaria	KY947273	KY947244	-

Chapter 3

Appendix I: Porifera species identified by ROV exploration and examining sampled material from 25 stations (see table 1, fig 1). Species are listed alphabetically according to order and family. Numbers in the table indicate number of collected individuals for sampling station (DR= dredge, BV= beam trawl). Missing stations (relative to fig 1; i.e., 25DR, 26DR, 45DR, 46DR) indicate that no sponge was collected. Species identified through ROV observations are indicated by "+". Order abbreviations are as it follows: At= Astrophorida; Dt= Dictyoceratida; Hd= Hadromerida; Hl= Halichondrida; Hp= Haplosclerida; Pc= Poecilosclerida; Sp= Spirophorida; Ly= Lyssacinosida; Ve= Verongida. Family abbreviations are as it follows: An= Ancorinidae; Ca= Calthropellidae; Ge= Geodiidae; Pa= Pacastrellidae; Th= Theneidae; Vu= Vulcanellidae; Dy= Dysideidae; Ir= Irciniidae; Spo= Spongiidae; Cl= Clionaidae; He= Hemiasterellidae; Pol= Polymastiidae; Spi= Spirastrellidae; St= Stelligeridae; Su= Suberitidae; Teh= Tethyidae; Ti= Timeidae; Ax= Axinellidae; Bu= Buvaridae; Di= Dictyonellidae; Hal= Halichondrida; Cha= Chalinidae; Ni= Niphatidae; Pe= Petrosiidae; Ros= Rossellidae; Ac= Acarnidae; Cho= Chondropsidae; Co= Coelosphaeridae; Cra= Crambeidae; Cre= Crellidae; De= Desmacellidae; Ham= Hamacanthidae; Hym= Hymedesmiidae; Mic= Microcionidae; Myx= Myxillidae; Pod= Podospongiidae; Ra= Raspailiidae; Ted= Tedaniidae; Tei: Tetillidae; Ia= Ianthellidae.

Order	Family	Species	Sampling stations																			
			ROV	02 DR	05 DR	07 DR	10 BV	11 BV	12 BV	13 BV	14 BV	15 BV	16 BV	17 BV	18 DR	20 DR	21 BV	27 BV	29 DR	30 BV	32 BV	33 BV	41 BV	44 DR
At	An	*Dercitus plicatus*		5		1																	1	
At	An	*Jaspis eudermis*					1																	
At	An	*Jaspis incrustans*											2					2						
At	An	*Stryphnus mucronatus*											2											
At	An	*Stryphnus ponderosus*	+																					
At	Ca	*Calthropella recondita*										1												
At	Ge	*Caminella intuta*																					1	
At	Ge	*Caminus vulcani*				1																		
At	Ge	*Erylus discophorus*							1			1	1										2	

Order	Family	Species	Sampling stations																						
			ROV	02 DR	05 DR	07 DR	10 BV	11 BV	12 BV	13 BV	14 BV	15 BV	16 BV	17 BV	18 DR	20 DR	21 BV	27 BV	29 DR	30 BV	32 BV	33 BV	41 BV	44 DR
At	Ge	*Penares helleri*										1												
At	Pa	*Characella tripodaria*																					1	
At	Pa	*Pachastrella monilifera*					1											1					1	
At	Th	*Thenea muricata*						1						1										
At	Vu	*Poecillastra compressa*							1		2		6	2				1			5		6	5
At	Vu	*Vulcanella aberrans*						1										2					5	
Dt	Dy	*Dysidea* cf. *fragilis*																		1			1	1
Dt	Ir	*Sarcotragus* cf. *pipetta*																1						
Dt	Spo	*Spongia officinalis*											1											
Hd	Cl	*Cliona rhodensis*			1																			
Hd	Cl	*Cliona viridis*		5	2																			
Hd	He	*Hemiasterella elongata*															1	1			2			
Hd	Pol	*Polymastia polytylota*																					1	
Hd	Pol	*Polymastia spp*															1							
Hd	Sp	*Diplastrella bistellata*				1																		
Hd	St	*Stelligera rigida*									3													
Hd	St	*Stelligera stuposa*									2													
Hd	Su	*Aaptos aaptos*									1								1					
Hd	Su	*Prosuberites longispinus*		1	1																			
Hd	Su	*Rhizaxinella elongata*									5	7										1	3	
Hd	Su	*Rhizaxinella gracilis*									1												1	
Hd	Su	*Suberites carnosus*				1													1					6
Hd	Su	*Terpios fugax*	+																					
Hd	Teh	*Tethya aurantium*										1				1							1	
Hd	Ti	*Timea unistellata*		6																				
Hl	Ax	*Axinella alborani* sp.nov.			3	2					2	6							4			14	1	2
Hl	Ax	*Axinella* cf. *cinnamomea*									1												1	

Order	Family	Species	Sampling stations																				
			ROV	02 DR	05 DR	07 DR	10 BV	11 BV	12 BV	13 BV	14 BV	15 BV	16 BV	17 BV	18 DR	20 DR	21 BV	27 BV	29 DR	30 BV	32 BV	33 BV	41 BV	44 DR
Hl	Ax	*Axinella damicornis*	+																					
Hl	Ax	*Axinella egregia*																				3	1	
Hl	Ax	*Axinella polypoides*																					1	
Hl	Ax	*Axinella pumila*									2													
Hl	Ax	*Axinella salicina*	+																					
Hl	Ax	*Axinella spatula* sp. nov.									3	9					5					4	2	
Hl	Ax	*Axinella vellerea*			2								1				1			1	1	1	3	9
Hl	Ax	*Phakellia robusta*						2			2										1			3
Hl	Ax	*Phakellia ventilabrum*																			2	3	1	4
Hl	Bu	*Bubaris vermiculata*																	2					1
Hl	Bu	*Rhabdobaris implicata*									1													
Hl	Di	*Acanthella acuta*																						1
Hl	Di	*Dictyonella incisa*								1														
Hl	Hal	*Spongosorites intricatus*											1										1	
Hp	Cha	*Dendroxea lenis*				2																		
Hp	Cha	*Haliclona angulata*		2								1							1	1				
Hp	Cha	*Haliclona* cf. *cinerea*								1				1										
Hp	Cha	*Haliclona* cf. *perlucida*				1																		
Hp	Cha	*Haliclona* cf. *subtilis*		2																				
Hp	Cha	*Haliclona fulva*				1																		
Hp	Cha	*Haliclona lacazei*											1											
Hp	Cha	*Haliclona mucosa*					1													1	1	1	1	
Hp	Ni	*Gelliodes fayalensis*				1																		
Hp	Pe	*Petrosia ficiformis*			1																			
Ly	Ros	*Asconema setubalense*	+																					

Order	Family	Species	Sampling stations																			
			ROV	02 DR	05 DR	07 DR	10 BV	11 BV	12 BV	13 BV	14 BV	15 BV	16 BV	17 BV	18 DR	20 DR	21 BV	27 BV	29 DR	30 BV	32 BV	33 BV	41 BV	44 DR
Pc	Ac	*Iophon nigricans*																	1					
Pc	Cho	*Batzella inops*				1																		
Pc	Co	*Lissodendoryx lundbecki*															2							
Pc	Cra	*Crambe tailliezi*		12																				
Pc	Cre	*Crella elegans*														1								
Pc	Cre	*Crella pyrula*																						1
Pc	Des	*Desmacella annexa*											1											
Pc	Des	*Desmacella inornata*											1				3			2			3	9
Pc	Des	*Dragmatella aberrans*								1		2	1	1								18		
Pc	Ham	*Hamacantha falcula*																	1					1
Pc	Hym	*Hymedesmia paupertas*																						3
Pc	Hym	*Hymedesmia peachi*				2																		
Pc	Hym	*Phorbas fictitius*														1								
Pc	Hym	*Phorbas topsenti*				1																		
Pc	Mic	*Antho involvens*		2		1																		
Pc	Myx	*Myxilla rosacea*														1								
Pc	Pod	*Podospongia lovenii*			4																			8
Pc	Ra	*Aulospongus spinosus*			1													1						
Pc	Ra	*Endectyon filiformis* sp. nov.															1							
Pc	Ra	*Endectyon delaubenfelsi*									2													
Pc	Ra	*Eurypon cinctum*				2																		
Pc	Ra	*Eurypon coronula*									1													
Pc	Ra	*Eurypon lacazei*				1																		
Pc	Ted	*Tedania* spp.													1									
Sp	Tei	*Craniella cranium*									1													
Ve	Ia	*Hexadella racovitzai*	+																					

Appendix II: Porifera species hitherto recorded from the Alboran Island and its surrounding bathyal bottoms. Species are listed alphabetically according to class, order, family, and species name.

Class CALCAREA
Order Clathrinida
Family Clathrinidae
Clathrina coriacea (Montagu, 1818)
Class DEMOSPONGIAE
Order Agelasida
Family Agelasidae
Agelas oroides (Schmidt, 1864)
Order Astrophorida
Family Ancorinidae
Dercitus (Stoeba) plicatus (Schmidt, 1868)
Jaspis eudermis Lévi & Vacelet, 1958
Jaspis incrustans (Topsent, 1890)
Jaspis johnstonii (Schmidt, 1862)
Stelletta hispida (Buccich, 1886)
Stelletta mediterranea (Topsent, 1893)
Stryphnus mucronatus (Schmidt, 1868)
Stryphnus ponderosus (Bowerbank, 1866)
Family Calthropellidae
Calthropella (Calthropella) pathologica (Schmidt, 1868)
Calthropella (Corticellopsis) recondita Pulitzer-Finali, 1983
Family Geodiidae
Caminella intuta (Topsent, 1892)
Caminus vulcani Schmidt, 1862
Erylus discophorus (Schmidt, 1862)
Erylus papulifer Pulitzer-Finali, 1983
Geodia anceps (Vosmaer, 1894)
Geodia cydonium (Jameson, 1811)
Penares candidata (Schmidt, 1868)
Penares helleri (Schmidt, 1864)
Family Pachastrellidae
Characella tripodaria (Schmidt, 1868)
Pachastrella monilifera Schmidt, 1868
Family Theneidae
Thenea muricata (Bowerbank, 1858)
Family Thoosidae
Alectona millari Carter, 1879
Delectona alboransis Rosell, 1996
Family Vulcanellidae
Poecillastra compressa (Bowerbank, 1866)
Vulcanella aberrans (Maldonado & Uriz, 1996)
Vulcanella gracilis (Sollas, 1888)
Order Chondrosida
Family Chondrillidae
Chondrosia reniformis Nardo, 1847
Order Dendroceratida
Family Darwinellidae
Aplysilla sulfurea Schulze, 1878
Darwinella viscosa Boury-Esnault, 1971
Family Dictyodendrillidae
Spongionella pulchella (Sowerby, 1804)
Order Dictyoceratida
Family Dysideidae
Dysidea fragilis (Montagu, 1818)
Pleraplysilla reticulata Maldonado & Uriz, 1999
Pleraplysilla spinifera (Schulze, 1879)
Family Irciniidae
Ircinia dendroides (Schmidt, 1862)
Ircinia variabilis (Schmidt, 1862)
Sarcotragus fasciculatus (Pallas, 1766)
Sarcotragus pipetta (Schmidt, 1868)
Sarcotragus spinosulus Schmidt, 1862
Family Spongiidae
Spongia (Spongia) agaricina Pallas, 1766
Spongia (Spongia) nitens (Schmidt, 1862)
Spongia (Spongia) officinalis Linnaeus, 1759
Spongia spinosula (Schmidt, 1868)
Spongia (Spongia) virgultosa (Schmidt, 1868)
Family Thorectidae
Fasciospongia cavernosa (Schmidt, 1862)
Hyrtios collectrix (Schulze, 1880)
Order Hadromerida
Family Clionaidae
Cliona celata Grant, 1826
Cliona rhodensis Rützler & Bromley, 1981
Cliona viridis (Schmidt, 1862)
Dotona pulchella mediterranea Rosell & Uriz, 2002
Pione vastifica (Hancock, 1849)
Spiroxya levispira (Topsent, 1898)
Family Hemiasterellidae
Hemiasterella elongata Topsent, 1928
Paratimea constellata (Topsent, 1893)
Family Polymstiidae
Polymastia mamillaris (Montagu, 1806)
Polymastia polytylota Vacelet, 1969
Polymastia spp
Pseudotrachya hystrix (Topsent, 1890)
Family Spirastrellidae
Diplastrella bistellata (Schmidt, 1862)
Spirastrella cunctatrix Schmidt, 1868
Family Stelligeridae
Stelligera rigida (Montagu, 1818)
Stelligera stuposa (Ellis & Solander, 1786)
Family Suberitidae
Aaptos aaptos (Schmidt, 1864)

Prosuberites longuispinus Topsent, 1893
Protosuberites rugosus (Topsent, 1893)
Pseudosuberites hyalinus (Ridley & Dendy, 1886)
Rhizaxinella elongata (Ridely & Dendy, 1886)
Rhizaxinella gracilis (Lendenfeld, 1898)
Suberites carnosus (Johnston, 1842)
Suberites domuncula (Olivi, 1792)
Pseudosuberites sulphureus (Bowerbank, 1866)
Terpios fugax Duchassaing & Michelotti, 1864
Family Tethyidae
Tethya aurantium (Pallas, 1766)
Family Timeidae
Timea cumana Pulitzer-Finali, 1978
Timea unistellata (Topsent, 1892)

Order Halichondrida
Family Axinellidae
Axinella alboranica sp. nov.
Axinella cf. *cinnamomea* (Nardo, 1833)
Axinella damicornis (Esper, 1974)
Axinella egregia sensu Topsent, 1892
Axinella polypoides Schmidt, 1862
Axinella pumila Babic, 1922
Axinella salicina Schmidt, 1868
Axinella spatula sp. nov.
Axinella vellerea Topsent, 1904
Axinella verrucosa (Esper, 1794)
Phakellia robusta Bowerbank, 1866
Phakellia ventilabrum (Linnaeus, 1767)
Family Bubaridae
Bubaris vermiculata (Bowerbank, 1866)
Cerbaris alborani (Boury-Esnault, Pansini & Uriz, 1994)
Rhabdobaris implicata Pulitzer-Finali, 1983
Family Dictyonellidae
Acanthella acuta Schmidt, 1862
Dictyonella incisa (Schmidt, 1880)
Dictyonella marsilii (Topsent, 1893)
Family Halichondriidae
Axinyssa aurantiaca (Schmidt, 1864)
Ciocalypta penicillus Bowerbank, 1862
Ciocalypta porrecta (Topsent, 1928)
Halichondria (Halichondria) bowerbanki Burton, 1930
Halichondria (Halichondria) panicea (Pallas, 1766)
Halichondria (Halichondria) semitubulosa Lieberkühn, 1859
Hymeniacidon perlevis (Montagu, 1818)
Spongosorites flavens Pulitzer-Finali, 1983
Spongosorites intricatus (Topsent, 1892)

Order Haploslcerida
Family Callyspongiidae
Siphonochalina balearica Ferrer-Hernandez, 1916
Siphonochalina coriacea Schmidt, 1868
Family Chalinidae
Chalinula limbata (Montagu, 1818)
Dendroxea lenis (Topsent, 1892)
Haliclona (Gellius) angulata (Bowerbank, 1866)
Haliclona (Gellius) flagellifera (Ridley & Dendy, 1886)
Haliclona (Gellius) lacazei (Topsent, 1893)
Haliclona (Halichoclona) fulva (Topsent, 1893)
Haliclona (Halichoclona) perlucida (Griessinger, 1971)
Haliclona (Haliclona) reptans (Griessinger, 1971)
Haliclona (Haliclona) simulans (Johnston, 1842)
Haliclona (Reniera) aquaeductus (Schmidt, 1862)
Haliclona (Reniera) cinerea (Grant, 1826)
Haliclona (Reniera) citrina (Topsent, 1892
Haliclona (Reniera) subtilis Griessinger, 1971
Haliclona (Soestella) implexa (Schmidt, 1868)
Haliclona (Soestella) mucosa (Griessinger, 1971)
Haliclona pocilliformis (Griessinger, 1971)
Family Niphatidae
Gelliodes fayalensis Topsent, 1892
Family Petrosiidae
Petrosia (Petrosia) ficiformis (Poiret, 1789)

Order Poecilosclerida
Family Acarnidae
Acarnus tortilis Topsent, 1892
Iophon hyndmani (Bowerbank, 1858)
Iophon nigricans (Bowerbank, 1858)
Family Chondropsidae
Batzella inops (Topsent, 1891)
Family Coelosphaeridae
Coelosphaera (Histodermion) cryosi (Boury-Esnault, Pansini & Uriz, 1994)
Forcepia (Leptolabis) brunnea (Topsent, 1904)
Forcepia (Leptolabis) luciensis (Topsent, 1888)
Forcepia (Leptolabis) megachela (Maldonado, 1992)
Lissodendoryx (Lissodendoryx) isodictyalis (Carter, 1882)
Lissodendoryx (Lissodendoryx) lundbecki Topsent, 1913

Family Crambeidae
Crambe crambe (Schmidt, 1862)
Crambe tailliezi Vacelet & Boury-Esnault, 1982
Crambe tuberosa Maldonado & Benito, 1991
Family Crellidae
Crella (Crella) elegans (Schmidt, 1862)
Crella (Grayella) pulvinar (Schmidt, 1868)
Crella (Pytheas) sigmata Topsent, 1925
Crella (Yvesia) pyrula (Carter, 1876)
Crella (Yvesia) rosea (Topsent, 1892)
Family Desmacellidae
Biemna parthenopea Pulitzer-Finali, 1978
Biemna variantia (Bowerbank, 1858)
Desmacella annexa Schmidt, 1870
Desmacella inornata (Bowerbank, 1866)
Dragmatella aberrans (Topsent, 1890)
Family Desmacididae
Desmacidon fruticosum (Montagu, 1818)
Family Esperiopsidae
Esperiopsis fucorum (Esper, 1794)
Ulosa stuposa (Esper, 1794)
Family Hamacanthidae
Hamacantha (Vomerula) falcula (Bowerbank, 1874)
Family Hymedesmiidae
Hemimycale columella (Bowerbank, 1874)
Hymedesmia (Hymedesmia) baculifera (Topsent, 1901)
Hymedesmia (Hymedesmia) pansa Bowerbank, 1882
Hymedesmia (Hymedesmia) paupertas (Bowerbank, 1866)
Hymedesmia (Hymesdemia) peachi Bowerbank, 1882
Hymedesmia (Stylopus) coriacea (Fristedt, 1885)
Phorbas dives (Topsent, 1891)
Phorbas fibulatus (Topsent, 1893)
Phorbas fictitius (Bowerbank, 1866)
Phorbas mercator (Schmidt, 1868)
Phorbas plumosus (Montagu, 1818)
Phorbas tenacior (Topsent, 1925)
Phorbas topsenti Vacelet & Perez, 2008
Family Latrunculiidae
Latrunculia (Biannulata) citharistae Vacelet, 1969
Sceptrella insignis (Topsent, 1890)
Family Microcionidae
Antho (Acarnia) cf. novizelanica (Ridley & Duncan, 1881)
Antho (Antho) involvens (Schmidt, 1864)
Clathria (Clathria) coralloides (Scopoli, 1772)
Clathria (Microciona) armata (Bowerbank, 1862)
Clathria (Microciona) duplex Sarà, 1958
Clathria (Microciona) gradalis Topsent, 1925
Clathria (Microciona) spinarcus (Carter & Hope, 1889)
Family Mycalidae
Mycale (Aegogropila) rotalis (Bowerbank, 1874)
Mycale (Aegogropila) syrinx (Schmidt, 1862)
Mycale (Carmia) macilenta (Bowerbank, 1866)
Mycale (Paresperella) serrulata Sarà & Siribelli, 1960
Family Myxillidae
Myxilla (Myxilla) rosacea (Lieberkühn, 1859)
Family Podospongiidae
Podospongia lovenii Bocage, 1869
Family Raspailiidae
Aulospongus spinosus (Topsent, 1927)
Endectyon (Endectyon) filiformis sp. nov.
Endectyon (Endectyon) delaubenfelsi Burton, 1930
Eurypon cinctum Sarà, 1960
Eurypon coronula (Bowerbank, 1874)
Eurypon lacazei (Topsent, 1891)
Raspailia agnata (Topsent, 1896)
Family Tedaniidae
Tedania (Tedania) anhelans (Vio in Olivi, 1792)
Tedania spp
Order Spirophorida
Family Tetillidae
Craniella cranium (Müller, 1776)
Order Verongida
Family Aplysinidae
Aplysina aerophoba Nardo, 1833
Aplysina cavernicola (Vacelet, 1959)
Family Ianthellidae
Hexadella racovitzai Topsent, 1896
Class HEXACTINELLIDA
Order Lyssacinosida
Family Rossellidae
Asconema setubalense Kent, 1870
Class HOMOSCLEROMORPHA
Order Homosclerophorida
Family Oscarellidae
Oscarella lobularis (Schmidt, 1862)
Family Plakinidae
Plakina monolopha Schulze, 1880
Plakina trilopha Schulze, 1880
Plakinastrella mixta Maldonado, 1992

Chapter 4

Appendix I: List of bibliographic sponge records from 1870 to present day. It comprises 18 studied areas from Macaronesia, southern Lusitanian, Gulf of Cádiz, Western and Central Mediterranean regions. Rows comprise the sponge species ordered by families. Within each family, genera and species names are alphabetically ordered. Columns represent locations of each record, depth range (m) and source data. The symbol "*" next to a depth range indicates approximate depth data. Sites for records are organized by ocean areas, from West to East, and within each area, references are order by publication year of the record, then by author last name.

Appendix I in Chapter 4 consists of an Excel file too big to fit in the appendix section of this volume and has been uploaded to Google Drive. Please follow this link to access the document:
https://drive.google.com/drive/folders/1xrYO42HBU9hom2UiwysB7ev5ZZx3g63a?usp=sharing

Appendix II: List of the Mediterranean and Atlantic deep-sea biogeographical areas considered in the presence/absence matrix of sponge species for the study of the biogeographic affinities across an Atlantic-Mediterranean gradient. It details the names of area, the area codes used to present results in graphs (with Mediterranean codes area ending with '-M' and Atlantic those ending with '-A') and the bibliographic references from which the sponge species records were extracted. References called OCEANA-2011/2013/2015/2016 indicate records from sponge samples retrieved during oceanographic campaigns performed by NGO OCEANA in 2011, 2013, 2015 and 2016 (further addressed in Chapter 5).

Area	Code	References
Azores	A-A	(Ridley & Dendy, 1887; Topsent, 1890, 1892, 1896, 1901, 1904b, 1913; Stephens, 1915; Topsent, 1924, 1928; Lévi & Vacelet, 1958; Tabachnick & Menshenina, 2007; Van Soest et al., 2010; Cárdenas et al., 2018; Carvalho & Pisera, 2019)
South Azores Banks	AB-A	(Cárdenas et al., 2018; Carvalho et al., 2020)
Cape Verde	CV-A	(Ridley & Dendy, 1887; Schulze, 1887; Sollas, 1888; Topsent, 1904a, 1928; Van Soest et al., 2012, 2013, 2014; Boury-Esnault et al., 2017; Hestetun et al., 2017)
Canary Islands	C-A	(Topsent, 1928, 1929; Burton, 1954; Weerdt & Van Soest, 1986; Samaai et al., 2006; Van Soest et al., 2013; Carvalho et al., 2015; Hestetun et al., 2017; Carvalho & Pisera, 2019; Carvalho et al., 2020)
Madeira	Ma-A	(Topsent, 1928; Weerdt & Van Soest, 1986; Samaai et al., 2006; Carvalho et al., 2015; Hestetun et al., 2017; Carvalho & Pisera, 2019)
Morocco	Mo-A	(Topsent, 1928; Barthel et al., 1996)
Lusitanian Banks	LB-A	(Kent, 1870; Poléjaeff, 1884; Topsent, 1928; Boury-Esnault et al., 2015; Cristobo et al., 2015; Carvalho et al., 2020)
Gulf of Cádiz	GC-A	(Thomson, 1873; Carter, 1876; Schulze, 1887; Sollas, 1888; Topsent, 1895; Arnesen, 1920; Topsent, 1928; Boury-Esnault et al., 1994; Van Soest et al., 2013, 2014)
Mud volcanoes	MV-A	(Díaz del Río et al., 2014; Chevaldonné et al., 2015; Sitjà et al., 2019; González-García et al., 2020)
Alboran Sea	Al-M	(Topsent, 1928; Vacelet, 1961; Templado et al., 1986; Boury-Esnault et al., 1994; Aguilar et al., 2011; Pardo et al., 2011; de la Torriente et al., 2014; Sitjà & Maldonado, 2014; Boury-Esnault et al., 2015) OCEANA-2011
Balearic Sea	B-M	(Uriz & Rosell, 1990; Maldonado et al., 2015; Boury-Esnault et al., 2017; Santín et al., 2018) OCEANA-2013
Gulf of Lion	GL-M	(Topsent, 1900, 1928; Vacelet, 1960, 1969, 1976; Uriz, 1981, 1982, 1983, 1984; Lent et al., 1987; Lastras et al., 2016; Boury-Esnault et al., 2017; Fourt et al., 2017; Hestetun et al., 2017)
Ligurian Sea	L-M	(Topsent, 1928, 1934, 1936; Vacelet, 1960, 1969; Pulitzer-Finali, 1983; Pansini & Musso, 1991; Bakran-Petricioli et al., 2007; Boury-Esnault et al., 2017; Fourt et al., 2017)
West Corsica	C-M	(Vacelet, 1969; Pansini, 1987a; Chevaldonné et al., 2015; Boury-Esnault et al., 2017; Fourt et al., 2017)
East Tyrrhenian Sea	T-M	(Vosmaer, 1894; Topsent, 1928; Magnino et al., 1999; Bakran-Petricioli et al., 2007; Aguilar et al., 2011; Pisera & Vacelet, 2011; Bertolino et al., 2019; Cardone et al., 2019)
Sicily Strait	S-M	(Topsent, 1928; Vacelet, 1961; Zibrowius & Taviani, 2005; Aguilar et al., 2011; Bo et al., 2012; Calcinai et al., 2013; Taviani et al., 2015; Taviani et al., 2017; Bertolino et al., 2019). OCEANA-2015, 2016
Gulf of Taranto	GT-M	(Pulitzer-Finali, 1983; Tursi et al., 2004; Longo et al., 2005; Schönberg & Beuck, 2007; Beuck et al., 2010; Mastrototaro et al., 2010; Vertino et al., 2010; Boury-Esnault et al., 2017)
Adriatic Sea	A-M	(Babiç, 1922; Pansini, 1987b; D'Onghia et al., 2015; Taviani et al., 2015).

References to appendix II:

Aguilar, R., López Correa, M., Calcinai, B., Pastor, X. and García, S. (2011) First records of *Asbestopluma hypogea* Vacelet and Boury-Esnault, 1996 (Porifera, Demospongiae Cladorhizidae) on seamounts and in bathyal settings of the Mediterranean Sea. *Zootaxa,* 2925, 33-40.

Arnesen, E. (1920) Spongia. Report on the Scientific Results of the "Michael Sars" North Atlantic Deep-Sea Expedition, 1910. 3(2), 1-29.

Babiç, K. (1922) Monactinellida und Tetractinellida des Adriatischen Meeres. *Zoologische Jahrbücher, Abteilung für Systematik, Geographie und Biologie der Tiere*, 46(2), 217-302.

Bakran-Petricioli, T., Vacelet, J., Zibrowius, H., Petricioli, D., Chevaldonné, P. and Rađa, T. (2007) New data on the distribution of the 'deep-sea' sponges *Asbestopluma hypogea* and *Oopsacas minuta* in the Mediterranean Sea. *Marine Ecology,* 28(suppl.1), 10-23.

Barthel, D., Tendal, O. S. and Thiel, H. (1996) A wandering population of the Hexactinellid sponge *Pheronema carpenteri* on the continental slope off Morocco, Northwest Africa. *Pubblicazioni della Stazione Zoologica di Napoli: Marine Ecology,* 17(4), 603-616.

Beuck, L., Freiwald, A. and Taviani, M. (2010) Spatiotemporal bioerosion patterns in deep-water scleractinians from off Santa Maria di Leuca (Apulia, Ionian Sea). *Deep-Sea Research Part II: Topical Studies in Oceanography,* 57, 458-470.

Bo, M., Bertolino, M., Bavestrello, G., Canese , S., Giusti, M., Angiolillo, M., Pansini, M. and Taviani, M. (2012) Role of deep sponge grounds in the Mediterranean Sea: a case study in southern Italy. *Hydrobiologia,* 687(1), 163-177.

Boury-Esnault, N., Pansini, M. and Uriz, M. J. (1994) Spongiaires bathyaux de la mer d'Alboran et du golfe ibéro-marocain. *Mémoires du Muséum National d'Histoire Naturelle,* 1601-174.

Boury-Esnault, N., Vacelet, J., Dubois, M., Goujard, A., Fourt, M., Pérez, T. and Chevaldonné, P. (2017) New hexactinellid sponges from deep Mediterranean canyons. *Zootaxa,* 4236, 118-134.

Boury-Esnault, N., Vacelet, J., Reiswig, H. M., Fourt, M., Aguilar, R. and Chevaldonné, P. (2015) Mediterranean hexactinellid sponges, with the description of a new *Sympagella* species (Porifera, Hexactinellida). *Journal of the Marine Biological Association of the United Kingdom,* 95 (Special Issue 07), 1353-1364.

Burton, M. (1954) Sponges. The "Rosaura" Expedition. *Bulletin of the British Museum (Natural History),* Zoology, 2(6), 215-239.

Calcinai, B., Moratti, V., Martinelli, M., Bavestrello, G. and Taviani, M. (2013) Uncommon sponges associated with deep coral bank and maerl habitats in the Strait of Sicily (Mediterranean Sea). *Italian Journal of Zoology,* 80(3), 412-423.

Cárdenas, P., Vacelet, J., Chevaldonné, P., Pérez, T. and Xavier, J. R. (2018) From marine caves to the deep sea, a new look at *Caminella* (Demospongiae, Geodiidae) in the Atlanto-Mediterranean region. *Zootaxa,* 4466(1), 174-196.

Carter, H. J. (1876) Descriptions and figures of deep-sea sponges and their spicules, from the Atlantic Ocean, dredged up on board H.M.S. "Porcupine", chiefly in 1869 (concluded). *Annals and Magazine of Natural History,* 4(18), 225-479.

Carvalho, F. C., Pomponi, S. A. and Xavier, J. R. (2015) Lithistid sponges of the upper bathyal of Madeira, Selvagens and Canary Islands, with description of a new species of *Isabella*. *Journal of the Marine Biological Association of the United Kingdom,* 95(7), 1287-1296.

Chevaldonné, P., Pérez, T., Crouzet, J.-M., Bay-Nouailhat, W., Bay-Nouailhat, A., Fourt, M., Almón, B., Pérez, J., Aguilar, R. and Vacelet, J. (2015) Unexpected records of 'deep-sea' carnivorous sponges *Asbestopluma hypogea* in the shallow NE Atlantic shed light on new conservation issues. *Marine Ecology,* 36(3), 475-484.

Cristobo, J., Ríos, P., Pomponi, S. A. and Xavier, J. (2015) A new carnivorous sponge, *Chondrocladia robertballardi* sp. nov. (Porifera: Cladorhizidae) from two north-east Atlantic seamounts. *Journal of the Marine Biological Association of the United Kingdom,* 95(7), 1345-1352.

D'Onghia, G., Capezzuto, F., Cardone, F., Carlucci, R., Carluccio, A., Chimienti, G., Corriero, G., Longo, C., Maiorano, P., Mastrototaro, F., Panetta, P., Rosso, A., Sanfilippo, R., Sion, L. and Tursi, A. (2015) Macro- and megafauna recorded in the submarine Bari Canyon (southern Adriatic, Mediterranean Sea) using different tools. *Mediterranean marine science,* 16(1), 180-196.

de la Torriente, A., Aguilar, R., Serrano, A., García, S., Fernández, L. M., García-Muñoz, M., Punzón, A., Arcos, J. M. and Sagarminaga, R. Sur de Almería - Seco de los Olivos. Proyecto LIFE+ INDEMARES. A. y. M. A. Fundación Biodiversidad del Ministerio de Agricultura. (2014).

Díaz del Río, V., Bruque, G., Fernández-Salas, L. M., Rueda, J. L., González, E., López, N., Palomino, D., López, F. J., Farias, C., Sánchez, R., Vázquez, J. T., Rittierott, C. C., Fernández, A., Marina, P., Luque, V., Oporto, T., Sánchez, O., García, M., Urra, J., Bárcenas, P., Jiménez, M. P., Sagarminaga, R. and Arcos, J. M. Volcanes de fango del golfo de Cádiz, Proyecto LIFE + INDEMARES. Fundación Biodiversidad del Ministerio de Agricultura, Alimentación y Medio Ambiente. (2014)

Fourt, M., Goujard, A., Pérez, T. and Chevaldonné, P. (2017) Guide de la faune profonde de la mer Méditerranée. Explorations des roches et des canyons sous-marins des côtes françaises. *Patrimoines naturels. Publications scientifiques du Muséum national d'Histoire naturelle Paris,* 751-184.

Hestetun, J. T., Tompkins-Macdonald, G. and Rapp, H. T. (2017) A review of carnivorous sponges (Porifera: Cladorhizidae) from the Boreal North Atlantic and Arctic. *Zoological Journal of the Linnean Society,* 181(1), 1-69.

Kent, S. (1870) On two new Siliceous Sponges taken in the late Dredging-Expedition of the Yacht 'Norma' off the Coasts of Spain and Portugal. *Annals and Magazine of Natural History,* (4) 6(33), 217-224.

Lastras, G., Canals, M., Ballesteros, E., Gili, J.-M. and Sanchez-Vidal, A. (2016) Cold-Water Corals and Anthropogenic Impacts in La Fonera Submarine Canyon Head, Northwestern Mediterranean Sea. *PLoS One,* 11(5), e0155729.

Lent, F. v., de Weerdt, W. H., Vacelet, J. and Boury-Esnault, N. (1987) The Haplosclerid sponge fauna of Banyuls-sur-Mer (Mediterranean), with a description of a new species. *In:* J. Vacelet and N. Boury-Esnault (Eds), *Taxonomy of Porifera,* G13. Springer-Verlag, Berlin, Heidelberg, pp. 125-148.

Lévi, C. and Vacelet, J. (1958) Eponges récoltées dans l'Atlantique Oriental par le "President Theodore Tissier" (1955-1956). *Revue des Travaux de l'Institut des Pêches Maritimes,* 22(2), 225-246.

Longo, C., Mastrototaro, F. and Corriero, G. (2005) Sponge fauna associated with a Mediterranean deep-sea coral bank. *Journal of the Marine Biological Association of the United Kingdom,* 85(06), 1341-1352.

Magnino, G., Gravina, M. F., Righini, P., Serena, F. and Pansini, M. (1999) Due demosponge Lithistidi nuove per i mari italiani. *Biologia marina mediterranea,* 6(1), 391-393.

Maldonado, M., Aguilar, R., Blanco, J., García, S., Serrano, A. and Punzón, A. (2015) Aggregated clumps of Lithistid sponges: A singular, reef-Like bathyal habitat with relevant paleontological connections. *PLoS One,* 10(5), e0125378.

Mastrototaro, F., D'Onghia, G., Corriero, G., Matarrese, A., Maiorano, P., Panetta, P., Gherardi, M., Longo, C., Rosso, A., Sciuto, F., Sanfilippo, R., Gravili, C., Boero, F., Taviani, M. and Tursi, A. (2010) Biodiversity of the white coral bank off Cape Santa Maria di Leuca (Mediterranean Sea): An update. *Deep-Sea Research Part II: Topical Studies in Oceanography,* 57(5-6), 412-430.

Pansini, M. (1987a) Littoral demosponges from the banks of the straits of Sicily and the Alboran Sea. *In:* J. Vacelet and N. Boury-Esnault (Eds), *Taxonomy of Porifera,* G13. Springer-Verlag, Berlin, Heidelberg, pp. 149-186.

Pansini, M. (1987b) Report on a collection of Demospongiae from soft bottoms of the Eastern Adriatic Sea. *In:* W. C. Jones (Ed), *European contributions to the taxonomy of sponges,* 1. Publications of the Sherkin Island Marine Station, pp. 41-53.

Pansini, M. and Musso, B. (1991) Sponges from trawl-exploitable bottoms of Ligurian and Thyrrhenian seas: distribution and ecology. *Pubblicazioni della Stazione Zoologica di Napoli: Marine Ecology,* 12(4), 317-329.

Pardo, E., Aguilar, R., García, S., de la Torriente, A. and Ubero, J. (2011) Documentación de arrecifes de corales de agua fría en el Mediterráneo occidental (Mar de Alborán). *Chronica Naturae,* 1, 20-34.

Poléjaeff, N. (1884) Report on the Keratosa collected by H.M.S. "Challenger" during the years 1873-1876. *Report of the Scientific Results of the Voyage of H.M.S."Challenger" 1873-76, Zoology*, 11(31), 1-88.

Pulitzer-Finali, G. (1983) A collection of Mediterranean Demospongiae (Porifera) with, in appendix, a list of the Demospongiae hitherto recorded from the Mediterranean Sea. *Annali del Museo Civico di Storia Naturale Giacomo Doria,* 84, 445-621.

Ridley, S. O. and Dendy, A. (1887) Report on the Monaxonida collected by H.M.S."Challenger" during the years 1873-1876. *Report of the Scientific Results of the Voyage of H.M.S."Challenger" 1873-76, Zoology*, 20(Part LIX), 1-275.

Santín, A., Grinyó, J., Ambroso, S., Uriz, M., Gori, A., Dominguez-Carrió, C. and Gili, J.-M. (2018) Sponge assemblages on the deep Mediterranean continental shelf and slope (Menorca Channel, Western Mediterranean Sea). *Deep-Sea Research Part I: Oceanographic Research Papers,* 131, 75-86.

Schönberg, C. H. L. and Beuck, L. (2007) Where Topsent went wrong: *Aka infesta* a.k.a. *Aka labyrinthica* (Demospongiae: Phloeodictyidae) and implications for other *Aka* species. *Journal of the Marine Biological Association of the United Kingdom,* 87, 1459–1476.

Schulze, M. F. E. (1887) Report on the Hexactinellida collected by H.M.S. "Challenger" during the years 1873-1876. *Report of the Scientific Results of the Voyage of H.M.S."Challenger" 1873-76*, Zoology, 211-513.

Sitjà, C. and Maldonado, M. (2014) New and rare sponges from the deep shelf of the Alboran Island (Alboran Sea, Western Mediterranean). *Zootaxa,* 3760(2), 141-179.

Sitjà, C., Maldonado, M., Farias, C. and Rueda, J. L. (2019) Deep-water sponge fauna from the mud volcanoes of the Gulf of Cadiz (North Atlantic, Spain). *Journal of the Marine Biological Association of the United Kingdom,* 99(4), 807-831.

Sollas, W. J. (1888) Report on the Tetractinellida collected by H.M.S. Challenger during the years 1873-76. *Report of the Scientific Results of the Voyage of H.M.S. Challenger 1873-76,* 25(part 63), 1-458.

Stephens, J. (1915) Atlantic sponges collected by the Scottish National Antarctic Expedition. *Transactions of the Royal Society of Edinburgh,* 50(2), 423-467.

Tabachnick, K. R. and Menshenina, L. L. (2007) Revision of the genus Asconema (Porifera: Hexactinellida: Rossellidae). *Journal of the Marine Biological Association of the United Kingdom,* 87(6), 1403-1429.

Taviani, M., Angeletti, L., Beuck, L., Campiani, E., Canese, S., Foglini, F., Freiwald, A., Montagna, P. and Trincardi, F. (2015) On and Off the Beaten Track: Megafaunal Sessile Life and Adriatic Cascading Processes. *Marine Geology,* 369, 273-287.

Taviani, M., Angeletti, L., Canese, S., Cannas, R., Cardone, F., Cau, A., Cau, A. B., Follesa, M. C., Marchese, F., Montagna, P. and Tessarolo, C. (2017) The "Sardinian cold-water coral province" in the context of the Mediterranean coral ecosystems. *Deep-Sea Research Part II: Topical Studies in Oceanography,* 145, 61-78.

Templado, J., García-Carrascosa, M., Baratech, L., Capaccioni, R., Juan, A., López-Ibor, A., Silvestre, R. and Massó, C. (1986) Estudio preliminar de la fauna asociada a los fondos coralígenos del mar de Alborán (SE de España). *Boletín del Instituto Español de Oceanografía,* 3(4), 93-104.

Thomson, C. W. (1873) *The depths of the sea.* Macmillan and Co., London. 527 pp.

Topsent, E. (1890) Notice préliminaire sur les spongiaires recueillis durant les campagnes de l'Hirondelle. *Bulletin de la Société Zoologique de France,* 15, 26-32, 65-71.

Topsent, E. (1892) Contribution a l'étude des Spongiaires de l'Atlantique Nord. *Résultats des Campagnes Scientifiques accomplies par le Prince Albert I.* Monaco, 21-165.

Topsent, E. (1895) Campagnes du Yacht "Princesse Alice". Notice sur les spongiaires recueillis en 1894 et 1895. *Bulletin de la Société Zoologique de France,* 20, 213-216.

Topsent, E. (1896) Campagnes du Yacht "Princess Alice". Sur deux curieuses espirellines des Açores. *Bulletin de la Société Zoologique de France,* 21, 147-150.

Topsent, E. (1900) Étude monographique des Spongiaires de France. III. Monaxonida (Hadromerina). *Archives de Zoologie Expérimentale et Générale,* (3) 81-331.

Topsent, E. (1901) Eponges nouvelles de Açores. *Mémoires de la Société Zoologique de France,* 14, 448-466.

Topsent, E. (1904a) Notes sur les Eponges du "Travailleur" et du "Talisman". III. *Bulletin du Muséum National d'Historie Naturelle,* Paris, 6, 372-378.

Topsent, E. (1904b) Spongiaires des Açores. *Résultats des Campagnes Scientifiques accomplies par le Prince Albert I.* Monaco*,* 251-279.

Topsent, E. (1913) Spongiaires provenant des campagnes scientifiques de la "Princess Alice" dans les Mers du Nord (1898-1899, 1906-1907). *Résultats des Campagnes Scientifiques accomplies par le Prince Albert I.* Monaco*,* 453-67.

Topsent, E. (1924) Révision des Mycales de l'Europe occidentale. *Annales de l'Institut Océanographique,* 1(3), 77-118.

Topsent, E. (1928) Spongiaires de l'Atlantique et de la Méditerranée, provenant des croisières de Prince Albert I de Monaco. *Résultats des Campagnes Scientifiques accomplies par le Prince Albert I.* Monaco, 741-376.

Topsent, E. (1929) Notes sur Helophloeina stylivarians n. g., n. sp. Mycaline à desmes des Canaries. *Bulletin de l'Institut Océanographique de Monaco,* 533, 1-8.

Topsent, E. (1934) Eponges observées dans les parages de Monaco. Première Partie. *Bulletin de l'Institut Océanographique de Monaco,* 650, 1-42.

Topsent, E. (1936) Eponges observées dans les parages de Monaco. Deuxième Partie. *Bulletin de l'Institut Océanographique de Monaco,* 686, 1-70.

Tursi, A., Mastrototaro, F., Matarrese, A., Maiorano, P. and D'Onghia, G. (2004) Biodiversity of the white coral reefs in the Ionian Sea (Central Mediterranean). *Chemistry and Ecology,* 20(suppl.1), 107-116.

Uriz, M. J. (1981) Estudio sistemático de las esponjas Astrophorida (Demospongia) de los fondos de pesca de arrastre, entre Tossa y Calella (Cataluña). *Boletín del Instituto Español de Oceanografía,* 6(320), 7-58.

Uriz, M. J. (1982) Estudio sistemático de las esponjas del orden Axinellida (Demospongia) de la Costa Brava (Cataluña). *Actas del II Simposio Ibérico del Estudio del Bentos Marino,* 2(3), 57-80.

Uriz, M. J. (1983) Monografía I. Contribución a la fauna de esponjas (Demospongia) de Cataluña. *Anales de la Sección de Ciencias del Colegio Universitario de Gerona,* 7, 1-220.

Uriz, M. J. (1984) Distribución y afinidades biogeográficas de las esponjas córneas del litoral catalán. *Investigación Pesquera,* 48(1), 51-58.

Uriz, M. J. and Rosell, D. (1990) Sponges from bathyal depths (1000-1750 m.) in the Western Mediterranean Sea. *Journal of Natural History,* 24, 373-391.

Vacelet, J. (1960) Eponges de la Méditerranée nord-occidentale récoltées par le "President Théodore Tissier" (1958). *Revue des Travaux de l'Institut des Pêches Maritimes,* 24(2), 257-272.

Vacelet, J. (1961) Quelques Eponges remarquables de Méditerranée. *Revue des Travaux de l'Institut des Pêches Maritimes,* 25(3), 351-354.

Vacelet, J. (1969) Eponges de la Roche du Large et de l'étage bathyal de Méditerranée (récoltées de la Soucoupe plongeante cousteau et dragages). *Mémoires du Muséum National d'Histoire Naturelle (France),* série A, 59(2), 145-219.

Vacelet, J. (1976) Inventaire des Spongiaires du Parc National de Port-Cros (Var). *Travaux scientifiques du Parc National de Port-Cros,* 2, 167-186.

Van Soest, R. M. W., Beglinger, E. J. and de Voogd, N. J. (2010) Skeletons in confusion: a review of astrophorid sponges with (dicho–)calthrops as structural megascleres (Porifera, Demospongiae, Astrophorida). *ZooKeys,* 6, 81-88.

Van Soest, R. M. W., Beglinger, E. J. and de Voogd, N. J. (2012) Sponges of the family Esperiopsidae (Demospongiae, Poecilosclerida) from Northwest Africa, with the descriptions of four new species. *European Journal of Taxonomy,* 18, 1-21.

Van Soest, R. M. W., Beglinger, E. J. and de Voogd, N. J. (2013) Microcionid sponges from Northwest Africa and the Macaronesian Islands (Porifera, Demospongiae, Poecilosclerida). *Zoologische mededeelingen,* 87, 275-404.

Van Soest, R. M. W., Beglinger, E. J. and de Voogd, N. J. (2014) Mycale species (Porifera: Poecilosclerida) of Northwest Africa and the Macaronesian Islands. *Zoologische mededeelingen,* 88(4), 59-109.

Vertino, A., Savini, A., Rosso, A., Di Geronimo, I., Mastrototaro, F., Sanfilippo, R., Gay, G. and Etiope, G. (2010) Benthic habitat characterization and distribution from two representative sites of the deep-water SML Coral Province (Mediterranean). *Deep-Sea Research Part II: Oceanographic Research Papers,* 57, 380-396.

Vosmaer, G. C. J. (1894) Preliminary notes on some Tetractinellids of the Bay of Naples. *Tijdschrift der Nederlandsche Dierkundige Vereeniging,* 4(2), 269-286.

Weerdt, W. H. d. and Van Soest, R. W. M. (1986) Marine shallow-water Haplosclerida (Porifera) from the South-Eastern part of the North Atlantic Ocean. *Zoologische Verhandelingen,* 22, 51-49.

Zibrowius, H. and Taviani, M. (2005) Remarkable sessile fauna associated with deep coral and other calcareous substrates in the Strait of Sicily, Mediterranean Sea. *In:* A. Freiwald and J. M. Roberts (Eds), *Cold-Water Corals and Ecosystems*. Springer Berlin Heidelberg, Berlin, Heidelberg, pp. 807-819.

Chapter 5

Appendix I: List of bibliographic sponge records from 1870 to present day. It comprises 18 studied areas from Macaronesia, southern Lusitanian, Gulf of Cádiz, Western, Central and Eastern Mediterranean regions. Rows comprise the sponge species ordered by families. Within each family, genera and species names are alphabetically ordered. Columns represent locations of each record, depth range (m) and source data. The symbol "*" next to a depth range indicates approximate depth data. Sites for records are organized by ocean areas, from West to East, and within each area, references are order by publication year of the record, then by author last name.

Appendix I in Chapter 5 consists of an Excel file too big to fit in the appendix section of this volume and has been uploaded to Google Drive. Please follow this link to access the document:
https://drive.google.com/drive/folders/1xrYO42HBU9hom2UiwysB7ev5ZZx3g63a?usp=sharing

This is the updated version of the data file previously created in Chapter 4 (see Appendix I and II of Chapter 4). References newly added to the present file are included in the main text of Chapter 5.

Confirmation of acceptance

Chapter 4 has been accepted for publication in *Deep-Sea Research Part I: Oceanographic Research Papers* as "Sitjà C., Maldonado M., Farias C. and Rueda J.L. (2020) Export of bathyal benthos to the Atlantic through the Mediterranean outflow: sponges from the mud volcanoes of the Gulf of Cádiz as a case study.

Document of acceptance:

Track Your Accepted Article

The easiest way to check the publication status of your accepted article

Export of bathyal benthos to the Atlantic through the Mediterranean outflow: sponges from the mud volcanoes of the Gulf of Cadiz as a case study

Article reference	DSRI_103326
Journal	Deep-Sea Research Part I
Corresponding author	Manuel Maldonado
First author	Cèlia Sitjà
Received at Editorial Office	7 Nov 2019
Article revised	15 May 2020
Article accepted for publication	3 Jun 2020

Last update: 3 Jun 2020 — Share via email

Status comment

- Your article has been received for production.

Production events

3 Jun 2020	Received for production

Complimentary items

- You are entitled to a Share Link for your article free of charge. The Share Link will be sent you as soon as the final article is published in an issue.

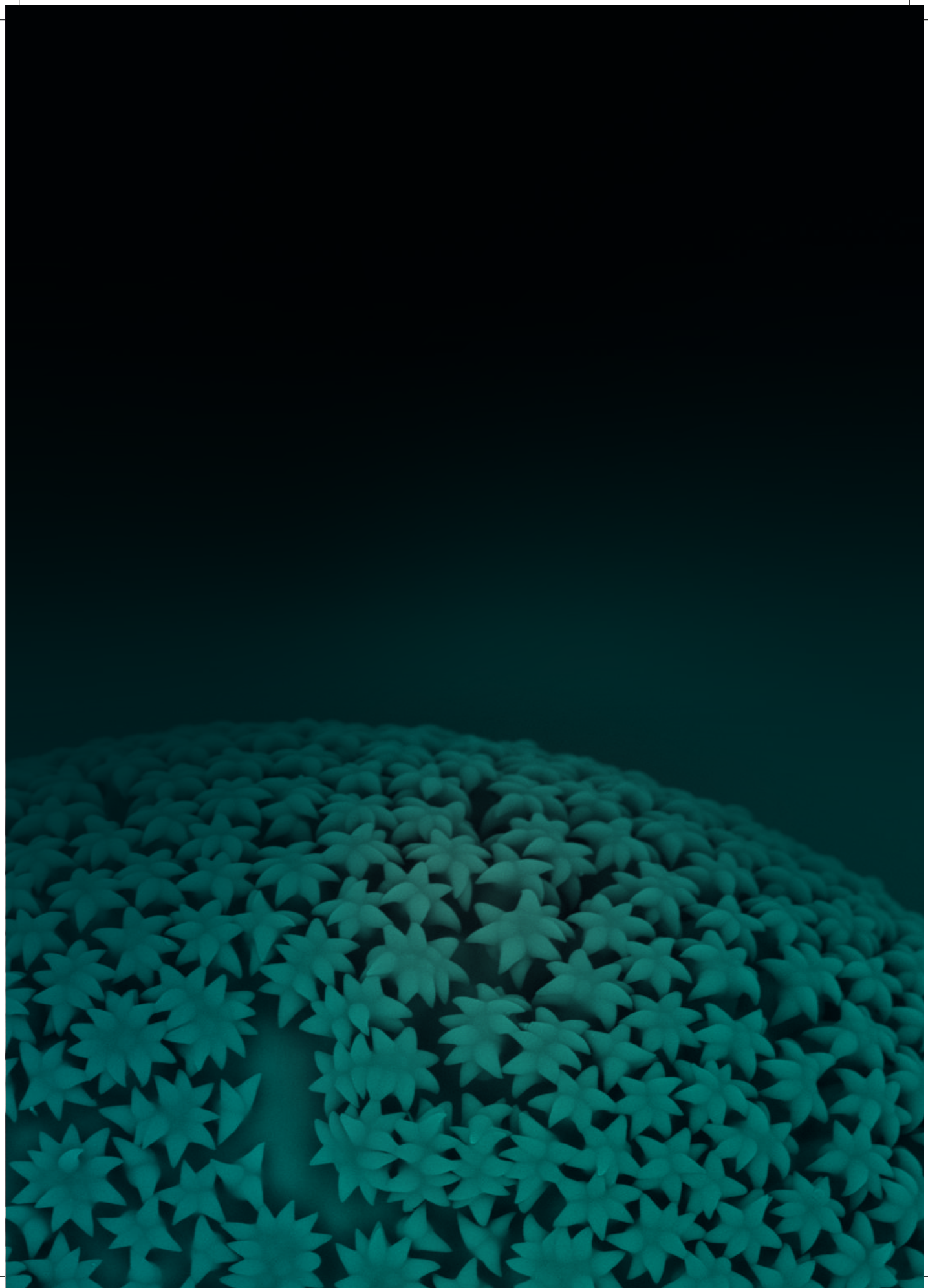

Published work

Zootaxa 3760 (2): 141–179
www.mapress.com/zootaxa/

Article

ISSN 1175-5326 (print edition)
ZOOTAXA
ISSN 1175-5334 (online edition)

http://dx.doi.org/10.11646/zootaxa.3760.2.2
http://zoobank.org/urn:lsid:zoobank.org:pub:E05CF7B1-8410-4482-AB7D-DC9833479CC3

New and rare sponges from the deep shelf of the Alboran Island (Alboran Sea, Western Mediterranean)

CÈLIA SITJÀ & MANUEL MALDONADO[1]

Department of Marine Ecology. Centro de Estudios Avanzados de Blanes (CEAB-CSIC), Acceso Cala St. Francesc 14, Blanes 17300, Girona, Spain

[1]*Corresponding author. E-mail: maldonado@ceab.csic.es*

Table of contents

Accepted by J. Hooper: 13 Dec. 2013; published: 31 Jan. 2014

Abstract

The sponge fauna from the deep shelf (70 to 200 m) of the Alboran Island (Alboran Sea, Western Mediterranean) was investigated using a combination of ROV surveys and collecting devices in the frame of the EC LIFE+ INDEMARES Grant aimed to designate marine areas of the Nature 2000 Network within Spanish territorial waters. From ROV surveys and 351 examined specimens, a total of 87 sponge species were identified, most belonging in the Class Demospongiae, and one belonging in the Class Hexactinellida. Twenty six (29%) species can be regarded as either taxonomically or faunistically relevant. Three of them were new to science (*Axinella alborana* **nov. sp.**; *Axinella spatula* **nov. sp.**; *Endectyon filiformis* **nov. sp.**) and 4 others were Atlantic species recorded for the first time in the Mediterranean Sea (*Jaspis eudermis* Lévi & Vacelet, 1958; *Hemiasterella elongata* Topsent, 1928; *Axinella vellerea* Topsent, 1904; *Gelliodes fayalensis* Topsent, 1892). Another outstanding finding was a complete specimen of *Rhabdobaris implicata* Pulitzer-Finali, 1983, a species only known from its holotype, which had entirely been dissolved for its description. Our second record of the species has allowed a neotype designation and a restitution of the recently abolished genus *Rhabdobaris* Pulitzer-Finally, 1983, also forcing a slight modification of the diagnosis of the family Bubaridae. Additionally, 12 species were recorded for the first time from the shelf of the Alboran Island, including a few individuals of the large hexactinellid *Asconema setubalense* Kent, 1877 that provided the second Mediterranean record of this "North Atlantic" hexactinellid. ROV explorations also revealed that sponges are an important component of the deep-shelf benthos, particularly on rocky bottoms, where they make peculiar sponge gardens characterized by a wide diversity of small, erect species forming a dense "undergrowth" among a scatter of large sponges and gorgonians. The great abundance and the taxonomic singularities of the sponge fauna occurring in these deep-shelf bottoms strongly suggest these habitats to be considered within the environmental protection of the Nature 2000 Network.

Key words: Atlantic immigrants, benthic communities, biodiversity, deep benthos, environmental protection, Mediterranean invasions, sponge gardens, Porifera

Introduction

The Alboran Sea occupies the westernmost basin of the Mediterranean. It is known to be a transitional region between the North Atlantic Ocean and the Mediterranean *sensu stricto*, in terms of both hydrography and organismal distributions. The influx of North Atlantic surface water during most of the Quaternary and in Recent times favors the penetration of many "Atlantic species" in this western Mediterranean zone (Péres & Picard 1964). Consequently, the sublittoral communities in this area often present high biodiversity relative to equivalent communities in nearby Lusitanian and Mauritanian areas (Templado *et al.* 2006; Coll *et al.* 2010).

At the heart of the Alboran basin, the Island of Alboran (Fig. 1), a tiny (642 m long and 265 m wide) islet made of volcanic rocks, emerges from a large (45 km long and 10 km wide) submerged shelf, remnant of an ancient (7–16 my old) volcanic cone. This cone is in turn part of an ancient submerged volcanic chain that crosses the Alboran basin with Northeast-Southwest direction. The bottom of the basin in this area reaches a maximum depth of 1500 m and consists of a thinned crustal microplate formed during the Lower Miocene (about 18 my ago) at an important seismic area where the Euroasian and African plates collided (Comas *et al.* 1992; Martínez-García *et al.* 2010).

Although the hydrography of the Alboran Sea is quite complex, it has been well documented that in the central area where the Alboran Island is located, the incoming Atlantic seawater forms a low-salinity (~36.5 ‰), 150–200 m thick, upper layer above the underlying Mediterranean water (~38.2‰), influencing to a varying extent all the communities on the shelf of the island. The singularity and ecological relevance of the benthic communities on the upper shelf (above 70 m) of the Alboran Island has long been recognized (reviewed in Templado *et al.* 2006), and the upper shelf is currently protected under both Spanish and European legislation by declaration of a Marine Reserve, a Fish Reserve, a Special Area of Mediterranean Importance (SPAMI), and a Site of Community Importance (SCI). Additionally, the shelf of the Alboran Island, due to its strategic location at the Mediterranean entry, may provide a unique reference site for early detection of migration and invasion processes into the Mediterranean by Atlantic organisms.

Previously available information on the sponge fauna of the Alboran Sea (Templado *et al.* 1986; Pansini *et al.* 1987; Maldonado & Benito 1991; Maldonado 1992; Boury-Esnault *et al.* 1994; Maldonado & Uriz 1996, 1999; Rosell & Uriz 2002; Templado *et al.* 2006) strongly suggests that sponges may be an important component of the benthos at the still ill-known deep shelf of the Alboran Island. Interestingly, the deep-shelf sponge fauna of the Alboran Island bears some similarities with that reported from the easternmost areas of the western Mediterranean,

such as the Ligurian Sea and the Strait of Sicily (Pansini *et al.* 1987; Maldonado & Uriz 1995; Bertolino *et al.* 2013a; Bertolino *et al.* 2013b). Additionally, some studies have suggested a continued input of sponge species from the Lusitanian region into the Alboran Sea over the Quaternary (Maldonado & Uriz 1995), despite sponges being sessile organisms with short-living planktonic larvae lacking recognizable strategies for long-distance dispersal (Maldonado 2006). Since global warming enhances northward migration of subtropical marine species (Coll *et al.* 2010), it is urgent to improve our knowledge of these deep-shelf Alboranian communities before the immigrants get integrated in them and further complicate both discrimination of the pre-warming original fauna and the understanding of future Mediterranean faunal shifts (Vermeij 2012).

Materials and methods

Within the frame of an EC Grant LIFE+ INDEMARES aimed to list and designate marine areas for the Nature 2000 Network in Spanish territorial waters, we explored the deep shelf (70 to 200 m) of the Alboran Island, using a remotely operated underwater vehicle (ROV) along with traditional dredging and trawling devices to collect benthic fauna.

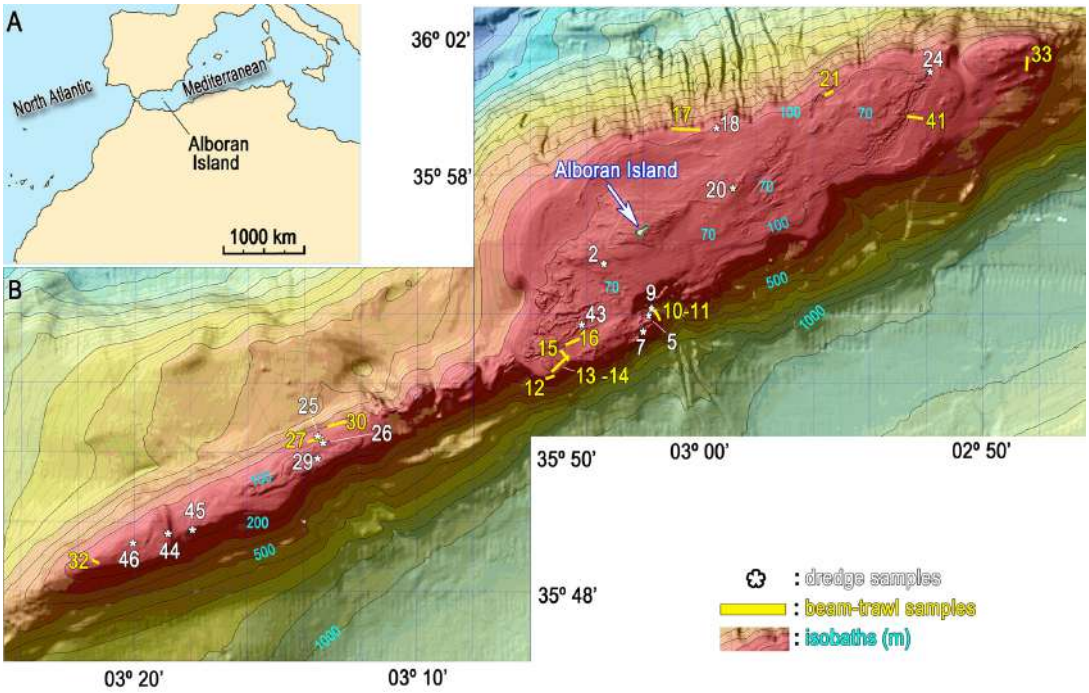

FIGURE 1. (A) Localization of the Alboran Island in the Mediterranean. (B) Distribution of the 25 studied sampling stations over the bathymetric map of the shelf of the Alboran Island.

Prior to any collecting tasks, scientific partners of the INDEMARES-Alboran grant developed a detailed bathymetric profiling of the island shelf using side scan sonar (Geotecnia, Hidrología and Medio Ambiente S.L.) and outlined the location of the most relevant benthic communities through suspended still video (information available through Juan Goutayer). Using this basic information, a first detailed assessment of the benthic communities at the deep shelf of the Alboran Island was carried out by running 9 video transects (19 hours of recording) at depths ranging from 65 to 205 m in September 2011, using a SEAEYE FALCON ROV. A second research stage involved collecting cruises in 2011 and 2012, during which a total of 44 sites were sampled in the 25–290 m depth range, using a small beam trawl on soft bottoms and a dredge on hard bottoms. Here we are reporting on the sponge fauna collected in 25 sampling stations (Fig. 1; Table 1), incorporating, whenever possible,

the information available from the video transects. Collected specimens were fixed in 4% formalin for 2–3 months, rinsed in distilled water, and subsequently transferred to 70% ethanol. Because of an initial fixation step in formalin, the collected sponge material is not suitable for molecular analysis. Taxonomic identifications were accomplished by considering the external morphology and skeleton, using standard techniques to prepare spongin fibres and spicules for light microscopy observation. Body features, spicules, and skeletal arrangements were described according to the thesaurus of sponge morphology (Boury-Esnault & Rützler 1997). When required, acid-cleaned spicules were mounted on aluminum stubs, gold-coated, and studied through a HITACHI TM3000 Scanning Electron Microscope (SEM), following standard protocols for sample preparation. Features of the collected material were compared, when required, to those of holotypes and additional material borrowed from sponge collections of the Muséum National d'Histoire Naturelle (MNHN) of Paris, the Musée Océanographique of Monaco (MOM), and the Museo Civico di Storia Naturale Giacomo Doria of Genoa (MSNG). All collected material during the INDEMARES-Alboran cruises, holotypes included, has been stored in the Invertebrate Collection of the National Museum of Natural Sciences (MNCN), Madrid, Spain.

Results and discussion

Taxonomic and ecological singularities. Taxonomic identification of 351 collected specimens along with additional identifications derived from ROV video monitoring yielded a list of 87 sponge species (Table 2), most belonging to the Class Demospongiae. The Hexactinellida were represented by only one species, *Asconema setubalense* Kent, 1870, identified through ROV recordings. Eleven specimens of Calcarea were collected, but they were not taxonomically investigated. The results of the present study have increased the previous number of sponge species known from the Alboran Island Platform and the bottoms of the surrounding abyssal plain by 33, leading to a total of 196 species (Table 6).

Twenty six (29%) out of 87 identified species were considered as relevant from either a taxonomical or faunistical point of view. Three of them were new to science (*Axinella alborana* **nov. sp.**; *Axinella spatula* **nov. sp.**; *Endectyon filiformis* **nov. sp.**) and 4 others were recorded in the Mediterranean Sea for the first time (*Jaspis eudermis* Lévi & Vacelet, 1958; *Hemiasterella elongata* Topsent, 1928; *Axinella vellerea* Topsent, 1904; *Gelliodes fayalensis* Topsent, 1892). Another outstanding finding was a complete specimen of *Rhabdobaris implicata* Pulitzer-Finali, 1983, a species only known from the holotype, which was entirely dissolved for the preparation of a spicule slide. Twelve additional species were recorded for the first time from the shelf of the Alboran Island: *Acanthella acuta* Schmidt, 1862; *Calthropella recondita* Pulitzer-Finali, 1983; *Dendroxea lenis* (Topsent, 1892); *Endectyon delaubenfelsi* Burton, 1930; *Erylus discophorus* (Schmidt, 1862); *Eurypon lacazei* (Topsent, 1891); *Prosuberites longispinus* Topsent, 1893; *Rhizaxinella gracilis* (Lendenfeld, 1898); *Spongosorites intricatus* (Topsent, 1892); *Hexadella racovitzai* Topsent, 1896; *Terpios fugax* Duchassaing & Michelotti, 1864; and *Asconema setubalense*. From a conservation point of view, there were 4 rare Mediterranean endemic species (*Axinella salicina* Schmidt, 1868; *Crambe tailliezi* Vacelet & Boury-Esnault, 1982; *Sarcotragus pipetta* Schmidt, 1868; *Vulcanella aberrans* (Maldonado & Uriz, 1996)), and 2 other species, *Tethya aurantium* (Pallas, 1766) and *Axinella polypoides* Schmidt, 1862, listed as vulnerable in the current environmental legislation (Templado *et al.* 2004).

Collecting devices and ROV explorations revealed that sponges are relevant or dominant benthic organisms in 3 major habitats of the deep shelf: 1) the rhodolith beds (60–120 m; Fig. 2A–B); 2) the rocky plains moderately sloping, which correspond to the flanks of the ancient volcanic cone (80–120 m; Fig. 2C–D); and 3) the isolated rocky outcrops surrounded by soft sediments (Fig. 2E–F).

The rhodolith beds occuppied vast areas in the 60–100 m depth range. Although the species composition of the general sessile fauna varied widely from one rhodolith to another, a wide variety of encrusting sponges was often abundant on them (Fig. 2B). Species such as *Bubaris vermiculata* (Bowerbank, 1866), *Diplastrella bistellata* (Schmidt, 1862), *Dercitus (Stoeba) plicatus* (Schmidt, 1868), and several members of the genera *Eurypon* Gray, 1867 were common. Small submassive and erect species of the genera *Axinella*, *Suberites*, *Phakellia* or *Poecillastra compressa* (Bowerbank, 1866) were also frequent.

The slopy rocky plains, which showed moderate charges of fine sediments, often hosted important populations of flabellate and lamellate, erect and massive sponges, typically including *Phakellia robusta Bowerbank,* 1866 (Fig. 2C), *Phakellia ventilabrum* (Linnaeus, 1767), *Poecillastra compressa* (Fig. 2C),

Characella pachastrelloides (Carter, 1876), *Pachastrella monilifera* Schmidt, 1868, *Vulcanella aberrans* (Fig. 2D), along with a lower abundance of other large astrophorids and halichondrids. Among the scatter of large sponges, there was a dense, peculiar "undergrowth" made of a variety of small erect sponges (Fig. 2C). Stipitate or lollipop morphologies, such as *Podospongia lovenii* Bocage, 1869, *Rhizaxinella elongata* (Ridley & Dendy, 1886), *Rhizaxinella gracilis* or *Crella (Yvesia) pyrula* (Carter, 1876), and digitate or branching morphologies, such as *Axinella vellerea* Topsent, 1904, *Axinella pumila* Babic, 1922, *Stelligera stuposa* (Ellis & Solander, 1786), and *Stelligera rigida* (Montagu, 1818), were common in the undergrowth (Fig. 2C–D, G–H). These communities can indeed be regarded as Mediterranean "sponge gardens", characterized by high diversity and abundance of small erect species growing among the large astrophorids and axinellids that typically build the "sponge gardens" or "sponge grounds" at similar depth ranges on North-Atlantic margins (Hogg *et al.* 2010). On the deepest zone of the sloping rocky flats some isolated individuals of the large hexactinellid *Asconema setubalense* also occurred (e.g., 181 m deep; 35º 53.190' N, 03º 02.111' W), providing the second Mediterranean record of this species. This hexactinellid had traditionally been reported from greater depths in the North-Atlantic ocean, but it was recently recorded first in the Mediterranean during the ROV exploration of another deep site (> 250 m) of the Alboran Sea, the "Seco de los Olivos" ("Chella" Seamount; Pardo *et al.* 2011). Whether a denser population of *A. setubalense* occurs deeper in the slope of the Alboran Island remains to be explored.

TABLE 1. Information on sampling stations, indicating station number, type of collecting device (DR= dredge; BV= beam trawl), geographical coordinates of starting and end point of sampling transects, depth range (m) during the transect, and bottom type (R= rock, G= gravel, OG= organogenic gravel, RH= rhodolith bed, LS= lava stone bed).

Station number	Collection device	Transect start point (lat. and long.)	Transect end point (lat. and long.)	Starting depth (m)	Ending depth (m)	Bottom type
02	DR	35º55.422'N 03º03.307'W	35º55.452'N 03º03.378'W	54	52	RH
05	DR	35º53.980'N 03º01.806'W	35º53.917'N 03º01.810'W	130	109	R
07	DR	35º53.506'N 03º02.092'W	35º53.416'N 03º02.051'W	87	92	RH
10	BV	35º53.990'N 03º01.570'W	35º54.116'N 03º01.610'W	214	290	G
11	BV	35º54.068'N 03º01.613'W	35º53.811'N 03º01.413'W	243	240	G
12	BV	35º52.222'N 03º05.215'W	35º52.167'N 03º05.388'W	120	112	OG
13	BV	35º52.379'N 03º05.182'W	35º52.825'N 03º04.591'W	99	95	G
14	BV	35º52.723'N 03º04.668'W	35º52.340'N 03º05.265'W	96	100	G
15	BV	35º52.668'N 03º04.656'W	35º52.900'N 03º04.924'W	96	96	G
16	BV	35º53.103'N 03º04.738'W	35º53.256'N 03º04.289'W	92	82	RH
17	BV	35º59.326'N 03º00.044'W	35º59.364'N 03º01.000'W	121	169	G
18	DR	35º59.395'N 02º59.396'W	35º59.386'N 02º59.460'W	92	94	R
20	DR	35º57.663'N 02º58.848'W	35º57.672'N 02º58.810'W	48	42	RH
21	BV	36º00.399'N 02º55.318'W	36º00.288'N 02º55.570'W	101	93	OG

.....continued on the next page

TABLE 1. (Continued)

Station number	Collection device	Transect start point (lat. and long.)	Transect end point (lat. and long.)	Starting depth (m)	Ending depth (m)	Bottom type
25	DR	35º50.413'N 03º13.390'W	35º50.421'N 03º13.491'W	111	114	OG
26	DR	35º50.294'N 03º13.248'W	35º50.251'N 03º13.304'W	94	97	OG
27	BV	35º50.415'N 03º13.245'W	35º50.398'N 03º13.722'W	109	100	OG
29	DR	35º49.768'N 03º13.090'W	35º49.996'N 03º13.432'W	93	94	OG /RH
30	BV	35º50.756'N 03º13.165'W	35º50.896'N 03º12.434'W	180	163	OG
32	BV	35º46.869'N 03º21.413'W	35º46.843'N 03º21.301'W	125	122	R
33	BV	36º01.034'N 02º48.487'W	36º01.397'N 02º48.433'W	173	134	G
41	BV	35º59.617'N 02º52.077'W	35º59.677'N 02º52.666'W	112	102	G
44	DR	35º47.716'N 03º17.986'W	35º47.820'N 03º17.902'W	152	135	R /G
45	DR	35º47.589'N 03º18.679'W	35º47.560'N 03º18.769'W	134	120	G
46	DR	35º47.404'N 03º19.984'W	35º47.437'N 03º20.037'W	103	104	G/ LS

The rocky outcrops standing out from soft bottoms, with their impressive rocky crests, walls, overhangs, and crevices, provided an optimal substrate for suspension feeders, often hosting a large variety of sponges, cnidarians, brachiopods, molluscs, sabellid tube worms, ascidians, etc (Fig. 2E). The ROV inspections revealed that encrusting, branching, and massive sponges often co-occurred on the outcrops, favored by the multiplicity of microhabitats that these tortuous rocky structures offer. Common sponges were *Dysidea fragilis* (Montagu, 1818), *Sarcotragus pipetta*, *Hexadella racovitzai*, *Penares helleri* (Schmidt, 1864*), Crambe tailliezi*, *Terpios fugax*, *Caminus vulcani* Schmidt, 1862, *Dercitus plicatus*, *Craniella cranium* (Müller, 1776), and also several species of *Suberites*, *Calthropella* Sollas, 1888, *Erylus* Gray, 1867, *Haliclona* Grant, 1836, *Spongosorites* Topsent, 1896, and *Phorbas* Duchassaing & Michelotti, 1864. Large astrophorids (Fig. 2F), such as *Geodia* spp*., Stelletta* spp*., Pacahastrella monilifera, Poecillastra compressa*, *Characella pachastrelloides*, *Vulcanella aberrans,* along with small digitate and stalked sponges were also present, though in lower abundance.

Large areas of the deep shelf were covered with soft bottom, particularly on the north side of the island. The substrate mostly consisted of coarse sand mixed with calcareous gravel, more rarely incorporating a low proportion of mud. In contrast to the above-described hard-bottom communities, the soft bottoms were poor in sponges. Nevertheless, despite their general low sponge abundance, this bottom type hosted scattered individuals of rare and/or endemic species, such as *Axinella salicina* (Fig. 2I) and a new species of the genus *Endectyon.*

A total of 631 demosponges *sensu lato*: (i.e., Demospongiae + Homoscleromorpha) have been listed for the Mediterranean (Voultsiadou 2009; Calcinai *et al.* 2013; the present study). Interestingly, the bottoms around the Alboran Island host 194 demosponge species (Table 6), which means about 30.4% of the total Mediterranean demosponge fauna. Such a remarkable percentage points clearly this island shelf to be a remarkable biodiversity hotspot in terms of demosponge fauna (and probably of several other groups of benthic invertebrates as well). Altogether, the abundance and taxonomic singularity of the sponge fauna occurring in these deep-shelf bottoms strongly suggest these habitats to be accommodated within the environmental protection of the Nature 2000 Network.

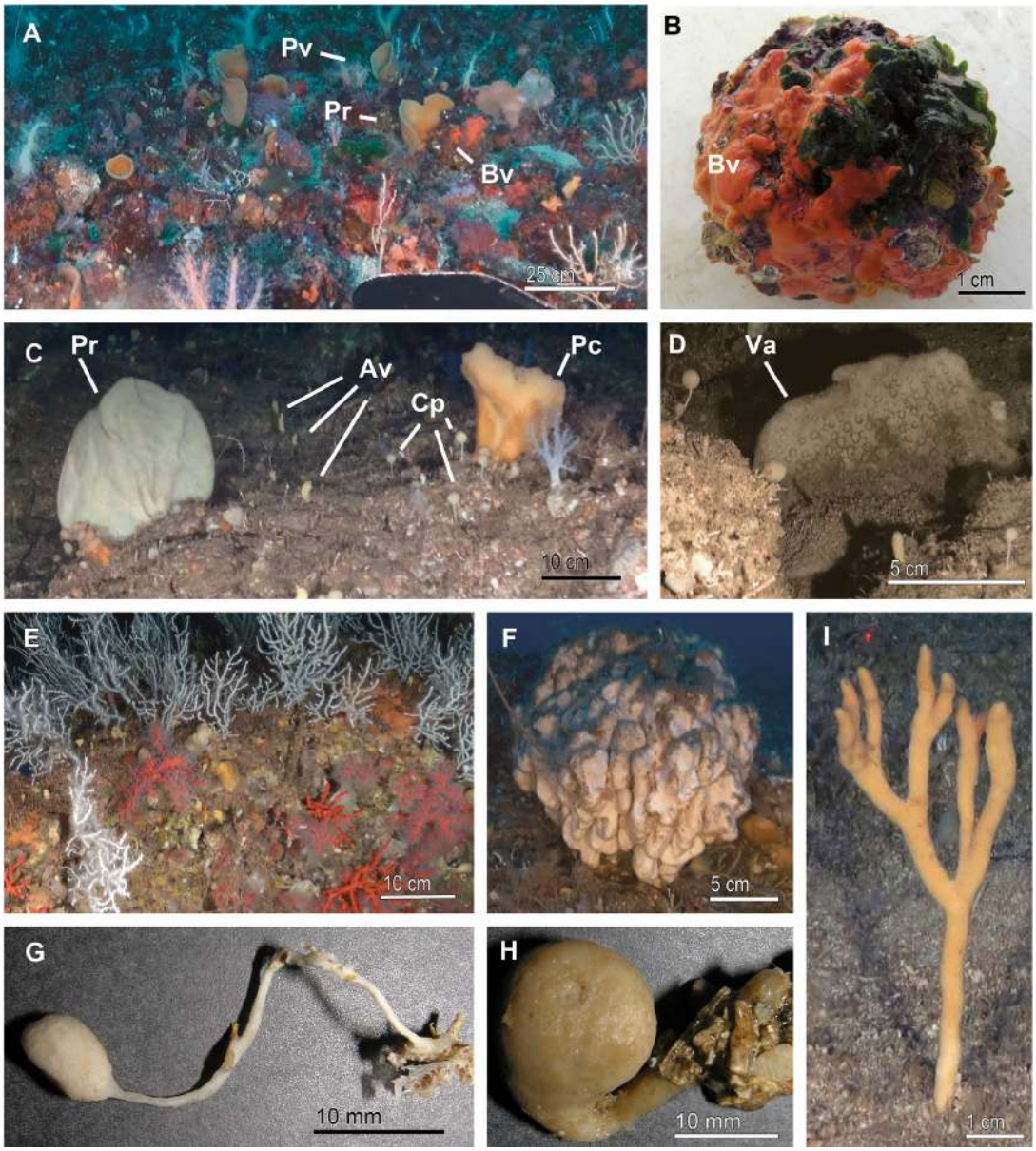

FIGURE 2. Benthic communities on the deep shelf of the Alboran Island in which sponges are important members. (A) View of a rhodolith bottom dominated by cnidarians and sponges. The most abundant sponges were *Phakellia ventilabrum* (Pv), *Phakellia robusta* (Pr), and *Bubaris vermiculata* (Bv). (B) Detail of a rhodolith, largely encrusted by *Bubaris vermiculata* (Bv). (C) View of a gently sloping rocky bottom, showing large specimens of *Phakellia robusta* (Pr) and *Poecillastra compressa* (Pc) together with a dense "canopy" of small digitiform, claviform and globiform sponges, such as *Axinella vellerea* (Av) and *Crella pyrula* (Cp). (D) Individual of *Vulcanella aberrans* (Va) surrounded by small globiform and digitiform sponges. (E) Benthic community on the outcrops dominated by cnidarians, including the octocoral *Corallium rubrum.* Abundant massive, submassive and encrusting sponges are common under the gorgonian forest. (F) Large astrophorid (*Geodia* spp.) sighted from the ROV on the top of an outcrop. (G) Collected specimen of *Crella (Yvesia) pyrula* (MNHN-Sp136-DR44). (H) Collected specimen of *Rhizaxinella gracilis* (MNHN-Sp22-BV14). (I) A solitary specimen of *Axinella salicina* located by the ROV on a coarse-sand and gravel bottom, a substrate type that generally shows low abundance of sponges.

Systematics

Here we provide taxonomic description of eight demosponges collected from the deep shelf of the Alboran Island, which we consider of special interest because they are new to science, are new records for the Mediterranean Sea or are exceptionally rare species.

Phylum PORIFERA Grant, 1836

Class DEMOSPONGIAE Sollas, 1885

Order ASTROPHORIDA Sollas, 1887

Family ANCORINIDAE Schmidt, 1870

Genus *Jaspis* Gray, 1867

Diagnosis. Encrusting or massive sponges without triaenes; choanosomal skeleton composed of oxeas irregularly interlaced, ectosomal skeleton formed by a layer of paratangential oxeas generally smaller than those in the choanosome; microscleres are euasters without a centrum; never being spherasters (*sensu* Uriz 2002).

Jaspis eudermis Lévi & Vacelet, 1958

(Figs. 3A, 4; Table 2)

Material examined. Specimen MNCN-Sp71-BV10 collected from Stn. 10 (Table 1; Fig. 1).

Comparative material: Holotype of *Jaspis eudermis* Lévi & Vacelet, 1957 (MNHN DCL-738) from Princess Alice Bank, Azores (Stn. 62; 37º47'N 29º03'W, 330 m deep, 1955–1956).

Macroscopic description. Creamy white (in alcohol), cushion-shaped sponge, being 45 x 23 mm in size (Fig. 3A). Consistency firm, but friable. Surface nearly glabrous, covered by a friable, detachable, thick membrane (crust-like), with no discernible aquiferous openings. At the zones where the ectosomal crust is lost, subdermal aquifer canals of up to 1mm in diameter are evident.

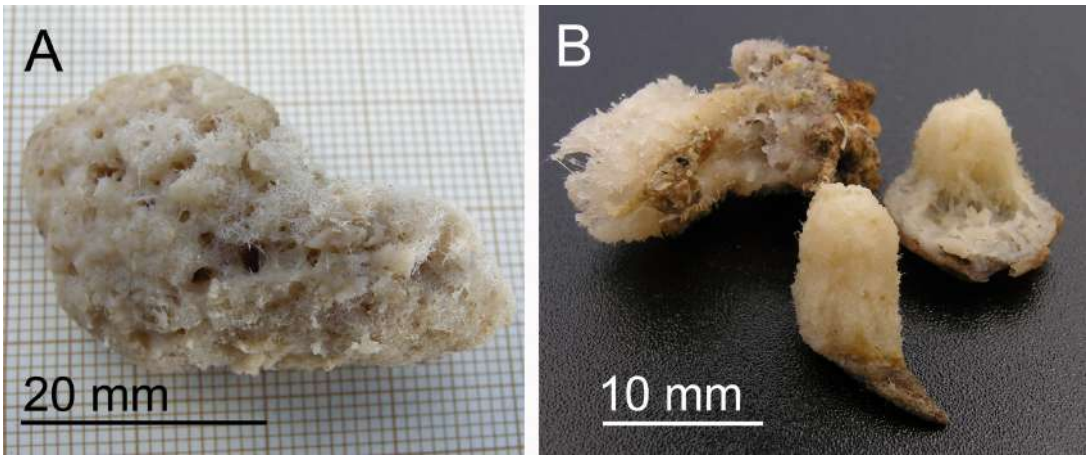

FIGURE 3. (A) Specimen of *Jaspis eudermis* Lévi & Vacelet, 1958 collected from the Alboran Sea and photographed on graphic paper (MNCN-Sp71-BV10). (B) Three Alboranian specimens of *Hemiasterella elongata* Topsent, 1928 (from left to right, MNCN-Sp66-BV21, MNCN-Sp66 B & A).

Skeleton. Megascleres are oxeas, which seem to occur in two categories. Oxeas I are 1125–2000 x 20–40 µm and fairly abundant. They are once or twice slightly bent, frequently asymmetric, usually with acerate tips, occasionally blunt (Fig. 4A–B). Oxeas I showing irregular shapes are also occasional (Fig. 4C). Oxeas II are 390–1500 x 5–10 µm, and comparatively quite scarce; they are slightly curved, sometimes centrotylote, and with conical or acerate ends (Fig. 4A). Microscleres are oxyasters, with 12–20 conical, smooth actines (Fig. 4A, D); their total diameter ranges from 20 to 65 µm, but with no discernible size categories.

There is an ectosomal, crust-like skeleton consisting of abundant oxyasters and tangential oxeas (mostly type II) irregularly disposed in small groups. The choanosomal skeleton consists of oxeas in disordered arrangement, along with abundant oxyasters.

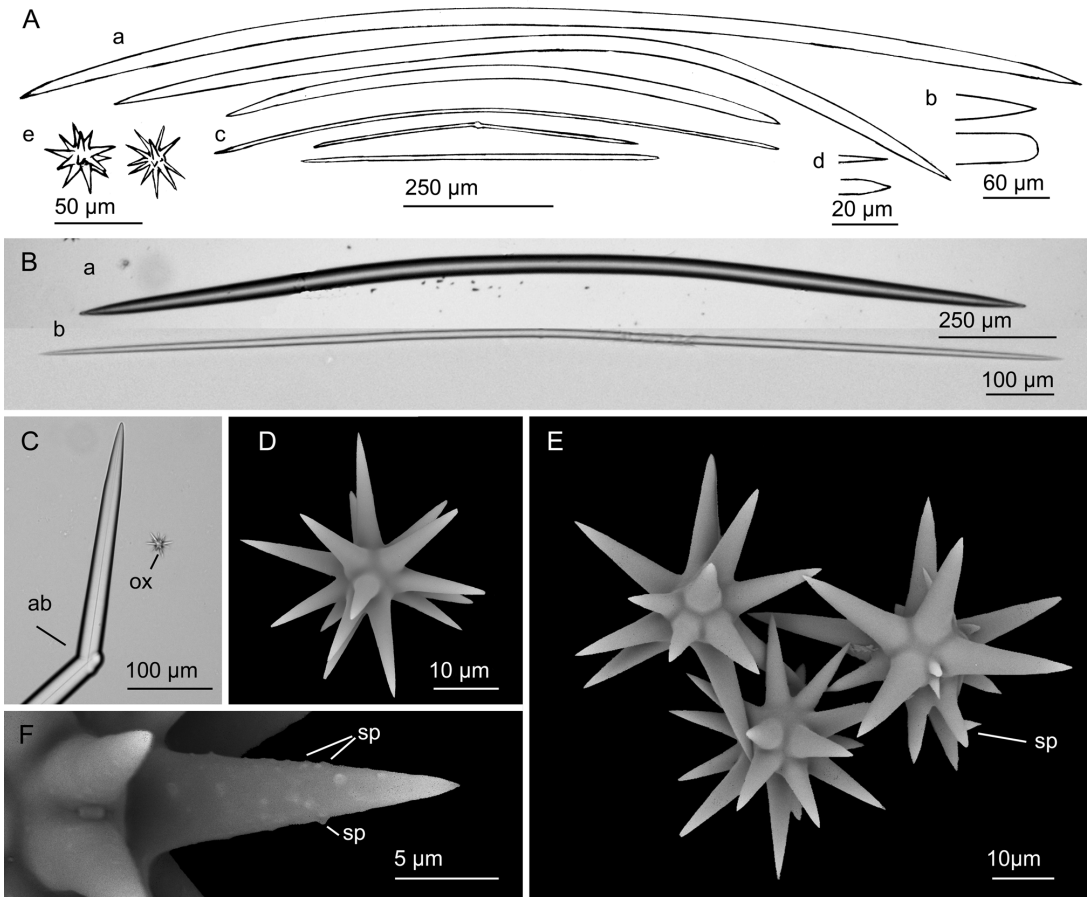

FIGURE 4. *Jaspis eudermis* Lévi & Vacelet, 1958: (A) Line drawing of the spicule complement of the Alboranian specimen (MNCN-Sp71-BV10), consisting of oxeas I (a) with acerate or blunt ends (b), oxeas II (c) with acerate or conical ends (d), and oxyasters (e). (B) Light microscope micrographs of oxeas I (a) and oxeas II (b). (C) An abnormal end (ab) of an oxea I next to an oxyaster (ox). (D) SEM micrograph of an entirely smooth oxyaster. (E) SEM image of several oxyasters of the holotype of *J. eudermis* (Stn. 62 MNHN DCL738), one having some large spines (sp) on some actines. (F) Detail of an oxyaster actine of the holotype showing minute spines (sp).

Distribution and ecology notes. Rare species, previously known only from Azores (eastern North Atlantic). The only specimen herein collected from a gravel bottom at depths of 214–290 m provides the first record of the species in the Mediterranean Sea.

Taxonomic remarks. Several species of *Jaspis* occur in the Mediterranean or/and in the adjacent eastern North-Atlantic zone, but most of them have spicules clearly smaller than those of *J. eudermis*. The only exception is *Jaspis incrustans* (Topsent, 1890), which has fairly large oxeas that reach 1250 µm in length. Nevertheless,

oxyasters of *J. incrustans* measure only up to 26 µm in total diameter and their actines are clearly spiny rather than smooth (Maldonado 1993).

Our material fits reasonably the only brief description available for *J. eudermis*, which corresponds to the holotype, a fragmentary, 2 x 2 x 1 cm, cushion-shaped sponge. It was reported to have a single category of 1200–1650 x 45 µm oxeas (versus two in our specimens) and 35–45 µm oxyasters. The oxyasters were pictured by Lévi & Vacelet (1958) as having more than 10 actines with a smooth (not spiny) surface. Our revision of the holotype indicates that there are indeed two size categories of oxeas, discernible not only because of their thickness (1225–1725 x 30–60 µm and 660–850 x 8–10 µm, with some occasional transitional stage), but also because of their shape, being the smaller category isodiametric and more markedly curved than the fusiform oxeas of the larger category. This reinterpretation of the oxea size distribution brings our specimen and the holotype in full skeletal agreement, as they also share the general traits of the macroscopic morphology and skeletal architecture. Furthermore, they both are the only *Jaspis* material in the Atlantic-Mediterranean region having large, "smooth" oxyasters with more than eleven actines. In this regard, our SEM re-examination of the holotype provides new interesting information. The oxyasters of the holotype measure 30–55 µm in total diameter and have 16 to 20 actines. Most of the actines are entirely smooth (Fig. 4E), as it also happens consistently in the Alboranian specimen (Fig. 4D). Nevertheless, under high SEM magnification approximately 20% of the oxyasters of the holotype show subtle microspines in one or more of their actines (Fig. 4F). In very few occasions, large, isolated spines also occur (Fig. 4E). Therefore, the "smooth" nature of the actines of *J. eudermis* is to be assessed in further detail when more specimens are collected.

Order HADROMERIDA Topsent, 1894

Family HEMIASTERELLIDAE Lendenfeld, 1889

Genus *Hemiasterella* Carter, 1879

Diagnosis. Hemiasterellidae with vasiform, plate-like, flattened branching or massive growth form; choanosomal and peripheral skeletons are loosely organized, vaguely plumoreticulate, without apparent axial compression or differentiation between axial and extra-axial regions. The spicule complement consists of styles and/or oxeas without functional arrangement to any particular part of skeleton and euasters predominantly located in peripheral region of the sponge but not forming a surface crust. The euasters typically show thick, acanthose, strongylote, curved, asymmetrical or branching actines; sometimes calthrop-like, reduced in number to 2–4 actines (sensu Hooper 2002a).

Hemiasterella elongata Topsent, 1928

(Figs. 3B, 5; Table 2)

Material examined. Four specimens collected: MNCN-Sp66-BV21 from Stn. 21; MNCN-Sp04-DR29 from Stn. 29 m; and MNCN-Sp20-BV33A & B from Stn. 33 (Table 1, Fig. 1).

Macroscopic description. Specimens with columnar shape, measuring 5–15 x 4–7 mm (Fig. 3B). The individuals are settled on rock pieces, over which slightly expand their base. The surface shows irregularly shallow folds and grooves, mostly running parallel to the longest body axis. The ectoderm is membrane-like and bears a sparse and uneven hispidation. Pore-like aquiferous openings are visible, especially in the lower half of the body. Color is bright to creamy white both in life and after preservation in ethanol.

Skeleton. Megascleres are styles, measuring 1316–2250 x 10–30 µm. They are straight, markedly curved, or just with a slight asymmetrical curvature (Fig. 5A–B). The round end of the styles may also be in a stronglyoxea fashion; the pointing end is regularly acerate or, less frequently, stepped, not very sharp (Fig. 5A–C). Styles with both ends modified into oxea are very rare (e.g., one of 1825 x 10 µm per slide) or absent, depending on the individuals. Microscleres are abundant spherostrongylasters, with only a moderately developed centrum and 10–15 strongylote, slightly conical, spiny actines (Fig. 5A, C–E). Spines are more dense toward the end of the actines. Spherostrongylasters range from 14 to 23 µm in total diameter.

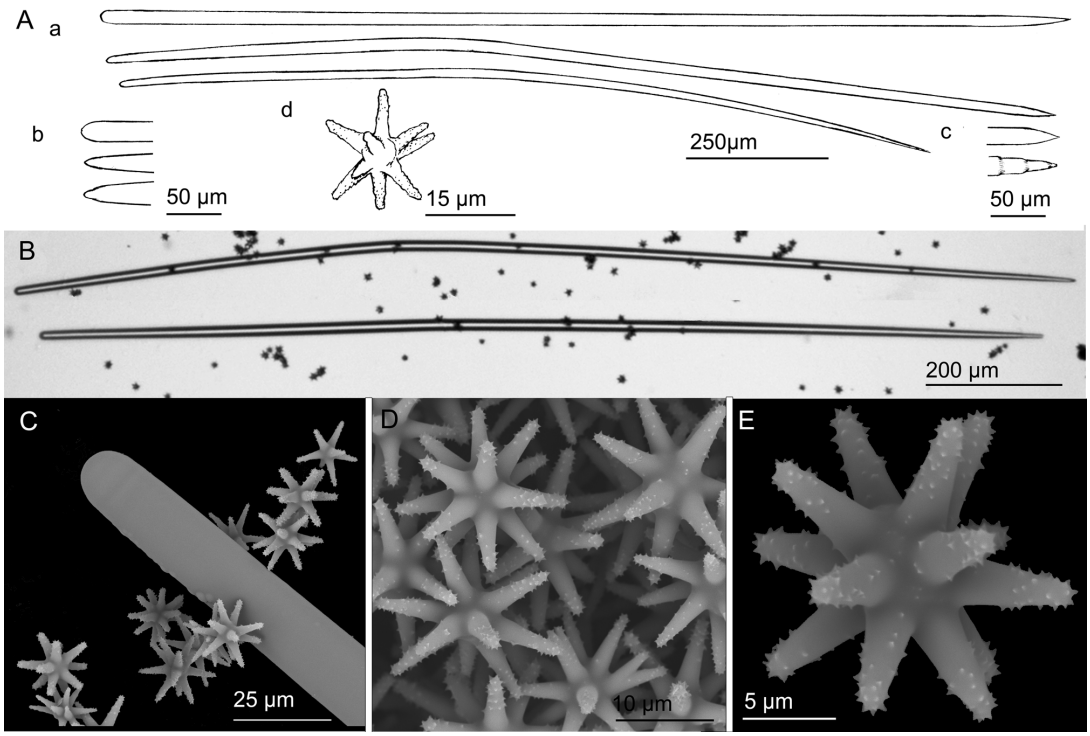

FIGURE 5. *Hemiasterella elongata Topsent, 1928: (A) Line drawing summarizing the skeletal complement of the Alboranian specimens, consisting of long, isodiametric styles (a) with a round to strongylote end (b) and an acerate or stepped distal end (c), and spiny spherostrongylasters (d). (B) Light microscope view of two differently curved styles. (C) SEM micrograph of a typical round end of a style surrounded by spherostrongylasters. (D–E) SEM details of spherostrongylasters, with spiny actines.*

The skeletal arrangement shows no axial condensation. Ascending plumose pauci- or multispiculate tracts of styles ramify below the ectosome and may end in plumose tufts that make an hispid surface. There is scarce spongin connecting and packing the spicules in the tracts. Spherostrongylasters are very abundant overall the skeleton, but especially at the periphery, where they make a layer reinforcing the ectosome.

Distribution and ecology notes. Rare species, previously known only from its holotype collected at Cape Verde Islands, eastern North Atlantic (Topsent 1928). The herein collected individuals provide the first record of the species for the Mediterranean Sea. All the collected specimens inhabited 93 to 173 m deep, soft bottoms rich in organogenic gravel, occasionally mixed with pieces of dead rhodoliths.

Taxonomic remarks. The collected specimens bear overall similarity with the holotype described by Topsent (1928). Nevertheless, some morphological differences occur. The holotype shows two incipient branches, while the Alboranian specimens show no sign of branching. Another difference is that the Alboranian individuals have thinner styles (10–30 µm) than the holotype (25–60 µm).

Hemiasterella aristoteliana Voultsiadou-Koukoura & Van Soest, 1991, the only *Hemiasterella* representative recorded in the Mediterranean previously, occurs in the northern Aegean Sea. Although it has also styles and strongylasters as the only spicule types, the species is clearly distinguishable from *H. elongata*, because the former has much longer styles (1800–3000 x 18–37 µm) and its asters are commonly reduced to forms with only 1 to 3 actines (Voultsiadou-Koukoura & van Soest 1991).

As noted by Topsent (1928), there are some similarities between *H. elongata* and *Hemiasterella vasiformis* (Kirkpatrick, 1903) from South Africa. Nevertheless, the latter has a caliculate body shape, many styles becoming tylostyles and strongyles, and a bit larger asters (up to 30 µm of diameter) (Kirkpatrick 1903).

Together with the Antarctic *Hemiasterella digitata* Burton, 1929, *H. elongata* shows an uncommon shape within the genus, but that of *H. digitata* is better described as palmo—digitate, with a surface strongly hispid in small patches and neither oscules nor pores visible (Burton 1929).

Order HALICHONDRIDA Gray, 1867

Family AXINELLIDAE Carter, 1875

Genus *Axinella* Schmidt, 1862

Diagnosis. Ramose, bushy or lamellate habit. Surface generally smooth, with choanosomal spicules projecting slightly. Oscules, when visible, with stellate morphology (i.e., superficial canals leading to opening 'imprinted' in superficial skeleton). Ectosome without specialized skeleton. Choanosomal skeleton differentiated in axial and extra-axial regions; axial skeleton compressed or vaguely reticulated. Extra-axial skeleton plumose or plumoreticulate. Megascleres styles, or styles and oxeas, or oxeas; when both present, one type may be rare; modifications of megascleres common in several species. Microscleres, if present, microraphides and raphides, mostly in tightly packed trichodragmata (*sensu* Alvarez & Hooper 2002).

Remarks. Recent molecular work based on 18S rRNA, 28S rRNA, and CO1 has suggested that the genus *Axinella* is polyphyletic, containing at least two major clades (Gazave *et al.* 2010; Morrow *et al.* 2012). One of the clades ? the proper "Axinella clade" ? revolves around the type species, *Axinella polypoides* Schmidt, 1862, while the other, which includes species such as *Axinella damicornis* (Esper, 1794), *Axinella verrucosa* (Esper, 1794), and *Axinella corrugata* (George & Wilson, 1919), shows greater affinities to agelasid sponges than to the *A. polypoides* clade. The name "Cymbaxinella clade" has been proposed to allude these latter molecular-based group, following the phylocode (Gazave *et al.* 2010). As no morphological synapomorphies can be found to decide when an "*Axinella*-like" species should be allocated to the "Cymbaxinella" clade or the "Axinella" clade (Gazave *et al.* 2010), whenever the molecular information is not available for a species, a serious practical gap rises between the phylocode proposal and the traditional Linnean classification. Subsequent work based on 28S rRNA and CO1 molecular markers has revealed that the "*Axinella*-like" members of the "Cymbaxinella" clade are closer to encrusting species, such as *Hymerhabdia typica* Topsent, 1892 (formerly in Bubaridae) and *Prosuberites* spp. (formerly in Suberitidae), than to *Agelas* spp. On those arguments, a new family Hymerhabdiidae was erected in the Order Agelasida to assemble together *Prosuberites* spp., *Hymerhabdia* spp., those "Axinella" species in the "Cymbaxinella" clade, and some species formerly in the genus *Stylissa* (Morrow *et al.* 2012). But again, no morphological clues have been provided to decide in the absence of molecular information when either a newly described or an old, revisited "Axinella-like" species could belong to this new family. Tentatively, Morrow and co-workers (2012) have suggested that "true *Axinella*" species, such as *A. polypoides*, have raphides in trichodragmata, while those in the "Cymbaxinella" clade of Agelasida "apparently lack this spicule type". Following this tentative argument, we cannot rule out the possibility that at least one of new species herein described as *Axinella* but lacking raphides (i.e., *Axinella alborana* **nov. sp.**) could be reallocated into another genus in the future if newly collected specimens can ever be analyzed by molecular methods and the emerging molecular clades are finally given taxonomic status. Likewise, this could also be the case of the rare *Axinella vellerea* Topsent, 1904, which is herein morphologically revisited in detail.

***Axinella alborana* nov. sp.**
(Figs. 6A–C, 7; Tables 2, 3, 4)

Etymology. This species is named after the Alboran Island, where it occurs abundantly.

Material examined. Holotype MNCN-Sp155-DR44A from type locality Stn. 44 (Table 1, Fig. 1), a rocky bottom at depths of 135 to 152 m on the Alboran Island shelf. Thirty-three paratypes designated: MNCN-Sp03DR05A to C from Stn. 5; MNCN-Sp13-DR07A & B from Stn. 7; MNCN-Sp14-BV13A & B from Stn. 13; MNCN-Sp34-BV14A to F from Stn. 14; MNCN-Sp19-DR29A to D from Stn. 29 m; MNCN-Sp146-BV33 A to N from Stn. 33; MNCN-Sp191-BV41 from Stn. 41; and MNCN-Sp155-DR44B from Stn. 44 (Table 1, Fig. 1).

Comparative material: Syntype material of *Axinella flustra* (Topsent, 1892) = *Tragosia flustra* Topsent, 1892, since no holotype was designated by Topsent (1892) for this species (Table 3). Syntypes were two specimens (MOM-040044) from Bay of Biscay (Stn. 58; 43º40'N 8º55'W, 134 m deep, 7 August 1886) and two specimens (MOM-040272) from Azores (Stn. 247; 38º23.500'N 30º20.333'W, 318 m deep, 30 August 1888).

TABLE 2. Porifera species identified by ROV exploration and examining sampled material from 25 stations (see Table 1, Fig. 1). Species are listed alphabetically according to order and family. Numbers in the Table indicate number of collected individuals for sampling station (DR = dredge, BV = beam trawl). Missing stations (relative to Fig. 1; i.e., 25DR, 26DR, 45DR, 46DR) indicate that no sponge was collected. Species identified through ROV observations are indicated by "+". Order abbreviations are as it follows: At = Astrophorida; Dt = Dictyoceratida; Hd = Hadromerida; Hl = Halichondrida; Hp = Haplosclerida; Pc = Poecilosclerida; Sp = Spirophorida; Ly = Lyssacinosida; Ve = Verongida. Family abbreviations are as it follows: An= Ancorinidae; Ca= Calthropellidae; Ge= Geodiidae; Pa= Pacastrellidae; Th= Theneidae; Vu= Vulcanellidae; Dy= Dysideidae; Ir= Irciniidae; Spo= Spongiidae; Cl= Clionaidae; He= Hemiasterellidae; Pol= Polymastiidae; Spi= Spirastrellidae; St= Stelligeridae; Su= Suberitidae; Teh= Tethyidae; Ti= Timeidae; Ax= Axinellidae; Bu= Buvaridae; Di= Dictyonellidae; Hal= Halichondrida; Cha= Chalinidae; Ni= Niphatidae; Pe= Petrosiidae; Ros= Rosellidae; Ac= Acarnidae; Cho= Chondropsidae; Co= Coelosphaeridae; Cra= Crambeidae; Cre= Crellidae; Des= Desmacellidae; Ham= Hamacanthidae; Hym= Hymedesmiidae; Mic= Microciionidae; Myx= Myxillidae; Pod= Podospongiidae; Ra= Raspailiidae; Ted= Tedaniidae; Tei= Tetillidae; Ia= Ianthellidae.

Order	Family	Species	Sampling stations																						
			ROV	02 DR	05 DR	07 DR	10 BV	11 BV	12 BV	13 BV	14 BV	15 BV	16 BV	17 BV	18 DR	20 DR	21 BV	27 BV	29 DR	30 BV	32 BV	33 BV	41 BV	44 DR
At	An	*Dercitus plicatus*		5		1																	1	
At	An	*Jaspis eudermis*					1																	
At	An	*Jaspis incrustans*											2					2						
At	An	*Stryphnus mucronatus*											2											
At	An	*Stryphnus ponderosus*	+																					
At	Ca	*Calthropella recondita*										1												
At	Ge	*Caminella intuta*																					1	
At	Ge	*Caminus vulcani*				1																		
At	Ge	*Erylus discophorus*							1			1	1										2	
At	Ge	*Penares helleri*										1												
At	Pa	*Characella tripodaria*																					1	
At	Pa	*Pachastrella monilifera*					1											1					1	
At	Th	*Thenea muricata*						1						1										
At	Vu	*Poecillastra compressa*							1		2		6	2				1			5		6	5
At	Vu	*Vulcanella aberrans*						1										2					5	
Dt	Dy	*Dysidea* cf. *fragilis*																		1			1	1
Dt	Ir	*Sarcotragus pipetta*																1						
Dt	Spo	*Spongia officinalis*											1											
Hd	Cl	*Cliona rhodensis*				1																		
Hd	Cl	*Cliona viridis*		5		2																		
Hd	He	*Hemiasterella elongata*															1		1			2		
Hd	Pol	*Polymastia polytylota*																					1	
Hd	Pol	*Polymastia* spp															1							
Hd	Sp	*Diplastrella bistellata*				1																		

.....continued on the next page

TABLE 2. (Continued)

Order	Family	Species	Sampling stations																						
			ROV	02 DR	05 DR	07 DR	10 BV	11 BV	12 BV	13 BV	14 BV	15 BV	16 BV	17 BV	18 DR	20 DR	21 BV	27 BV	29 DR	30 BV	32 BV	33 BV	41 BV	44 DR
Hd	St	*Stelligera rigida*									3													
Hd	St	*Stelligera stuposa*									2													
Hd	Su	*Aaptos aaptos*									1								1					
Hd	Su	*Prosuberites longispinus*		1		1																		
Hd	Su	*Rhizaxinella elongata*									5	7										1	3	
Hd	Su	*Rhizaxinella gracilis*									1												1	
Hd	Su	*Suberites carnosus*				1													1					6
Hd	Su	*Terpios fugax*	+																					
Hd	Teh	*Tethya aurantium*										1				1							1	
Hd	Ti	*Timea unistellata*		6																				
Hl	Ax	*Axinella alborana* nov. sp.			3	2				2	6								4			14	1	2
Hl	Ax	*Axinella* cf. *cinnamomea*								1												1		
Hl	Ax	*Axinella damicornis*	+																					
Hl	Ax	*Axinella egregia*																				3	1	
Hl	Ax	*Axinella polypoides*																					1	
Hl	Ax	*Axinella pumila*									2													
Hl	Ax	*Axinella salicina*	+																					
Hl	Ax	*Axinella spatula* nov. sp.									3	9					5					4	2	
Hl	Ax	*Axinella verrerea*			2																	1	1	9
Hl	Ax	*Phakellia robusta*						2			2										1			3
Hl	Ax	*Phakellia ventilabrum*																			2	3	1	4
Hl	Bu	*Bubaris vermiculata*																	2					1
Hl	Bu	*Rhabdobaris implicata*									1													
Hl	Di	*Acanthella acuta*																						1
Hl	Di	*Dictyonella incisa*								1														
Hl	Hal	*Spongosorites intricatus*											1										1	
Hp	Cha	*Dendroxea lenis*				2																		
Hp	Cha	*Haliclona angulata*		2								1							1	1				
Hp	Cha	*Haliclona* cf. *cinerea*								1				1										
Hp	Cha	*Haliclona* cf. *perlucida*				1																		
Hp	Cha	*Haliclona* cf. *subtilis*		2																				

.....continued on the next page

TABLE 2. (Continued)

Order	Family	Species	Sampling stations																						
			ROV	02 DR	05 DR	07 DR	10 BV	11 BV	12 BV	13 BV	14 BV	15 BV	16 BV	17 BV	18 DR	20 DR	21 BV	27 BV	29 DR	30 BV	32 BV	33 BV	41 BV	44 DR
Hp	Cha	*Haliclona fulva*				1																		
Hp	Cha	*Haliclona lacazei*											1											
Hp	Cha	*Haliclona mucosa*					1													**1**	1	**1**	1	
Hp	Ni	*Gelliodes fayalensis*				1																		
Hp	Pe	*Petrosia ficiformis*			1																			
Ly	*Ros*	*Asconema setubalense*	+																					
Pe	Ae	*Iophon nigricans*																	1					
Pe	Cho	*Batzella inops*				1																		
Pe	Co	*Lissodendoryx lundbecki*															2							
Pe	Cra	*Crambe taillezi*		12																				
Pe	Cre	*Crella elegans*														1								
Pe	Cre	*Crella pyrula*																						1
Pe	Des	*Desmacella anneva*											1											
Pe	Des	*Desmacella inornata*											1				3			2			3	9
Pe	Des	*Dragmatella aberrans*								1		2	1	1								18		
Pe	Ham	*Hamacantha falcula*																	1					1
Pe	Hym	*Hymedesmia paupertas*																						3
Pe	Hym	*Hymedesmia peachi*				2																		
Pe	Hym	*Phorbas fictitius*														1								
Pe	Hym	*Phorbas topsenti*				1																		
Pe	Mic	*Antho involvens*		2		1																		
Pe	Myx	*Myxilla rosacea*														1								
Pe	Pod	*Podospongia lovenii*			**4**																			8
Pe	Ra	*Aulospongus spinosus*			1													**1**						
Pe	Ra	*Endectyon filiformis* **nov. sp.**															1							
Pe	Ra	*Endectyon delaubenfelsi*									**2**													
Pe	Ra	*Eurypon cinctum*				2																		
Pe	Ra	*Eurypon coronula*									1													
Pe	Ra	*Eurypon lacazei*				1																		
Pe	Ted	*Tedania* spp.													1									
Sp	Tei	*Craniella cranium*									1													
Ve	*Ia*	*Hexadella racovitzai*	+																					

TABLE 3. Comparative data of *Axinella* spp. previously described from the Atlantic-Mediterranean region and skeletally and/or morphologically related to those reported in the present study (bottom of species list). Numbers in brackets following the species name indicate bibliographic references, as it follows: (1) Descatoire 1966; (2) present study; (3) Topsent 1892; (4) Topsent 1896; (5) Topsent 1928; (6) Lendenfeld 1897; (7) Lévi 1957; (8) Pulitzer - Finali 1983; (9) Babic 1922; (10) Boury-Esnault *et al.*1994; (11) Pansini 1984; (12) Topsent1904; (13) Burton 1931. Dashes refer to the absence of data in the references and blanks in the "Styles" or "Oxeas" columns indicate the absence of a particular spicule type. Abbreviations for skeletal structure are: pl= plumose; pr= plumoreticulate.

Axinella spp. (reference)	Specimen location	Shape and size (length x width in mm)	Color	Styles (µm)	Oxeas (µm)	Trichodragmata (µm)	Skeletal structure
A. alba (1)	Glénan Islands (Atlantic Ocean)	encrusting base (25mm long) with 3 erect processes (15 x 5-8)	white	250-1200 x 15-18 (I) 260-950 x 3-10 (II)	700-1000 x 15-18	40-60 (length)	pl
A. alborana nov.sp. (2)	Alboran Island (Mediterranean Sea)	erect, stalked , and flattened, sometimes with incipient branches (10-28 x 2-19)	pale to bright orange (in alcohol)	630-2375 x 5-20	260-650 x 5-20		pr
A. flustra (3)	Bay of Biscay, Azores (Atlantic Ocean)	erect, stalked, with flattened branches (50 x 50)	beige (in alcohol)	870 x 16	185 x 7 (axis) 255 x 13 (body)		pr
A. flustra, herein revised (2)	Bay of Biscay, Azores (Atlantic Ocean)	erect, stalked , with 1-8 flattened branches (24-50 x 30-50)	yellowish white (in alcohol)	190->900 x 10-20	160-340 x 7.5-15	47-50 (length)	pr
A. flustra, as *A. padina* (4)	Golf of Lion (Mediterranean Sea)	erect, foliaceous , with 4 spatula-shaped lobes (40X35)	____	650-900 x 8-10	250-275 x 3-6	40 (length)	pr
A. flustra, as *Tragosia flustra* (5)	Cape Verde (Atlantic Ocean)	erect, stalked, foliaceous (30-40 x 35-40)	orange yellow (in vivo)	300- >1000 x 10-20	160-320 x 3-15	25-36 x 3-5	pr
A.infundibuliformis, as *Trachytragophora infundibuliformis* (6)	Rockall bank (Atlantic Ocean)	flabellate or caliculate (no size given)		300-600 x 12-16	250-500 x 10-15	15-20 x 5-6	pr
A. minuta (7)	Gabes Gulf , Alexandria (Western Mediterranean)	cushion-shaped encrusting base from which some processes rise up (2 x 2)		120-300 (I) 1200 (II)	120-300		pr
A. minuta (8)	Corse (Mediterranean Sea)	incipiently and irregularly branched (15 x 11)	____	150-490 x 5.5-14 (I) 1300-1700 x 11.5-30 (II)	180-600 x 4.5-14		____
A. pumila (9)	Adriatic Sea (Mediterranean Sea)	encrusting, resembling a grass lawn (no size given)	yellowish pink (in alcohol)	255-935 x 8-6 (I) 2000 x 19 (II)	170-730 x 2-18		____
A. pumila (10)	Alboran Sea (Mediterranean)	massive (no size given)	white (in alcohol)	790-1300 x 20-25	350-520 x 12-15		pr
A. spatula nov.sp.; beige (2)	Alboran Island (Mediterranean Sea)	erect, flabellate, undivided or with 2 branches (35-75 x 6-13)	beige (in alcohol)	119-1400 x 3-30	180-750 x 2.5-20	25-35 x 5-7.5	pr
A. spatula nov.sp.: black (2)	Alboran Island (Mediterranean Sea)	erect, flabellate, undivided or with 2-3 branches (35-100 x 2-8)	black (in alcohol)	350-1400 x 5-20	120-500 x 2.5-20	25-30 x 6-10	pr
A. cavelea (11)	Portofino, Marseille, Marconi Gulf (Mediterranean Sea)	flabellate (50-60 x 40-50)	orange (in vivo); white (in alcohol)	270-1450 x 2.5-14	250-370 x 2-12		pl
A. casoumda (12)	Azores (Atlantic Ocean)	erect, with a narrow base, mostly ramified (30-60 x 15-20)	yellowish white (in alcohol)	>1000 x 20	>1500 x 50		pr
A. vellerea (12)	Azores (Atlantic Ocean)	clavate or stalked and branched (45-90 x 17)	yellowish white (in alcohol)	1000 x 30-40 (I) 1800 (II)			pl
A. vellerea, herein revised (2)	Azores (Atlantic Ocean)	markedly or slightly branched (45-97 x 18-40)	ochre (in alcohol)	825-1625 x 12-35			pl
A vellerea (13)	Folden Fiord (Norwegian Sea)	massive, as incipient, erect columns (no size given)	yellowish white (in alcohol)	____	____		____
A. vellerea (2)	Alboran Island (Mediterranean Sea)	columnar, undivided or with 2-3 incipient lobule-like branches (10-30 x 5-8)	ochre to light brown (in alcohol)	470-1725 x 11-30	700-1120 x 5-20		pr

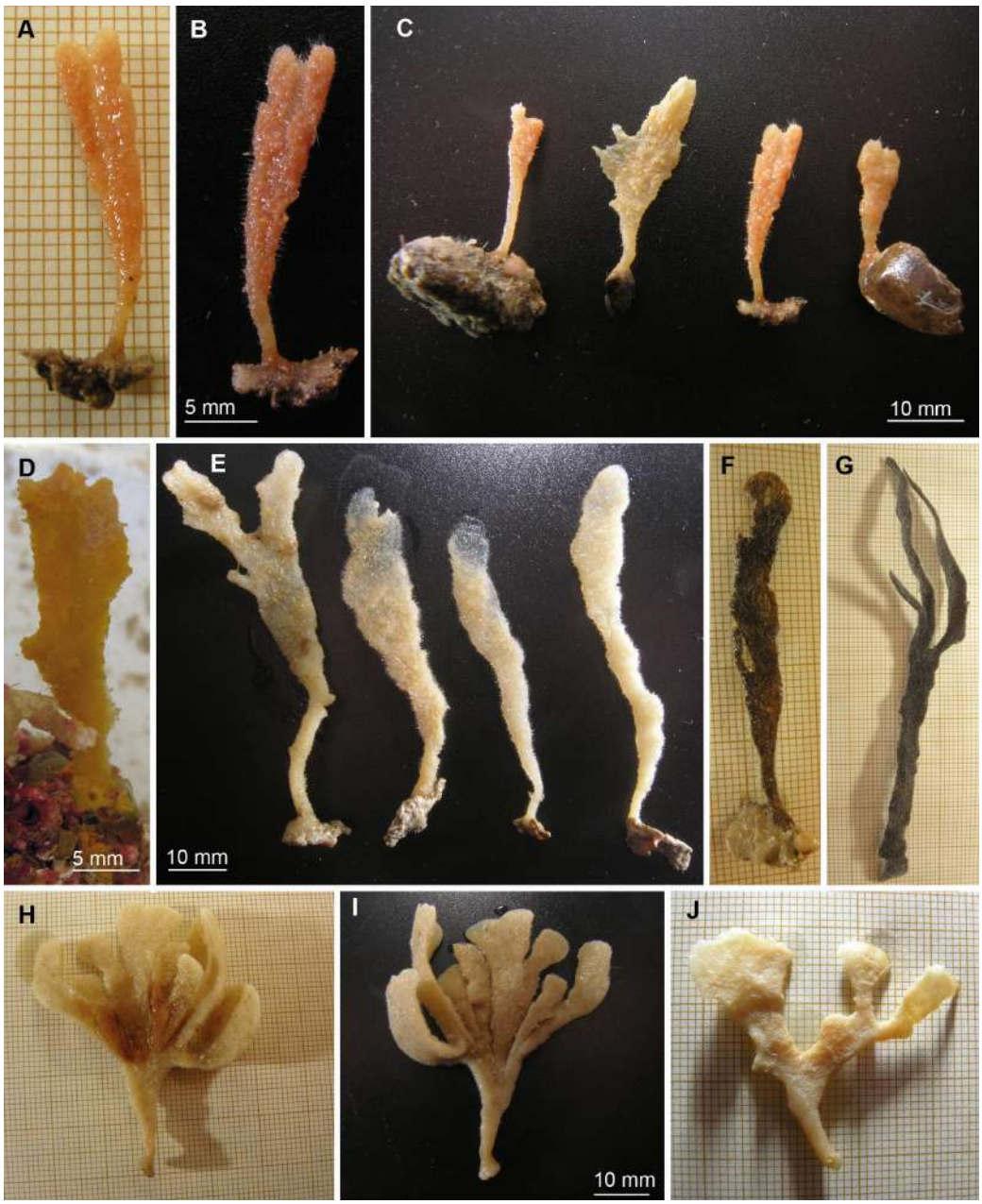

FIGURE 6. (A–B) Holotype of *Axinella alborana* **nov. sp.** seen from its both sides (MNCN-Sp155-DR44A). (C) Holotype and 3 additional, collected specimens of *A. alborana* **nov. sp.** (from left to right, MNCN-Sp3-DR05A, MNCN-Sp146-BV33A, MNCN-Sp155-DR44A, MNCN-Sp146-BV33B). (D) Specimen of *Axinella spatula* **nov. sp.**, photographed on board immediately after collection. (E) Preserved specimens of *A. spatula* **nov. sp.**, being the first (from left to right) the holotype (MNCN-Sp145); the remaining specimens are BV33B, MNCN-Sp116-BV15A & B, and MNCN-Sp65-BV21B. (F–G) Blackish specimens (MNCN-Sp57-BV21A and MNCN-Sp57-BV21B, respectively) of *A. spatula* **nov. sp.** The former shows an incipient branching, while the latter is clearly branched and with no narrowing at the stalk. (H–J) Syntypes of *Tragosia flustra* (Topsent, 1892) collected by Topsent in 1888 (Stn. 247. M. O. M. 040272) and in 1886 (Stn. 58. M. O. M. 040044), respectively. The former (H–I) is shown on its both sides, being profusely ramified, while the latter (J) shows only 3 branches.

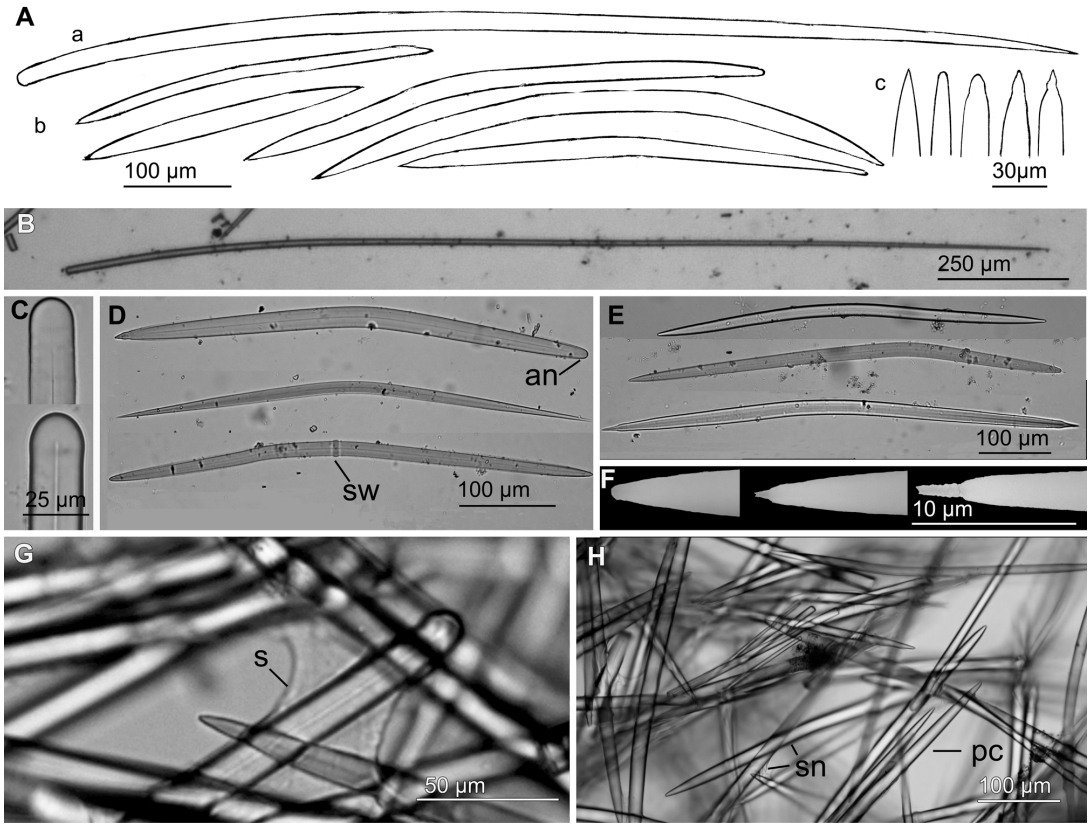

FIGURE 7. *Axinella alborana* **nov. sp.**: (A) Line drawing summarizing the skeletal complement of the Alboranian specimens, consisting of styles (a) and oxeas (b) with acerate, blunt or mucronate ends (c). (B–C) Light microscope view of a style, with examples of the round end. (D–E) Light microscope views of oxeas. Note the varying curving angle, the anisoxea (an) character in some spicules, and the annular swelling (sw) of others. (F) SEM details of oxea ends, being typically either blunt or mucronate. (G) Light microscope view of the skeletal arrangement, showing a style embedded in spongin (s) in the extra-axial skeleton. (H) Light microscope view of oxeas at the extra-axial plumoreticulate skeleton occurring either in paucispicular tracts (pc) or free (sn).

Macroscopic description. Erect, stalked, flattened sponge, typically attached to small fragments of rocks or shell fragments (Fig. 6A–C; Table 4). The stalk is either cylindrical or compressed, no longer than one quarter of the total sponge length, and hardly recognizable in some specimens. The flattened part of the body is flexible and relatively rectangular, except for the apical margin of the lamina that may be irregularly lobate. Some specimens show an incipient, terminal ramification; none is markedly divided nor further branched. The sponges measure 10–28 mm in height, with a lamina up to 19 mm in wideness and 1–2 mm in thickness. The surface is irregularly hispid, with no aquiferous opening discernible. The color ranges from creamy to reddish orange in life, clearing after preservation in ethanol.

Skeleton. Megascleres are styles and oxeas (Table 4). Styles are slightly curved at a third of their length (Fig. 7A–B), with a regular round end that occasionally forms one or two slight subtyles and/or annular swellings (Fig. 7C). The pointed end is usually sharp, but rarely blunt ends occur. Styles measure 630–2375 x 5–20 µm, although two specimens showed a low proportion (<1%) of abnormally shorter or longer styles, measuring respectively down to 580 µm and up to 3000 µm in length (Table 1). Oxeas are slightly or markedly fusiform, curved once or twice, either symmetrically or asymmetrically (Fig. 7A, D). Points are usually acerate; anisoxeas are fairly common and variations like mucronate and blunt ends are frequent, depending on the specimen (Fig. 7D). Occasionally they are centrotylote, with annular or subspherical swellings (Fig. 7D) being smooth or rarely rugose.

They measure 260–650 x 5–20 µm, but shorter oxeas, down to 180 and 125 µm in length, occur respectively in 2 of the studied specimens. As a rule of thumb, oxeas are more abundant than styles.

An axial skeleton is discernible in the stalk, made of ascending compact tracts of oxeas embedded by spongin and crossed by isolated (i.e., not packed) oxeas arranged confusedly. From the axial skeleton, an extra-axial plumoreticulate skeleton emerges, consisting of ascending loose pauci—and multispicular tracts of oxeas reinforced with some spongin (Fig. 7G). In the extra-axial region, there are isolated inter-crossed oxeas forming a confusing reticule-like arrangement (Fig. 7H). Long styles, either isolated or in small groups (2–4), project outward from the spongin cover of the extra-axial tracts, piercing the sponge surface to make it hispid.

TABLE 4. Comparative data of *Axinella alborana* **nov. sp.** specimens, including branching level, color after preservation, and size range of styles and oxeas.

Specimen	Branching	Color (alcohol)	Styles (µm)	Oxeas (µm)
MNCN-Sp03-DR05A	unbranched	orange	990–1800 x 10–20	270–560 x 5–20
MNCN-Sp03-DR05B	2 incipient branches	reddish orange	1100–2375 x 1–20	180–580 x 7.5–15
MNCN-Sp14-BV13A	2 incipient branches	pale orange	630–2075 x 5–20	260–650 x 5–20
MNCN-Sp34-BV14A	2 incipient branches	pale orange	580–1300 x 10–20	125–620 x 5–15
MNCN-Sp34-BV14B	2 incipient branches	whitish orange	975–2000 x 10–20	360–630 x 10–20
MNCN-Sp19-DR29A	damaged	pale orange	710–1625 x 7.5–15	360–610 x 7.5–20
MNCN-Sp146-BV33A	2 incipient branches	pale orange	630–1400 x 7.5–20	290–580 x 10–20
MNCN-Sp146-BV33B	2 incipient branches	pale orange	730–2250 x 5–20	280–620 x 5–20
MNCN-Sp191-BV41A	unbranched	whitish orange	825–1750 x 7.5–20	350–550 x 10–20
MNCN-Sp155-DR44A	2 incipient branches	reddish orange	1000–3000 x 10–20	390–600 x 15–20

Distribution and ecology notes. The individuals were collected at the deep shelf (87 to 173 m) of the Alboran Island, from rocky, detritic-organogenic gravel, and rhodolith bottoms.

Taxonomic remarks. No previously known *Axinella* spp. in the Atlantic-Mediterranean area have characteristics similar to those of the new species (Table 3). The external morphology of *A. alborana* **nov. sp.** bears some external resemblance to *A. flustra* (Fig. 6H–J), especially to Topsent's (1904) syntypes from Stn. 247 (Fig. 6H–I). Nevertheless, both species strongly differ skeletally, having *A. flustra* trichodragmata and shorter oxeas (Table 3). *Axinella vaceleti* Pansini, 1984 is also a flabellate species, but with a marked fan-shaped, undulating lamina, which is also larger (50–60 mm high) and thicker (4–5 mm) than that of the *A. alborana* **nov. sp.** specimens. Additionally, *A. vaceleti* has smaller spicules, specially the styles, ranging from 270 to 1450 µm (Pansini 1984).

Specimens of *Axinella alborana* **nov. sp.** were investigated for the first time about twenty years ago, as part of a study on the deep-shelf Alboranian sponges carried out by Maldonado (1993). Nevertheless, no description of material was published at that time because of the risk that the small individuals now described as *A. alborana* **nov. sp.** might correspond to juvenile stages of some poorly known, large *Axinella* spp. growing at the ill-known deep shelf. However, our recent exploration of those deep-shelf habitats using an ROV has revealed that there is no dense population of any other large *Axinella* spp. in the areas where *A. alborana* **nov. sp.** occurs. In the light of these findings, the idea that the dense undergrowth of small individuals might correspond to juvenile sponges makes no sense and these small sponges can indeed be identified as adults of *A. alborana* **nov. sp.**

***Axinella spatula* nov. sp.**
(Figs. 6D–G, 8; tables 2, 3, 5)

Etymology. The species is named after the "spatula" tool (a diminutive form of the Latin "spatha"), which bears resemblance to the external shape of the specimens.

Material examined. Holotype MNCN-Sp145-BV33B collected from type locality Stn. 33 (Table 1, Fig. 1), a 134 to 173 m deep, gravel bottom at the deep shelf of the Alboran Island.

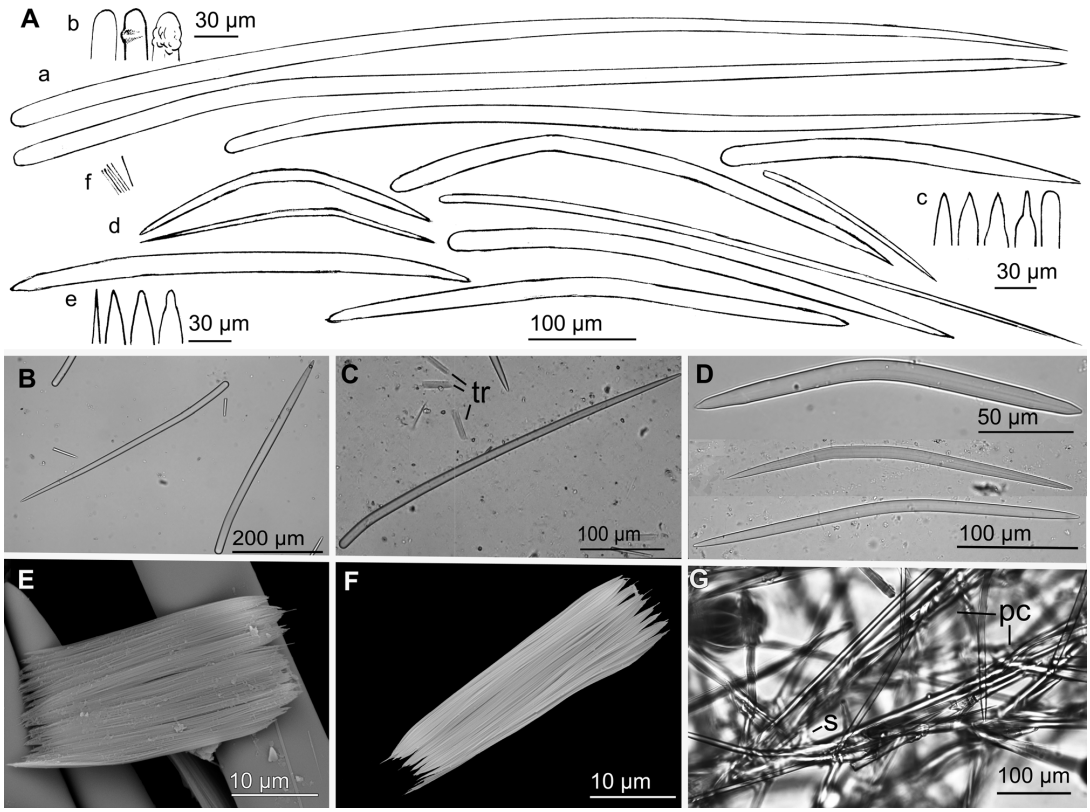

FIGURE 8. *Axinella spatula* **nov. sp.**: (A) Line drawing summarizing the skeletal complement of the Alboranian specimens. It consists of styles (a) in a wide range of sizes, with a round end that occasionally shows one or more swellings (b) and a distal end that can be acerate, stepped or blunt (c). Oxeas of varying shape (d), with acerate to mucronate ends (e). Raphides (f) are in trichodragmata. (B–C) Light microscope views of styles and trichodragmata (tr). (D) Light microscope view of oxeas. (E) SEM micrograph of the flattened trichodragmata typically found in the beige specimens (e.g., in MNCN-Sp65-BV21A). (F) SEM micrograph of a more cylindrical trichodragmata typically found in blackish specimens (e.g., in MNCN-Sp57-BV21A). (G) Detail of the plumoreticulate and somewhat irregular skeletal arrangement at the lamina region of the sponge. Note the spongin (s) is embedding the paucispicular tracts (pc).

Twenty-two paratypes designated: MNCN-Sp28-BV14A to C from Stn. 14; MNCN-Sp116-BV15A to I from Stn.15; MNCN-Sp57-BV21A to C (blackish specimens) and MNCN-Sp65-BV21A & B from Stn. 21; MNCN-Sp145-BV33A & C to D from Stn. 33; MNCN-Sp188-BV41A & B from Stn. 41 (Table 1, Fig. 1).

Comparative material: Syntype material of *Axinella flustra* (Topsent, 1892) = *Tragosia flustra* Topsent, 1892, since no holotype was designated by Topsent (1892) for this species (Table 3). Syntypes were two specimens (MOM-040044) from Bay of Biscay (Stn. 58; 43º40'N 8º55'W, 134 m deep, 7 August 1886) and two specimens (MOM-040272) from Azores (Stn. 247; 38º23.500'N 30º20.333'W, 318 m deep, 30 August 1888).

Macroscopic description. Erect, flabellate sponges (Fig. 6E–G; Table 5). They are 35–100 mm in height, with a basal stalk-like region in which the lamina progressively increases in wideness from the attachment point up to about 1/4 of the height, where it becomes approximately rectangular (3–9 mm in wideness). The lamina is thin (1–1.5 mm) and flexuous. It can be undivided, or, in some individuals, forming two or three flattened branches, all with a regular apical margin (Fig. 6E). The sponge surface is porous to the dissecting microscope, largely and irregularly hispid. Most collected individuals are pale orange when alive, turning into yellowish white to beige after ethanol preservation. Nevertheless, three of the specimens show remarkable color dissimilarity, being dark brown to black, at least after preservation in ethanol (Fig. 6F–G). Some of these blackish specimens (part of the paratype series) also account for the largest sizes (up to100 mm in height) and have the stalk-like region more flattened than the orange-beige individuals.

TABLE 5. Comparative data of *Axinella spatula* **nov. sp.** specimens, including branching level, color after preservation, and size range of styles and oxeas.

Specimen	Branching	Color (alcohol)	Styles (μm)	Oxeas (μm)	Trichodragmata (μm)
MNCN-Sp28- BV14A	unbranched	beige	170–1300 x 8–20	180–430 x 5–12	22.5–32.5 x 8–10
MNCN-Sp28- BV14B	unbranched	beige	310–1250 x 5–10	210–450 x 4–10	25–28 x 5–8
MNCN-Sp57- BV21A	unbranched	black	350–1400 x 5–20	220–500 x 2.5–20	25–30 x 6.25–10
MNCN-Sp57- BV21B	2 incipient branches	black	245–1225 x 8–18	120–432 x 9–12	25–30 x 6–10
MNCN-Sp65 -BV21A	unbranched	beige	220–1100 x 5–30	220–520 x 5–10	25–30 x 9–10
MNCN-Sp145-BV33A	2 incipient branches	beige	165–1050 x 3–15	180–520 x 2.5–15	25–30 x 5–8
MNCN-Sp188- BV41A	unbranched	beige	119–1400 x 4–15	190–750 x 5–20	25–35 x 5–8

Skeleton. Megascleres are styles and oxeas (Table 5). Styles occur in a wide variety of size and shape, with abundant intermediate forms that prevent making putative categories. Styles are often slightly curved, either symmetrically or asymmetrically; sometimes they have more than one flexion point and can even be angulated and, more rarely, slightly sinuous (Fig. 8A–C). The round end is usually regular, occasionally with an annular swelling (Fig. 8A). The distal end is of variable morphology, from sharp hastate or acerate type to stepped, mucronate, and almost blunt (strongyloxea-like) type (Fig. 8A). Styles measure 119–1400 x 3–30 μm, not being further categorizable according to their size. They are also difficult to separate according to their location, but most of those in the choanosomal region are not larger than 550–620 x 10–20 μm. Styles in the black specimens have a size range (245–1400 x 5–20 μm) virtually identical to that of the orange-beige individuals, although predominating sizes are usually over 800 x 10 μm. Oxeas, some more abundant than the styles, are also relatively variable in size and shape, but variability ranges are similar among specimens. They can be slightly or markedly curved, once or twice, and symmetrically or asymmetrically (Fig. 8A, D). Tips are usually acerate or blunt, although mucronate ends also occur (Fig. 8A). They measure 180–750 x 2.5–20 μm in the orange-beige specimens and 120–500 x 2.5–20 μm in blackish individuals. Microscleres in both orange-beige and blackish individuals are raphides in highly packed trichodragmata (Fig. 8E–F), measuring 22.5–35 x 5–13.7 μm. Although no evident size difference exists in trichodragmata between orange-beige and blackish individuals, their shape can be flattened or cylindrical in the orange-beige ones (Fig. 8E), but only cylindrical trichodragmata (Fig. 8F), and in higher abundance, are found in the blackish ones.

The skeletal structure is plumoreticulate. There is an evident axial skeleton in the stalk-like region, built by multispiculate tracts of oxeas. In the thin lamina there is no clear distinction between axial and extra-axial skeleton. Rather, there are pauci—and multispicular, ascending and ramifying tracts, compressed in the sense of the lamina and consisting of mainly oxeas, with sparse styles (Fig. 8G). These tracts are looser than in the axial skeleton of the stalk, and are connected each other by an irregular reticule that becomes more apparent in the thinnest parts of the lamina. In the three blackish specimens, the styles in the ascending tracts are somewhat more abundant and usually slightly longer than those in the orange-beige specimens. There are peripheral styles with their round end embedded in the tracts, piercing perpendicularly surface and making it hispid. The hispidating styles are usually long and occur isolated or in plumose tufts of up to 7 styles. Trichodragmata are predominantly located near the surface, especially in the blackish specimens. Spongin is abundant in the axial skeleton although it does not entirely embed all the spicules. It occurs moderately in the plumose tracts of the lamina (Fig. 8G).

Distribution and ecology notes. All the collected specimens came from gravel bottoms, sometimes with organogenic components, at depths ranging from 93 to173 m.

Taxonomic remarks. Except for color, the morphological and skeletal differences between the orange-beige individuals and the blackish ones are minor (Table 5) and we judged them not enough to support a differentiation into two separated species. Both color varieties share relevant features, such as similar body morphology and plumoreticulate skeleton with the same spicule categories and similar size ranges. In addition to the obvious color differences, it can be noticed: 1) a higher abundance of cylindrical trichodragmata in the blackish individuals; 2) a slightly more organized reticule-like arrangement linking the plumose tracts in the orange-beige individuals; and 3)

higher frequencies of short styles in the orange-beige specimens. Even though we are herein assuming that these differences correspond to ill-known aspects of intraspecific variation, we cannot discard that future studies based on molecular features of new collections and/or "in vivo" observations may led to a species split.

Trichodragmata similar to those in *A. spatula* **nov. sp.** are also found in some other *Axinella* spp. (Table 3), such as *Axinella infundibuliformis* (Linnaeus, 1759). Nevertheless, this latter species has a caliculate or fan-like body shape, a plumoreticulate skeleton of oxeas and styles clearly smaller (300–600 x 12–16 μm), as well as smaller (15–20 μm long) trichodragmata (Lendenfeld 1897; Arndt *et al.* 1935). It is also worth noting that the earliest descriptions of *A. infundibuliformis* were little accurate and apparently overlooked the small trichodragmata (Johnston 1842; Bowerbank 1866; Hansen *et al.* 1885; Fristedt 1887). *Axinella alba* (Descatoire, 1966) also shows trichodragmata, but it is an encrusting species and has oxeas (700–1000 x 15–18 μm) longer than those of *A. spatula* **nov. sp.** Trichodramata and styles also occur in *Axinella flustra* (Descatoire 1966), but, again, although these styles and trichodragmata are in a size range similar to those of *A. spatula* **nov. sp.**, the branching body shape (Fig. 6H–J) and shorter oxeas make *A. flustra* easily distinguishable (Table 3).

Some members of the axinellid genus *Dragmacidon* Hallman, 1917 (Table 3) bear some vague resemblance to *A. spatula* **nov. sp.**, namely occurrence of raphides and the absence of a clear axial and extra-axial skeleton differentiation. Furthermore, phylogenetic analyses based on 18SrRNA, 28S rRNA and CO1 have brought *Dragamacidon* species and raphide-bearing *Axinella* species into a same clade (Gazave *et al.* 2010; Morrow *et al.* 2012). *Dragmacidon tuberosum* (Topsent, 1928) is the only geographically close species in the genus having trichodragmata, but those are distinctive, having the raphides projecting from each side of the packets; besides, this species has shorter styles (Topsent 1928).

Axinella vellerea Topsent, 1904

(Figs. 2B, 9, 10; Tables 2, 3)

Material examined. Thirteen specimens collected from the deep shelf of Alboran Island: MNCN-Sp51-DR05A & B from Stn. 5; MNCN-Sp148-BV33 from Stn. 33; MNCN-Sp196-BV41 from Stn. 41; MNCN-Sp142-DR44 A to I from Stn. 44 (Table 1, Fig. 1)

Comparative material: Syntype material of *Axinella vellerea* Topsent, 1904 (since no holotype was originally designated by Topsent), consisting of two specimens from Stn. 866 at Azores Islands (38º52.833'N 27º23.083'W; water depth: 599 m; 2 August 1897), and currently stored at the Monaco Museum (MOM-040631).

Macroscopic description. Specimens are erect, columnar, undivided or with two-tree incipient, lobule-like ramifications (Fig. 9A–H). The sponges measure 10–30 x 5–8 mm. The consistency is fleshy but hardly flexible. The surface is irregular, grooved, and porous. In some specimens, the oscules can be observed in the translucent epithelium folding the grooves, which run usually vertically, parallel to the longest axis of the body. The hispidation of the ectosome is short and not very dense, mostly verifiable under the dissecting microscope. The animal color in ethanol is ochre or pale brown.

Skeleton. Megascleres are only styles and, in some individuals, a very low number of oxeas. Styles occur in a wide range of shapes and sizes, but without making discernible categories. They are slightly curved to somewhat angulate, some curved nearly the round end, similarly to rhabdostyles (Fig. 10A–B). The round end may be regular, but subtyles and annular swellings are also common, either in terminal or subterminal position (Fig. 10A–C). The point is usually acerate, but sometimes stepped or even blunt (Fig. 10A). Spicule malformations occasionally occur as well. Styles measure 470–1725 x 11–30 μm, but diameters smaller than 15 μm are uncommon. Some scattered oxeas have been observed in some specimens, in which case they are angulated or have a two-point curvature (Fig. 10D), sometimes asymmetrical; they may also be centrotylote. When present, they measure 700–1120 x 5–20 μm.

The skeletal arrangement consists of a somewhat central, compressed, plumoreticulate axis from which a plumoreticulate extra-axial skeleton spreads (Fig. 10E). The ascending extra-axial tracts become thinner as they reach the surface, and their terminal styles pierce the ectosome causing hispidation. Moderate spongin embeds the spicules but without forming fibres (Fig. 10F); spongin becomes less abundant in the extra-axial region.

Distribution and ecology notes. The individuals were collected from depths ranging from 102 to 173 m, on rock, gravel or dead rhodolith pieces. The collected material makes the first Mediterranean record of this rare species. To date only four specimens had previously been reported: three of them collected from a 599 m deep,

gravel bottom at Azores (Topsent 1904), and one from 200–290 m depths at the Folden fiord of the Norwegian Sea (Burton 1931).

Taxonomic remarks. The size of the examined syntypes of *A. vellerea* (97 x 40 mm and 45 x 18 mm) is slightly larger than that of any of the Alboranian individuals, being the remaining aspects of the external morphology notably similar between both specimen groups (Fig. 9A–H). The largest syntype also shows two branches better developed (Fig. 9F–G) than the incipient branches often characterizing the Alboranian individuals (Fig. 9A–E). Regarding the spicules, the Alboranian specimens and the syntypes of *A. vellerea* show styles in nearly identical size and shape ranges (Table 3). A small skeletal difference is that oxeas are not found in neither the original description by Topsent (1904) nor in our re-examination of the syntypes. Burton (1931) did report occasional "oxeote styles" in his Norwegian specimen. In the Alboranian, specimens, we found oxeas in only a minority of individuals and always in low abundance. Therefore, the oxeas appear to be a variable element in the spicule complement of *A. vellerea*, as it is also the case of other *Axinella* spp.

As previously noticed by Topsent (1904), *A. vellerea* and *Axinella vasonuda* Topsent, 1904 bear similarity in both their external morphology and the skeletal organization. Nevertheless, *A. vasonuda* is characterized by having oxeas as main spicule type, showing only scarce styles, the occurrence of which is limited to the peripheral zones of the skeleton.

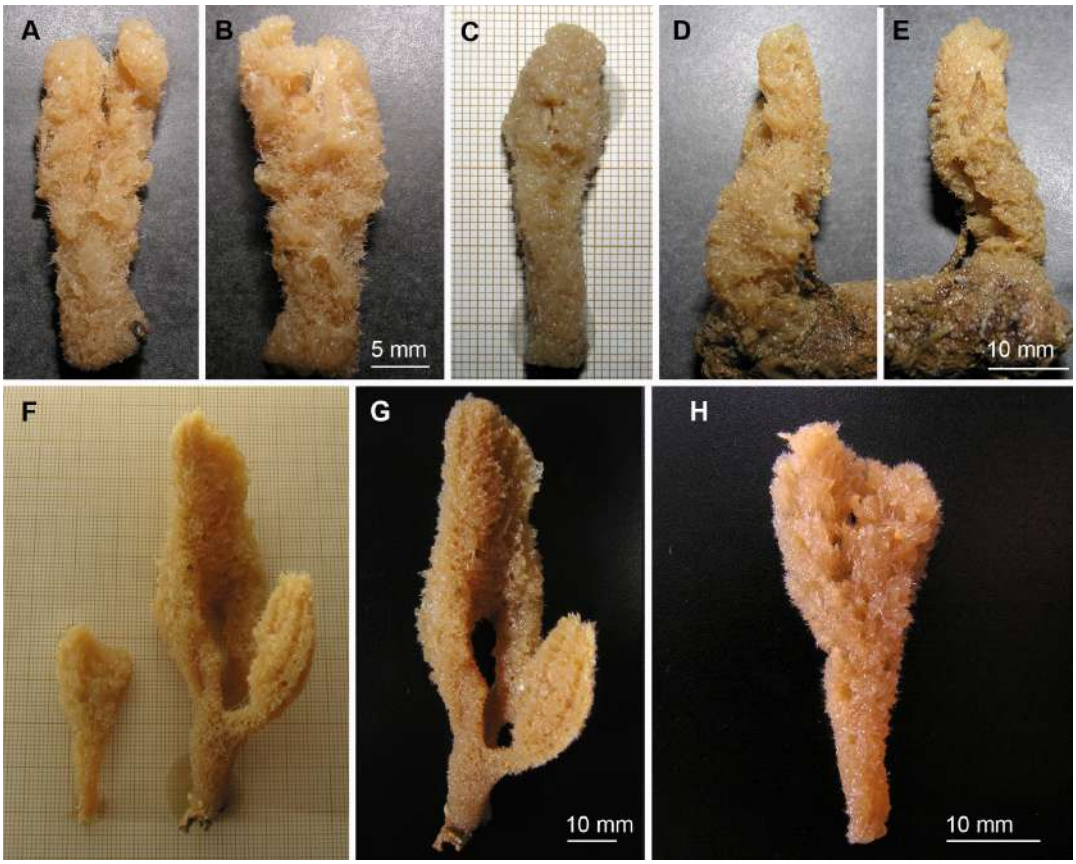

FIGURE 9. *Axinella vellerea* Topsent, 1904. (A–B) One of the collected Alboranian specimens (MNCN-Sp51-DR05A) shown on its both sides and bearing an incipient branching. (C) A branchless Alboranian specimen (MNCN-SP51-DR05B) of *A. vellerea* photographed on graphic paper. (D-E) Another unbranched Alboranian specimen (MNCN-Sp142-DR44A) attached to a piece of gravel, shown on its both sides. (F) Photograph of the holotype (the large sponge to the right) and the syntype (to the left) of *A. vellerea*, collected by Topsent in 1897 (Stn. 866. M. O. M. 040631). (G) Close up of the holotype of *A. vellerea*, being clearly ramified and larger than most specimens collected from the Alboran Island. (H) Close up of the syntype of *A. vellerea*, showing an incipient branch.

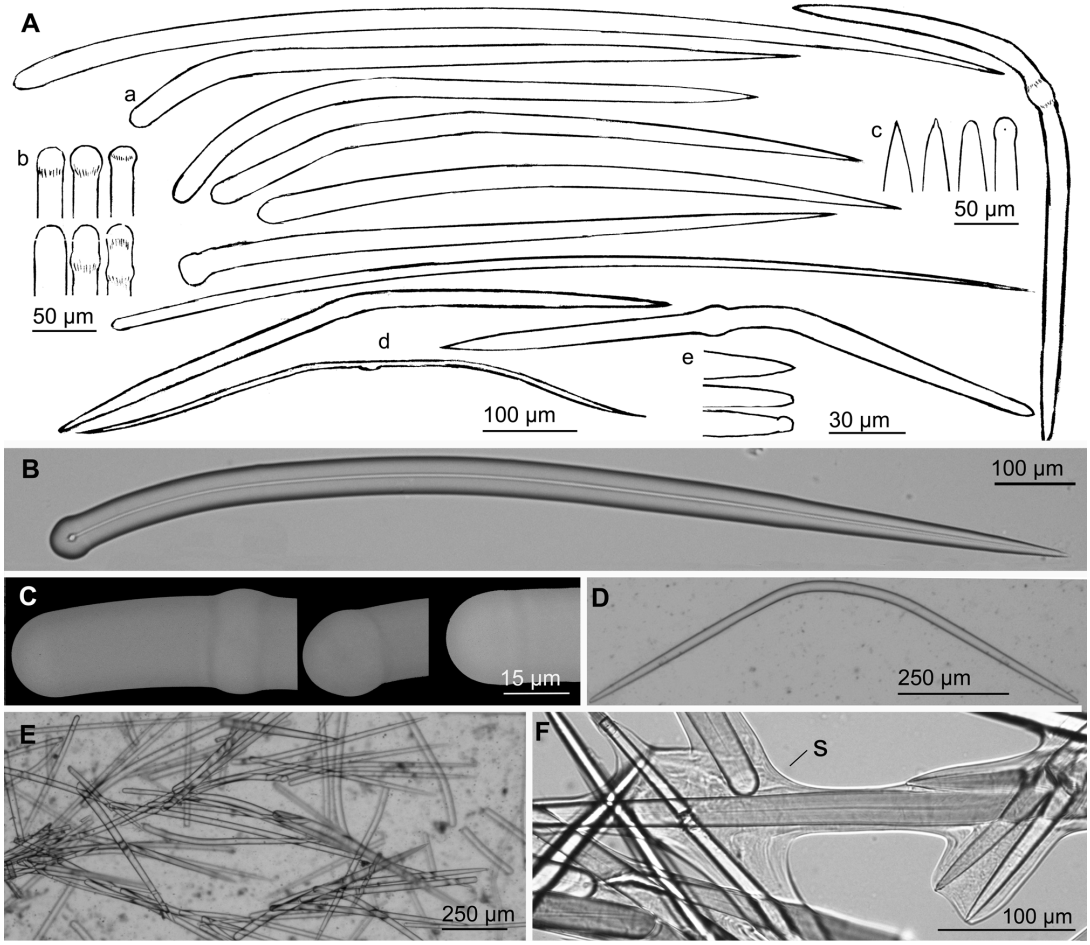

FIGURE 10. *Axinella vellerea* Topsent, 1904: (A) Line drawing summarizing the skeletal complement of the Alboranian specimens. Styles (a) are in a wide variety of shapes, with a round end that can be regular or showing one or more swellings (b) and a distal end (c) that can be regular to blunt, sometimes with mucronate variations. Oxeas (d) occur in varying size and shapes, with ends ranging from acerate to mucronate (e). (B) Light microscope view of a style with a subtylote end. (C) SEM detail of three typical morphologies (i.e., subterminal ring, subtylote, and regular) of the round end of styles. (D) Light microscope view of a double-bent oxea. (E) Light microscope view of plumose arrangement in the extra-axial skeleton. (F) Detail of styles embedded by spongin (s).

Family BUBARIDAE Topsent, 1894

Genus *Rhabdobaris* Pulitzer-Finali, 1983

Diagnosis. Monotypic genus of Bubaridae, characterized by stalked and flabellate body shape, possessing long hispidating styles and a plumoreticulate internal skeleton made of choanosomal rhabdostyles, oxeas, and strongyles, with smooth and spiny forms co-occurring. Microscleres are raphides in trichodragmata (genus diagnosis herein redefined after *Rhabdobaris* being restituted as a valid genus; not a junior synonym of *Cerbaris* Topsent, 1898).

Remarks. See the "Taxonomic remarks" section of *Rhabdobaris implicata* for further discussion and concerns about the morphological affinity of the herein restituted genus *Rhabdobaris* and members of the family Raspailiidae.

***Rhabdobaris implicata* Pulitzer-Finali, 1983**
(Figs. 11A–B, 12; Table 2)

Synonymy. Cerbaris implicatus (Pulitzer-Finali, 1983): Alvarez & Van Soest 2002, 751–752.

Material examined. Only one individual (MNCN-Sp23-BV14) collected from Stn. 14 (Table 1, Fig. 1), a 96–100 m deep, gravel bottom on the deep shelf of the island. The collected individual is herein designated the neotype, given that the previously available holotype specimen was entirely acid-dissolved to obtain a spicule slide. We are reasoning herein (see the *Taxonomic remarks* section) that type material in which the macroscopic body features and the skeletal arrangement can be evaluated is crucial to recognize the distinct nature of the monotypic genus *Rhabodobaris* within the family Bubaridae and, therefore, to support the nomenclatorial restitution of the genus. These "exceptional circumstances" strongly advice the neotype designation to preserve the stability of the nomenclature, following article 75 of the International Code of Zoological Nomenclature.

Comparative material: Original holotype of *Rhabdobaris implicata* Pulitzer-Finali, 1983. The only available material of the original holotype is the spicule slide (MSNG-47170) resulting from boiling in nitric acid the small specimen collected off Calvi, N-W of Corse, at 121–149 m depth (Pulitzer-Finali 1983).

Macroscopic description. Stalked, flabellate sponge (Fig. 11A–B), with a thin lamina measuring 15 mm long x 25 mm wide x 1 mm thick; the stalk, somewhat compressed, measures 7 mm in length x 2.5 mm in wideness. There are 3 and 4 reinforcement ribs at each side of the lamina (Fig. 11A–B), making the lamina poorly flexible. There are no aquiferous openings discernible to the naked eye. The surface of the lamina is markedly hispid, with long spicules protruding uniformly at moderated density. The stalk is less hispid. The color of the alcohol-preserved specimen is creamy white.

Skeleton. Megascleres are in seven categories: long hispidating styles, rhabdostyles, oxeas, styrongyles, acanthoxeas, acanthostyles, acanthostrongyles. Microscleres are raphides in trichodragmata. Hispidating styles are long, gently conical, nearly straight or softly curved, with a regular round end and a sharp, acerate or hastate point (Fig. 12A–B). They are 754–1557 µm long and 8–16 µm wide. Rhabdostyles have a slight to marked curvature on their first ¼ of their length (Fig. 12A, C), rarely becoming regular styles. Other variations occurring in the rhabdostyles are annular or irregular swellings in the vicinity of the round end and polyaxial malformations in the vicinity of the pointing end (Fig. 12C); the points can be acerate, stepped, or even bifid (Fig. 12A). Rhabdostyles measure 137–304 x 5–13 µm, although some thinner, growing stages (Fig. 12A) can occasionally be observed, measuring 107–212 x 3–6 µm. Oxeas are isodiametric, in a wide range of morphologies, showing from one to three flexion points, and more asymmetrical (Fig. 12A, E); they can occasionally be centrotylote, sometimes with the swelling placed asymmetrically. Oxea ends are acerate, conical, mucronate or stepped, with bifid and polyaxonic malformations also occurring (Fig. 12A, E). Oxeas measure 222–405 x 5–10 µm, although, as it happens in the rhabdostyles, thinner growing stages (Fig. 12A) measuring 185–285 x 1–3 µm occasionally occur. Strongyles are curved once or twice, regularly or irregularly (Fig. 12A), occasionally symmetrically or asymmetrically centrotylote, measuring 160–310 x 14–15 µ. Strongyles are clearly less abundant than rhabdostyles and oxeas.

The rhabdostyles, the oxeas and the strongyles have "acanthose versions", which usually are slightly smaller and less abundant than their respective smooth counterparts. Acanthorhabdostyles measure 125–187 x 6–11 µm and show from scarce to abundant small spines, equally or unequally distributed along the spicule and not necessarily confined to one of the ends (Fig. 12D). Acanthoxeas measure 120–280 x 7–9 µm and show few to abundant spines, often more concentrated towards the ends (Fig. 12A, F). In few acanthoxeas, the spines were relatively thick and blunt, becoming a sort of tubercles. Acanthostrongyles measure 129–409 x 5–12 µm, being entirely or partially spiny (Fig. 12A). Microscleres are toxiform raphides, occurring in trichodragmata (Fig. 12A, H) that measure 22–50 x 10–20 µm.

The skeletal architecture is plumoreticulate. The stalk contains a compact plumoreticulate skeleton with ascending multispiculate tracts including all categories of choanosomal megascleres (i.e., except the long hispidating styles) embedded in moderate spongin. Nevertheless, in order not to damage the stalk, we only sampled a tiny peripheral portion of stalk tissue and cannot discard the occurrence of a pure axial skeleton in its central region. In the lamina, the ascending tracts ramify and reticulate irregularly, compressed in the plane of the lamina; there are also free oxeas and styles arranged obliquely to the ascending tracts. Long hispidating styles with their round end embedded in the ascending tracts protrude largely the surface of the sponge at the lamina. Additionally,

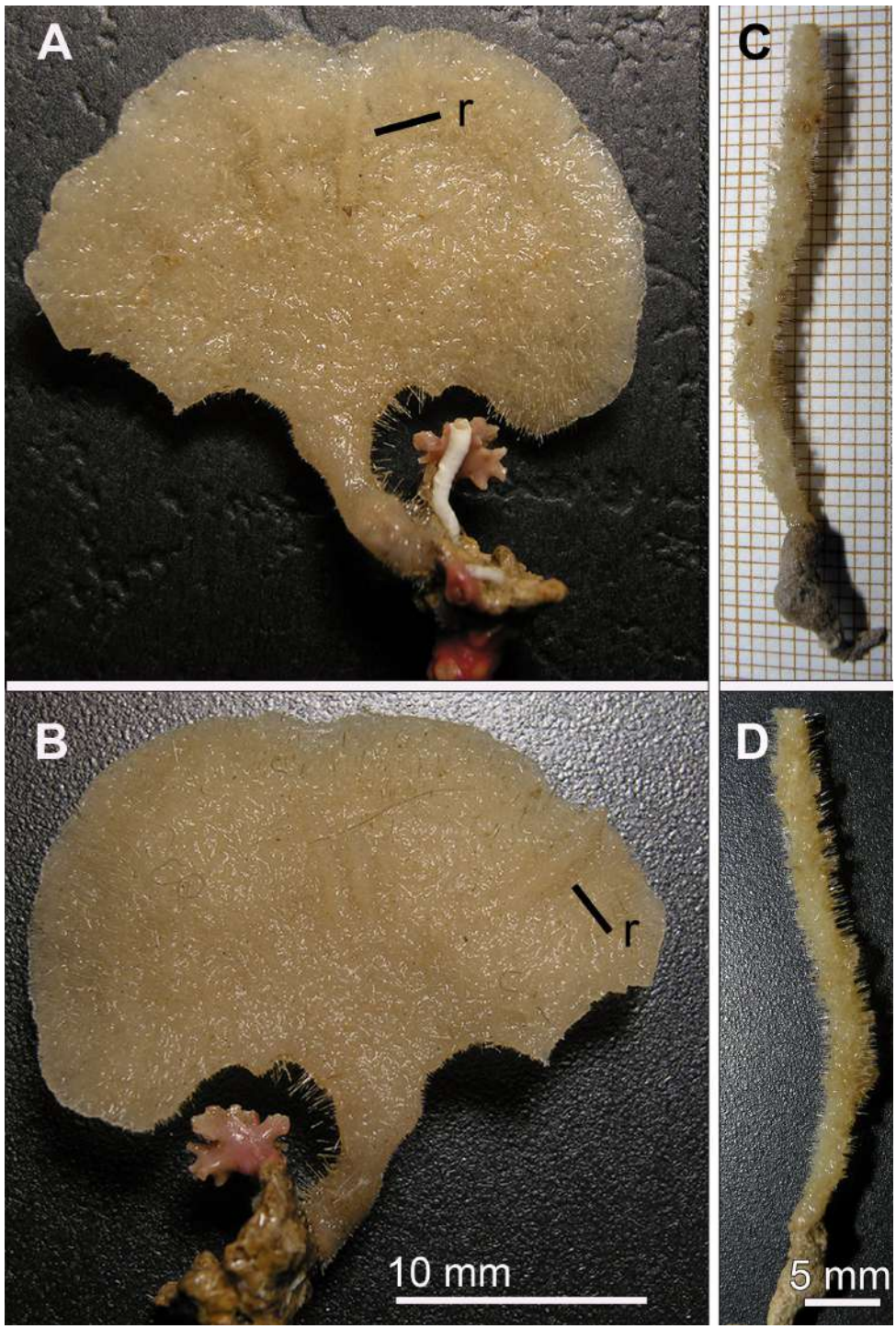

FIGURE 11. (A–B) Neotype (MNCN-Sp23-BV14) of *Rhabdobaris implicata* Pulitzer-Finali, 1983 collected from the Alboran Island and photographed on its both sides. Note some ribs (r) on the lamina. (C–D) Holotype of *Endectyon (Hemectyon) filiformis* **nov. sp.** (MNCN-Sp69 BV21) attached on a small piece of gravel, photographed on its both sides.

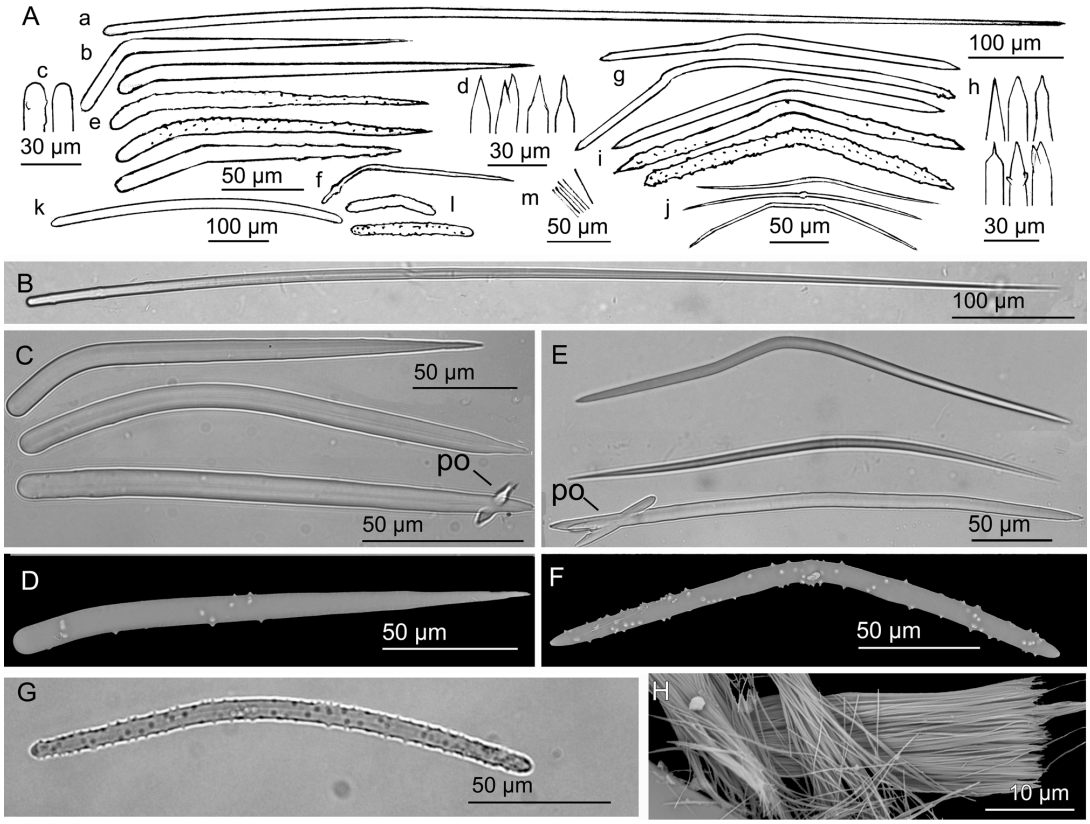

FIGURE 12. *Rhabdobaris implicata* Pulitzer-Finali, 1983: (A) Line drawing summarizing the skeletal complement of the Alboranian specimen (MNCN-Sp23-BV14), consisting of hispidating styles (a), smooth rhabdostyles (b) with a regular or swollen round end (c) and acerate, bifid to polyactinal, or stepped distal end (d), acanthostyles (e), small styles (f), smooth oxeas (g) with acerate, stepped, mucronate or polyactinal ends (h), acanthoxeas (i), developing stages of oxeas (j), strongyles (k), acanthostrongyles (l), and toxiform raphides in trichodragmata (m). (B–D) Light microscope views of an hispidating style (B) and choanosomal rhabdostyles (C), sometimes with abnormal, polyactinal points (po). (D) SEM view of an acanthostyle. (E) Light microscope view of oxeas in various shapes, sometimes showing polyactinal ends (po). (F) SEM micrograph of an acanthoxea. (G) Light microscope view of an acanthostrongyle of the holotype *Rhabdobaris implicata* Pulitzer-Finali, 1983 (MSNG-47170). (H) SEM image of two overlapped trichodragmata of toxiform raphides in the Alboranian specimen.

among the long hispidating styles, there is also a short, dense and uniform hispidation caused mostly by non-acanthose rhabdostyles and oxeas. Likewise, the hispidation of the stalk is only due to these shorter spicules, lacking the long hispidating styles.

Distribution and ecology notes. Rare species, only known previously from the holotype (Pulitzer-Finali 1983), a specimen collected at 121–149 m, off Calvi (Corse Island, Western Mediterranean). Our Alboranian specimen, collected from a 96–100 m deep, gravel bottom with a very rich associated invertebrate fauna, provides the second record of the species in the Mediterranean.

Taxonomic remarks. The body shape and the spicule complement of the newly collected material matches notably well with the original description of *Rhabdobaris implicata* by Pulitzer-Finali (1983), who indicated that it was a new "stipitate" genus in the family Bubaridae. The only difference is that acanthostrongyles (Fig. 12G) are more abundant than acanthoxeas in the holotype, while it is the opposite in the Alboranian individual.

The genus *Rhabdobaris* Pulitzer-Finali, 1983 was declared a junior synonym of *Cerbaris* by Alvarez & Van Soest (2002) on the argument that they both share the occurrence of acanthose diactines in the basal, choanosomal skeleton. However, the features of the newly collected individual of *R. implicata* make clear that it does not fit the genus diagnosis of *Cerbaris* provided by Alvarez & Van Soest (2002). *Cerbaris*, among other traits, is

characterized by encrusting sponges, with a choanosomal skeleton consisting of a basal layer of acanthose and smooth diactines and monactines projecting perpendicularly to the substratum. Therefore, the current diagnosis of *Cerbaris* reflects several major mismatches relative to the features of *Rhabdobaris implicata*: 1) *R. implicata* is a stalked, flabellate sponge (Fig. 11A–B), rather than an encrusting form; 2) the skeleton is not a basal layer, but consists of a plumoreticulate structure of ascending tracts; 3) it lacks the distinct ceroxas (M-shaped oxeas) of *Cerbaris*; 4) *Rhabdobaris implicata* has acanthostyles in great abundance, a spicule type often missing in *Cerbaris*. Altogether, the differences in body shape, spicule complement and skeletal organization advice to re-establish the original genus *Rhabdobaris* erected by Pulitzler-Finali (1983) in the family Bubaridae. Likewise, the existence of *Rhabdobaris* makes compulsory a modification of the current definition for family Bubaridae, as it is currently defined by Alvarez & Van Soest (2002) only to host sponges with an encrusting growth habit supported by a basal layer of interlacing choanosomal diactines.

A comparison of the spicule complement of our Alboranian specimen to *Cerbaris* spp. occurring in or near the Western Mediterranean region reveals only vague resemblance to *Cerbaris* (formerly *Bubaropsis*) *curvisclera* (Lévi & Vacelet 1958) from Azores and *Cerbaris* (formerly *Rhabdoploca*) *curvispiculifer* (Carter 1880), originally described from the Indian Ocean (Gulf of Manaar) and subsequently found in Azores (Topsent 1904) and Banyuls (Vacelet 1969). These two latter *Cerbaris* species are encrusting forms that also lack the plumoreticulate skeleton. In addition, C. *curvispiculifer* lacks raphides, having a spicule complement that varies across described specimens. For instance, it lacks both smooth and acanthose oxeas in the Indian and North-Atlantic specimens, but not in the Mediterranean material. *Cerbaris curvisclera* has raphides and smooth oxeas, but lacks any kind of style or acanthostyle. Therefore, *R. implicata* is clearly distinguishable from these *Cerbaris* species.

Although the genus *Rhabdobaris* is herein restituted within the original family in which it was erected, that is Bubaridae, there are concerns that *Rhabdobaris* could be a raspailiid. Indeed, the body shape, the spicule complement, and the general skeletal organization match better the traits characterizing the family Raspailiidae than those of the family Bubaridae. Nevertheless, *Rhabdobaris* lacks the hispidating bouquets around the long hispidating styles, which typically characterize most—but not all—raspailiids. Therefore, a definitive family assignation may require further inference of the phylogenetic relationships of *Rhabdobaris* using molecular markers.

Order POECILOSCLERIDA Topsent, 1928

Suborder MIICROCIONINA Hajdu, van Soest & Hooper, 1994

Family RASPAILIIDAE Nardo, 1833

Subfamily RASPAILIINAE Nardo, 1833

Genus *Endectyon* Topsent, 1920

Diagnosis. Prominently hispid, conulose surface, and typically arborescent growth form. Skeleton with marked axial and extra-axial differentiation; axial skeleton with well-developed spongin fibres forming a compressed reticulation, cored by stout choanosomal styles; extra-axial subectosomal skeleton being radial or plumose, with multi- or paucispicular tracts of long subectosomal styles (subgenus *Endectyon*) or choanosomal styles (subgenus *Hemectyon*), sometimes connected by unispicular tracts forming hexagonal meshes, usually protruding the surface. Ectosomal skeleton varies from typical raspailiid condition, with thin ectosomal styles grouped in brushes around protruding subectosomal styles (subgenus *Endectyon*), to surface brushes composed of subectosomal styles only (nominal genus *Basiectyon*), to brushes of acanthostyles surrounding choanosomal styles (subgenus *Hemectyon*). Erect brushes of echinating acanthostyles located on the outer margin of the axial skeleton, making a boundary between the extra-axial and axial regions, or forming plumose brushes along the length of the extra-axial tracts, or localized exclusively at the base of the sponge (nominal genus *Basiectyon*). Structural megascleres are smooth styles of 2–3 size categories, along with echinating acanthostyles and/or acanthostrongyles with peculiar strongly curved (clavulate) hooks on the shaft, base, and/or apex. Microscleres are absent (*sensu* Hooper 2002b).

Subgenus *Hemectyon* Topsent, 1920

Diagnosis. Erect, probably undivided (see "Taxonomic Remarks"), growth form. Skeletal organization with recognizable axial, extra-axial and ectosomal regions. Axial skeleton of multispiculate-cored fibres densely reticulated. Extra-axial skeleton consisting of a more lax reticulum of pauci- to multispicular radiating primary tracts intercrossed by uni- to paucispicular secondary tracts. Spongin fibres and tracts of the axial and extra-axial regions are cored by smooth choanosomal styles; the radiating primary tracts of the extra-axial skeleton may be sparsely echinated by acanthostyles, particularly in their subectosomal regions. In the subectosomal region, the peripheral nodes of the extra-axial network serve as basis for small bouquets of longer (subectosomal) styles, which pierce the sponge ectosome to make a long, dense hispidation. At the point where each of these protruding bouquets of styles pierce the sponge ectosome, a surrounding brush consisting mostly of acanthostyles (but also incorporating some choanosomal styles) occurs, being this skeletal trait a distinct character for the subgenus *Hemectyon* (modified herein to accommodate the features of the new species).

***Endectyon (Hemectyon) filiformis* nov. sp.**
(Figs. 11C–D, 13; Table 2)

Etymology. This species is named after its erect, undivided body shape.

Material examined. Holotype: Specimen MNCN-Sp69 BV21, from type locality Stn. 21 (Table 1, Fig. 1), a 93 to 101 m deep, gravel bottom on the deep shelf of the island.

Macroscopic description. Flexible, slender, thread-like sponge, measuring 54 mm in height and 3 mm in diameter, attached to a gravel piece. The surface is densely and markedly hispid (Fig. 11C–D), with no obvious oscules. The color in life is bright orange, turning into creamy white in ethanol.

Skeleton. Megascleres in 4 spicule categories: Subectosomal styles, choanosomal styles, occasional oxeas, and acanthostyles. The subectosomal styles are long and slender, slightly curved at the centre or near the round end, with a regular round end, and an acerate point that can be sometimes softly stepped or, in the thinner growth stages, hastate (Fig. 13A); they measure 713–1465 x 3.2–20 µm. The choanosomal styles measure 187.4–272.5 x 6.4–9 µm, being irregularly curved once or twice, sometimes in a rhabdostyle fashion, with hastate or acerate points (Fig. 13A–B). These styles may show a slight swelling either near the round end or towards central positions. The oxeas are less common than the previous categories, typically curved at the middle, with sharp conical ends that can be slightly different (Fig. 13A, C), measuring 234–277 x 3–9 µm. The acanthostyles are nearly straight or slightly curved and show scarce, large, conical spines. Spines are usually sparse over the spicule length, mostly making a sort of verticillate cluster at the round end, producing a clavulate acanthostyle; the spines very rarely appear around the sharp end of the spicule. The number of spines varies from one to four at the round end and from one to ten over the shaft length, and they can be straight, curved toward the spicule points or in the opposite direction (Fig. 13A, D). The acanthostyles are far less abundant than the choanosomal styles and measure 114–150 x 6–7 µm.

Axial and extra-axial skeleton are poorly differentiated. The axial skeleton is a relatively more compact reticule of pauci- and multispicular tracts of choanosomal styles surrounded by moderate spongin (Fig. 13F). The reticule becomes progressively less compact towards the periphery (extra-axial region?) and is built with thinner tracts (pauci- and unispiculate) of choanosomal styles and occasional oxeas. From the periphery of this extra-axial network, groups of 2 to 10, long subectosomal styles project radially (Fig. 13E), piercing the surface and causing the long hispidation of the surface. At the point where one of these radiating tracts of long subectosomal styles pierces the sponge ectosome, a surrounding brush consisting mostly of acanthostyles (but also incorporating some oxea or choanosomal style) occurs (Fig. 13E); this skeletal trait is a diagnostic character for the subgenus *Hemectyon.*

Distribution and ecology notes. The only individual of *Endectyon (Hemectyon) filiformis* **nov. sp.** was collected from a 93 to 100 m deep, organogenic-gravel bottom.

Taxonomic remarks. Members of the genus *Endectyon* are the only raspailiids having echinating acanthostyles with clavulate morphology and located outside the axial skeleton (Hooper 1991; Hooper 2002b). Within the subgenus *Hemectyon,* only one species had been described to date: *Endectyon (Hemectyon) hamatum* (Schmidt, 1870). This species was originally reported from the Caribbean (Schmidt 1870; Topsent 1920). It was subsequently cited from the East Africa (North Kenya) by Pulitzer-Finali (1993), but a revision of that specimen assignation would be advisable, as it contains abundant raphides and the brief skeletal description suggests it to be a raspailiid different from *Endectyon* spp.

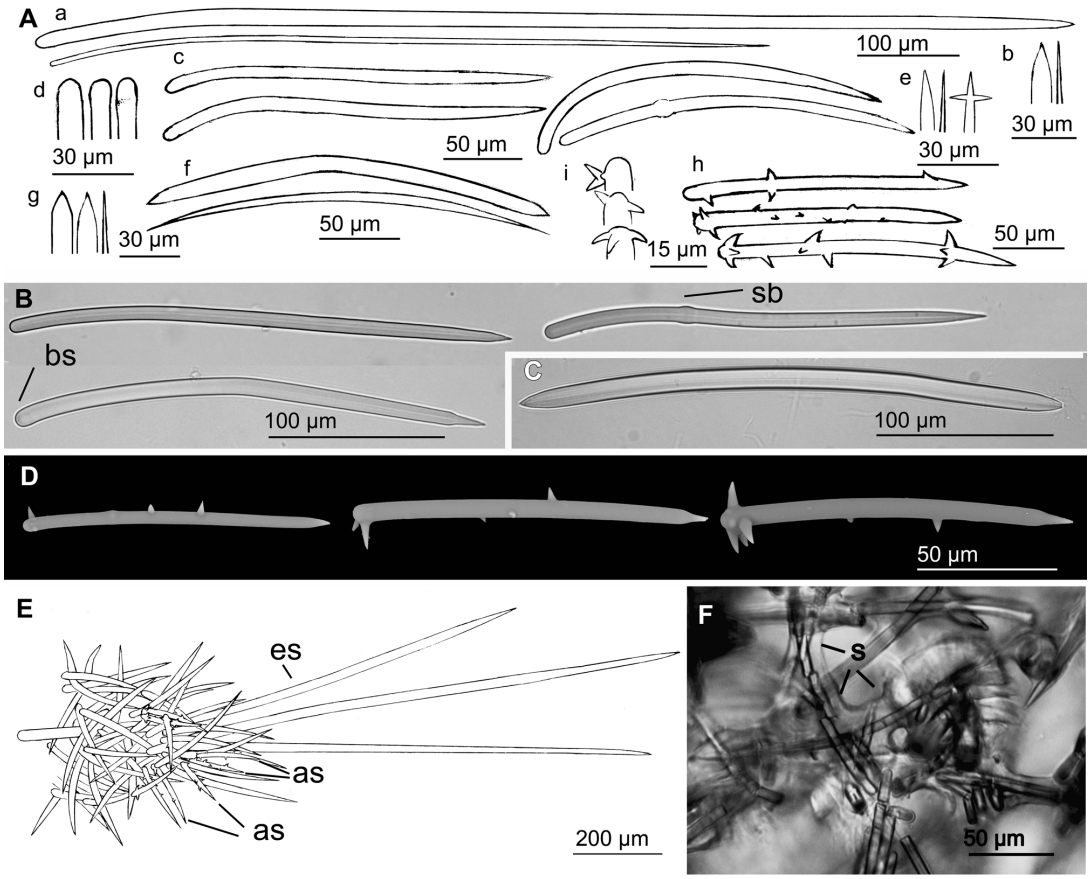

FIGURE 13. *Endectyon (Hemectyon) filiformis* **nov. sp.**: (A) Line drawing summarizing the spicule complement of the holotype (MNCN-Sp69-BV21). There are subectosomal styles (a) with a round end and an acerate or hastate distal end (b) and choanosomal styles with a regular or swollen round end (d) and an acerate, hastate or polyaxonic distal end (e). There are also oxeas (f) with conical to hastate ends (g) and acanthostyles (h) with large spines that can be clavulate at the round end (i). (B) Light microscope view of choanosomal styles, with slight subterminal swelling (bs) or a subtle subtyle (sb). (C) Light microscope view of an oxea. (D) SEM micrographs of acanthostyles. (E) Line drawing sketching the organization of the ectosomal skeleton, which consists of the subectosomal styles (es) surrounded by an hispidating brush of acanthostyles (as). (F) Light microscope view of the choanosomal skeleton where spongin (s) can be observed embedding the choanosomal styles.

The occurrence of acanthostyle brushes surrounding the groups of hispidating styles clearly indicates that the newly described Alboranian material belongs to the subgenus *Hemectyon*, making the second known species in this subgenus. The differences between *E. (H.) hamatum* and *E. (H.) filifomis* **nov. sp.** are clear: 1) the axial and extra-axial differentiation is less marked in the new species, as well as the differentiation between radiating primary tracts and secondary intercrossing tracts; 2) the primary radiating tracts are only very rarely echinated by the acanthostyles in the new species; 3) the acanthostyles do not have clavulate spines at the round end in *E. (H.) hamatum*, but they do have them in the new species; 4) The hispidating styles in *E. (H.) hamatum* are relatively small (220–275 x 2 µm) and shorter than those coring the choanosomal fibres and tracts (270–615 x 6–18 µm), whereas they are notably longer (up to 1465 x 20 µm) in the new species; and 5) the new species contains occasional oxeas, while they do not occur in *E. (H.) hamatum.* Indeed, oxeas are an uncommon spicule type in *Endectyon* spp., although occasional modifications of styles into oxeas and strongyles have already been recorded in *Endectyon (Endectyon) tenax* (Schmidt, 1870) from North Carolina by Wells *et al.* (1960) and *Endectyon (Endectyon) multidentatum* (Burton, 1948) from Congo Coast (Burton 1948).

To accommodate the skeletal features of this new species, it has been necessary to modify herein the last accepted diagnosis of subgenus *Hemectyon*, which was proposed by Hooper (2002b) on the basis of the only species available at that time. An additional reason to revise the subgenus diagnosis is the growth habit. Originally, *Hemectyon* was erected on a partial sponge fragment that was assumed to be part of a larger, branched individual (Schmidt 1870; Topsent 1920). Ever since, the successive genus diagnoses have included terms such as "rameuse" (Topsent 1920) or "arborescent" (Hooper 2002b), a branching condition that has never been corroborated objectively. Given that the holotype of *E. (H.) hamatum* is an undivided cylindrical fragment (23mm x 3.5) and that the complete holotype of *E. (H.) filiformis* **nov. sp.** is also an undivided, digit-like growth form, there is no reason to support any longer that the sponges of the subgenus *Hemectyon* are arboresecent. Rather, they should be postulated as erect, branchless growth forms, at least until future collections of new material disprove it.

Order HAPLOSCLERIDA Topsent, 1928

Suborder HAPLOSCLERINA Topsent, 1928

Family NIPHATIDAE Van Soest, 1980

Genus *Gelliodes* Ridley, 1884

Diagnosis. Thickly incrusting to massive, tubular growth form, intricately branching, long cylindrical stems irregularly ramified and anastomosing at points of contact (single branches attain a length of about 100 mm), rampant or erect, arising from a common basal portion. Oscules usually numerous, unevenly scattered over the surface and often conspicuous. Surface uneven, membranous, strongly aculeated at intervals of about 2–5mm, sustained by strong, slender, sharp ramified spines, 2–3 mm long surface may be also ridged or tuberculate or smooth, and finely hispid or velvety. Texture very hard. Ectosomal skeleton is a tangential network of secondary fibres, free oxeas and abundant sigmas, often interrupted by the ends of the strong primary longitudinal fibres protruding from the choanosomal skeleton to form the spines. Choanosomal skeleton composed of primary longitudinal-radial multispicular and ramified primary fibres, distinct and very compact. Primary fibres form rectangular to rounded meshes, subdivided irregularly by secondary fibres, and mesh containing abundant free spicules. Megascleres consist of robust oxeas with sharp apices. Microscleres are abundant sigmata (*sensu* Desqueyroux-Fáundez & Valentine 2002).

***Gelliodes fayalensis* Topsent, 1892**
(Figs. 14, 15; Table 2)

Synonymy. Adocia fayalensis (Topsent, 1892): (Burton 1956,)145.

Material examined. Specimen MNCN-Sp137 DR07 collected from Stn. 7 (Table 1, Fig. 1).

Macroscopic description. Ovate, cushion-shaped sponge, attached to a small piece of rhodolith (Fig. 14A–B). It measures 30 x 20 mm and is fouled around its basal region by a thickly encrusting individual of *Haliclona* sp. Surface is smooth, consisting of a thin, delicate, translucent membrane. The ectosomal membrane is damaged in many areas of the body, showing a highly cavernous subectosomal tissue. Ectosome damage makes difficult to discriminate the occurrence of oscules from ectosome breakages. The consistency is hard but friable. The color in alcohol is beige.

Skeleton. Megascleres are oxeas in a size range that could well represent two categories. The oxeas in the large category measure 280–400 x 10–15 µm and are slightly curved, typically showing two flexion points (Fig. 15A–B, E). The ends are acerate, with occasional malformations (Fig. 15A, C). The oxeas in the small category are less abundant, measure 200–270 x 2–5 µm, are regularly curved over their entire length (Fig. 15A, D–E), and have relatively regular hastate ends (Fig. 15A). Nevertheless, we cannot discard that the smaller oxeas are early developing stages of the larger oxeas. Microscleres are abundant sigmata, 15–27 µm in maximum length (Fig. 15A, E–F).

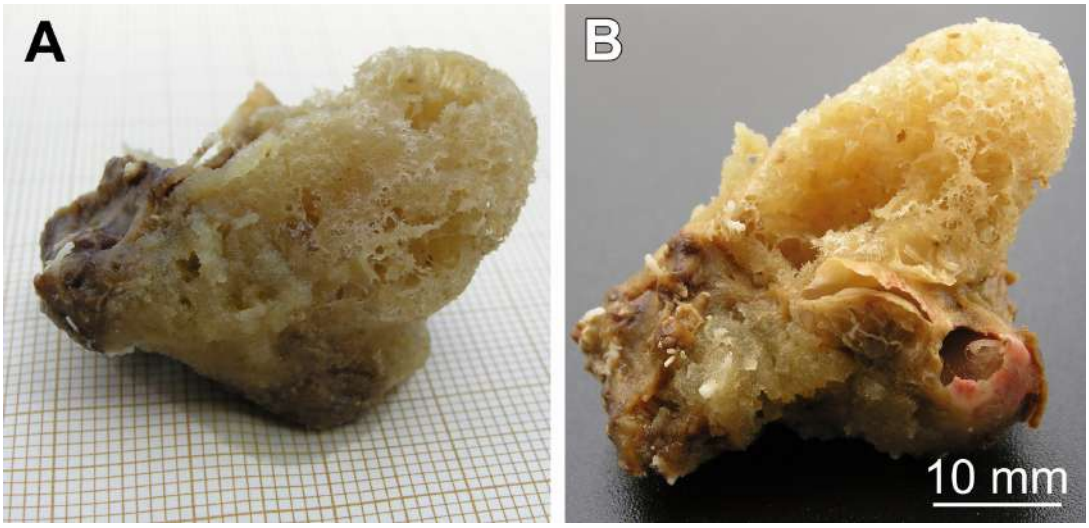

FIGURE 14. *Gelliodes fayalensis* Topsent, 1892. Specimen from the Alboran Island (MNCN-Sp137-DR07), photographed on its both sides while attached to a rhodolith fragment.

The ectosomal skeleton is a reticule of tangential oxeas made of uni- or paucispicular lines. The choanosomal skeleton is an irregular network (Fig. 15G) consisting of compact, primary multispicular tracts of oxeas with moderate spongin (Fig. 15H), which branch and subdivide when running from the deep choanosome towards the periphery. Primary tracts are 250–625 µm wide and connect each other by secondary, pauci- or multispicular secondary tracts, which are 125–200 µm wide. Microscleres are abundant at the subectosomal region, also occurring in the choanosome, some partially embedded in the oxea tracts.

Distribution and ecology notes. Rare species, known from the original description of 5 individuals from Azores (Topsent 1892, 1904), all coming from the Fayal Channel (Azores), growing on gravel bottoms rich in organogenic elements, at depths of 98–100 m. The herein described Alboranian specimen, collected from a rhodolith bottom at depths ranging from 109 and 130 m, provides the first record of the species in the Mediterranean Sea.

Taxonomic remarks. The spicule complement, the spicule size, and the skeletal organization of the Alboranian individual are strongly similar to those of *Gelliodes fayalensis* Topsent, 1892. A minor difference is that Topsent (1892) did not split the oxeas of *G. fayalensis* into two size categories. Nevertheless, we are not completely certain that the smaller oxeas that we are herein describing are a size category themselves; they could rather be early growth stages. The only size data for oxeas in Topsent's description (1892) is 270 x 9 µm, which approximately represents the median of the size range found in the oxeas of the Alboran specimen.

All specimens described from Azores by Topsent (1892, 1904) were reported to have several distinct oscules. The preservation condition of our Alboranian specimen did prevent us to discriminate oscules from the frequent ectosomal breakages and, indeed, hindered a relevant comparison in terms of external morphology features.

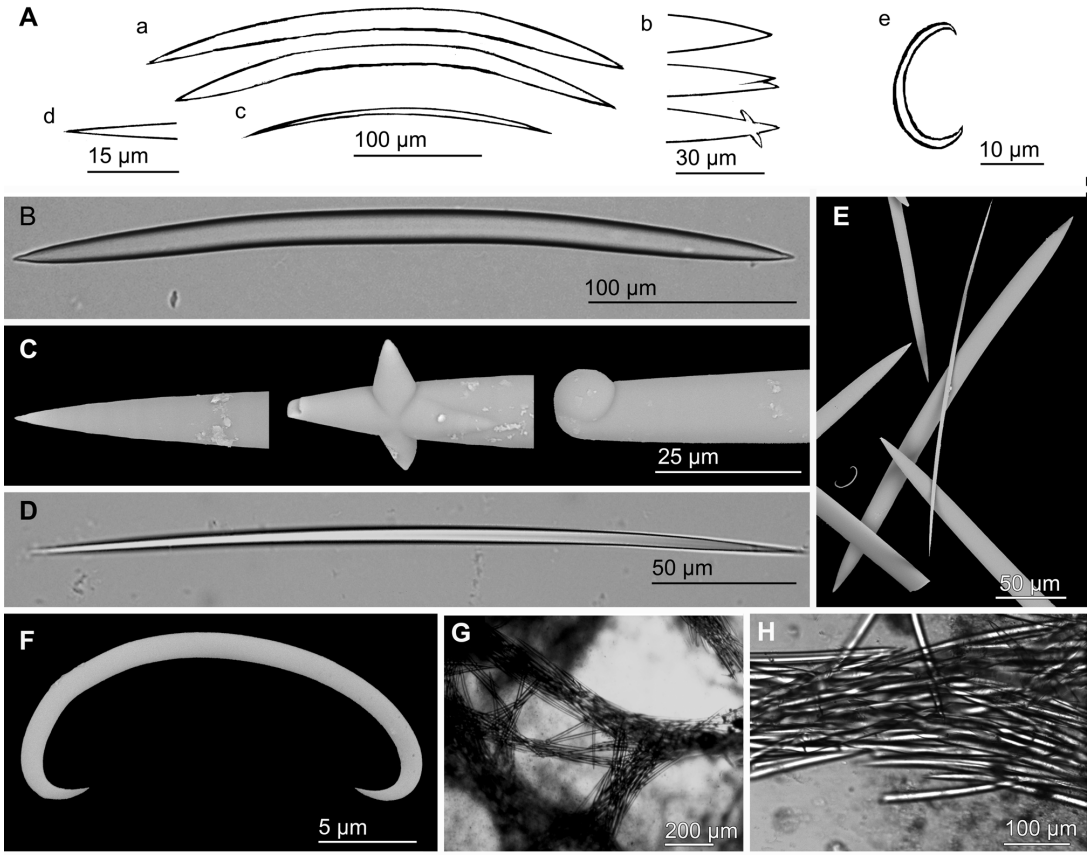

FIGURE 15. *Gelliodes fayalensis* Topsent, 1892: (A) Line drawing summarizing the spicule complement of the Alboranian specimen (MNCN-Sp137-DR07), consisting of fusiform oxeas I (a) with acerate to malformed ends (b), isodiametric oxeas II (c) with acerate ends (d), and sigmata (e). (B) Light microscope view of Oxea I. (C) SEM detail of regular and abnormal ends of oxea I. (D) Light microscope view of isodiametric Oxea II. (E) SEM view oxeas I and II and a sigma. (F) SEM detail of a sigma. (G) Light microscope view of multispiculate tracts of oxeas I and II forming a network. (H) Light microscope detail of a multispiculate tract.

Concluding remarks

The bottoms of the Alboran Island are characterized by elevated sponge richness and substantial diversity, hosting representatives of about 30 % of the known Mediterranean demosponges (Table 6). Among this fauna, there are also a good number of Mediterranean endemisms and rare species, along with numerous "Atlantic" species that appear to have penetrated in this westernmost Mediterranean area and that, surprisingly, may reach notable abundances (e.g. *Axinella vellerea*). While recent invasions of shallow habitats by sponges have relatively been easy to detect in several oceans and seas (e.g., *Mycale* (*Mycale) grandis* Gray, 1867; *Terpios hoshinota* Rützler & Muzik, 1993; *Paraleucilla magna* Klautau, Monteiro & Borojevic, 2004), faunal expansions taking place in deep-sea habitats can go unnoticed for decades. It remains unclear whether the common occurrence of "North-Atlantic" deep-shelf immigrants that has been detected in this and previous sponge studies at the Alboran Island reflects only vestiges of ancestral faunal expansions during the Quaternary interglacial periods or it is also partially derived from recent northward expansions favored by man-driven global warming. While the former mechanism is more likely the main cause, our results contribute to reinforce the idea that the Alboran shelf provides a privileged natural laboratory from where to document past, present, and future biotic exchange between the Atlantic and the Mediterranean (Aguilar *et al.* 2011; Vermeij 2012). From this notion, two major actions would be advisable for the

immediate future: 1) to complete timely an exhaustive, global characterization of the benthic assemblages of the deep shelf of the Alboran Island, establishing a crucial baseline for further monitoring steps; 2) to extend the environmental protection currently given to the shallow-shelf communities of the Alboran Island to the singular and ecologically valuable deep-shelf bottoms, taking the opportunity of the currently developing frame of the Nature 2000 Network.

TABLE 6. Porifera species hitherto reported from the Alboran Island Platform and the bottoms of the surrounding abyssal plain. Species are listed alphabetically according to class, order, family, and species name.

Class CALCAREA
Order Clathrinida
Family Clathrinidae
Clathrina coriacea (Montagu, 1818)

Class DEMOSPONGIAE
Order Agelasida
Family Agelasidae
Agelas oroides (Schmidt, 1864)
Order Astrophorida
Family Ancorinidae
Dercitus (Stoeba) plicatus (Schmidt, 1868)
Jaspis eudermis Lévi & Vacelet, 1958
Jaspis incrustans (Topsent, 1890)
Jaspis johnstonii (Schmidt, 1862)
Stelletta hispida (Buccich, 1886)
Stelletta mediterranea (Topsent, 1893)
Stryphnus mucronatus (Schmidt, 1868)
Stryphnus ponderosus (Bowerbank, 1866)
Family Calthropellidae
Calthropella (Calthropella) pathologica (Schmidt, 1868)
Calthropella (Corticellopsis) recondita Pulitzer-Finali, 1983
Family Geodiidae
Caminella intuta (Topsent, 1892)
Caminus vulcani Schmidt, 1862
Erylus discophorus (Schmidt, 1862)
Erylus papulifer Pulitzer-Finali, 1983
Geodia anceps (Vosmaer, 1894)
Geodia cydonium (Jameson, 1811)
Penares candidata (Schmidt, 1868)
Penares helleri (Schmidt, 1864)
Family Pachastrellidae
Characella tripodaria (Schmidt, 1868)
Pachastrella monilifera Schmidt, 1868
Family Theneidae
Thenea muricata (Bowerbank, 1858)
Family Thoosidae
Alectona millari Carter, 1879
Delectona alboransis Rosell, 1996
Family Vulcanellidae
Poecillastra compressa (Bowerbank, 1866)
Vulcanella aberrans (Maldonado & Uriz, 1996)
Vulcanella gracilis (Sollas, 1888)
Order Chondrosida
Family Chondrillidae
Chondrosia reniformis Nardo, 1847
Order Dendroceratida
Family Darwinellidae
Aplysilla sulfurea Schulze, 1878
Darwinella viscosa Boury-Esnault, 1971
Family Dictyodendrillidae
Spongionella pulchella (Sowerby, 1804)
Order Dictyoceratida
Family Dysideidae
Dysidea fragilis (Montagu, 1818)
Pleraplysilla reticulata Maldonado & Uriz, 1999
Pleraplysilla spinifera (Schulze, 1879)
Family Irciniidae
Ircinia dendroides (Schmidt, 1862)
Ircinia variabilis (Schmidt, 1862)
Sarcotragus fasciculatus (Pallas, 1766)
Sarcotragus pipetta (Schmidt, 1868)
Sarcotragus spinosulus Schmidt, 1862
Family Spongiidae
Spongia (Spongia) agaricina Pallas, 1766
Spongia (Spongia) nitens (Schmidt, 1862)
Spongia (Spongia) officinalis Linnaeus, 1759
Spongia spinosula (Schmidt, 1868)
Spongia (Spongia) virgultosa (Schmidt, 1868)
Family Thorectidae
Fasciospongia cavernosa (Schmidt, 1862)
Hyrtios collectrix (Schulze, 1880)
Order Hadromerida
Family Clionaidae
Cliona celata Grant, 1826
Cliona rhodensis Rützler & Bromley, 1981
Cliona viridis (Schmidt, 1862)
Dotona pulchella mediterranea Rosell & Uriz, 2002
Pione vastifica (Hancock, 1849)
Spiroxya levispira (Topsent, 1898)
Family Hemiasterellidae
Hemiasterella elongata Topsent, 1928
Paratimea constellata (Topsent, 1893)
Family Polymstiidae
Polymastia mamillaris (Montagu, 1806)
Polymastia polytylota Vacelet, 1969
Polymastia spp.
Pseudotrachya hystrix (Topsent, 1890)
Family Spirastrellidae
Diplastrella bistellata (Schmidt, 1862)
Spirastrella cunctatrix Schmidt, 1868

.....continued on the next page

TABLE 6. (continued)

Family Stelligeridae
Stelligera rigida (Montagu, 1818)
Stelligera stuposa (Ellis & Solander, 1786)
Family Suberitidae
Aaptos aaptos (Schmidt, 1864)
Prosuberites longuispinus Topsent, 1893
Protosuberites rugosus (Topsent, 1893)
Pseudosuberites hyalinus (Ridley & Dendy, 1886)
Rhizaxinella elongata (Ridely & Dendy, 1886)
Rhizaxinella gracilis (Lendenfeld, 1898)
Suberites carnosus (Johnston, 1842)
Suberites domuncula (Olivi, 1792)
Pseudosuberites sulphureus (Bowerbank, 1866)
Terpios fugax Duchassaing & Michelotti, 1864
Family Tethyidae
Tethya aurantium (Pallas, 1766)
Family Timeidae
Timea cumana Pulitzer-Finali, 1978
Timea unistellata (Topsent, 1892)

Order Halichondrida
Family Axinellidae
Axinella alborana **nov. sp.**
Axinella cf. *cinnamomea* (Nardo, 1833)
Axinella damicornis (Esper, 1974)
Axinella egregia sensu Topsent, 1892
Axinella polypoides Schmidt, 1862
Axinella pumila Babic, 1922
Axinella salicina Schmidt, 1868
Axinella spatula **nov. sp.**
Axinella vellerea Topsent, 1904
Axinella verrucosa (Esper, 1794)
Phakellia robusta Bowerbank, 1866
Phakellia ventilabrum (Linnaeus, 1767)
Family Bubaridae
Bubaris vermiculata (Bowerbank, 1866)
Cerbaris alborani (Boury-Esnault, Pansini & Uriz, 1994)
Rhabdobaris implicata Pulitzer-Finali, 1983
Family Dictyonellidae
Acanthella acuta Schmidt, 1862
Dictyonella incisa (Schmidt, 1880)
Dictyonella marsilii (Topsent, 1893)
Family Halichondriidae
Axinyssa aurantiaca (Schmidt, 1864)
Ciocalypta penicillus Bowerbank, 1862
Ciocalypta porrecta (Topsent, 1928)
Halichondria (Halichondria) bowerbanki Burton, 1930
Halichondria (Halichondria) panicea (Pallas, 1766)
Halichondria (Halichondria) semitubulosa Lieberkühn, 1859
Hymeniacidon perlevis (Montagu, 1818)
Spongosorites flavens Pulitzer-Finali, 1983
Spongosorites intricatus (Topsent, 1892)

Order Haploslcerida
Family Callyspongiidae
Siphonochalina balearica Ferrer-Hernandez, 1916
Siphonochalina coriacea Schmidt, 1868
Family Chalinidae
Chalinula limbata (Montagu, 1818)
Dendroxea lenis (Topsent, 1892)
Haliclona (Gellius) flagellifera (Ridley & Dendy, 1886)
Haliclona (Gellius) lacazei (Topsent, 1893)
Haliclona (Halichoclona) fulva (Topsent, 1893)
Haliclona (Halichoclona) perlucida (Griessinger, 1971)
Haliclona (Haliclona) reptans (Griessinger, 1971)
Haliclona (Haliclona) simulans (Johnston, 1842)
Haliclona (Reniera) aquaeductus (Schmidt, 1862)
Haliclona (Reniera) cinerea (Grant, 1826)
Haliclona (Reniera) citrina (Topsent, 1892
Haliclona (Reniera) subtilis Griessinger, 1971
Haliclona (Soestella) implexa (Schmidt, 1868)
Haliclona (Soestella) mucosa (Griessinger, 1971)
Haliclona pocilliformis (Griessinger, 1971)
Family Niphatidae
Gelliodes fayalensis Topsent, 1892
Family Petrosiidae
Petrosia (Petrosia) ficiformis (Poiret, 1789)

Order Poecilosclerida
Family Acarnidae
Acarnus tortilis Topsent, 1892
Iophon hyndmani (Bowerbank, 1858)
Iophon nigricans (Bowerbank, 1858)
Family Chondropsidae
Batzella inops (Topsent, 1891)
Family Coelosphaeridae
Coelosphaera (Histodermion) cryosi (Boury-Esnault, Pansini & Uriz, 1994)
Forcepia (Leptolabis) brunnea (Topsent, 1904)
Forcepia (Leptolabis) luciensis (Topsent, 1888)
Forcepia (Leptolabis) megachela (Maldonado, 1992)
Lissodendoryx (Lissodendoryx) isodictyalis (Carter, 1882)
Lissodendoryx (Lissodendoryx) lundbecki Topsent, 1913
Family Crambeidae
Crambe crambe (Schmidt, 1862)
Crambe tailliezi Vacelet & Boury-Esnault, 1982
Crambe tuberosa Maldonado & Benito, 1991
Family Crellidae
Crella (Crella) elegans (Schmidt, 1862)
Crella (Grayella) pulvinar (Schmidt, 1868)
Crella (Pytheas) sigmata Topsent, 1925
Crella (Yvesia) pyrula (Carter, 1876)
Crella (Yvesia) rosea (Topsent, 1892)
Family Desmacellidae
Biemna parthenopea Pulitzer-Finali, 1978
Biemna variantia (Bowerbank, 1858)
Desmacella annexa Schmidt, 1870
Desmacella inornata (Bowerbank, 1866)
Dragmatella aberrans (Topsent, 1890)
Family Desmacididae
Desmacidon fruticosum (Montagu, 1818)
Family Esperiopsidae
Esperiopsis fucorum (Esper, 1794)
Ulosa stuposa (Esper, 1794)
Family Hamacanthidae
Hamacantha (Vomerula) falcula (Bowerbank, 1874)

.....continued on the next page

TABLE 6. (continued)

Family Hymedesmiidae
Hemimycale columella (Bowerbank, 1874)
Haliclona (Gellius) angulata (Bowerbank, 1866)
Hymedesmia (Hymedesmia) baculifera (Topsent, 1901)
Hymedesmia (Hymedesmia) pansa Bowerbank, 1882
Hymedesmia (Hymedesmia) paupertas (Bowerbank, 1866)
Hymedesmia (Hymesdemia) peachi Bowerbank, 1882
Hymedesmia (Stylopus) coriacea (Fristedt, 1885)
Phorbas dives (Topsent, 1891)
Phorbas fibulatus (Topsent, 1893)
Phorbas fictitius (Bowerbank, 1866)
Phorbas mercator (Schmidt, 1868)
Phorbas plumosus (Montagu, 1818)
Phorbas tenacior (Topsent, 1925)
Phorbas topsenti Vacelet & Perez, 2008
Family Latrunculiidae
Latrunculia (Biannulata) citharistae Vacelet, 1969
Sceptrella insignis (Topsent, 1890)
Family Microcionidae
Antho (Acarnia) cf. novizelanica (Ridley & Duncan, 1881)
Antho (Antho) involvens (Schmidt, 1864)
Clathria (Clathria) coralloides (Scopoli, 1772)
Clathria (Microciona) armata (Bowerbank, 1862)
Clathria (Microciona) duplex Sarà, 1958
Clathria (Microciona) gradalis Topsent, 1925
Clathria (Microciona) spinarcus (Carter & Hope, 1889)
Family Mycalidae
Mycale (Aegogropila) rotalis (Bowerbank, 1874)
Mycale (Aegogropila) syrinx (Schmidt, 1862)
Mycale (Carmia) macilenta (Bowerbank, 1866)
Mycale (Paresperella) serrulata Sarà & Siribelli, 1960
Family Myxillidae
Myxilla (Myxilla) rosacea (Lieberkühn, 1859)
Family Podospongiidae
Podospongia lovenii Bocage, 1869
Family Raspailiidae
Aulospongus spinosus (Topsent, 1927)
Endectyon (Hemectyon) filiformis **nov. sp.**
Endectyon (Endectyon) delaubenfelsi Burton, 1930
Eurypon cinctum Sarà, 1960
Eurypon coronula (Bowerbank, 1874)
Eurypon lacazei (Topsent, 1891)
Raspailia agnata (Topsent, 1896)
Family Tedaniidae
Tedania (Tedania) anhelans (Vio in Olivi, 1792)
Tedania spp.
Order Spirophorida
Family Tetillidae
Craniella cranium (Müller, 1776)
Order Verongida
Family Aplysinidae
Aplysina aerophoba Nardo, 1833
Aplysina cavernicola (Vacelet, 1959)
Family Ianthellidae
Hexadella racovitzai Topsent, 1896

Class HEXACTINELLIDA
Order Lyssacinosida
Family Rossellidae
Asconema setubalense Kent, 1870

Class HOMOSCLEROMORPHA
Order Homosclerophorida
Family Oscarellidae
Oscarella lobularis (Schmidt, 1862)
Family Plakinidae
Plakina monolopha Schulze, 1880
Plakina trilopha Schulze, 1880
Plakinastrella mixta Maldonado, 1992

Acknowledgments

The authors thank Dr. Serge Gofas (University of Malaga), Dr. Carmen Salas (University of Malaga), Dr. Ángel Luque (Autonomous University of Madrid) and Juan Goutayer for organizing the logistic of collecting and ROV cruises and providing help with bathymetric maps, community maps, and video material. Scientists and technicians participating in the cruise, along with crewmembers and ROV crew, are thanked for their help on board. Gustavo Carreras (CEAB) helped with line drawings and María J. Carbonell (CEAB) assisted with SEM observations. Dr. Isabelle Domart-Coulon (Muséum national d'Histoire naturelle, Paris), Dr. Maria Tavano (Museo Civico di Storia Naturale Giacomo Doria di Genoa, Genoa, Italy), and Michèle Bruni (Musée océanographique de Monaco, Monaco) are thanked for the loan of comparative materials. Dr. Maurizio Pansini kindly provided information on *Axinella vaceleti* Pansini, 1984 and Dr. Rob Van Soest did so on *Axinella pumila* Babic, 1922. Dr. S. Gofas, Dr. A. Luque, Dr. Jose Templado (MNCN), Dr. Christine Morrow (National Museums Northern Ireland), Dr. Bernard Picton (National Museums Northern Ireland), and two anonymous reviewers provided useful, constructive comments on draft stages of the manuscript. This research has benefited from funds of a European Community grant LIFE+ Indemares (through the Fundación Biodiversidad Project 46P.PR9999), an Intramural CSIC Research Grant (PIE, PN-2013), and a grant of Spanish Ministry of Economy and Competitiveness (CTM2012-37787).

References

Aguilar, R., Aksissou, M., Templado, J. & Romani, M. (2011) Scientific rationale for the proposed CIESM Near Atlantic Marine Peace Park - A CIESM proposal. *In:* Briand, F. (Ed.), *Marine peace parks in the Mediterranean*. CIESM, Monaco, pp. 43–49.

Alvarez, B. & Hooper, J.N.A. (2002) Family Axinellidae Carter, 1875. *In:* Hooper, J.N.A. & Van Soest, R.W.M. (Eds.), *Systema Porifera: A guide to the classification of sponges*. Kluwer Academic/Plenum Publishers, New York, pp. 724–747.

Alvarez, B. & Van Soest, R.W.M. (2002) Family Bubaridae Topsent, 1894. *In:* Hooper, J.N.A. & Van Soest, R.W.M. (Eds.), *Systema Porifera. A guide to the classification of sponges*. Kluwer Academic/ Plenum Publishers, New York, pp. 748–754.

Arndt, W., Grimpie & Wagler. (1935) *Porifera. Die Tierwelt der Nord-und Ostsee*. Berlin, 140 pp.

Babic, K. (1922) Monactinellida und Tetractinellida des Adriatischen Meeres. *Zoologische Jahrbücher*, Abt. Systematik, 46, 217–302.

Bertolino, M., Bo, M., Canese, S., Bavestrello, G. & Pansini, M. (2013a) Deep sponge communities of the Gulf of St Eufemia (Calabria, southern Tyrrhenian Sea), with description of two new species. *Journal of the Marine Biological Association of the United Kingdom*, FirstView, 1–17.

Bertolino, M., Cerrano, C., Bavestrello, G., Carella, M., Pansini, M. & Calcinai, B. (2013b) Diversity of Porifera in the Mediterranean coralligenous accretions, with description of a new species. *ZooKeys*, 336, 1–37. http://dx.doi.org/10.3897/zookeys.336.5139

Boury-Esnault, N., Pansini, M. & Uriz, M.J. (1994) Spongiaires bathyaux de la mer d'Alboran et du golfe ibéro-marocain. *Mémoires. Muséum National d'Histoire Naturelle*, 160, 1–174.

Boury-Esnault, N. & Rützler, K. (1997) Thesaurus of sponge morphology. *Smithsonian Contributions to Zoology*, 596, 1–55. http://dx.doi.org/10.5479/si.00810282.596

Bowerbank, J.S. (1866) *A monograph of the British Spongiadae. II. Synopsis of Genera*. Ray Society of London, London, 388 pp.

Burton, M. (1929) Porifera. Part II. Antarctic Sponges. *British Antarctic Terra Nova Expedition. 1910-1913*, Zool., 6, 393–458.

Burton, M. (1931) The Folden Fiord. Report on the sponges collected by Mr. Soot-Ryven in the Folden Fiord in the year 1923. *Tromsø Museum Skrifter*, 1, 1–8.

Burton, M. (1948) Marine sponges of Congo coast. *Institut Royal Colonial Belge Bulletin des Séances* 19, 753–758.

Burton, M. (1956) The Sponges of West Africa. *Atlantide Report. Scientific Results of the Danish Expedition to the Coasts of Tropical West Africa, 1945-1946*, 4, 111–147.

Calcinai, B., Moratti, V., Martinelli, M., Bavestrello, G. & Taviani, M. (2013) Uncommon sponges associated with deep coral bank and maerl habitats in the Strait of Sicily (Mediterranean Sea). *Italian Journal of Zoology*, 80, 412–423. http://dx.doi.org/10.1080/11250003.2013.786763

Carter, H.J. (1880) Report on Specimens dredged up from the Gulf of Manaar and presented to the Liverpool Free Museum by Capt. W. H. Cawne Warren. *Annals and Magazine of Natural History*, 5–6, 437–457, 35–61, 126–156.

Coll, M., Piroddi, C., Steenbeek, J., Kaschner, K., Ben Rais Lasram, F., Aguzzi, J., Ballesteros, E., Bianchi, C.N., Corbera, J., Dailianis, T., Danovaro, R., Estrada, M., Froglia, C., Galil, B.S., Gasol, J.M., Gertwagen, R., Gil, J., Guilhaumon, F., Kesner-Reyes, K., Kitsos, M.-S., Koukouras, A., Lampadariou, N., Laxamana, E., López-Fé de la Cuadra, C.M., Lotze, H.K., Martin, D., Mouillot, D., Oro, D., Raicevich, S., Rius-Barile, J., Saiz-Salinas, J.I., San Vicente, C., Somot, S., Templado, J., Turon, X., Vafidis, D., Villanueva, R. & Voultsiadou, E. (2010) The biodiversity of the Mediterranean Sea: Estimates, patterns, and threats. *PLoS One*, 5, e11842. http://dx.doi.org/10.1371/journal.pone.0011842

Comas, M.C., García-Dueñas, V. & Jurado, M.J. (1992) Neogene tectonic evolution of the Alboran Sea. *Geo-Marine Letters*, 12, 157–164. http://dx.doi.org/10.1007/bf02084927

Descatoire, A. (1966) Sur quelques Démosponges de l'Archipel de Glénan. *Cahiers de Biologie Marine*, 7, 231–246.

Desqueyroux-Fáundez, R. & Valentine, C.A. (2002) Family Niphatidae Van Soest, 1980. *In:* Hooper, J.N.A. & Van Soest, R.W.M. (Eds.), *Systema Porifera. A guide to the classification of sponges*. Kluwer Academic/ Plenum New York, pp. 874–890.

Fristedt, K. (1887) Sponges from the Atlantic and Arctic Oceans and the Behring Sea. Vega-Expeditionens Vetenskap. *Iakttagelser (Nordenskiöld)*, 4, 401–471.

Gazave, E., Carteron, S., Chenuil, A., Richelle-Maurer, E., Boury-Esnault, N. & Borchiellini, C. (2010) Polyphyly of the genus *Axinella* and of the family Axinellidae (Porifera: Demospongiaep). *Molecular Phylogenetics and Evolution*, 57, 35–47. http://dx.doi.org/10.1016/j.ympev.2010.05.028

Hansen, G.A., Grondal & Sons, B. (1885) *Spongiadae. Den Norske Nordhavs-Expedition 1876-1878*. Grondal & Sons Bogtrykkeri, Christiania, 25 pp.

Hogg, M.M., Tendal, O.S., Conway, K.W., Pomponi, S.A., van Soest, R.W.M., Gutt, J., Krautter, M. & Roberts, J.M. (2010) *Deep-sea sponge grounds: Reservoirs of biodiversity.* UNEP-WCMC, Cambridge, 84 pp.

Hooper, J.N.A. (1991) Revision of the Family Raspailiidae (Porifera: Demospongiae), with Description of Australian Species. *Invertebrate Taxonomy*, 5, 1179–1418. http://dx.doi.org/10.1071/it9911179

Hooper, J.N.A. (2002a) Family Hemiasterellidae Lendenfeld, 1889. *In:* Hooper, J.N.A. & Van Soest, R.W.M. (Eds.), *Systema Porifera: a guide to the classification of sponges*. Kluwer Academic/Plenum Publishers, New York, pp. 186–195.

Hooper, J.N.A. (2002b) Family Raspailiidae Hentschel, 1923. *In:* Hooper, J.N.A. & Van Soest, R.W.M. (Eds.), *Systema Porifera. Guide to the classification of sponges*. Kluwer Academic/ Plenum New York, pp. 469–510.
Johnston, G. (1842) *A history of British sponges and lithophytes.* W.H. Lizars, Edinburgh, 1–264 pp.
Kirkpatrick, R. (1903) Descriptions of South African sponges. Part III. *Marine Investigations in South Africa*, 2, 233–261.
Lendenfeld, R.V. (1897) On the Spongida. Notes on Rockall Island and Banks. *Transactions of the Royal Irish Academy*, 31, 82–88.
Lévi, C. (1957) Spongiaires des côtes d'Israel. *Bulletin of the Research Council of Israel*, 6 B, 201–212.
Lévi, C. & Vacelet, J. (1958) Eponges récoltées dans l'Atlantique Oriental par le "President Theodore Tissier" (1955-1956). *Revue des Travaux de l'Institut des Pêches Maritimes*, 22, 225–246.
Maldonado, M. (1992) Demosponges of the red coral bottoms from the Alboran Sea. *Journal of Natural History*, 26, 1131–1161.
http://dx.doi.org/10.1080/00222939200770661
Maldonado, M. (1993) Demosponjas litorales de Alborán. Faunística y Biogeografía, Ph.D. University of Barcelona, Barcelona, 496 pp.
Maldonado, M. (2006) The ecology of the sponge larva. *Canadian Journal of Zoology (Journal Canadien de Zoologie)*, 84, 175–194.
Maldonado, M. & Benito, J. (1991) *Crambe tuberosa* n. sp. (Demospongiae, Poecilosclerida): a new Mediterranean poecilosclerid with lithistid affinities. *Cahiers de Biologie Marine*, 32, 323–332.
Maldonado, M. & Uriz, J.M. (1995) Biotoic affinities in a transitional zone between the Atlantic and the Mediterranean: a biogeographical approach based on sponges. *Journal of Biogeography*, 22, 89–110.
Maldonado, M. & Uriz, M.J. (1996) A new species of *Sphinctrella* (Demospongiae: Astrophorida) and remarks on the status of the genus in the Mediterranean. *Bulletin de l'Institut Royal des Sciences Naturelles de Belgique*, 66 suppl., 175–184.
Maldonado, M. & Uriz, M.J. (1999) A new dendroceratid sponge with reticulate skeleton. *Memoirs of the Queensland Museum*, 44, 353–359.
Martínez-García, P., Soto, J.I. & Comas, M. (2010) Structural analysis and recent tectonics in the central Alboran Sea. *Trabajos de Geología, Universidad de Oviedo*, 30, 44–48.
Morrow, C.C., Picton, B.E., Erpenbeck, D., Boury-Esnault, N., Maggs, C.A. & Allcock, A.L. (2012) Congruence between nuclear and mitochondrial genes in Demospongiae: A new hypothesis for relationships within the G4 clade (Porifera: Demospongiae). *Molecular Phylogenetics and Evolution*, 62, 174–190.
http://dx.doi.org/10.1016/j.ympev.2011.09.016
Pansini, M. (1984) Notes on some Mediterranean *Axinella* with description of two new species. *Bollettino dei Musei e degli Istituti Biologici della Università di Genova*, 50 (51), 79–98.
Pansini, M., Vacelet, J. & Boury-Esnault, N. (1987) Littoral demosponges from the banks of the straits of Sicily and the Alboran Sea. *In: Taxonomy of Porifera*. Springer Verlag, Berlin, Heidelberg, pp. 149–186.
Pardo, E., Aguilar, R., García, S., de la Torriente, A. & Ubero, J. (2011) Documentación de arrecifes de corales de agua fría en el Mediterráneo occidental (Mar de Alborán). *Chronica Naturae*, 1, 20–34.
Péres, J.M. & Picard, J. (1964) Nouveau manuel de bionomie benthique de la mer Méditerranée. *Recueil des Travaux de la Station Marine d'Endoume*, 31, 1–137.
Pulitzer-Finali, G. (1983) A collection of Mediterranean Demospongiae (Porifera) with, in appendix, a list of the Demospongiae hitherto recorded from the Mediterranean Sea. *Annali del Museo Civico di Storia Naturale Giacomo Doria*, 84, 445–621.
Pulitzer-Finali, G. (1993) A collection of marine sponges from East Africa. *Annali del Museo Civico di Storia Naturale Giacomo Doria*, 89, 247–350.
Rosell, D. & Uriz, M.J. (2002) Excavating and endolithic sponge species (Porifera) from the Mediterranean: species descriptions and identification key. *Organisms, Diversity & Evolution*, 55–86.
http://dx.doi.org/10.1078/1439-6092-00033
Schmidt, O. (1870) *Grundzüge einer Spongien-Fauna des Atlantischen Gebietes*. Leipzig, 88 pp.
Templado, J., Calvo, M., Luque, A.A., Garvía, A., Maldonado, M. & Moro, L. (2004) *Guía de invertebrados y peces marinos protegidos por la legislación nacional e internacional*. Ministerio de Medio Ambiente/Consejo Superior de Investigaciones Científicas, Madrid, 214 pp.
Templado, J., Calvo, M., Moreno, D., Flores, A., Conde, F., Abad, R., Rubio, J., López-Fé, C.M. & Ortiz, M. (2006) *Flora y fauna de la reserva marina y reserva de pesca de la isla de Alborán*. Ministerio de Agricultura, Pesca y Alimentación. Secretaría General de Pesca Marítima, Madrid, 126 pp.
Templado, J., García-Carrascosa, M., Baratech, L., Capaccioni, R., Juan, A., López-Ibor, A., Silvestre, R. & Massó, C. (1986) Estudio preliminar de la fauna asociada a los fondos coralígenos del mar de Alborán (SE de España). *Boletin del Instituto Español de Oceanografía*, 3, 93–104.
Topsent, E. (1892) Contribution a l'étude des Spongiaires de l'Atlantique Nord. *Résultats des Campagnes Scientifiques accomplies par le Prince Albert I. Monaco*, 2, 1–165.
Topsent, E. (1896) Matériaux pour servir à l'étude de la Faune des Spongiaires de France. *Mémoires de la Société Zoologique de France*, 9, 113–133.
Topsent, E. (1904) Spongiaires des Açores. *Résultats des Campagnes Scientifiques accomplies par le Prince Albert I. Monaco*, 25, 1–279.

Topsent, E. (1920) Spongiaires du Musée Zoologique de Strasbourg. Monaxonides. *Bulletin de l'Institut Océanographique de Monaco*, 381, 1–36.
Topsent, E. (1928) Spongiaires de l'Atlantique et de la Méditerranée, provenant des croissières du Prince Albert I de Monaco. *Résultats des Campagnes Scientifiques accomplies par le Prince Albert I. Monaco*, 74, 1–376.
Uriz, M.J. (2002) Family Ancorinidae Schmidt, 1870. *In:* Hooper, J.N.A. & Van Soest, R.W.M. (Eds.), *Systema Porifera: a guide to the classification of Sponges*. Kluwer Academic/Plenum Publishers, New York, pp. 108–126.
Vacelet, J. (1969) Eponges de la Roche du Large et de l'étage bathyal de Méditerranée (récoltées de la Soucoupe plongeante cousteau et dragages). *Mémoires du Muséum National d'Histoire Naturelle*, série A, 59, 145–219.
Vermeij, G.J. (2012) The tropical history and future of the Mediterranean biota and the West African enigma. *Journal of Biogeography*, 39, 31–41.
Voultsiadou-Koukoura, E. & van Soest, R.W.M. (1991) *Hemiasterella aristoteliana* n. sp. (Porifera, Hadromerida) from the Aegean Sea with a discussion on the family Hemiasterellidae. *Bijdragen tot de Dierkunde*, 61, 43–49.
Voultsiadou, E. (2009) Reevaluating sponge diversity and distribution in the Mediterranean Sea. *Hydrobiologia*, 628, 1–12. http://dx.doi.org/10.1007/s10750-009-9725-9
Wells, H.W., Wells, M.J. & Gray, I.E. (1960) Marine sponges of North Carolina. *Journal of the Elisha Mitchell Scientific Society*, 76, 200–245.

Journal of the Marine Biological Association of the United Kingdom

cambridge.org/mbi

Original Article

Cite this article: Sitjà C, Maldonado M, Farias C, Rueda JL (2019). Deep-water sponge fauna from the mud volcanoes of the Gulf of Cadiz (North Atlantic, Spain). *Journal of the Marine Biological Association of the United Kingdom* **99**, 807–831. https://doi.org/10.1017/S0025315418000589

Received: 14 November 2017
Revised: 29 June 2018
Accepted: 3 July 2018
First published online: 13 September 2018

Key words:
Bathyal benthos; continental slope; deep-sea biodiversity; environmental conservation; methane seeps; Porifera; sponge aggregations

Author for correspondence:
Manuel Maldonado
E-mail: maldonado@ceab.csic.es

Deep-water sponge fauna from the mud volcanoes of the Gulf of Cadiz (North Atlantic, Spain)

C. Sitjà[1], M. Maldonado[1], C. Farias[2] and J. L. Rueda[3]

[1]Department of Marine Ecology, Centro de Estudios Avanzados de Blanes (CEAB-CSIC), Acceso Cala St. Francesc 14, Blanes 17300, Girona, Spain; [2]Centro Oceanográfico de Cádiz, Instituto Español de Oceanografía (IEO), Puerto Pesquero, Muelle de Levante, s/n, 11006 Cádiz, Spain and [3]Centro Oceanográfico de Málaga, Instituto Español de Oceanografía (IEO), Puerto Pesquero s/n, Apdo. 285, Fuengirola 29640, Málaga, Spain

Abstract

Mud volcanoes are singular seafloor structures classified as 'sensitive habitats'. Here we report on the sponge fauna from a field of eight mud volcanoes located in the Spanish margin of the northern Gulf of Cadiz (North-eastern Atlantic), at depths ranging from 380 to 1146 m. Thirty-eight beam-trawl samplings were conducted (covering over 61,000 m^2) from 2010 to 2012, in the frame of a EC-LIFE + INDEMARES grant. A total of 1659 specimens were retrieved, belonging to 82 species, from which 79 were in the Class Demospongiae and three in Hexactinellida. Two species were new to science (*Jaspis sinuoxea* sp. nov.; *Myrmekioderma indemaresi* sp. nov.) and three others recorded for the first time in the Atlantic Ocean (*Geodia anceps*, *Coelosphaera cryosi* and *Petrosia raphida*). Five additional species were 'Atlantic oddities', since this study provides their second record in the Atlantic Ocean (*Lanuginella* cf. *pupa*, *Geodia* cf. *spherastrella*, *Cladocroce spathiformis*, *Cladocroce fibrosa* and *Haliclona pedunculata*). Basic numerical analyses indicated a significant linear relationship between the species richness per m^2 and the number of sponge individuals per m^2, meaning that in most volcanoes many species occur in equivalent, moderate abundance. Likewise, sponge species richness increased with depth, while the abundance of hard substrata resulting from carbonate precipitation and the fishing activities around the volcanoes had no detectable effect on the sponge fauna. However, in the latter case, a negative trend – lacking statistical support – underlaid the analyses, suggesting that a more extensive sampling would be necessary to derive more definitive conclusions in this regard.

Introduction

The confluence of the Atlantic Ocean and the Mediterranean Sea is an area of special interest to monitor the flux of invasive marine fauna in either direction and to identify natural patterns of North Atlantic *vs* Mediterranean endemicity (Pérès & Picard, 1964; Bouchet & Taviani, 1992; Coll *et al.*, 2010). Biodiversity studies have shown how the taxonomic composition of the benthic fauna of the westernmost zone of the Mediterranean Sea (i.e. the Alboran Sea) is naturally influenced by the North Atlantic Surface Water (NASW) inflow (0 to about 100 m depth), which has historically imported shallow-water Atlantic species into the Alboran Sea (Pérès & Picard, 1964; Templado *et al.*, 2006). This general pattern has also been confirmed specifically for the sponge fauna of the Alboran Sea (Topsent, 1928; Templado *et al.*, 1986; Pansini, 1987; Maldonado, 1992, 1993; Maldonado & Uriz, 1995; Sitjà & Maldonado, 2014), including the African Mediterranean coasts (Schmidt, 1868; Topsent, 1901, 1938; Maldonado *et al.*, 2011). However, the reverse effect is little studied. How the outflow of Intermediate Mediterranean water (MOW), originated at 500 m depth, impacts on the diversity and taxonomic composition of the benthic faunal assemblages at the Atlantic side of the Gilbraltar Strait remains poorly investigated. The MOW deviates north along the Portuguese continental margin upon passing the Camarinal Sill (280 m depth) of the Gibraltar Strait. Although the MOW is thoroughly mixed north of the Iberian Peninsula, its physical characteristics have been hypothesized to somehow positively affect the development of cold-water coral communities as distant to the north as the Galicia Bank seamount, Aviles Canyon, Le Danois Bank seamount and Porcupine Seabight (de Mol *et al.*, 2005; Van Rooij *et al.*, 2010; Sánchez *et al.*, 2014). However, the impact on the fauna of the bathyal bottoms at the Gulf of Cadiz, where the MOW might have an important influence because there it remains unmixed, has seldom been addressed, particularly regarding the sponge fauna (Arnesen, 1920; Topsent, 1927, 1928). Most of the available information on the deep-water sponge fauna in that Atlantic region derives from the Azores archipelago due to intensive sampling by French cruises (Topsent, 1892, 1898, 1904, 1928) and some more recent Portuguese initiatives (Carvalho *et al.*, 2015; Xavier *et al.*, 2015). The Azores archipelago is, however, too distant from the Gibraltar Strait to reflect clearly the role of the MOW in exporting benthic fauna. Therefore, to our knowledge, there is only a single study dealing with the deep-water sponge fauna from Atlantic locations close to the Gibraltar Strait (Boury-Esnault *et al.*, 1994).

In the last decade of the 20th century, an exciting, new deep-water habitat was discovered in the Gulf of Cadiz: fields of mud volcanoes extending between the Moroccan, Portuguese and Spanish continental margins (Kenyon *et al.*, 2000; Gardner, 2001; Pinheiro *et al.*, 2003). More than 60 mud volcanoes have been identified to date, distributed in four main fields, which constitute one of the most extensive gas seepage areas of the North-east Atlantic (Gardner, 2001; Pinheiro *et al.*, 2003; León *et al.*, 2007; Medialdea *et al.*, 2009; Palomino *et al.*, 2016). The bubbling of methane (and other hydrocarbons seeping in smaller amounts, such as propane, butane and ethane) provides the carbon that highly specialized microorganisms (i.e. methanotrophic) will consume anaerobically. This process results in precipitation of methane-derived authigenic carbonates (MDAC), such as slabs and chimneys (Levin, 2005; Suess, 2014). These structures generated by carbonate precipitation around the methane seeps are a source of new hard substrate suitable for colonization by deep-sea sessile fauna (sponges, gorgonians, cold-water corals, etc.), which in turn appears to attract demersal fauna, unchaining a global increase of benthic biodiversity (León *et al.*, 2007; Rueda *et al.*, 2012; Palomino *et al.*, 2016). In European waters, mud volcanoes are classified as sensitive habitats: habitat 1180 'Submarine structures made by leaking gases' (Habitats Directive 92/43/EEC), and, to date, the sponge fauna occurring in these mud volcano systems remains largely unexplored. The main objective of this study is to describe the diversity of the sponge fauna at some of the mud volcanoes, with the subsequent purpose (work in preparation) of assessing quantitatively its relationships with sponge faunas of bathyal bottoms in both Northern Atlantic and Western Mediterranean adjacent areas.

Materials and methods

In the frame of the EC Grant LIFE + INDEMARES – leg CHICA (Chimneys of Cadiz) – the mud volcanoes of the Spanish margin of the Gulf of Cadiz were explored and subsequently declared a SCI (Site of Community Importance), which has now become part of the Nature 2000 Network in Spanish territorial waters. The current study has benefited from a variety of tasks conducted by the research consortium during four oceanographic cruises (INDEMARES CHICA 0610 – IEO, 0211 – IEO, 1011 – IEO, 0412 – IEO) in 2010, 2011 and 2012, as follows: (1) Elaboration of a high-resolution bathymetric profile of the mud volcano fields at the upper and medium continental slope using a sound velocity sensor SV Plus, a multibeam echosounder Simrad EM-3002D, a multifrequency echosounder EK-60 and a topographic parametric sonar TOPAS PS 28 (Figures 1; and (2) video recording of the benthic communities of the SCI using both the towed observation vehicle, VOR 'Aphia 2012', and the ROV 'Liropus 2000'. These tasks resulted in about 28 VOR and seven ROV digital video transects, involving about 14 and 12 h of seafloor recordings, respectively. Information from mapping and video records has been used to complement this study of the sponge fauna.

The sponge specimens herein examined were collected using a 2 m-wide beam trawl at a total of 38 sampling stations distributed across eight mud volcanoes, namely Gazul, Anastasya, Tarsis, Pipoca, Chica, Hespérides, Almazán and Aveiro (Figure 1). The total trawled area across the mud volcano field accounted for over 61,000 m^2. The exact location of each trawl is depicted in Figure 1 and additional details (pathway coordinates, depth, trawled area, type of bottom, etc.) are summarized in Table 1. The sampled mud volcanoes were located at different depths, ranging from 380 to 1146 m (Table 2).

In addition to depth, there were also between-volcano differences in the abundance of methane-derived authigenic carbonate (MDAC) formations. Samples retrieved by the trawls were used to assess between-volcano differences in the abundance of MDAC formations, such as chimneys, crusts and slabs (Table 2). This information, when possible, was confronted with underwater images obtained during ROV transects. The abundance of these hard substrata is a factor hypothesized to locally favour sponge abundance and species richness. The MDAC abundance was semiquantitatively categorized from 0 to 3 for each of the beam trawls, according to the following criteria: 0 = no MDAC piece retrieved per trawl, 1 = 1 MDAC piece retrieved per trawl, 2 = two to five MDAC pieces retrieved, and 3 = more than five MDAC pieces retrieved, often larger than 50 cm in length. Finally, the abundance of MDAC formations for a given volcano was calculated as the mean (±SD) of the semi-quantitative value for the set of beam trawl transects conducted in each mud volcano.

Besides depth and MDAC differences, there were also between-volcano differences in the intensity of the fishing activity by the trawling fleet. The intensity of trawling activity has herein been quantified by tracking the activity of each vessel in the fleet for the period January to December 2011 using the Vessel Monitoring System (VMS) data sets supplied by the Spanish General Secretary of Fisheries (Spanish Ministry of Agriculture and Fisheries). The value of fishing activity at each mud volcano (Table 2) was then calculated as the mean (±SD) of the semi-quantitative value inferred for each of the beam trawl transects in that volcano, according to the following criteria: 0 = no trawling vessel operating in that area during 2011; 1 = 1 trawling vessel; 2 = 2–5 trawling vessels; 3 = >5 trawling vessels.

The relationship between the values of species richness (i.e. number of species) and sponge abundance (i.e. number of individuals) found in each mud volcano and normalized per the extension of the sampled area were analysed by Pearson correlation. The relationships between each of these two faunal variables, the average volcano depth, the MDAC abundance, and the level of fishing activity in each mud volcano (Table 2) were also examined pairwise using the Spearman rank correlation.

Immediately after beam-trawl retrieval, the sponges were directly preserved in 70% ethanol. In some cases, the sponges were damaged in diverse grade during trawling. Taxonomic identification of the stored material followed the standard protocols for phenetic taxonomy, based on features of the external morphology and skeleton using dissecting and compound light microscopes. When high-resolution observations of skeletal elements were required, spicules were nitric acid-cleaned, mounted on aluminium stubs, dried and then gold-coated to be examined through a Hitachi TM3000 scanning electron microscope (SEM). Molecular approaches have also been conducted for a minority of species, but the results will be reported elsewhere.

Description of body features, spicules and skeletal arrangements have been made according to the sponge morphology thesaurus (Boury-Esnault & Rützler, 1997). When required, the features of the collected material were compared to those of holotypes and additional material borrowed from the sponge collections of the Muséum National d'Histoire Naturelle of Paris (MNHN) and the Museo Civico di Storia Naturale Giacomo Doria of Genoa (MSNG). All material herein described as part of INDEMARES-CHICA cruises, holotypes included, will be stored in the Invertebrate Collection of the National Museum of Natural Sciences (MNCN), Madrid, Spain.

Results

General faunal assessment

Out of the 38 sampling stations, seven provided no sponges and the remaining 31 retrieved a total of 1659 sponges. A total of

https://doi.org/10.1017/S0025315418000589

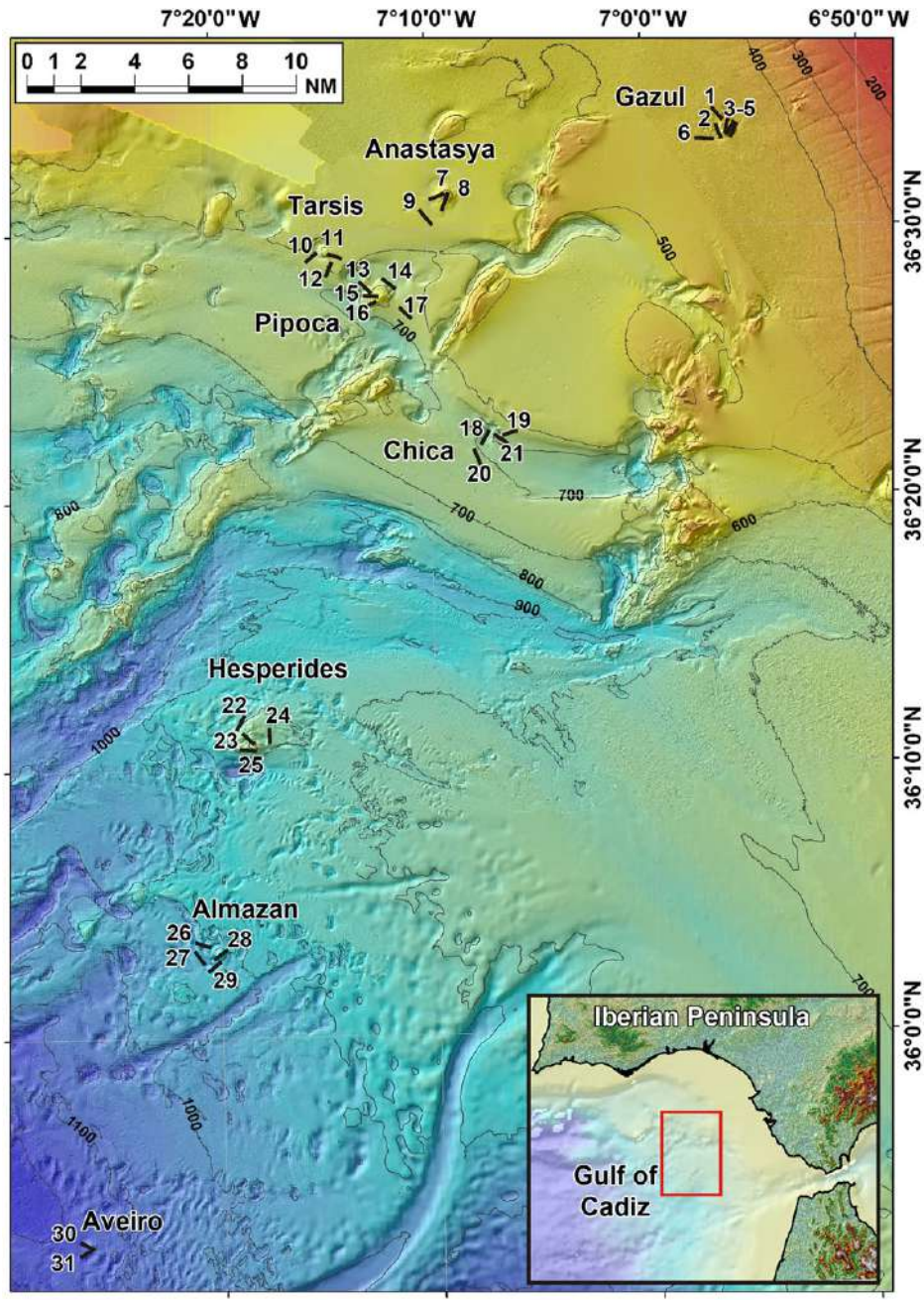

Fig. 1. Location of the 31 studied beam trawl transects (see also Table 1). Transect numbers in map correspond to trawling codes at the data base of the Spanish Institute of Oceanography (IEO) cruises as it follows: 1: 10BT03; 2: 10BT04; 3: 10BT06; 4: 10BT08; 5: 10BT07; 6: 10BT02; 7: 11BT08; 8: 11BT01; 9: 11BT14; 10: 11BT10; 11: 11BT02; 12: 11BT11; 13: 11BT16; 14: 11BT15; 15: 11BT18; 16: 11BT17; 17: 11BT20; 18: 11BT31; 19: 11BT05; 20: 11BT19; 21: 11BT06; 22: 11BT21; 23: 11BT24; 24: 11BT22; 25: 11BT23; 26: 11BT30; 27: 11BT26; 28: 11BT29; 29: 11BT25; 30: 11BT27; 31: 11BT28.

https://doi.org/10.1017/S0025315418000589

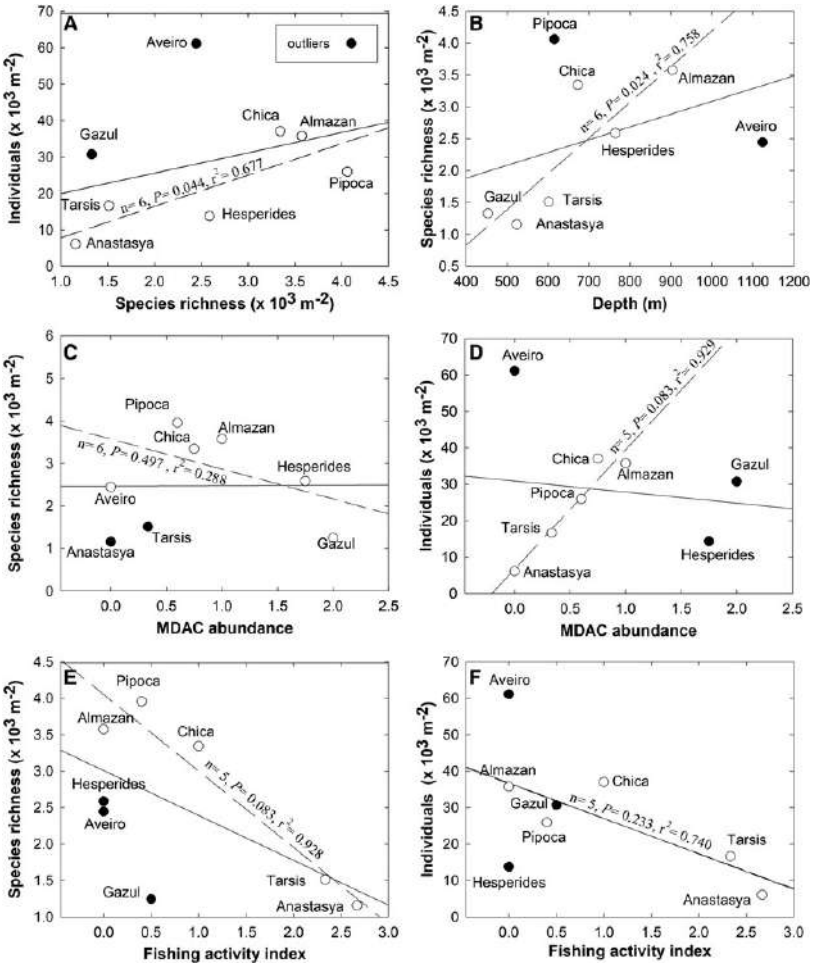

Fig. 2. Pairwise relationships between the faunal parameters (species richness per m^2 and abundance of individuals per m^2) and some features of the volcanoes (average depth, abundance of methane-derived authigenic carbonates, and fishing activity). In each graph, the solid line represents a correlation analysis (either Pearson or Spearman, as explained in the Method section) involving the eight studied volcanoes. The dashed line represents a 'revised' version of the correlation analysis after excluding the outliers (i.e. those volcanoes indicated with solid circles), for which the basic test statistics are given adjacent to the correlation line.

675 specimens were preserved, while 984 others, which were easily identifiable as representatives of common species already preserved, were only counted as collected material and returned to the sea. The collected sponges represented a total of 82 species, as listed in Appendix I. Most of them belonged to the class Demospongiae (79 species), the class Hexactinellida being represented by three species only, *Asconema setubalense* Kent, 1870; *Pheronema carpenteri* (Thomson, 1869) and *Lanuginella* cf. *pupa* Schmidt, 1870. Calcarea and Homoscleromorpha species were not collected. Such a species richness increases the number of previously recorded species (77 spp.) in the Gulf of Cadiz by 43 leading to a total of 120 spp. and representing a 35% increase. Ten species were considered as taxonomically or faunally relevant (12% of the total identified species) and are herein described in detail. Two of them are new to science (*Jaspis sinuoxea* sp. nov.; *Myrmekioderma indemaresi* sp. nov.). Three others are recorded in the Atlantic Ocean for the first time; *Geodia anceps* (Vosmaer, 1894) previously known from the Western Mediterranean, *Coelosphaera* (*Histodermion*) *cryosi* (Boury-Esnault, Pansini & Uriz, 1994), from the Mediterranean Moroccan coast, and *Petrosia* (*Petrosia*) *raphida* (Boury-Esnault, Pansini & Uriz, 1994), hitherto known only from deep Mediterranean waters close to the Gibraltar Strait. *Geodia anceps* was found at Almazán mud volcano, while both *C. cryosi* and *P. raphida* were found at Pipoca mud volcano, which largely meet the MOW, so these records could reflect a natural species transfer from the Mediterranean to the Atlantic. Five other species are considered as rare because this study provides their second record for the Atlantic Ocean: the hexactinellid *Lanuginella* cf. *pupa* Schmidt, 1870 and the demosponges *Geodia* cf. *spherastrella* Topsent, 1904, *Cladocroce spathiformis* Topsent, 1904, *Cladocroce fibrosa* (Topsent, 1890) and *Haliclona* (*Rhizoniera*) *pedunculata* (Boury-Esnault, Pansini & Uriz, 1994).

Another relevant finding was a 'micro-aggregation' of the carnivorous sponge *Lycopodina hypogea* (Vacelet & Boury-Esnault,

https://doi.org/10.1017/S0025315418000589

Table 1. Summary of beam-trawl sampling stations that retrieved sponges

			Beam trawl start			Beam trawl end				
Map code	Haul	Mud volcano	Latitude	Longitude	Depth (m)	Latitude	Longitude	Depth (m)	Sampled area (m^2)	Seabed characteristics
1	10BT03	Gazul	36°34.02′N	6°56.17′W	462	36°34.26′N	6°56.41′W	460	1864	Muddy medium sand with sea urchins, *Flabellum chunii* & sponges
2	10BT04	Gazul	36°33.48′N	6°56.31′W	495	36°°33.20′N	6°°56.19′W	483	1902	Gravel coarse and fine sand with MDAC, *Cidaris cidaris* & *Hyalinoecia tubicola*
3	10BT06	Gazul	36°33.33′N	6°56.07′W	422	36°°33.59′N	6°°55.59′W	450	1778	Fine sand with MDAC, *Leptometra phalangium*, sponges & *Madrepora oculata*
4	10BT08	Gazul	36°33.27′N	6°56.01′W	380	36°°33.54′N	6°55.44′W	455	1990	Muddy gravel and fine sand with MDAC, *L. phalangium*, sponges & *M. oculata*
5	10BT07	Gazul	36°33.22′N	6°55.51′W	420	36°33.52′N	6°56.36′W	459	2088	Muddy fine sand with MDAC, *L. phalangium*, sponges & *M. oculata*
6	10BT02	Gazul	36°33.17′N	6°56.43′W	477	36°33.19′N	6°57.27′W	478	2424	Medium and fine sand with *Actinauge richardi*
7	11BT08	Anastasya	36°31.37′N	7°9.23′W	478	36°31.56′N	7°8.59′W	550	2155	Sandy mud with seapens (*Kophobelemnon stelliferum, Funiculina quadrangularis*)
8	11BT01	Anastasya	36°31.14′N	7°8.86′W	489	36°31.76′N	7°8.67′W	546	2424	Sandy mud with seapens (*K. stelliferum, F. quadrangularis*) & *Thenea muricata*
9	11BT14	Anastasya	36°30.70′N	7°10.00′W	540	36°31.20′N	7°10.50′W	539	2343	Sandy mud with seapens (*K. stelliferum, F. quadrangularis*)
10	11BT10	Tarsis	36°29.37′N	7°15.12′W	639	36°29.71′N	7°14.64′W	598	1911	Sandy mud with seapens and *F. chunii*.
11	11BT02	Tarsis	36°29.24′N	7°14.27′W	579	36°29.19′N	7°14.99′W	620	2159	Sandy mud with seapens (*K. stelliferum, F. quadrangularis*)
12	11BT11	Tarsis	36°28.85′N	7°14.19′W	591	36°29.30′N	7°13.91′W	584	1882	Muddy sand with seapens (*K. stelliferum, F. quadrangularis*) & bamboo coral (*Isidella*)
13	11BT16	Pipoca	36°28.18′N	7°12.98′W	627	36°28.57′N	7°13.47′W	719	2051	Muddy sand with seapens (*K. stelliferum, F. quadrangularis*) & *T. muricata*
14	11BT15	Pipoca	36°28.28′N	7°11.88′W	675	36°28.62′N	7°12.40′W	670	1987	Muddy sand with *Cidaris cidaris*
15	11BT18	Pipoca	36°27.74′N	7°12.48′W	565	36°27.70′N	7°11.87′W	557	1805	Sandy mud with MDAC, sponges & small gorgonians (*Acanthogorgia hirsuta*)
16	11BT17	Pipoca	36°27.38′N	7°12.52′W	573	36°27.61′N	7°11.97′W	530	1848	Sandy mud with MDAC, sponges & small gorgonians (*A. hirsuta*)
17	11BT20	Pipoca	36°27.18′N	7°11.12′W	625	36°27.54′N	7°11.60′W	616	1914	Muddy sand with seapens (*K. stelliferum, F. quadrangularis*) & *T. muricata*
18	11BT31	Chica	36°22.60′N	7°7.22′W	729	36°23.02′N	7°6.88′W	604	1863	Sandy mud with MDAC, *C. cidaris*, sponges & gorgonians
19	11BT05	Chica	36°22.38′N	7°6.41′W	655	36°22.23′N	7°7.08′W	682	2212	Muddy sand with seapens (*K. stelliferum, F. quadrangularis*) & *F. chunii*
20	11BT19	Chica	36°21.88′N	7°7.86′W	690	36°22.36′N	7°8.11′W	690	1935	Sandy mud with *C. cidaris* & *A. richardi.*
21	11BT06	Chica	36°22.56′N	7°6.79′W	660	36°22.86′N	7°7.31′W	673	2065	Muddy sand with MDAC, *T. muricata*, seapens & gorgonians
22	11BT21	Hespérides	36°12.21′N	7°18.73′W	817	36°12.66′N	7°18.42′W	845	1897	Muddy sand with *Radicipes* cf. *fragilis* & *F. chunii*

(*Continued*)

Table 1. (*Continued.*)

			Beam trawl start			Beam trawl end				
Map code	Haul	Mud volcano	Latitude	Longitude	Depth (m)	Latitude	Longitude	Depth (m)	Sampled area (m^2)	Seabed characteristics
23	11BT24	Hespérides	36°11.17′N	7°18.42′W	704	36°10.82′N	7°17.95′W	734	1876	Muddy sand with MDAC, CWC remains, *F. chunii,* gorgonians & black corals
24	11BT22	Hespérides	36°11.22′N	7°17.50′W	758	36°10.76′N	7°17.48′W	801	1713	Muddy sand with MDAC, CWC remains, *F. chunii,* gorgonians & black corals
25	11BT23	Hespérides	36°10.83′N	7°18.69′W	703	36°10.87′N	7°19.31′W	756	1856	Muddy sand with MDAC, CWC remains, hydrozoans, siboglinids, *F. chunii* & black corals
26	11BT30	Almazán	36°3.67′N	7°20.15′W	912	36°3.52′N	7°19.56′W	904	1842	Sandy mud with *R.* cf. *fragilis, Isidella* & *Pheronema carpenteri*
27	11BT26	Almazán	36°2.90′N	7°20.59′W	941	36°2.48′N	7°20.22′W	893	1892	Sandy mud with MDAC, CWC remains, *Isidella*, *R.* cf. *fragilis* and gorgonians.
28	11BT29	Almazán	36°3.17′N	7°20.33′W	860	36°2.88′N	7°20.87′W	928	1948	Sandy mud with MDAC, CWC remains, *P. carpenteri, Isidella*, gorgonians & black corals
29	11BT25	Almazán	36°3.29′N	7°19.72′W	894	36°3.61′N	7°19.22′W	896	1871	Sandy mud with MDAC, CWC remains, gorgonians, *C. cidaris*, siboglinids & crinoids
30	11BT27	Aveiro	35°52.03′N	7°25.83′W	1099	35°51.79′N	7°25.30′W	1114	1809	Mud with siboglinids, *Isidella* & *Nymphaster arenatus*
31	11BT28	Aveiro	35°51.74′N	7°26.72′W	1146	35°51.51′N	7°27.28′W	1136	1871	Sandy mud with *T. muricata, Isidella* & *P. carpenteri*

MDAC, Methane-derived authigenic carbonates; CWC, Cold-water corals.

Table 2. Summary of features of the mud volcanoes, including N = number of beam-trawl transects conducted, total sampled area (m^2), mean (±SD) depth of trawls (m), abundance of methane-derived authigenic carbonates (MDAC), level of intensity of benthic fishing activity (trawling) in the sampled areas, total number of sponge species identified, and total number of individuals retrieved. The MDAC abundance and fishing intensity in each mud volcano have been calculated as semiquantitative indexes (mean ± SD) from the values of each beam-trawl transect (see Methods)

Mud volcano	*N*	Sampled area (m^2)	Mean depth (m)	MDAC abundance	Fishing intensity	Species richness	Abundance (ind.)
Gazul	6	12,046	453 ± 32	2.00 ± 0.89	0.50 ± 0.84	15	370
Anastasya	3	6923	524 ± 32	0.00 ± 0.00	2.67 ± 0.58	8	42
Tarsis	3	5954	602 ± 23	0.33 ± 0.58	2.33 ± 1.15	9	99
Pipoca	5	9608	616 ± 60	0.60 ± 0.89	0.40 ± 0.89	38	249
Chica	4	8078	673 ± 36	0.75 ± 0.50	1.00 ± 1.41	27	299
Hespérides	4	7344	765 ± 52	1.75 ± 1.50	0.00 ± 0.00	19	105
Almazan	4	7555	904 ± 25	1.00 ± 0.82	0.00 ± 0.00	27	270
Aveiro	2	3681	1124 ± 21	0.00 ± 0.00	0.00 ± 0.00	9	225

1996): a total of 71 individuals in close proximity to each other on a flattened MDAC boulder of 35 cm^2 collected from Gazul mud volcano at a depth of about 490 m. The presence of this species in this same mud volcano had previously been suggested from a ROV study based on video recording (Chevaldonné *et al*., 2015). Deep-water records of this species in the Mediterranean are scarce and it is rarely found in such high densities (Chevaldonné *et al*., 2015). Because this sponge has been mostly reported from the Mediterranean and from shallow Atlantic waters, a detailed description of the skeleton of these deep-water individuals was considered worthwhile to contribute to the understanding of intraspecific skeletal variability.

Regarding abundances, the most abundant species was the demosponge *Thenea muricata* (Bowerbank, 1858) with 366 collected individuals. Because of its relatively small size and the capability to form aggregations on soft bottoms (which are extensive in the studied fields of mud volcanoes), these high abundances are not surprising. The only demosponge forming real aggregations was *Petrosia* (*Petrosia*) *crassa* (Carter, 1876), represented in the samples by 169 individuals. The demosponge *Desmacella inornata* (Bowerbank, 1866) was also very abundant, with 110 individuals. The abundance of two hexactinellids, *Pheronema carpenteri* (Thomson, 1869), with 181 individuals, and *Asconema setubalense* Kent, 1870, with 117 individuals, showed that aggregations of these large species also occur in these bottoms even when methane seeping occurs (see online Appendix I).

A comparison of the species richness and total sponge abundance (individual counts) revealed large between-volcano differences in those parameters (Table 2). Yet there are also large differences in the sampling effort between mud volcanoes (Table 2), the sampled area (12,046 m^2) in Gazul (the shallowest and best sampled mud volcano) being almost 4-fold larger than that sampled (3681 m^2) in Aveiro (the deepest and least sampled volcano). When species richness and abundance were normalized by sampled area, the mud volcano Pipoca (located at an intermediate depth) emerged as hosting the highest species richness per square metre and Aveiro (the deepest one) as having the highest abundance per square metre (Table 2; Figure 2). A Pearson correlation involving the eight mud volcanoes revealed no relationship between the species richness and the average density of sponges per m^2 of sampled bottom (N = 8, $r^2 = 0.130$, $P = 0.379$; Figure 2A). The main reason for the lack of correlation is that the pattern is largely disrupted by the sponge fauna of the shallowest (Gazul) and the deepest (Aveiro) volcanoes. The Aveiro fauna consists of a moderate number of species per m^2 but a very high number of individuals. This is because the species *Thenea muricata* occurs in this mud volcano forming dense aggregations, represented in the samples by a total of 139 individuals. On the other hand, the Gazul fauna consists of a low number of species but several of them represented with high abundances, such as *Asconema setubalense* (54 individuals), *Poecillastra compressa* (54), *Lycopodina hypogea* (71) and *Petrosia crassa* (149). Both ROV and VOR images and collected material confirmed that most of these sponges are able to form aggregations at some point, as also documented preliminarily for some of them in a technical report of the grant results (Díaz del Río *et al*., 2014). When the Gazul and Aveiro mud volcanoes were excluded from the correlation analysis for being outliers, a significant positive linear relationship between species richness per m^2 and abundance of individuals per m^2 emerged for the remaining mud volcanoes (N = 6, $P = 0.044$, $r^2 = 0.677$; Figure 2A). Such a relationship means that, in most volcanoes, most of the species are not spatially overrepresented through aggregations, but just scattered with low or moderate abundances that do not differ much between species. When the species richness per m^2 was plotted *vs* the average depth of each mud volcano (Figure 2B), no significant correlation emerged (N = 8, $P = 0.301$, $r^2 = 0.175$), but it became statistically significant when the outlier volcanoes Pipoca and Aveiro were excluded from the analysis (N = 6, $P = 0.024$, $r^2 = 0.758$; Figure 2B). This shift indicates that, as a general trend, the species richness per m^2 increases with increasing depth within the bathymetric range of these mud volcanoes. Such a pattern was altered by the fauna of Pipoca, which is richer than expected given its intermediate depth, and by the fauna of Aveiro, which is poorer than expected given that it is the deepest mud volcano. This general pattern appears to support the classical view that biodiversity of benthic fauna peaks at intermediate depths on the continental slope.

The underwater images revealed marked between-transect differences in the intensity of the seeping activity in the different mud volcanoes. Likewise, the number of fragments of MDAC formations retrieved by the beam trawl also varied across transects (Table 2). The highest mean abundance of MDAC structures was found in Gazul (averaged as 2), followed by Hespérides (1.75) and Almazán (1). MDAC abundance was comparatively low at Chica, Pipoca and Tarsis (averaged as 0.75, 0.60 and 0.33, respectively). The rest of the volcanoes (i.e. Anastasya and Aveiro) lacked MDAC formations (scored as 0). The abundance of hard substrate is a feature that was predicted to affect the general composition and abundance of the sponge fauna. Yet when the pairwise relationship between abundance of MDAC formations in each mud volcano and its respective species richness

https://doi.org/10.1017/S0025315418000589

and abundance of sponges per m^2 were examined through rank correlation, no significant pattern was revealed, even when two and up to three outliers were eliminated (Figure 2C, D).

When the faunal parameters were compared against the level of impact that the trawling activity in each of the mud volcanoes may have, a negative general trend was noticed, suggesting that the greater the fishery activity the smaller the sponge richness (Figure 2E) and abundance (Figure 2F). Yet, this trend was never statistically significant, even when up to three outliers were progressively eliminated (Figure 2E, F).

Systematics

Phylum PORIFERA Grant, 1836
Class HEXACTINELLIDA Schmidt, 1870
Subclass HEXASTEROPHORA Schulze, 1886
Order LYSSACINOSIDA Zittel, 1877
Family ROSSELLIDAE Schulze, 1885
Genus *Lanuginella* Schmidt, 1870
DIAGNOSIS: (Tabachnick, 2002)
Lanuginella cf. *pupa* Schmidt, 1870
(Figures 3A & 4).

Material examined

One specimen collected from Station 20: P75-11BT19.

Macroscopic description

Ovate specimen measuring 6 mm in length and 3 mm in diameter, attached to a rock, basiphytose, with smooth surface and a single oscule. Consistency is fragile and colour after preservation in ethanol is white (Figure 3A).

Skeletal structure

Choanosomal skeleton is composed of diactins, hexactins and microscleres. Hypodermal pentactins are tangential to the surface with their proximal ray directed inwards to the body of the sponge. Dermalia is mainly composed of stauractins, and sometimes pentactins, tauactins and hexactins. The atrialia presents hexactins smaller and less rough than the choanosomal ones.

Spicules

Spicules are diactins, often flexuous, with four centrally located tubercles, and rough pointed ends (Figure 4A, B). They measure 325–3000 × 3.75–6.8 μm. Choanosomal hexactins occur bearing rays of different lengths, sometimes flexuous, with smooth or rough pointed ends (Figure 4A, C). Size of the rays is 250–850 × 5.6–12.5 μm. Hypodermal pentactins are common (Figure 4A, D), characterized by rays with acerate ends measuring 170–850 × 4–10 μm and a proximal ray measuring 242–950 × 7.5–11.5 μm with microspinned end. Abundant stauractins occur (Figure 4A, E–G) along with scarce pentactins, tauactins and hexactins (Figure 4A). They are evenly microspined, with conical ends and rays measuring 42.5–140 × 2–5.64 μm. Atrialia hexactins moderately occur (Figure 4A, H), being less rough than the dermalia spicules, almost smooth, and measuring 46.46–150 × 2–6.25 μm. Microscleres are discohexasters showing a total diameter of 30–70 μm, with a primary rosette being 6.3–10.45 μm in diameter and discs of 3–5 points (Figure 4A, I, J). Strobiloplumicomes were not observed.

Skeletal structure

Choanosomal skeleton is composed of diactins, hexactins and microscleres. Hypodermal pentactins are tangential to the surface with their proximal ray directed inwards to the body of the sponge. Dermalia is mainly composed of stauractins, and sometimes pentactins, tauactins and hexactins. The atrialia presents hexactins smaller and less rough than the choanosomal ones.

Distribution and ecology notes

Specimen collected from depths of 690 m, growing on a small MDAC slab from a sandy mud bottom from the Chica mud volcano (Table 1). It makes the second record of the species in the Atlantic Ocean, 12 specimens having previously been recorded from Cape Verde by Schmidt (1870) and Tabachnick (2002). Ijima (1904) reported some specimens from the Pacific Ocean but that assignation to *L. pupa* is currently considered 'inaccurate' according to the World Porifera Database (van Soest *et al.*, 2018).

Taxonomic remarks

Since the holotype of the species is not available, the features of our specimen were compared with those reported in the original description (Schmidt, 1870). This holotype description being somewhat imprecise, a more complete and accurate description of another specimen off Palmeira, Cape Verde was also consulted (Tabachnick, 2002). According with them, our specimen shares the same habit and skeletal structure, the skeletal composition being mostly coincident but with two small differences: (1) the atrialia hexactins (46.46–150 × 2–6.25 μm) from our specimen were slightly smaller than those from the Cape Verde specimens (68–243 × 7 μm); and (2) strobiloplumicomes were neither observed in our specimen nor mentioned in the holotype, while they were described by Tabachnick (2002).

Regarding other species from subfamily Lanuginellinae, they all bear strobiloplumicomes, and none of them resembles the rest of skeletal features better than *Lanuginella pupa.*

Class DEMOSPONGIAE Sollas, 1885
Subclass HETEROSCLEROMORPHA Cárdenas, Perez and Boury-Esnault, 2012
Order POECILOSCLERIDA Topsent, 1928
Family CLADORHIZIDAE Dendy, 1922
Genus *Lycopodina* Lundbeck, 1905
DIAGNOSIS: (Hestetun *et al.*, 2016)
Lycopodina hypogea (Vacelet and Boury-Esnault, 1996)
(Figures 3B & 5).

Material examined

Three of 71 specimens collected from Station 2: P203-10BT04 A-BS.

Macroscopic description

Oval body, 0.72–1.5 mm long and 0.58–1 mm in diameter, with a stalk of 1.2–1.83 mm in length and 0.09–0.18 mm in diameter. Filaments project from the body, varying in number and length among individuals, depending on the digestive stage. Whitish colour after preservation in ethanol (Figure 3B).

Skeletal structure

The stalk contains a central axis of styles and subtylostyles, which branches radially at the body, forming progressively thinner tracts that finally enter the filamentous, feeding projections. The main ramifications of the axis are surrounded by styles and subtylostyles in confusion. Anisochela are abundant, projecting the largest ala from the epithelium of the hunting filaments. The attachment base contains smaller subtylostyles and/or styles in confusion and desma were never found.

Spicules

Megascleres are styles and subtylostyles (Figure 5A, B), measuring 200–550 × 2.5–6.6 μm. Megascleres in the stalk are slightly thinner while those at the basal plate are shorter (100–300 μm) and more robust (4.5–6 μm). Microscleres are abundant palmate anisochela, 8.75–11.5 μm in length, with a frontal long tooth of

https://doi.org/10.1017/S0025315418000589

Fig. 3. Photographs showing the general aspect of some studied specimens: (A) *Lanuginella* cf. *pupa* (P75-11BT19) growing on a small rock. (B) Some representatives of the specimens of *Lycopodina hypogea* (P203-10BT04) growing in close proximity on a boulder. (C) *Coelosphaera* (*Histodermion*) *cryosi* (P03C-11BT18). (D) Specimen of *Jaspis sinuoxea* sp. nov. designed as holotype (P70-11BT17A). (E) Specimen of *Geodia anceps* (P224-11BT25) growing on a rock, marked as 'Ga'. (F) Fragment of a specimen of *Geodia* cf. *spherastrella* (P14E-11BT17A) showing what remains of its hispidation, ectosome and choanosome. (G) Specimen of *Myrmekioderma indemaresi* sp. nov. designed as holotype (P10-10BT06) with a patent cerebriform surface. (H) Fragment of *Petrosia* (*Petrosia*) *raphida* (P200-11BT17) attached to a rock. (I-J) Specimen of *Cladocroce fibrosa* (P54-11BT17). (K) Specimen of *Cladocroce spathiformis* (P05-10BT03A). (L) Specimens of *Haliclona* (*Rhizoniera*) *pedunculata* (from left to right P23B-11BT20D, P23B-11BT20C and P23B-11BT20D) showing slightly different morphologies, that on the left being the most common.

https://doi.org/10.1017/S0025315418000589

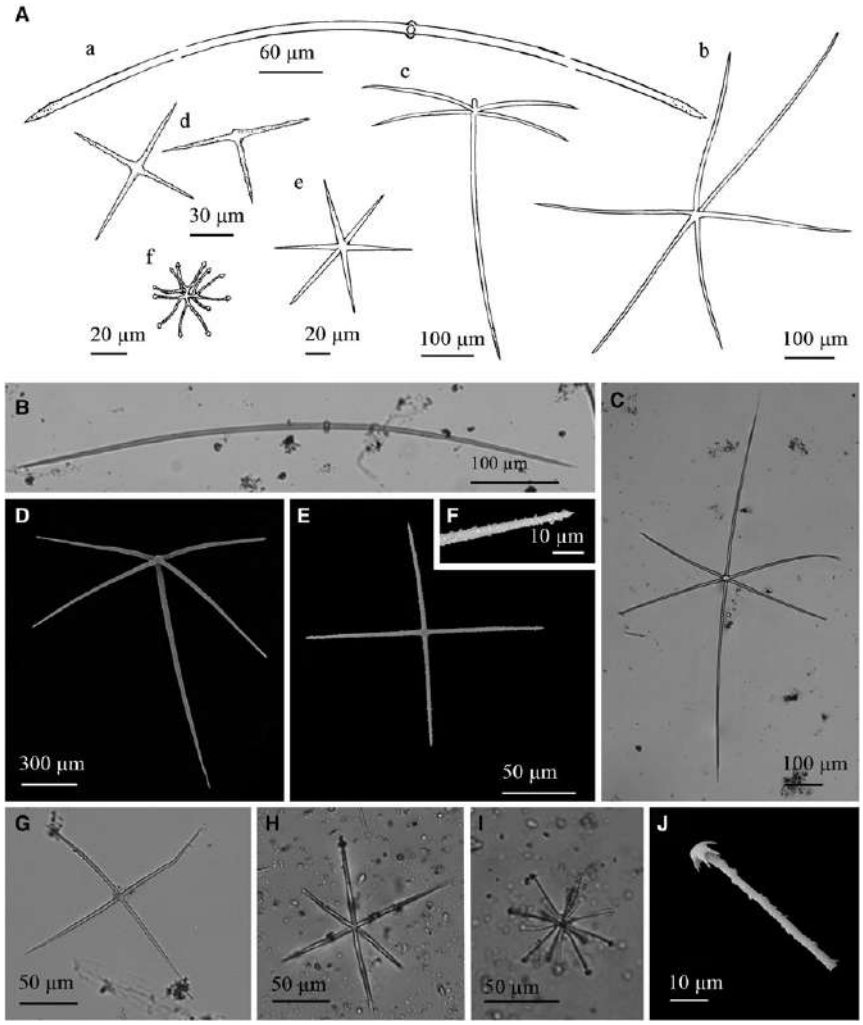

Fig. 4. *Lanuginella* cf. *pupa* Schmidt, 1870: (A) Line drawing summarizing the skeletal complement of the specimen herein described. Diactins are (a) bent or flexuous and show four tubercles at the centre of their shaft. Choanosomal hexactins (b) also occur with often differently sized rays, as well as hypodermal pentactins (c). Dermalia is mainly formed by microspined stauractins and, less frequently other variations as tauactins (d), while the atrialia contains hexactins, smoother than the previous (e). Microscleres are microspined discohexasters (f). (B) Light microscope view of a diactine. (C) Light microscope view of a choanosomal hexactine, with differently long, somewhat flexuous rays. (D) SEM view of an hypodermal pentactine. (E) SEM view of a tauractine. (F) SEM detail of a spined ray of a tauractine. (G) Light microscope view of a tauractine with an abnormal ray. (H) Light microscope view of an atrialia hexactine. (I) Light microscope view of a discohexaster. (J) SEM detail of a ray of a discohexaster in which the microspines can be observed.

4.4–5.86 × 2.17–3.09 µm (Figure 5C). No forceps was observed, suggesting absence of reproductive elements at the time of collection.

Distribution and ecology notes

Noticeable aggregation of 71 individuals on a flattened slab of only 35 cm^2 from Gazul mud volcano, at depths of 483–495 m (Table 1). Previously, *L. hypogea* had been reported from the Mediterranean and shallow depths in the Atlantic. The bathyal occurrence of the species in the area had only tentatively been proposed from a ROV video record (Chevaldonné *et al.*, 2015). All previous Mediterranean deep-water records report individuals in low numbers rather than in aggregations.

Taxonomic remarks

Some of the previously described shallow-water specimens of *L. hypogea* show longer subtylostyles in the stalk than in the body (Vacelet and Boury-Esnault, 1996; Chevaldonné *et al.*, 2015), while some others show no length differences (Chevaldonné *et al.*, 2015).

https://doi.org/10.1017/S0025315418000589

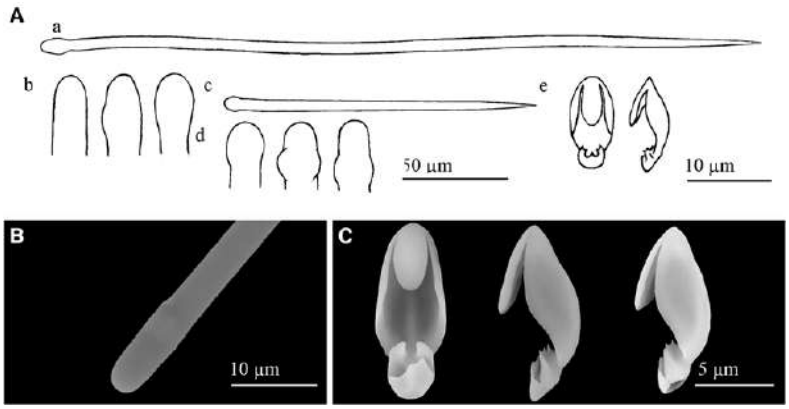

Fig. 5. *Lycopodina hypogea*: (A) Line drawing summarizing the skeletal complement of the species. Megascleres are (subtylo-)styles (a) with blunt to faintly subtylote ends (b). The basal plate of the sponge shows shorter subtylostyles (c) with more evident subtyles (d). Microscleres are palamate anisochela (e). (B) SEM detail of a blunt end of a style with a very subtle subterminal swelling. (C) SEM detail of anisochelae.

Family COELOSPHAERIDAE Dendy, 1922
Genus *Coelosphaera* Thomson, 1873
Subgenus *Coelosphaera* (*Histodermion*) Topsent, 1927
DIAGNOSIS: (van Soest, 2002)
Coelosphaera (*Histodermion*) *cryosi* (Boury-Esnault, Pansini & Uriz, 1994)
(Figures 3C & 6).

Material examined

Two specimens, collected from Station 13: P03C-11BT16 and Station 15: P03C-11BT18.

Macroscopic description

Specimen with a body collapsed as a result of being trawled and exposed to air on board during its collection process. The sponge looks coated, with an irregular shape, covering a surface of 15 mm in length and 30 mm in width. It shows an evident ectosome and a loose, somewhat hollow choanosome. Surface is smooth and shows 12 fistulas with no patent openings. Oscules and pores are not observed, consistency is fragile and easy to steer with tweezers, and colour after preservation in ethanol is cream (Figure 3C).

Skeletal structure

Choanosomal skeleton is formed by loose bundles of strongyles echinated by some acanthostyles. Microscleres are present over all the choanosome and are especially abundant at the base, where also some acanthostyles lie perpendicularly to the substrate. Ectosome is a tangential and compact layer of strongyles and microscleres, the fistula showing the same structure.

Spicules

Megascleres are abundant iso- and anisostrongyles (Figure 6A–C) with variable strongylote ends that range from narrow to lanceolate (Figure 6A, D). Fusiform and slightly sinuous shapes sometimes occur, as well as tylote developing stages (Figure 6A–C). They measure 335–470 µm in length and 8.75–15 µm in diameter. Accessory megascleres are subtylote acanthostyles, straight or slightly bent, with conspicuous spines curved upwards at the shaft (Figure 6A, E, F). They measure 60–240 µm in length by 10–15 µm in diameter. Microscleres are abundant, arcuate isochelae that sometimes bear sparse microspines (Figure 6A, G, H), measuring 27.5–37.5 µm in length and 3.5–7.5 µm in width, and C and S shaped sigmata (Figure 6A, I, J). Sigmata occur in two categories, the smallest measuring 22.5–50 µm in length and 1.8–2.5 µm in diameter, while the largest comprises sizes of 58.5–85 µm in length and 1.8–2.5 µm in width, and sometimes shows bifid ends.

Distribution and ecology notes

The specimens were collected from Pipoca mud volcano, growing on small MDAC pieces found on muddy sand (627–719 m deep) and sandy mud (565–557 m deep) bottoms respectively (Table 1). This is the second record for this species, being previously reported from the Mediterranean Moroccan coast, at a 170 m-deep bottom of shell debris (Boury-Esnault *et al*., 1994).

Taxonomic remarks

The collected specimen fits closely the diagnosis of the genus *Coalosphaera* (*Histodermion*), sharing most of its characteristics with *C. cryosi* except for two minor differences. Our specimen has ectosomal diactines with ends widely variable in shape, from narrowing to lanceolated, to even tylote. In the holotype all the ectosomal diactines have tylote ends. Differences in the isochelae also occur, our specimen showing a single category which can show microspines, while the holotype shows two categories with no reported microspines. These differences are here considered to be intraspecific variability, since tylote stages of megascleres occur in both the studied and the type material and the isochela size of our specimen falls between the two size categories described in the holotype, suggesting that the existence or not of the two categories could also have resulted from a subjective author criterion during categorization.

Regarding body shape, the mud volcano specimen resembles *Coelosphaera* (*Histodermion*) *dividuum* (Topsent, 1927) from Azores, which is the only other species in this subgenus hitherto recorded from the Atlantic. They both bear anisostrongyles and only one category of isochelae. Nevertheless, our specimen only has anisostrongyles while *C. dividuum* has anisostrongyles and tylotes, the latter measuring 425–740 × 8–15 µm (size of anisostrongyles is not specified in the original description). Also the acanthostyles of our specimen are smaller than those of *C. dividuum*, which measure 450–470 × 13–16 µm, and it bears two categories of sigmata while *C. dividuum* lacks them.

https://doi.org/10.1017/S0025315418000589

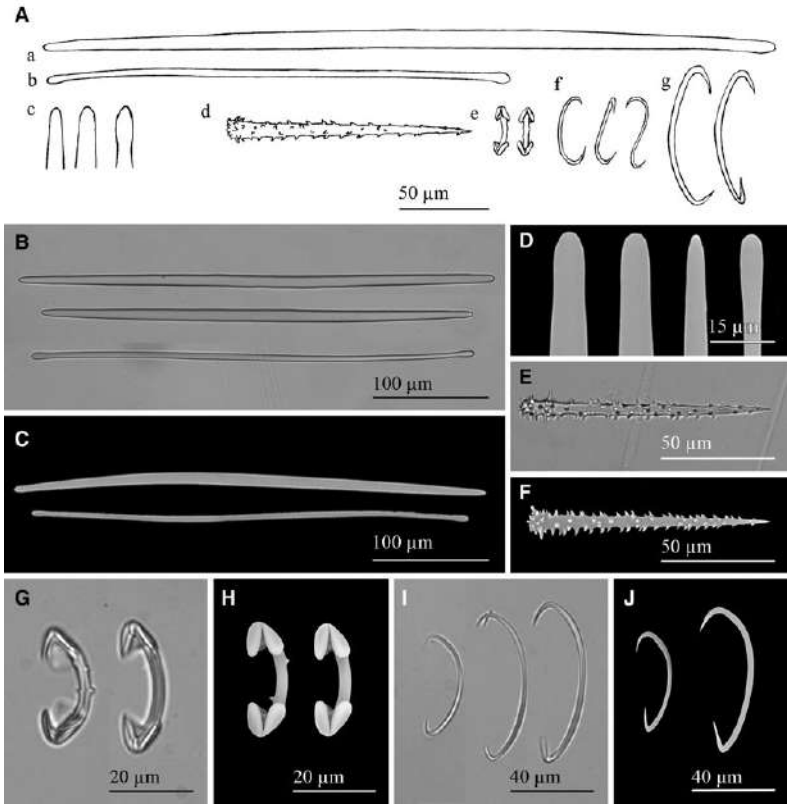

Fig. 6. *Coelosphaera* (*Histodermion*) *cryosi*: (A) Line drawing summarizing the skeletal complement of the species. Megascleres are abundant iso- and anisostrongyles (a) that sometimes occur in thinner shapes (b). Their ends range from narrow to lanceolate, and are tylote in the thinner shapes (c). Accessory megascleres are subtylote acanthostyles with conspicuous spines curved upwards at the shaft (d). Microscleres are arcuate isochelae that sometimes bear sparse microspines (e) and C and S shaped sigmata in two size categories (f–g). (B) Light microscope view of anisostrongyles. (C) SEM view of anisostrongiles. (D) SEM detail of different strongyle tips. (E) Light microscope view of an acanthostyle. (F) SEM view of an acanthostyle. (G) Light microscope view of a spiny and a smooth isochelae. (H) SEM view of a spiny and a smooth isochelae. (I) Light microscope view of sigmata in two size categories with regular and bifid tips. (J) SEM view of sigmata in two size categories.

Order TETRACTINELLIDA Marshall, 1876
Family ANCORINIDAE Schmidt, 1870
Genus *Jaspis* Gray, 1867
DIAGNOSIS: (Uriz, 2002)
Jaspis sinuoxea sp. nov.
(Figures 3D & 7).

Material examined

Holotype P70-11BT17A from Station 16 (36° 27.38′N 7°12.52′W – 36°27.61′N 7°11.97′W). Four paratypes designated: P70-11BT17B & C from Station 16; P70-11BT18 A & B from Station 15 (36°27.74′N 7°12.48′W – 36°27.70′N 7°11.87′W).

Etymology

This species is named after the evident sinuous shape of its oxeas.

Macroscopic description

Encrusting to thickly encrusting, patchily growing on small rocks. Some fragmented specimens collected with no attached substrate. They measure 3–25 mm in length, 5–50 mm in width and 1–3 mm in thickness. Oscules only observed in holotype as two non-elevated 'pores' of 0.25 mm in diameter and with some faint radiating 'veins'. Sponge surface is smooth, although large megascleres from the choanosome occasionally hispidate it. Consistency is friable, especially in the choanosome, colour after preservation in ethanol is whitish beige (Figure 3D).

Skeletal structure

Ectosome is a crust-like layer of tangential and compacted ectosomal oxeas and oxyasters. The organization of the choanosomal skeleton is in confusion, with all spicule types arranged without a recognizable pattern.

Spicules

Megascleres are oxeas in a wide size range (Figure 7A), not divisible into discrete size categories but by location and shape. Choanosomal oxeas (Figure 7A–D) measure 450–2875 × 8.5–75 µm, they are more or less fusiform, bent or more often sinuous, the ends are usually softly mucronated (Figure 7E) or blunt, resulting in strongyloxeas (Figure 7A); sometimes they are acerate. Centrotylotism is fairly common and scarce spines at the ends may occasionally occur as well. Ectosomal oxeas

https://doi.org/10.1017/S0025315418000589

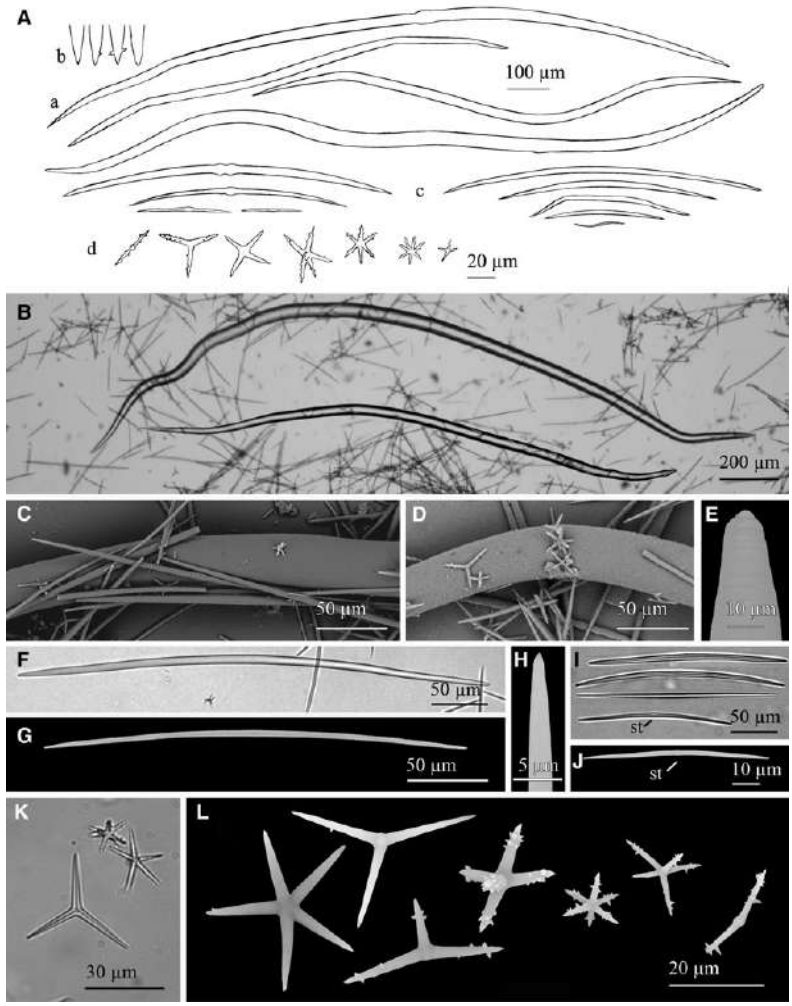

Fig. 7. *Jaspis sinuoxea* sp. nov.: (A) Line drawing summarizing the skeletal complement of the species. Choanosomal oxeas are from bent to sinuous, sometimes with a subtyle more or less centrally located (a) and with acerate or mucronate ends that occasionally bear one or two spines (b). Ectosomal oxeas are once or twice slightly or evenly bent, occasionally slightly sinuous and sometimes show centrotylotism (c). Microscleres are oxyasters in a wide size range, with few to abundant spines, rarely smooth (d). (B) Light microscope view of sinuous choanosomal oxeas, which can be hardly to evenly sinuous. (C-D) SEM detail of choanosomal oxea sections surrounded by ectosomal oxeas and oxyasters. (E) SEM detail of a choanosomal oxea mucronate end. (F) Light microscope view of an ectosomal oxea. (G) SEM view of an ectosomal oxea. (H) SEM detail of an ectosomal oxea conical end. (I) Light microscope view of small ectosomal oxeas, which are from straight to softly bent and sometimes bear a faint subtyle (st). (J) SEM detail of a small ectosomal oxea with a central subtyle (st). (K) Light microscope view of widely variable oxyasters, from large with three smooth actines to small and bearing seven spined actines. (L) SEM detail of oxyasters in a wide range of shapes and sizes. All kind of shapes can be found independently from size, but large oxyasters frequently show few nearly smooth actines while smaller ones generally bear abundant spined actines.

(Figure 7A, F, G, I, J) measure 65–550 × 1.25–12.5 µm, they are from slightly to evenly fusiform, once or twice slightly or markedly bent. Occasionally they are subtly sinuous, and can show centrotylotism. Ends are acerate or conical (Figure 7H). Microscleres are oxyasters variable in shape and size but with no discernible categories (Figure 7A, K, L). They measure 7.5–45 µm in diameter and bear 2–9 conical actines, which can be either smooth or spiny. Generally oxyasters smaller than 15–30 µm in diameter (depending on the specimen) show spines, while those of larger diameters can be either smooth or spiny, but most of the largest ones are actually entirely or almost entirely smooth.

Distribution and ecology notes

The individuals were collected at 530–573 m from a deep sandy mud bottom with MDAC at Pipoca mud volcano (Table 1).

Taxonomic remarks

The specimens from the volcanoes fit the diagnosis of genus *Jaspis*, which in the Atlantic and the Mediterranean is represented

https://doi.org/10.1017/S0025315418000589

by species lacking sinuous oxeas. However, sinuous megascleres have been recorded in *Jaspis stellifera* (Carter, 1879) from Australia and *Jaspis serpentina* Wilson, 1925 from Philippines. The former has slightly flexuous oxeas (Kennedy, 2000) and the latter more markedly sinuous strongyles or oxeas. Yet the microscleres from those two species do not match the features of those in our specimens. Interestingly, a combination of euasters and sinuous diactines occurs in some species of the genus *Paratimea* Hallman, 1917. However, the global spicule complement and skeletal arrangement in the specimens here collected do not meet those characterizing *Paratimea* spp.

Family GEODIIDAE Gray, 1867
Genus *Geodia* Lamarck, 1815
DIAGNOSIS: (Cárdenas *et al.*, 2013)

Geodia anceps (Vosmaer, 1894)
(Figures 3E & 8).

Material examined

One specimen: P224-11BT25 from Station 29.

Macroscopic description

Irregularly globular shape, measuring 65 mm in height, and 50 mm × 25 mm in width. Smooth surface, with uniporal oscules and ostioles. Some small buds occur scattered on the sponge surface. Consistency is slightly compressible and colour in ethanol is beige (Figure 3E).

Skeletal structure

The inner choanosome shows oxea and oxyasters in confusion, becoming radially arranged in loose bundles towards the ectosome. The cortex is 500 µm thick, the inner cortex being reinforced by oxea and clads of triaenes, with their rhabdomes towards the choanosome.

The external cortex consists of two layers, an inner layer of sterrasters and an outer layer of oxyspherasters. Anatrianes project their clads out from the sponge surface.

Spicules

Megascleres are oxeas, orthotriaenes and dichotriaenes. Oxeas, softly curved and fusiform with slightly blunt ends, measure 2122–3406 × 16–42.3 µm (Figure 8A, B). Orthotriaenes show clads of 96.8–580 × 12–68.86 µm and a rhabdome of 375–2770 × 13.5–70 µm (Figure 8A, C). Dichotriaenes with rhabdomes measuring 800–2700 × 30–55 µm and protoclads and deuteroclads measuring respectively 122–378 × 30–53.4 µm and 121–338 × 39–53 µm (Figure 8A, D). Anatriaenes (Figure 8A) have been mostly observed as broken, isodiametric and somewhat flexuous rhabdomes of 6–8 µm in diameter and lengths of up to 1500 µm. Microscleres are somewhat compressed sterrasters, with a diameter of 76.6–91.1 µm (Figure 8A, F). Also smooth oxyasters in two categories. The first one consisting of scarce oxyasters with a diameter of 30.8–50 µm (generally smaller than 36 µm) and only 2–5 actines (Figure 8Af, E); the second one, being a more abundant category of oxyasters with diameter of 18–30 µm and 6–8 actines and a centrum slightly thicker (Figure 8Ag, E, G). Spheroxyasters of 13.2–28.5 µm in total diameter, with a large centrum (6.2–14.5 µm in diameter) and abundant actines which can show sparse microspines (Figure 8Ah, H).

Distribution and ecology notes

The specimen was collected from Almazán mud volcano, on a sandy mud bottom with MDAC at a depth of 894–896 m (Table 1). It represents the first record for the species in the Atlantic Ocean, although it is noteworthy to mention that several specimens were recently found by Ríos and Cárdenas in the Avilés Canyon, Atlantic northern coast of Spain (personal communication). To date, it was only recorded from the Mediterranean, that is, from the Bay of Naples at 150–200 m depth (Vosmaer, 1894) and, from the same area, at a 120−135 m deep muddy bottom with stones (Pulitzer-Finali, 1970). Maldonado (1992) provided another record from 70–120 m deep bottom in Alboran Sea with red coral. Also, it was recorded from a white coral reef located south of Cape S. Maria di Leuca (southern Italy) at 738–809 m depth (Longo *et al.*, 2005).

Taxonomic remarks

The skeletal structure and composition of our specimen fits that of *Geodia anceps*. Sterrasters were found to be somewhat bigger than those from the holotype with a larger centrum. Specimens recently found in the Avilés canyon by Ríos and Cárdenas are also characterized by comparatively larger sterrasters (Cárdenas, personal communication); this could represent a common character of the Atlantic specimens. Also remarkable is the presence of small buds at the sponge surface of the collected specimen, which, to our knowledge, makes this the first budding report in this species.

Geodia cf. *spherastrella* Topsent, 1904
(Figures 3F & 9).

Material examined

Four specimens: P14E-11BT17A to D from Station 16.

Comparative material examined

Geodia spherastrella Topsent, 1904. Holotype: A spicules slide (MNHN no. D.T. 842 122P.A. 1897); Princesse-Alice cruise to Azores, station 866 (Terceira Island: 38°52′50″N 27°23′05″W); collected on 2 August 1897 from a coarse sand bottom at 599 m depth.

Macroscopic description

Two cushion-shaped specimens of 2–3 mm in diameter, with no discernible openings, sparse, long hispidation, and hard consistency. A third specimen only conserved its base and part of the lateral body wall, showing a 0.5 mm thick cortex and an unevenly distributed hispidation and three sparse ostia (Figure 3F). A fourth individual only had its base (30 mm in diameter) preserved.

Skeletal structure

The deepest choanosome skeleton consists mostly of oxeas in confusion and sparse microscleres, but the structure becomes more radially arranged towards the ectosome. Oxeas often hispidate the surface and orthotrianes are placed with clads in the ectosome without crossing it. Ectosome consists of highly packed sterrasters together with spheroxyasters and sphero-strongylasters.

Spicules

Megascleres are oxeas, fusiform and softly bent, with acerate to blunt ends, sometimes mucronate, measuring 445–4153 × 9–22.5 µm (Figure 9A, B). Those longer than 2500–3000 µm are often hispidating and sometimes show a slightly flexuous shape, but no categories can be established since size overlapping occurs between hispidating and choanosomal oxeas. Orthotriaenes also occur, with clads measuring 165–360 × 15–23 µm and rhabdomes of 752–1149 × 16.5–29 µm (Figure 9A, C). Microscleres are abundant sterrasters with ellipsoidal shape and a maximum diameter of 100–130 µm (Figure 9A, D, G), often being observed developing stages which measure down to 60 µm. Sparse spheroxyasters of 17.8–27 µm in diameter occur, showing a marked centrum and smooth and microspined actines (Figure 9A, E, H). Moderately abundant sphero-strongylasters are also present,

https://doi.org/10.1017/S0025315418000589

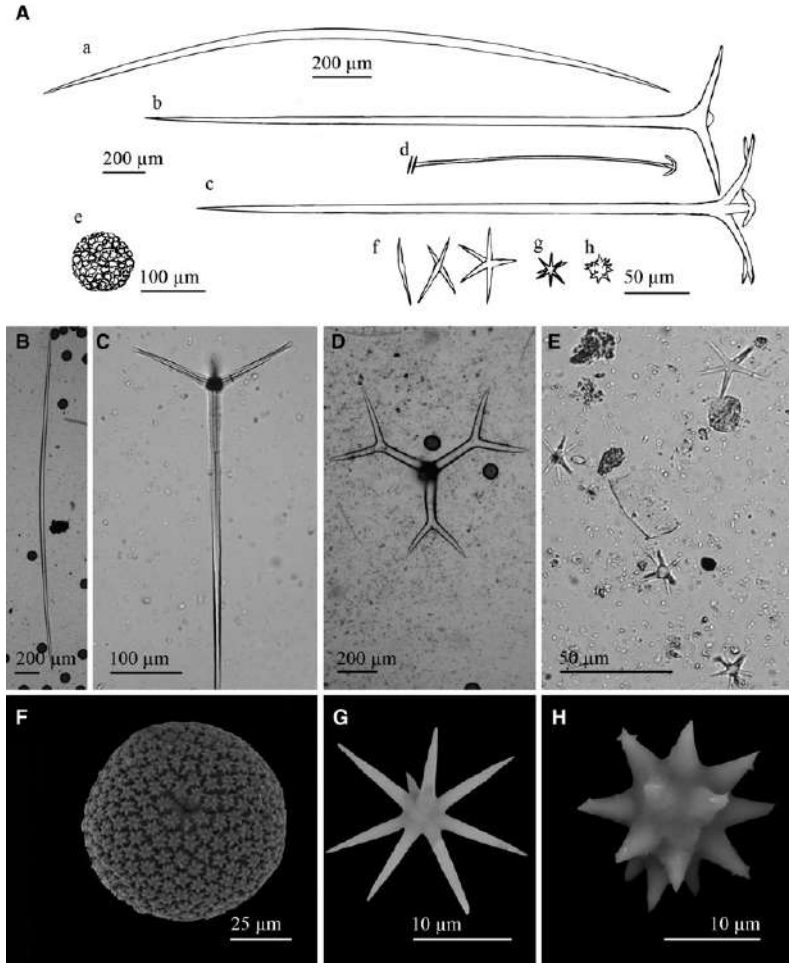

Fig. 8. *Geodia anceps* (Vosmaer, 1894): (A) Line drawing summarizing the skeletal complement of the species. Megascleres are fusiform oxeas (a), orthotriaenes (b), dichotriaenes (c) and flexuous anatriaenes (d). Microscleres are sterrasters (e), oxyasters in two different categories, oxyasters I, scarce and bigger (f) and oxyasters II, more abundant, smaller and with more actines (g), and spheroxyasters with abundant spines (h). (B) Light microscope view of a softly bent oxea. (C) Light microscope view of a orthotriaene. (D) Light microscope view of a dichotriaene. (E) Light microscope view of an oxyaster I on the upper left and three smaller oxyasters II. (F) SEM view of a sterraster. (G) SEM view of an oxyaster II. (H) SEM view of a spheroxyaster with sparse microspines.

measuring 8.5–11.6 µm in diameter and bearing more or less regular actines, which can be short to slightly long and always with spined ends (Figure 9A, E, I).

Distribution and ecology notes

The specimens were collected from Pipoca mud volcano, all from a sandy mud bottom with MDAC at a depth of 530–573 m (Table 1). This material makes the second record of this species in the Atlantic Ocean, one specimen being previously known from the vicinities of Terceira Island in Azores that was collected at a coarse sand bottom at 599 m depth (Topsent, 1904).

Taxonomic remarks

The skeletal composition of our specimens strongly resembles that of the holotype of *Geodia spherastrella*, which is represented only by a spicules slide. The examination of the type slide revealed oxeas of 558.7–3519 × 27.6–40.32 µm, similar in shape to those of the collected specimens. Orthotrianes were not observed in the holotype slide although Topsent (1904) mentioned them in the original description of the species. For this reason, we consider that the lack of orthotrianes in the type slide is an unfortunate mishap that subsequent authors should keep in mind if using it. Microscleres from the holotype also coincide in shape and size with those of our specimens, measuring sterrasters 90–125.5 µm in diameter, spheroxyasters 19.3–30.2 µm, and sphero-strongylasters, 7.6–14.8 µm. It is worth noting that, in the type description from Topsent (1904), 'sterraster-like ends' of the sphero-strongylaster actines were mentioned, and they were observed both in the holotype slide through light microscope and in our specimens through scanning microscopy (Figure 9I).

https://doi.org/10.1017/S0025315418000589

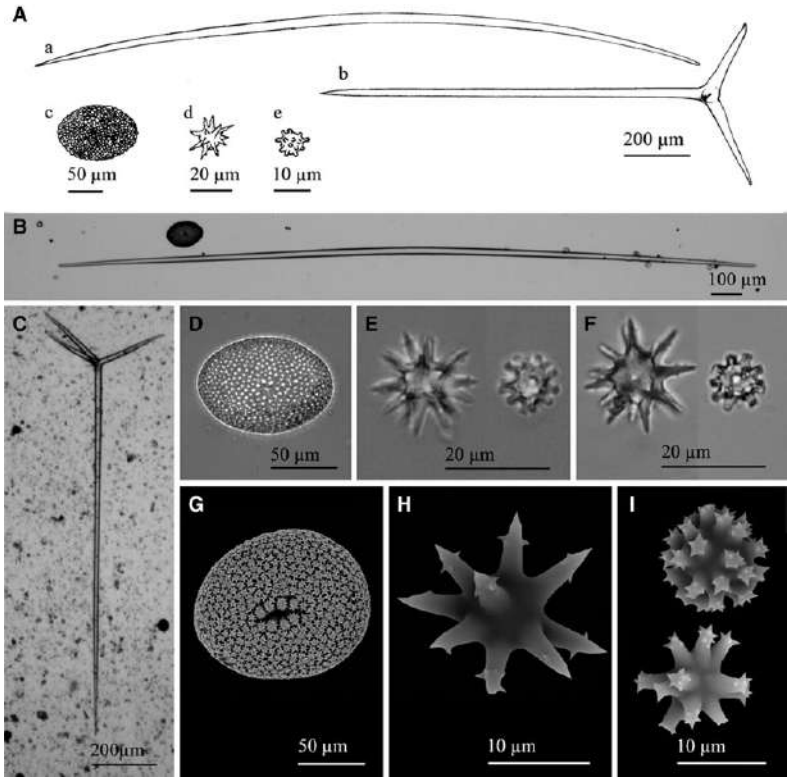

Fig. 9. *Geodia* cf. *spherastrella* Topsent, 1904: (A) Line drawing summarizing the skeletal complement of the species. Megascleres are oxeas, normally fusiform and bent (a), and orthotrianes (b). Microscleres are ellipsoid sterrasters (c), spheroxyasters (d) and sphero-strongylasters (e). (B) Light microscope view of a softly bent oxea. (C) Light microscope view of an orthotriaene. (D) Light microscope view of an sterraster. (E) Light microscope view of a spheroxyaster and a sphero-strongylaster. (F)) Light microscope view from the type material of a spheroxyaster and a sphero-strongylaster. Note the similarities between 'E' and 'F'. (G) SEM view of a sterraster. (H) SEM view of a spherostrongylaster. (H) SEM view of two sphero-strongylasters. Note the differences on the length of the rays and their spined ends.

Little is known about the habit and skeletal structure of the type. According to the original description, it was irregularly shaped, white, smooth and with encrusted small pebbles. The specimens collected from the mud volcanoes conserved a small part of their surface and it seems to be smooth with some irregularly hispid regions and no encrusted pebbles.

Order AXINELLIDA Lévi, 1953
Family HETEROXYIDAE Dendy, 1905
Genus *Myrmekioderma* Elhers, 1870
DIAGNOSIS: (Hooper, 2002)
Myrmekioderma indemaresi sp. nov.
(Figures 3G & 10).

Material examined

Two specimens collected: Holotype P10-10BT06 from Station 3 (36° 33.33′N 6°56.07′W – 36°33.59′N 6°55.59′W); paratype P10-10BT08 from Station 4 (36°33.27′N 6°56.01′W – 36°33.54′N 6°55.44′W).

Comparative material examined

Holotype of *Myrmekioderma spelaea* (Pulitzer – Finali, 1983) originally designated as *Raphisia spelaea* Pulitzer-Finali, 1983; MSNG – (PTRE12) from Cala Sorrentino, Tremiti Island, 2–3 m deep.

Etymology

This species is named after the acronym (i.e. INDEMARES) of the EC LIFE + grant that funded the exploration and sampling of the mud volcanoes.

Macroscopic description

Massive nearly entire individuals, measuring 40–60 mm in height, 40–65 mm in width, and 5–20 mm in thickness. Four oscules observed in P10-10BT08 being 2–3 mm in diameter. Ostioles not evident. Surface is cerebriform (where it is well preserved), shortly hispid, incorporating sparse debris. Colour after preservation in ethanol is creamy-white. Consistency is firm and fleshy, somewhat friable (Figure 3G).

Skeletal structure

Ectosome shows a layer of oxeas perpendicular to surface (Figure 10I), sometimes hispidating it. The choanosome shows multispicular tracts of oxeas, with some sparse oxeas in between that become more evident in the subectosomal region, where they run radially to surface. A moderate amount of collagen is

https://doi.org/10.1017/S0025315418000589

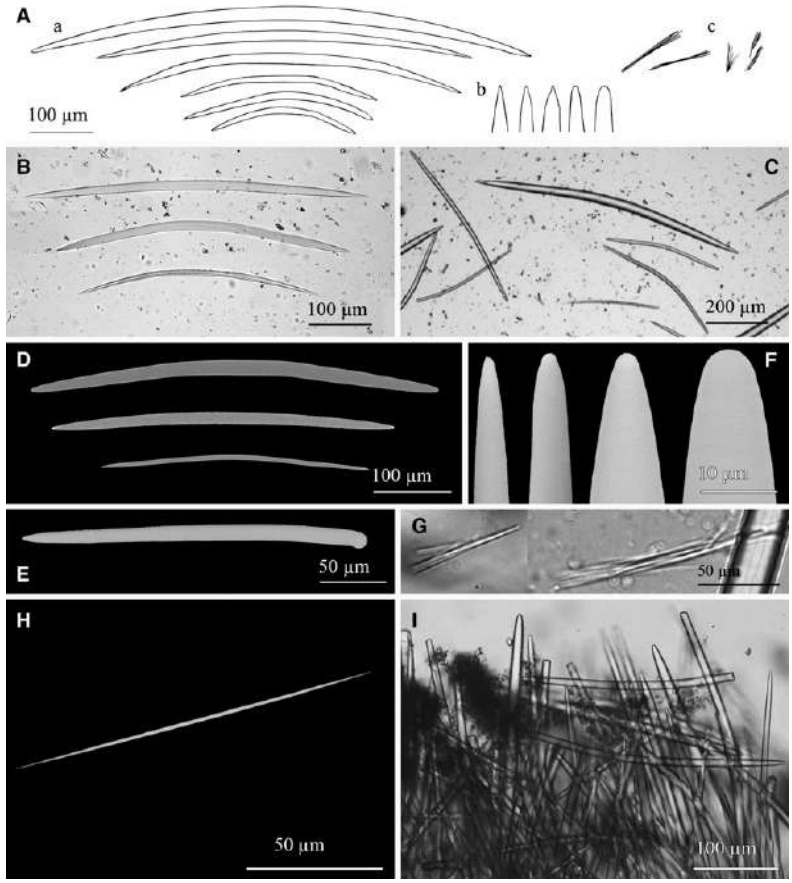

Fig. 10. *Myrmekioderma indemaresi* sp. nov.: (A) Line drawing summarizing the skeletal complement of the species. Oxeas occur in a wide variety of sizes and are once or twice bent (a) with variable ends that can be acerate, mucronate, stepped or blunt (b). Raphides occur in wispy trichodragmata in two different categories (c). (B) Light microscope view of oxeas once and twice bent. (C) Light microscope view of oxeas of different sizes. (D) SEM view of oxeas nearly straight and softly bent. (E) SEM view of an oxea with a blunt, almost subtylote end modification. (F) SEM detail of slight to even blunt ends of oxeas. (G) Raphides in trichodragmata. (H) SEM view of a raphide. (I) Light microscope view of ectosomal oxeas perpendicular to surface.

present in the tracts. Trichodragmata occur in all regions of the skeleton.

Spicules

Megascleres are oxeas in a wide size range of 200–1020 × 3.5–30 µm. They are from slightly to evenly, once or twice, bent, with acerate ends (Figure 10A, D) that sometimes are blunt (Figure 10F, E), mucronated or stepped. Oxeas located in the ectosome are shorter, showing a maximum size of 520 × 15 µm. Microscleres are moderately abundant raphides in wispy trichodragmata (Figure 10G, H). Raphides are from straight to slightly sinuous and measure 35–212.5 × 1.2–1.4 µm.

Distribution and ecology notes

The specimens were collected from Gazul mud volcano. One of them from a fine sand with MDAC bottom at a depth of 422–450 m. The other individual was from a bottom of muddy gravel and fine sand with MDAC at 380–455 m depth (Table 1). The collected material makes the first deep-sea record of this genus, since its deepest record is 73 m depth. To date *Myrmekioderma* species were known from the Indian and Pacific Oceans, the western Atlantic and the Mediterranean. This is the first record of *Myrmekioderma* in the eastern Atlantic.

Taxonomic remarks

Among the *Myrmekioderma* species from the Atlantic and Mediterranean, the spicule complement of the collected specimens shows some resemblance with that of *Myrmekioderma spelaea* (Pulitzer – Finali, 1983) from the Mediterranean. However, the examination of the holotype of *M. spelaea* has revealed a smooth non-tuberculated surface, the presence of often anisostrongylote oxea measuring 82.5–680 × 2.5–25 µm and trichodragmata measuring 30–150 × 5–8 µm. Its choanosome is confused while its ectosome is arranged tangentially and easily detachable. Also its distribution in depth is different, since it is recorded from 5 m depth. The specimens here described also coincide in showing similar oxeas and trichodragmata with *Epipolasis spissa* (Topsent, 1892), recorded from Azores and Mediterranean. But

https://doi.org/10.1017/S0025315418000589

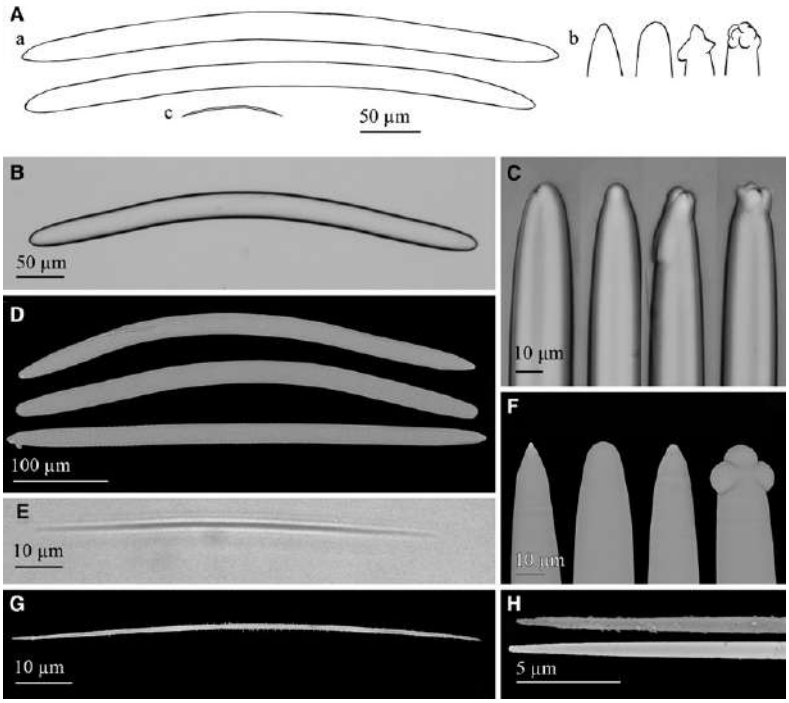

Fig. 11. *Petrosia* (*Petrosia*) *raphida* Boury-Esnault, Pansini & Uriz, 1994: (A) Line drawing summarizing the skeletal complement of the volcano specimen. Strongyloxeas (a) are usually bent and show variable ends from slightly to markedly strongylote and sometimes polyactine or tuberculate (b). Raphides (c) are strait or centrally bent and microspined. (B) Light microscope view of a strongyloxea. (C) Light microscope view of strongylote, mucronate or polyactine strongyloxea ends. (D) SEM view showing the variable shapes and ends of strongyloxeas. (E) Light microscope view of a raphide. (F) SEM detail of conic, strongylote, mucronated and tuberculate ends of strongyloxeas. (G) SEM view of a raphide with microspines. (H) SEM detail of raphides ends with spines, and with nearly absent spines.

it bears toxas (Topsent, 1892, 1904) and its skeletal structure is described as a subhalichondroid reticule (De Weerdt, 2002). Since no other species comparable to the collected specimens have been hitherto described, we consider them to constitute a species new to science.

There is little doubt that our two specimens fit the diagnosis of genus *Myrmekioderma*, concerning habit and spicules complement. However, during our examination of the holotype of *M. spelaea*, we have noticed that this species appears to fit better in the current diagnosis of the genus *Epipolasis* than in *Myrmekioderma*. Van Soest *et al.* (1990) transferred *Raphisia spelaea* to *Myrmekioderma spelaea* when the latter was still considered a halichondrid and genus *Epipolasis* a synonym of *Myrmekioderma*. Given the noticed similarities between the holotype of *M. spelaea*, including a detachable ectosome, and current *Epipolasis* diagnosis (Erpenbeck and van Soest, 2002), a genus transfer for such a species, that is, *Epipolasis spelaea* (Pulitzer-Finali, 1983), should be advisable.

Order HAPLOSCLERIDA Topsent, 1928
Family PETROSIIDAE van Soest, 1980
Genus *Petrosia* Vosmaer, 1885
DIAGNOSIS: (Desqueyroux-Fáundez & Valentine, 2002)
Petrosia (*Petrosia*) *raphida* Boury-Esnault, Pansini & Uriz, 1994
(Figures 3H & 11).

Material examined

Specimen P200-11BT17 collected from Station 16.

Macroscopic description

Fragment of a specimen, measuring 20 mm in length, 10 mm in width and 1–5 mm in thickness, attached to a rock. Oscules are not observed (probably due to the fragment condition of the specimen) but ostioles of 0.2–0.5 mm in diameter are abundantly scattered over the scarce areas of preserved surface, which is smooth to the touch and crust-like in consistency. Choanosome is friable and somewhat loose. Colour after preservation in ethanol is creamy beige (Figure 3H).

Skeletal structure

The skeleton of the ectosome is a tangential net of multispicular tracts of a diameter of 150–300 µm made by strongyloxeas and raphides. Choanosome is a three-dimensional net of multispicular tracts of strongyloxeas and raphides forming more or less roundish meshes of 50–165 µm in width. Spongin not observed.

Spicules. Megascleres are strongyloxeas (Figure 11A, B, E), moderately once or twice bent, although nearly straight and marked curvatures sometimes occur. They are mostly isodiametric, with ends ranging from slightly acerate to strongylote. Both iso- and anisoxeas occur, the first being the usual form. Conical, mucronated, stepped, polyactine and tuberculated ends are fairly common (Figure 11A, C, F). Size is 290–500 × 20–25 µm and diameters down to 7.5 µm are occasional. Microscleres are abundant raphides (Figure 11A, D, G), from straight to centrally bent, with microspines, regularly spread or more abundant at the ends.

https://doi.org/10.1017/S0025315418000589

More rarely, the microspination is nearly lacking (Figure 11H). Raphides measure 75–100 × 0.95–1.15 µm.

Distribution and ecology notes

The specimen was collected from depths of 530–573 m, growing on a small MDAC piece from a sandy mud bottom at Pipoca mud volcano (Table 1). It makes the first record of the species in the Atlantic Ocean, two individuals being known so far from the Mediterranean side of the Strait of Gibraltar, at 580 m depth (Boury-Esnault *et al*., 1994).

Taxonomic remarks

Our specimen fits the holotype description of *P. raphida*, with two minor differences. One relates to megascleres tips, those of the type specimen usually being strongylote, sometimes varying to narrower or swollen ends. The other difference is the presence of microspines in raphides, not reported in the original description, although, admittedly, these spines are only observable through scanning electron microscopy. Since the collected material fits the spicule complement and skeletal structure of *P. raphida* and it was collected not geographically far from the holotype collection site, the two minor differences reported above are considered as intraspecific variability of those characters.

The literature of additional *Petrosia* species recorded from the Atlantic and the Mediterranean have been considered, being *Petrosia* (*Strongylophora*) *davilai* (Alcolado, 1979), from Cuba, the only one which bears raphides. Nevertheless, it shows smaller strongyles (29–311 × 3–9 µm) and microxeas, which are not present in our specimens.

The genus *Petrosia* is currently divided in two subgenera, mainly differentiated by: (i) the number of size categories of oxeas or strongyles (subgenus *Petrosia* shows 2–3 categories while subgenus *Strongylophora* Dendy, 1905 shows 3–5); (ii) the ectosomal skeleton architecture (unispicular ectosomal network in *Petrosia* and dense irregular tangential ectosomal reticulation of free strongyles and oxeas of different sizes echinated by small centrangulate microxeas in *Strongylophora*); (iii) absence and presence of microscleres in *Petrosia* and *Strongylophora* respectively (Desqueyroux-Fáundez & Valentine, 2002). It is worth noting that *P. raphida* is close to the current diagnosis of subgenus *Petrosia* but it differs from it by having only a category of megascleres, microscleres and a multispicular tangential network. Therefore, a readjustment of the subgenus diagnosis would be advisable, as it is herein suggested: Subgenus *Petrosia* characterized by a tangential specialized ectosomal uni- or multispicular network, and a very dense lamellate-isotropic choanosomal skeletal network of thickly crowded spicule tracts producing rounded meshes, forming layers parallel to the surface. A dense interstitial reticulation of free spicules gives the sponge a stony texture. Megascleres are in 1–3 distinct size categories of oxeote or strongylote spicules. Microscleres occasionally present.

Family CHALINIDAE Gray, 1867
Genus *Cladocroce* Topsent, 1892
DIAGNOSIS: (De Weerdt, 2002)
Cladocroce fibrosa (Topsent, 1890)
(Figures 3I, J, 12).

Material examined

One of four specimens collected from the mud volcanoes of Gulf of Cadiz: P54-11BT17 from Station 16; P54-11BT06A to C from Station 21.

Macroscopic description

Foliaceous body, erect on a cylindrical stalk. Its body measures 130 mm in length, 50 mm in width and 2 mm thick. The stalk is 80 mm in height and 3 mm in diameter at its base, reaching up to 11 mm at the junction with the body, where it ramifies in three main branches. The surface at the best preserved areas is hispid and pores of 0.5–3 mm are abundantly spread on both faces. The body is flexible but collapses outside the water while the stalk is robust and keeps its shape. Colour after preservation in ethanol is beige, the stalk being darker than the body (Figure 3I, J).

Skeletal structure

The skeleton of the stalk is made of highly compacted oxeas longitudinally arranged, with moderately abundant spongin in-between. The skeleton of the stalk ramifies at its upper extreme in three main multispicular tracts that run longitudinally along the body. They anastomose in thinner multispicular tracts, which are connected by uni- and paucispicular tracts and single oxeas that make a diffuse triangular net with oval meshes (Figure 12E, F). As a consequence, the skeleton of the body is reticulate. There is no ectosomal skeleton differentiated.

Spicules

Oxeas softly bent, sometimes straight or markedly bent, occasionally asymmetric (Figure 12A–C). Ends are acerate, more or less sharp (Figure 12D). They measure 410–610 × 10–17 µm.

Distribution and ecology notes

The specimen was collected from a 530–573 m depth range, on a sandy mud bottom with MDAC from Pipoca mud volcano (Table 1). It makes the second Atlantic record. One specimen was previously collected on sand and mud bottom at 1300 m depth in Azores (Topsent, 1892), and two more individuals from a mud bottom of Planier Canyon, off Marseille, at 352 m depth, in the western Mediterranean (Vacelet, 1996). Also, Fourt *et al.* (2017) provided seven records off the Mediterranean French coasts (Calvi, Cassidaigne, Planier, Porquerolles and Sicié Canyons and Banc de Magaud) and Corse (Ajaccio Canyon) between 250–510 m depth.

Taxonomic remarks

Several species of *Cladocroce* occur in the Atlantic, and some of them show a lamellate habit: *Cladocroce spatula* (Lundbeck, 1902), *Cladocroce spathiformis* Topsent, 1904 and *Cladocroce osculosa* Topsent, 1927, the last one lacking a stalk. Nevertheless, *C. fibrosa* is the only one bearing evident, thick, oxea fibres that rise from the base and ramify longitudinally as they become thinner. Likewise, none of the *Cladocroce* spp. has oxeas out of the size range 62–375 × 2–25 µm, except for *C. fibrosa*. The oxeas of the latter are reported to measure 600 × 18 µm by Topsent (1892) and 445–570 × 14–20 µm by Vacelet (1996), data which are also consistent with the sizes in our specimen.

Cladocroce spathiformis Topsent, 1904
(Figures 3K & 13).

Material examined

Eight specimens collected from the mud volcanoes of Gulf of Cadiz: P05-10BT03A to E from Station 1; P05-11BT17 from Station 16; P05-11BT18 from Station 15 and P05-11BT31 from Station 18.

Macroscopic description

Lamellar fragments of 58 mm in length, 47 mm in width and 8 mm thick, one is conserving the attachment base. The surface is porous, and oscula of 1–2 mm in diameter are all located at one face. The surface is slightly hispid and shows spared sand

https://doi.org/10.1017/S0025315418000589

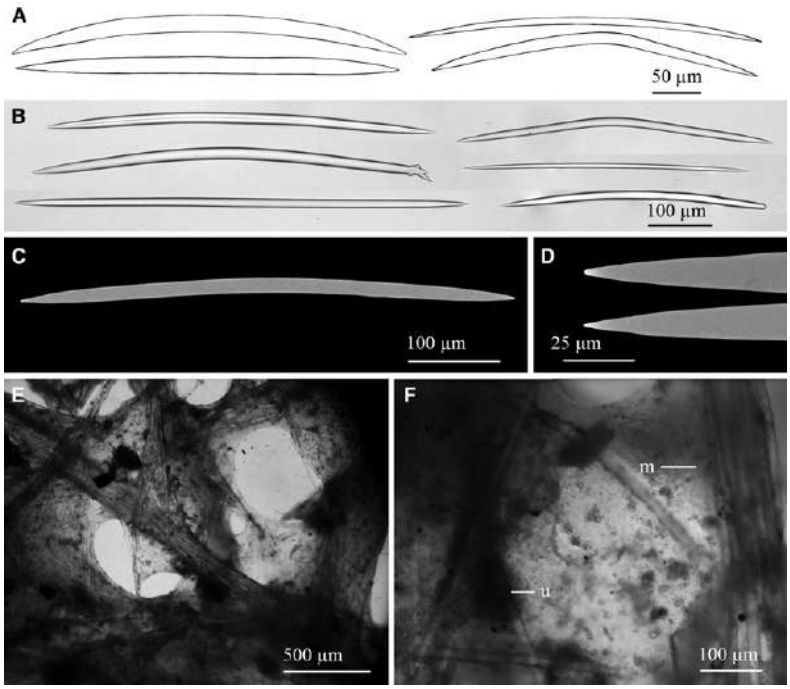

Fig. 12. *Cladocroce fibrosa* (Topsent, 1890): (A) Line drawing summarizing the skeletal complement of the volcano specimen. Oxeas are usually slightly bent but range from straight to markedly bent, with normally acerate ends. (B) Light microscope view of oxeas variable in shape and ends. (C) SEM view of an oxea. (D) SEM detail of more or less sharpened acerate ends of oxeas. (E) Light microscope view of skeletal structure of the body with multispicular tracts of oxeas in between which single oxeas form a diffuse triangular net. (F) Light microscope detail of a multispicular tract (m) and three unispicular tracts (u) forming a triangular net.

rests observed under binocular microscope. Consistency is fleshy, firm and friable, poorly flexible. Colour after preservation in ethanol ranges from beige to brown (Figure 3K).

Skeletal structure

Ectosomal skeleton is a tangential, triangular reticule of uni- and paucispicular tracts, also with some debris. Spongin is only visible at nodes. The choanosomal skeleton at the base of the body is an anisotropic reticule of multispicular (Figure 13F) tracts of oxea, measuring about 60–175 µm in diameter, connected by paucispicular (Figure 13E), some unispicular tracts and free spicules. At the upper part of the body multispicular tracts are scarce, being mainly pauci- and unispicular along with free oxeas. They form a more or less triangular mesh with some detrital inclusions in some specimens.

Spicules. Isodiametric oxeas, usually softly bent (Figure 13A–C), sometimes straight or markedly bent once or twice. Ends are often mucronate, stepped, or sometimes strongylote (Figure 13D). They measure 312–422 × 5–17 µm.

Distribution and ecology notes

The specimens were collected from 460–729 m. Five came from a muddy medium sand bottom from Gazul mud volcano, two others were collected from sandy mud bottoms with MDAC from Pipoca, and an eighth one came from a sandy mud with MDAC bottom from Chica mud volcano (Table 1). They constitute the second record of the species, hitherto only one specimen being known, collected from a muddy sand bottom at 1165 m depth in Azores (Topsent, 1904).

Taxonomic remarks

The collected specimens fit the holotype of *C. spathiformis*, which was described to be brown and lamellate, with several aquiferous openings and oxeas measuring 375 × 17 µm. The collected material slightly resembled *Cladocroce osculosa* Topsent, 1927, recorded from the Ibero-Moroccan Gulf (Topsent, 1928), in being lamellate and brown with numerous aquiferous openings, but our specimens are much thicker than those of *C. osculosa* (1.5 mm thick) and show larger oxea than *C. osculosa* (225 × 9 µm). Similarly, our specimens share a lamellate habit with *Cladocroce spatula* (Lundbeck, 1902), recorded from Iceland and Greenland, but our specimens have larger oxeas than those of *C. spatula* (190–220 × 10–12 µm). They also have multi-spicular choanosomal tracts, distinguishable from uni- or paucispicular primary tracts characterizing *C. spatula* choanosomal skeleton (Lundbeck, 1902).

Genus *Haliclona* Grant, 1836
DIAGNOSIS: (De Weerdt, 2002)
Subgenus *Haliclona* (*Rhizoniera*) Griessinger, 1971
Haliclona (*Rhizoniera*) *pedunculata* (Boury-Esnault, Pansini & Uriz, 1994)
(Figures 3L & 14, Table 3).

Material examined

Seven of 49 specimens collected from the mud volcanoes of Gulf of Cadiz: P23B-11BT01 from Station 8; P23B-11BT05A to J from

https://doi.org/10.1017/S0025315418000589

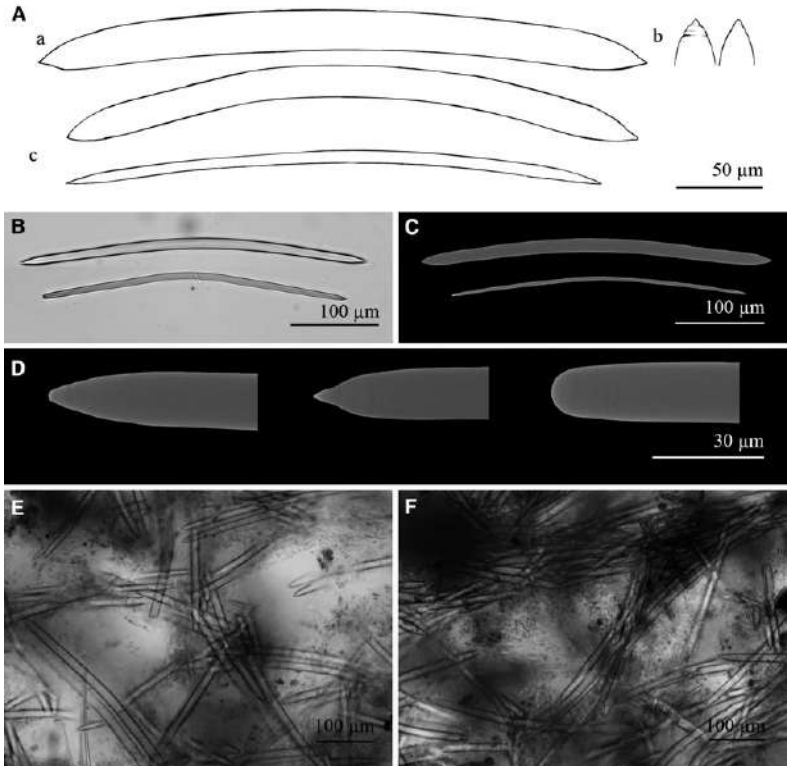

Fig. 13. *Cladocroce spathiformis* Topsent, 1904: (A) Line drawing summarizing the skeletal complement of the volcano specimen. Oxeas are usually once or twice softly bent (a) and often show mucronate and stepped ends (b). Thinner oxea sometimes occur (c). (B) Light microscope view of two oxea. (C) SEM view of two oxea. (D) SEM detail of slightly stepped, mucronate and strongylote oxea ends. (E) Light microscope view of paucispicular tracts of oxea. (F) Light microscope view of multispicular tracts of oxea.

Station 19; P23B-11BT06A to N from Station 21; P23B-11BT11A to H from Station 12; P23B-11BT16A & B from Station 13; P23B-11BT20A to N from Station 17.

Comparative material examined

Holotype of *Haliclona* (*Rhizoniera*) *rhizophora* (Vacelet, 1969) as *Reniera rhizophora* (MNHN-JV-68-13) from Standia, North of Crete (Station 12; 35°29′7″N 25°14′6″E, 150 m depth, 1984); Holotype of *Haliclona* (*Rhizoniera*) *pedunculata* (Boury-Esnault, Pansini & Uriz, 1994) as *Rhizoniera pedunculata* (MNHN D-NBE.MP.MV-3) from off Sant Vincent Cape, Portugal (Station DW16-187; 36.7°N 9.4°W, 1280–1285 m depth, 1984).

Macroscopic description

Stalked, with inverted pyriform and somewhat compressed body, which is 8–15 mm long and 5–8 mm wide (one specimen showed an irregularly shaped, flattened body measuring 13 mm wide). The stalk is flexible and cylindrical, measuring 4–17 mm long and 0.3–1.5 mm wide. At its distal extreme, the stalk divides radially along the body base so that it forms a supporting structure. The stalk also ramifies at its basal end in 2–7 rhizomes that are 4–25 mm long and 0.1–1 wide. Some specimens show partially or totally broken rhizomes and one of them bears two stalks. Oscule normally not observed, probably contracted, with the exception of one individual with an oscular tube. Surface shows abundant pores of up to 0.75 mm. Texture is spongy and fragile, colour after preservation in ethanol is light brown at the body and beige at the stalk (Figure 3L).

Skeletal structure

There is no ectosomal skeleton differentiated. The choanosomal skeleton is an anisotropic somewhat irregular reticule of paucispicular tracts of oxeas forming primary lines which are interconnected by a net of unispicular tracts of oxeas (Figure 14H, I). Spongin is hardly observed and microscleres are scattered all over the body. Stalk is made of densely packed ascending multispicular tracts of oxeas.

Spicules

Megascleres are oxeas softly bent, sometimes straight (Figure 14A, B, D), with acerate ends (Figure 14A, E). They are 350–470 × 8–12.5 µm. Thin developing stages (Figure 14D) are sometimes observed in some specimens, measuring down to 270 × 2.5 µm. Microscleres generally are fairly abundant toxas, markedly bent and with ends curved upwards (Figure 14A, C, G). They measure 47.43–74 × 1–1.9 µm. There are also abundant sigmata, with a slightly angulate shape at the centre of their shaft (Figure 14A, C, F), measuring 13.75–24 × 0.6–1.6 µm. Yet, although the seven specimens studied in full detail consistently showed a single sigmata category and presence of toxa, some variability was noticed

https://doi.org/10.1017/S0025315418000589

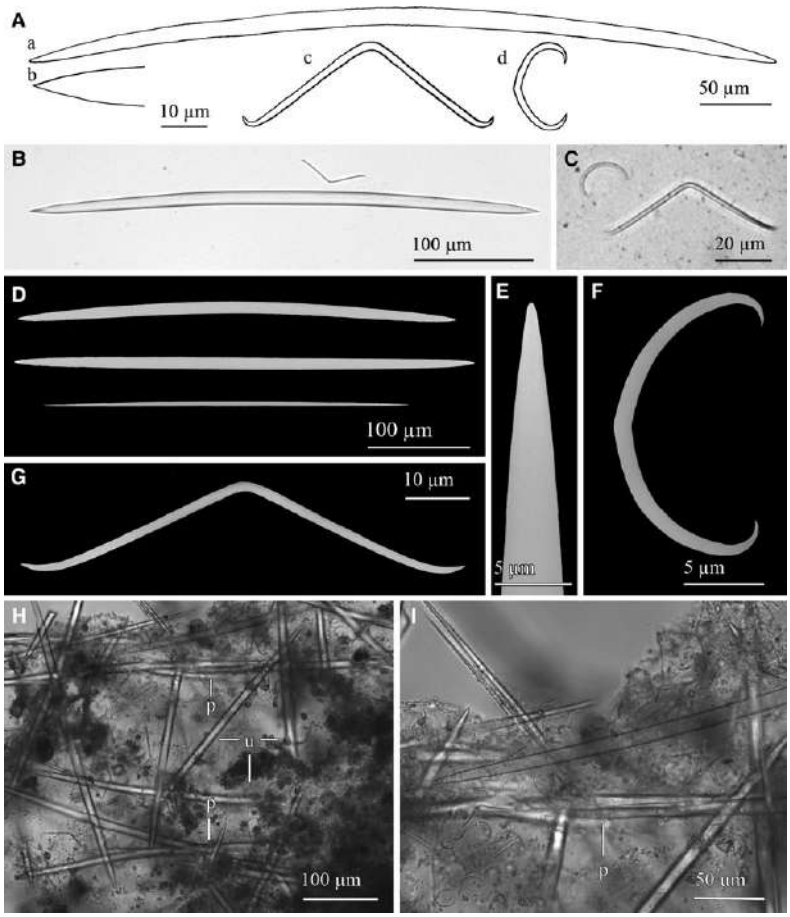

Fig. 14. *Haliclona* (*Rhizoniera*) cf. *pedunculata* (Boury-Esnault, Pansini & Uriz, 1994): (A) Line drawing summarizing the skeletal complement of the collected specimens. Oxeas (a) are somewhat fusiform and softly bent with acerate ends (b). Microscleres are toxas (c) markedly bent and sigmata (d) slightly angulate. (B) Light microscope view of an oxea and a toxa. (C) Light microscope view of a toxa and a sigma. (D) SEM view of slightly different oxeas and a developing one. (E) SEM detail of an end of an oxea. (F) SEM detail of a sigma. (G) SEM detail of a toxa. (H) Light microscope view of the reticulate skeleton with paucispicular tracts (p) connected by unispicular tracts of oxeas or single oxeas (u). (I) Light microscope detail of a paucispicular tract. Note microscleres spared all around the skeleton.

regarding the microscleres when the microscleres of the remaining 43 specimens were examined. A total of four specimens showed not one but two size categories of sigmata (12.5–25 × 1.5–2.5 µm and 27.5–37.5 × 1.25–2 µm for pooled data; for individual data see Table 3), two other specimens had a single sigmata category but lacked toxa, one of them showing a wide size range of sigmata not discernible in two categories (Table 3).

Distribution and ecology notes

The individuals were collected at muddy sand and sandy mud bottoms at depths between 489–719 m from Anastasya, Tarsis, Pipoca and Chica mud volcanoes (Table 1). Despite being notably common across different mud volcanoes, the collected specimens constitute the second record for the species, which had previously been recorded from a nearby area of the Atlantic (36°43′N 9° 24′W), where three specimens were collected from depths of 1141 and 1283 m (Boury-Esnault *et al.*, 1994).

Taxonomic remarks

The collected specimens fit well the features of subgenus *Haliclona* (*Rhizoniera*) (De Weerdt, 2002) except, in some of them, for the presence of microscleres. However, the variability in the microscleres across the herein studied individuals indicated that their presence/absence can be a matter of intraspecific variability. Examination of the holotype revealed that the stalk was broken, for which rhizomes could not be observed, and that toxas were actually present but scarce, measuring 64–74.28 × 1.6–2.5 µm. This result is important because it is modifying the original description of the species, which was thought to lack toxa. Yet there are two minor differences between the collected and the type material. The holotype bears a small oscular tube, which has been only observed in one of the specimens from the Gulf of Cadiz and is therefore assumed to be contracted in the rest of them. The other difference concerns the sigmata, since the holotype shows two categories with a wider size range (16.25–29.35 × 0.7–1.4 µm and 35–70 × 2–3.75 µm). Four of the

https://doi.org/10.1017/S0025315418000589

Table 3. Summary of microsclere size in the six individuals of *Haliclona* (*Rhizoniera*) *pedunculata* that showed an atypical microsclere composition out of the 49 collected individuals

Specimen	Sigmata I (μm)	Sigmata II (μm)	Toxa (μm)
P23B-11BT05A	12.5–25.0 × 2.0–2.5	32.5–37.5 × 1.25–2.0	60.6–70.0 × 1.3–1.7
P23B-11BT05B	17.5–20.0 × 2.0–2.5	30.0–35.0 × 1.25–2.0	53.8–66.1 × 1.4–1.8
P23B-11BT05C	15.0–21.0 × 2.0–2.5	27.5–33.2 × 1.20–2.0	56.4–70.4 × 1.5–2.6
P23B-11BT06A	15.0–23.0 × 1.5–2.0	27.5–36.0 × 1.25–1.5	58.2–65.4 × 1.3–2.0
P23B-11BT06B	20.0–27.0 × 1.3–1.8	Absent	Absent
P23B-11BT06C	16.1–32.5 × 1.0–1.8	Absent	Absent

Gulf of Cadiz specimens have been found to show two categories as well, but two others had only one category and lacked toxa, one of them showing sigmata in a wide size range not separable in categories. Therefore, the microsclere spicule complement is assumed to be subject to important intraspecific variability.

Due to the high number of collected specimens, it is no longer possible to consider *H. pedunculata* as an isolated case of a microscleres-bearing individual in the subgenus *Rhizoniera*. Rather, an amendment of its current diagnosis is suggested as follows to consider that stalked species with microscleres are to be included in this subgenus: Sponges thickly encrusting, cushion-shaped with oscular chimneys or mounds, or massive, rarely stalked. Consistency soft to moderately firm, sometimes viscous. Surface frequently slightly hispid through projecting spicules of the primary lines. Colour brown, pink, purple or bluish-grey. Megascleres usually slender oxeas with acerated points. Microscleres are rarely present sigmas and toxas. Consistency soft to moderately firm (amended from De Weerdt, 2002).

Discussion

The study of the sponge fauna of eight mud volcanoes from the Gulf of Cadiz resulted in the identification of 1659 specimens belonging to 82 species. Two of them were new to science and several others were little known previously. Apart from the taxonomic value of the gathered collection, three of the species, *Geodia anceps*, *Coelosphaera* (*Histodermion*) *cryosi* and *Petrosia* (*Petrosia*) *raphida* were hitherto known from the Alboran Sea. Their present discovery in the Gulf of Cadiz mud volcanoes bathed by the MOW could well testify for a natural export towards the Atlantic of deep-sea Mediterranean benthic fauna. The occurrence of *G. anceps* in the Avilés Canyon (Cantabrian Sea) has also been recently corroborated (Ríos and Cárdenas, personal communication), which suggests dispersal from the Mediterranean following the northwards MOWs along Portuguese coasts. A similar effect has been detected for crinoids, with large bathyal fields of the typically Mediteranean species *Leptometra phlangium* growing at the Pipoca mud volcano (Palomino *et al*., 2016), which is located in the pathway of the MOW. In contrast, in those bathyal areas of the Gulf of Cadiz that are located out of the MOW pathway, the crionid aggregations are formed by a typically Atlantic species, *Leptometra celtica* (Fonseca *et al*., 2014). According to the scarce available information, the natural transfer of Mediterranean species towards the Gulf of Cadiz could be interpreted as being of much lower intensity than the other way around. In the only previous study addressing this issue (Boury-Esnault *et al*., 1994), it was found that the Atlantic stations bathed by the outgoing MOW did not show noticeable values of species richness. Only about 18% of the species collected in that study were present in both the Atlantic and the Mediterranean side of the Gibraltar Strait. Six species considered to that date as Mediterranean endemisms were collected for the first time in the Gulf of Cadiz (Boury-Esnault *et al*., 1994). Combining this literature data and our new records, it appears that out of the 62 species known to occur both in the north-eastern Atlantic and the western Mediterranean, about 26 are from deep-sea locations bathed by the MOW. Therefore, it could be that the natural export of Mediterranean deep-sea benthos by the MOW is more important than previously believed from the few available studies.

Some elemental numerical analyses of the species richness and sponge abundance have been made, but the results have to be interpreted very cautiously since the gathered sponge collection is affected by large between-volcano differences in sampling effort. Because of logistical limitations, the deep mud volcanoes were systematically sampled less extensively than the shallow ones. For this reason, the possibility cannot be discarded that the fauna of some of the deeper volcanoes could be seriously underrepresented in the gathered sponge collection. From the available data, it appears that most of the sponge species occur in low to moderate abundance in the mud volcanoes and are not spatially overrepresented, with the exception of Gazul and Aveiro which show small aggregations of species such as *Petrosia crassa* and *Thenea muricata*. The analyses also suggest that those mud volcanoes located at mid depths on the continental slope seem to host a richer sponge fauna than those placed in shallower or deeper waters. A previous study using a manned submersible to record sponge abundance over a transect along the upper part of a tropical continental slope found a moderated increase in the species richness between 400 and 500 m depths (Maldonado & Young, 1996). From the present approach, the abundance of MDAC, which was *a priori* predicted to act as a source of new hard substrate suitable for sessile fauna, emerges as having no significant role in increasing the species richness per m^2 in the sponge fauna of the mud volcanoes. Likewise, the abundance of MDAC substrate did not correlate positively with the number of sponge individuals. Rather, sponge abundance per m^2 peaked in areas of soft bottom, where highly specialized species are known to form large aggregations. This situation is paradigmatically summarized by the mud volcano Aveiro, which, despite lacking authigenic carbonates, holds the highest values of sponge abundance due to the high abundance of *Thenea muricata* individuals. Therefore, the theoretical role of MDAC in somehow favouring the sponge fauna cannot be demonstrated in practice, at least from the available data.

Likewise, from the current data, no statistically significant effect can be put forward for the fishing activity concerning either the species richness or the sponge abundance, beyond slightly negative trends which lack statistical support (Figure 2D, E). These trends would suggest that both the species richness and the abundance would decrease with increasing fishing activity, except for some mud volcanoes where the faunal parameters are low despite being subjected to no or very low fishing activity. Yet, to derive more definitive conclusion in this regard a more extensive and homogeneous sampling of the mud volcanoes

https://doi.org/10.1017/S0025315418000589

located deeper than 500 m would be necessary, as well as the inclusion of a greater number of mud volcanoes in the analyses.

The combined effect of depth, occurrence of MDAC formations and fishing activity on the sponge communities of the volcanoes has not been assessed here, these multivariate analyses being part of a further, separate study (in preparation) that is specifically dealing with faunal and biogeographic affinities.

Supplementary material. The supplementary material for this article can be found at https://doi.org/10.1017/S0025315418000589.

Acknowledgements. The authors thank Dr Victor Díaz del Río, Dr Luis Miguel Fernández Salas and Dr Nieves López González from the Instituto Español de Oceanografía for organizing and conducting the collecting cruises. Scientists, technicians and crew members of the RV 'Emma Bardán' and RV 'Cornide de Saavedra' are gratefully acknowledged for their work on board. Dr Paco Cárdenas is especially thanked for identifying the *Geodia anceps* specimen and providing valuable data on this and other unpublished specimens from the Avilés Canyon. We also thank Gustavo Carreras (CEAB-CSIC) for help with line drawings and Maria García (CEAB-CSIC) for sputtering of SEM samples. Dr Isabelle Domart-Coulon (Muséum National d'Historie naturelle, Paris) and Dr Maria Tavano (Museo Civico di Storia Naturale Giacomo Doria, Genoa, Italy) are thanked for their assistance with loans of museum specimens. We thank both the General Secretary of Fisheries (Spanish Ministry of Agriculture and Fisheries) for providing access to Vessel Monitoring System data for monitoring the activity of the trawling fleet at the Gulf of Cádiz during 2011 and Emilio González García (University of Málaga) for the analysis of those data.

Financial support. This research has benefited from funds of two grants of the European Community (LIFE + INDEMARES 07/NAT/E/000732 and INTEMARES LIFE15 IPE/ES/000012) awarded to co-authors at the IEO. Likewise, this research has benefited from funds of a Spanish Ministry of Economy and Competitiveness grant (MINECO– CTM2015-6722-1R) and a European Union Horizon 2020 SponGES (no. 679849) grant awarded to the CEAB-CSIC.

References

Arnesen E (1920) Spongia. *Report on the Scientific Results of the 'Michael Sars' North Atlantic Deep-Sea Expedition 1910, 3, Part II*, 1–29.

Bouchet P and Taviani M (1992) The Mediterranean deep-sea fauna: pseudo-populations of Atlantic species. *Deep Sea Research* **39**, 169–148.

Boury-Esnault N, Pansini M and Uriz MJ (1994) Spongiaires bathyaux de la mer d'Alboran et du golfe ibéro-marocain. *Mémoires Muséum National d'Histoire Naturelle* **160**, 1–174.

Boury-Esnault N and Rützler K (1997) Thesaurus of sponge morphology. *Smithsonian Contributions to Zoology* **596**, 1–55.

Cárdenas P, Rapp HT, Klitgaard AB, Best M, Thollesson M and Tendal OS (2013) Taxonomy, biogeography and DNA barcodes of *Geodia* species (Porifera, Demospongiae, Tetractinellida) in the Atlantic boreo-Arctic region. *Zoological Journal of the Linnean Society* **169**, 251–311.

Carvalho FC, Pomponi SA and Xavier JR (2015) Lithistid sponges of the upper bathyal of Madeira, Selvagens and Canary Islands, with description of a new species of *Isabella*. *Journal of the Marine Biological Association of the United Kingdom* **95**, 1287–1296.

Coll M, Piroddi C, Steenbeek J, Kaschner K, Ben Rais Lasram F, Aguzzi J, Ballesteros E, Bianchi CN, Corbera J, Dailianis T, Danovaro R, Estrada M., Froglia C, Galil BS, Gasol JM, Gertwagen R, Gil J, Guilhaumon F, Kesner-Reyes K, Kitsos M-S, Koukouras A, Lampadariou N, Laxamana E, López-Fé de la Cuadra CM, Lotze HK, Martin D, Mouillot D, Oro D, Raicevich S, Rius-Barile J, Saiz-Salinas JI, San Vicente C, Somot S, Templado J, Turon X, Vafidis D, Villanueva R and Voultsiadou E (2010) The biodiversity of the Mediterranean Sea: estimates, patterns, and threats. *PLoS ONE* **5**, e11842.

Chevaldonné P, Pérez T, Crouzet J-M, Bay-Nouailhat W, Bay-Nouailhat A, Fourt M, Almón B, Pérez J, Aguilar R and Vacelet J (2015) Unexpected records of 'deep-sea' carnivorous sponges *Asbestopluma hypogea* in the shallow NE Atlantic shed light on new conservation issues. *Marine Ecology* **36**, 475–484.

de Mol B, Henriet JP and Canals M (2005) Development of coral banks in Porcupine Seabight: do they have Mediterranean ancestors? In Freiwald A and Roberts JM (eds), *Cold-water Corals and Ecosystems*. Berlin: Springer, pp. 515–533.

De Weerdt WH (2002) Family Chalinidae Gray, 1867. In Hooper JNA and van Soest RWM (eds), *Systema Porifera. A Guide to the Classification of Sponges*, vol. 1. New York, NY: Kluwer Academic/Plenum, pp. 852–873.

Desqueyroux-Fáundez R and Valentine CA (2002) Family Niphatidae van Soest, 1980. In Hooper JNA and van Soest RWM (eds), *Systema Porifera. A Guide to the Classification of Sponges*, vol. 1. New York, NY: Kluwer Academic/Plenum, pp. 874–890.

Díaz del Río V, Bruque G, Fernández-Salas LM, Rueda JL, González E, López N, Palomino D, López FJ, Farias C, Sánchez R, Vázquez JT, Rittierott CC, Fernández A, Marina P, Luque V, Oporto T, Sánchez O, García M, Urra J, Bárcenas P, Jiménez MP, Sagarminaga R and Arcos JM (2014) Volcanes de fango del Golfo de Cádiz, Proyecto LIFE + INDEMARES. *Fundación Biodiversidad. Ministerio de Agricultura, Alimentación y Medio Ambiente*, 1–128.

Erpenbeck D and van Soest RWM (2002) Family Halichondriidae Gray, 1867. In Hooper JNA and van Soest RWM (eds), *Systema Porifera. A Guide to the Classification of Sponges*, vol. 1. New York, NY: Kluwer Academic/Plenum, pp. 787–816.

Fonseca P, Abrantes F, Aguilar R, Campos A, Cunha M, Ferreira D, Fonseca TP, García S, Henriques V, Machado M, Mechó A, Relvas P, Rodrigues CF, Salgueiro E, Vieira R, Weetman A and Castro M (2014) A deep-water crinoid *Leptometra celtica* bed off the Portuguese south coast. *Marine Biodiversity* **44**, 223–228.

Fourt M, Goujard A, Pérez T and Chevaldonné P (2017) Guide de la faune profonde de la mer Méditerranée. Explorations des roches et des canyons sous-marins des côtes françaises. *Patrimoines naturels. Publications scientifiques du Museum national d'Histoire naturelle Paris* **75**, 1–184.

Gardner JM (2001) Mud volcanoes revealed and sampled on western Moroccan continental margin. *Geophysical Research Letters* **28**, 339–342.

Hestetun JT, Vacelet J, Boury-Esnault N, Borchiellini C, Kelly M, Ríos P, Cristobo J and Rapp HT (2016) The systematics of carnivorous sponges. *Molecular Phylogenetics and Evolution* **94**, Part A, 327–345.

Hooper JNA (2002) Family Desmoxyidae Hallmann, 1916. In Hooper JNA and van Soest RWM (eds), *Systema Porifera. A Guide to the Classification of Sponges*, vol. 1. New York, NY: Kluwer Academic/Plenum, pp. 755–772.

Ijima I (1904) Studies on the Hexactinellida. Contribution IV. (Rossellidae). *Journal of the College of Science, Imperial University of Tokyo* **18**, 1–307.

Kennedy JA (2000) Resolving the '*Jaspis stellifera*' complex. *Memoirs of the Queensland Museum* **45**, 453–476.

Kenyon NH, Ivanov MK, Akhmetzhanov AM and Akhmanov GG (2000) Multidisciplinary study of geological processes on the North East Atlantic and Western Mediterranean margins. *UNESCO*, 127.

León R, Somoza L, Medialdea T, González FJ, Díaz-del-Río V, Fernández-Puga MC, Maestro A and Mata MP (2007) Sea-floor features related to hydrocarbon seeps in deepwater carbonate-mud mounds of the Gulf of Cádiz: from mud flows to carbonate precipitates. *Geo-Marine Letters* **27**, 237–247.

Levin LA (2005) Ecology of cold seep sediments: interactions of fauna with flow, chemistry and microbes *Oceanography and Marine Biology. Annual Review* **43**, 1–46.

Longo C, Mastrototaro F and Corriero G (2005) Sponge fauna associated with a Mediterranean deep-sea coral bank. *Journal of the Marine Biological Association of the United Kingdom* **85**, 1341–1352.

Lundbeck W (1902) Porifera. I. Homorrhaphidae and Heterorhaphidae. *Danish Ingolf Expedition 1895–1896* **6**, 1–108.

Maldonado M (1992) Demosponges of the red coral bottoms from the Alboran Sea. *Journal of Natural History* **26**, 1131–1161.

Maldonado M (1993) Demosponjas litorales de Alborán. Faunística y Biogeografía. PhD. dissertation. University of Barcelona, Barcelona.

Maldonado M, Sánchez-Tocino L, López-Acosta M and Sitjà C (2011) Invertebrados claves del sistema infralitoral y circalitoral rocoso de las Islas Chafarinas: estudio con vistas a futuras estrategias de conservación. *Centro de Estudios Avanzados (CSIC)/Organismo Autónomo de Parques Naturales (OAPN)*, 1–84.

Maldonado M and Uriz JM (1995) Biotoic affinities in a transitional zone between the Atlantic and the Mediterranean: a biogeographical approach based on sponges. *Journal of Biogeography* **22**, 89–110.

Maldonado M and Young CM (1996) Effects of physical factors on larval behavior, settlement and recruitment of four tropical demosponges. *Marine Ecology Progress Series* **138**, 169–180.

Medialdea T, Somoza L, Pinheiro LM, Fernández-Puga MC, Vázquez JT, León R, Ivanov MK, Magalhaes V, Díaz-del-Río V and Vegas R (2009) Tectonics and mud volcano development in the Gulf of Cádiz. *Marine Geology* **261**, 48–63.

Palomino D, López-González N, Vázquez JT, Fernández-Salas LM, Rueda JL, Sánchez-Leal R and Díaz-del-Río V (2016) Multidisciplinary study of mud volcanoes and diapirs and their relationship to seepages and bottom currents in the Gulf of Cádiz continental slope (northeastern sector). *Marine Geology* **378**, 196–212.

Pansini M (1987) Littoral demosponges from the banks of the straits of Sicily and the Alboran Sea. In Vacelet J and Boury-Esnault N (eds), *Taxonomy of Porifera*, vol. G 13. Berlin: Springer Verlag, pp. 149–186.

Pérès JM and Picard J (1964) Nouveau manuel de bionomie benthique de la mer Méditerranée. *Recueil des Travaux de la Station Marine d'Endoume* **31**, 1–137.

Pinheiro LM, Ivanov MK, Sautkin A, Akhmanov G, Magalhães VH, Volkonskaya A, Monteiro JH, Somoza L, Gardner J, Hamouni N and Cunha MR (2003) Mud volcanism in the Gulf of Cádiz: results from the TTR-10 cruise. *Marine Geology* **195**, 131–151.

Pulitzer-Finali G (1970) Report on a collection of sponges from the Bay of Naples. I. Sclerospongiae, Lithistida, Tetractinellida, Epipolasida. *Pubblicazioni della Stazione Zoologica di Napoli: Marine Ecology* **38**, 328–354.

Rueda JL, Díaz-del-Río V, Sayago-Gil M, López-González N, Fernández-Salas LM and Vázquez JT (2012) Fluid venting through the seabed in the Gulf of Cadiz (SE Atlantic Ocean, Western Iberian Peninsula): geomorphic features, habitats, and associated fauna. In Harris PT and Baker EK (eds), *Seafloor Geomorphology as Benthic Habitat*. London: Elsevier, pp. 831–841.

Sánchez F, González-Pola C, Druet M, García-Alegre A, Acosta J, Cristobo J, Parra S, Ríos P, Altuna Á, Gómez-Ballesteros M, Muñoz-Recio A, Rivera J. and del Río GD (2014) Habitat characterization of deep-water coral reefs in La Gaviera Canyon (Avilés Canyon System, Cantabrian Sea). *Deep Sea Research Part II: Topical Studies in Oceanography* **106**, 118–140.

Schmidt O (1868) *Die Spongien der Küste von Algier. Mit Nachträgen zu den Spongien des Adriatischen Meeres*. Leipzig: W. Engelmann.

Schmidt O (1870) *Grundzüge Einer Spongien-Fauna des Atlantischen Gebietes*. Leipzig: W. Engelmann.

Sitjà C and Maldonado M (2014) New and rare sponges from the deep shelf of the Alboran Island (Alboran Sea, Western Mediterranean). *Zootaxa* **3760**, 141–179.

Suess E (2014) Marine cold seeps and their manifestations: geological control, biogeochemical criteria and environmental conditions. *International Journal of Earth Sciences* **103**, 1889–1916.

Tabachnick KP (2002) Family Rossellidae Schulze, 1885. In Hooper JNA and van Soest RWM (eds), *Systema Porifera. A Guide to the Classification of Sponges*, vol. 2. New York, NY: Kluwer Academic/Plenum, pp. 1441–1505.

Templado J, Calvo M, Moreno D, Flores A, Conde F, Abad R, Rubio J, López-Fé CM and Ortiz M (2006) *Flora y fauna de la reserva marina y reserva de pesca de la isla de Alborán*. Madrid: Ministerio de Agricultura, Pesca y Alimentación. Secretaría General de Pesca Marítima.

Templado J, García-Carrascosa M, Baratech L, Capaccioni R, Juan A, López-Ibor A, Silvestre R and Massó C (1986) Estudio preliminar de la fauna asociada a los fondos coralígenos del mar de Alborán (SE de España). *Boletín del Instituto Español de Oceanografía* **3**, 93–104.

Topsent E (1892) Contribution a l'étude des Spongiaires de l'Atlantique Nord. *Résultats des Campagnes Scientifiques accomplies par le Prince Albert I. Monaco* **2**, 1–165.

Topsent E (1898) Eponges nouvelles des Açores. (Première serie). *Mémoires de la Société Zoologique de France* **11**, 225–255.

Topsent E (1901) Considérations sur la faune des Spongiaires des côtes d'Algerie. Eponges de La Calle. *Archives de Zoologie Expérimentale et Générale*, *3eme série* **9**, 327–370.

Topsent E (1904) Spongiaires des Açores. *Résultats des Campagnes Scientifiques accomplies par le Prince Albert I. Monaco* **25**, 1–279.

Topsent E (1927) Diagnoses d'Eponges nouvelles recueillies par le Prince Albert I de Monaco. *Bulletin de l'Institut Océanographique de Monaco* **502**, 1–19.

Topsent E (1928) Spongiaires de l'Atlantique et de la Méditerranée, provenant des croissières du Prince Albert I de Monaco. *Résultats des Campagnes Scientifiques accomplies par le Prince Albert I. Monaco* **74**, 1–376.

Topsent E (1938) Contribution nouvelle à la connaisance des Eponges des côtes d'Algerie. Les espéces nouvelles d'O. Schmidt, 1868. *Bulletin de l'Institut Océanographique de Monaco* **758**, 1–32.

Uriz MJ (2002) Family Ancorinidae Schmidt, 1870. In Hooper JNA and van Soest RWM (eds), *Systema Porifera. A Guide to the Classification of Sponges*, vol. 1. New York, NY: Kluwer Academic/Plenum Publishers, pp. 108–126.

Vacelet J (1996) Nouvelles signalisations d'éponges profondes en Méditerranée. *Mésogée* **55**, 107–114.

Vacelet J and Boury-Esnault N (1996) A new species of carnivorous sponge (Demospongiae: Cladorhizidae) from a Mediterranean cave. *Bulletin de l'Institut Royal des Sciences Naturelles de Belgique* **66**(suppl.), 109–115.

Van Rooij D, De Mol L, Le Guilloux E, Reveillaud J, Hernández-Molina FJ, Llave E, Léon R, Estrada F, Mienis F, Moeremans R, Blamart D, Vanreusel A and Henriet J (2010) Influence of the Mediterranean outflow water on benthic ecosystems: answers and questions after a decade of observations. *GeoTemas* **11**, 179–180.

van Soest RWM (2002) Family Coelosphaeridae Dendy, 1922. In Hooper JNA and van Soest RWM (eds), *Systema Porifera. A Guide to the Classification of Sponges*, vol. 1. New York, NY: Kluwer Academic/Plenum, pp. 528–546.

van Soest RWM, Boury-Esnault N, Hooper JNA, Rützler K, de Voogd NJ, Alvarez B, Hajdu E, Pisera AB, Manconi R, Schönberg C, Klautau M, Picton B, Kelly M, Vacelet J, Dohrmann M, Díaz M-C, Cárdenas P, Carballo JL, Ríos P and Downey R (2018) World Porifera database. Available at http://www.marinespecies.org/porifera (accessed on 24.5.2018).

van Soest RWM, Díaz MC and Pomponi SA (1990) Phylogenetic classification of the Halichondrids (Porifera, Demospongiae). *Beaufortia. Series of Miscellaneous Publications* **40**, 15–62.

Vosmaer GCJ (1894) Preliminary notes on some Tetractinellids of the Bay of Naples. *Tijdschrift der Nederlandsche Dierkundige Vereeniging* **4**, 269–286.

Xavier JR, Cárdenas P, Cristobo J, van Soest R and Rapp HT (2015) Systematics and biodiversity of deep-sea sponges of the Atlanto-Mediterranean region. *Journal of the Marine Biological Association of the United Kingdom* **95**, 1285–1286.